

Revisions of the *clavipes* and *pruni* species groups of the genus *Merodon* Meigen, 1803 (Diptera, Syrphidae)

Ante Vujić¹, Snežana Radenković¹, Laura Likov¹, Nataša Kočiš Tubić¹, Grigory Popov^{2,3}, Ebrahim Gilasian⁴, Mihajla Djan¹, Marina Janković Milosavljević¹, Jelena Ačanski⁵

¹ University of Novi Sad, Faculty of Sciences, Department of Biology and Ecology, Trg Dositeja Obradovića 2, 21000 Novi Sad, Serbia

² I.I. Schmalhausen Institute of Zoology, National Academy of Sciences of Ukraine, Bohdan Khmelnytsky Street 15, UA-01030 Kyiv, Ukraine

³ Department of Environmental Sciences and Natural Resources, University of Alicante, PO Box. 99, 03080 Alicante, Spain

⁴ Insect Taxonomy Research Department, Iranian Research Institute of Plant Protection, Agricultural Research, Education and Extension Organization, Tehran, 19395-1454, Iran

⁵ University of Novi Sad, BioSense Institute, Dr Zorana Đinđića 1, 21000 Novi Sad, Serbia

Corresponding author: Jelena Ačanski (acanski@biosense.rs)

Abstract

This study focuses on the *avidus-nigritarsis* lineage within the genus *Merodon*, exploring morphological, genetic, and distributional aspects of two related assemblies within this lineage: the *clavipes* and *pruni* species groups. An integrative taxonomic approach was followed to ensure comprehensive species identification and validation, using adult morphology, wing geometric morphometrics, and genetic analysis of the mtDNA COI gene. In the *clavipes* group, seven species were identified, including three new species: *M. aenigmaticus* Vujić, Radenković & Likov, **sp. nov.**, *M. latens* Vujić, Radenković & Likov, **sp. nov.**, and *M. rufofemoris* Vujić, Radenković & Likov, **sp. nov.** In the *pruni* group, our revision revealed a new species, *M. aequalis* Vujić, Radenković & Likov, **sp. nov.**, and the revalidation of *Merodon obscurus* Gil Collado, 1929, **stat. rev.** *Merodon pallidus* Macquart, 1842 is redescribed. Diagnoses, identification keys to species, and distribution maps are provided, and neotypes for *Syrphus clavipes* Fabricius, 1781 and *Merodon quadrinotatus* (Sack, 1931) are designated. Additionally, the following new synonyms are proposed: *M. clavipes albus* **syn. nov.**, *M. clavipes ater* **syn. nov.**, *M. clavipes niger* **syn. nov.**, and *M. splendens* **syn. nov.** are junior synonyms of *M. clavipes*; and *M. velox armeniacus* **syn. nov.** and *M. velox anathema* **syn. nov.** are junior synonyms of *M. velox*.

Key words: Geometric morphometrics, hoverflies, integrative taxonomy, mtDNA COI gene, new species, new synonym



Academic editor: Ximo Mengual

Received: 15 January 2024

Accepted: 22 March 2024

Published: 28 May 2024

ZooBank: <https://zoobank.org/C1A2654B-7DC3-4451-91B7-49B29304FBED>

Citation: Vujić A, Radenković S, Likov L, Tubić NK, Popov G, Gilasian E, Djan M, Milosavljević MJ, Ačanski J (2024) Revisions of the *clavipes* and *pruni* species groups of the genus *Merodon* Meigen, 1803 (Diptera, Syrphidae). ZooKeys 1203: 1–69. <https://doi.org/10.3897/zookeys.1203.118842>

Copyright: © Ante Vujić et al.
This is an open access article distributed under terms of the Creative Commons Attribution License (Attribution 4.0 International – CC BY 4.0).

Introduction

The genus *Merodon* Meigen, 1803 (tribe Merodontini) is one of the most species-rich hoverfly genera, distributed across the Palaearctic and Afrotropical Regions and comprising 193 described and 41 yet-to-be formally described species (Vujić et al. 2021a). The Mediterranean Basin hosts the highest species diversity (Vujić et al. 2012) with approximately 140 known species (Vujić pers. comm. 21 February 2024), which has been linked to the high diversity of bulb plant species in this region that serve as larval host plants (Ricarte et al.

2008, 2017; Andrić et al. 2014; Preradović et al. 2018). The regions harbouring the greatest species richness are the Iberian, Balkan and especially the Anatolian peninsulas (Vujčić et al. 2021a). Asia Minor and Eastern Europe are considered hot spots and regions displaying high endemism levels for the genus (Kaloveloni et al. 2015), as documented by several studies in the Eastern Mediterranean Basin (Vujčić et al. 2007, 2011, 2013a, 2015, 2020a, 2020b, 2020c; Ståhls et al. 2009, 2016; Radenković et al. 2011, 2020; Kaloveloni et al. 2015; Ačanski et al. 2016, 2017; Kočiš Tubić et al. 2018; Likov et al. 2020). Central Asia and Pakistan also have numerous endemics with potential significance for the phylogeny of the genus *Merodon* (Vujčić et al. 2021a). In contrast, the Afrotropical and Eastern Palaearctic Regions are characterised by having less *Merodon* species (Vujčić et al. 2021a).

Vujčić et al. (2019) recognised five monophyletic lineages within the genus *Merodon*, i.e., *albifrons*, *aureus*, *avidus–nigritarsis*, *desuturinus*, and *natans* lineages, condensing previous studies from Šašić et al. (2016) and Radenković et al. (2018a). Inside the *avidus–nigritarsis* lineage, based on the morphological characters and molecular data, ten species groups have been established (*aberrans*, *aurifer*, *avidus*, *clavipes*, *fulcratus*, *italicus*, *nigritarsis*, *pruni*, *serrulatus*, and *tarsatus* groups) together with eight individual taxa without grouping affinities (*M. auronitens* Hurkmans, 1993, *M. caudatus* Sack, 1913, *M. clunipes* Sack, 1913, *M. crassifemoris* Paramonov, 1925, *M. eumerusi* Vujčić et al. 2019, *M. hirtus* Sack, 1932, *M. murinus* Sack, 1913, and *M. ottomanus* Hurkmans, 1993) (Likov et al. 2020; Vujčić et al. 2021a). Some of these groups were recently revised, such as the *aurifer* (Vujčić et al. 2021b), *avidus* (Likov et al. 2020), *nigritarsis* (Vujčić et al. 2013a; Likov et al. 2020), *serrulatus* (Vujčić et al. 2020b), *aberrans* (Vujčić et al. 2022), and *tarsatus* species group (Vujčić et al. 2023).

Hurkmans (1988) defined the *clavipes* species group of *Merodon* based on a single apomorphy, i.e., the structure of the anterior surstylar lobe, and he assigned several representatives: *M. aberrans* Egger, 1860, *M. brevis* Paramonov, 1926, *M. clavipes* (Fabricius, 1781), *M. cupreus* Hurkmans, 1988, *M. dzhalitae* Paramonov, 1927, *M. hamifer* Sack, 1913, *M. karadaghensis* Zimina, 1989, *M. lusitanicus* Hurkmans, 1988, *M. quadrinotatus* Sack, 1931, *M. splendens* Hurkmans, 1988, *M. velox* Loew, 1869, and *M. warnckei* Hurkmans, 1988. Nevertheless, Likov et al. (2020) presented this group in a much narrower sense, including large species (15–20 mm) with long body pilosity and a broad metafemur covered with long pile. Likov et al. (2020) only assigned two taxa to the *clavipes* group, namely *M. clavipes* and *M. velox*. Vujčić et al. (2021a) mentioned a few additional diagnostic features, such as that the constituent species all: are large and bumble bee-like (15–20 mm) with long body pilosity and a broad metafemur with long pile; have an elongated basoflagellomere; and the male genitalia are well-characterised with large anterior and posterior surstylar lobes. Accordingly, *M. quadrinotatus* and *M. vanderghooti* Hurkmans, 1993 were added to the *clavipes* species group.

Hurkmans (1988) established the *pruni* species group based on the structure of the male genitalia, a narrow vertex angle (angle between eyes on male vertex), and the extensive yellow coloration of the abdomen, and he included the nominal species and the variety *M. pruni* var. *obscurus* Gil Collado, 1929 as members of this group. In contrast, both Likov et al. (2020) and Vujčić et al. (2021a) defined the *pruni* species group based on a completely different set of diagnostic char-

acters: short body pilosity, short basoflagellomere, and the metatrochanter having a distinct calcar. Likov et al. (2020) assigned two species to the *pruni* group, namely *M. pallidus* Macquart, 1842 and *M. pruni* Rossi, 1790, whereas Vujčić et al. (2021a) recognised four species in this group, i.e., *M. cupreus* Hurkmans, 1993, *M. pallidus*, *M. pruni*, and one undescribed species from Israel.

Integrative taxonomy, or the use of different sources of information (molecular, morphometric, morphological characters) in the identification and delineation of taxa, has become a widely accepted approach in the taxonomic studies on the genus *Merodon* during the last 15 years. Examples are many for different groupings, like the *avidus* species complex (Popović et al. 2015; Ačanski et al. 2016), and several species groups such as the *ruficornis* (Vujčić et al. 2012), *desuturinus* (Vujčić et al. 2018), *aureus* (Milankov et al. 2008; Francuski et al. 2011; Šašić et al. 2016; Veselić et al. 2017; Radenković et al. 2018b; Ačanski et al. 2022), *nigritarsis* (Likov et al. 2020), *nanus* (Kočiš Tubić et al. 2018), *serrulatus* (Vujčić et al. 2020b), *constans* (Vujčić et al. 2020a), *rufus* (Radenković et al. 2020), *natans* (Vujčić et al. 2021c), *aberrans* (Vujčić et al. 2022), and *tarsatus* species groups (Vujčić et al. 2023).

The objectives of the present study are: 1) to review the *clavipes* and *pruni* species group; 2) to define morphological characters for both groups and their constituent species; 3) to study the type material of the species of both groups to resolve nomenclatural issues and to propose appropriate synonyms; 4) to use an integrative taxonomic approach involving molecular and geometric morphometric tools to describe the hidden taxonomic complexity of the taxa in both groups; 5) to describe the new taxa within these groups; 6) to provide identification keys and distributional maps for the species of both groups.

Materials and methods

Morphological study

In total 947 specimens of the *clavipes* species group and 722 specimens of the *pruni* species group were studied. The examined material belongs to the following institutions and private collections:

BA coll. - Barendregt Aat collection, the Netherlands; **BM coll.** - Bartak Miroslav Collection, Czech Republic; **CWM coll.** - de Courcy Williams Michael collection, Greece; **DD coll.** - Doczkal Dieter collection, Germany; **DJ coll.** - Dils Jos collection, Belgium; **EMIT** - Entomological Museum of Isparta, Isparta, Turkey; **FSUNS** - Faculty of Sciences, Department of Biology and Ecology, University of Novi Sad, Novi Sad, Serbia; **GLAHM** - Hunterian Zoology Museum, University of Glasgow, Glasgow, UK; **HM coll.** - Hauser Martin collection, USA; **HMIM** - Hayk Mirzayans Insect Museum, Insect Taxonomy Research Department, Iranian Research Institute of Plant Protection, Tehran, Iran; **IRSNB** - Institut royal des Sciences naturelles de Belgique, Brussels, Belgium; **IZY** - Institute of Zoology, Scientific Center of Zoology and Hydroecology, National Academy of Sciences of the Republic of Armenia, Yerevan, Armenia; **LAU** - Musée Zoologique, Lausanne, Switzerland; **LMR coll.** - Lyszkowski M. Richard collection, Bridge of Allan, UK; **LSF** - Museo Zoologico La Specola, Firenze, Italy; **LT coll.** - Lebard Thomas collection, France; **MAegean** - The Melissotheque of the Aegean, University of the Aegean, Mytilene, Greece; **MNCN** - Museo Nacional de Ciencias

Naturales, Madrid, Spain; **MNHN** – Musee National d’Histoire Naturelle, Paris, France; **MZH** – Finnish Museum of Natural History, University of Helsinki, Helsinki, Finland; **MZLS** – Natural History Museum, Zoological Section La Specola, Florence, Italy; **MZLU** – Museum of Zoology Lund University, Lund, Sweden; **NHMB** – Natural History Museum Belgrade, Belgrade, Serbia; **NHMUK** – Natural History Museum, London, UK; **NHMW** – Naturhistorisches Museum Wien, Vienna, Austria; **NMPC** – National Museum Prague, Prague, Czech Republic; **NMS** – National Museum of Scotland, Edinburgh, UK; **PMCG** – Natural History Museum of Montenegro, Podgorica, Montenegro; **RMNH** – Naturalis Biodiversity Center, Leiden, the Netherlands; **SA coll.** – Ssymank Axel collection, Germany; **SD coll.** – Sommaggio Daniele collection, Italy; **SJ coll.** – van Steenis Jeroen collection, the Netherlands; **SIZK** – I. I. Schmalhausen Institute of Zoology, National Academy of Sciences of Ukraine, Kyiv, Ukraine; **SJH coll.** – Stuke Jens-Hermann collection, Germany; **SJM coll.** – Smart J. Malcolm collection, UK; **SZMN** – The Siberian Zoological Museum of the Institute of Systematics and Ecology of Animal Siberian Branch of the Russian Academy of Sciences, Novo Sibirsk, Russia; **TAU** – Tel Aviv University, Tel Aviv, Israel; **THM** – Tullie House Museum & Art Gallery, Carlisle, UK; **TJM coll.** – Taylor J. Mike collection, UK; **USNM** – The Department of Entomology, of the National Museum of Natural History, Smithsonian Institution, Washington, DC, USA; **VWG coll.** – Van de Weyer Guy collection, Belgium; **WK coll.** – Watt Kenneth collection, Aberdeen, UK; **WML** – World Museum Liverpool, Liverpool, UK; **ZFMK** – Museum Koenig, LIB, Bonn, Germany; **ZHMB** – Zoologisches Museum of the Humboldt University, Berlin, Germany; **ZIS** – Zoological Institute and Museum, Sofia, Bulgaria; **ZMBH** – National Museum of Bosnia and Herzegovina, Sarajevo, Bosnia and Herzegovina; **ZMUC** – Zoological Museum, Natural History Museum of Denmark, University of Copenhagen, Copenhagen, Denmark.

The terminology adopted in the morphological descriptions follows Thompson (1999), except terms according to male genitalia which follows Marcos-García et al. (2007), “fasciate maculae” follows Vujčić et al. (2021a), and the term “fossette” follows Doczkal and Pape (2009).

In order to study the male genitalia, dry specimens were relaxed in a humidity chamber, and the genitalia were separated from the rest of the specimen using an entomological pin. Genitalia were cleared by boiling them individually in tubes of 10% KOH solution for a few minutes. This process was followed by brief immersion in acetic acid to neutralise the KOH, followed by immersion in ethanol to remove the acid. Genitalia were stored in microvials containing glycerol.

Nikon SMZ18 binocular microscope was used for morphological examination and drawing, while photographs were made using Nikon Digital Sight 10 digital camera. Afterwards, the photographs were stacked in CombineZ software (Hadley 2006). Measurements were taken with an eyepiece graticule or micrometer.

The distribution maps were generated with the mapping software ArcGIS v. 10.3 (ESRI 2014).

Molecular study

Genomic DNA of 47 hoverfly specimens belonging to the *clavipes* species group (27 specimens) and *pruni* species group (20 specimens) was obtained for the present study. DNA was extracted from meso- and metalegs using the

SDS extraction protocol described by Chen et al. (2010). DNA vouchers of the specimens are deposited at the Department of Biology and Ecology, Faculty of Sciences, University of Novi Sad (FSUNS). Two fragments (the 3'-end and 5'-end) of the mitochondrial COI gene were amplified using C1-J-2183 and TL2-N-3014 primer pair (Simon et al. 1994) and LCO-1490 and HCO-2198 primer pair (Folmer et al. 1994), respectively. The PCR reactions were carried out according to Kočič Tubić et al. (2018). Amplification products were enzymatically purified using Exonuclease I and Shrimp Alkaline Phosphatase enzymes (ThermoScientific, Lithuania) according to the manufacturer's instructions and then commercially sequenced in the forward direction by the MacroGen EZ-Seq service (MacroGen Europe, Amsterdam, Netherlands).

Chromatograms of sequences produced for this study were edited for base-calling errors using BioEdit v. 7.2.5. (Hall 1999) and adjusted manually. Additional sequences of species representing the main *Merodon* lineages following Vujčić et al. (2021a), as well as sequences of *Platynochaetus macquarti* Loew, 1862 and *Eumerus grandis* Meigen, 1822 species serving as outgroups, were retrieved from GenBank and joined to the sequence dataset. The details and GenBank accession numbers of all analysed species and outgroups are presented in Supplementary information (Suppl. material 1). The COI gene sequences of all analysed samples were aligned by the Clustal W algorithm (Thompson et al. 1994) implemented in BioEdit 7.2.5. (Hall 1999). The sequence matrix of concatenated indel-free 3'-end and 5'-end COI gene fragments was used for the construction of two trees: Maximum Parsimony (MP) and Maximum Likelihood (ML). The MP analysis was performed in NONA (Goloboff 1999), spawned with the aid of ASADO, v. 1.85 (Nixon 2008), using the heuristic search algorithm (settings: mult*1000, hold/100, max trees 100000, TBR branch swapping). The ML tree was constructed using MEGA 7.0 software (Kumar et al. 2016) under the general time-reversible evolutionary model (Nei and Kumar 2000) using a discrete Gamma distribution with five rate categories and by assuming that a certain fraction of sites is evolutionarily invariable (GTR+G+I). Nodal support values were estimated using nonparametric bootstrapping with 1000 replicates for both (MP and ML) trees. The trees were rooted on *Platynochaetus macquarti*.

Geometric morphometrics

Landmark-based geometric morphometric analysis of wing shape was conducted on 87 male specimens of the following species: *Merodon clavipes* ($n = 23$); *M. latens* sp. nov. ($n = 10$); *M. obscurus* stat. rev. ($n = 9$); and *M. pruni* ($n = 45$). Female specimens were not available for the analysis. The right wing of each specimen was removed using a micro-scissors and then mounted in Hoyer's medium on a microscopic slide. Wings have been archived and labelled with a unique code in FSUNS, together with other data relevant to the specimens. Eleven homologous landmarks that could be reliably identified at vein intersections or terminations were selected using TpsDig 2.05 software (Rohlf 2017a) (Table 1). Generalised least squares Procrustes superimposition on the raw coordinates was conducted in TpsRelw v. 1.68 (Rohlf 2017b) to minimise non-shape variations in wing location, scale and orientation and to superimpose the wings in a common coordinate system (Rohlf and Slice 1990; Zelditch et al. 2004).

Table 1. Results from discriminant analysis of wing shape differences among investigated species. Above diagonal *p* values. Below diagonal *F* values. **p* < 0.05, ***p* < 0.01.

	<i>M. pruni</i>	<i>M. obscurus</i>	<i>M. latens</i> sp. nov.	<i>M. clavipes</i>
<i>M. pruni</i>		0.000171**	0.000000**	0.000000*
<i>M. obscurus</i>	3.35056		0.000000**	0.000000**
<i>M. latens</i> sp. nov.	27.44203	16.65196		0.000016**
<i>M. clavipes</i>	66.27740	28.59318	4.03195	

We performed two separate analyses. First, we assessed wing shape variation among species. Second, we quantified phenotypic differences among geographically-defined groups of specimens (herein treated as populations). Specimens from Italy, Cyprus and France were not included in our population level analysis due to respective small sample sizes, which may interfere with the statistical analysis.

To explore wing-shape variation among the species and populations, we employed discriminant function (DA) and canonical variate (CVA) analyses on a partial warp scores TpsRelw v. 1.68 (Rohlf 2017b). A Gaussian naïve Bayes classifier was also used to delimit species boundaries based on wing shape variation without a priori-defined groups. Phenetic relationships among the species and populations were characterised using an unweighted pair group method with arithmetic mean cluster analysis (UPGMA) based on squared Mahalanobis distances computed from the DA. Superimposed outline drawings produced in MorphoJ v. 2.0 (Klingenberg 2011) were used to visualise differences in wing shape between species pairs. All statistical analyses were performed in Statistica for Windows v. 13 (TIBCO Software Inc. 2018).

Results

Taxonomic account

Merodon clavipes species group

Diagnosis. The *clavipes* species group belongs to *M. avidus-nigritarsis* lineage, characterised by the mesocoxa without long pile on the posterior section. This group includes large bumble bee-like species (15–20 mm), usually with long body pilosity on thorax, femora and abdomen (Fig. 1B, C); basoflagellomere elongated, > 2× longer than wide (as in Fig. 2); scutum without or with very weak and narrow pollinose vittae (as in Fig. 3) and fascia of completely black or intermixed yellow and black pile between wing bases (as in Fig. 1A, C, E); metatrochanter in male angular (as in Fig. 4F); metafemur broad, covered with very long pile, especially ventrally (Fig. 4); terga black in male, except for the male of *M. rufofemoris* sp. nov. that has tergum 2 with reddish lateral maculae; terga black in females of all species with reddish lateral maculae on tergum 2; terga usually covered with stripes of pile in different combinations of colours (white, yellow or black) (Fig. 5); terga 2–4 with a pair of distinct whitish grey pollinose fasciate maculae (Fig. 6); sternum 4 in male with medial, circular or triangular incision on posterior margin (Fig. 7). Male genitalia: surstylus with well-defined and large anterior and posterior lobes (as in Fig. 8A: al, pl); anterior surstylar lobe large, elongated and sickle-like (Fig. 8A: al); posterior surstylar lobe more

or less rectangular (Fig. 8A: pl), in some species with an apicolateral bulge; cercus rectangular (Fig. 8A: c); hypandrium sickle-shaped; lingula distinct, with tapering tip, in some species peak-like (Fig. 8D: l).

The *clavipes* group comprises six species presented here, distributed in the Mediterranean Region and more to the east up to Iran.

Subgroups

The *clavipes* species group of *Merodon* contains two subgroups based on the structure of male genitalia, colour of legs and basoflagellomere, and pilosity of posterior margin of scutellum. The *vandergooti* subgroup is characterised by completely or partly orange-yellowish tibiae, tarsi and femora, with bright orange-yellow basoflagellomere, the posterior margin of scutellum without long pile medially (as in Figs 2D, E, 3A, C, 4C, E, G), and posterior surstylar lobe without dorsal prominence (as in Figs 9A: pl, 11A: pl, 10A: pl). This subgroup includes *M. vandergooti* and two species described here, *M. aenigmaticus* sp. nov. and *M. rufofemoris* sp. nov. The other subgroup is the *clavipes* subgroup, whose members have black to dark brown legs and basoflagellomere, and pilosity on posterior margin of scutellum not interrupted medially (as in Figs 2A, 3B, 4A), and the posterior surstylar lobe has a dorsal prominence (as in Fig. 8A: dp, pl, C: pl). This subgroup contains three previously known species, *M. clavipes*, *M. quadrinotatus*, *M. velox* and one species described here, *Merodon latens* sp. nov.

***Merodon aenigmaticus* Vujčić, Radenković & Likov, sp. nov.**

<https://zoobank.org/A5E500DF-C71A-4127-966E-25B7B759C2F0>

Figs 1A, 3A, 4G, 7A, 9, 12C

Type material examined. Holotype. Male in MNHN. The specimen had no label or information about its origin. FSUNS ID 04325.

Diagnosis (only male known). Similar to *Merodon vandergooti* (Fig. 4C) from which differs with less broad metafemur (in *M. aenigmaticus* sp. nov. is $\sim 3.5\times$, while in *M. vandergooti* is $\sim 2.5\times$ longer than wide) (Fig. 4G), less curved metafemur and metatibia (Fig. 4G), and quite rounded posterior surstylar lobe (Fig. 9A: pl, marked with red arrow), while posterior surstylar lobe is strongly angulated ventrally in *M. vandergooti* (Fig. 10A: pl, marked with red arrow). It differs from *M. rufofemoris* sp. nov. by partly black femora (Fig. 4G) (orange-yellow in *M. rufofemoris* sp. nov.; Fig. 4E), and quite rounded posterior surstylar lobe (Fig. 9A: pl) (strongly angulate ventrally in *M. rufofemoris* sp. nov.; Fig. 11A: pl, marked with red arrow).

Description. Male. Head. Basoflagellomere orange-yellow (Fig. 12C), elongated, $\sim 2\times$ longer than wide, and $\sim 2.2\times$ longer than pedicel, convex dorsally; fossette dorsolateral; arista reddish to brown and thickened at basal third; arista $\sim 1.5\times$ longer than basoflagellomere; face and frons black with whitish pollinosity, while face covered with dense whitish pilosity; pile on frons dense, greyish white; oral margin small, black, sparsely pollinose; lunula shining black to brown, bare; eye contiguity ~ 12 facets long; vertical triangle isosceles, black, shiny, except grey pollinose anterior corner, covered with greyish white pilosity; ocellar triangle equilateral; occiput with a grey-yellow pile, densely covered with grey pollinosity along eyes; eyes covered with short, whitish grey pile (Fig. 12C).

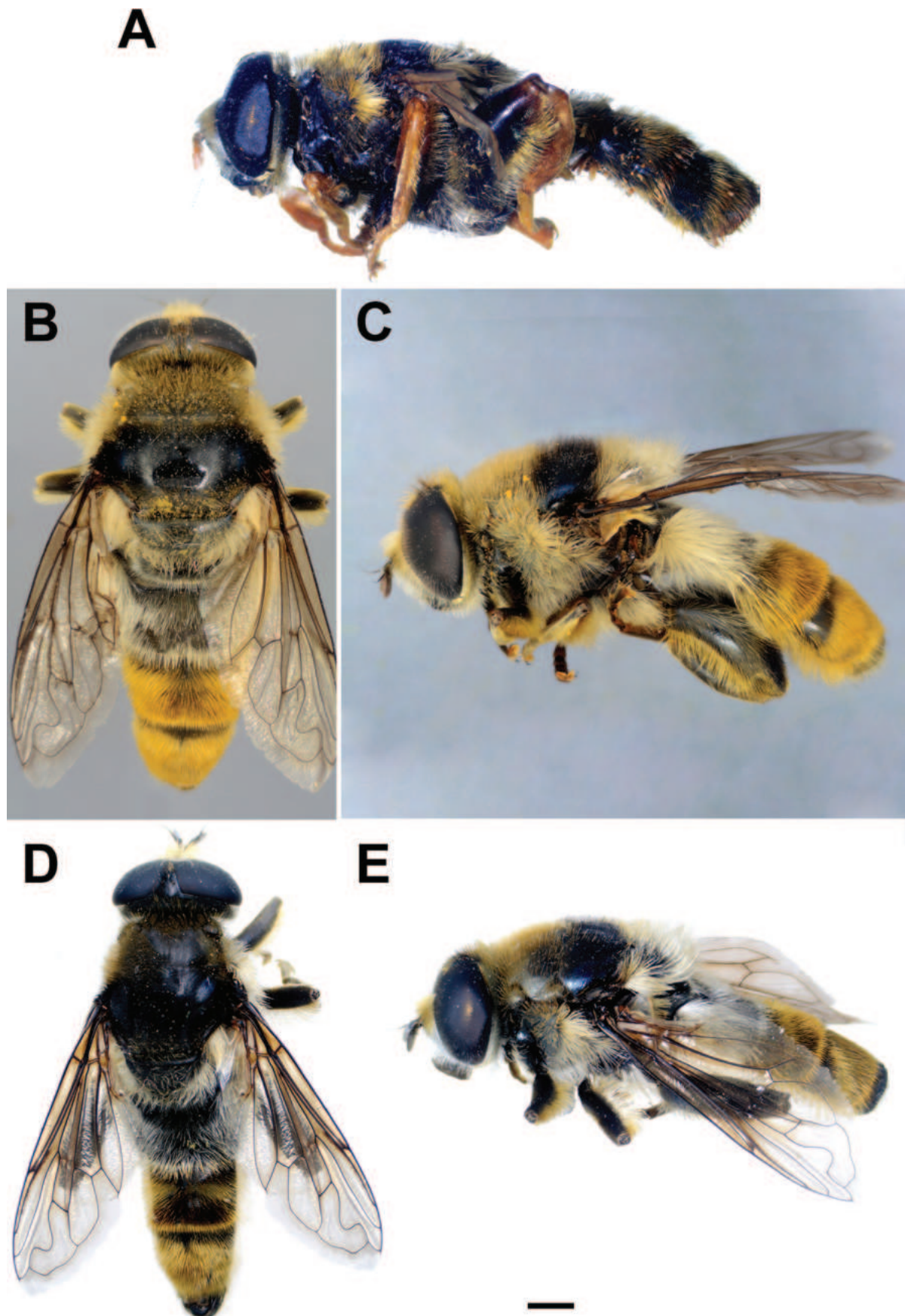


Figure 1. Body of male **A** *M. aenigmaticus* sp. nov. **B–C** *M. clavipes* **D, E** *M. latens* sp. nov. **B, D** dorsal view **A, C, E** lateral view. Scale bar: 2 mm.

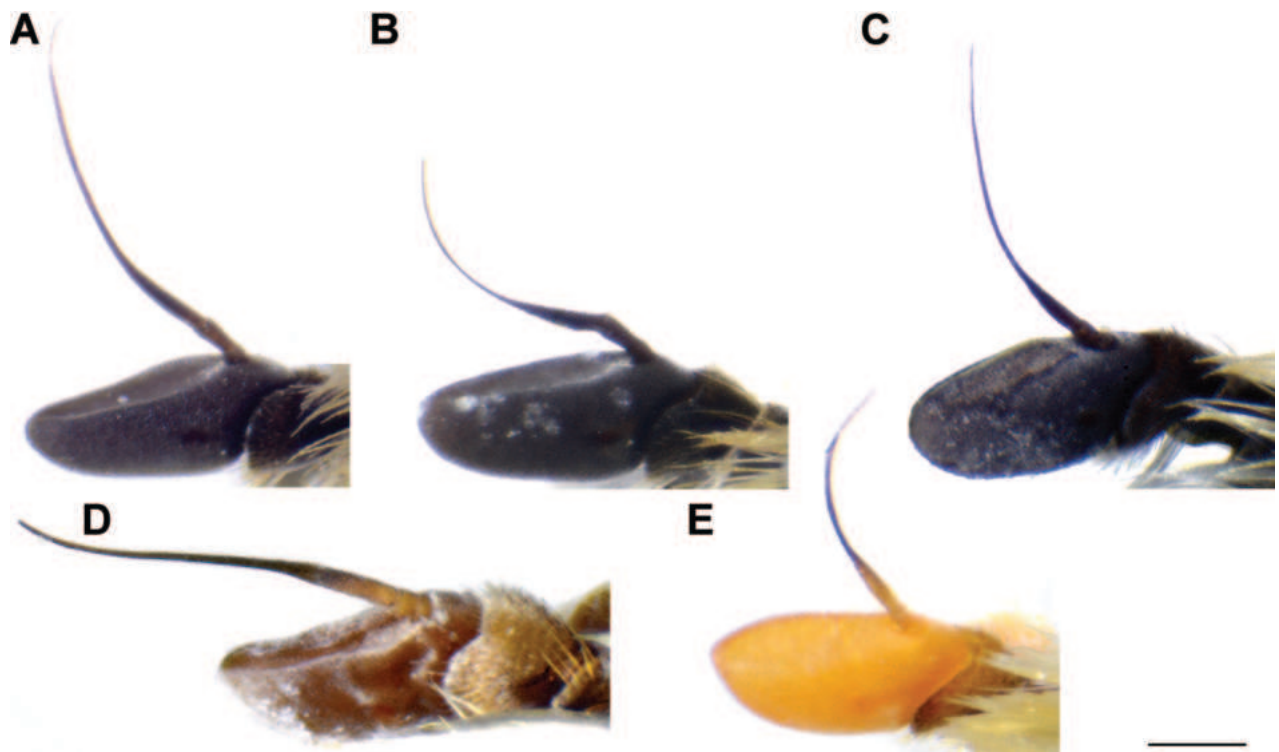


Figure 2. Basoflagellomere of male, lateral view **A** *M. clavipes* **B** *M. latens* sp. nov. **C** *M. quadrinotatus* **D** *M. rufofemoris* sp. nov. **E** *M. vandergooti*. Scale bar: 0.5 mm.

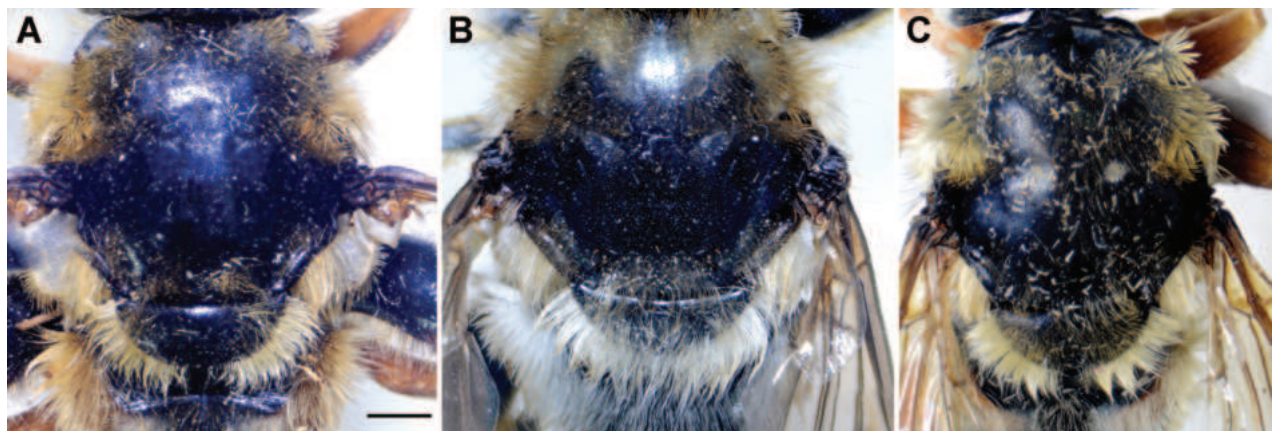


Figure 3. Thorax of male, dorsal view **A** *M. aenigmaticus* sp. nov. **B** *M. latens* sp. nov. **C** *M. rufofemoris* sp. nov. Scale bar: 1 mm.

Thorax. Scutum and scutellum black with bronze lustre, covered with short, reddish yellow pile; pilosity between wing bases mostly black; scutum with indistinct pollinose vittae; posterior margin of scutellum with very long reddish yellow to whitish pilosity, reduced medially (Fig. 3A); posterodorsal part of anterior anepisternum, posterior anepisternum (except anteroventral angle), anterior anepimeron, dorsomedial anepimeron, and posterodorsal and anteroventral parts of katepisternum with long, dense greyish white pile; wings mostly covered with microtrichia; wing veins yellowish to brown; calypteres whitish yellow; halteres yellowish; legs reddish yellow, except black basal half of pro- and mesofemora, and basal 4/5 of metafemur; metafemur broad, covered with long, whitish yellow pilosity (Fig. 4G).

Abdomen. Elongated (Fig. 1A), ~ 1.3× longer than mesonotum; terga black, except lateral sides of tergum 2 with reddish yellow maculae; terga 2–4 with broad, distinct silver-grey pollinose fasciate maculae interrupted medially; pile on terga reddish yellow to whitish; sterna black, covered with whitish grey pile; posterior margin of sternum 4 with characteristic posteromedial incision (Fig. 7A).

Male genitalia (Fig. 9). Anterior surstylar lobe large, elongated (up to 3× longer than wide) and sickle-like (Fig. 9A: al); posterior surstylar lobe rectangular with quite rounded ventral margin (Fig. 9A: pl), ~ 1.5× longer than wide, covered with short pile; cercus rectangular (Fig. 9B: c); hypandrium sickle-shaped, without lateral projections; lingula short and tapering (Fig. 9D: l).

Female. Unknown.

Distribution. Unknown. The species is described based on a male holotype from the MNHN collection lacking any label or information about the origin of the specimen.

Etymology. The name *aenigmaticus* derives from the Latin adjective, meaning 'enigmatic, like an enigma', in the masculine form. This term describes the absence of any information related to the holotype, including collecting place, date or collector. Species epithet to be treated as an adjective.

***Merodon clavipes* (Fabricius, 1781)**

Syrphus clavipes Fabricius, 1781: 427.

Musca clauda Villers, 1789: 463.

Musca curvipes Gmelin, 1790: 2871.

Syrphus gravipes Rossi, 1790: 286.

Merodon curvipes Meigen, 1803: 274.

Merodon senilis Meigen, 1822: 356.

Merodon canipilus Rondani, 1865: 131.

Merodon clavipes var. *alba* Paramonov, 1926: 90.

Merodon clavipes var. *atra* Paramonov, 1926: 91.

Merodon clavipes var. *niger* Paramonov, 1926: 90.

Merodon clavipes albus Peck, 1988: 169 (sic! non Paramonov), syn. nov.

Merodon clavipes ater Peck, 1988: 169 (sic! non Paramonov), syn. nov.

Merodon clavipes niger Peck, 1988: 169 (sic! non Paramonov), syn. nov.

Merodon splendens Hurkmans, 1993: 182, syn. nov.

***Syrphus clavipes* Fabricius, 1781: 427**

Type locality. ITALY. The original description (Fabricius 1781) was based on an unspecified number of syntypes. The lectotype was designated by Hurkmans (1993: 178): male in Sehestedt and Tonder Lund collection (ZMUC). Unfortunately, the type material was destroyed (AV pers. obs.). Two pins from the type collection possess only labels: [*Syrphus clavipes*] and [P 195-1].

Neotype (designated here). Male, Italy, Sicily, 20.vi.1914, leg. Trautmann (ZMUC).

A neotype was designated to clarify the taxonomic status of *Merodon clavipes*. Lectotype was designated by Hurkmans (1993) in his revisionary work on genus *Merodon*, but has been destroyed. Data and description are sufficient to

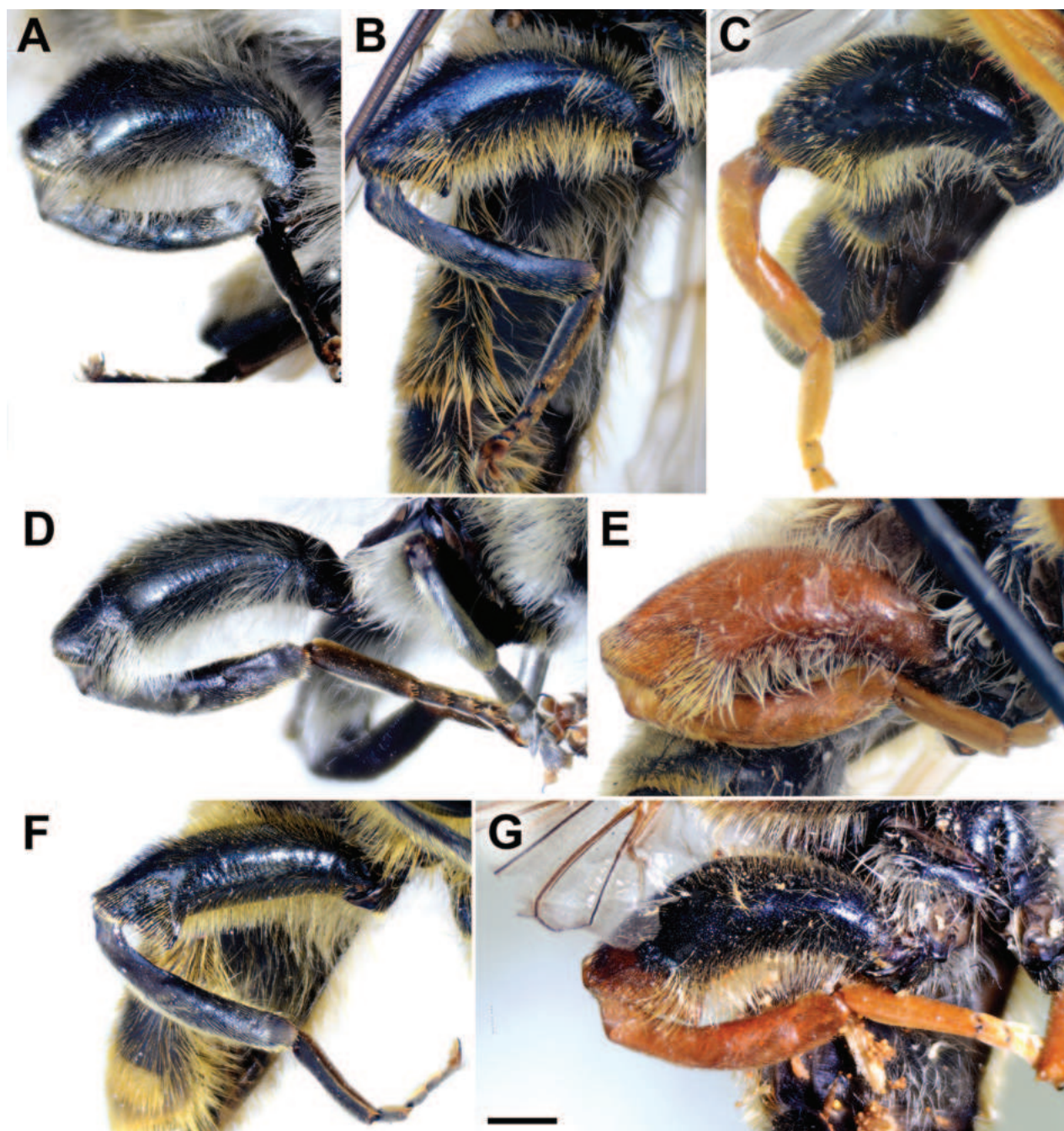


Figure 4. Metaleg of male, lateral view A *M. clavipes* B *M. latens* sp. nov. C *M. vanderhooti* D *M. quadrinotatus* E *M. rufofemoris* sp. nov. F *M. velox* G *M. aenigmaticus* sp. nov. Scale bar: 1 mm.

ensure recognition of the specimen designated, and the neotype is consistent with what is known of the former name-bearing type from the original description and latter revision. Neotype belongs to the same country (Italy) cited as the original type locality and it is deposited in the same Museum where lectotype was kept (ZMUC).

***Musca clauda* Villers, 1789: 463**

Type locality. FRANCE. Synonymy with *Merodon clavipes* was cited in Peck (1988: 168) and Hurkmans (1993: 178). Type material presumably lost.



Figure 5. Abdomen of male, dorsal view **A** *M. clavipes* **B** *M. latens* sp. nov. **C** *M. rufofemoris* sp. nov. **D** *M. quadrinotatus* **E** *M. vanderhooti* **F** *M. velox*. Scale bar: 2 mm.

***Syrphus gravipes* Rossi, 1790: 286**

Type locality. Italy. Synonymy with *Merodon clavipes* was cited in Peck (1988: 168) and Hurkmans (1993: 178). Type material presumably lost.

***Merodon senilis* Meigen, 1822: 356**

Type locality. Italy. Synonymy with *Merodon clavipes* was cited in Peck (1988: 168) and Hurkmans (1993: 178). Lectotype was designated by Hurkmans (1993: 178): female “*senilis*” (NHMW) (not found).

***Merodon canipilus* Rondani, 1865: 131**

Type locality. Italy. Synonymy with *Merodon clavipes* was cited in Peck (1988: 168) and Hurkmans (1993: 178). Lectotype was designated by Hurkmans (1993: 178): male in Rondani collection [52] (LSF) (examined).

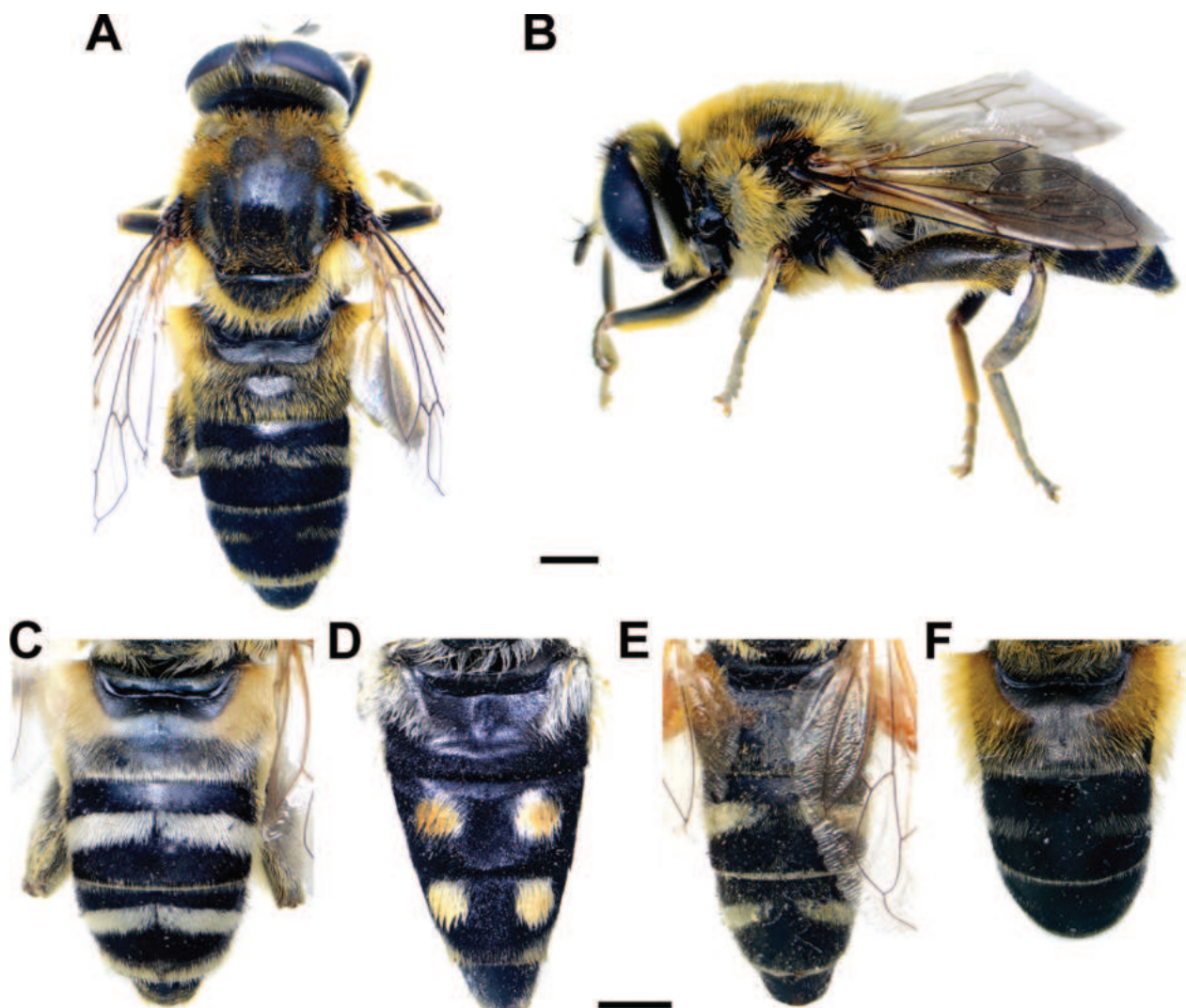


Figure 6. A, B *M. latens* sp. nov. C *M. clavipes* D *M. quadrinotatus* E *M. vandergooti* F *M. velox*. A, B body of female C–F abdomen of female. A, C–F dorsal view B lateral view. Scale bar: 2 mm.

***Merodon clavipes* var. *alba* Paramonov, 1926a: 90**

Merodon clavipes albus Peck, 1988: 169 (sic! non Paramonov), syn. nov.

Holotype (examined). Female with labels: white, handwritten, bold ink [N 327]; yellowish, handwritten, pale ink, with bluish typographical frame [Valegotsulovo / d. Balta / g. Odessa / 2.vi.25], 47.566923; 29.9389105, Ukraine; pink, handwritten, pale ink, with double typographical frame [*Merodon / clavipes* Fabr. / var. *alba* ♀ / Typus var. nov.] (SIZK).

Notes. This taxon was described from a single female, but the specimen storage location was not indicated (Paramonov 1926a: 90) and, until recently, it was not known (Liepa 1969: 4, 20; Hurkmans 1993: 179 “types of either of the varieties ... are considered to be lost”, 205 “lost”, 206). The original description is based on a single specimen, which is the holotype according to article 73.1.2 ICZN (1999) and it is kept in the SIZK collection (Popov 2011). Type locality: Ukraine. The species name is clearly infrasubspecific (1.3.4, 10.2 ICZN 1999) because, as stated by Paramonov himself, the specimen was collected together with the nominal taxon (45.6.1, 45.6.4 ICZN 1999, also see Lingafelter and Nearn 2013).

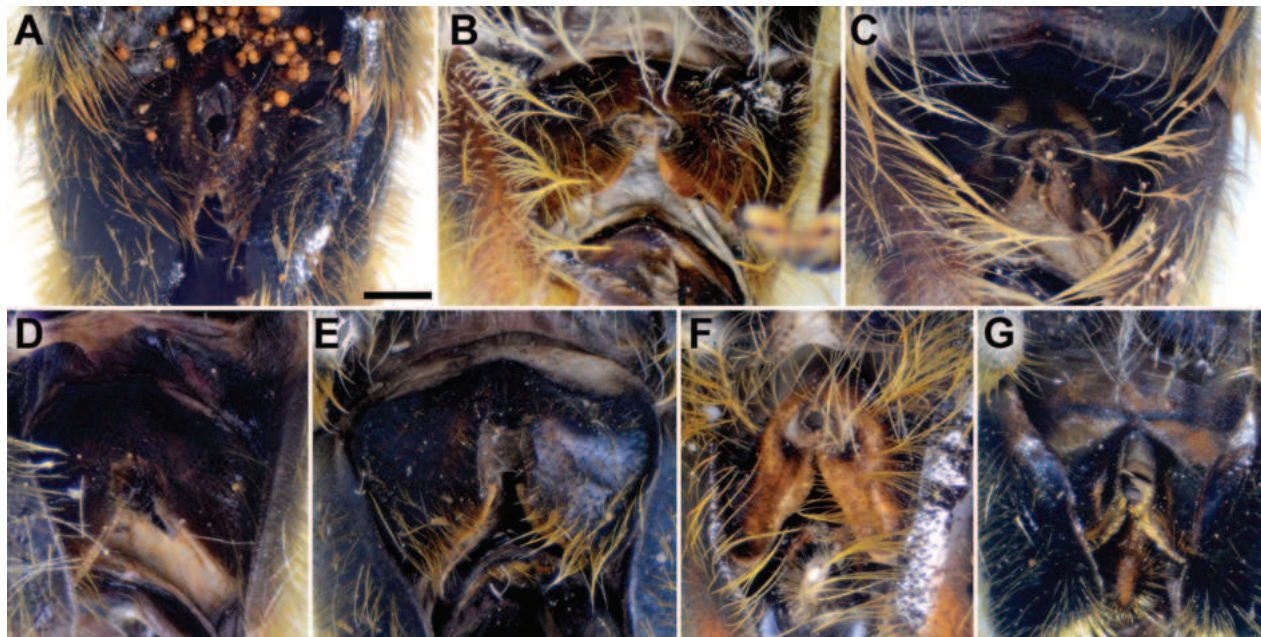


Figure 7. Sternum 4 of male, dorsal view **A** *M. aenigmaticus* sp. nov. **B** *M. clavipes* **C** *M. latens* sp. nov. **D** *M. quadrinotatus* **E** *M. rufofemoris* sp. nov. **F** *M. vanderhooti* **G** *M. velox*. Scale bar: 1 mm.

Therefore, this name is not subject to Code 45.6.4.1 (ICZN 1999). The name was first given subspecies rank in Peck's Catalogue (1988: 169), i.e., «*M. clavipes albus* Paramonov» (the original gender ending was incorrect and changed, see Article 34.2, ICZN 1999), according to article 45 (g) (ii) ICZN (1985), now corresponding to 45.6.4 (ICZN 1999) (see 45.6.4.1 of ICZN, 1999). However, this is a violation of article 45 (f) (ii) ICZN (1985), now corresponding to 45.6.1, 45.6.4 (ICZN 1999). According to article 45.5.1 (ICZN 1999), Peck adopts authorship of this species name, so we present it as *Merodon clavipes albus* Peck, 1988, which is a syn. nov. for *M. clavipes* (Fabricius 1781). Later, Hurkmans (1993: 178) erroneously indicated that Peck (1988: 169) listed the name as a "variety". He also erroneously indicated that S. Ya. Paramonov published the name in 1927 and that the single specimen is a syntype. He left the ranking "variety" for the name (Hurkmans 1993: 179). Colour varieties of *M. clavipes* have been found in multiple populations of this species, similar to the variations reported for *Merodon equestris* (Conn 1976; Han et al. 2018).

***Merodon clavipes* var. *atra* Paramonov, 1926a: 91**

Merodon clavipes atra Peck, 1988: 169 (sic! non Paramonov), syn. nov.

Notes. This variety was established without reference to the type material, for the male specimens that were in the possession of P. Sack (Germany, now his collection is conserved in the Naturmuseum Senckenberg, Frankfurt am Main) (Paramonov 1926a: 91). The number of types was not given in the original description and their storage location was not indicated, nor were they discovered subsequently (Liepa 1969: 4, 20). The type locality is also unknown. The types of this variety were also not found in the SIZK Department of Entomology collection (G. Popov, in prep.), where the vast majority of Paramonov's types are stored.

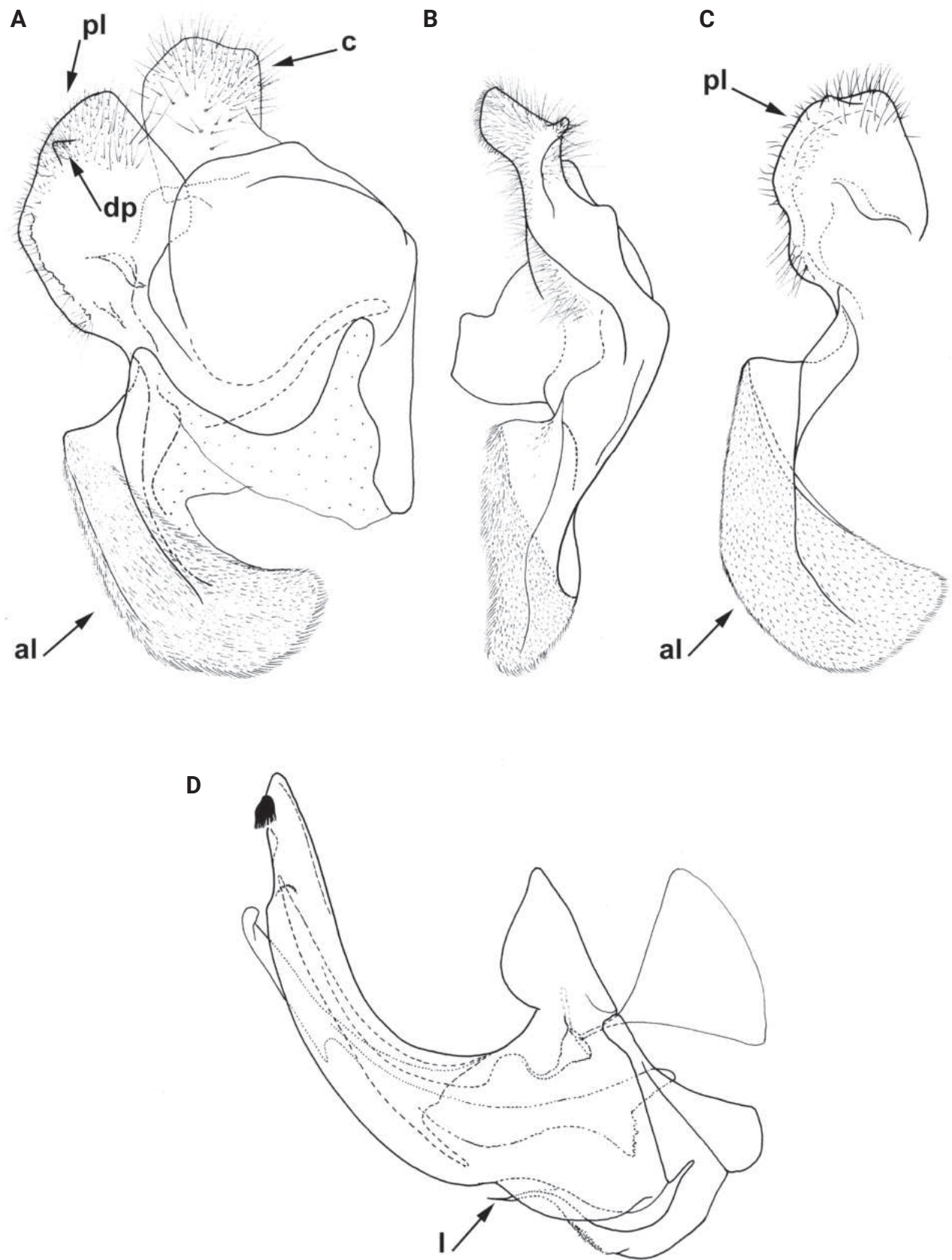


Figure 8. Male genitalia **A, B, D** *M. clavipes* **C** *M. latens* sp. nov. **A–C** epandrium **D** hypandrium. **A, C, D** lateral view **B** ventral view. Abbreviations: al-anterior surstylar lobe, c-cercus, l-lingula, pl-posterior surstylar lobe. Scale bar: 0.5 mm.

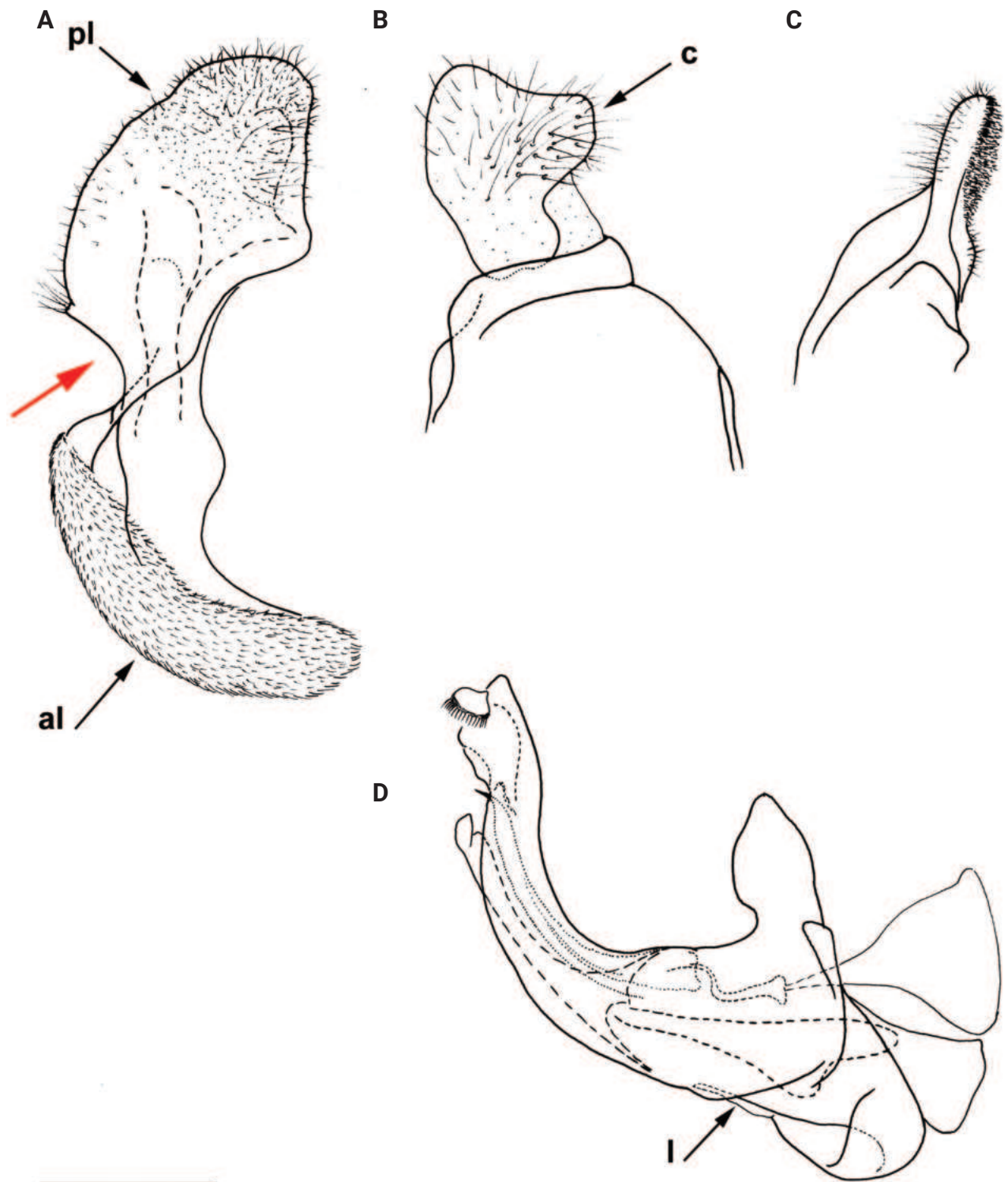


Figure 9. Male genitalia *M. aenigmaticus* sp. nov. **A** surstylar lobe **B** cercus **C** posterior surstylar lobe **D** hypandrium. Rounded posterior surstylar lobe marked with red arrow. **A**, **B**, **D** lateral view **C** ventral view. Abbreviations: al-anterior surstylar lobe, c-cercus, l-lingula, pl-posterior surstylar lobe. Scale bar: 0.5 mm.

Thus, the types are considered lost, as already indicated by W. Hurkmans (1993: 178, 179, 205).

The name "*atra*" by Paramonov is clearly infrasubspecific (see Articles 1.3.4 and 10.2, ICZN 1999), because S. Paramonov (Paramonov 1926a) placed this

variety together with others he described for this species (see Articles 45.6.1 and 45.6.4, ICZN 1999). Moreover, he did not report the type locality (see the same Articles; also see Lingafelter and Nearn 2013). Therefore, this name is not subject to the Code (see Article 45.6, ICZN 1999).

The name was given subspecies rank for the first time (see Article 45.6.4.1, ICZN 1999), «*M. clavipes ater* Paramonov» (the original gender ending was incorrect and changed, see Article 34.2, ICZN 1999), in Peck's Catalogue (1988: 169) according to article 45 (g) (ii) ICZN (1985), now corresponding to Article 45.6.4 (ICZN 1999). However, this is a violation of Article 45 (f) (ii) ICZN (1985), now corresponding to Articles 45.6.1 and 45.6.4 (ICZN 1999). So, according to the Articles 45.5.1 and 50.3.1 (ICZN 1999), L. Peck established her own authorship of this name, and we use subspecies name *ater* Peck, 1988 that we consider to be a new synonym (syn. nov.) for *M. clavipes* (Fabricius, 1781), since according to our data, this colour form has no geographical reference and is inherent to some specimens of the species throughout the range. Colour varieties of *M. clavipes* have been found in multiple populations of this species, similar to variations described for *Merodon equestris* (Conn 1976; Han et al. 2018).

***Merodon clavipes* var. *nigra* Paramonov, 1926a: 90**

Merodon clavipes niger Peck, 1988: 169 (sic! non Paramonov), syn. nov.

Holotype (examined). Female with labels: white, handwritten, bold ink [N 328]; yellowish, handwritten, pale ink, with bluish typographical frame [Valegozulovo / d. Balta / g. Odessa / 28.v.25.], 47.566923; 29.9389105, Ukraine; pink, handwritten, pale ink, with double typographical frame [*Merodon / clavipes* Fabr. / var. *nigra* ♀ / Typus. var. nov.] (SIZK).

Notes. The situation for variety *niger* is identical to that described above for variety *alba* (see above *clavipes* var. *alba* Paramonov, 1926). The taxon was described from a single female, but the specimen storage place was not indicated (Paramonov 1926a) and, until recently, it was not known (Liepa 1969; Hurkmans 1993). The original description is based on a single specimen, which is the holotype that is kept in the SIZK collection (Popov 2011). Type locality: Ukraine. This name is clearly infrasubspecific because, as indicated by Paramonov himself, the specimen was collected together with the nominal taxon. Therefore, this name is not subject to Code 45.6.4.1 (ICZN 1999). The name was given subspecific rank for the first time in Peck's Catalogue (1988), i.e., «*M. clavipes niger* Paramonov» (the original gender ending was incorrect and changed, see Article 34.2, ICZN 1999). Thus, Peck assumes authorship of this name, so we use *Merodon clavipes niger* Peck, 1988, which is a syn. nov. for *M. clavipes* (Fabricius, 1781). Later, Hurkmans (1993) mistakenly indicated that Peck (1988) listed the name as a "variety", that Paramonov published the name in 1927, and that the single specimen is a syntype. He left the rank variety for the name (Hurkmans 1993). Colour varieties of *M. clavipes* have been found in multiple populations of this species, similar to variations described for *Merodon equestris* (Conn 1976; Han et al. 2018).

***Merodon splendens* Hurkmans, 1993: 182, syn. nov.**

Type locality. Italy, Sardinia. The original description was based on a male holotype (Hurkmans 1993) from Lausanne Museum (LAU). Holotype (designated by Hurkmans): male, Italy, Sardinia (LAU), [specimen dry pinned]. Original labels: [Sardaigne St. Ussassai 16.v.1977 P. Goeldlin], [Holotype of *Merodon splendens* Hurkmans]. The holotype is conspecific with *Merodon clavipes* (examined).

Diagnosis. Male: legs black (Fig. 4A); antennae black (Fig. 2A); metafemur extremely broad (~ 2–2.5× longer than wide) and curved basally (Fig. 4A); tergum 3 with a pair of rectangular pollinose fasciate maculae, ending close to lateral margins (Fig. 1C). Female with a pair of reddish lateral maculae on tergum 2 (Fig. 6C). Male genitalia in Fig. 8. Similar to *M. latens* sp. nov. from which differs by a broader metafemur, ~ 2–2.5× longer than wide (Fig. 4A) (~ 3–3.5× in *M. latens* sp. nov.; Fig. 4B), and the posterior surstylar lobe more straight ventrally (Fig. 8A: pl) (more arcuate ventrally in *M. latens* sp. nov.; Fig. 8C: pl).

Distribution and biology. From northern France to the Mediterranean (including Corsica, Sardinia, Sicily and Crete); from Italy through central and southern Europe to Greece, countries of the former Yugoslavia, as well as Albania, Romania, Ukraine (Odesa region, Zakarpattia region), and southern areas of the European parts of Russia and Turkey. Speight (2020) also mentioned North Africa and the Iberian Peninsula as within the species range. Specimens from North Africa were unavailable to us for examination, so we could not confirm if they indeed belong to *Merodon clavipes*. In terms of the Iberian specimens, we assert that they belong to *M. latens* sp. nov. (Fig. 13; Suppl. material 2). The preferred environment of *Merodon clavipes* in the Mediterranean is sparsely-vegetated open ground in semi-arid environments, typified by unimproved stony pasturage and open grassy areas within thermophilous *Quercus* forest (Speight 2020). In the more temperate zone of Europe, the preferred environments are steppe grasslands and open areas near thermophilous forests. In Ukraine, at the northern edge of its range, this species occurs in rocky steppe on the margin of *Quercus* forest (locus typicus of Paramonov's varieties). Hurkmans (1985) described the territorial behaviour of males and, in Hurkmans (1993), he also noted that females fly close to the soil and through the vegetation. Flowers visited: Umbellifers; *Euphorbia*, *Leontodon* and *Solidago* (Speight 2020). Flight period: March/August depending on climatic zone (in central Europe adults appear during shorter period in early summer, while in southern Europe there can be two generations, spring and summer ones). Developmental stages: undescribed (Speight 2020).

***Merodon latens* Vujčić, Radenković & Likov, sp. nov.**

<https://zoobank.org/6FEF8C5C-26F2-4141-9FC7-DE8BFCE237AC>

Figs 1D, E, 2B, 3B, 4B, 5B, 6A, B, 7C, 8C, 12A, B, 13, 14B, 15, 17

Type material examined. Holotype: SPAIN • 1 ♂; Sierra Nevada, second valley; 37.102778, -3.455277; 17 Jun. 2014; leg. A. Vujčić, S. Radenković, S. Pérez-Bañón; in FSUNS. **Paratypes.** SPAIN • 7 ♂♂, 3 ♀♀; Andalusia, Almirajara, Corbijolo los Capotes; 36.879, -3.7317; 11 Jun. 2003; leg. D. Doczkal; in DD collection. Spain, Andalusia, Granada, 37.25, -3.25, 29–31 May 1925, leg. Zerny, 1 male in NHMW • 1 ♀; Andalusia, Granada; 1 Jun. 1925; leg. Zerny; in NHMW • 1 ♂, 1 ♀;

Andalusia, Puerto de Santa Maria; 36.6401, -6.2596; Apr. 1933; leg. S. Hering; in ZHMB • 1 ♀; Andalusia, Sierra de Baza; 37.422222, -2.851944; 9 Jun. 2003; leg. D. Doczkal; in DD collection • 2 ♂♂; Andalusia, Sierra de Segura, Casas de Carrasco; 38.156666, -2.678333; 7 Jun. 2003; leg. D. Doczkal; in DD collection • 1 ♂; Barcelona; 41.414247, 2.127128; May 1918; leg. H. Teunissen; in RMNH • 1 ♂; Burgos, Espinosa de Cervera; 12 Jun. 1992, 41.897516, -3.467732; leg. M. Hull; in WML • 1 ♂; Castilla la Mancha, Sierra de Alcaraz, Riopar; 38.504722, -2.46; 14 Jun. 2003; leg. D. Doczkal, in DD collection • 3 ♂♂, 2 ♀♀; Ciudad Real, Sierra de Santa Maria, Viso del Marques; 38.966666, -3.916666; 20 Apr. 1999; leg. M.E. Irwin; in HM collection • 1 ♂; Cortes de la Frontera, way to Grazalema, 36.593904, -5.312444, 6 May 2015; leg. A. Vujčić; in FSUNS • 1 ♂, 1 ♀; Cortijo los Capotes, Almijara; 36.878889; -3.731667; 11 Jun 2003; leg. A. Ssymank; in SIZK • 1 ♂; Granada, Rio Lanjaron, near Lanjaron; 36.9437, -3.469431; 28. Apr. 1966; leg. Lyneb. Martin, Langemark; in ZMUC • 3 ♂♂, 2 ♀♀; Granada, Sierra Nevada, near Padul; 37.083333, -3.166667; 4 May 1966; leg. Martin; Langemark; in ZMUC • 1 ♂; Grazalema 2, Puerto Alamillo; 36.722683, -5.333724; 8 May 2015; leg. A. Vujčić; in FSUNS • 1 ♂; Leon, Mirantes de Luna; 42.841438, -5.861399; 3 Jun. 1987; leg. M.A. Marcos-García; in FSUNS • 1 ♂; Lugros, Sierra Nevada; 37.183056, -3.257778; 18 Jun. 2014, leg. A. Vujčić, S. Radenković, S. Pérez-Bañón; in FSUNS • 1 ♂; Malaga, Alhaurin el Grande; 36.633333, -4.683333; 1 May 1979; leg. H. Teunissen; in RMNH • 1 ♂; Malaga, Ronda; 16 Apr. 1955; leg. I.H.H. Yarow; in NHMUK • 1 ♂; Prov. Salamanca, Villar de Ciervo; 40.741661, -6.741098; 24 May 1987; leg. Tschorsnig; in ZFMK • 1 ♂, 1 ♀; Sierra Nevada, first valley; 37.127777, -3.445555; 17 Jun. 2014; leg. A. Vujčić, S. Radenković, S. Pérez-Bañón; in FSUNS • 1 ♂; Sierra Nevada, Rio Lanjaron 2; 38.125555, -3.870833; 28 Apr. 2019; leg. A. Vujčić, S. Radenković; in FSUNS • 1 ♂, 1 ♀; Sierra Nevada N. P., road to San Jeronimo; 37.240277, -3.48; 17 Jun. 2014, leg. X. Mengual; in ZFMK • 1 ♂; SW Spain, 4 km SE of Antequera; 37.002352, -4.517977; 7 May 1981; leg. A.E. Stubbs; in NHMUK • 1 ♂; Puertollano; 38.697473, -4.090701; in MNHN.

Diagnosis. Similar to *Merodon clavipes* from which differs by the less broad metafemur of the male (from lateral view ~ 4× longer than wide; Fig. 4B) (< 3× longer than wide in *M. clavipes*; Fig. 4A), less curved metafemur basally (strongly curved in *M. clavipes*; Fig. 4A), and ventral pilosity on metafemur < 2× longer than dorsolateral (Fig. 4B) (while > 2× longer in *M. clavipes*; Fig. 4A). Male genitalia are very similar to *M. clavipes* (Fig. 8A), with the single difference in the shape of surstylus, especially of the posterior surstylar lobe: more arcuate ventrally in *M. latens* sp. nov. (Fig. 8C: pl), and more or less straight in *M. clavipes* (Fig. 8A: pl). Female of *M. latens* sp. nov. has less dense ventral pilosity on metafemur, with ventral pile as long as a dorsolateral pile (Fig. 14B), while female of *M. clavipes* has denser and longer ventral pilosity on metafemur (Fig. 13A). Molecular and morphometric data clearly separated these two species (Figs 15, 16, 17 and Suppl. material 3). *Merodon latens* sp. nov. is an Iberian endemic.

Description. Male. Head. Basoflagellomere dark brown (Fig. 2B), elongated, ~ 2× longer than wide, and ~ 2.3× longer than pedicel, convex dorsally; fossette dorsolateral; arista brown and thickened at basal third; arista ~ 1.3× longer than basoflagellomere (Fig. 2B); face and frons black, with whitish grey pollinosity; face covered with dense whitish pilosity; pile on frons dense, grey-yellow; oral margin small, black, sparsely pollinose; lunula shining black to brown, bare; eye contiguity ~ 13–15 facets long; vertical triangle isosceles, black, shiny, except

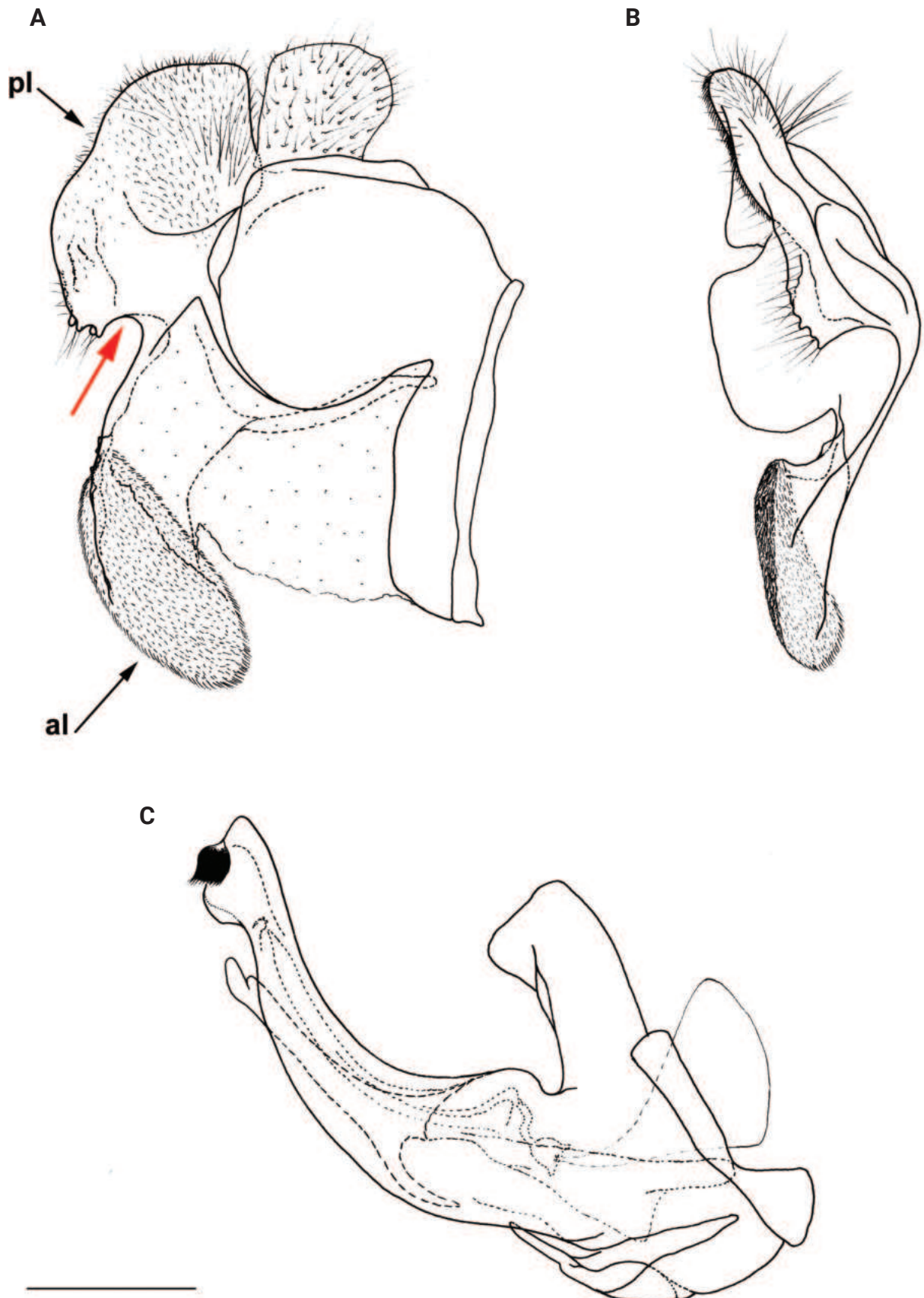


Figure 10. Male genitalia *M. vandergooti* **A, B** epandrium, **C** hypandrium. **A, C** lateral view **B** ventral view. Strongly angulated ventral part of posterior surstylar lobe marked with red arrow. Abbreviations: al-anterior surstylar lobe, pl-posterior surstylar lobe. Scale bar: 0.5 mm.

grey pollinose anterior corner, covered with both black and yellow pile; ocellar triangle equilateral; occiput with grey-yellow, dense pollinosity; eyes densely covered with whitish grey pile (Fig. 12A).

Thorax. Scutum and scutellum black with bronze lustre, covered with short, greyish yellow pile in anterior half; pilosity between wing bases entirely or mostly black; scutum with indistinct pollinose vittae; transverse suture with two medial pollinose maculae; posterior margin of scutum and all scutellum with long whitish pilosity (Fig. 3B); posterodorsal part of anterior anepisternum, posterior anepisternum (except anteroventral angle), anterior anepimeron, dorsomedial anepimeron, and posterodorsal and anteroventral parts of katepisternum with long, dense, whitish pile; wings mostly covered with microtrichia; wing veins brown to black; calypteres whitish yellow; halteres yellow to brown; legs black; metafemur moderately broad, from lateral view ~ 4× longer than wide, covered with long, whitish, yellow, and black pile (Fig. 4B).

Abdomen. Elongated (Fig. 5B), as long as mesonotum; terga black; terga 3 and 4 with distinct silver-grey pollinose fasciate maculae interrupted medially; pile on terga 1 and 2 whitish, while on terga 3–5 grey-yellow to reddish; sterna black, covered with whitish yellow pile; posterior margin of sternum 4 with characteristic circular posteromedial incision (Fig. 7C).

Male genitalia (Fig. 8C). Anterior surstylar lobe large, elongated and sickle-like (Fig. 8C: al); posterior surstylar lobe rectangular, arcuate ventrally (Fig. 8C: pl).

Female (Fig. 6A, B). Similar to the male except for typical sexual dimorphism and the following characteristics: frons with broad pollinose vittae along eyes, occupying ~ 1/3 of the width of the frons from frontal view (Fig. 12B); scutum between wing bases without black pilosity, only wing basis with few black pile in some specimens (Fig. 6B); metafemur narrower (~ 3.5× longer than wide), with ventral pilosity shorter than in male (Fig. 14B); lateral sides of tergum 2 with reddish yellow maculae (Fig. 6A); terga 3–5 with short adpressed black pilosity medially.

Distribution and biology. The species range is limited to the Iberian Peninsula (Spain) (Fig. 13). It preferentially occurs in open sparsely-vegetated semi-arid environments, typically unimproved stony pasturage and open grassy areas within thermophilous *Quercus* forest. Adult males and females both showed territorial behaviour, flying close to the soil and through the vegetation. Flowers visited by adults are mostly umbellifers and *Euphorbia*. Flight period: April/June. Developmental stages: undescribed.

Etymology. The name *latens* derives from the Latin adjective meaning hidden, secret, not revealed. This term refers to the discovery of Iberian populations, previously cited as *Merodon clavipes*, as distinct species. Species epithet to be treated as an adjective.

***Merodon quadrinotatus* (Sack, 1931)**

Lampetia quadrinotata Sack, 1931: 324.

Type locality. “Mesopotamia” (Iraq according to Peck 1988). The original description was based on one female (holotype) (Sack 1931). The holotype is considered lost (Hurkmans 1993).

Neotype (designated here): female, Iran, (HMIM), [specimen dry pinned]. Original labels: [IRAN-Fars-Meimand/Firouzabad-Tange riz/N 28 56 00 2670m/E 052 50 07.6/Leg. Gilasian/15.iv.2006], [*Merodon quadrinotatus*/(Sack, 1931)/det. A. Vujčić 2019], [Loan Vujčić 2007/Gilasian 32] [NEOTYPE of *Merodon quadrinotatus* Sack / designated by Vujčić A.]. A neotype for *Lampetia quadrinotata* is here designated to fix and ensure the universal and consistent interpretation of the name. This designation was based on the good condition of the specimen; a well-preserved female with clearly visible characters which are conspecific with the holotype. This species possesses a unique character, a pair of tear like white pilose maculae on terga 2 and 3, especially distinct in females (Fig. 6D).

Notes. This species was described based on a single female. Here we present the first description for the male.

Diagnosis. Male similar to *Merodon clavipes* (Figs 4A, 5A) from which differs by the metafemur slightly broad (in *M. quadrinotatus* is 3.75×, while in *M. clavipes* is 2× longer than wide) and less curved basally (Fig. 4D) and by tergum 3 with a pair of tear-like, pollinose fasciate maculae separated from lateral margins (Fig. 5D) (in *M. clavipes* tergum 3 with a pair of rectangular pollinose fasciate maculae, ending close to lateral margins). Female with black terga and very characteristic pairs of pollinose, rounded maculae covered with dense whitish pile on terga 3 and 4 (Fig. 6D); a unique abdominal pattern in *Merodon*. Male genitalia as in Fig. 18.

Description. Male. Head. Basoflagellomere dark-brown (Fig. 2C), elongated, ~ 2× longer than wide, and ~ 1.9× longer than pedicel, convex dorsally; fossette dorsolateral; arista reddish to brown and thickened at basal third; arista ~ 1.5× longer than basoflagellomere; face and frons black, with greyish pollinosity; face covered with dense whitish to yellowish pilosity; pile on frons dense, yellowish; oral margin small, black, not pollinose; lunula shining black to brown, bare; eye contiguity ~ 15 facets long; vertical triangle isosceles, brown-black, shiny, except grey pollinose anterior corner, covered with greyish white and black pilosity; ocellar triangle equilateral; occiput with grey-yellow pile, densely covered with grey pollinosity along eyes; eyes covered with short, whitish grey pile.

Thorax. Scutum black with bronze lustre, covered with greyish yellow pile; pilosity between wing bases mostly black; scutum with indistinct pollinose vittae; scutellum covered with whitish pile; posterior margin of scutellum with very long grey-yellow to whitish pilosity, reduced medially (as on Fig. 3C); posterodorsal part of anterior anepisternum, posterior anepisternum (except anteroventral angle), anterior anepimeron, dorsomedial anepimeron, and posterodorsal and anteroventral parts of katepisternum with long, dense whitish to greyish white pile; wings mostly covered with microtrichia; wing veins yellowish to brown; calypteres whitish; halteres brownish; legs black; metafemur moderate broad, ~ 3.75× longer than wide, covered with long, whitish pilosity (Fig. 4D).

Abdomen. Elongated (Fig. 5D), ~ 1.3× longer than mesonotum; terga black; terga 3 and 4 with a pair of broad, tear-like, distinct silver-grey pollinose fasciate maculae; pile on tergum 2 and lateral sides of terga 3 and 4 grey-yellow to whitish; terga 3 and 4 medially with short, golden-yellow pile (Fig. 5D); sterna black, covered with whitish grey pile; posterior margin of sternum 4 with characteristic posteromedial incision (Fig. 7D).

Male genitalia (Fig. 18). Anterior surstylar lobe short (~ 1.4× longer than wide) and rectangular (Fig. 18A: al); posterior surstylar lobe rectangular, with a dorsal prominence (Fig. 18A: dp); cercus rectangular (Fig. 18A: c); hypandrium

sickle-shaped, without lateral projections; lingula short, with tapering narrow tip (Fig. 18C: l).

Female. Similar to the male except for normal sexual dimorphism and the following characteristics: face and frons covered with white pilosity; frons with broad pollinose vittae along eyes and a narrow shiny central stripe; scutum with short erect white pilosity, except for broad fascia of black pile between wing bases; long whitish pilosity on metafemur absent; metafemur covered with short black pilosity and few longer black pile ventrally; terga covered with short black pilosity, except for long white pile on lateral sides of terga 2–4, posterior margin of tergum 4, and pairs of pollinose, rounded maculae covered with dense whitish pile on terga 3 and 4 (Fig. 6D).

Distribution and biology. The range of this species includes Turkey, Iran and Iraq (Fig. 19; Suppl. material 2). *Merodon quadrinotatus* has been recorded predominantly in Iranian ecoregions, specifically, forest steppe of the Zagros Mountains, Eastern Anatolian montane steppe, and woodlands and forest steppe of Kopet Dag (Kopeh Dag) (Olson et al. 2001) but also in nearby localities within Iraq and Turkey. The Iranian localities are typified by arid and semi-arid forest ecosystems with *Quercus brantii* Lindl. as the dominant vegetation type, as well as cold and arid semi-steppe scrubland and grasslands (*Astragalus* spp.) (Azizi Jalilian et al. 2020). The preferred environment is sparsely-vegetated open ground in semi-arid regions, with unimproved stony pasturage and open grassy areas within thermophilous forest being typical. Flight period: April/June. Developmental stages: undescribed.

***Merodon rufofemoris* Vujčić, Radenković & Likov, sp. nov.**

<https://zoobank.org/85A45AAA-5D78-4914-A8CC-A3E0F8C4DA4A>

Figs 2D, 3C, 4E, 5C, 7E, 11, 12D, 13, 20A, B

Type material examined. Holotype: IRAN • 1 ♂; Fars prov., Dasht-e Ajran; 29.552, 51.942; 5 May 2015; leg. M. Kafka; in BM collection.

Diagnosis (only male known). Similar to *Merodon vandergooti* from which differs by all femora completely reddish yellow (Figs 4E, 20B), while in males of *M. vandergooti* pro- and mesofemora are partly orange-yellowish and metafemur is almost completely black (Figs 4C, 20D), a less curved metafemur (Fig. 4E), and an elongated anterior surstyler lobe in *M. rufofemoris* sp. nov. (Fig. 11A: al) (shorter in *M. vandergooti*; Fig. 10A: al). It differs from *M. aenigmaticus* sp. nov. by the reddish yellow femora (Fig. 4E) (partly black in *M. aenigmaticus* sp. nov.; Fig. 4G), and the posterior surstyler lobe angulate ventrally (Fig. 11A: pl) (rounded in *M. aenigmaticus* sp. nov.; Fig. 9A: pl).

Description. Male. Head. Basoflagellomere orange-yellow (Fig. 2D), elongated, ~ 2× longer than wide, and ~ 1.9× longer than pedicel, convex dorsally; fessette dorsolateral; arista reddish to brown and thickened at basal third; arista ~ 1.5× longer than basoflagellomere; face and frons black, with whitish pollinosity; face covered with dense whitish pilosity; pile on frons dense, whitish; oral margin small, black, sparsely pollinose; lunula shining black to brown, bare; eye contiguity ~ 10 facets long; vertical triangle isosceles, black, shiny, except grey pollinose anterior corner, covered with greyish white pilosity; ocellar triangle equilateral; occiput with grey-yellow to reddish pile, densely covered with grey pollinosity along eyes; eyes covered with short, whitish grey pile (Fig. 12D).

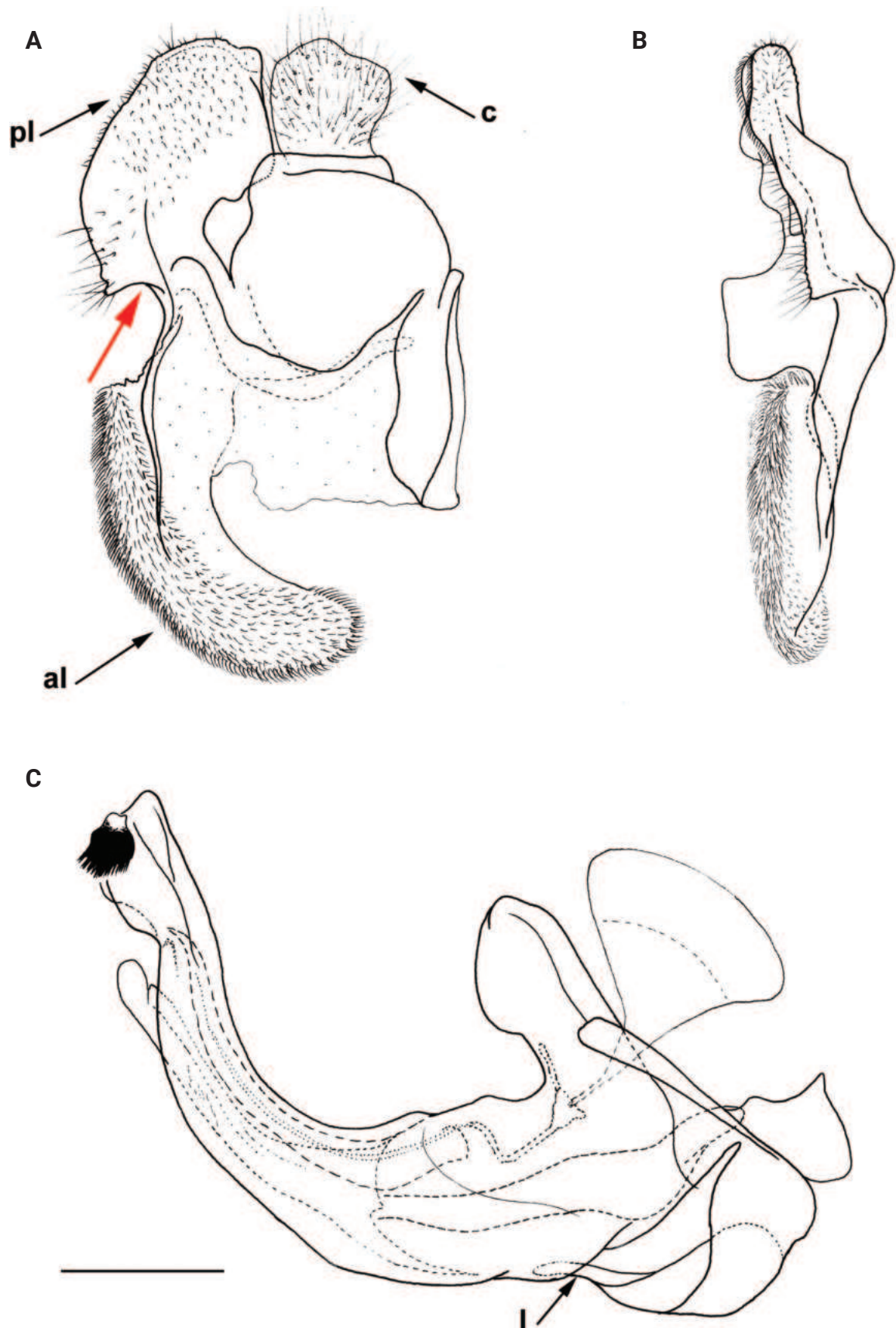


Figure 11. Male genitalia *M. rufofemoris* sp. nov. **A, B** epandrium **C** hypandrium **A, C** lateral view **B** ventral view. Strongly angulated ventral part of posterior surstylar lobe marked with red arrow. Abbreviations: al-anterior surstylar lobe, c-cercus, l-lingula, pl-posterior surstylar lobe. Scale bar: 0.5 mm.

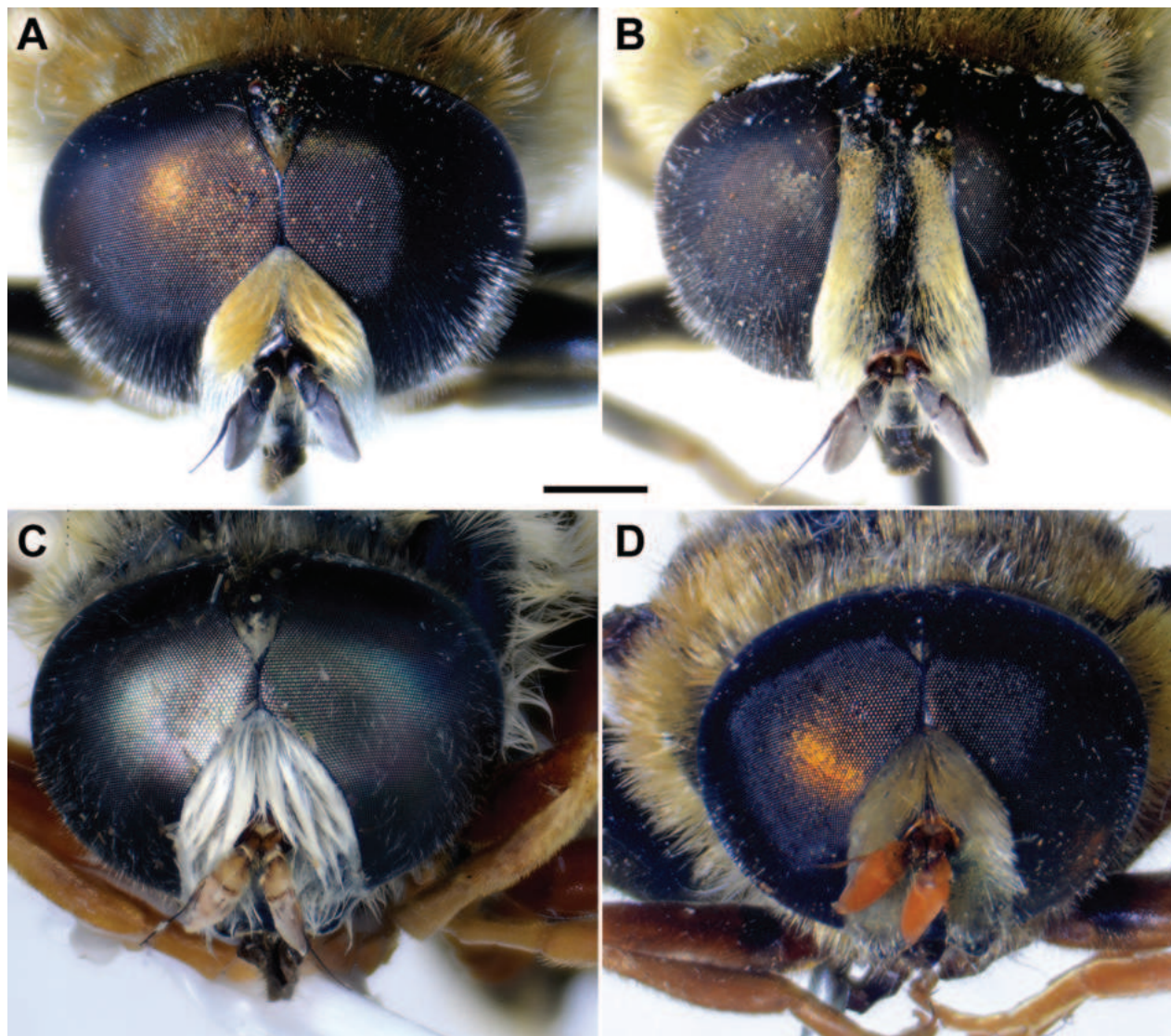


Figure 12. Head, frontal view **A, B** *M. latens* sp. nov. **C** *M. aenigmaticus* sp. nov. **D** *M. rufifemoris* sp. nov. **A, C–D** male **B** female. Scale bar: 1 mm.

Thorax. Scutum and scutellum black with bronze lustre, covered with short, greyish yellow pile; pilosity between wing basis mostly black; scutum with indistinct pollinose vittae; transverse suture with two medial pollinose maculae (Figs 3C, 20A); posterior margin of scutellum with very long grey-yellow to whitish pilosity, reduced medially (Fig. 3C); posterodorsal part of anterior anepisternum, posterior anepisternum (except anteroventral angle), anterior anepimeron, dorsomedial anepimeron, and posterodorsal and anteroventral parts of katepisternum with long, dense greyish white pile; wings mostly covered with microtrichia; wing veins yellowish to brown; calypteres whitish yellow; halteres yellow to white; legs reddish yellow; metafemur broad, ~ 3.5× longer than wide, covered with long, whitish yellow pilosity (Fig. 4E).

Abdomen. Elongated (Fig. 5C), ~ 1.3× longer than mesonotum; terga black, except lateral sides of tergum 2 with reddish yellow maculae; terga 3 and 4 with a pair of broad, distinct silver-grey pollinose fasciate maculae; pile on terga grey-yellow to whitish; sterna black, covered with whitish grey pile; posterior margin of sternum 4 with characteristic posteromedial incision (Fig. 7E).

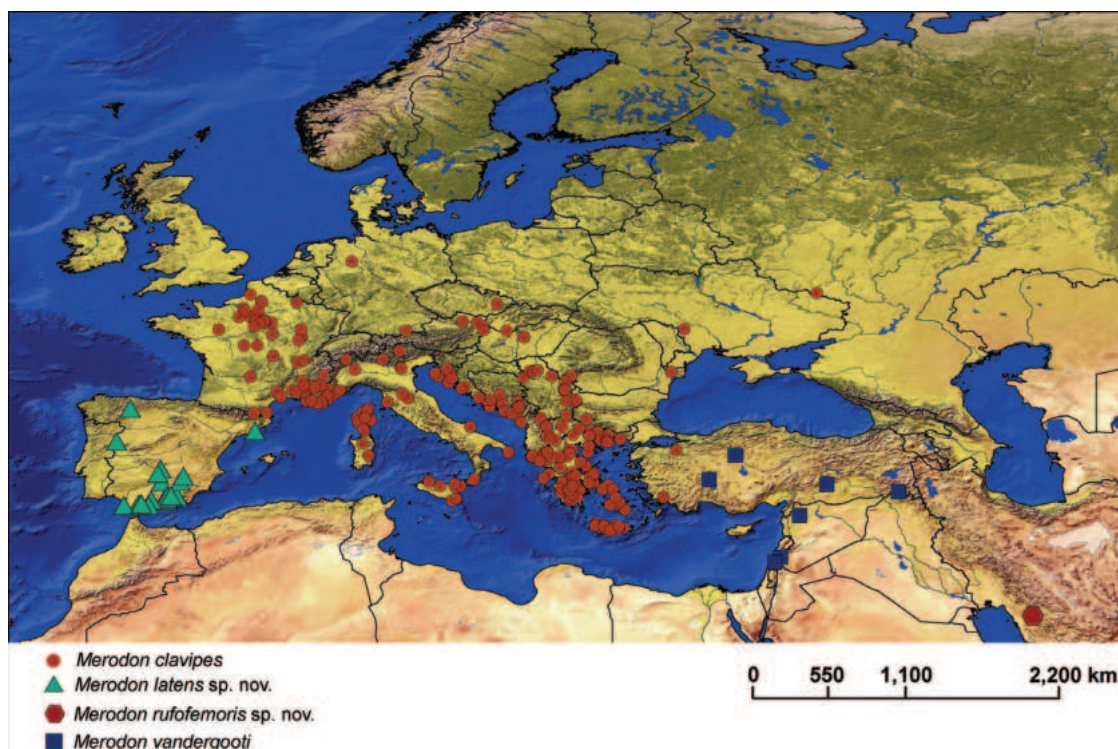


Figure 13. Distribution map of *Merodon clavipes*, *M. latens* sp. nov., *M. rufefemoris* sp. nov. and *M. vandergooti*.

Male genitalia (Fig. 11). Anterior surstylar lobe large, elongated (~ 3.5× longer than wide) and sickle-like (Fig. 11A: al); posterior surstylar lobe rectangular (Fig. 11A: pl, marked with red arrow); cercus rectangular (Fig. 11A: c); hypandrium sickle-shaped, without lateral projections; lingula short, with tapering but rounded tip (Fig. 11C: l).

Female. Unknown.

Distribution and biology. This species is only found in the Fars Province of Iran (Fig. 13). This Iranian locality lies within the Zagros Mountains forest steppe ecoregion (Olson et al. 2001), representing an arid and semi-arid forest ecosystem with *Quercus brantii* as the dominant vegetation type (Azizi Jalilian et al. 2020). Flight period: May. Developmental stages: undescribed.

Etymology. The name is derived from the Latin adjective *rufus* (red, reddish) and inflection of the noun femur in genitive singular (*femoris*) and refers to the reddish yellow colour of femora. Species epithet to be treated as an adjective.

***Merodon vandergooti* Hurkmans, 1993**

Merodon aureotibia Hurkmans, 1993: 203.

Merodon vandergooti Hurkmans, 1993: 188.

Type locality. TURKEY, “Hakkari”. The original description was based on a male holotype and ~ 40 male paratypes (all in RMNH) (Hurkmans 1993). Holotype (designated by Hurkmans): male, Turkey, Hakkari (RMNH), [specimen dry pinned]. Original labels: [Turkey, Hakkari, Süvarihalil geçidi, 1250 m W side near Halub Deresi, 13.vi.1984 leg. J. A. W. Lucas], [Holotype of *Merodon vandergooti* Hurkmans] (examined).

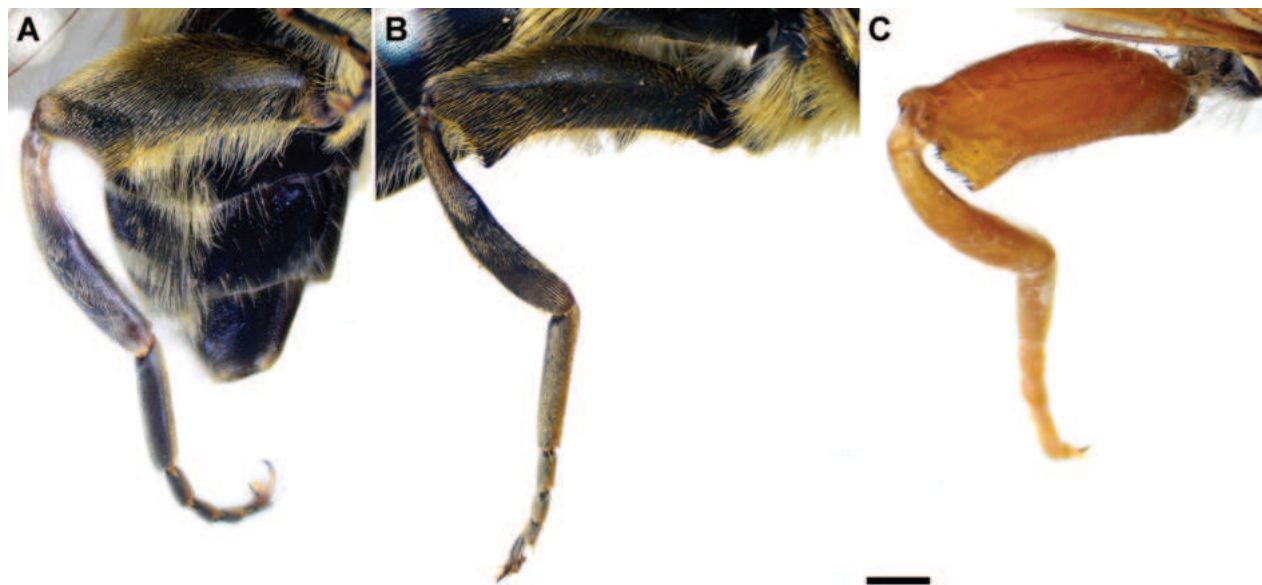


Figure 14. Metaleg of female, lateral view **A** *M. clavipes* **B** *M. latens* sp. nov. **C** *M. vandergooti*. Scale bar: 1 mm.

***Merodon aureotibia* Hurkmans, 1993: 203**

Type locality. TURKEY, “Adiyaman”. The original description was based on a female holotype and three female paratypes (all in RMNH) (Hurkmans 1993). Holotype (designated by Hurkmans): female, Turkey, Adiyaman (RMNH), [specimen dry pinned]. Original labels: [Turkey, Adiyaman, Nemrut Dağı, 1.vi.1983, leg. M. Kuhbandner], [Holotype of *Merodon aureotibia* Hurkmans] (examined).

Notes. *Merodon vandergooti* and *M. aureotibia* were described in the same publication (Hurkmans 1993): *M. vandergooti* from a large number of males and *M. aureotibia* based only on females. Hurkmans (1993) considered *M. vandergooti* is the only member of the *vandergooti* group and *M. aureotibia* as part of the *alagozicus* group. The type material of the two taxa belongs to the same species, and Vujčić et al. (2011) retained *M. vandergooti* (Hurkmans 1993: 188) as the valid name for this species and designated *M. aureotibia* (Hurkmans 1993: 203) as a synonym.

Diagnosis. Tibiae and tarsi plus all femora in female (Fig. 14C) while pro- and mesofemora in males partly, orangish yellow (Fig. 20C, D); male metafemur very broad (~ 2.5× longer than wide) and strongly curved, covered with long and dense yellow pile ventrally (Fig. 4C). Male genitalia in Fig. 10.

Distribution and biology. The species range includes Israel, Syria and Turkey (Fig. 13; Suppl. material 2). The preferred environment of *Merodon vandergooti* is Eastern Mediterranean conifer-sclerophyllous-broadleaf forests. In Israel, this species has been registered from the Hermon and Meiron mountains where the montane forest is dominated by *Quercus infectoria* subsp. *veneris* (A. Kern.) Meikle, *Q. libani* G. Olivier, *Juniperus drupacea* Labill., and *Acer monspessulanum* subsp. *microphyllum* (Boiss.) Bornm., as well as in Mediterranean maquis and semi-steppe bathas (Danin 1988). In Turkey, the species range covers warm temperate grassland and shrubland/woodland (Evrendilek and Gulbeyaz 2008). Flight period: April/July. Developmental stages: undescribed.

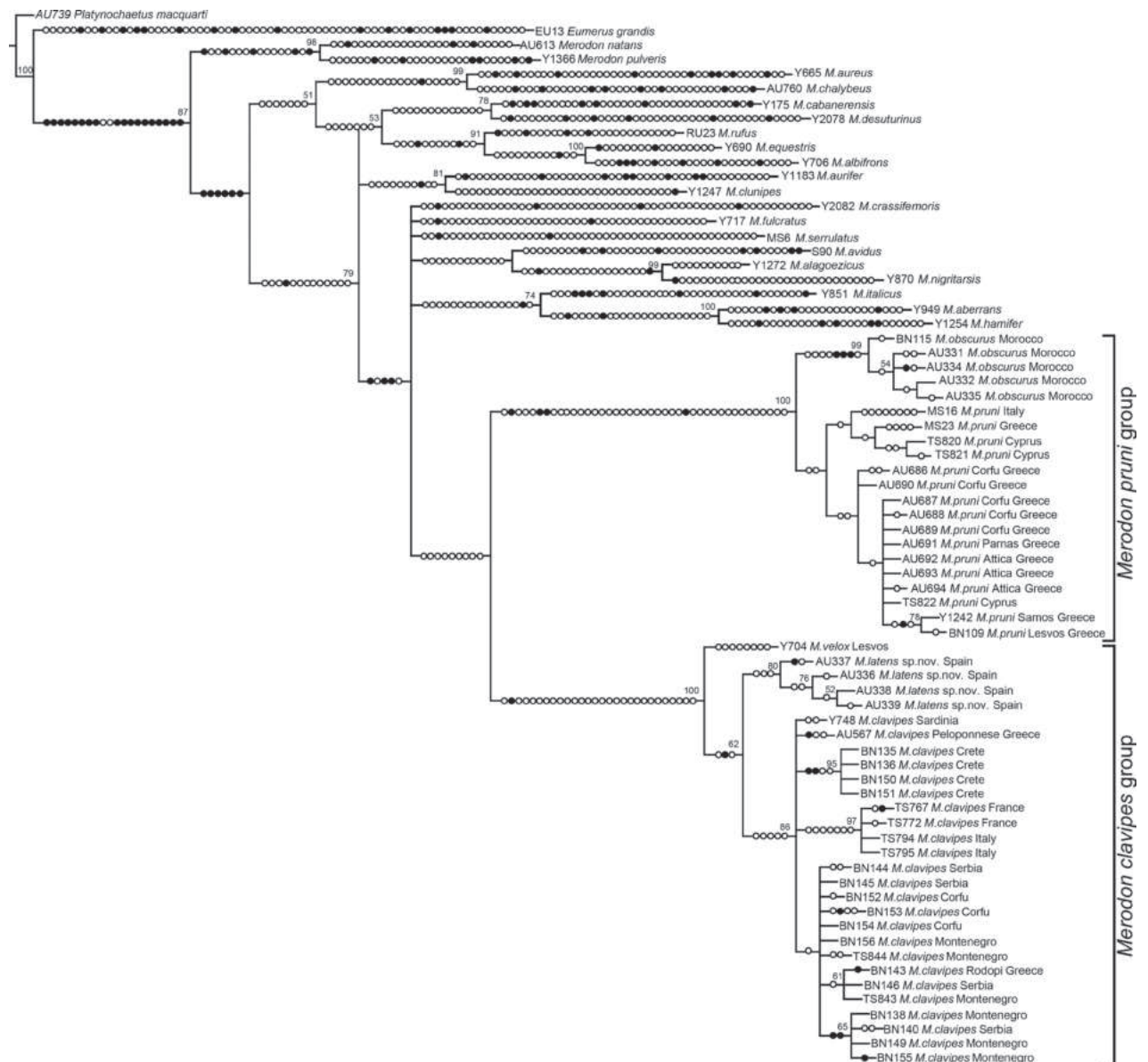


Figure 15. Maximum Parsimony strict consensus tree based on nine equally parsimonious trees, length 1443 steps, consistency index (CI) 38, retention index (RI) 75. Filled circles represent non-homoplasious changes and open circles are homoplasious changes. Bootstrap supports are depicted near nodes (≥ 50).

***Merodon velox* Loew, 1869**

Merodon velox Loew, 1869: 253.

Merodon velox var. *anathema* Paramonov, 1926: 149.

Merodon velox var. *armeniaca* Paramonov, 1926: 147.

Merodon velox anathemus Peck, 1988: 175 (sic! non Paramonov), syn. nov.

Merodon velox armeniacus Peck, 1988: 175 (sic! non Paramonov), syn. nov.

***Merodon velox* Loew, 1869: 253**

Type locality. TURKEY, “Smyrna = Izmir” and Greece (Rhodus = Rhodos). The original description (Loew 1869) was based on seven males and an unspecified number of female syntypes from the Vienna collection (RMNH).

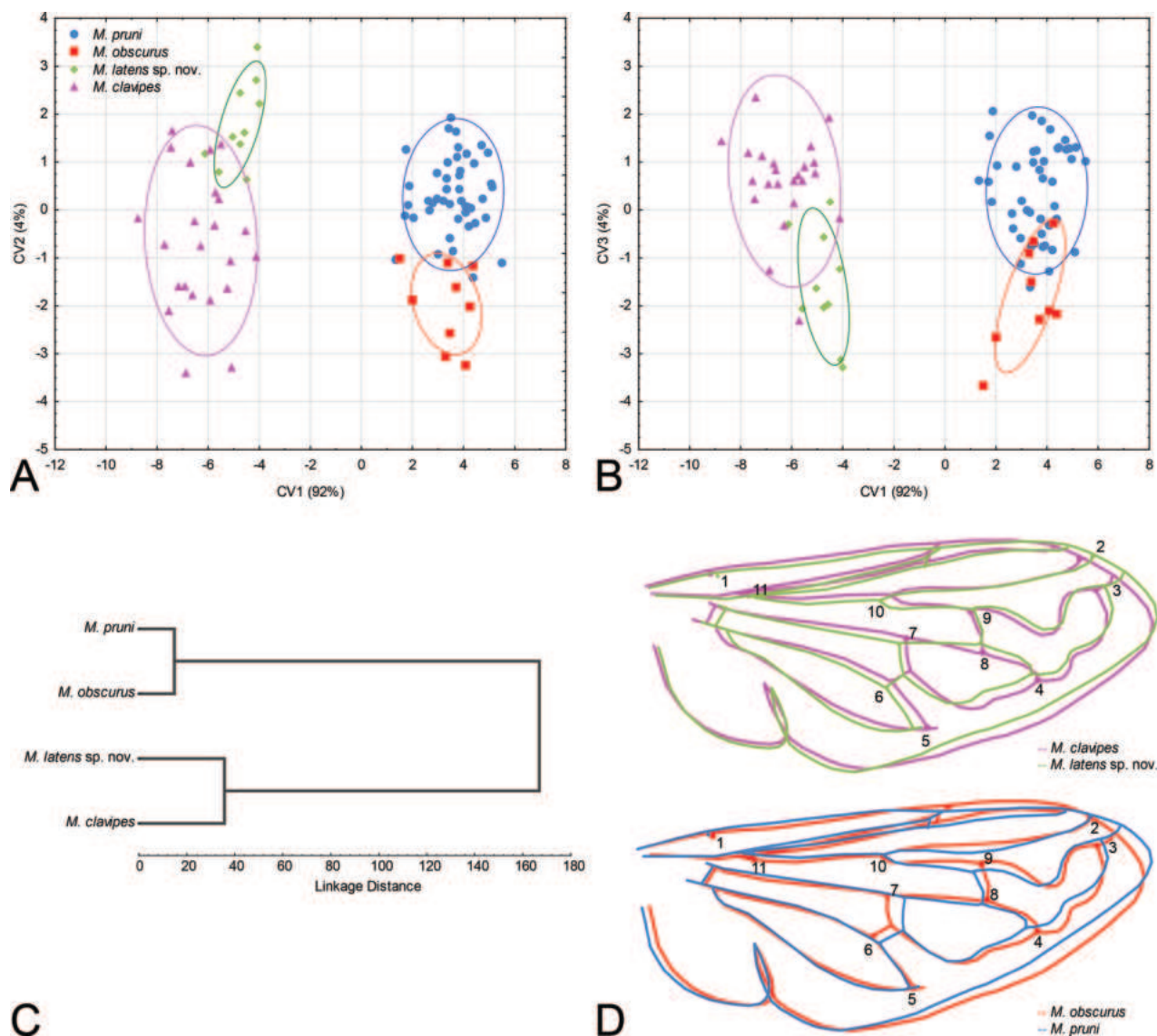


Figure 16. Geometric morphometric analysis of the wing shape in males of *Merodon clavipes*, *M. latens* sp. nov., *M. obscurus*, and *M. pruni* **A** Position of male specimens in the space defined by CV1 and CV2 axes **B** Position of male specimens in the space defined by CV1 and CV3 axes **C** UPGMA phenogram constructed using squared Mahalanobis distances of wing shape **D** Drawings showing differences in wing shape for each species pair; differences between the species were exaggerated 5-fold to make them more discernible.

Lectotype (designated by Hurkmans 1993: 183): male, Greece, Rhodes (NHWM), [specimen dry pinned]. Original label: [Rhodus / Alte Sammlung] (examined).

***Merodon velox* var. *anathema* Paramonov 1926b: 149**

Merodon velox anathemus Peck, 1988: 175 (sic! non Paramonov), syn. nov.

Holotype (examined). Female with labels: white, handwritten, bold ink [N 340]; printed [mons Takältu / prope Kulp. / 28...V.....13.], = Tekaltı Dağı mountain, near Kulp (Turkey), 38.516667; 41.016667; pink, handwritten, pale ink, with double typographical frame [*Merodon / anathema / n. sp. ♀* Typus / Paramonov d.].

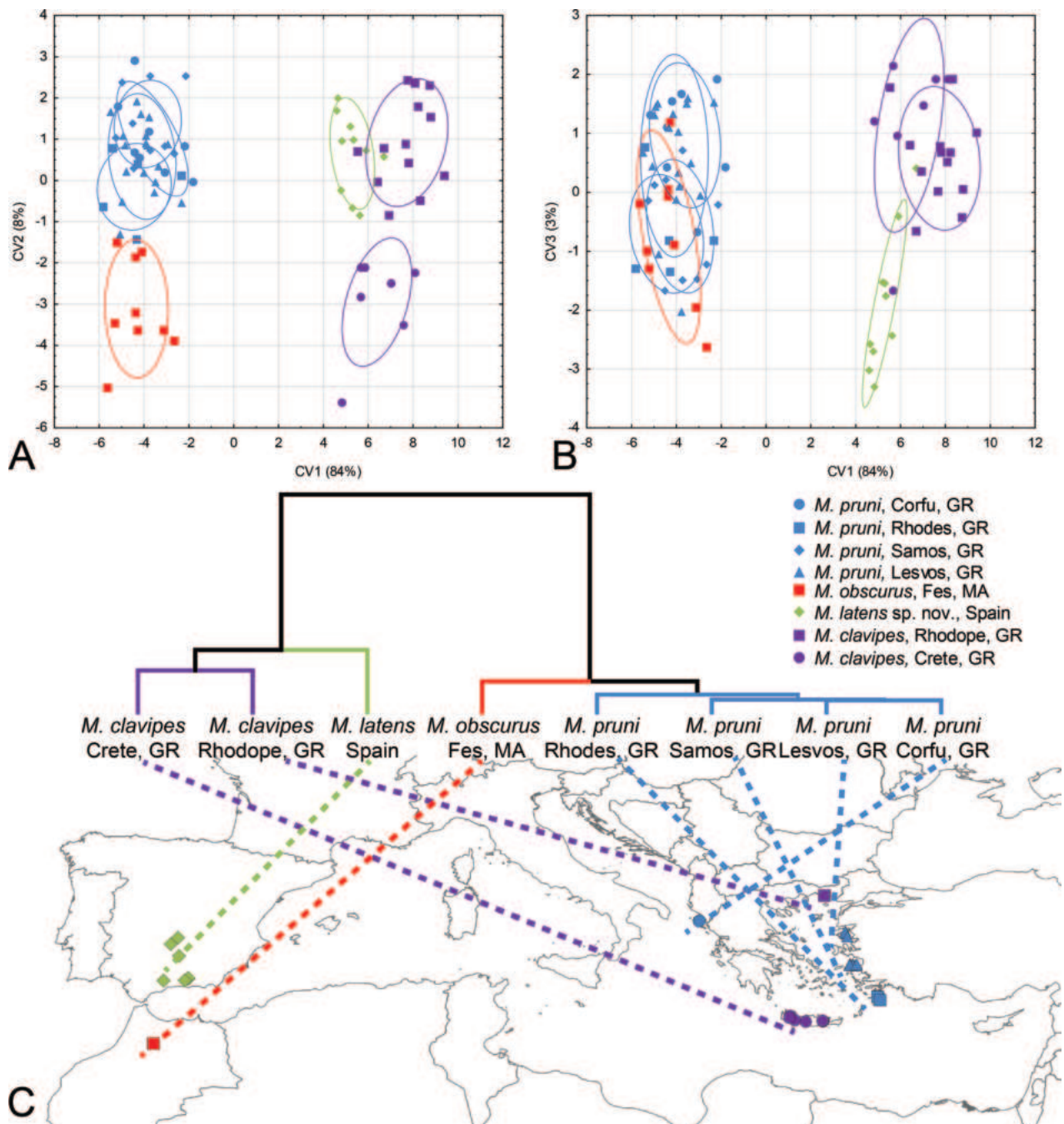


Figure 17. Wing shape differences among populations of *Merodon clavipes*, *M. latens* sp. nov., *M. obscurus* and *M. pruni* **A** Scatter plot of individual scores of CV1 and CV2 **B** Scatter plot of individual scores of CV1 and CV3 **C** UPGMA phenogram constructed using squared Mahalanobis distances of wing shape plotted on the map of Mediterranean basin showing the distribution of populations used in the analysis.

Notes. The taxon was described as a “var.” from a single female, which is the holotype according to article 73.1.2 ICZN (1999). Paramonov indicated that the type is kept in his personal collection (Paramonov 1926b: 149). Type locality: Turkey. Later, S. Ya. Paramonov gave the species as “*M. anathema* sp. n.” (Paramonov 1927: 15). Until recently, the type was believed to be lost (Liepa 1969: 4, 20; Hurkmans 1993: 183 “holotype ... not examined, probably lost”, 205 “lost”, 206), but it has since been found at the SIZK (Popov 2011).

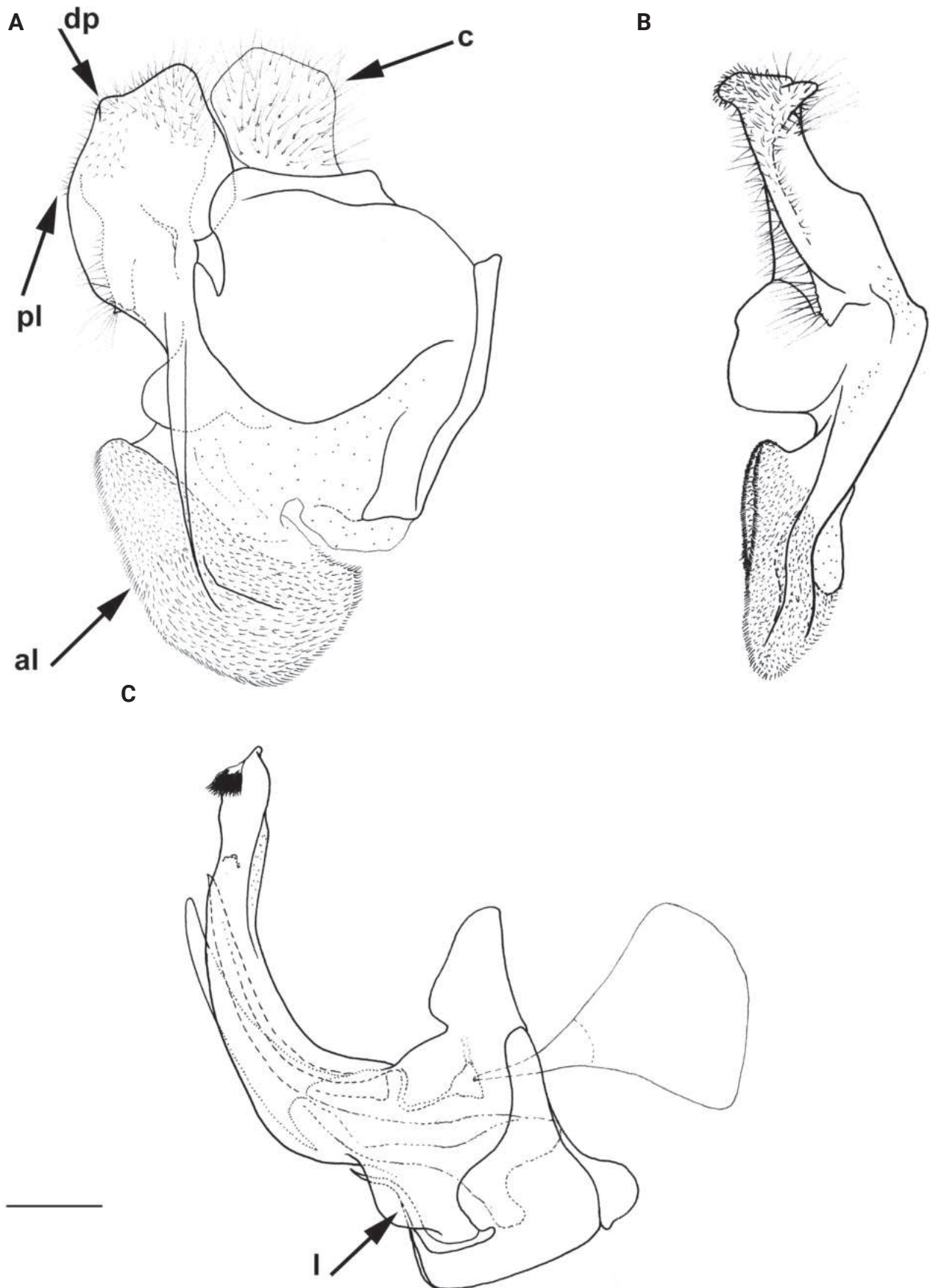


Figure 18. Male genitalia *M. quadrinotatus* **A, B** epandrium **C** hypandrium. **A, C** lateral view **B** ventral view. Abbreviations: al-anterior surstyler lobe, c-cercus, dp-dorsal prominence, l-lingula, pl-posterior surstyler lobe. Scale bar: 0.5 mm.

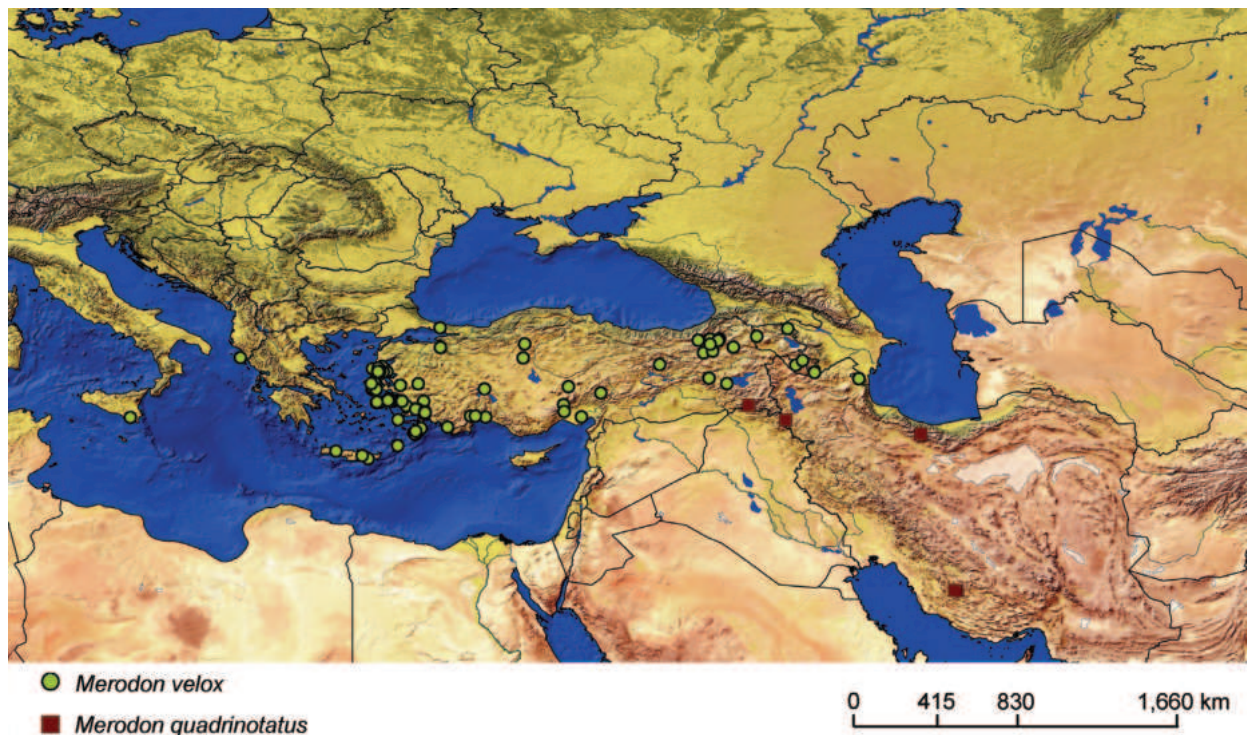


Figure 19. Distribution map of *Merodon velox* and *M. quadrinotatus*.

The name was correctly (see also Lingafelter and Nearn 2013) given a subspecific rank for the first time in Peck's Catalogue (1988: 175), «*Merodon velox anathemus* Paramonov», according to 45 (g) (ii) ICZN (1985), now 45.6.4 (ICZN 1999), but the original feminine name *anathema* was incorrectly changed contrary to article 31 (b) (ii) (ICZN 1985), now 31.2.1, 34.2.1 (ICZN 1999). Hurkmans (1993: 184) left the rank variety for the name. The study of the *Merodon velox* material revealed that character of this subspecies are not outside the limits of species variability in other parts of the species' range, so we consider *anathema* syn. nov. for *M. velox* Loew, 1869.

***Merodon velox* var. *armeniaca* Paramonov 1926b: 147**

Merodon velox armeniacus Peck, 1988: 175 (sic! non Paramonov), syn. nov.

Lectotype (examined). Male with labels: white, handwritten, bold ink [N 341]; pale ink [Армения / Эривань / 24.v.24.], = Yerevan (Armenia), 40.166667; 44.516667; pink, handwritten, pale ink, with double typographical frame [*Merodon / velox* Lw. ♂ / var. *armeniaca* / var. nov. / Paramonov det.] (SIZK).

Paralectotype (examined): female with labels: white, handwritten, bold ink [N 342]; pale ink [Армения / Ордубад / 7.VI.24.], = Ordubad (Azerbaijan), 38.908056N 46.027778E; pink, handwritten, pale ink, with double typographical frame [*Merodon / velox* Lw ♀ / var. *armeniaca* / var. nov. / Paramonov det.].

Notes. Paramonov indicated that the male types (12 specimens) are kept in two localities, "Typus in meiner Sammlung und im Museum von Armenien" (Paramonov 1926b: 148), with the only female type being kept in his personal collection (ibid.: 149). The exact location of the types was not known, and it was thought that they had possibly been lost (Liepa 1969: 4, 20; Hurkmans 1993:

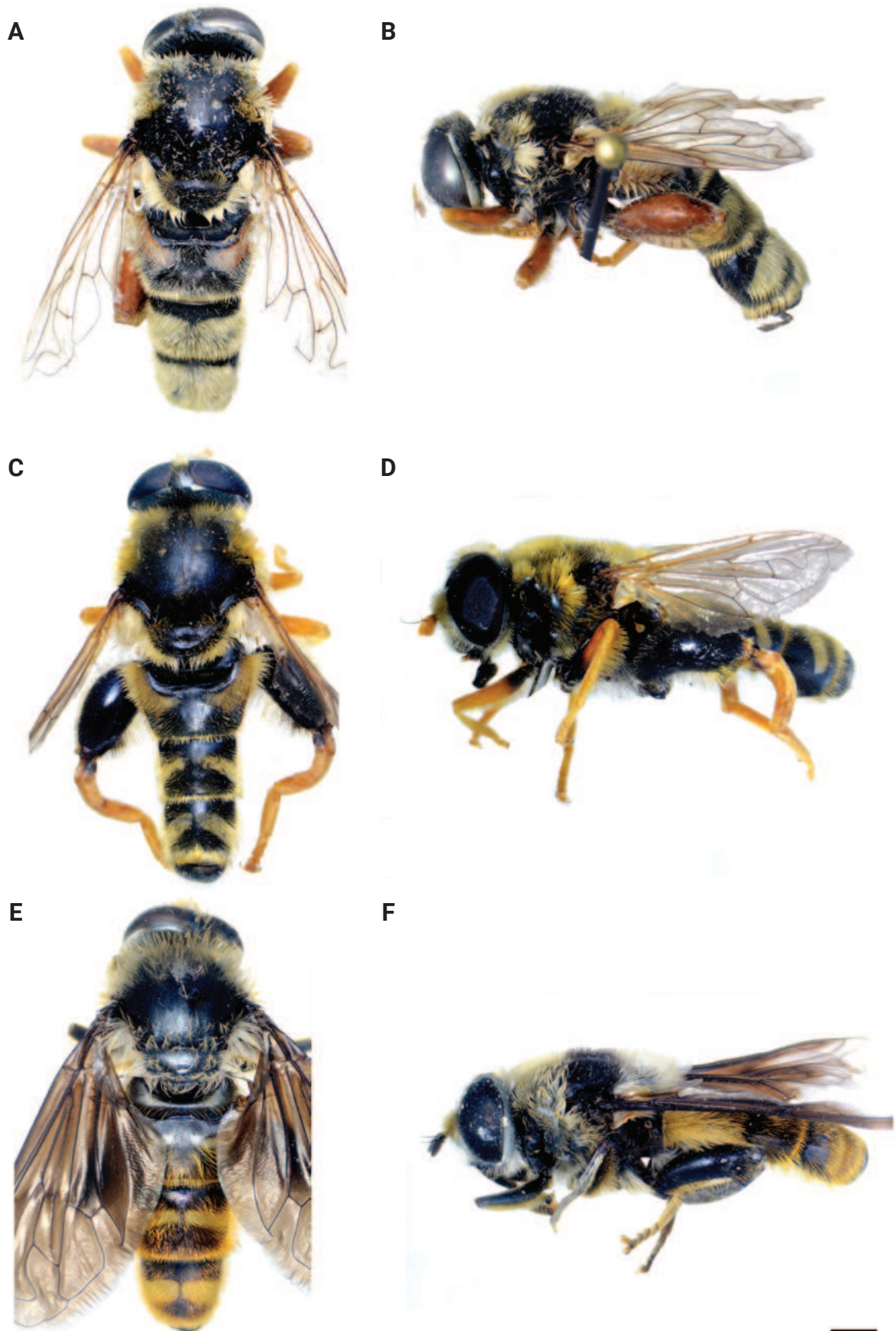


Figure 20. Body of male **A, B** *M. rufofemoris* sp. nov. **C–D** *M. vanderhooti* **E, F** *M. velox*. **A, C, E** dorsal view **B, D, F** lateral view. Scale bar: 1 mm.

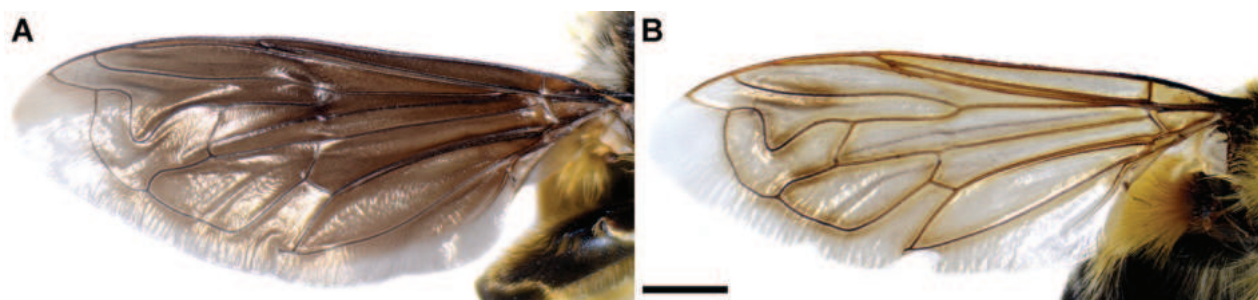


Figure 21. Wing of *Merodon velox*, dorsal view **A** male **B** female. Scale bar: 1 mm.

183 “syntypes ... not examined, probably lost”, 205 “lost”, 206). Two syntypes of 13 have been preserved in SIZK (Popov 2011). It was assumed that some of the syntypes had been preserved at the current IZY (Liepa 1969: 4, 20 “Museum of Natural History of the Armenian SSR, Yerevan”; Hurkmans 1993: 184 “possibly some of the material might be present in the collection of the Museum of Armenia, Erivan”). According to personal communication with Mark G. Kalashyan (Yerevan), a single specimen of *Merodon velox* is deposited in the IZY collection and was examined by S. Ya. Paramonov, hosting two labels, [Armenia, prope Beuk-Vedi, 1.vi.1926, A. Schelk.] = Vedi, Armenia, 39.910556; 44.727778, and [*Merodon velox* Lw., ♂, Paramonov d.]. This specimen is not the type. The name was correctly given a subspecific rank for the first time in Peck’s Catalogue (1988: 175) (see also Lingafelter and Nearn 2013), «*Merodon velox armeniacus* Paramonov», according to article 45 (g) (ii) ICZN (1985), now corresponding to 45.6.4 (ICZN, 1999). Hurkmans (1993: 184) left the rank of variety for the name. According to article 74 ICZN (1999), we designate the male as the lectotype and the female as the paralectotype. Type locality: Armenia (76.2 ICZN 1999). Paramonov later mentioned this name (Paramonov 1927: 15), but erroneously indicated the wrong year of collection for the types (1925). In fact, 1924 is specified in the original description and indicated on the type labels. The study of the *M. velox* material revealed that characters of this subspecies are not outside the limits of the species variability in other parts of the species range, so we consider *armeniacus* syn. nov. for *M. velox* Loew, 1869.

Diagnosis. Male: wings brown-black except extreme apical part (Figs 20E, F, 21A); female: wing in basal half with yellow, while in apical half with brown veins; wing covered along veins with dark brown microtrichia (Fig. 21B). Male genitalia as in Fig. 22. Similar to *Merodon clavipes* and *M. latens* sp. nov. from which male differs by brown-black wing (hyaline wing in *M. clavipes* and *M. latens* sp. nov.) and a narrower metafemur (Fig. 4F), < 2× broader than the metatibia (metafemur is > 2× broader than the metatibia in *M. clavipes* (Fig. 4A) and *M. latens* sp. nov. (Fig. 4B)); female differs by wing covered along veins with dark brown microtrichia (Fig. 21B), clear in *M. clavipes* and *M. latens* sp. nov.

Distribution and biology. The species range includes Armenia, Azerbaijan, Georgia, Greece, Italy, and Turkey. Hurkmans (1993) also lists Yugoslavia, but those records could not be confirmed (Fig. 20; Suppl. material 2). The preferred environment of *Merodon velox* is forest or open ground, typically thinly-vegetated and stony semi-arid areas, unimproved grasslands, and open areas in *Abies* forest, as well as *Castanea* forest (Speight 2020). This species apparently resembles a small *Xylocopa* in the field and continues to fly at temperatures above 35 °C. Males are strongly territorial, and both sexes fly low and fast through ground vegetation

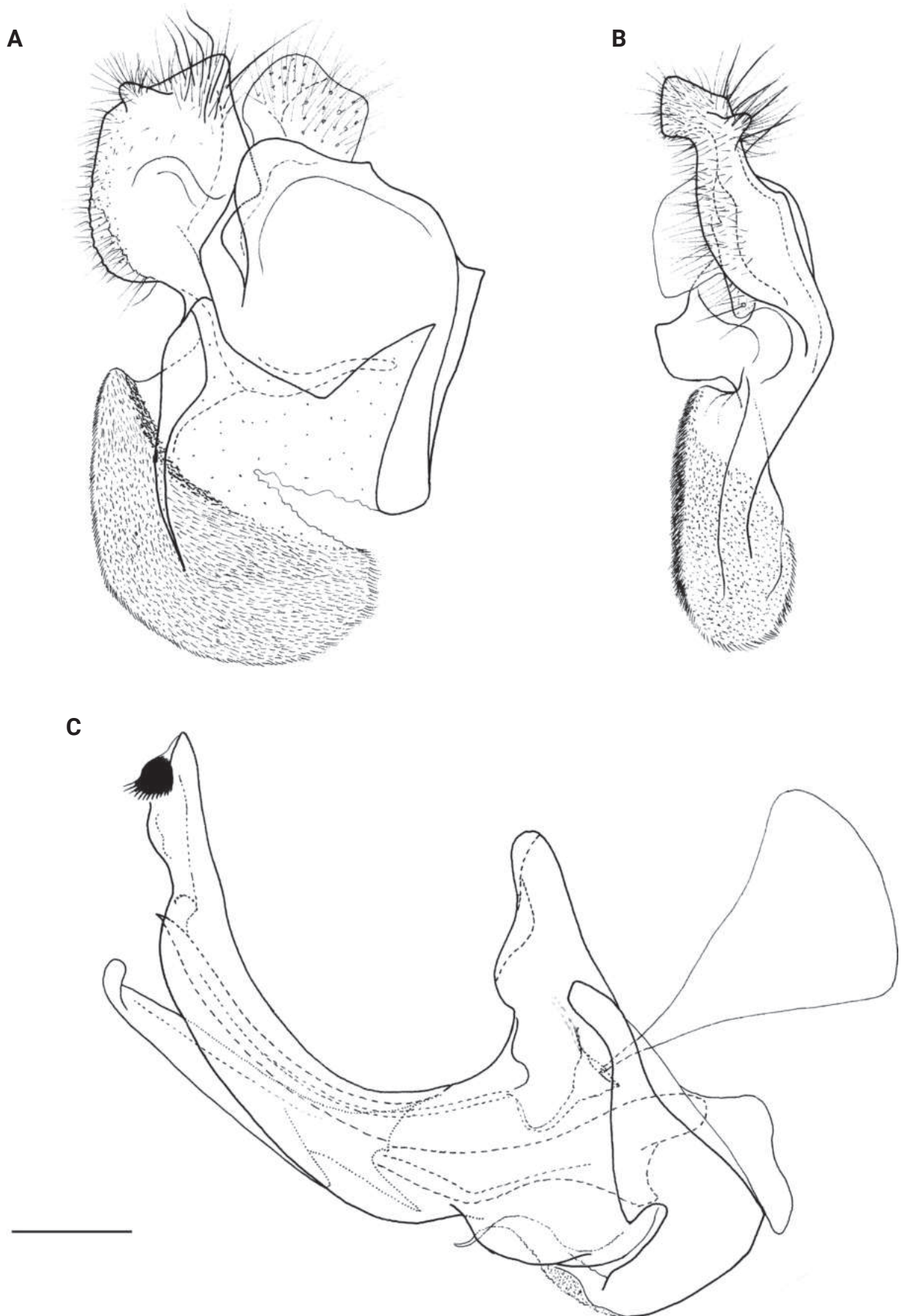


Figure 22. Male genitalia *M. velox* **A, B** epiandrium **C** hypandrium. **A, C** lateral view **B** ventral view. Scale bar: 0.5 mm.

(Hurkmans and Hayat 1997). The species has been found drinking at the edge of a small stream in the evening on a hot day (Reemer and Smit 2007). Flowers visited: umbellifers; *Euphorbia* (Zimina 1960; Hurkmans and Hayat 1997). Flight period: March/September. Developmental stages: not described (Speight 2020).

Key for the *Merodon* species of the *clavipes* species group

- 1 Basoflagellomere orange-yellow; tibiae, tarsi and all femora in female (females of *Merodon aenigmaticus* sp. nov. and *M. rufofemoris* sp. nov. are unknown) and pro- and mesofemora in males completely or partly orange-yellowish (as in Fig. 4C, E); posterior margin of scutellum medially without long pile (Fig. 3C) (*vandergooti* subgroup).....**2**
 - Legs and basoflagellomere black to dark brown; posterior margin of scutellum with long pilosity, not interrupted medially (as in Fig. 3B) (*clavipes* subgroup).....**4**
- 2 Metafemur reddish yellow (Fig. 4E); anterior surstylar lobe more elongated, ~ 3.5× longer than wide (Fig. 11A: al) ***Merodon rufofemoris* sp. nov.**
 - Metafemur mostly black (as in Fig. 4C); anterior surstylar lobe shorter (as in Fig. 9A: al), < 3× longer than wide**3**
- 3 Metafemur narrower and less curved, ~ 3.5× longer than wide (Fig. 4G); posterior surstylar lobe rounded (Fig. 9A: pl) ***Merodon aenigmaticus* sp. nov.**
 - Metafemur extremely broad and more curved, ~ 2.5× longer than wide (Fig. 4C); posterior surstylar lobe angular ventrally (Fig. 10A: pl) ***Merodon vandergooti* Hurkmans, 1993**
- 4 Wings membrane in males black, except extreme apical part (Fig. 21A); wing membrane in females with yellow veins on basal half, and with brown veins on apical half; wing along veins covered with dark brown microtrichia (Fig. 21B).....***Merodon velox* Loew, 1869**
 - Wing mostly hyaline (as in Fig. 1).....**5**
- 5 Tergum 3 in male with a pair of tear drop-shaped pollinose fasciate maculae separated from lateral margins (Fig. 5D); in female tergum 2 black; terga 3 and 4 with very characteristic pairs of pollinose, rounded maculae covered with dense whitish pile (Fig. 6D) ***Merodon quadrinotatus* (Sack, 1931)**
 - Tergum 3 in male with a pair of rectangular, pollinose fasciate maculae, ending close to lateral margins (as in Fig. 5A); in female tergum 2 with pair of lateral reddish yellow maculae (as in Fig. 6C) and without or with a pair of rectangular, pollinose fasciate maculae covered with grey pile on terga 3 and 4 (as in Fig. 6C)**6**
- 6 Male with broad (~ 2–2.5× longer than wide) and curved metafemur (Fig. 4A); posterior surstylar lobe more straight ventrally (Fig. 8A: pl); distribution: from northern France to the Mediterranean, and from Italy through central and southern Europe to Greece, former Yugoslav countries, Albania, Romania, Ukraine, European Russia, and Turkey (Fig. 13) ***Merodon clavipes* (Fabricius, 1781)**
 - Male with less broad (~ 3–3.5× longer than wide) and less curved metafemur (Fig. 4B); posterior surstylar lobe more arcuate ventrally (Fig. 8C: pl); distribution: Iberian Peninsula and south western France (Fig. 13) ***Merodon latens* sp. nov.**

***Merodon pruni* species group**

Diagnosis. The *pruni* species group belongs to the *M. avidus–nigritarsis* lineage, characterised by mesocoxa without a long pile on the posterior section. This group includes large species (10–18 mm) characterised by short body pilosity (except for *M. cupreus*) especially on scutum and abdomen (as in Fig. 23), short basoflagellomere, as long as broad (Fig. 24), and pleurae usually covered with distinct whitish to yellowish pilosity; scutum with well-defined or indistinct, narrow, pollinose vittae, and some species may have a fascia with mostly black pile between wing bases; metatrochanter usually with more or less distinct calcar (Fig. 25); metafemur covered with medium to long outstanding pile (Fig. 25); tergum 2 at least partly reddish or yellow laterally (as in Fig. 26A, D), except for *M. cupreus* that has all terga black (Fig. 26C); terga 2–4 with a pair of very distinct whitish grey pollinose fasciate maculae (as in Fig. 27); sternum 4 with medial, circular incision on posterior margin (Fig. 28); male genitalia: anterior surstylar lobe small, approximately as long as wide, triangular or rectangular (as in Fig. 29A: al); posterior surstylar lobe enlarged (several times longer than wide) and broad (as in Fig. 29A: pl); cercus more or less rectangular (as in Fig. 29A: c); hypandrium with filamentous prolongation on ejaculatory sack (as in Fig. 29C: marked with red arrow); lingula medium sized and narrow (as in Fig. 29C: l). Five species belong to this species group: *Merodon pruni* is distributed in most of the Mediterranean, *M. obscurus* stat. rev. is endemic to North Africa, and the other three species are more allocated to the east, from Turkey to Israel and Pakistan.

***Merodon aequalis* Vujjić, Radenković & Likov, sp. nov.**

<https://zoobank.org/204E1669-2E84-4938-A8B4-C30015D9B6BE>

Figs 23, 24A, E, F, 25A, 26A, B, 28A, 30A, 31A, 32, 33, 34

Type material examined. Holotype. STATE OF PALESTINE • 1 ♂; Wadi Kabala Judean hills; 30 Apr. 1947; in TAU. **Paratypes.** ISRAEL • 1 ♂; Golan, Qunaitra; 19 May 1983; leg. F. Kaplan; in RMNH • 1 ♂; Golan, 5 km south Qunaitra; 19.v.1983; leg. F. Kaplan; in TAU • 1 ♀; Ekron; 28 May 1921; in TAU • 1 ♀; Jerusalem; 6 May 1922; leg. P.A. Buxton; in RMNH • 1 ♂; Mrar; 14 May 1974; leg. M. Kaplan; in TAU • 1 ♀; Rehovot; 28 Sep. 1920; in RMNH • 1 ♀; Rehovot, 28 Apr. 1920; in TAU • 1 ♂, 2 ♀♀; in TAU • 1 ♂; 9 May 1925; in RMNH. STATE OF PALESTINE • 1 ♂; Tikenias; 13 Oct. 1931; leg. U. Suenberg; in NHMUK • 1 ♂; 8 May; O. Theodor; in TAU.

Diagnosis. Sternum 3 with long, equally distributed pilosity (Fig. 30A). In male the metatrochanter has a small calcar, almost absent (Fig. 25A); metafemur broad, ~ 3.5× longer than wide, strongly curved, covered with long and dense pilosity ventrally (Fig. 25A); sternum 4 on Fig. 28A. Female with rounded metatrochanter (Fig. 31A) and shorter but dense pilosity on metafemur ventrally than in male (Fig. 31A). Similar to *Merodon pallidus* stat. rev. from which differs by sternum 3 with equally distributed pilosity of the same length (Fig. 30A) (in *M. pallidus* stat. rev. with a conspicuous area of very long pilosity medially; Fig. 30D: marked with arrow), the shape of sternum 4 of male (Fig. 28A) (slightly different in *M. pallidus* stat. rev.; Fig. 28D), small calcar on metatrochanter in male, almost absent (Fig. 25A) (male of *M. pallidus* has a distinct calcar; Fig. 25D, while female of *M. pallidus* stat. rev. has the metatrochanter angular; Fig. 31C).

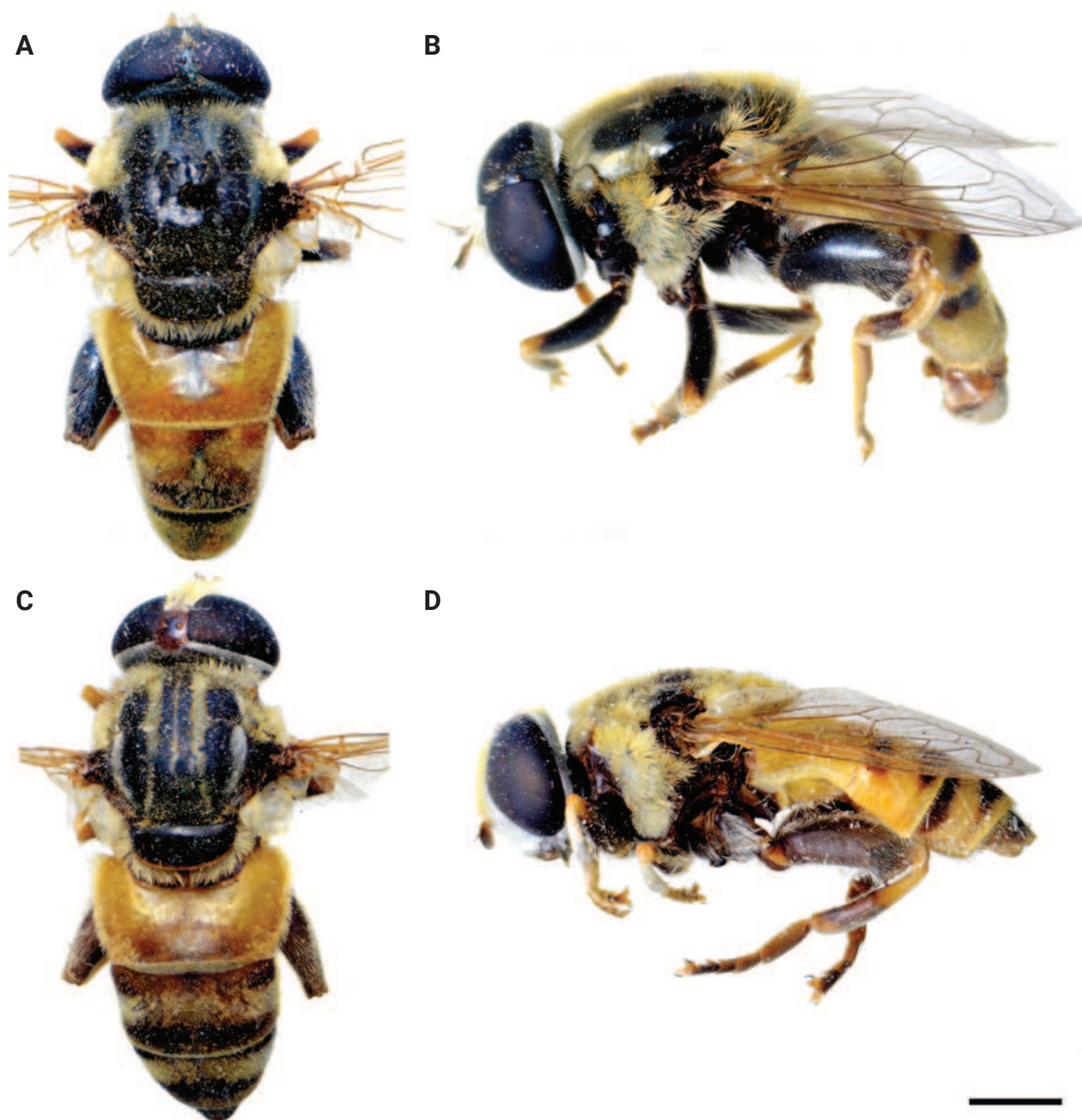


Figure 23. Body of *M. aequalis* sp. nov. **A, B** male **C–D** female. **A, C** dorsal view **B, D** lateral view. Scale bar: 2 mm.

Description. Male. Head (Fig. 24A, E). Pedicel and scapus reddish yellow; basoflagellomere from reddish yellow to brown (Fig. 24A), short, oval, $\sim 1.3\times$ longer than wide, and $\sim 2\times$ longer than pedicel, concave dorsally; fossette large, dorsolateral; arista reddish to brown and thickened at basal third; arista $\sim 2.5\times$ longer than basoflagellomere; face and frons black, with dense whitish pollinosity; face covered with dense whitish pilosity; pile on frons yellow-whitish; oral margin shiny black, without pollinosity; lunula reddish to brown, bare; eye contiguity $\sim 10\text{--}12$ facets long; vertical triangle isosceles, shiny, black, covered with grey-yellowish pilosity mixed with black pile around equilateral ocellar triangle; occiput with grey-yellow to whitish pile, and grey pollinose; eyes covered with short, whitish grey pile (Fig. 24E).

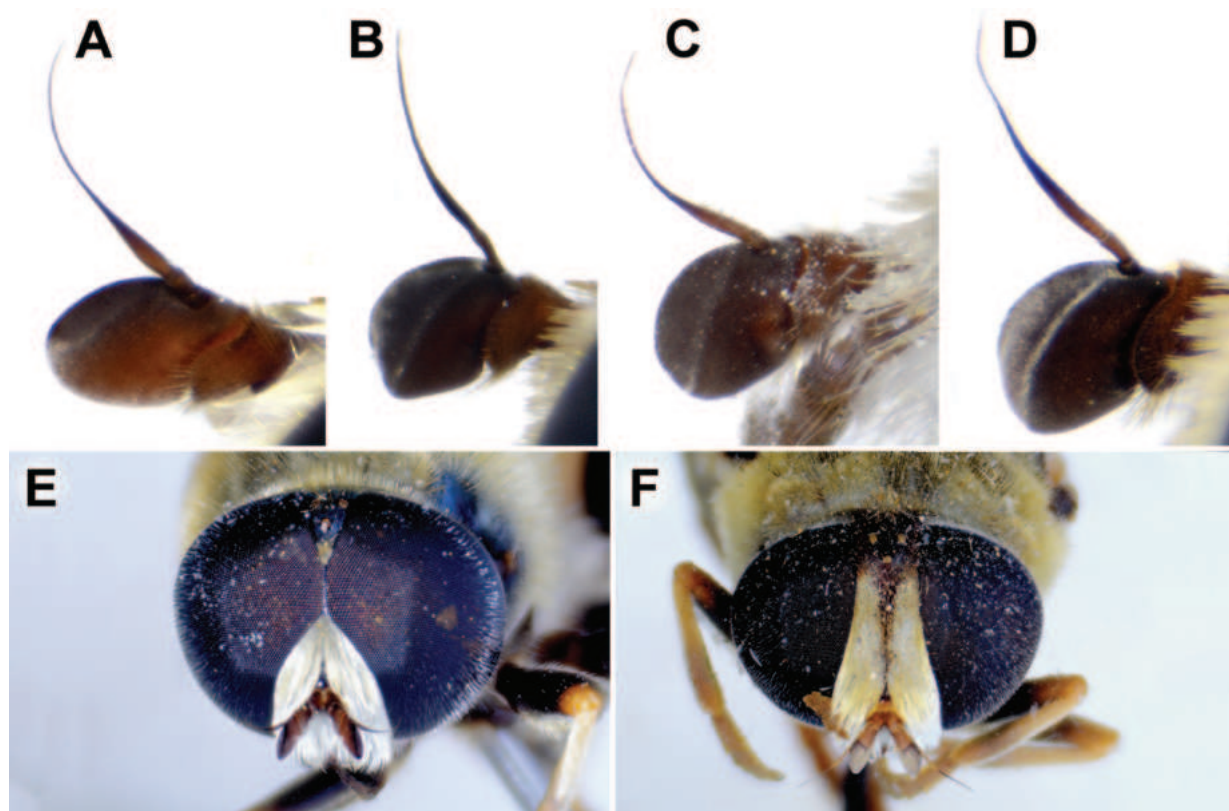


Figure 24. **A–D** basoflagellomera, lateral view **A** *M. aequalis* sp. nov. **B** *M. obscurus* **C** *M. pallidus* **D** *M. pruni*. **E, F** head of *M. aequalis* sp. nov., frontal view **A–E** male **F** female. Scale bar: 0.5 mm (**A–D**); 1 mm (**E, F**).

Thorax (Fig. 32A). Scutum and scutellum black with brownish lustre, covered with short, grey-yellow to whitish pile; pilosity between wing basis mostly black, at least around wing basis; lateral sides of scutum, excluding wing basis covered with long, golden to yellowish pile; scutum with two narrow pollinose vittae; posterior margin of scutellum with long yellowish pilosity (Fig. 32A); posterodorsal part of anterior anepisternum, posterior anepisternum (except anteroventral angle), anterior anepimeron, dorsomedial anepimeron, and posterodorsal and anteroventral parts of katepisternum with longer, dense whitish to yellow pile; wings mostly covered with microtrichia; wing veins yellowish to light brown; calypteres and halteres whitish yellow; angular calcar on metatrochanter small, almost absent; femora black except yellowish apex; metafemur broad, ~ 3.5× longer than wide, sparsely covered with long ventral pilosity (Fig. 25A); tibiae yellow to reddish, except brown medial ring; tarsi yellowish red, in some specimens brown dorsally.

Abdomen. Elongated, ~ 1.3× longer than mesonotum; tergum 1 black, terga 2–4 reddish yellow, medially partly brown; terga with a pair of broad, distinct silver-grey pollinose fasciate maculae; pile on terga yellow to whitish, medially short, adpressed, in some specimens black pile present on dark parts of terga 3 and 4 medially (Fig. 26A); sterna brown, covered with long, equally distributed whitish pile (Fig. 30A); posterior margin of sternum 4 with characteristic posteromedial circular incision (Fig. 28A).

Male genitalia (Fig. 33). Anterior surstylar lobe rectangular (Fig. 33A: al); posterior surstylar lobe large and broad, ~ 1.5× longer than wide (Fig. 33A: pl); cercus rectangular (Fig. 33A: c); hypandrium sickle-shaped, without lateral projections; lingula short (Fig. 33C: l).

Female. Similar to the male except for normal sexual dimorphism and the following characteristics: frons with broad pollinose vittae along eyes or completely pollinose, and reddish at the level of the ocellar triangle (Fig. 24F); scutum with five distinct pollinose vittae (Fig. 32B); metatrochanter rounded; pilosity on the ventral surface of metafemur shorter but denser than in male (Fig. 31A); tergum 2 all reddish, while terga 3–5 more brownish (Fig. 26B).

Distribution and biology. The range is restricted to Israel and the State of Palestine (Fig. 34). Its preferred environment is Eastern Mediterranean conifer-sclerophyllous-broadleaf forests. The vegetation of this ecoregion includes maquis, coniferous forests of *Pinus halepensis* Mill. and *P. brutia* Ten., dry *Quercus* spp. woodlands and steppe formations (WWF 2022). Flight period: April/October. Developmental stages: not described.

Etymology. Adjective *aequalis* meaning equal, similar, refers to the equally distributed pilosity of the same length on sternum 3 in males opposite to the related species *Merodon pallidus* stat. rev. with a conspicuous area of very long pilosity medially. Species epithet to be treated as an adjective.

***Merodon cupreus* Hurkmans, 1993**

Merodon cupreus Hurkmans, 1993: 179.

Type locality. Turkey, “Kars”. Original description was based on a male holotype and a high number of male and female paratypes (all in RMNH) (Hurkmans 1993: 179). Holotype (designated by Hurkmans): male, Turkey, Kars (RMNH), [specimen dry pinned]. Original labels: [Turkey, Kars, Handere 2100–2200 m, 20 km W of Saricamiş, 1.viii.1983, leg. J. A. W. Lucas], [Holotype of *Merodon cupreus* Hurkmans] (examined).

Diagnosis. Bumble bee mimic species (similar to species from *clavipes* species group) with pile on scutum longer than basoflagellomere (shorter in other species of the *pruni* species group); mesonotum with whitish pile except for broad black-pilose fascia between wing bases (Fig. 27B); tergum 2 black (mostly reddish yellow in other species of the *pruni* group); tergum 2 with whitish to yellow pile, and terga 3 and 4 covered with yellow to reddish pilosity (Fig. 26C); legs black; calcar on metatrochanter distinct; metafemur curved and covered with long, dense pilosity (Fig. 25B); sternum 3 medially with distinct pilosity (Fig. 30B: marked with arrow); sternum 4 in Fig. 28B. Male genitalia in Fig. 35. Similar to *Merodon clavipes* and *M. quadrinotatus* from which it clearly differs by its short basoflagellomere, which is as long as broad (as on Fig. 24A) (basoflagellomere > 2× longer than wide in *M. clavipes* (Fig. 2A) and *M. quadrinotatus* (Fig. 2C)).

Distribution and biology. The species is solely distributed in Turkey (Fig. 34; Suppl. material 2), including the eastern Pontic and Taurus mountains belonging to the Irano-Anatolian hotspot. These chains of high mountains form a natural barrier between the Mediterranean Basin and the dry plateaux of Western Asia. This topographically complex and extensive system of mountains and closed basins includes major parts of central and eastern Turkey. Historically, the mountains have served both as refuge and corridor between the eastern Mediterranean and western Asia, giving rise to multiple patches of local

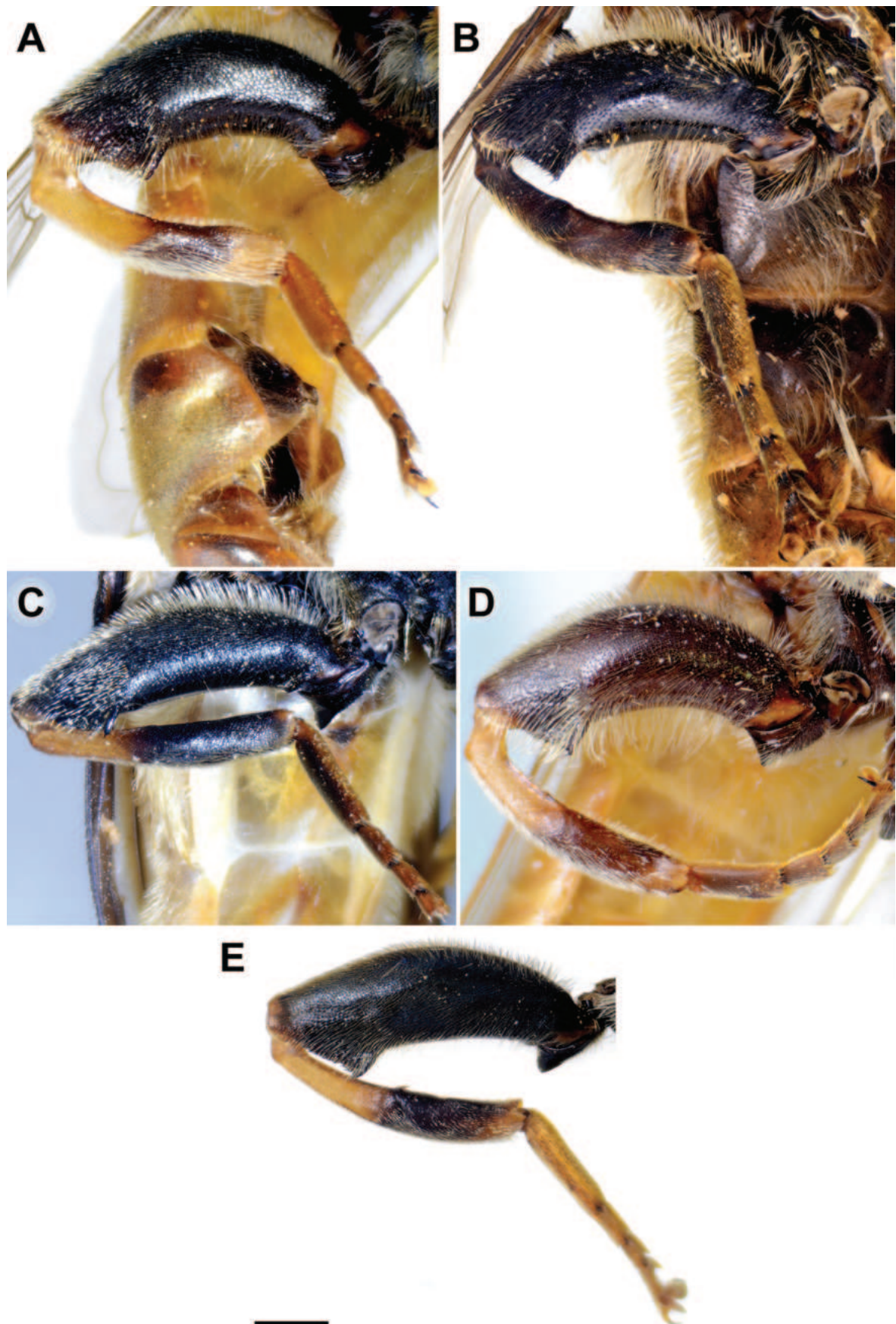


Figure 25. Metaleg of male, lateral view **A** *M. aequalis* sp. nov. **B** *M. cupreus* **C** *M. pruni* **D** *M. pallidus* **E** *M. obscurus*. Scale bar: 1 mm.

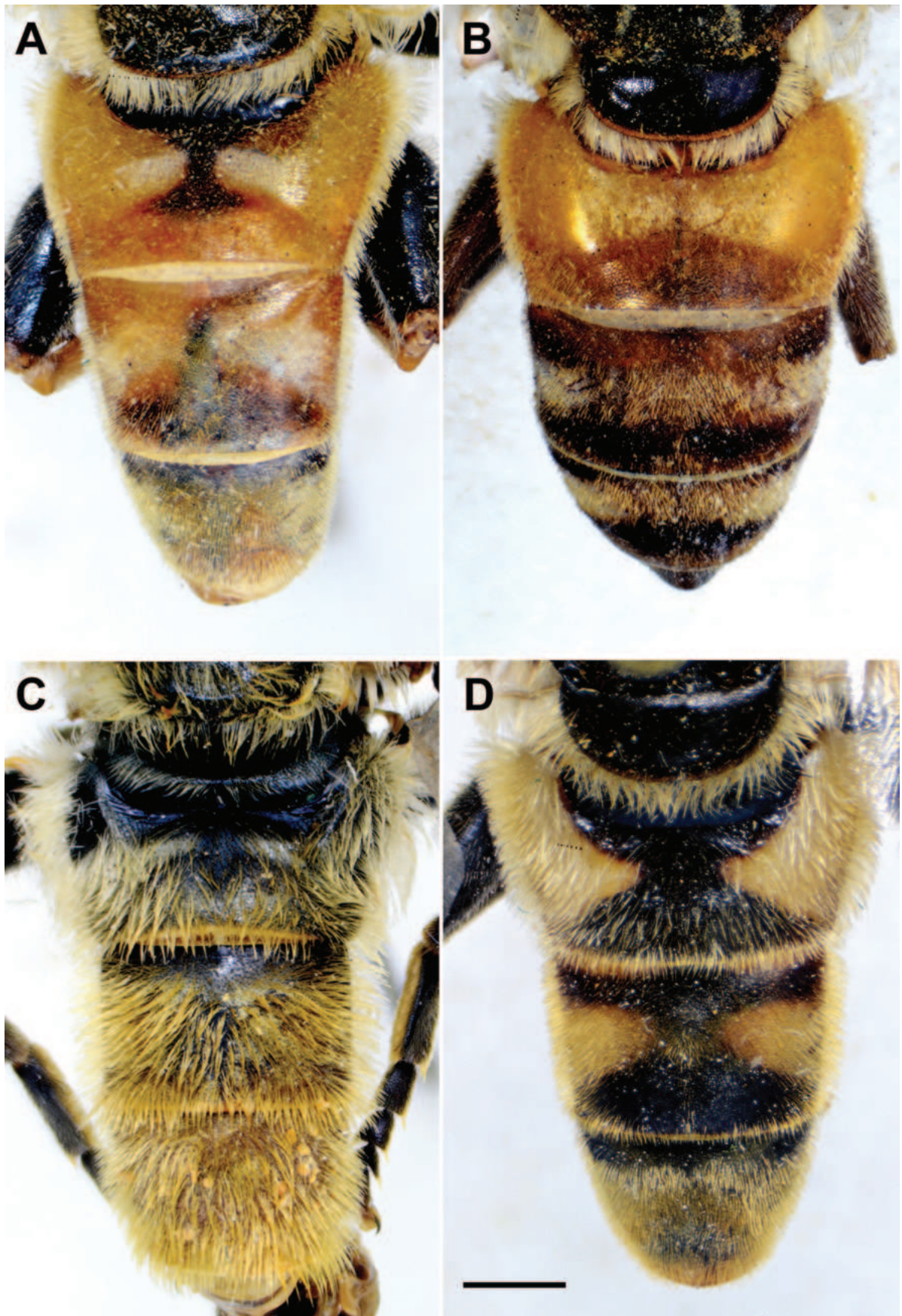


Figure 26. Abdomen, dorsal view **A, B** *M. aequalis* sp. nov. **C** *M. cupreus* **D** *M. pruni* **A, C–D** male **B** female. Scale bar: 1 mm.

endemism. The principal habitat of the species inside the hotspot is mountainous forest steppe, supporting oak-dominant (*Quercus* spp.) deciduous forests (CEPF 2022). Flight period: June/August. Developmental stages: not described.

***Merodon obscurus* Gil Collado, 1929, stat. rev.**

Merodon pruni var. *obscurus* Gil Collado, 1929: 407.

Type locality. MOROCCO (“Tanger”). *Merodon obscurus* was described as a variety of *M. pruni*. Holotype: male, Morocco, (MNCN) [specimen dry pinned]. Original label: [Tanger, Mz. Escalera / *M. pruni* var. *obscurus* Gil Tipo, Gil Collado det. / M.N.C.N. Madrid] (examined).

Notes. This species was listed as synonym of *Merodon pruni* by Peck (1988: 173) and Hurkmans (1993: 185). Based on our morphometry and molecular data, this is a valid taxon distributed in North West Africa, far from the range of *M. pruni* in the Eastern Mediterranean (Fig. 37).

Diagnosis. Sternum 3 with long, equally distributed pilosity (Fig. 30C). In male calcar at metatrochanter distinct (Fig. 25E); metafemur medium broad, ~ 5× longer than wide, with ventral margin slightly curved and covered with sparse pilosity ventrally (Fig. 25E); sternum 4 in Fig. 28C. Female with angular metatrochanter and sparse pile on metafemur ventrally (Fig. 31B). Male genitalia in Fig. 36. Similar to *Merodon pruni* except for the posterior surstylar lobe that is broader (~ 2.2× longer than wide) and more rounded apically (Fig. 36A: pl) (in *M. pruni* the posterior surstylar lobe is ~ 2.5× longer than wide and tapering to the tip; Fig. 29A: pl). *Merodon obscurus* stat. rev. occurs in North Africa, while *M. pruni* is an Eastern Mediterranean species (Fig. 37). Molecular and morphometric data clearly separated these two species (Figs 15, 16, 17, Suppl. material 3).

Distribution and biology. This species occurs in Algeria, Libya and Morocco (Fig. 37; Suppl. material 2). The preferred environment of *Merodon obscurus* stat. rev. includes sparsely-vegetated open ground and dry/semi-arid grassland with scattered tall herbs. Flowers visited: *Ferula*, *Foeniculum*. Flight period: April/September. Developmental stages: not described.

***Merodon pallidus* Macquart, 1842, stat. rev.**

Merodon pallidus Macquart, 1842: 70.

Type locality. Iraq (Baghdad). The original description was based on a single female specimen (holotype identified by Vockeroth in 1969, unpublished). The holotype is located in the Paris Museum (MNHN): female, Iraq, Baghdad, [specimen dry pinned]. Original labels: [No. 1187. / *Merodon* / *pallidus*] [label handwritten], [Bagdad] [label handwritten], [HOLOTYPE / Vockeroth ‘69’, ‘*Merodon pallidus* / Macquart 1842 / det. Vujčić 2008] [red label] (examined).

Notes. Peck (1988: 173) and Hurkmans (1993: 185) cited *Merodon pallidus* as a synonym of *M. pruni*. Hurkmans (1993: 185) designated a “lectotype” of *M. pallidus* based on incorrect interpretation of a male specimen from Baghdad deposited in an unknown collection. *Merodon pallidus* was described based on

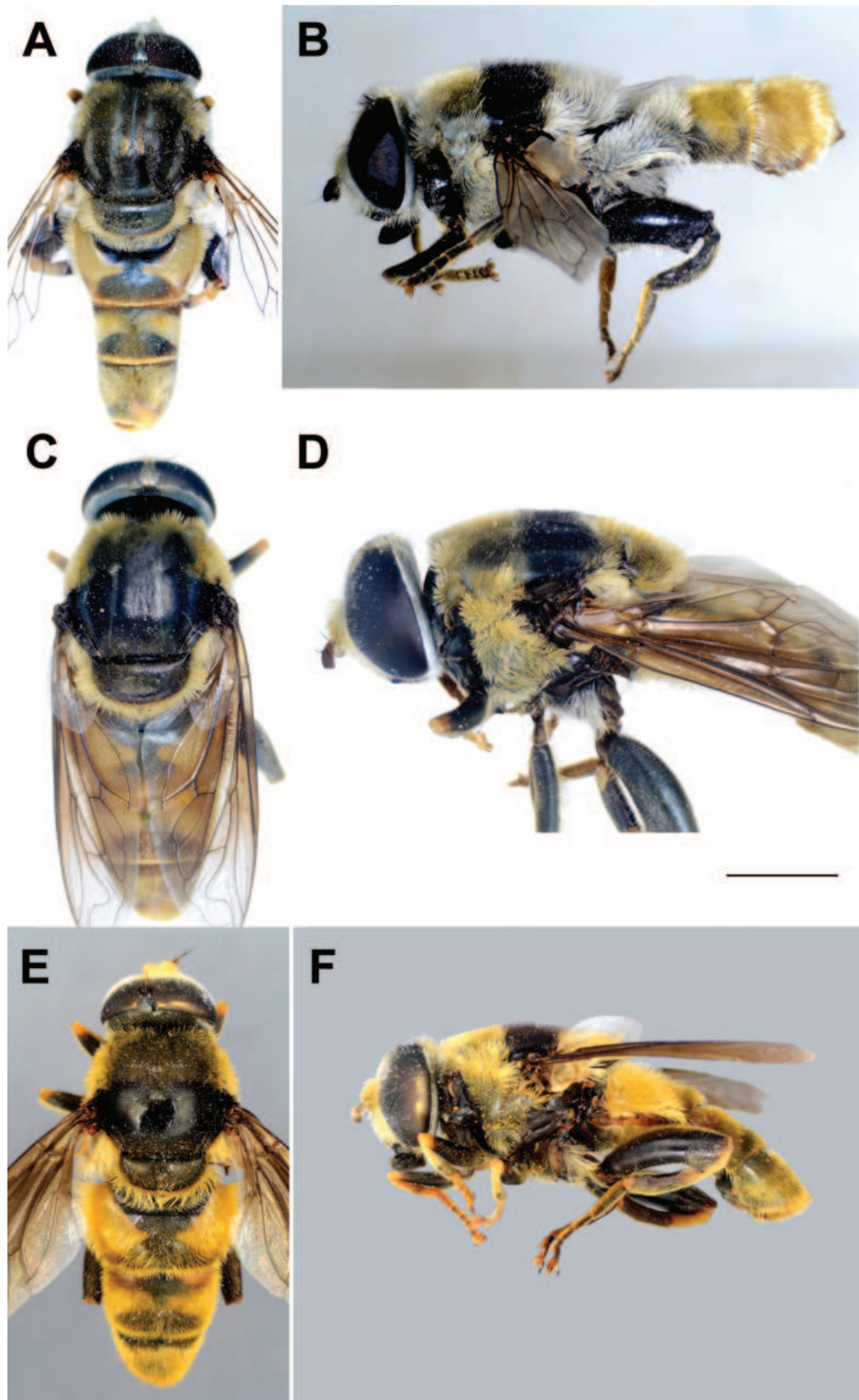


Figure 27. Body of male **A** *M. pallidus* **B** *M. cupreus* **C–D** *M. obscurus* **E, F** *M. pruni* **A, C, E** dorsal view **B, D, F** lateral view. Scale bar: 3 mm.

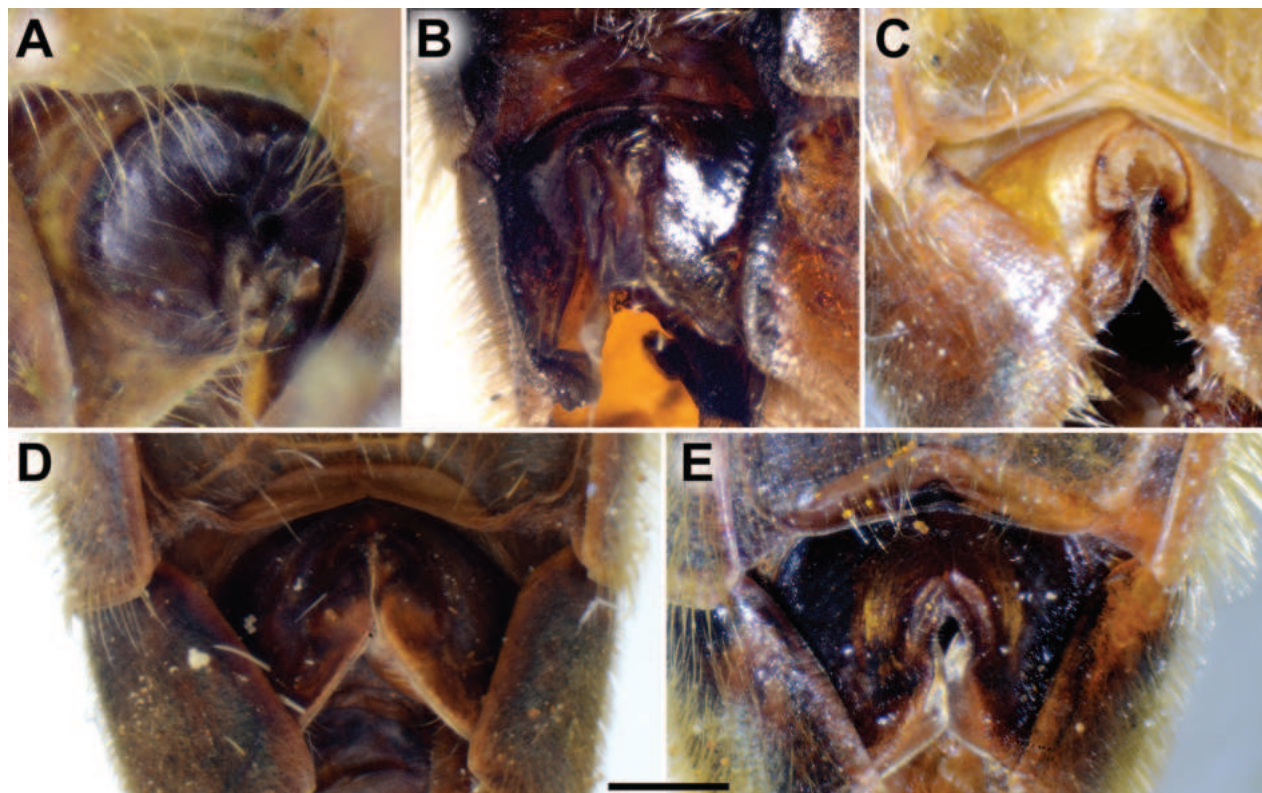


Figure 28. S4 of male, dorsal view **A** *M. aequalis* sp. nov. **B** *M. cupreus* **C** *M. obscurus* **D** *M. pallidus* **E** *M. pruni*. Abbreviations: al-anterior surstyliar lobe, c-cercus, l-lingula, pl-posterior surstyliar lobe. Scale bar: 1 mm.

one female and there are no indications that the specimen mentioned in Hurkmans (1993) belongs to the type material. A lectotype may be designated from syntypes (ICZN 1999), but Hurkmans “lectotype” was erroneously designated as the type. The identity of the Hurkmans “lectotype” could not be validated because this specimen is not located in any museum. Based on our assessment of morphological data, *M. pallidus* is a valid taxon, which we redefine herein. Based on our analysis of material belonging to distinct individuals collected from Iran, Israel, Pakistan, Palestine and Turkey (10 females, 7 males), the females are conspecific with the holotype of *M. pallidus*, so we re-describe the male herein.

Diagnosis. Sternum 3 with long and dense pile medially (Fig. 30D: marked with arrow). In male the metatrochanter has a less distinct calcar (Fig. 25D); metafemur broad (~ 3× longer than wide), strongly curved, covered with long and dense pilosity ventrally (Fig. 25D); sternum 4 in Fig. 28D. Female with angular metatrochanter and long and sparse pile on metafemur ventrally (Fig. 31C). Male genitalia in Fig. 38. Similar to *Merodon aequalis* sp. nov. from which differs by sternum 3 with an area of long pilosity medially (Fig. 30D: marked with arrow) (in *M. aequalis* sp. nov. sternum 3 has equally distributed pilosity of the same length; Fig. 30A); the shape of sternum 4 of male (Fig. 28D), which is slightly different in *M. aequalis* sp. nov. (Fig. 28A); and a distinct calcar on the metatrochanter of the male (Fig. 25D) and female with an angular metatrochanter (Fig. 31C) (in *M. aequalis* sp. nov. the calcar is almost absent in both sexes; Figs 25A, 31A).

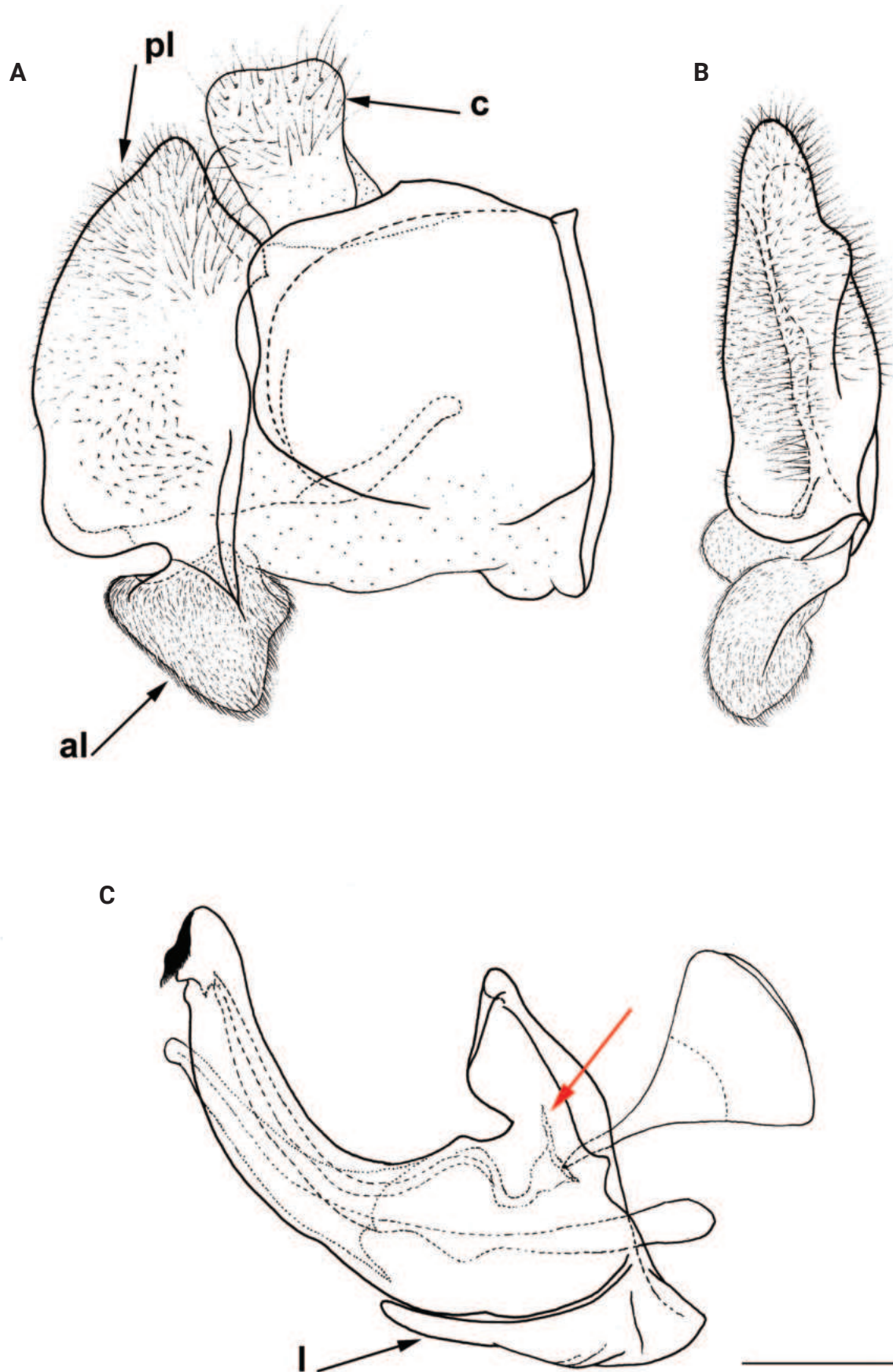


Figure 29. Male genitalia *M. pruni* **A, B** epandrium **C** hypandrium **A, C** lateral view **B** ventral view. Filamentous prolongation on ejaculatory sack marked with red arrow. Scale bar: 0.5 mm.

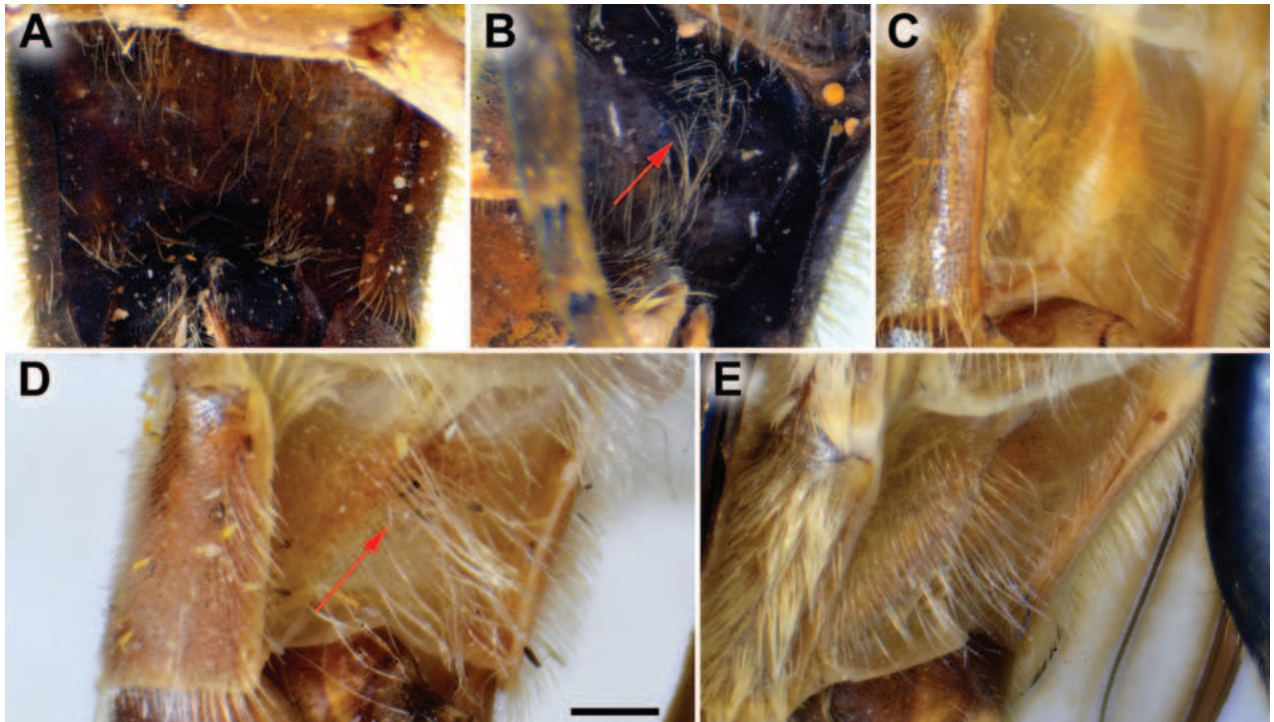


Figure 30. S3 of male, dorsolateral view **A** *M. aequalis* sp. nov. **B** *M. cupreus* **C** *M. obscurus* **D** *M. pallidus* **E** *M. pruni*. **B, D** area with distinct long pile marked with arrow. Scale bar: 1 mm.

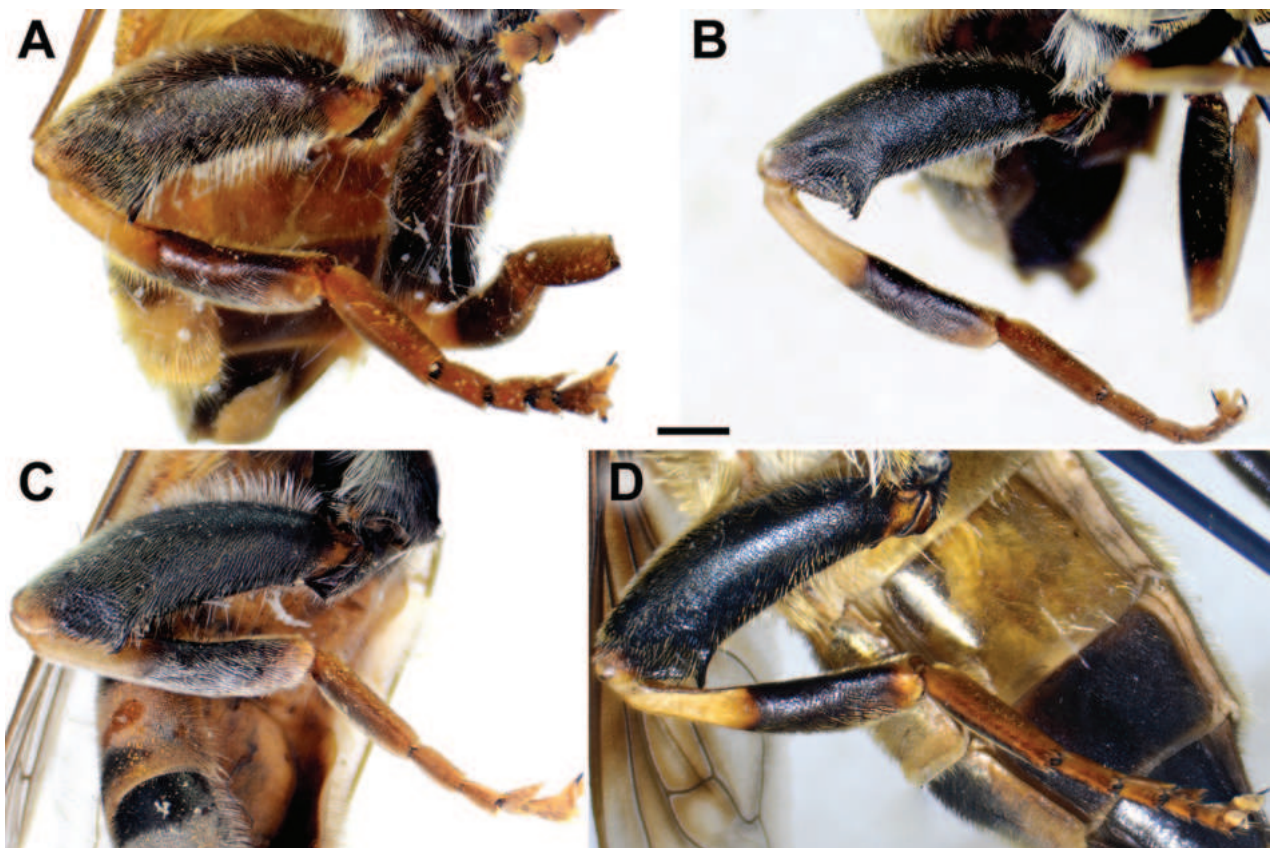


Figure 31. Metaleg of female, lateral view **A** *M. aequalis* sp. nov. **B** *M. obscurus* **C** *M. pallidus* **D** *M. pruni*. Scale bar: 1 mm.

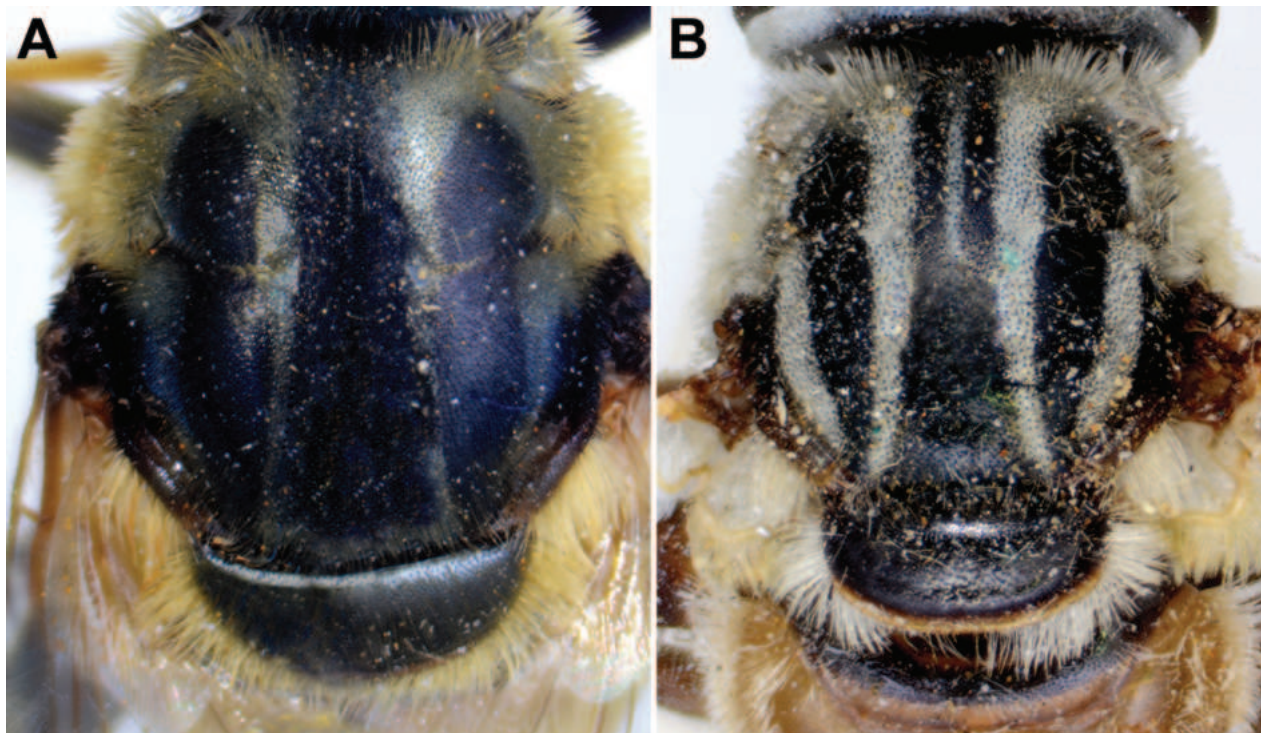


Figure 32. Thorax of *M. aequalis* sp. nov., dorsal view **A** male **B** female. Scale bar: 1 mm.

Re-description. Male. Head. Pedicel and scapus reddish yellow; basoflagellomere from reddish yellow to brown (Fig. 24C), short, oval, $\sim 1.3\times$ longer than wide, and $\sim 2\times$ longer than pedicel, concave dorsally; fossette large, dorsolateral; arista reddish to brown and thickened at basal third; arista $\sim 2.5\times$ longer than basoflagellomere; face and frons black, with dense whitish pollinosity; face covered with dense whitish pilosity; pile on frons yellow-whitish; oral margin shiny black, with sparse pollinosity; lunula reddish to brown, bare; eye contiguity ~ 12 facets long; vertical triangle isosceles, shiny, black, covered with grey-yellowish pilosity; ocellar triangle isosceles; occiput with grey-yellow to whitish pile, and grey pollinose; eyes covered with short, whitish grey pile.

Thorax. Scutum and scutellum black with brownish lustre, covered with short, greyish white pile; pilosity near wing bases mostly black; lateral sides of scutum covered with long, golden to the greyish white pile; scutum with five distinct pollinose vittae (Fig. 27A); posterior margin of scutellum with long pilosity; posterodorsal part of anterior anepisternum, posterior anepisternum (except anteroventral angle), anterior anepimeron, dorsomedial anepimeron, and posterodorsal and anteroventral parts of katepisternum with dense greyish white pile; wings mostly covered with microtrichia; wing veins yellowish to light brown; calypteres and halteres whitish yellow; angular calcar on metatrochanter distinct; femora black except yellowish apex; metafemur broad, $\sim 3\times$ longer than wide, covered with long whitish pilosity (Fig. 25D); tibiae yellow to reddish, except brown medial ring; tarsi yellowish red, in some specimens brown dorsally.

Abdomen. Elongated, $\sim 1.3\times$ longer than mesonotum; tergum 1 black, terga 2–4 usually reddish yellow, in some specimens medially partly black; terga with a pair of broad, distinct silver-grey pollinose fasciate maculae (Fig. 27A); pile

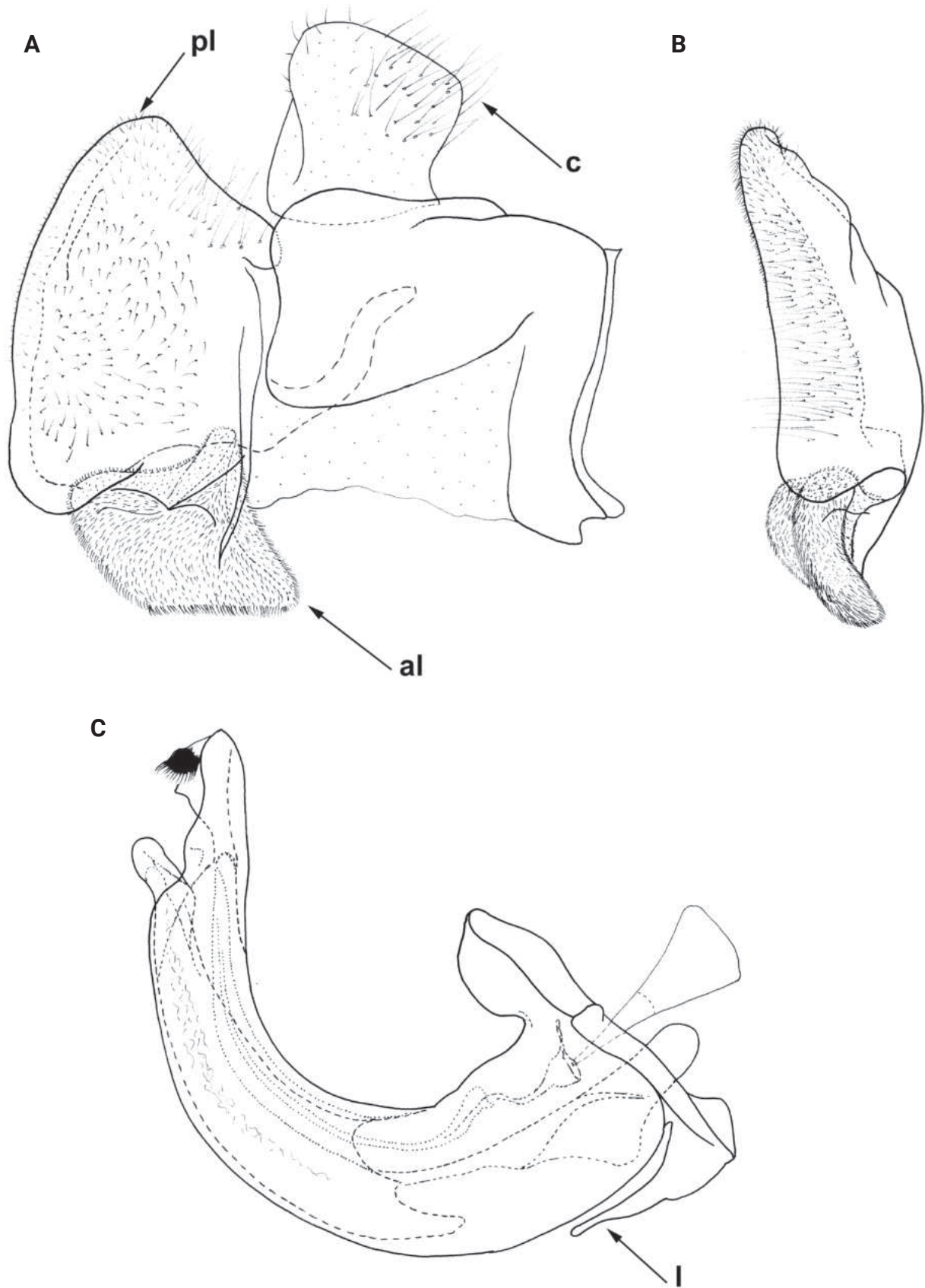


Figure 33. Male genitalia *M. aequalis* sp. nov. **A, B** epandrium **C** hypandrium. **A, C** lateral view **B** ventral view. Abbreviations: al-anterior surstylar lobe, c-cercus, l-lingula, pl-posterior surstylar lobe. Scale bar: 0.5 mm.

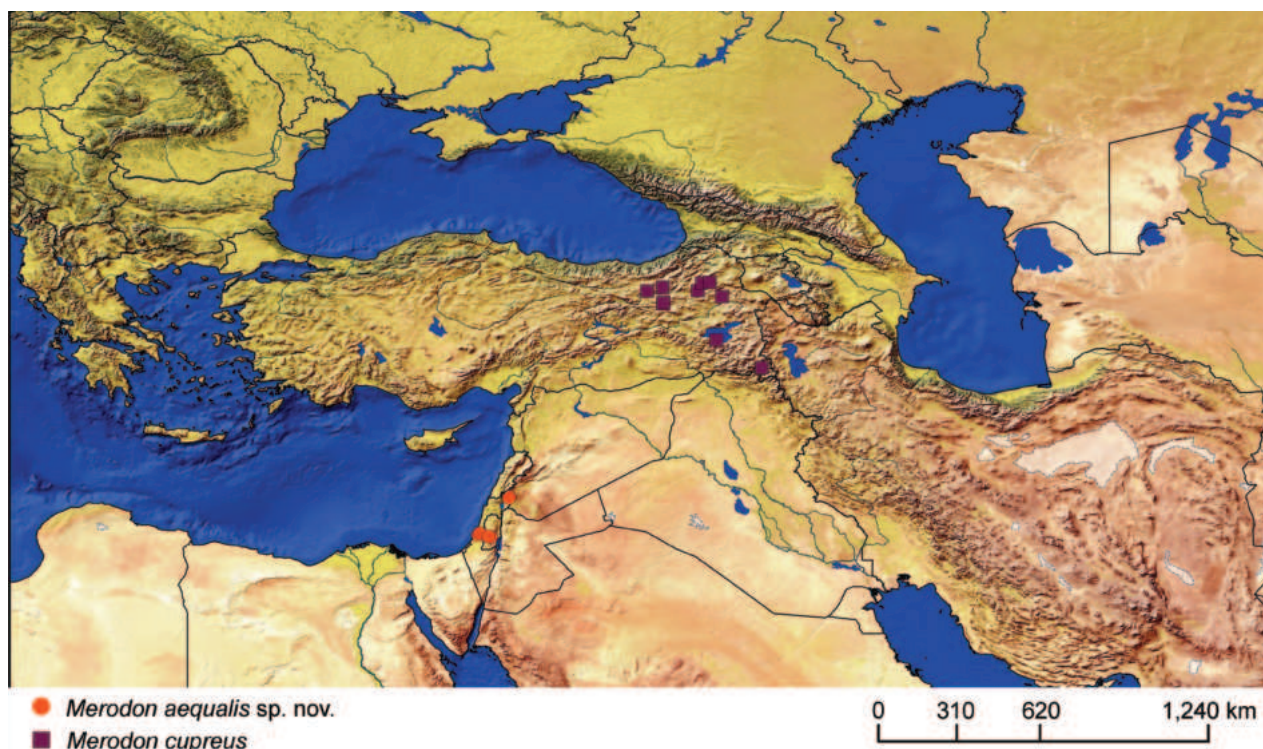


Figure 34. Distribution map of *Merodon aequalis* sp. nov. and *M. cupreus*.

on terga whitish, medially short, adpressed; sterna brown, covered with long, whitish pile; sternum 3 with an area of long pilosity medially (Fig. 30D: marked with arrow); posterior margin of sternum 4 with characteristic medial circular structure (Fig. 28D).

Male genitalia (Fig. 38). Anterior surstylar lobe triangular (Fig. 38A: al); posterior surstylar lobe large and broad (~ 2× longer than wide) (Fig. 38A: pl); cercus trapezoid (Fig. 38A: c); hypandrium sickle-shaped, without lateral projections; lingula long (Fig. 38C: l).

Female. Similar to the male except for normal sexual dimorphism and the following characteristics: frons covered with whitish pollinosity; scutum between wing bases with more black pilosity; metafemur narrower (~ 3.5× longer than wide), with ventral pilosity shorter than in male (Fig. 31C); terga 3 and 4 with short adpressed black pilosity medially on dark parts.

Distribution and biology. The species range includes Iran, Israel, Pakistan, the State of Palestine and Turkey (Fig. 39; Suppl. material 2). In Iran, it has been recorded within arid and semi-arid forest ecosystems where *Quercus brantii* is the dominant vegetation type (Azizi Jalilian et al. 2020) belonging to the Elburz range forest steppe ecoregion (Olson et al. 2001). The western part of the range of *Merodon pallidus* (Turkey, State of Palestine and Israel) belongs to the Eastern Mediterranean conifer-sclerophyllous-broadleaf forests ecoregions. The vegetation of this ecoregion includes maquis, coniferous forests of *Pinus halepensis* Mill. and *P. brutia* Ten., dry *Quercus* spp. woodlands and steppe formations (WWF 2022). In Pakistan, *M. pallidus* occurs in warm conifer/mixed forests (Siddiqui et al. 1999). Flight period: April/August. Developmental stages: not described.

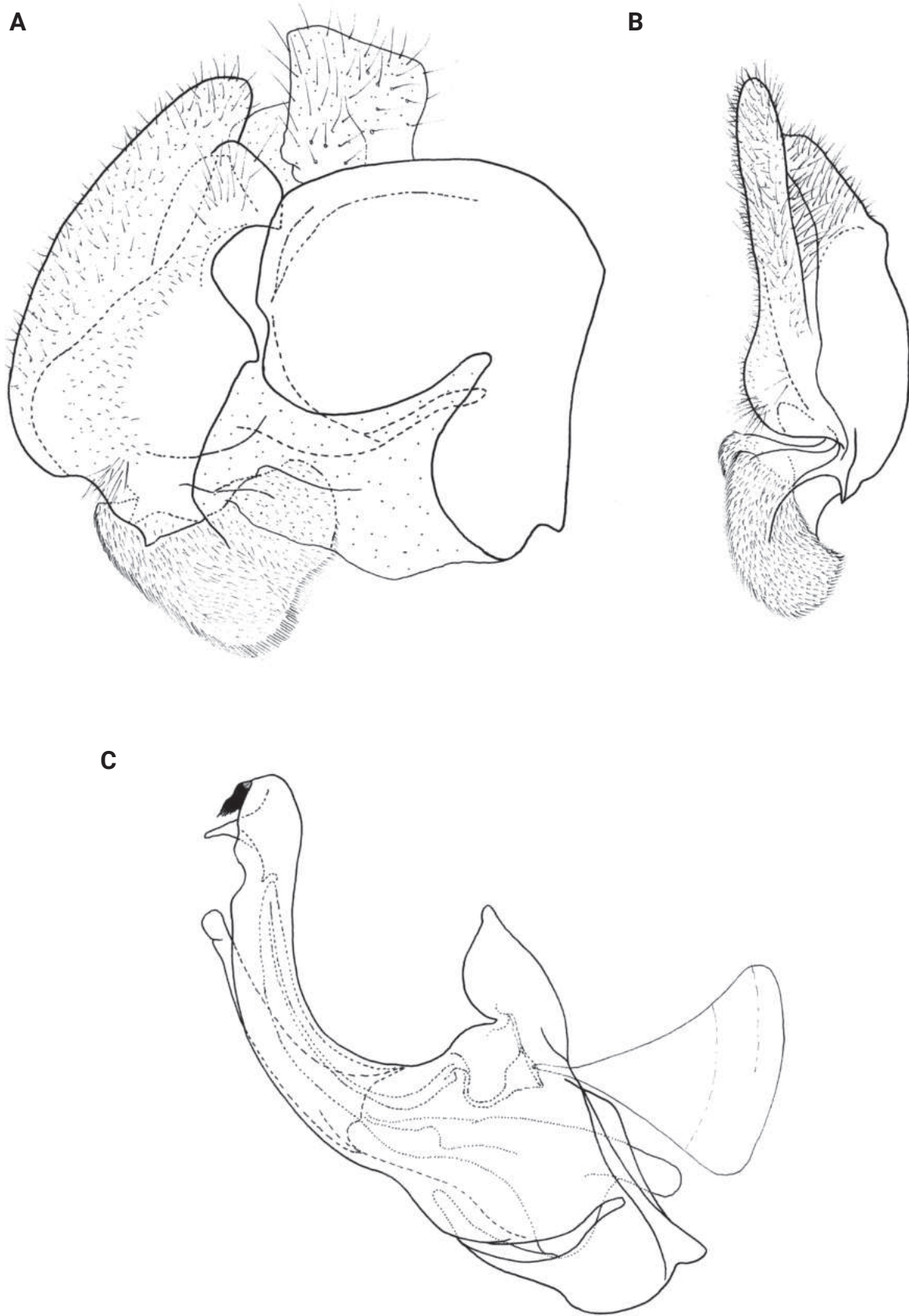


Figure 35. Male genitalia *M. cupreus* **A, B** epandrium **C** hypandrium **A, C** lateral view **B** ventral view. Scale bar: 0.5 mm.

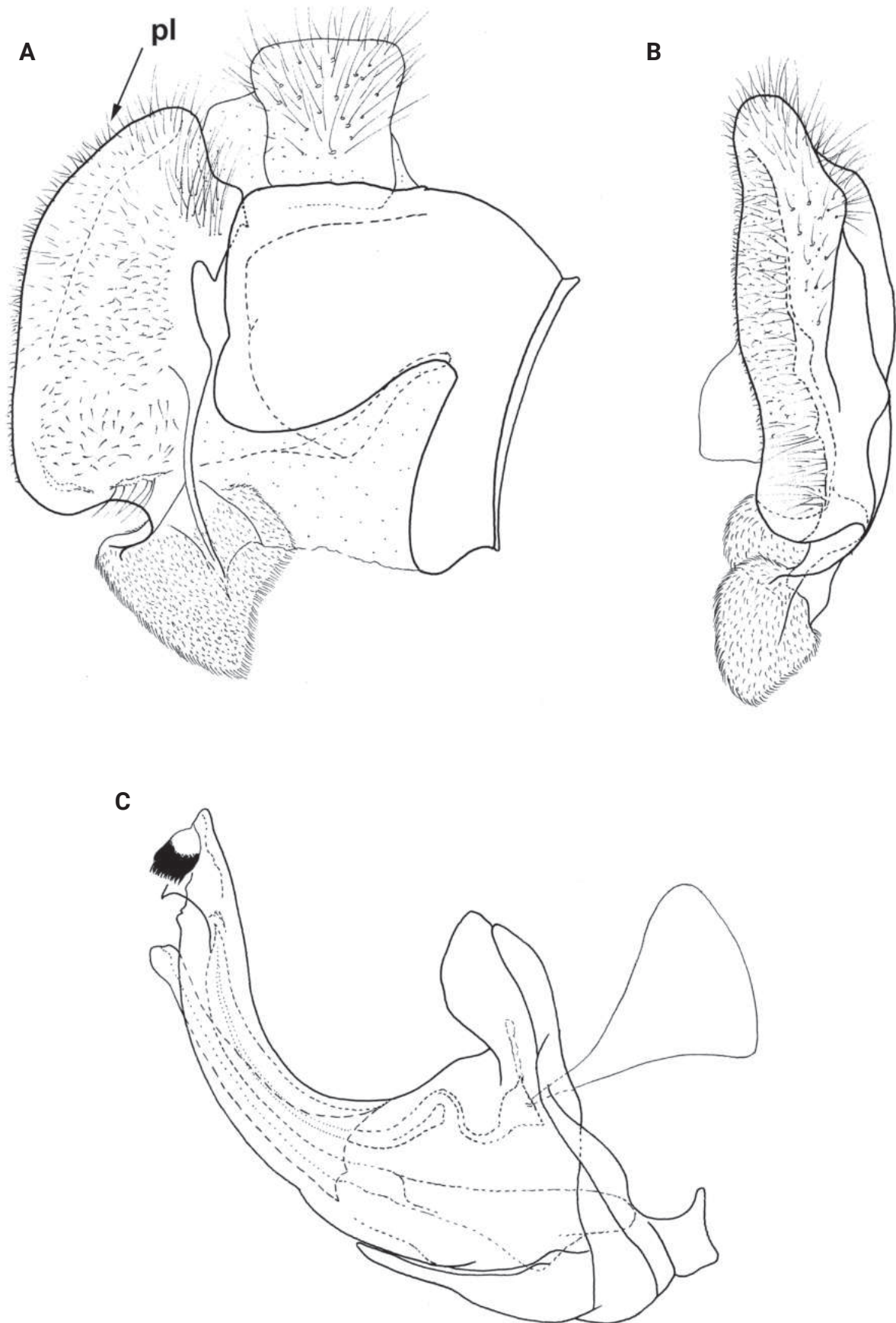


Figure 36. Male genitalia *M. obscurus* **A, B** epandrium **C** hypandrium **A, C** lateral view **B** ventral view. Abbreviations: pl-posterior surstylar lobe. Scale bar: 0.5 mm.

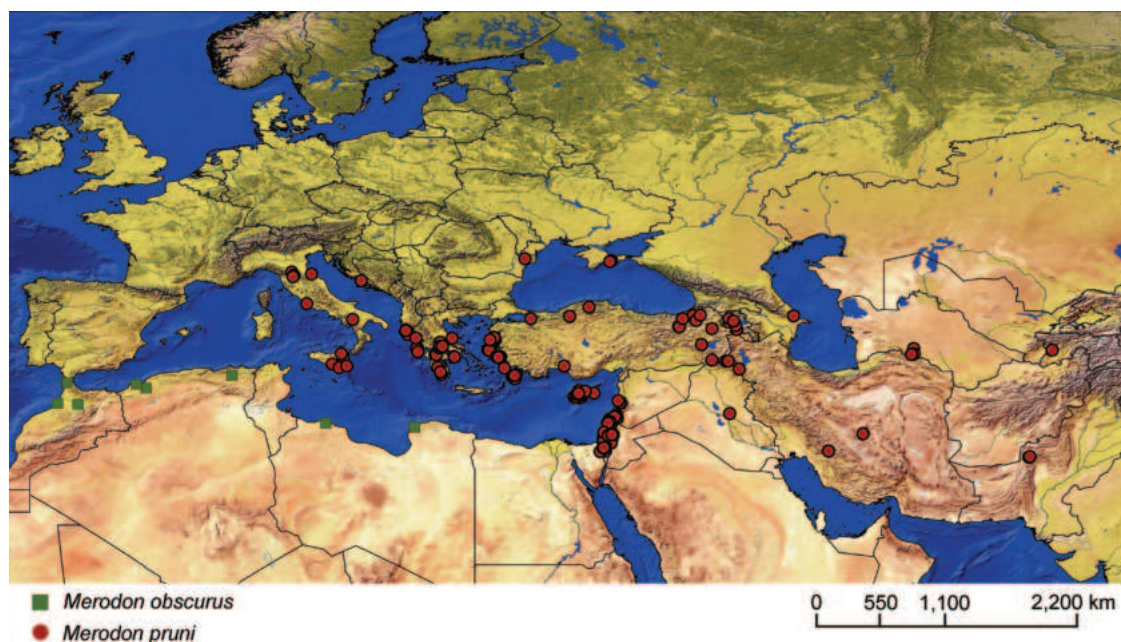


Figure 37. Distribution map of *Merodon pruni* and *M. obscurus*.

***Merodon pruni* (Rossi, 1790)**

Syrphus pruni Rossi, 1790: 293.

Merodon fulvus Macquart, 1834: 514.

Merodon sicanus Rondani, 1845: 258, 264.

Merodon fuscinervis Von Röder, 1887: 73.

***Syrphus pruni* Rossi, 1790: 293**

Type locality. ITALY (Toscana). The original description was based on an unspecified number of syntypes (Rossi 1790: 293). Type material could not be traced ‘in provinciis Florentina et Pisana’ [Firenze and Piza, Italy] [not located, not examined]. Based on the description and figure from the original publication (Rossi 1790), the identity of types is clear and fits the actual concept of species presented in Hurkmans (1993: 185). This species was cited in recent European publications (e. g. Speight 2020; Vujčić et al. 2021a).

***Merodon fulvus* Macquart, 1834: 514**

Type locality. FRANCE (“France méridionale”). Synonymy with *Merodon pruni* was cited in Sack (1931), Peck (1988: 172) and Hurkmans (1993: 185). Type material presumably lost.

***Merodon sicanus* Rondani, 1845: 258, 264**

Type locality. Italy, “Sicilia”. The original description was based on two female syntypes. One syntype was designated as a lectotype by Hurkmans (1993: 185): Original label [58] [number referring to the description of *Merodon sicanus* in the museum’s catalogue of Rondani collection]. This designation was based on syntype (examined) deposited in the LSF.

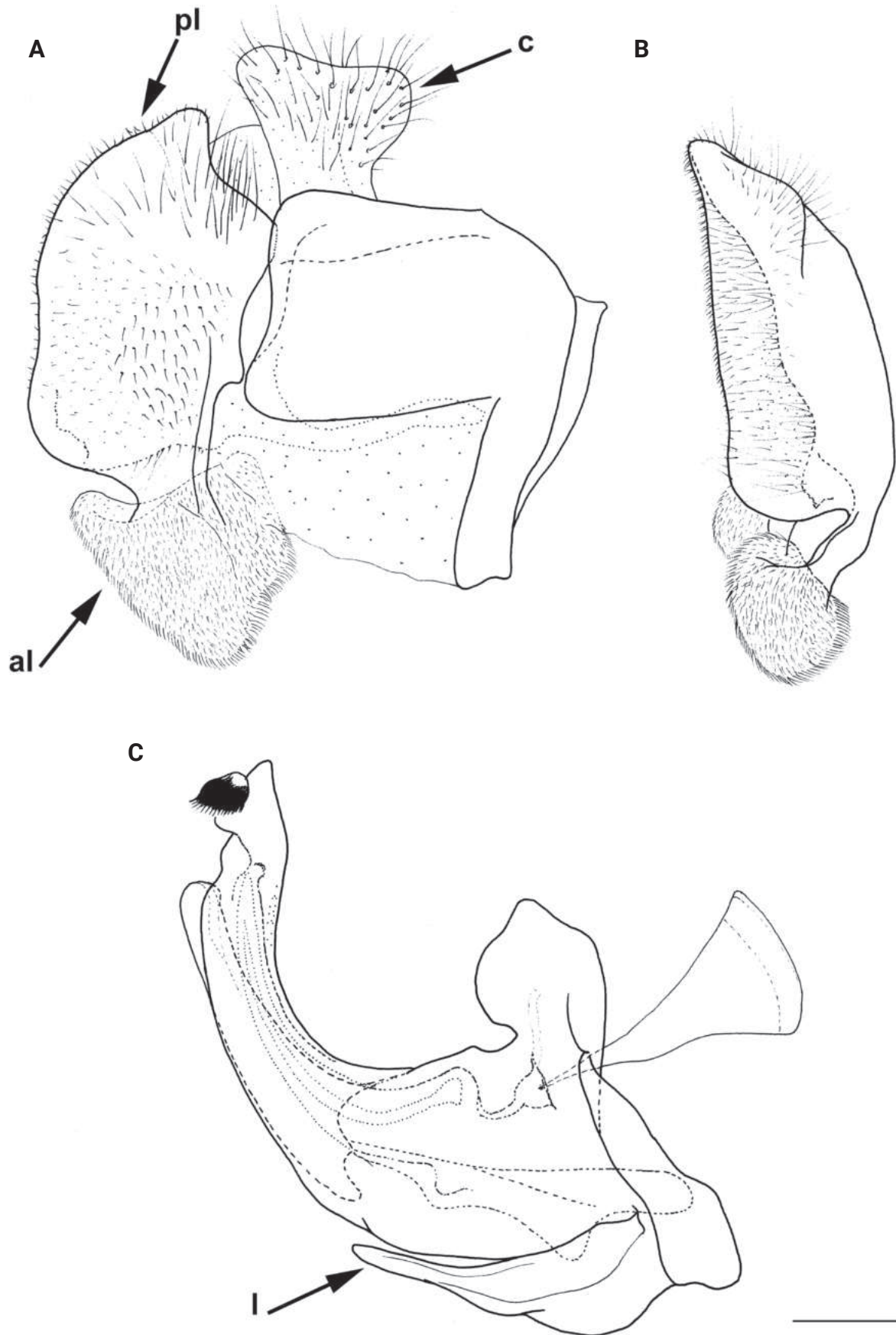


Figure 38. Male genitalia *M. pallidus* **A, B** epandrium **C** hypandrium **A, C** lateral view **B** ventral view. Abbreviations: al-anterior surstylar lobe, c-cercus, l-lingula, pl-posterior surstylar lobe. Scale bar: 0.5 mm.

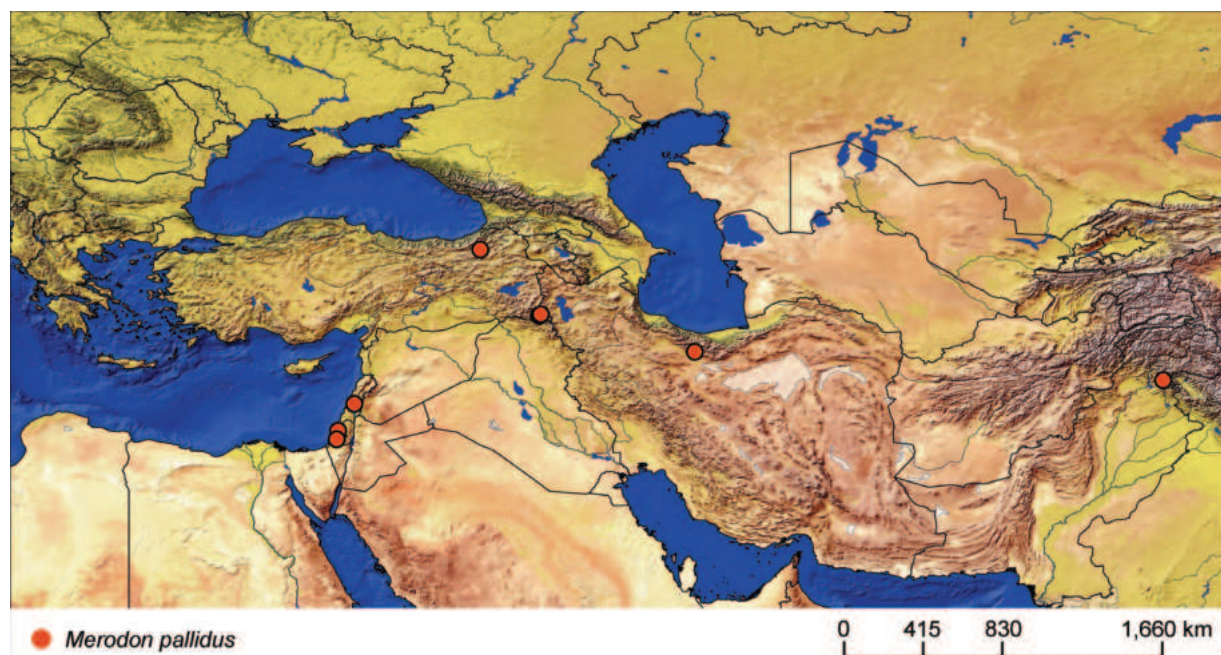


Figure 39. Distribution map of *Merodon pallidus*.

***Merodon fuscinervis* Von Röder, 1887: 73**

Type locality. GREECE (“Crete”). Synonymy with *Merodon pruni* was cited in Sack (1913), Peck (1988) and Hurkmans (1993). Type material presumably lost.

Diagnosis. Sternum 3 with more or less equally distributed pilosity (Fig. 30E). In male calcar at metatrochanter distinct (Fig. 25C); metafemur medium broad (~ 4.5× longer than wide), ventral margin slightly curved, and covered with sparse pilosity ventrally (Fig. 25C); sternum 4 in Fig. 28E. Female with angular metatrochanter and sparse pile on metafemur ventrally (Fig. 31D). Male genitalia in Fig. 29. Similar to *Merodon obscurus* stat. rev. from which differs by posterior surstylar lobe tapering to the tip (Fig. 29A: pl) (rounded apically in *M. obscurus* stat. rev.; Fig. 36A: pl) and its distribution in the Eastern Mediterranean (*M. obscurus* stat. rev. is restricted to North Africa).

Distribution and biology. It occurs throughout much of southern Europe (Italy, Croatia, Greece, Cyprus, Romania), eastwards to Ukraine, Turkey, Armenia, Azerbaijan, Iran, Iraq, Israel, State of Palestine, Lebanon, Pakistan, Turkmenistan, and Tajikistan. Hurkmans (1993) lists North Africa as part of the species range, but those specimens most likely belong to *Merodon obscurus*. Speight (2020) also mentions Austria and southern France (with the remark that it is most probably extinct), but species presence in those countries could not be confirmed (Fig. 37; Suppl. material 2). The preferred environment of species *M. pruni* is sparsely-vegetated open ground, dry/semi-arid grassland with scattered tall herbs, open areas in low-altitude *Abies cephalonica* forest on limestone, and *Castanea* forest (Speight 2020). At the northern edge of its range, i.e., in Ukraine, the species occurs in steppe habitats. Hurkmans (1985) provides some information on male territorial behaviour; also stating that females fly fast and very close to the ground and are much less noticeable than the males. Both sexes fly silently (Speight 2020). Flowers visited: *Ferula*, *Foeniculum*. Flight period: May/October, with peaks in May and September. Developmental stages: not described (Speight 2020).

Key for the *Merodon* species of the *pruni* species group

(The separation of females of *Merodon pruni* and *M. obscurus* is uncertain based on morphological characters, but it can be done based on molecular and morphometric data and by the geographic range)

- 1 Bumble bee mimic species (Fig. 27B) with pile on scutum longer than basoflagellomere; tergum 2 black (Fig. 26C); mesonotum with whitish pile, except broad black-pilose fascia between wing bases (Fig. 27B); tergum 2 with whitish pile; terga 3 and 4 covered with yellow to reddish pilosity (Fig. 26C); legs black; calcar on metatrochanter distinct (Fig. 25B); metafemur curved, covered with long, dense pilosity (Fig. 25B); sternum 3 medially with distinct pilosity; sternum 4 as in Fig. 28B ***Merodon cupreus* Hurkmans, 1993**
 - Species with shorter body pilosity; pile on scutum shorter than basoflagellomere; tergum 2 mostly reddish.....**2**
- 2 Metafemur with sparse ventral pilosity (as in Fig. 25C) **4**
 - Metafemur with long and dense ventral pilosity (as in Fig. 25D).....**3**
- 3 Sternum 3 medially with equally distributed pilosity (Fig. 30A); sternum 4 of male in Fig. 28A; calcar on metatrochanter in male small, almost absent (Fig. 25A); in female metatrochanter rounded (Fig. 31A).....
 - ***Merodon aequalis* sp. nov.**
 - Sternum 3 with area of long pilosity medially (Fig. 30D: marked with arrow); sternum 4 of male in Fig. 28D; calcar on metatrochanter in male distinct (Fig. 25D); in female metatrochanter angular (Fig. 31C).....
 - ***Merodon pallidus* Macquart, 1842, stat. rev.**
- 4 Posterior surstylar lobe tapering to the tip (Fig. 29A: pl); distribution: Eastern Mediterranean ***Merodon pruni* (Rossi, 1790)**
 - Posterior surstylar lobe more rounded apically (Fig. 36A: pl): distribution: North Africa ***Merodon obscurus* Gil Collado, 1929, stat. rev.**

Molecular analyses

The molecular analyses of the two studied *Merodon* species groups involved 72 nucleotide sequences in total including outgroups. We studied the dataset of the concatenated 3' and 5' fragments of the COI gene which comprised a total of 1273 characters (612 nucleotide positions of 5'-end fragment of COI gene and 661 of 3'-end fragment of this gene), of which 336 were parsimony informative. All positions containing missing data were excluded from the analysis. In the analyses, we involved the representatives of previously described *Merodon* lineages by Vujčić et al. (2021a). All five lineages clearly resolved as clades on both obtained trees, Maximum Parsimony (Fig. 15) and Maximum Likelihood (Suppl. material 3): *natans* (with bootstrap value MP = 98, ML = 99), *albifrons* (MP = 91, ML = 98), *desuturinus* (MP = 78, ML = 83), *aureus* (MP = 99, ML = 98), and *avidus-nigritarsis* lineage (MP = 79, ML = 96). Within *M. avidus-nigritarsis* lineage, both analysed species groups resolved as monophyletic with high bootstrap support (MP = 100 and ML = 99 for both groups). Comparing MP and ML trees, applied methods resulted in similar tree topologies within analysed species groups, with slight differences in bootstrap values. Within *clavipes* group samples from Spain clearly separated (with bootstrap support MP = 80 and ML = 94) from the other analysed species of the group (*M. clavipes* and

M. velox). This confirms the existence of additional new species of the group, named *M. latens* sp. nov. *Merodon obscurus* is proved to be valid species and is resolved in a separated clade within the *pruni* species group with 99 bootstrap support value on the two inferred trees, and clearly distinct from *M. pruni*.

Geometric morphometrics

Our species-based discriminant analysis (DA) provided evidence for highly significant wing shape differences among all species pairs (Table 1). Additionally, cross-validation of that analysis based on wing shape revealed highly accurate species assignment (95.4%). Of 87 specimens, only four were misclassified: one *Merodon obscurus* as *M. pruni*, two *M. latens* sp. nov. as *M. clavipes* and one *M. clavipes* as *M. latens* sp. nov. All specimens of *pruni* species group were correctly classified. We obtained a congruent classification based on the Gaussian naive Bayes classifier, with two *M. obscurus* misclassified as *M. pruni*, one *M. latens* sp. nov. as *M. clavipes* and two *M. clavipes* as *M. latens* sp. nov.

The species-based CVA conducted on wing shape parameters generated three highly significant canonical axes (CV1: Wilks' = 0.01199, $\chi^2 = 331.7617$, $p < .01$; CV2: Wilks' = 0.27443, $\chi^2 = 96.9786$, $p < .01$; CV3: Wilks' = 0.54099, $\chi^2 = 46.0769$, $p < .01$). The first canonical axis represents the majority of wing shape variation (92%) and clearly differentiates the *clavipes* and *pruni* groups (Fig. 16A, B). The second and third axes reflect intra-group variability and they clearly differentiated species *M. latens* sp. nov. from *M. clavipes* and *M. obscurus* from *M. pruni* (Fig. 16A, B). The same pattern of wing shape similarity was depicted in the phenogram based on squared Mahalanobis distances (Fig. 16C).

Pairwise differences in average wing shape were visualised for species within the groups using superimposed outline drawings (Fig. 16D). Differences inside the *clavipes* group were attributable to displacements of all landmarks. In contrast, differences between species *M. pruni* and *M. obscurus* were associated with highly prominent landmark displacements in central and distal parts of their wings (Fig. 16D).

Population-level geometric morphometrics analysis

Our population-based DA generated an overall correct classification of 89.8% for the specimens. All *Merodon obscurus* were correctly classified, whereas all misclassified specimens of *M. pruni* (4 out of 40) were assigned to conspecific populations. Regarding *M. latens* sp. nov., only two specimens out of ten were misclassified as *M. clavipes* from Rhodope, Greece. All specimens of *M. clavipes* were correctly classified.

Our population-based CVA produced four significant CV axes, from which the first three were informative in species delimitation. The first CV axis describes differences in wing shape between the *clavipes* and *pruni* species groups (Fig. 17A, B). Moreover, CV1 indicated wing shape differences between species *M. latens* sp. nov. and *M. clavipes* from Rhodope, Greece (Fig. 17A). CV2, representing 8% of total shape variation, clearly separated *M. pruni* populations from *M. obscurus* (Fig. 17A). This axis also clearly separated *M. clavipes* specimens from Crete, Greece, from both *M. clavipes* specimens from Rhodope, Greece

and *M. latens* sp. nov. (Fig. 17A). The third axis, representing 3% of total shape variation, separated species in the *clavipes* group (Fig. 17B).

We used a UPGMA phenogram constructed from squared Mahalanobis distances to summarise differences in wing shape among the investigated populations (Fig. 17C). The resulting phenogram revealed two main clusters, one for the *clavipes* group and another for the *pruni* group (Fig. 17C). All conspecific populations were grouped within their respective cluster.

Discussion

Systematics and taxonomy

The *clavipes* and *pruni* species groups comprise large hoverfly species, indeed the largest in size of the *avidus-nigritarsis* lineage. Bumble bee-like taxa from the *clavipes* group are characterised by their long body pilosity and elongated basoflagellomere (> 2× longer than wide), contrasting with the short body pilosity and short basoflagellomere (approximately as long as wide) of species in the *pruni* group. The nominal species of this latter group, *M. pruni*, is covered with very short pile, although one group representative (*M. cupreus*) exhibits an extremely similar appearance to the bumble bee-like species of the *clavipes* group. Representatives of both groups possess varying structures of the basoflagellomere and male genitalia, especially in terms of the shape of the surstylar lobe, which is characteristic for each group. In our molecular study, these two groups clearly resolved as being monophyletic within the *avidus-nigritarsis* lineage, with high bootstrap support for monophyly using both methodologies (MP = 100 and ML = 99).

The *clavipes* group includes four species previously described (*M. clavipes*, *M. quadrinotatus*, *M. vandergooti* and *M. velox*), as well as three species recognised herein. Two of those latter species are described based on newly discovered material held in different museum collections (*M. aenigmaticus* sp. nov. and *M. rufofemoris* sp. nov.). Discovery of the third species, *M. latens* sp. nov., is attributable to the integrative taxonomic approach we applied. Previous indications of the potential existence of divergent species on the Iberian Peninsula based on minor morphological differences among Iberian populations previously identified as *M. clavipes* are supported by our molecular and geometric morphometrics analyses. We also confirm the validity of *M. latens* sp. nov. as a new species through our combined morphological, molecular and geometric morphometrics analyses. Based on our analysis of the COI gene, *M. latens* sp. nov. is clearly different from the other two analysed species of the *clavipes* species group (i.e., *M. clavipes* and *M. velox*), as illustrated in both the Maximum-Parsimony and Maximum-Likelihood trees. This Iberian endemic displays a significantly different wing shape from *M. clavipes*, both in terms of species and population analyses. As revealed by many previous integrative hoverfly studies, wing shape is a reliable character for cryptic and sibling species delimitation. The strength of wing shape as a taxonomic character lies in its strong heritability (Moraes et al. 2004), with previous wing shape analyses proving concordant with molecular data (Vujčić et al. 2013b, 2020a; Ačanski et al. 2016; Šašić et al. 2016; Radenković et al. 2018b; Kočič Tubić et al. 2018; Chroni et al. 2018). Here, the high percentage of correct classification for specimens of *M. latens* sp. nov. and *M. clavipes* again validate that wing shape is a

reliable diagnostic character for species assignment. Importantly, differences in the morphological characters used to formulate the key presented herein enable proper identification of all species from the *clavipes* group.

The *pruni* species group comprises two well-known species (*M. cupreus* and *M. pruni*), one new species (*Merodon aequalis* sp. nov.), and a previously described taxon, whose status has now been revised. Classically, *M. pallidus* was considered a synonym of *M. pruni*. This species was described based on the female holotype discovered during our research in the Paris Museum. Based on newly found specimens from different collections conspecific with the type, we characterised morphological traits that confirmed the status of *M. pallidus* stat. rev. as a valid independent taxon, redefined herein. *Merodon obscurus* was described as a variety of *M. pruni*, and synonymy with *M. pruni* was cited in recent literature. Based on the results of our morphological, molecular and geometric morphometrics analyses, *M. obscurus* stat. rev. represents an independent taxon distributed in North West Africa, i.e., far from the Eastern Mediterranean range of *M. pruni*. Moreover, our integrative taxonomic approach successfully resolved the taxonomic status of *M. obscurus*. Both our MP- and ML-based molecular analyses clearly resolved specimens of *M. obscurus* as a separate clade, with strong bootstrap support (99) distinguishing it from species *M. pruni*. Furthermore, our geometric morphometric analysis successfully separated *M. pruni* from *M. obscurus* based on wing shape, both in our species and population analyses. The accurate classification success rate for *M. obscurus* specimens further supports their distinctiveness, with only one specimen of *M. obscurus* being misclassified.

Distribution

The two species groups we have examined herein, *clavipes* and *pruni*, have partially overlapping distributions. Both groups have diversified across the Mediterranean Basin. Several *Merodon* groups display similar patterns. For example, the *avidus* complex and the *natans* group are widespread in the Mediterranean Basin, but also have representatives on the Iberian Peninsula and in North Africa. Both those taxonomic clusters were the subject of recent integrative analyses and, as in our study, wing shape and molecular data successfully revealed their hidden diversity (Ačanski et al. 2016; Vujčić et al. 2021c). Ačanski et al. (2016) deduced their diversification processes, likely a response to repeated isolation in parts of the Mediterranean Basin during glacial-interglacial cycles (Hewitt 1999, 2001; Konstantinov et al. 2009). Later, the Pyrenees probably acted as a geographical barrier to prevent dispersal of *M. obscurus* stat. rev. and *M. latens* sp. nov. to other European areas.

In the case of both species groups, nominal species (i.e., *Merodon clavipes* and *M. pruni*) display the most widespread distributions; – that of *clavipes* group stretches from France throughout most of central and southern Europe to Ukraine, south Russia and Turkey, while *pruni* group occupies most of southern Europe through to Ukraine and Turkey and extending further eastwards into Tajikistan and Pakistan. Looking closely at species distributional patterns, it is evident that the range of species in the *pruni* group is slightly more easterly than that of the *clavipes* group. In fact, only species *M. pruni* occurs in Europe, and all other species in the *pruni* group primarily occur in the Middle East and Central Asia. Furthermore, species *M. obscurus* stat. rev. occurs in North Africa,

making it the only species in the two groups that is distributed here. *Merodon cupreus* and *M. aequalis* sp. nov. display the narrowest distributions of all species belonging to the *pruni* group, with *M. cupreus* only occurring in the eastern part of Turkey and *M. aequalis* sp. nov. being restricted to a few localities in Israel and the State of Palestine.

Regarding the *clavipes* group, the respective ranges of three out of its seven species include at least part of Europe. One of those three species (*M. latens* sp. nov.) is restricted to the Iberian Peninsula, whereas the other two (*M. clavipes* and *M. velox*) occur across central and southern Europe. The ranges of the other species in the *clavipes* group (*M. rufofemoris* sp. nov., *M. quadrinotatus* and *M. vandergooti*) are somewhat restricted to the Middle East and Central Asia. The distribution of *M. aenigmaticus* sp. nov. is puzzling, as the name suggests, but based on the distribution of its two closely related species (*Merodon rufofemoris* sp. nov. and *M. vandergooti*, distributed in Turkey and Iran), it is likely to be in the Middle East.

The fact that the distributions of the two species groups studied herein overlap in the Mediterranean Basin centres on the fact that this region represents one of the world's 25 biodiversity hotspots (Myers et al. 2000). More specifically, this region serves as a centre of *Merodon* diversity (Vujčić et al. 2012) probably due to its high diversity of bulbous plant species, which proved to be host plants for known larval stages (Andrić et al. 2014; Ricarte et al. 2017; Preradović et al. 2018). Unfortunately, host plant(s) for species of *pruni* group and *clavipes* group are still unknown and immature stages undescribed. Turkey displays the highest species diversity for both species groups assessed herein, hosting three of five *pruni*-group species and four of seven *clavipes*-group species, confirming its status as having the greatest diversity and endemism of the genus *Merodon* in the Mediterranean Basin (Vujčić et al. 2015). Although the Middle East and Central Asia appears to be less diverse and species-rich, greater research effort focused on these regions in recent years has highlighted the prevalence of *Merodon* species there (Vujčić et al. 2013a; Vujčić et al. 2019; Likov et al. 2020).

Conclusions

Our revision of two closely-related *Merodon* species groups from the *avidus-nigritarsis* lineage, i.e., *pruni* and *clavipes*, uncovers four new species (*M. aenigmaticus* sp. nov., *M. aequalis* sp. nov., *M. latens* sp. nov. and *M. rufofemoris* sp. nov.) and confirms the status of six previously well-known species. In addition, we redescribe *M. pallidus* stat. rev., re-instating it as a valid species from synonymy with *Merodon pruni*. The integrative taxonomic approach we adopted again demonstrated its power in resolving hoverfly taxonomy. A combination of morphological, molecular and geometric morphometric analyses revealed the divergence between *M. latens* sp. nov. and *M. clavipes*, as well as *M. obscurus* stat. rev. and *M. pruni*. The two studied species groups display partially overlapping distributions, albeit with that of the *pruni* group being slightly more eastward relative to that of the *clavipes* group. The Anatolian Peninsula hosts three of the five *pruni*-group species and four of the seven *clavipes*-group species, representing the area with the highest *Merodon* diversity and endemism across the Mediterranean Basin, Middle East and Central Asia.

Acknowledgements

The linguistic revision was carried out by John O' Brian. We sincerely thank Yevhen V. Rutjan (Kyiv, Ukraine), Volodymyr L. Perepetchayenko, Olexander I. Gubin (Donetsk, Ukraine), Denis G. Kasatkin (Rostov-on-Don, Russia), Axel Ssymank (Bonn, Germany), and Gunilla Ståhls (Helsinki, Finland) for the material loaned for the study. We are very grateful to Valery O. Korneyev (Kyiv, Ukraine) and Neal L. Evenhuis (Honolulu, USA) for fruitful discussions on the dating of Serhiy Ya. Paramonov's publications and for valuable comments during our work. We are also grateful to Mark G. Kalashyan (Yerevan) for searching and researching specimens from the Paramonov's collection at the IZY.

Additional information

Conflict of interest

The authors have declared that no competing interests exist.

Ethical statement

No ethical statement was reported.

Funding

This study was financially supported by the Ministry of Science, Technological Development and Innovation of the Republic of Serbia (Grant No. 451-03-66/2024-03/200125 and Grant No. 451-03-66/2024-03/200358), the Science Fund of the Republic of Serbia, #GRANT No 7737504, project Serbian Pollinator Advice Strategy - for the next normal - SPAS, and H2020 Project "ANTARES" (Grant agreement ID: 739570, <https://doi.org/10.3030/739570>).

Author contributions

Ante Vujić, Snežana Radenković and Nataša Kočiš Tubić conceived and designed the study; all authors performed the data analyses and took part in a draft preparation: Ante Vujić, Snežana Radenković, Grigory Popov and Laura Likov did the descriptions and produced the figures; Mihajla Djan and Nataša Kočiš Tubić performed the molecular analyses; Marina Janković Milosavljević was engaged in distribution; Jelena Ačanski was in charge for geometric morphometric analysis; while Ebrahim Gilasian and Grigory Popov contributed also to taxonomic discussions during preparation of the paper and participated in critical revision of the manuscript. All authors read, commented on, and approved the final version of the manuscript.

Author ORCIDs

Ante Vujić  <https://orcid.org/0000-0002-8819-8079>

Snežana Radenković  <https://orcid.org/0000-0002-7805-9614>

Laura Likov  <https://orcid.org/0000-0002-7215-1006>

Nataša Kočiš Tubić  <https://orcid.org/0000-0002-6077-7378>

Grigory Popov  <https://orcid.org/0000-0002-2519-1937>

Mihajla Djan  <https://orcid.org/0000-0002-2427-0676>

Marina Janković Milosavljević  <https://orcid.org/0000-0002-2136-815X>

Jelena Ačanski  <https://orcid.org/0000-0003-1745-6410>

Data availability

The data that support this study are available in the article and accompanying online Supplementary information. Nucleotide sequence data that support this study are available in GenBank at <https://www.ncbi.nlm.nih.gov/genbank/>.

References

- Ačanski J, Vujčić A, Djan M, Obreht-Vidaković D, Ståhls G, Radenković S (2016) Defining species boundaries in the *Merodon avidus* complex (Diptera, Syrphidae) using integrative taxonomy, with the description of a new species. *European Journal of Taxonomy* 237(237): 1–25. <https://doi.org/10.5852/ejt.2016.237>
- Ačanski J, Miličić M, Likov L, Milić D, Radenković S, Vujčić A (2017) Environmental niche divergence of species from *Merodon ruficornis* group (Diptera: Syrphidae). *Archives of Biological Sciences* 69(2): 247–259. <https://doi.org/10.2298/ABS160303095A>
- Ačanski J, Vujčić A, Šašić Zorić L, Radenković S, Djan M, Markov Ristić Z, Ståhls G (2022) *Merodon chalybeus* subgroup: An additional piece of the *M. aureus* group (Diptera, Syrphidae) puzzle. *Annales Zoologici Fennici* 59(1): 79–109. <https://doi.org/10.5735/086.059.0109>
- Andrić A, Šikoparija B, Obreht D, Đan M, Preradović J, Radenković S, Pérez-Bañón C, Vujčić A (2014) DNA barcoding applied: Identification of the larva of *Merodon avidus* (Diptera: Syrphidae). *Acta Entomologica Musei Nationalis Pragae* 54: 741–757.
- Azizi Jalilian M, Shayesteh K, Danehkar A, Salmanmahiny A (2020) A new ecosystem-based land classification of Iran for conservation goals. *Environmental Monitoring and Assessment* 192(3): 1–17. <https://doi.org/10.1007/s10661-020-8145-1>
- CEPF (2022) Irano-Anatolian Hotspot. <https://www.cepf.net/our-work/biodiversity-hotspots/irano-anatolian>
- Chen H, Rangasamy M, Tan SY, Wang H, Siegfried BD (2010) Evaluation of five methods for total DNA extraction from western corn rootworm beetles. *PLoS ONE* 5(8): e11963. <https://doi.org/10.1371/journal.pone.0011963>
- Chroni A, Grković A, Ačanski J, Vujčić A, Radenković S, Veličković N, Djan M, Petanidou T (2018) Disentangling a cryptic species complex and defining new species within the *Eumerus minotaurus* group (Diptera: Syrphidae), based on integrative taxonomy and Aegean palaeogeography. *Contributions to Zoology (Amsterdam, Netherlands)* 87(4): 197–225. <https://doi.org/10.1163/18759866-08704001>
- Conn DLT (1976) Evidence of restricted mimetic colour polymorphism in the large narcissus bulb fly, *Merodon equestris* fab. (Diptera: Syrphidae), in the Pyrenees. *Heredity* 36(2): 185–189. <https://doi.org/10.1038/hdy.1976.23>
- Danin A (1988) Flora and vegetation of Israel and adjacent areas. The zoogeography of Israel 30: 251–276.
- Doczkal D, Pape T (2009) *Lyneborgimyia magnifica* gen. et sp. n. (Diptera: Syrphidae) from Tanzania, with a phylogenetic analysis of the Eumerini using new morphological characters. *Systematic Entomology* 34(3): 559–573. <https://doi.org/10.1111/j.1365-3113.2009.00478.x>
- ESRI (2014) ArcGIS Desktop: Release 10.3. Environmental Systems Research Institute, Redlands, CA.
- Evrendilek F, Gulbeyaz O (2008) Deriving vegetation dynamics of natural terrestrial ecosystems from MODIS NDVI/EVI data over Turkey. *Sensors* 8(9): 5270–5302. <https://doi.org/10.3390/s8095270>

- Fabricius JC (1781) *Species insectorum, exhibentes eorum differentias specificas, synonyma auctorum, loca natalia, metamorphosin, adjectis observationibus, descriptionibus*. Vol. 1. CE Bohnii, Hamburgi et Kilonii, 494 pp. <https://doi.org/10.5962/bhl.title.36509>
- Folmer O, Black M, Hoeh W, Lutz R, Vrijenhoek R (1994) DNA primers for amplification of mitochondrial cytochrome c oxidase subunit I from diverse metazoan invertebrates. *Molecular Marine Biology and Biotechnology* 3(5): 294–299.
- Francuski Lj, Ludoški J, Vujčić A, Milankov V (2011) Phenotypic evidence for hidden biodiversity in the *Merodon aureus* group (Diptera: Syrphidae) on the Balkan Peninsula: conservation implication. *Journal of Insect Conservation* 15(3): 379–388. <https://doi.org/10.1007/s10841-010-9311-5>
- Goloboff PA (1999) NONA computer program version 2.0. Published by the author, Tucumán, Argentina.
- Hadley A (2006) CombineZ version 5. Published by the author.
- Hall T (1999) BioEdit: A user-friendly biological sequence alignment editor and analysis program for Windows 95/98/NT. *Nucleic Acids Symposium Series* 41: 95–98. <http://brownlab.mbio.ncsu.edu/JWB/papers/1999Hall1.pdf>
- Han T, Park H, Kim SH, Park IG, Choi DS (2018) Discovery of the large narcissus fly, *Merodon equestris* (Fabricius), (Diptera, Syrphidae) in South Korea. *International Journal of Industrial Entomology* 36(2): 42–48.
- Hewitt GM (1999) Post-glacial re-colonization of European biota. *Biological Journal of the Linnean Society*. *Linnean Society of London* 68(1–2): 87–112. <https://doi.org/10.1111/j.1095-8312.1999.tb01160.x>
- Hewitt GM (2001) Speciation, hybrid zones and phylogeography - or seeing genes in space and time. *Molecular Ecology* 10(3): 537–549. <https://doi.org/10.1046/j.1365-294x.2001.01202.x>
- Hurkmans W (1985) Territorial behaviour of two *Merodon* species (Diptera: Syrphidae). *Entomologische Berichten* 45(6): 69–70.
- Hurkmans W (1988) Ethology and ecology of *Merodon* in Turkey (Diptera: Syrphidae). *Entomologische Berichten* 48(7): 107–114.
- Hurkmans W (1993) A monograph of *Merodon* (Diptera: Syrphidae). Part 1. *Tijdschrift voor Entomologie* 136(2): 147–234.
- Hurkmans W, Hayat R (1997) Ethology and ecology of *Merodon* (Diptera, Syrphidae) in Turkey II: Descriptions of new species and notes on other syrphid flies. *Dipterists Digest* 3: 62–79.
- ICZN [International Commission on Zoological Nomenclature] (1985) *International Code of Zoological Nomenclature*, 3rd edn. London, 1–339: The International Trust for Zoological Nomenclature. <https://www.biodiversitylibrary.org/item/107166#page/5/mode/1up> [accessed 10 Sept 2021]
- ICZN [International Commission on Zoological Nomenclature] (1999) *International Code of Zoological Nomenclature*, 4th edn. London: The International Trust for Zoological Nomenclature. <https://www.iczn.org/the-code/the-international-code-of-zoological-nomenclature/the-code-online/> [accessed 10 Sept 2021]
- Kaloveloni A, Tscheulin T, Vujčić A, Radenković S, Petanidou T (2015) Winners and losers of climate change for the genus *Merodon* (Diptera: Syrphidae) across the Balkan Peninsula. *Ecological Modelling* 313: 201–211. <https://doi.org/10.1016/j.ecolmodel.2015.06.032>
- Klingenberg CP (2011) MorphoJ: An integrated software package for geometric morphometrics. *Molecular Ecology Resources* 11(2): 353–357. <https://doi.org/10.1111/j.1755-0998.2010.02924.x>

- Kočiš Tubić N, Ståhls G, Ačanski J, Djan M, Obreht Vidaković D, Hayat R, Khaghaninia S, Vujčić A, Radenković S (2018) An integrative approach in the assessment of species delimitation and structure of the *Merodon nanus* species group (Diptera: Syrphidae). *Organisms, Diversity & Evolution* 18(4): 479–497. <https://doi.org/10.1007/s13127-018-0381-7>
- Konstantinov AS, Korotyaev BA, Volkovitsh MG (2009) Insect biodiversity in the Palearctic Region. In: Footitt RG, Adler PH (Eds) *Insect Biodiversity: Science and Society*. Wiley-Blackwell, Oxford, 107–162. <https://doi.org/10.1002/9781444308211.ch7>
- Kumar S, Stecher G, Tamura K (2016) MEGA7: Molecular Evolutionary Genetics Analysis version 7.0 for bigger datasets. *Molecular Biology and Evolution* 33(7): 1870–1874. <https://doi.org/10.1093/molbev/msw054>
- Liepa ZR (1969) Lists of the scientific works and described species of the late Dr. S. J. Paramonov, with locations of types. *Journal of the Entomological Society of Australia N.S.W.* 5: 3–22.
- Likov L, Vujčić A, Kočiš Tubić N, Đan M, Veličković N, Rojo S, Pérez-Bañón C, Veselić S, Barkalov A, Hayat R, Radenković S (2020) Systematic position and composition of *Merodon nigratarsis* and *M. avidus* groups (Diptera, Syrphidae) with a description of four new hoverflies species. *Contributions to Zoology (Amsterdam, Netherlands)* 89(1): 74–125. <https://doi.org/10.1163/18759866-20191414>
- Lingafelter SW, Nearn EH (2013) Elucidating Article 45.6 of the International Code of Zoological Nomenclature: A dichotomous key for the determination of subspecific or infrasubspecific rank. *Zootaxa* 3709(6): 597–600. <https://doi.org/10.11646/zootaxa.3709.6.9>
- Loew H (1869) Beschreibung europäischer Dipteren. Systematische Beschreibung der bekannten europäischen zweiflügeligen Insecten, von Johann Wilhelm Meigen. Vol. 1. Halle, 310 pp.
- Marcos-García MÁ, Vujčić A, Mengual X (2007) Revision of Iberian species of the genus *Merodon* (Diptera: Syrphidae). *European Journal of Entomology* 104(3): 531–572. <https://doi.org/10.14411/eje.2007.073>
- Milankov V, Ståhls G, Vujčić A (2008) Genetic diversity of populations of *Merodon aureus* and *M. cinereus* species complexes (Diptera, Syrphidae): Integrative taxonomy and implications for conservation priorities on the Balkan Peninsula. *Conservation Genetics* 9(5): 1125–1137. <https://doi.org/10.1007/s10592-007-9426-8>
- Moraes EM, Manfrin MH, Laus AC, Rosada RS, Bomfin SC, Sene FM (2004) Wing shape heritability and morphological divergence of the sibling species *Drosophila mercatorum* and *Drosophila paranaensis*. *Heredity* 92(5): 466–473. <https://doi.org/10.1038/sj.hdy.6800442>
- Myers N, Mittermeier RA, Mittermeier CG, da Fonseca GAB, Kent J (2000) Biodiversity hotspots for conservation priorities. *Nature* 403(6772): 853–858. <https://doi.org/10.1038/35002501>
- Nei M, Kumar S (2000) *Molecular Evolution and Phylogenetics*. Oxford University Press, New York, 348 pp. <https://doi.org/10.1093/oso/9780195135848.001.0001>
- Nixon KC (2008) ASADO version 1.85 TNT-MrBayes Slaver version 2; mxram 200 (v1.5.30). Made available through the author (previously named WinClada, version 1.00.08 (2002)).
- Olson DM, Dinerstein E, Wikramanayake ED, Burgess ND, Powell GV, Underwood EC, D'Amico JA, Itoua I, Strand HE, Morrison JC, Loucks CJ, Allnutt TF, Ricketts TH, Kura Y, Lamoreux JF, Wettengel WW, Hedao P, Kassem KR (2001) *Terrestrial Ecoregions of the World: A New Map of Life on Earth* A new global map of terrestrial ecoregions

- provides an innovative tool for conserving biodiversity. *Bioscience* 51(11): 933–938. [https://doi.org/10.1641/0006-3568\(2001\)051\[0933:TEOTWA\]2.0.CO;2](https://doi.org/10.1641/0006-3568(2001)051[0933:TEOTWA]2.0.CO;2)
- Paramonov SJ [= Парамонов С] (1926a) Про деякі нові види та варієтети двокрильців (= Ueber einige neue Arten und Varietaeten von Dipteren (Fam. Stratiomyiidae et Syrphidae)). Записки Фізично-Математичного Відділу, Українська Академія Наук (= Bulletin de la Classe des Sciences Physiques et Mathématiques, Académie des Sciences de l'Ukraine) 2(1): 87–93.
- Paramonov SJ (1926b) Zur Kenntnis der Gattung *Merodon*. *Encyclopédie Entomologique Diptera (B II)* 2(3): 143–160. [was dated 1925]
- Paramonov SJ (1927) Fragmente zur Kenntnis der Dipteren-fauna Armeniens. *Societas entomologica. Internationale entomologische Fachzeitschrift* 42(4): 15–16.
- Peck LV (1988) Family Syrphidae. In: Soós Á, Papp L (Eds) *Catalogue of Palaearctic Diptera, Vol. 8 (Syrphidae – Conopidae)*. Elsevier Science Publishers & Akadémiai Kiadó, Amsterdam, Budapest, 11–230.
- Popov GV (2011) The type specimens of Syrphidae in Ukraine. Sixth International Symposium on the Syrphidae, 5–7th August 2011, the Hunterian (Zoology Museum), University of Glasgow. The book of abstracts, Glasgow, 28–29.
- Popović D, Ačanski J, Djan M, Obreht D, Vujčić A, Radenković S (2015) Sibling species delimitation and nomenclature of the *Merodon avidus* complex (Diptera: Syrphidae). *European Journal of Entomology* 112(4): 790–809. <https://doi.org/10.14411/eje.2015.100>
- Preradović J, Andrić A, Radenković S, Zorić LŠ, Pérez-Bañón C, Campoy A, Vujčić A (2018) Pupal stages of three species of the phytophagous genus *Merodon* Meigen (Diptera: Syrphidae). *Zootaxa* 4420(2): 229–242. <https://doi.org/10.11646/zootaxa.4420.2.5>
- Radenković S, Vujčić A, Ståhls G, Pérez-Bañón C, Rojo S, Petanidou T, Šimić S (2011) Three new cryptic species of the genus *Merodon* Meigen (Diptera: Syrphidae) from the island of Lesbos (Greece). *Zootaxa* 2735(1): 35–56. <https://doi.org/10.11646/zootaxa.2735.1.5>
- Radenković S, Veličković N, Ssymank A, Obreht Vidaković D, Djan M, Ståhls G, Veselić S, Vujčić A (2018a) Close relatives of Mediterranean endemo-relict hoverflies (Diptera, Syrphidae) in South Africa: Morphological and molecular evidence in the *Merodon melanocerus* subgroup. *PLoS ONE* 13(7): e0200805. <https://doi.org/10.1371/journal.pone.0200805>
- Radenković S, Šašić Zorić L, Djan M, Obreht Vidaković D, Ačanski J, Ståhls G, Veličković N, Markov Z, Petanidou T, Kočiš Tubić N, Vujčić A (2018b) Cryptic speciation in the *Merodon luteomaculatus* complex (Diptera: Syrphidae) from the eastern Mediterranean. *Journal of Zoological Systematics and Evolutionary Research* 56(2): 170–191. <https://doi.org/10.1111/jzs.12193>
- Radenković S, Vujčić A, Obreht Vidaković D, Djan M, Milić D, Veselić S, Ståhls G, Petanidou T (2020) Sky island diversification in the *Merodon rufus* group (Diptera, Syrphidae)—Recent vicariance in south-east Europe. *Organisms, Diversity & Evolution* 20(3): 345–368. <https://doi.org/10.1007/s13127-020-00440-5>
- Reemer M, Smit JT (2007) Some hoverfly records from Turkey (Diptera, Syrphidae). *Volucella* 8: 135–146.
- Ricarte A, Marcos-García MÁ, Rotheray GE (2008) The early stages and life histories of three *Eumerus* and two *Merodon* species (Diptera: Syrphidae) from the Mediterranean region. *Entomologica Fennica* 19(3): 129–141. <https://doi.org/10.33338/ef.84424>
- Ricarte A, Souba-Dols GJ, Hauser M, Marcos-García MÁ (2017) A review of the early stages and host plants of the genera *Eumerus* and *Merodon* (Diptera: Syrphidae),

- with new data on four species. PLoS One 12(12): e0189852. <https://doi.org/10.1371/journal.pone.0189852>
- Rohlf FJ (2017a) tpsDig version 2.31. Department of Ecology and Evolution, State University of New York, Stony Brook, NY.
- Rohlf FJ (2017b) TpsRelv version 1.69. Department of Ecology and Evolution, State University of New York, Stony Brook, NY.
- Rohlf FJ, Slice DE (1990) Extensions of the Procrustes method for the optimal superimposition of landmarks. Systematic Zoology 39(1): 40–59. <https://doi.org/10.2307/2992207>
- Rossi P (1790) Fauna etrusca sistens Insecta quae in provinciis Florentina et Pisana praesertim collegit. Tomus secundus. Thomae Masi et Sociorum, Liburni, 348 pp. [+ 10 pl.] <https://doi.org/10.5962/bhl.title.15771>
- Sack P (1913) Die Gattung *Merodon* Meigen (*Lampetia* Meig. olim.). Abhandlungen der Senckenbergischen Naturforschenden Gesellschaft 31: 427–462.
- Sack P (1931) Syrphidae. In: Lindner E (Ed.) Die Fliegen der paläarktischen Region. E. Schweizerbart'sche Verlagsbuchhandlung, Stuttgart, 4(6): 289–336.
- Šašić Lj, Ačanski J, Vujčić A, Ståhls G, Radenković S, Milić D, Obreht-Vidaković D, Đan M (2016) Molecular and morphological inference of three cryptic species within the *Merodon aureus* species group (Diptera: Syrphidae). PLoS ONE 11(8): e0160001. <https://doi.org/10.1371/journal.pone.0160001>
- Siddiqui KM, Mohammad I, Ayaz M (1999) Forest ecosystem climate change impact assessment and adaptation strategies for Pakistan. Climate Research 12(2–3): 195–203. <https://doi.org/10.3354/cr012195>
- Simon C, Frati F, Beckenbach A, Crespi B, Liu H, Flook P (1994) Evolution, weighting and phylogenetic utility of mitochondrial gene-sequences and a compilation of conserved polymerase chain-reaction primers. Annals of the Entomological Society of America 87(6): 651–701. <https://doi.org/10.1093/aesa/87.6.651>
- Speight MCD (2020) Species accounts of European Syrphidae, 2020. Syrph the Net, the database of European Syrphidae (Diptera). Syrph the Net publications, Dublin, 314 pp.
- Ståhls G, Vujčić A, Pérez-Bañón C, Radenković S, Rojo S, Petanidou T (2009) COI barcodes for identification of *Merodon* hoverflies (Diptera, Syrphidae) of Lesvos Island, Greece. Molecular Ecology Resources 9(6): 1431–1438. <https://doi.org/10.1111/j.1755-0998.2009.02592.x>
- Ståhls G, Vujčić A, Petanidou T, Cardoso P, Radenković S, Ačanski J, Pérez-Bañón C, Rojo S (2016) Phylogeographic patterns of *Merodon* hoverflies in the Eastern Mediterranean region: Revealing connections and barriers. Ecology and Evolution 6(7): 2226–2245. <https://doi.org/10.1002/ece3.2021>
- Thompson FC (1999) A key to the genera of the flower flies (Diptera: Syrphidae) of the Neotropical Region including descriptions of new genera and species and a glossary of taxonomic terms. Contributions to Entomology International 3: 321–378.
- Thompson JD, Higgins DG, Gibson TJ (1994) Clustal W: Improving the sensitivity of progressive multiple sequence alignment through sequence weighting, position-specific gap penalties and weight matrix choice. Nucleic Acids Research 22(22): 4673–4680. <https://doi.org/10.1093/nar/22.22.4673>
- TIBCO Software Inc (2018) Statistica (data analysis software system), version 13. <http://tibco.com>
- Veselić S, Vujčić A, Radenković S (2017) Three new Eastern-Mediterranean endemic species of the *Merodon aureus* group (Diptera: Syrphidae). Zootaxa 4254(4): 401–434. <https://doi.org/10.11646/zootaxa.4254.4.1>

- Vujčić A, Pérez-Bañón C, Radenković S, Ståhls G, Rojo S, Petanidou T, Šimić S (2007) Two new species of the genus *Merodon* Meigen 1803 (Diptera: Syrphidae) from the island of Lesbos (Greece), the eastern Mediterranean. *Annales de la Société Entomologique de France* 43(3): 319–326. <https://doi.org/10.1080/00379271.2007.10697527>
- Vujčić A, Marcos-García MÁ, Sarıbiyik S, Ricarte A (2011) New data on the *Merodon* Meigen, 1803 fauna (Diptera: Syrphidae) of Turkey, including description of a new species and changes in the nomenclatural status of several taxa. *Annales de la Société Entomologique de France* 47(1–2): 78–88. <https://doi.org/10.1080/00379271.2011.10697699>
- Vujčić A, Radenković S, Ståhls G, Ačanski J, Stefanović A, Veselić S, Andrić A, Hayat R (2012) Systematics and taxonomy of the *ruficornis* group of genus *Merodon* (Diptera: Syrphidae). *Systematic Entomology* 37(3): 578–602. <https://doi.org/10.1111/j.1365-3113.2012.00631.x>
- Vujčić A, Radenković S, Likov L, Trifunov S, Nikolić T (2013a) Three new species of the *Merodon nigratarsis* group (Diptera: Syrphidae) from the Middle East. *Zootaxa* 3640(3): 442–464. <https://doi.org/10.11646/zootaxa.3640.3.7>
- Vujčić A, Ståhls G, Ačanski J, Bartsch H, Bygebjerg R, Stefanović A (2013b) Systematics of Pipizini and taxonomy of European *Pipiza* Fallén: Molecular and morphological evidence (Diptera, Syrphidae). *Zoologica Scripta* 42(3): 288–305. <https://doi.org/10.1111/zsc.12005>
- Vujčić A, Radenković S, Ačanski J, Grković A, Taylor M, Şenol SG, Hayat R (2015) Revision of the species of the *Merodon nanus* group (Diptera: Syrphidae) including three new species. *Zootaxa* 4006(3): 439–462. <https://doi.org/10.11646/zootaxa.4006.3.2>
- Vujčić A, Radenković S, Likov L (2018) Revision of the Palaearctic species of the *Merodon desuturinus* group (Diptera, Syrphidae). *ZooKeys* 771: 105–138. <https://doi.org/10.3897/zookeys.771.20481>
- Vujčić A, Radenković S, Likov L, Andrić A, Gilasian E, Barkalov A (2019) Two new enigmatic species of the genus *Merodon* Meigen (Diptera: Syrphidae) from the north-eastern Middle East. *Zootaxa* 4555(2): 187–208. <https://doi.org/10.11646/zootaxa.4555.2.2>
- Vujčić A, Radenković S, Likov L, Andrić A, Janković M, Ačanski J, Popov G, de Courcy Williams M, Šašić Zorić L, Djan M (2020a) Conflict and congruence between morphological and molecular data: revision of the *Merodon constans* group (Diptera : Syrphidae). *Invertebrate Systematics* 34: 406–448. <https://doi.org/10.1071/IS19047>
- Vujčić A, Likov L, Radenković S, Kočiš Tubić N, Djan M, Šebić A, Pérez-Bañón C, Barkalov A, Hayat R, Rojo S, Andrić A, Ståhls G (2020b) Revision of the *Merodon serrulatus* group (Diptera, Syrphidae). *ZooKeys* 909: 79–158. <https://doi.org/10.3897/zookeys.909.46838>
- Vujčić A, Speight MCD, de Courcy Williams M, Rojo S, Ståhls G, Radenković S, Likov L, Miličić M, Pérez-Bañón C, Falk S, Petanidou T (2020c) Atlas of the Hoverflies of Greece. Brill, Leiden, The Netherlands, 368 pp. <https://doi.org/10.1163/9789004334670>
- Vujčić A, Radenković S, Likov L, Veselić S (2021a) Taxonomic complexity in the genus *Merodon* Meigen, 1803 (Diptera, Syrphidae). *ZooKeys* 1031: 85–124. <https://doi.org/10.3897/zookeys.1031.62125>
- Vujčić A, Likov L, Popov S, Radenković S, Hauser M (2021b) Revision of the *Merodon aurifer* group (Diptera: Syrphidae) with new synonyms of *M. testaceus* Sack, 1913. *Journal of Asia-Pacific Entomology* 24(4): 1301–1312. <https://doi.org/10.1016/j.aspen.2021.08.014>
- Vujčić A, Tot T, Andrić A, Ačanski J, Šašić Zorić L, Pérez-Bañón C, Aracil A, Veselić S, Arok M, Mengual X, van Eck A, Rojo S, Radenković S (2021c) Review of the *Merodon*

- natans* group with description of a new species, a key to the adults of known species of the *natans* lineage and first descriptions of some preimaginal stages. *Arthropod Systematics & Phylogeny* 79: 343–378. <https://doi.org/10.3897/asp.79.e65861>
- Vujić A, Radenković S, Kočiš Tubić N, Likov L, Popov G, Rojo S, Miličić M (2022) Integrative taxonomy of the *Merodon aberrans* (Diptera, Syrphidae) species group: Distribution patterns and description of three new species. *Contributions to Zoology (Amsterdam, Netherlands)* 92(1): 51–96. <https://doi.org/10.1163/18759866-bja10037>
- Vujić A, Radenković S, Barkalov A, Kočiš Tubić N, Likov L, Tot T, Popov G, Prokhorov A, Gilasian E, Anjum S, Djan M, Kakar B, Andrić A (2023) Taxonomic revision of the *Merodon tarsatus* species group (Diptera, Syrphidae). *Arthropod Systematics & Phylogeny* 81: 201–256. <https://doi.org/10.3897/asp.81.e93570>
- WWF (2022) Ecoregions. <https://www.worldwildlife.org/>
- Zelditch ML, Swiderski DL, Sheets HD, Fink WL (2004) Geometric morphometrics for biologists: a primer. Elsevier Academic Press, London, 443 pp.
- Zimina LV (1960) On the hoverfly (Diptera, Syrphidae) fauna of the Transcaucasia. *Entomological Review* 39(3): 662–665. [In Russian]

Supplementary material 1

List of molecular samples

Authors: Ante Vujić, Snežana Radenković, Laura Likov, Nataša Kočiš Tubić, Grigory Popov, Ebrahim Gilasian, Mihajla Djan, Marina Janković Milosavljević, Jelena Ačanski

Data type: xlsx

Explanation note: List of molecularly analysed samples with GenBank accession numbers (in boldface: newly generated sequences within this study).

Copyright notice: This dataset is made available under the Open Database License (<http://opendatacommons.org/licenses/odbl/1.0/>). The Open Database License (ODbL) is a license agreement intended to allow users to freely share, modify, and use this Dataset while maintaining this same freedom for others, provided that the original source and author(s) are credited.

Link: <https://doi.org/10.3897/zookeys.1203.118842.suppl1>

Supplementary material 2

Material listed with occurrences

Authors: Ante Vujić, Snežana Radenković, Laura Likov, Nataša Kočiš Tubić, Grigory Popov, Ebrahim Gilasian, Mihajla Djan, Marina Janković Milosavljević, Jelena Ačanski

Data type: xlsx

Explanation note: List of studied specimens, except type material cited in main document.

Copyright notice: This dataset is made available under the Open Database License (<http://opendatacommons.org/licenses/odbl/1.0/>). The Open Database License (ODbL) is a license agreement intended to allow users to freely share, modify, and use this Dataset while maintaining this same freedom for others, provided that the original source and author(s) are credited.

Link: <https://doi.org/10.3897/zookeys.1203.118842.suppl2>

Supplementary material 3

DNA data

Authors: Ante Vujjić, Snežana Radenković, Laura Likov, Nataša Kočiš Tubić, Grigory Popov, Ebrahim Gilasian, Mihajla Djan, Marina Janković Milosavljević, Jelena Ačanski

Data type: pdf

Explanation note: Maximum-Likelihood tree based on the General Time Reversible model.

The tree with the highest log likelihood (-8297.00) is shown. A discrete Gamma distribution was used to model evolutionary rate differences among sites (5 categories (+G, parameter = 1.1113)). The rate variation model allowed for some sites to be evolutionarily invariable ([+I], 59.56% sites). Bootstrap values ≥ 50 are depicted near nodes.

Copyright notice: This dataset is made available under the Open Database License (<http://opendatacommons.org/licenses/odbl/1.0/>). The Open Database License (ODbL) is a license agreement intended to allow users to freely share, modify, and use this Dataset while maintaining this same freedom for others, provided that the original source and author(s) are credited.

Link: <https://doi.org/10.3897/zookeys.1203.118842.suppl3>

Larval and adult morphology of *Photuris elliptica* Olivier (Coleoptera, Lampyridae) and a Halloweeny case of cave-dwelling firefly larva feeding on bat guano

Paula M. Souto¹, Simone P. Rosa², Robson de A. Zampaulo³, Sara C. Rivera⁴, Thais G. Pellegrini⁵, Luiz F. L. da Silveira⁴

1 Centre for Functional Ecology, Department of Life Sciences, Associated Laboratory TERRA, University of Coimbra, Coimbra, Portugal

2 Instituto de Recursos Naturais, Universidade Federal de Itajubá, Itajubá – MG, Brazil

3 Observatório Espeleológico, Belo Horizonte, Minas Gerais, Brazil

4 Western Carolina University, Biology Department, 1 University Drive, Cullowhee, NC 28723, USA

5 Laboratório de Ecologia Florestal, Departamento de Ciências Florestais, Universidade Federal de Lavras, Lavras, Brazil

Corresponding author: Simone P. Rosa (simonepollicena@unifei.edu.br)

Abstract

The predatory firefly *Photuris elliptica* is common throughout the Atlantic Forest and has been proposed as a biomonitor due to the species' narrow niche and elevational range. However, the species is only known from adults, and a more effective monitoring of its populations hinges on the lack of knowledge on their immature stages. Recent sampling in ferruginous caves and inserted in other lithologies, on sites in the Atlantic Forest and Cerrado, have led to the capture of firefly larvae later reared to adults in the lab. Firefly larvae have been reported in South American caves before; however, they have only been identified to family due to the adult-biased taxonomy of Lampyridae. Here, we provide an updated diagnosis of *Photuris elliptica*, describe its immature stages for the first time, and update the distribution of the species. The larvae of *Photuris elliptica* were observed to interact with guano of several bat species, including that of vampire bats. These observations are consistent with the less specialized feeding preferences of photurine larvae, unlike most other firefly taxa, which specialize in gastropods and earthworms. It is yet unclear whether *P. elliptica* are cave specialists. However, since its occurrence outside caves remains unknown, protecting cave environments must be considered in conservation strategies for this important biomonitor species.

Key words: *Bicellonycha*, cave fauna, coprophagy, Photurinae, predatory fireflies



Academic editor: Hume Douglas

Received: 6 February 2024

Accepted: 5 April 2024

Published: 28 May 2024

ZooBank: <https://zoobank.org/FC6F1DA1-FF7F-41C6-939C-A67499F46677>

Citation: Souto PM, Rosa SP, de A. Zampaulo R, Rivera SC, Pellegrini TG, da Silveira LFL (2024) Larval and adult morphology of *Photuris elliptica* Olivier (Coleoptera, Lampyridae) and a Halloweeny case of cave-dwelling firefly larva feeding on bat guano. ZooKeys 1203: 71–94. <https://doi.org/10.3897/zookeys.1203.120341>

Copyright: © Paula M. Souto et al.
This is an open access article distributed under terms of the Creative Commons Attribution License (Attribution 4.0 International – CC BY 4.0).

Introduction

Fireflies (Coleoptera, Lampyridae) spend most of their lives as larvae, when they specialize on eating soft-bodied invertebrates such as gastropods and earthworms (Riley et al. 2021). For most species, except for the predatory ones (subfamily Photurinae), this is the only part of their life cycles responsible for obtaining and incorporating nutrients, since the adults usually do not eat (Faust 2017; Souto et al. 2019). Yet, firefly larvae tend to have highly diverse and specialized habitat preferences, including aquatic (freshwater, marine, or brackish

water), semi-aquatic (in marshes, ponds, or bromeliads), and terrestrial (in leaf litter or soil) environments (reviewed by Riley et al. 2021). Given the importance of understanding and conserving firefly species, it is surprising that the immature stages of 94% of all firefly species remain completely unknown. Therefore, studies documenting the occurrence, behavior, morphology, and life cycle of larval forms are needed to fill out this Haeckelian gap (Faria et al. 2021).

The predatory fireflies in the genus *Photuris* Dejean, 1833 have been extensively studied for their complex adult behaviors (reviewed by Faust 2017; Lloyd 2018; Souto et al. 2019; Maquitico et al. 2022), remarkably including kleptoparasitism (Faust et al. 2012) and aggressive mimicry (“femme fatale”) (Lloyd 1965; Buschman 1974; Lloyd and Ballantyne 2003). This genus is divided in three subgenera, including *Photuris* (*Photuris*) commonly found throughout the New World from Canada to Argentina, with about 120 species (Olivier 1886; McDermott 1966; Souto et al. 2019; Heckscher 2021, 2023; Perez-Hernandez et al. 2022). However, their immature counterparts are comparatively neglected from a systematic standpoint despite their usually high local abundance, and studies on material reliably identified to species level are scarce (despite important work on ultrastructural morphology; e.g. Smith 1963; Strause et al. 1979). Aside from Rosa’s (2007) detailed work on the morphology and bionomy of *Photuris femoralis* Curtis, 1839 (there misidentified as *Photuris fulvipes* (Blanchard, 1837)), comparative works of taxonomic relevance are lacking for this genus, and for subfamily at large (but see Costa et al. 1988, for descriptions of the immature stages of an undetermined species of *Bicellonycha* Motschulsky, 1853). Studies on undetermined (i.e. unidentified to species) *Photuris* larvae (e.g. Oertel et al. 1975; Domagala and Ghiradella 1984; Murphy and Moiseff 2019) highlight the challenge of identifying larvae and the need for comparative work on reliably identified species to foster further studies on this group.

The predatory firefly *Photuris elliptica* Olivier, 1886 has been identified as an ideal flagship species to monitor environmental changes in the Atlantic Rainforest, given their narrow environmental niches (Colares et al. 2021). Adults of this species have been commonly collected in montane forests (Silveira et al. 2020), but their larvae have been elusive. Recent fieldwork by our group found photurine larvae dwelling in caves and grottos (small caves) across several spots at the Atlantic Rainforest and the Cerrado biomes. Most of the collections were carried out by RZ as part of various monitoring and research works on cave communities for environmental licensing purposes. The ubiquitous presence of these larvae caught the attention of RZ who managed to raise them to adults and allow us to reliably identify them as *Photuris elliptica*. This is not only the first report of reliably identified firefly larvae in caves, but also the first documentation of these organisms feeding on bat guano. Here, we provide the first description of the larva of *P. elliptica* and document their habitat and feeding behavior. We also provide updated diagnoses and a distribution map for this species.

Materials and methods

Collecting and rearing larvae. Larvae were collected from the cave RF_0071 (Brazil, Minas Gerais state, Barão dos Cocais municipality) using fine-tip brushes and transported alive to the laboratory in plastic containers with a sample of clay sediments from the cave (Figs 1, 2). The largest last instar larvae were

chosen for this procedure to maximize rearing success. The containers were kept at room temperature and light, and the substrate was kept moist. Larvae were fed with fish food until they reached adult forms, which took approximately 30 days. The fish food was predominantly composed of soybean meal, fish meal, creamed corn, and squid meal. The larvae were raised together in the same container without any observed intraspecific predation behaviors (cannibalism). In their last stage, the larvae built chambers in the substrate (Fig. 2B) (as commonly known in other photurine larvae; e.g. Rosa 2007), where they pupated and laid until emerged as adults. On this occasion, we were unable to preserve the pupa before the adult emerged, which is why we did not describe it here.

Material preparation. Study of the larval morphology was based on examination of whole specimens and head, mouthparts, and legs dissected after being boiled in water. Dissected larva and whole immature instar specimens were mounted in temporary slides in Hoyer's medium. Adults were soaked in 10% KOH for 24 hours, then dissected and examined. Drawings were made with a camera lucida adapted to a stereomicroscope Zeiss Discovery V8 or after photographs taken through the eyepiece of a microscope Zeiss Primo Star. Photographs were taken with a Canon EOS Rebel T6 camera with a Canon EF 100 mm f/2.8 lens and Leica M165C, extension tubes, and a LED illumination system (Kawada and Buffington 2016). Images were processed using Helicon



Figure 1. General aspect of the landscape and ferruginous caves in the Quadrilátero Ferrífero, state of Minas Gerais **A** Serra da Moeda **B, C** Caves inserted in the iron formation.

Focus 4.03 and Adobe Photoshop 24.2.1 software. The material studied are deposited in the following institutions: Museu de Zoologia da Universidade de São Paulo, São Paulo (**MZUSP**), Coleção de Invertebrados Subterrâneos de Lavras da Universidade Federal de Lavras, Minas Gerais (**ISLA**), Coleção Professor José Alfredo Dutra da Universidade Federal do Rio de Janeiro (DZRJ), and Muséum National d’Histoire Naturelle, Paris (**MNHN**).

Taxonomy and terminology. We based our identification on the original description (Olivier 1886) and by comparison to the holotype, deposited at Muséum National d’Histoire Naturelle, Paris, France (**MNHN**). Terminology followed Souto et al. (2019) and Novák (2018) for adults and immature stages, respectively. Accordingly, the terms tergum and epipleura of larva in Rosa (2007) are here corrected for mediotergite and laterotergite, respectively.

Results

Taxonomy

Photuris elliptica E. Olivier, 1886

Figs 2–11

Comparative diagnosis. Larva (Figs 2–4). Larvae of *Photuris elliptica* are remarkably different from other known congeneric larvae in its color pattern, with thoracic and abdominal mediotergites ochre with black trapezoidal spots medially, which are sometimes medially split (Figs 2A–D, 3A). Other species are brown, reddish brown or black with paler or darker lateral spots (Buschman 1984; Rosa 2007). The chaetotaxy of *Photuris elliptica* and *P. femoralis* is similar, differing by the presence of long, stout setae on anterior margin of pronotum in *P. elliptica* and shape of the longer stouter setae on posterior corners of mediotergite and laterotergite (Fig. 3A, B), which are stiff and acute in *P. elliptica* and subfoliaceous (somewhat flat, tip blunt) in *P. femoralis*. What is more, *P. elliptica* has one pair of parasagittal stouter, longer setae near midlength of pronotum (Fig. 3A) and the ventral stout setae of tibia is longer (about 5 times longer than fine setae) (Fig. 3E), while *P. femoralis* has two parasagittal pairs of setae near midlength of pronotum and ventral stout setae of tibia about 3 times longer than fine setae (see Rosa 2007).

Adult (Figs 5–11). *Photuris elliptica* is very similar to *P. funesta* Gorham, 1880, a common species of the tropical Andes in Colombia (Olivier 1886; LS pers. ob.). Both species share a relatively large size (12–13 mm in *P. elliptica*, ~15–20 mm in *P. funesta*), an overall elongate body and similar color pattern (body dull black, except for the yellow pronotum [with a black spot on the disc in *P. funesta*]). *Photuris elliptica* can be readily distinguished from *P. funesta* by the lack of a black dot at the pronotal disc, obtuse posterior angles of the pronotum (projected and acute in *P. funesta*), and more elliptical elytron (subparallel in *P. funesta*).

In the Atlantic Rainforest of southeastern Brazil, *P. elliptica* is somewhat similar to *P. velox* Olivier, 1886—both species are relatively large, have obtuse posterior corners of the pronotum and elliptical elytra (Silveira et al. 2020). However, *P. velox* has a very different color pattern, with body overall dark brown to black, except for pale yellow pronotal and elytral expansions.



Figure 2. *Photuris elliptica* Olivier, 1886, mature larvae **A** larva eating carnivorous bat guano **B** larvae in the plastic container with fine sediment; arrows indicate pupal chambers.

Photuris elliptica also overlaps in distribution with *P. femoralis* Curtis and *P. lugubris* Gorham, 1881. *Photuris elliptica* can be distinguished from *P. femoralis* by the elliptical elytral outline (lacking outward lateral expansions in *P. femoralis*) and color pattern (pronotum pale yellow) (Souto et al. 2019; Silveira et al. 2020). *Photuris elliptica* also has a thinner mandible that evenly tapers throughout (larger and constricted by the basal third in *P. femoralis*). *Photuris elliptica* is similar to *P. lugubris*, with a notched posterior margin of the sternal VII, the central tooth on the labrum much longer than the others, and similar color pattern (pronotum yellow, elytron black). *Photuris elliptica* can be distinguished from *P. lugubris* by its yellow pro- and mesocoxae (black in *P. lugubris*), as well as for the more conspicuous marginal costa (less developed in *P. lugubris*).

For overall morphological comparison within the genus, *P. elliptica* shows considerable differences from other *Photuris* with which they do not co-occur, including *P. frontalis* LeConte, 1852, *P. tenuisignathus* Zaragoza-Caballero, 1995, and the *P. versicolor* (Fabricius, 1798) complex (Zaragoza-Caballero 1995). Based on the availability of published material and references therein, members of the *P. versicolor* group (including *P. quadrifulgens* (Barber, 1951), *P. trivittata* Lloyd & Ballantyne, 2003, *P. versicolor*, and *P. walldoxeyi* Faust, 2019) are deemed morphologically similar and will be treated as a single group for comparison (Barber 1951; McDermott 1967; Faust and Davis 2019).

Photuris elliptica mandibles are thinner and evenly tapered throughout, compared to the thicker mandibles of *P. femoralis* and the *P. versicolor* group which are constricted by the basal third (Fig. 6A). The antennal sockets are very close, nearly contiguous in *P. elliptica* instead of separated by half a socket width in other *Photuris* (Fig. 6C). The labial palp of *P. elliptica* is triangular rather than C-shaped in congeners (Fig. 6C). The pronotum of *P. elliptica* is wide (1.5 times wider than long) and has a shorter anterior expansion with a distinct dorsal bend as seen in lateral view (Fig. 7A, E), while other *Photuris* feature longer pronota with long, straight anterior expansions. The elytron of *P. elliptica* are also wider, equally wide in the 1st and 2nd thirds, with lateral expansions more pronounced slightly after the humerus (Fig. 7M–O). This is distinct from

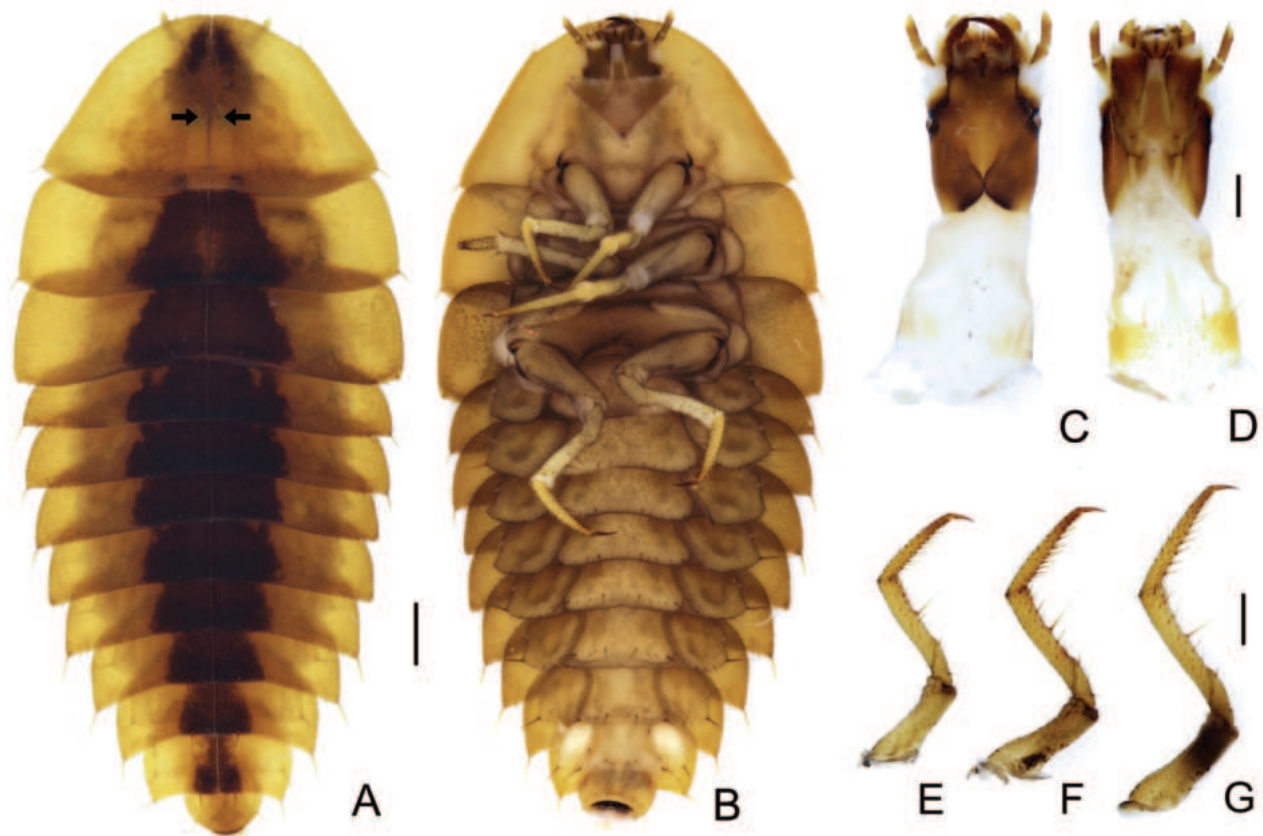


Figure 3. *Photuris elliptica* Olivier, larval morphology, mature larva **A** habitus dorsal view **B** habitus ventral view **C** head dorsal view **D** head ventral view **E–G** right pro-, meso- and metalegs lateral view. Black arrows indicate the parasagittal pair of stout setae. Scale bars: 1.0 mm (**A, B**); 0.5 mm (**C–G**).

P. femoralis, with straight, narrow elytra, and *P. versicolor* group, with elytra that are slightly convergent throughout. The legs have less prominent trochanters than the other *Photuris* species illustrated in the literature (Fig. 7L). The male lantern covers the entire sterna VI and VII, both of which are much longer than sternum V, unusual for *Photuris* (Fig. 5C). The median projection of the sternum VIII is remarkably longer (a fifth of sternum greater length) than that of *P. femoralis*, *P. lugubris*, and *P. versicolor* group (a sixth), but narrower than *P. frontalis* (roughly a fourth) (Fig. 8B). The posterior margin of the pygidium in *P. elliptica* is truncate (Fig. 8A), similar to *P. versicolor* group, instead of rounded in *P. femoralis*, *P. frontalis*, and *P. lugubris*. The arms of the sternum IX are separated by half the sternum width where it meets the syntergite (Fig. 8C), while the arms in other *Photuris* are separated by a fourth of the sternum IX width or less. Similar to *P. femoralis* and *P. tenuisignathus*, and unlike the other ones mentioned, the aedeagus of *P. elliptica* is distinct for lacking the basal lobes at the base of the paramere (Fig. 8H). The tip (apical fifth) of the phallus is also wider (Fig. 8E), similar to *P. frontalis* and *P. lugubris*, rather than constricted in *P. femoralis* and *P. versicolor* group.

Due to lack of published data on *Photuris* females, *P. elliptica* can only be compared to *P. femoralis* (Souto et al. 2019) and *P. versicolor* group (Figs 9–11). The mandibles of *P. elliptica* have smoother inner margins than *P. femoralis* and *P. versicolor* group and are much longer than the latter (Fig. 9A). The median tooth on the labrum is twice as long as the lateral teeth, while *P. femoralis* has

teeth all the same size and *P. versicolor* group has a median tooth 1.5 times as long as the lateral teeth (Fig. 9A). The labial palps of *P. elliptica* are less emarginate (less C-shaped) than those of other *Photuris* females (Fig. 9B). *Photuris elliptica* has a slightly depressed vertex of the head (flat in congeners) (Fig. 9D, E) and antennal sockets that are wider than long (round in congeners) (Fig. 9C). *Photuris elliptica* and *P. femoralis* also share a wider, shorter pronotum compared to the longer *P. versicolor* group pronotum (Fig. 10A). The *P. elliptica* lanterns are similar to *P. femoralis*, compared with *P. versicolor* group lanterns which are longer and thinner, especially on sternum VI (Fig. 5F). The sternum VIII is lightly sclerotized, similar to *P. versicolor* group, while *P. femoralis* has a strongly sclerotized sternum VIII (Fig. 11A). The arms of the ovipositor in *P. elliptica* are longer than the rest of the ovipositor, resulting in much longer arms than its congeners (Fig. 11B). Given that no other photurine species have had their bursal anatomy described before, cross-species comparisons are not possible, but we trust even a simple description would help future comparisons. The bursa copulatrix (Fig. 11E, F) of *P. elliptica* has a long and broad spermatophore digesting gland (wider and longer than bursal core), with a basal long and slender pouch, and no distinct bursal sclerites. A spermatheca could not be clearly determined but, if present, it would be very different from other known lampyrid spermathecae (e.g. Fu and Ballantyne 2021; Zeballos et al. 2023).

Holotype examined. Minas Gerais, Caraça, 1/II/1885, male, E. Gounelle col. (MNHN – France, Paris, Muséum National d’Histoire Naturelle). The holotype, confirmed by MNHN curator A. Mantilleri, has the author’s original identification label, but lacks an original type label.

Material examined (adults). BRAZIL – **Minas Gerais** • 1 ♂; Barão dos Cocais, cave RF_0071; 19°55'21.57"S, 43°30'43.37"W (WGS84); alt. 908 m; 24.III.2014, afótica; Zampaulo R.A. leg.; ISLA without catalog number • 2 ♂; Catas Altas, Vale, Mina Fábrica Nova, cave FN_0001; 20°12'26.69"S, 43°26'18.45"W (WGS84); 18.IX.2020; Eq. Spelayon et al. leg.; ISLA 84748 • 1 ♂; Presidente Olegário, Gruta da Caieira; 18°19'23.99"S, 46°5'16.00"W (WGS-84); 11.X.2010; without collector; ISLA 3102 • 1 ♂; Arcos/Pains, Agrimg (AGR), 002_001_003; 20°20'21.27"S, 45°34'36.87"W (WGS84); Eq. Spelayon et al. leg.; ISLA 51729 • 1 ♂; Monte Verde; 11.XII.1969; J. Halik leg., MZUSP 9482 • 1 ♀; same locality; 27.XI.1969; J. Halik leg.; MZUSP 9122 – **São Paulo** state • 2 ♂; Campos do Jordão; 18.XII.1944; F. Lane leg.; MZUSP without catalog number • 1 ♂; Monte Alegre, Fazenda Santa Maria; 1100 m elev.; 28–30.XII.1942; Zoppei & Dente leg.; MZUSP without catalog number • 1 ♂; Santo Antônio do Pinhal (Pindamonhangaba, sic), Estação Eugênio Lefevre; 1200 m elev.; 24.I.1963; Exp. Dep. Zool. leg.; *Photuris*, Silveira det. 2012; MZUSP without catalog number – **Rio de Janeiro** state • 1 ♂, 1 ♀; Teresópolis, Parque Nacional da Serra dos Órgãos, represa do Rio Beija-flor; 14–17.I.2015; Silveira leg.; DZRJ 3543.

Pupa. Unknown.

First instar to mature larva (possibly 6th instar) (Figs 2–4). Body dorsal view (from anterior margin of pronotum to posterior margin of abdominal tergite IX) 2.5–14 mm long, about 2 times longer than wide, oblong (pronotum semi-circular, widest at metathorax and gradually decreasing in width posteriorly from abdominal segment III, dorsoventrally flattened. Head dark brown, median region in front of frontal suture paler (Fig. 3C); dorsal surface of body

ochre, pronotum medially with a pair of brown elongate spots on anterior half (sometimes almost contiguous), a parasagittal pair of shorter brown spots on posterior margin (sometimes obsolete), mesothoracic, metathoracic and abdominal tergites I–VIII with median trapezoidal brown spot from anterior to posterior margins, about 1/3 as wide as tergite (Fig. 3A, B). Tegument with setae of four types: most surface covered with dense, yellow short decumbent (lying on surface), semi erect and erect setae; edges with few darker stouter and longer setae. (Fig. 3A, B). **Head** (Figs 3C, D, 4A, B). About 1.5 times longer

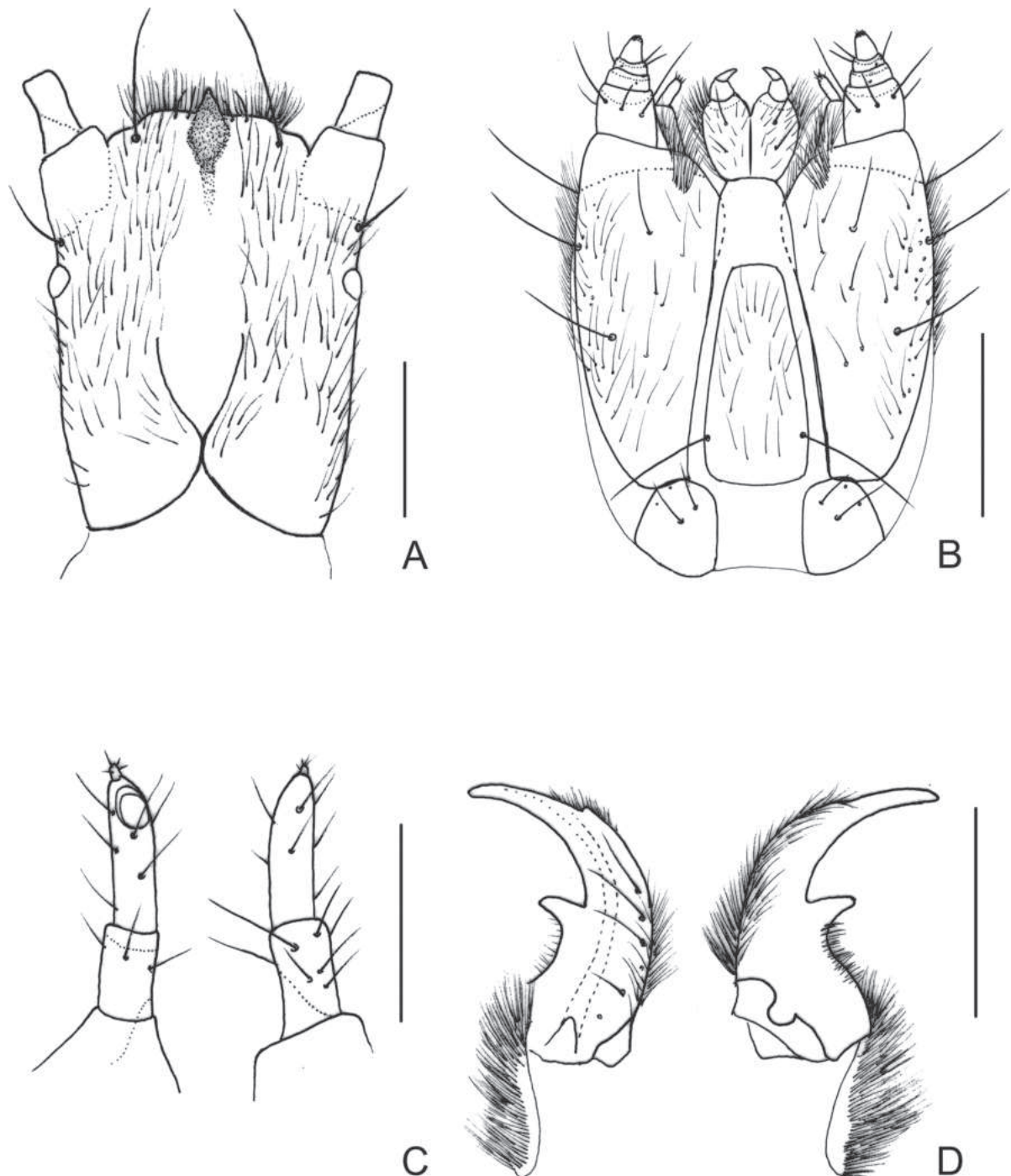


Figure 4. *Photuris elliptica* Olivier, larval morphology, mature larva **A** head dorsal view **B** maxillolabial complex ventral view **C** left antenna ventral and dorsal views **D** right mandible ventral and dorsal views. Scale bars: 1.0 mm (**A, B**); 0.5 mm (**C, D**).

than wide (length up to nasale), almost entirely retractable into prothorax (only mandibles and antenna visible in dorsal view when head retracted), sides weakly converging posteriorly, posterior margin with wide triangular notch (Figs 3C, 4A); laterodorsal surface with long, fine setae, one stemma with convex lens laterally at base of antennifer (Fig. 4A); antennifer membranous, as long as basal antennomere (Fig. 4A). Frontal arms V-shaped, well impressed posteriorly, almost reaching $\frac{1}{2}$ length of head (Figs 3C, 4A); epicranial stem very short; clypeolabrum fused to frons, each lateral part darkly sclerotized with anterior edge bisinuous, median part translucent, with dark fusiform plate at middle; plate with anterior part fused to head capsule, forming acute tooth; posterior part fused to epipharynx and visible through translucent cuticle (Fig. 3A, B). Antennae elongate, with three antennomeres, antennomere I partially sclerotized, sparsely setose, cylindrical; antennomere II 1.4–1.7 times longer than I, fully sclerotized, sparsely setose, laterally flattened, apex ventrally with elliptical, flattened sensorium; antennomere III 0.2× as long as antennomere II, attached dorsally to antennomere II, digitiform, subapically one seta and one dome-like projection, apically three spiniform projections (Fig. 4C). Epipharynx with cross-shaped sclerite and two triangular striate plates; plates with anterior margin densely covered with fine setae and two orifices at lateral margins; hypopharynx with anterior part bilobed, densely setose; median part triangular darkly sclerotized, glabrous; posterior part elongate, semitubular. Mandibles symmetrical, falcate, with a channel opening near apex at outer edge, lateroventral edge with dense row of fine setae from base to channel opening; ventromesal margin posteriorly to retinaculum with shorter setae; retinaculum well developed, forming a large, acute tooth; mesal membranous extension densely setose (Fig. 4D). Maxillolabial complex separated from ventral head capsule by narrow membrane; maxillae with cardo as long as wide, 0.25 times as long as stripes; stipites about 2.5 times longer than narrow, with short membranous area on anterior margin, covered with fine setae irregularly distributed, denser laterally, four stouter setae (three laterally, one anteromedially); palpus 4-segmented, tapering toward apex, with sparse fine setae, palpomere I 1.1–1.2 times wider than long, palpomeres II and III transverse, about $\frac{1}{5}$ – $\frac{1}{4}$ as long as I, palpomere IV conical 3 times longer than III; galea 2-articulated: basal palpomere triangular, as wide as long; apical palpomere digitiform, 3 times longer than wide, with one stouter long seta apically (as long as palpomere IV) and few shorter setae; lacinia consisting of densely structure connected to dorsomesal stipital edge; labium: prementum covered with fine setae, one stouter setae near each palpus, anterior edge emarginated between palpi, long dark endocarina at midline; palpus two segmented, apical palpomere as long as the basal one, strongly tapered apicad; mentum with anterior $\frac{1}{3}$ membranous; posterior $\frac{2}{3}$ sclerotized with pair of long setae posteriorly; submentum and gula membranous (Fig. 4B). Post-occipital membrane as long as head, with elongate lateral sclerotization wider and contiguous on prothoracic collar. **Thorax** (Fig. 3A, B): dorsal surface covered with short decumbent, semierect and erect setae, tip of posterior angle with one stouter, longer setae (about 4–5 times longer than fine setae), one parasagittal pair of longer stout setae on posterior edge, ventral surface evenly weakly sclerotized, except by darkly sclerotized thin strand at base of coxae (Fig. 3A, B). Pronotum semielliptical 1.6–1.9 times wider than long, posterior margin slightly curved posterad,

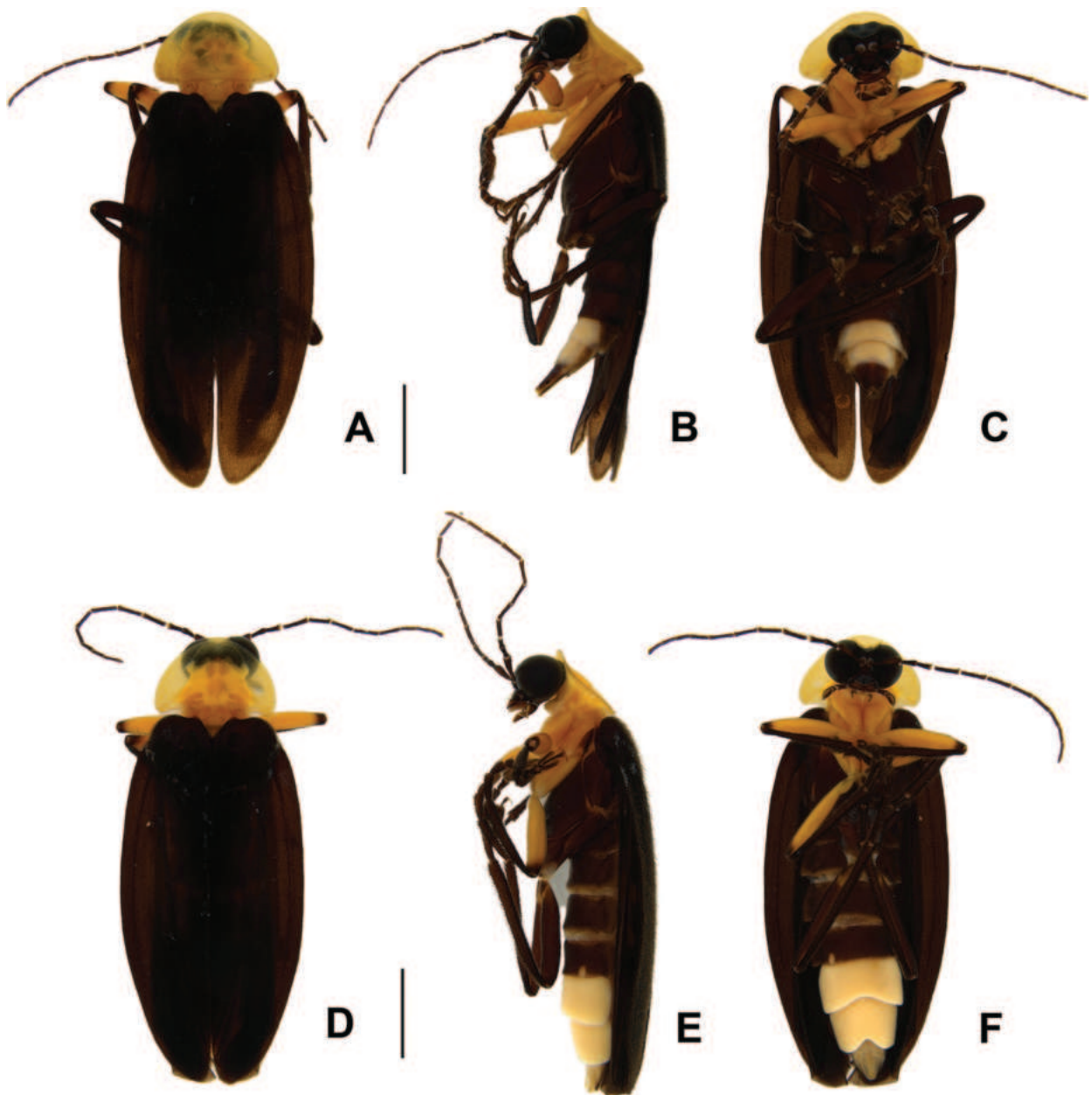


Figure 5. *Photuris elliptica* Olivier, adult habitus **A–C** male habitus: **A** dorsal view **B** lateral view **C** ventral view **D–F** female habitus: **D** dorsal view **E** lateral view **F** ventral view. Scale bars: 2.5 mm.

anterior margin with two pairs anteriorly and one pair anterolaterally of stouter, longer setae (3–5 times longer than fine setae), one pair of parasagittal stouter, longer setae (3 times longer than fine setae) at midlength (Fig. 3A); prothoracic collar weakly sclerotized, ventrally covered with short setae, two pairs of longer, stouter setae anteriorly (Fig. 3C, D); prosternum weakly sclerotized, covered with short setae, each anterior corner with one stouter, longer setae (Fig. 3D). Mesonotum as long as metanotum, both transverse, with anterior and posterior angles almost straight, with transverse pigmented impression parallel to anterior edge (Fig. 3A); mesonotum 3.0–3.3 times wider than long (Fig. 3A); metanotum 3.8–4.0 times wider than long (Fig. 3A); mesepisternum with a functional biforous spiracle on anterior corner. **Legs** (Fig. 3E–G): evenly sclerotized, pretarsus darker, with short spiniform setae becoming stiffer and darker

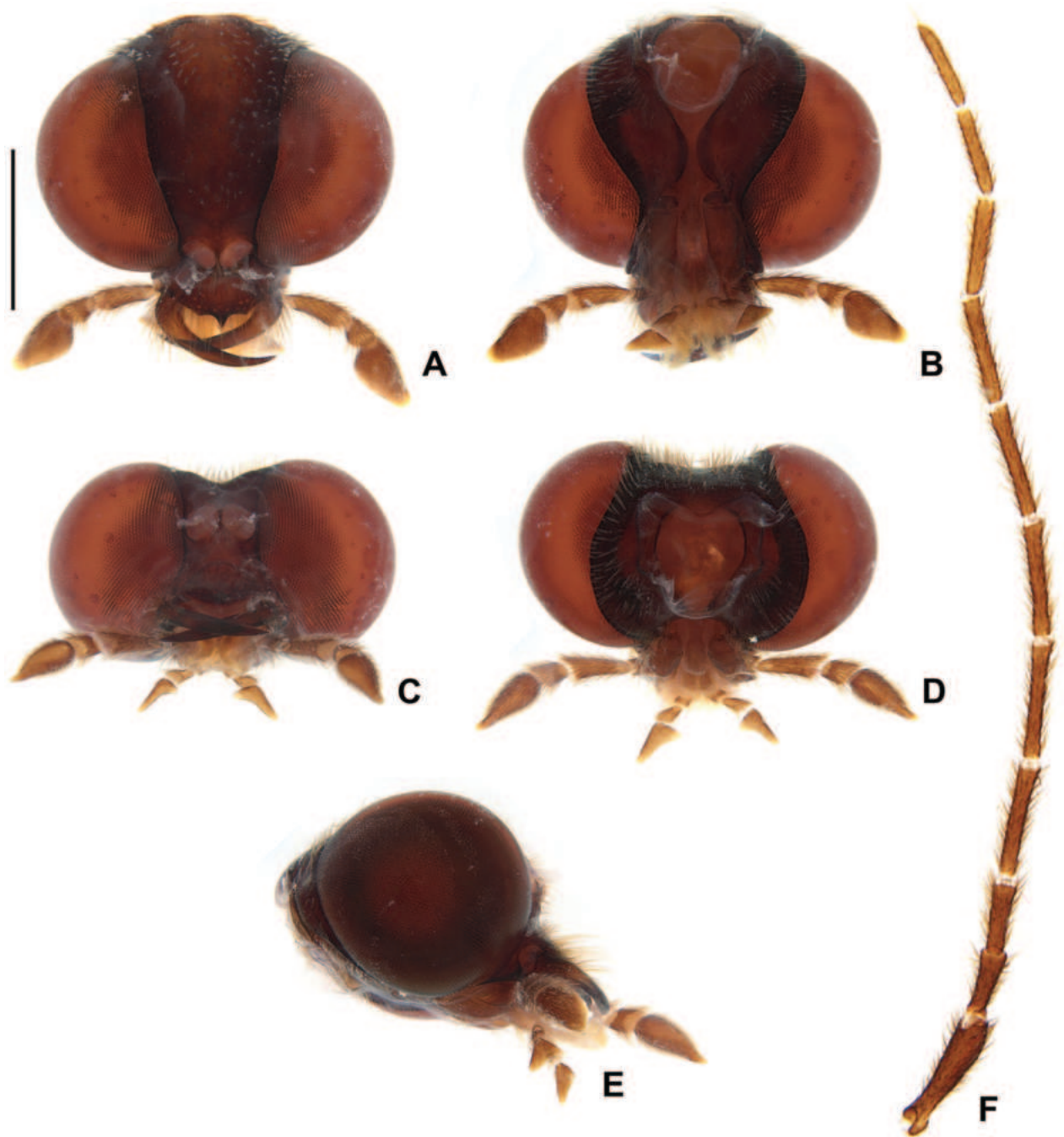


Figure 6. *Photuris elliptica* Olivier, male head **A–E** head capsule: **A** dorsal view **B** ventral view **C** frontal view **D** occipital view **E** lateral view **F** antenna dorsal. Scale bar: 1 mm.

from coxa to tarsus, tibia with one longer stouter seta ventrally (about 5 times longer than short setae); pretarsus with one seta on each side at base (Fig. 3D). **Abdomen** (Fig. 3A, B) dorsal surface covered with short decumbent, semierect and erect setae, tip of posterior angle with one stouter, longer setae (about 4–5 times longer than fine setae), one pair of longer stouter setae parasagittally; median tergites transverse, gradually narrowed posterad from segment III; I–VIII with anterior angles rounded, posterior angles acute, and transverse pigmented impression parallel to anterior edge, median tergite IX almost circular (dorsal visible part semicircular), about 0.5 times as long as VIII, margin

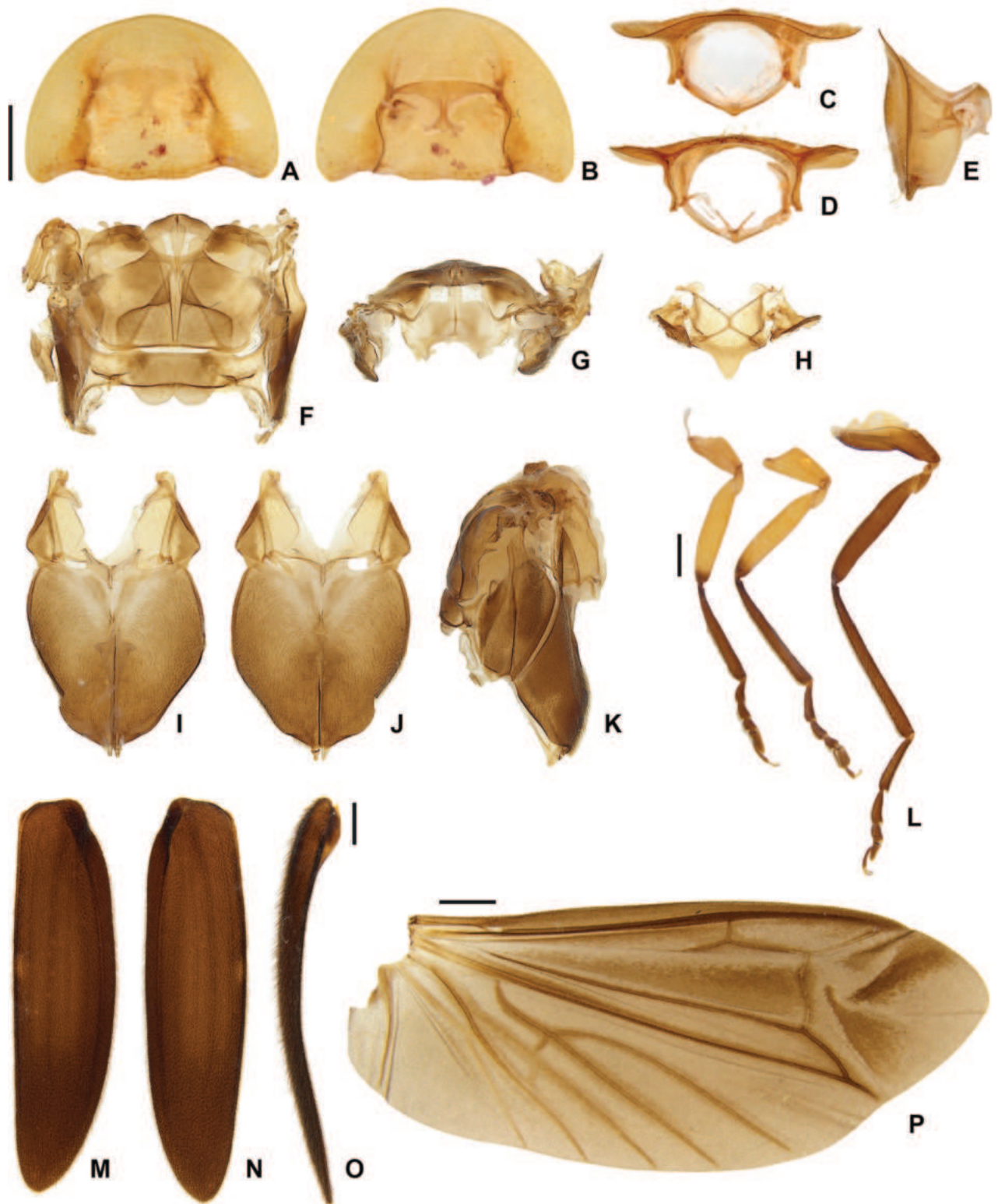


Figure 7. *Photuris elliptica* Olivier, male thorax **A–E** pronotum: **A** dorsal view **B** ventral view **C** anterior view **D** posterior view **E** lateral view **F–G** alinotum: **F** dorsal view **G** anterior view **H** mesoscutellum view **I–K** pterothorax: **I** ventral view **J** dorsal view **K** lateral view **L** proleg, mesoleg, metaleg **M–O** elytron: **M** dorsal view **N** ventral view **O** lateral view **P** wing. Scale bars: 1 mm.

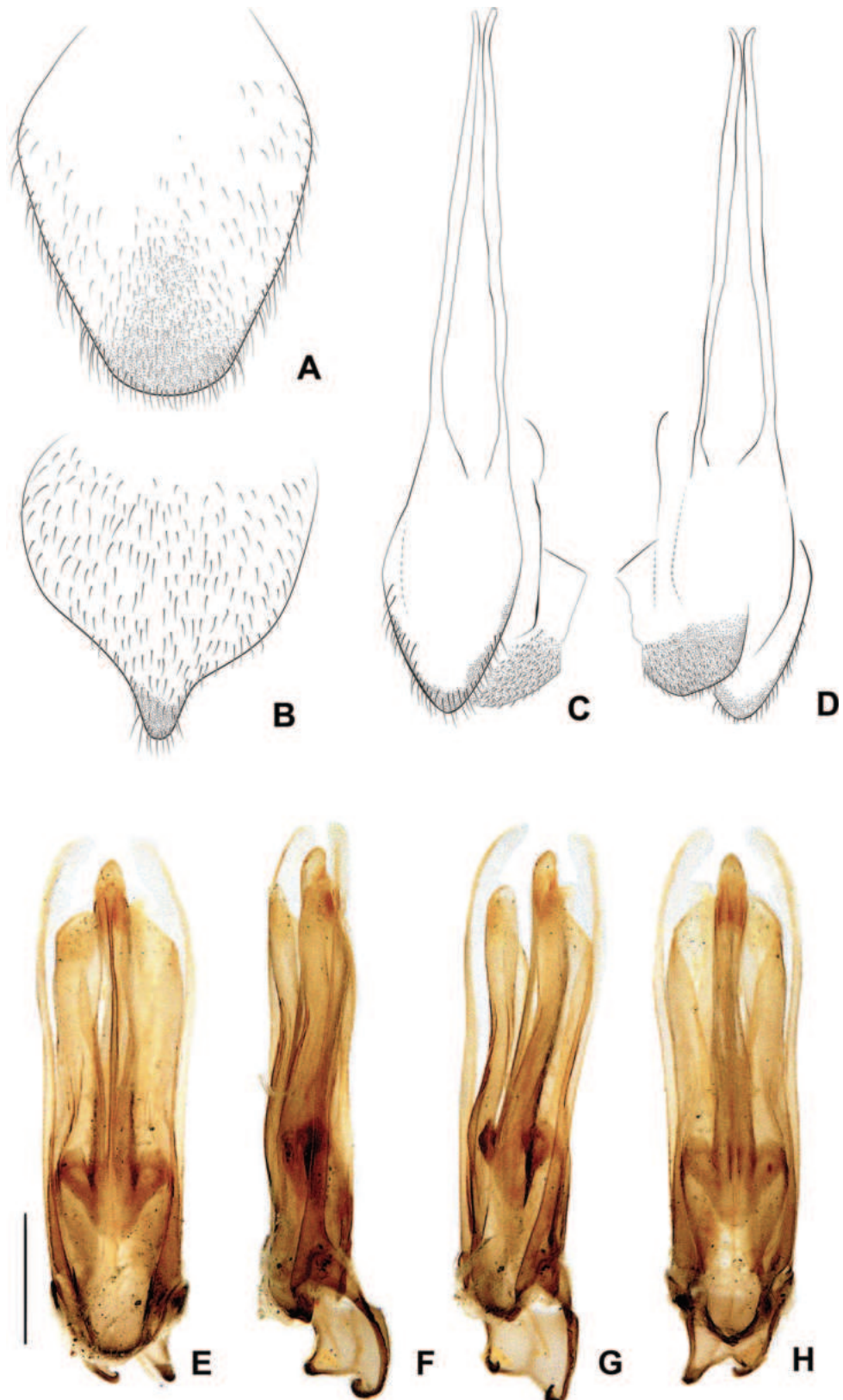


Figure 8. *Photuris elliptica* Olivier, male abdomen **A** pygidium dorsal view **B** sternum VIII ventral view **C** syntergite dorsal view **D** sternum IX ventral view **E–H** aedeagus: **E** dorsal view **F** lateral view **G** oblique view **H** ventral view. Scale bar: 0.5 mm.

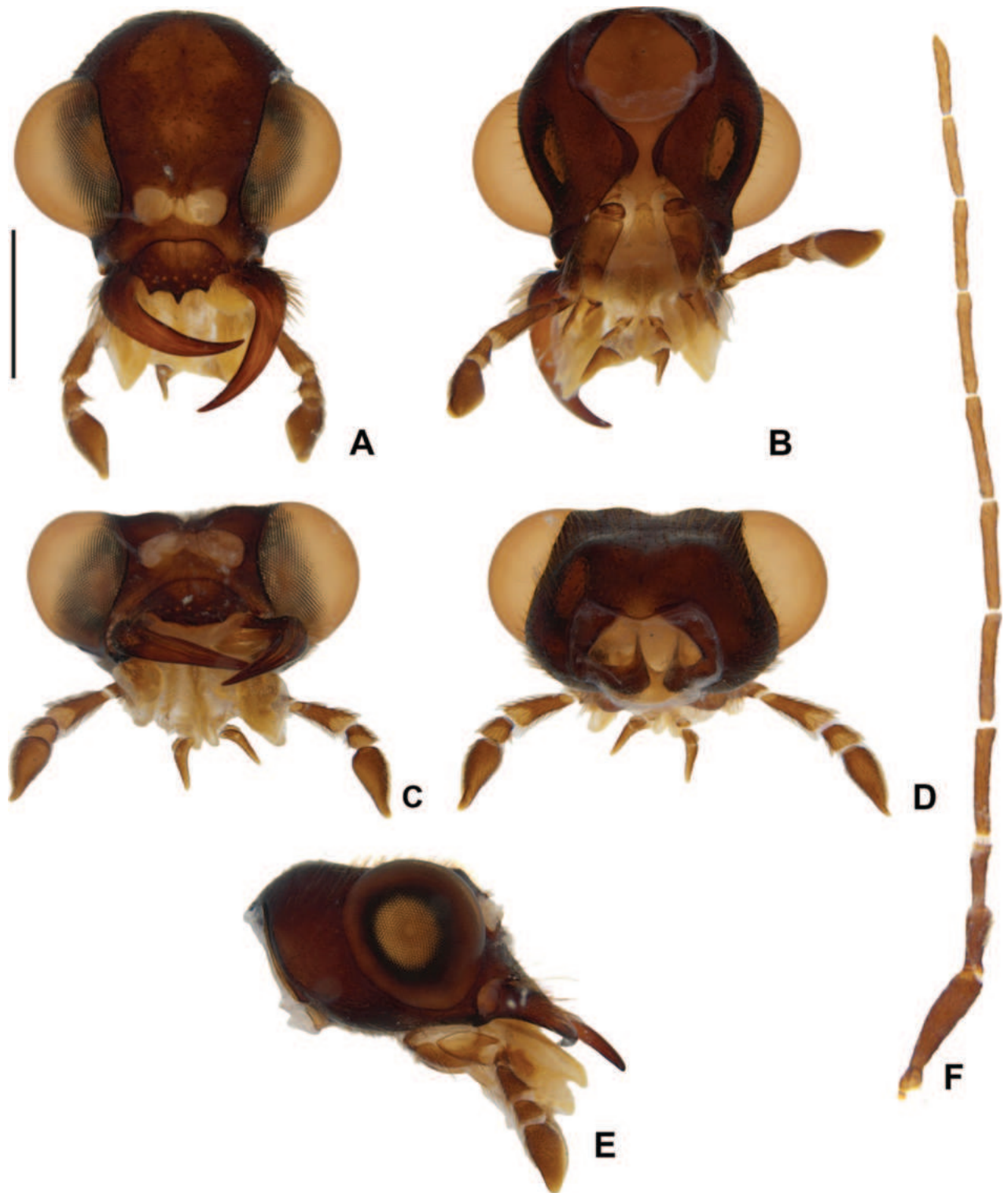


Figure 9. *Photuris elliptica* Olivier, female head **A–E** head capsule: **A** dorsal view **B** ventral view **C** frontal view **D** occipital view **E** lateral view **F** antenna dorsal view. Scale bar: 1 mm.

with one pair of stouter longer seta lateroposteriorly (Fig. 3A). Ventral surface evenly sclerotized, covered with light brown, fine, decumbent and semi-erect setae; laterotergites as long as wide, 0.5–0.8 times as wide as median sternites (widened apicad), inner edge overlapping the lateral edge of the median sternite, posterior edge with 6–7 stouter, longer setae (1.5–2.0 times longer than fine

semi erect seta), posterior angle with one stouter, long seta (about 5.0 times longer than fine semi-erect setae), spiracles on lateral edge at midlength; whitish spot (photic organ) occupying almost entirely the laterotergite VIII; median sternites I–VIII trapezoidal, posterior edge with several stouter setae, two pairs of setae 3–4 times longer than fine semi-erect setae (one pair parasagittal, one pair lateral); median sternite IX 1.5 times longer than VIII; segment X ventroapical, membranous, except for a darkly sclerotized transverse strand; pygopodia finger-like, with several dense rows of minutely sclerotized hooks (Fig. 3B).

Material examined (larvae). BRAZIL – **Minas Gerais** • 19 larvae; Mariana, Vale – Mina Fabrica Nova, cave FN_0005; 20°13'18.36"S, 43°26'2.91"W (WGS84); 2–3.XII.2020; Eq. Spelayon et al. leg; ISLA 83940 (6 larvae 12–14 mm length), ISLA 78905, 83917 [antigo] (1 larvae 4 mm length), ISLA 83939 (5 larvae 10–13 mm length), ISLA 83918 (1 larva 2.5 mm length), ISLA 83913 (1 larva cut in half), ISLA 83919 (1 larva 3.0 mm length), ISLA 83915 (1 larva 11 mm length), ISLA 83916 (3 larvae 4–14 mm); • 6 larvae; same data, but cave FN_0004; 20°13'18.35"S, 43°26'2.63"W (WGS84); 01.XII.2020; ISLA 83934 (1 larva 3 mm length), ISLA 83931 (1 larva 3 mm length), ISLA 83938 (2 larvae 12–13 mm), ISLA 83932 (1 larva 8 mm length) • 1 larva; same data, but cave FN_0027; 20°13'25.55"S, 43°26'15.00"W; 24.IX–09.X.2020; ISLA 83956 (12 mm length) • 1 larvae; same data, but cave FN_0006; 20°13'7.12"S, 43°25'49.72"W (WGS84); ISLA 83957 (10 mm length) • 6 larvae; same data, but cave FN_0025; 20°13'0.57"S, 43°26'35.61"W (WGS84); 24.IX–30.X.2020; ISLA 83947 (1 larva 13 mm length), ISLA 83945 (2 larvae 11–12 mm length), ISLA 83903 (1 larva 11 mm length), ISLA 83946 (2 larvae 10–13 mm length) • 6 larvae; same data, but cave FN_0003; 20°13'19.20"S, 43°26'2.76"W (WGS84); 03–04.XII.2020; ISLA 83926 (1 larva 2.5 mm length); ISLA 83924 (5 larvae 10–13 mm length) • 2 larvae; same data, but cave FN_0002; 20°13'38.49"S, 43°25'52.23"W (WGS84); 04.XII.2020; ISLA 83937 (1 larva 4 mm length), ISLA 83935 (1 larva 11 mm length) • 7 larvae; Dores de Guanhões, G. Energia, cave CAV 05; 19° 1'32.90"S, 42°53'27.24"W (WGS84); 30.I–03.II.2017; Eq. Spelayon et al. leg.; ISLA 52343 (11–13 mm length); • 1 larva; same data, but 29–31.V.2017; ISLA 52341 (13 mm length); • 2 larvae; same data but CAV 008; Lat. 19,0640/Long. 42,9270; ISLA 52344 (7–9 mm length) • 1 larva; same data, but cave DGN005; 19°2'25.09"S, 42°51'54.36"W (WGS84); 11–15.XII.2015; ISLA 45434 (7–10 mm length) • 1 larva; same data but, Energia cave SPT 004; 19°1'42.61"S; 42°55'27.13"W (WGS84); 11–12.XII.2015; ISLA 45513 (8–10 mm length) • 1 larva; same data, but G.E.-S2_NOVA 004; 18°58'59.54"S, 42°55'40.10"W (WGS84); 5–7.VII.2016; ISLA 45596 (5 mm length); • 3 larvae; same data but NOVA_003; 18°59'28.68"S, 42°55'57.75"W (WGS84); ISLA 45595 (6–12 mm length); • 1 larva; same data, but G. Energia SPT 004; 19°1'42.61"S, 42°55'27.13"W (WGS84); 17–20.VII.2015; ISLA 45514 (9 mm length); • 1 larva; same data, but G.Energia, cave DGN 005, DGN005; 19°2'25.09"S, 42°51'54.36"W (WGS84); 19–21.VII.2015; ISLA 45436 (10 mm length) • 2 larvae; Barão dos Cocais, cave CAV 01; 19°59'53.63"S, 43°33'56.52"W (WGS84); 06.III.2016; Fábio Bondezan leg; ISLA 47284 (13 mm length); • 1 larva; same data, but cave RF_0092; 19°55'51.44"S, 43°31'47.09"W (WGS84); 18.IX.2014; Eq. Ativo Ambiental leg.; ISLA 471 (12 mm length); • 1 larva; same data, but CAV 11; 20°0'21.44"S, 43°34'4.08"W (WGS84); 7.III.2016; ISLA 47283 (5 mm length); • 1 larva; São Gonçalo do Rio Abaixo, VALE Brucutu, cave BRU_0002; 19°53'21.55"S, 43°26'16.11"W (WGS84); 16.V.2020; Spelayon

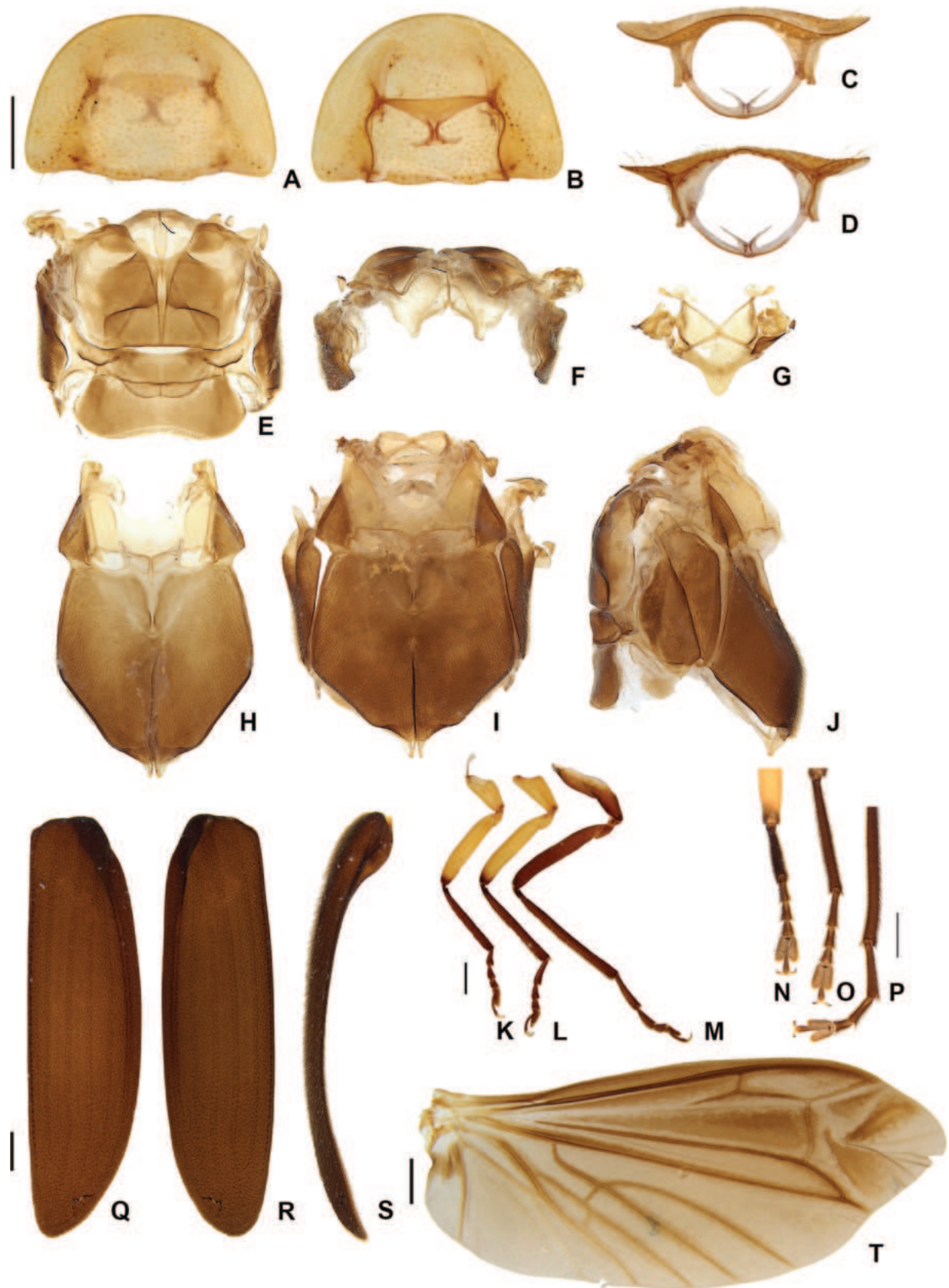


Figure 10. *Photuris elliptica* Olivier, female thorax morphology **A–D** pronotum: **A** dorsal view **B** ventral view **C** anterior view **D** posterior view **E** alinotum dorsal view **F** alinotum anterior view **G** mesoscutellum ventral view **H** meso- and metaventrite ventral view **I** intact pterothorax ventral view **J** intact pterothorax lateral view **K** proleg **L** mesoleg **M** metaleg **N–P** detail of tarsi and claws **N** proleg **O** mesoleg **P** metaleg **Q–S** elytron **Q** dorsal view **R** ventral view **S** lateral view **T** wing. Scale bars: 1 mm.

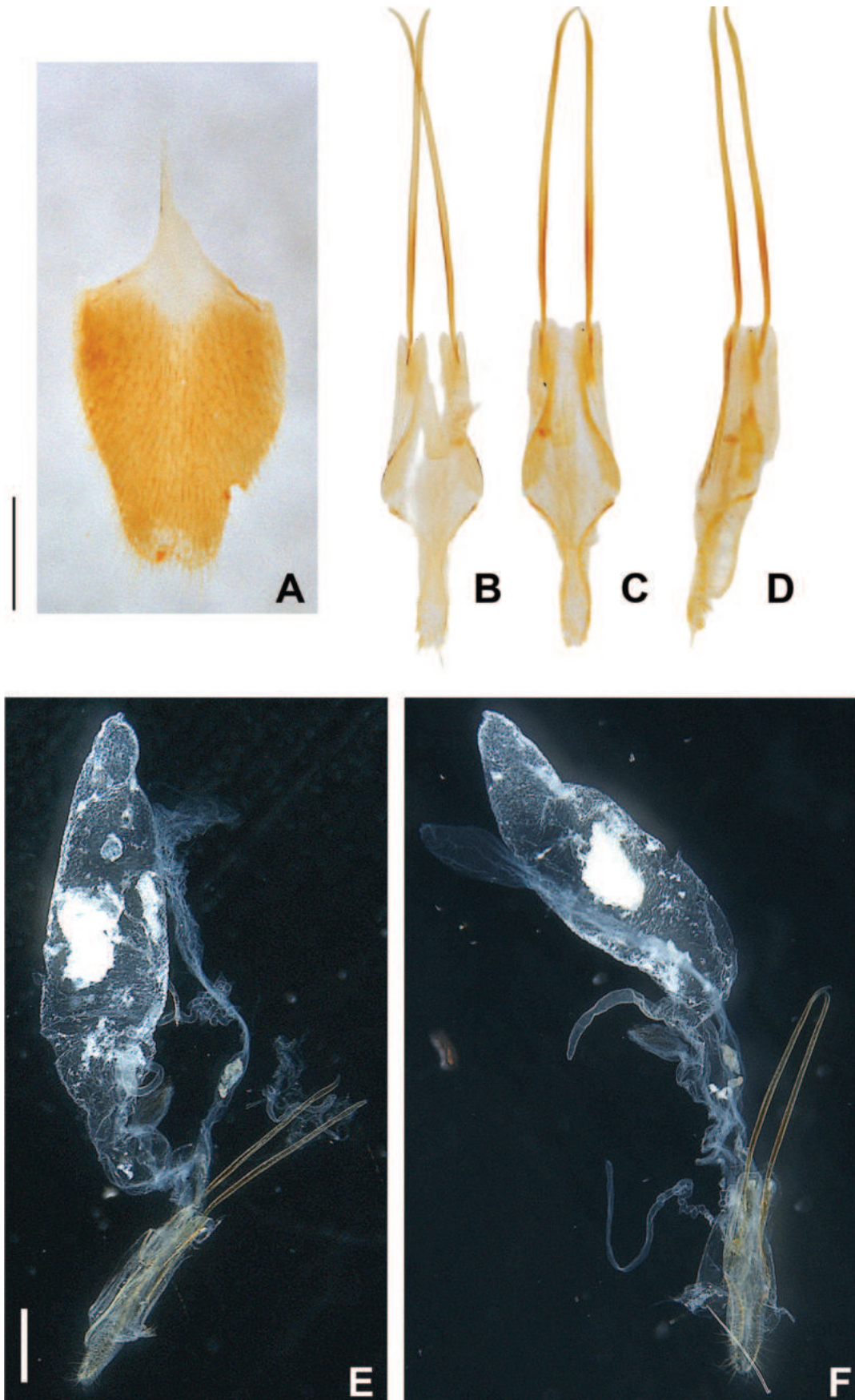


Figure 11. *Photuris elliptica* Olivier, female abdomen **A** sternum VIII ventral view **B–D** ovipositor **B** dorsal view **C** ventral view **D** lateral view **E, F** internal anatomy **E** dorsolateral view **F** lateral view. Scale bars: 0.5 mm.

et al. leg.; ISLA 81940 (7 mm length); • 1 larva; same data, but cave BRU_0008; S 19°52'33.74"S, 43°25'3.11"W (WGS84); 19–23.VIII.2020; ISLA 82162 (11 mm length); • 1 larva; Santana do Riacho, Gruta da Viola; 19°17'44.67"S, 43°37'0.33"W (WGS84); 17.IV.2017; Proj. MG/Rabelo et al. leg.; ISLA 78921 (12 mm length); • 5 larvae; Coração de Jesus, Gruta Sumitumba; 16°39'47.90"S, 44°22'8.42"W (WGS84); 29.I.2015; ISLA 78709 (3 larvae 3–5 mm, 2 larvae 13 mm length) • 1 larva; Lima Duarte, Parque Estadual do Ibitipoca, Gruta Manequinho; 21°43'11.64"S, 43°54'11.16"W (WGS84); ISLA 78708 (10 mm length); • 1 larva; Rio Pardo de Minas, Peixe Bravo, cave Lago; 15°59'55.17"S, 42°44'42.63"W (WGS84); ISLA 78904 (13 mm length).

Biology and life cycle. The larvae of *Photuris elliptica* were collected only inside caves located in different lithologies, mainly ferruginous rocks (mostly), but also limestone, quartzite, and granite (see above). In general, the larvae are found in aphotic zones, under blocks or on the surface where the floor is formed by fine sediment (sand or clay), places where it is possible to build chambers for their metamorphosis. Regarding food, larvae were observed feeding on guano from insectivorous, carnivorous, and hematophagous bats (Fig. 2). Although immature forms are recurrent in caves, adult forms are rarer, and adults are therefore expected to disperse to surface environments after hatching. Inside the cave, bioluminescence was quite difficult to observe. The larvae emitted a very faint greenish light for only a few seconds and then went for a long time without emitting light. The light from the flashlights and human approach (disturbance) seemed to inhibit the larvae from glowing. There were a few observations of luminescence, just after remaining still and keeping the flashlight off for several minutes.

Many larvae of different sizes were collected, but only mature larvae (those one 12–14 mm length) were reared until adult stages, and, thus, we could not count the exact number of instars. Still, compared with *Photuris femoralis*, *P. elliptica* is a little smaller (*P. femoralis* first instar larva is 2.7 mm, 6th instar larva 12.2 mm, adults 10.0–10.6 mm, while *P. elliptica* larvae ranged from 2.5–14.0 mm and adults 12.0–13.0 mm length), suggesting that *P. elliptica* has the same number of larval instars as *P. femoralis* (usually six, rarely seven instars). Thus, we probably examined all larval instars, being first instar 2.5–3.0 mm length and sixth 13.0–14.0 mm length. What is more, this indicates that at least the entire larval stage occurs inside caves.

Distribution (Fig. 12). Most of the observations of the species were made in caves (larvae) and surface ecosystems (epigeal) located in mountainous areas at altitudes of above 1000 m. However, some occurrences were observed in regions at lower altitudes in the north and center-west regions of Minas Gerais. Furthermore, *P. elliptica* species can be found in the Atlantic Forest and Cerrado biomes, located in the states of São Paulo, Rio de Janeiro, and Minas Gerais, Brazil.

Discussion

Are *Photuris elliptica* larvae cave specialists?

Caves have unique environmental conditions that set them apart from surface ecosystems. These conditions include higher humidity, the complete absence of light, and a lower availability of food (Poulson and White 1969; Culver 1982). Thus, cave ecosystems are selective environments where only species with mor-

phological, physiological, or behavioral pre-adaptations can successfully colonize and establish viable populations over time (Culver 1982). However, caves are attractive environments due to the scarcity of specialized predators (Gibert and Deharveng 2002; Fernandes et al. 2016) and, thus, are ideal for laying and development of eggs of those species able to survive in these environments.

Lampyrid larvae occupy a wide array of environments (see above; reviewed by Riley et al. 2021), but our observations are to our knowledge the first report of a

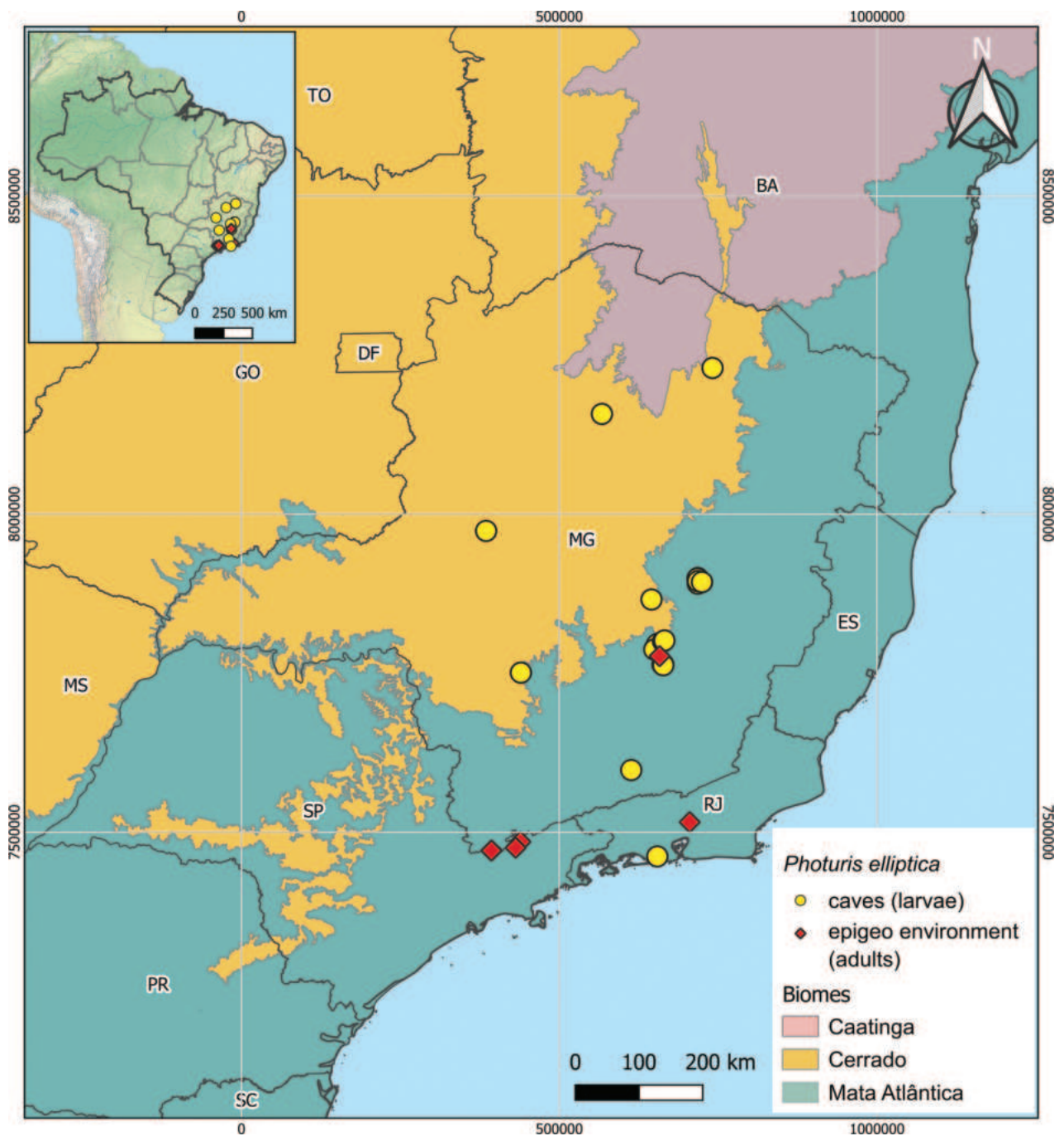


Figure 12. Political and biogeographic map of Brazil, showing the spatial distribution of *Photuris elliptica* Olivier, which occurs in two different Brazilian continental biomes, the Mata Atlântica and Cerrado. Letters on the map correspond to Brazilian states. Abbreviations: BA, Bahia; DF, Distrito Federal; ES, Espírito Santo; GO, Goiás; MG, Minas Gerais; MS, Mato Grosso do Sul; PR, Paraná; RJ, Rio de Janeiro; SC, Santa Catarina; SP São Paulo

lampyrid larvae dwelling in caves. A few traits of this species' larva may be adaptations to a cave life. For instance, the brighter, less pigmented *P. elliptica* larval color pattern could be the outcome of relaxed selection for camouflage patterns in the aphotic zone of caves (Fig. 2). Similar phenotypes are common in cave beetles (e.g. Luo et al. 2018). Likewise, the longer leg setae (Fig. 3E–G) could indicate greater reliance on chemical and physical cues, compared to dwellers of open environments, as found elsewhere in beetles (e.g. Luo et al. 2023). Both observations are yet to be tested by field observations and experiments. Yet, the broader diet of *Photuris* larvae may be a key factor allowing their widespread occurrence in caves.

Caves are oligotrophic environments, with limited availability of food items, partly due to lack of light and, consequently, of photosynthetic organisms (Culver and Pipan 2009). Therefore, cave food webs depend on their connectivity to surrounding surface environments (Kováč 2018). In this context, bat guano is a key source of energy for cave environments.

Photuris are unique among lampyrid larvae in having a comparatively broader menu. Most firefly larvae specialize in gastropods and or/earthworms, whereas *Photuris* larvae will readily eat arthropods, and even plants. For example, Buschman (1984) reported 21 food records from field observations for *Photuris* larvae: five were snails and slugs, 11 were insects (caterpillars, membracids, adult cerambycids, and dipteran larvae), four were fallen berries, and one was an earthworm. Likewise, Faust and Faust (2014) reported *Photuris* larvae eating milkweed rhizomes—a chemically defended plant—and no adverse reactions were observed. All *P. elliptica* larvae in the field were seen eating bat guano, of different kinds (see above), and nothing else, despite the presence of slugs and earthworms. However, it cannot be ruled out that these larvae have a broader menu. In fact, it is yet unknown whether guano is even a preferred rather than tolerated food item. Nevertheless, the fact that these larvae can live on bat guano for several weeks, until they managed to successfully pupate and emerge from the pupa, may facilitate their occurrence in caves.

Most of the larvae analyzed in the present work were collected in ferruginous caves. A possible gateway to caves for *Photuris* larvae would be the roots of trees or even the natural porosity of the rock, especially in iron ore caves, which are often relatively shallow or close to the surface (Ferreira et al. 2015). Thus, generalist organisms such as *Photuris* larvae could easily access and colonize underground environments.

We therefore encourage future firefly surveys to include underground environments, hoping that this will help mitigate the staggering knowledge shortfall on lampyrid larvae, as well as provide a better understanding of the ecological and evolutionary condition of the use of these environments by firefly species.

Conclusions

Photuris elliptica larvae dwell in caves of differing lithologies, where they were observed to feed on bat guano of diverse compositions. Although these larvae have some interesting deviations from other known *Photuris* larvae—including lesser pigmentation and unique or longer setae—it is yet unclear whether they are cave specialists. *Photuris elliptica* adults were rarely seen and are yet to be collected in caves, although they are locally abundant elsewhere in forested sites of the Atlantic rainforest.

Acknowledgements

We thank Muséum national d'Histoire naturelle curators A. Taghavian and A. Mantilleri for hosting L. Silveira and granting access to type materials in 2015 and 2019; Museu Nacional de História Natural e da Ciência de Lisboa (MNHNC, Portugal) for kindly allowing the use of stereoscopic microscopes for dissection of adult specimens, as well as the use of the Leica M165C for photographing them; VALE's speleology management and Spelayon Consultoria that collected part of the specimens, and "Coleção de Invertebrados Subterrâneos de Lavras da Universidade Federal de Lavras", Minas Gerais (ISLA) for sending material. We thank the Center for Functional Ecology – Science for People & the Planet (CFE), University of Coimbra, for financial assistance in publishing this work, and all reviewers and the editor for their insightful and constructive reviews.

Additional information

Conflict of interest

The authors have declared that no competing interests exist.

Ethical statement

No ethical statement was reported.

Funding

SRC and LFLS were funded by NSF#2001683 CSBR: Natural History: Development of the Catamount, and LFLS is now funded by # 2323041 ARTS: Deploying integrative systematics to untangle Lucidota, the Gordian knot of Neotropical firefly taxonomy.

Author contributions

Conceptualization: LFLS, SPR, RAZ, TGGP. Data curation: TGGP, RAZ, PMS, SPR. Formal analysis: SPR, PMS, SCR, RAZ, LFLS. Funding acquisition: PMS. Investigation: SCR, SPR, LFLS, PMS, RAZ. Methodology: PMS, RAZ. Supervision: LFLS. Writing – original draft: LFLS, PMS, SPR, RAZ, SCR. Writing – review and editing: TGGP, RAZ, LFLS, SCR, PMS, SPR.

Author ORCIDs

Paula M. Souto  <https://orcid.org/0000-0001-6995-9146>

Luiz F. L. da Silveira  <https://orcid.org/0000-0002-0648-3993>

Data availability

All of the data that support the findings of this study are available in the main text.

References

- Barber HS (1951) North American fireflies of the genus *Photuris*. Smithsonian Miscellaneous Collections 117: 1–58.
- Buschman LL (1974) Flash behavior of a Nova Scotian firefly, *Photuris fairchildi* Barber, during courtship and aggressive mimicry (Coleoptera, Lampyridae). Coleopterists Bulletin 28(1): 27–31. <https://www.jstor.org/stable/3999531>

- Buschman LL (1984) Larval biology and ecology of *Photuris* fireflies (Lampyridae: Coleoptera) in northcentral Florida. *Journal of the Kansas Entomological Society* 57(1): 7–16. <https://www.jstor.org/stable/25084474>
- Colares C, Roza AS, Mermudes JRM, Silveira LFL, Khattar G, Mayhew PJ, Monteiro RF, Nunes MFSQC, Macedo MV (2021) Elevational specialization and the monitoring of the effects of climate change in insects: Beetles in a Brazilian rainforest mountain. *Ecological Indicators* 120: 106888. <https://doi.org/10.1016/j.ecolind.2020.106888>
- Costa C, Vanin SA, Casari-Chen SA (1988) *Larvas de Coleoptera do Brasil*. Museu de Zoologia, Universidade de São Paulo, São Paulo, 282 pp. <https://doi.org/10.5962/bhl.title.100233>
- Culver DC (1982) *Cave Life*. Harvard University Press, Cambridge, 189 pp. <https://doi.org/10.4159/harvard.9780674330214>
- Culver DC, Pipan T (2009) *The Biology of Caves and Other Subterranean Habitats*. Oxford University Press, Oxford, 259 pp. <https://doi.org/10.1093/oso/9780198820765.001.0001>
- Domagala P, Ghiradella H (1984) Structure and function of the terminal abdominal appendages (pygypodia) of photurid firefly larvae. *The Biological Bulletin* 166(2): 299–309. <https://doi.org/10.2307/1541218>
- Faria LRR, Pie MR, Salles FF, Soares EDG (2021) The Haeckelian shortfall or the tale of the missing semaphoronts. *Journal of Zoological Systematics and Evolutionary Research* 59(2): 359–369. <https://doi.org/10.1111/jzs.12435>
- Faust LF (2017) *Fireflies, Glow-worms, and Lightning Bugs: Identification and Natural History of the Fireflies of the Eastern and Central United States and Canada*. University of Georgia Press, Athens, 360 pp.
- Faust LF, Davis J (2019) A new species of *Photuris* Dejean (Coleoptera: Lampyridae) from a Mississippi cypress swamp, with notes on its behavior. *Coleopterists Bulletin* 73(1): 97–113. <https://doi.org/10.1649/0010-065X-73.1.97>
- Faust L, Faust H (2014) The occurrence and behaviors of North American fireflies (Coleoptera: Lampyridae) on milkweed, *Asclepias syriaca* L. *Coleopterists Bulletin* 68(2): 283–291. <https://doi.org/10.1649/0010-065X-68.2.283>
- Faust LF, De Cock R, Lewis S (2012) Thieves in the night: kleptoparasitism by fireflies in the genus *Photuris* Dejean (Coleoptera: Lampyridae). *Coleopterists Bulletin* 66(1): 1–6. <https://doi.org/10.1649/072.066.0101>
- Fernandes CS, Batalha MA, Bichuette ME (2016) Does the cave environment reduce functional diversity? *PLoS ONE* 11(3): e0151958. <https://doi.org/10.1371/journal.pone.0151958>
- Ferreira RL, Oliveira MPA, Souza-Silva M (2015) Biodiversidade subterrânea em geossistemas ferruginosos. In: Carmo FF, Kamino LHY (Eds) *Geossistemas Ferruginosos do Brasil: áreas prioritárias para conservação da diversidade geológica e biológica, patrimônio cultural e serviços ambientais*. 3i, Belo Horizonte, 195–232.
- Fu X, Ballantyne L (2021) Reproductive systems, transfer and digestion of spermatozoa in two Asian Luciolinae fireflies (Coleoptera: Lampyridae). *Insects* 12(4): 365. <https://doi.org/10.3390/insects12040365>
- Gibert J, Deharveng L (2002) Subterranean ecosystems: A truncated functional biodiversity. *Bioscience* 52(6): 473–481. [https://doi.org/10.1641/0006-3568\(2002\)052\[0473:SEATFB\]2.0.CO;2](https://doi.org/10.1641/0006-3568(2002)052[0473:SEATFB]2.0.CO;2)
- Heckscher CM (2021) Four new species of North American fireflies from isolated peatlands with reference to species determination of *Photuris* Dejean (Coleoptera: Lampyridae). *Northeastern Naturalist* 28(3): 277–295. <https://doi.org/10.1656/045.028.0304>

- Heckscher CM (2023) Two new species of mid-Atlantic *Photuris* Fireflies (Coleoptera: Lampyridae) from Pennsylvania and Delaware. *Northeastern Naturalist* 30(4): 440–448. <https://doi.org/10.1656/045.030.0407>
- Kawada R, Buffington ML (2016) A scalable and modular dome illumination system for scientific microphotography on a budget. *PLoS ONE* 11(5): e0153426. <https://doi.org/10.1371/journal.pone.0153426>
- Kováč L (2018) Caves as oligotrophic ecosystems. In: Moldovan OT, Kováč L, Halse S (Eds) *Cave Ecology*. Springer, Cham, 297–307. <https://doi.org/10.1007/978-3-319-98852-8>
- Lloyd JE (1965) Aggressive mimicry in *Photuris*: Firefly femmes fatales. *Science* 149(3684): 653–654. <https://doi.org/10.1126/science.149.3684.653>
- Lloyd JE (2018) *A Naturalist's Long Walk Among Shadows: of North American Photuris – Patterns, Outlines, Silhouettes ... Echoes*. 2nd edn. Self-published, Gainesville, 477 pp. <https://entnemdept.ufl.edu/lloyd/firefly/>
- Lloyd JE, Ballantyne LA (2003) Taxonomy and behavior of *Photuris trivittata* sp. n. (Coleoptera: Lampyridae: Photurinae); redescription of *Aspisoma trilineata* (Say) comb. n. (Coleoptera: Lampyridae: Lampyrinae: Cratomorphini). *The Florida Entomologist* 86(4): 464–473. [https://doi.org/10.1653/0015-4040\(2003\)086\[0464:TABOPT\]2.0.CO;2](https://doi.org/10.1653/0015-4040(2003)086[0464:TABOPT]2.0.CO;2)
- Luo XZ, Wipfler B, Ribera I, Liang HB, Tian MY, Ge SQ, Beutel RG (2018) The thoracic morphology of cave-dwelling and free-living ground beetles from China (Coleoptera, Carabidae, Trechinae). *Arthropod Structure & Development* 47(6): 662–674. <https://doi.org/10.1016/j.asd.2018.09.001>
- Luo XZ, Gabelaia M, Faille A, Beutel R, Ribera I, Wipfler B (2023) New insights into the evolution of the surface antennal sensory equipment in free-living and cave-dwelling beetles (Leiodidae: Leptodirini). *Arthropod Systematics & Phylogeny* 81: 1089–1102. <https://doi.org/10.3897/asp.81.e98166>
- Maquitico Y, Vergara A, Villanueva I, Camacho J, Cordero C (2022) *Photuris lugubris* female fireflies hunt males of the synchronous firefly *Photinus palaciosi* (Coleoptera: Lampyridae). *Insects* 13(10): 915. <https://doi.org/10.3390/insects13100915>
- McDermott FA (1966) Lampyridae. In: Steel OW (Ed.) *Coleopterorum Catalogus Supplementa*. Pars 9 (editio secunda). W. Junk, 's-Gravenhage, 149 pp.
- McDermott FA (1967) The North American fireflies of the genus *Photuris* DeJean, a modification of Barber's Key (Coleoptera; Lampyridae). *Coleopterists Bulletin* 21: 106–116. <https://www.jstor.org/stable/3999313>
- Murphy F, Moiseff A (2019) Anatomy of the stemmata in the *Photuris* firefly larva. *Journal of Comparative Physiology. A, Neuroethology, Sensory, Neural, and Behavioral Physiology* 205(1): 151–161. <https://doi.org/10.1007/s00359-018-01312-2>
- Novák M (2018) Redescription of immature stages of central European fireflies, part 2: *Lamprohiza splendidula* (Linnaeus, 1767) larva, pupa and notes on its life cycle and behaviour (Coleoptera: Lampyridae). *Zootaxa* 4378(4): 516–532. <https://doi.org/10.11646/zootaxa.4378.4.4>
- Oertel D, Linberg KA, Case JF (1975) Ultrastructure of the larval firefly light organ as related to control of light emission. *Cell and Tissue Research* 164(1): 27–44. <https://doi.org/10.1007/BF00221693>
- Olivier E (1886) Études sur les lampyrides. II. *Annales de la Société Entomologique de France* 6(6): 201–216.
- Perez-Hernandez CX, Zaragoza-Caballero S, Romo-Galicia A (2022) Updated checklist of the fireflies (Coleoptera: Lampyridae) of Mexico. *Zootaxa* 5092(3): 291–317. <https://doi.org/10.11646/zootaxa.5092.3.3>

- Poulson TL, White WB (1969) The cave environment. *Science* 165(3897): 971–981. <https://doi.org/10.1126/science.165.3897.971>
- Riley WB, Rosa SP, Silveira LFL (2021) A comprehensive review and call for studies on firefly larvae. *PeerJ* 9: e12121. <https://doi.org/10.7717/peerj.12121>
- Rosa SP (2007) Description of *Photuris fulvipes* (Blanchard) immatures (Coleoptera, Lampyridae, Photurinae) and bionomic aspects under laboratory conditions. *Revista Brasileira de Entomologia* 51(2): 125–130. <https://doi.org/10.1590/S0085-56262007000200001>
- Silveira LFL, Khattar G, Vaz S, Wilson VA, Souto PM, Mermudes JRM, Stanger-Hall KF, Macedo MV, Monteiro RF (2020) Natural history of the fireflies of the Serra dos Órgãos mountain range (Brazil: Rio de Janeiro) – one of the ‘hottest’ firefly spots on Earth, with a key to genera (Coleoptera: Lampyridae). *Journal of Natural History* 54(5–6): 275–308. <https://doi.org/10.1080/00222933.2020.1749323>
- Smith DS (1963) The organization and innervation of the luminescent organ in a firefly, *Photuris pennsylvanica* (Coleoptera). *The Journal of Cell Biology* 16(2): 323–359. <https://doi.org/10.1083/jcb.16.2.323>
- Souto PM, Campello L, Khattar G, Mermudes JRM, Monteiro RF, Silveira LFL (2019) How to design a predatory firefly? Lessons from the Photurinae (Coleoptera: Lampyridae). *Zoologischer Anzeiger* 278: 1–13. <https://doi.org/10.1016/j.jcz.2018.10.006>
- Strause LG, DeLuca M, Case JF (1979) Biochemical and morphological changes accompanying light organ development in the firefly, *Photuris pennsylvanica*. *Journal of Insect Physiology* 25(4): 339–347. [https://doi.org/10.1016/0022-1910\(79\)90022-2](https://doi.org/10.1016/0022-1910(79)90022-2)
- Zaragoza-Caballero S (1995) La familia Lampyridae (Coleoptera) en la Estación de Biología Tropical “Los Tuxtlas”. *Publicaciones especiales del Instituto de Biología. Unam* 14: 7–93.
- Zeballos LF, Roza AS, Campello-Gonçalves L, Vaz S, Da Fonseca CRV, Rivera SC, Silveira LFL (2023) Phylogeny of *Scissicauda* species, with eight new species, including the first Photinini fireflies with biflabellate antennae (Coleoptera: Lampyridae). *Diversity* 15(5): 620. <https://doi.org/10.3390/d15050620>

An integrated taxonomic revision of *Ctonoxylon* (Coleoptera, Curculionidae, Scolytinae) reveals new Malagasy species originating from multiple recent colonisations of the island

Bjarte H. Jordal¹ 

¹ Department of Natural History, University Museum of Bergen, University of Bergen, P.O. 7800, NO-5020 Bergen, Norway
Corresponding author: Bjarte H. Jordal (bjarte.jordal@uib.no)

Abstract

Ctonoxylon is a strictly Afrotropical genus of bark beetles breeding under bark of rainforest trees and lianas. A taxonomic revision of the genus included a molecular phylogenetic analysis of ten species based on three gene fragments and was compared to a morphology-based tree topology for all 24 currently recognised species. Four species are described as new to science: *Ctonoxylon torquatum*, **sp. nov.**, *Ctonoxylon tuberculatum*, **sp. nov.**, *Ctonoxylon quadrispinum*, **sp. nov.**, all from Madagascar, and *Ctonoxylon pilosum*, **sp. nov.** from Cameroon. *Ctonoxylon hirsutum* Hagedorn, 1910, **stat. rev.** is resurrected from synonymy with *C. flavescens* Hagedorn, 1910, and *C. atrum* Browne, 1965 **stat. rev.** from its synonymy with *C. methneri* Eggers, 1922 (as *C. hamatum* Schedl, 1941). The following species have new synonymies suggested: *Ctonoxylon festivum* Schedl, 1941 (= *C. dentigerum* Schedl, 1941, **syn. nov.**), *C. methneri* Eggers, 1922 (= *C. hamatum* Schedl, 1941, **syn. nov.**, = *C. griseum* Schedl, 1941, **syn. nov.**), *C. montanum* Eggers, 1922 (= *C. longipilum* Eggers, 1935, **syn. nov.**, = *C. nodosum* Eggers, 1940, **syn. nov.**), *C. camerunum* Hagedorn, 1910 (= *C. conradti* Schedl, 1939, **syn. nov.**), and *C. spinifer* Eggers, 1920 (= *C. setifer* Eggers, 1920, **syn. nov.**). New country records are noted for *C. festivum* (Tanzania), *C. flavescens* (Uganda), *C. camerunum* (Liberia), *C. crenatum* Hagedorn, 1910 (Democratic Republic of the Congo), *C. spathifer* Schedl, 1941 (Ghana), *C. atrum* (Cameroon), and *C. spinifer* (Madagascar), with patterns in distribution and colonisation of Madagascar discussed. An identification key with pictures of all species is provided.

Key words: Afrotropical, bark beetles, biogeography, Madagascar, taxonomy, Xyloctonini



Academic editor:

Miguel Alonso-Zarazaga
Received: 22 March 2024
Accepted: 10 May 2024
Published: 28 May 2024

ZooBank: <https://zoobank.org/6FE93D4B-8104-45F4-850A-C1B78CA10A9D>

Citation: Jordal BH (2024) An integrated taxonomic revision of *Ctonoxylon* (Coleoptera, Curculionidae, Scolytinae) reveals new Malagasy species originating from multiple recent colonisations of the island. ZooKeys 1203: 95–130. <https://doi.org/10.3897/zookeys.1203.123757>

Copyright: © Bjarte H. Jordal.
This is an open access article distributed under terms of the Creative Commons Attribution License (Attribution 4.0 International – CC BY 4.0).

Introduction

The Afrotropical genus *Ctonoxylon* Hagedorn, 1910 is a member of the bark beetle tribe Xyloctonini Eichhoff, 1878. Although some dubious records have been noted from Madagascar (Schedl 1977), the large majority of collections are from western parts of Africa and particularly the Congolese basin (Schedl 1956, 1957, 1961). Only two species are restricted to the eastern Zambezi and southern African parts of the Afrotropics and five primarily western species extend their distribution to the eastern tropical Africa (Table 1). As for most Afrotropical bark beetles, knowledge about this genus was previously limited to a few commonly collected species.

Table 1. Currently valid species of *Ctonoxylon* Hagedorn, and their validated distribution (DRC = Democratic Republic of the Congo).

<i>Ctonoxylon acuminatum</i> Schedl, 1957	Nigeria, DRC (Dem. Rep. Congo)
<i>Ctonoxylon amanicum</i> Hagedorn, 1912	Cameroon, Tanzania
<i>Ctonoxylon atrum</i> Browne, 1965	Cameroon, Nigeria
<i>Ctonoxylon auratum</i> Hagedorn, 1910	Cameroon, DRC
<i>Ctonoxylon bosqueiae</i> Schedl, 1962	Ghana
<i>Ctonoxylon camerunum</i> Hagedorn, 1910	Ivory Coast, Ghana, Nigeria, Cameroon, DRC
<i>Ctonoxylon caudatum</i> Schedl, 1971	DRC
<i>Ctonoxylon cornutum</i> Eggers, 1943	Cameroon
<i>Ctonoxylon crenatum</i> Hagedorn, 1910	Nigeria, Cameroon
<i>Ctonoxylon festivum</i> Schedl, 1941	Cameroon, Eq. Guinea
<i>Ctonoxylon flavescens</i> Hagedorn, 1910	Tropical/subtropical Africa
<i>Ctonoxylon hirsutum</i> Hagedorn, 1910	Ghana, Cameroon
<i>Ctonoxylon hirtellum</i> Schedl, 1971	DRC
<i>Ctonoxylon kivuensis</i> Schedl, 1957	DRC
<i>Ctonoxylon methneri</i> Eggers, 1922	Kenya, Tanzania, S. Africa
<i>Ctonoxylon montanum</i> Eggers, 1922	Tropical Africa
<i>Ctonoxylon pilosum</i> Jordal, sp. nov.	Cameroon
<i>Ctonoxylon pygmaeum</i> Eggers, 1920	Cameroon
<i>Ctonoxylon quadrispinum</i> Jordal, sp. nov.	Madagascar
<i>Ctonoxylon spathifer</i> Schedl, 1951	Ivory Coast, Tanzania
<i>Ctonoxylon spinifer</i> Eggers, 1920	Tropical Africa, Madagascar
<i>Ctonoxylon torquatum</i> Jordal, sp. nov.	Madagascar
<i>Ctonoxylon tuberculatum</i> Jordal, sp. nov.	Madagascar
<i>Ctonoxylon uniseriatum</i> Schedl, 1965	Namibia, S. Africa

Ctonoxylon is a peculiar group of species which are readily recognised by having divided eyes, a rounded pea-like body shape, impressions on lateral sclerites of the metathorax to accommodate the legs in resting position, and likewise, their tibiae have furrows for hiding the tarsi. As in the similar and related genera *Xyloctonus* Eichhoff, 1872, *Cryphalomimus* Eggers, 1927 and *Scolytomimus* Blandford, 1895, they have evident behavioural and morphological adaptations to avoid predators such as ants (Jordal 2024). The odd morphology inspired Eichhoff (1878), Hopkins (1915), and Schedl (1961) to elevate the tribe to subfamily or family status.

Ctonoxylon is the sister group to three other genera in subtribe Xyloctonina, based on molecular and morphological phylogenetic analyses (Jordal 2023, 2024), and is the most species rich. Approximately 29 species are listed in Wood and Bright (1992), with a few synonyms subsequently suggested or restated by Beaver (2011). Many more synonyms and new species are anticipated. Very few taxonomic revisions have been made over the last century, with mainly single species descriptions published and no keys were ever produced to enable proper identification of species. This study revises the genus, describes four species as new to science, and summarises known ecological and biological features of the genus. Three dozen new records are reported, many with new country or host plant records. An identification key is provided and is illustrated by photos of all species.

Materials and methods

Type material and newly recorded samples were studied and deposited in the following collections:

CAS	California Academy of Science, San Francisco, USA
CMNC	Canadian Museum of Nature, Ottawa, Canada
MNHN	Muséum National d'Histoire Naturelle, Paris, France
MSUC	Michigan State University, AJ Cook arthropod research collection, East Lansing, USA
NHMK	The Natural History Museum, London, UK
NHMW	Naturhistorisches Museum, Vienna, Austria
RMCA	Musee Royal de l'Afrique Centrale, Tervuren, Belgium
SDEI	Senckenberg Deutsches Entomologisches Institut, Munchenberg, Germany
USNM	National Museum of Natural History, Washington D.C., USA
ZFMK	Zoologisches Forschungsmuseum "Alexander Koenig", Bonn, Germany
ZMHB	Museum für Naturkunde der Humboldt-Universität, Berlin, Germany
ZMUB	University Museum of Bergen, Norway

New specimens were collected during several field expeditions to Madagascar and to several African countries between 2006 and 2019. A few unidentified samples were collected by other researchers, in flight intercept or Malaise traps, or by light traps. Beetles collected by the author were dissected from dead woody materials, including lianas, seeds, twigs, branches, and tree trunks. Due to the distinct engravings by the beetles under bark, or in the wood, their family structure, brood size and stage was noted, and whether or not parents stayed with their progeny during their development.

Morphological characters which are important for distinguishing species groups were included in a phylogenetic analysis (Tables 2, 3). Several of these characters are, despite their peculiar expression, new in taxonomic work on the genus. All *Ctonoxylon* species have divided eyes but the distance between the eyes varies much more than previously reported (Figs 1–6). Certain groups also have an eye scraper associated with the eye partition; it is shaped as a projection from the anterior lateral margin of the prothorax and fits in line with a tiny carina located between the two eye parts (Figs 1, 2). Another overlooked character includes a circular or slightly transverse groove just above the procoxa, reminiscent of a mycangium (Figs 5–7). It is not evident which purpose this groove may have, if any. Just above the procoxa, but in front of the just mentioned groove, a remarkable feature appears in some species in which they have a pitted collar running along the anterior margin of the prothorax (Figs 3–6). Other species have just a single vertically elongated pit (Fig. 7) or a longer groove parallel to the front margin (Fig. 3). Yet another group of species have in the same position a long vertical carina, replacing the groove or series of pits.

Phylogenetic analyses of molecular and morphological data were executed in MrBayes. Molecular data from the three gene fragments mitochondrial cytochrome oxidase 1 (COI), elongation factor 1 alpha (EF-1a), and the large ribosomal subunit (28S), were previously analysed and reported in Jordal (2023). New morphological data were analysed with MrBayes using 5 million

Table 2. Morphological characters coded for *Ctonoxylon* and hypothetical outgroup.

1. Eyes: 0, each eye part separated by little more than scapus thickness; 1, separated by width of upper eye or more.
2. Eye scraper on the prothorax margin: 0, absent; 1, a small, rounded nodule; 2, an acuminate shaped tooth.
3. Frons vestiture: 0, fine hair-like setae; 1, scale-like setae; 2, glabrous.
4. Anterior margin of the pronotum: 0, smooth; 1, with a single fused tooth; 2, with pair of sub-contiguous teeth; 3, with four teeth.
5. Pronotal setae: 0, fine hair-like setae only; 1, scattered coarse setae, sometimes mixed with finer setae; 2, glabrous.
6. Just inside the anterior lateral margin of the prothorax: 0=smooth; 1, long carina from eye scraper to procoxa; 2, carina replaced by an elongated cavity; 3, replaced by a series of deep pits.
7. Propleuron, just above procoxa: 0, smooth; 1, with deep elongate or circular pit.
8. Main setae on the elytral interstriae: 0, hairlike; 1, scalelike; 2, absent.
9. Interstitial ground vestiture: 0, hair-like; 1, scale-like; 2, absent.
10. Elytral apex: 0, emarginate; 1, rounded; 2, pronged.
11. Setae on the posterior part of the metaventrite: 0, hairlike; 1, short and broad; 2, very long and broad.
12. Metaventrite: 0, smooth; 1, with a vertical curved swollen edge demarcating the posterior position of the mesotibia.
13. Elytral suture locking mechanism: 0, normal straight; 1, buckled suture at elytral midlength.
14. Protibial groove on its anterior face: 0, tiny or absent; 1, shallow, no more than half the width of protibia; 2, as deep as width of tibia.

Table 3. Data matrix based on coded character states from Table 2.

outgroup	0	0	0	0	0	0	0	0	0	0	0	0	0	0	0	0	0	0	0
<i>Ctonoxylon hirtellum</i>	0	0	0	2	0	1	0	0	2	0	0	1	0	2					
<i>C. festivum</i>	1	2	0	2	0	1	0	0	0	0	0	1	0	2					
<i>C. flavescens</i>	1	2	0	2	0	1	0	0	2	0	0	1	0	2					
<i>C. tuberculatum</i>	1	2	0	2	0	1	0	0	2	0	0	1	0	2					
<i>C. hirsutum</i>	1	2	0	2	0	1	0	0	0	0	0	1	0	2					
<i>C. bosqueiae</i>	1	2	0	2	0	1	0	0	2	0	0	1	0	2					
<i>C. montanum</i>	1	2	0	2	0	1	0	0	2	2	0	1	0	2					
<i>C. cornutum</i>	1	2	0	2	0	1	0	1	1	0	1	1	1	2					
<i>C. camerunum</i>	1	2	0	2	0	1	0	1	1	0	1	1	1	2					
<i>C. torquatum</i>	0	0	0	2	0	3	1	1	1	2	0	0	0	1					
<i>C. pilosum</i>	0	0	0	2	0	3	1	1	0	0	0	0	0	1					
<i>C. auratum</i>	0	0	1	1	0	3	1	1	0	0	0	0	0	1					
<i>C. caudatum</i>	1	1	2	2	2	2	1	1	1	2	0	0	0	1					
<i>C. pygmaeum</i>	0	1	2	2	1	3	1	1	2	2	0	0	1	2					
<i>C. crenatum</i>	1	1	0	2	2	2	1	2	2	2	0	0	0	?					
<i>C. kivuensis</i>	1	1	0	2	0	2	1	0	2	1	0	0	0	?					
<i>C. spathifer</i>	1	0	0	1	0	2	1	1	1	1	0	0	0	1					
<i>C. quadrispinum</i>	1	1	0	4	0	2	1	1	1	0	0	0	1	2					
<i>C. methneri</i>	1	1	0	2	0	2	1	1	1	0	1	0	1	2					
<i>C. atrum</i>	1	1	0	2	0	2	1	1	1	0	1	0	1	2					
<i>C. acuminatum</i>	1	1	0	2	0	2	1	1	2	1	0	0	1	2					
<i>C. amanicum</i>	0	0	1	2	1	2	1	1	2	1	2	0	1	2					
<i>C. spinifer</i>	1	1	1	2	1	2	1	1	2	1	2	0	1	2					
<i>C. uniseriatum</i>	1	0	1	2	1	2	1	1	2	1	2	0	1	2					

generations of four chains run in parallel with one cold chain of $\text{temp}=0.3$; character variation followed a gamma distribution of variable rates. These data were also analysed by parsimony in PAUP* using implied weighting (e.g., in Goloboff et al. 2018) to increase resolution in the tree topology.

Biogeographical inference is based on a recently published study (Jordal 2024) on the related genus *Xyloctonus*. The definition of ancestral areas is based on a statistical clustering algorithm for plants and four animal groups (Linder et al. 2012). This classification is very similar to more traditional classifications (e.g. Morrone and Ebach 2022) but is firmly founded on statistical similarity in fauna and flora.

Results and discussion

Phylogeny and biogeography

Bayesian and parsimony analyses of 14 morphological characters coded for all valid species in the genus resulted in a poorly resolved tree topology. Using implied weights, the parsimony tree was more fully resolved (Fig. 10). A dichotomy appeared between a group of taxa related to *C. flavescens*, and taxa related to *C. methneri*, respectively. Species in these two clades differ consistently by the presence of a carina along the anterior lateral margin of the prothorax as seen in the *flavescens* group (versus grooves or deep pits), in the absence of a propleural pit above the procoxae as seen in all species in the *methneri* clade, and the demarcation of the mesotibiae in resting position in the *flavescens* clade, which imprints a glabrous and swollen area on the anterior half of the metaventricle and metanepisternum. Species in the *flavescens* group, with one exception, have a sharp eye scraper pointing from the anterior lateral margin of the prothorax, in line with a fine horizontal carina between the two eye parts (Fig. 1).

Bayesian analysis of nucleotides from three gene fragments partially supported the two main groups described above (Fig. 11). A major difference from the morphological analyses was the grouping of *C. uniseriatum*, *C. spinifer*, and *C. amanicum* as sister to the *flavescens* group, albeit without any strong node support. The separation of *C. pilosum* sp. nov. and a group consisting of *C. methneri*, *C. atrum*, and *C. quadrispinum* is also consistent with morphology. It is furthermore notable that *C. atrum* separates from *C. methneri*, with which it was previously synonymised, and instead forms a sister relationship with *C. quadrispinum* sp. nov., documenting considerable genetic divergence between the three species. A similar degree of genetic divergence was found between the morphologically very similar species in the *flavescens* clade (Table 4), and in the *spinifer* clade (Fig. 11). These data suggest that rather minor morphological variation warrants studies on genetics to test species validity and potential cryptic speciation.

Recent biogeographical and phylogenetic analysis of Xyloctonini (Jordal 2023, 2024), including the morphology-based analyses in this study (Fig. 10), revealed three putatively recent origins of undescribed species in Madagascar. Reconstruction of ancestral areas using molecular data for two of these species strongly supported a Congolese distribution of their ancestors. This is also the most likely hypothesis for the third species, *C. torquatum* sp. nov., for which DNA data was not possible to obtain. Based on morphological analysis, this species is closely related to the two Congolese species *C. auratum* and *C. pilosum* sp. nov., strongly suggesting an origin in that area.

Biology

All species of *Ctonoxylon* observed in the field during this study established monogynous pairs under bark. The female first initiated a tunnel opening and thereafter let one of the many wandering males mates with her, in or near the entrance. The male stayed with the female for some time during which the female engraved a tunnel where eggs were laid in designated pits along the tunnel wall. In two species the tunnel was made longitudinally to the wood grain, whereas in three other species they cut tunnels transversely to the grain (Table 5). Brood sizes ranged from fewer than 10 eggs up to more than 50 and did not generally correlate with host plant diameter, except always low for *C. uniseriatum* breeding in very thin lianas. Males left the tunnel system early in all observed species, usually before the first eggs hatched, otherwise at early larval stage. The female also left her offspring before they were completely developed, approximately at late larval or pupal stage.

Host plants were rarely identified in past studies, but host selection appears to be broad in *C. flavescens*, and in this study always found in branches of fallen trees. One of the host plant families previously recorded for this species, Apocynaceae, was also recorded for *C. acuminatum* (see Schedl 1961), which may indicate some generality across species. It should also be noted that *C. flavescens* has been recorded most frequently from fig trees, indicating a likely important host plant. Similarly, *C. methneri* was in this study repeatedly collected from cape olive trees (*Olea capensis* L.), where they often breed in huge trunks with very thick bark. Yet other species, such as *C. uniseriatum*, *C. amanicum* and *C. quadrispinum*, were found only in thin lianas, demonstrating huge variability in host preferences across the genus.

Table 4. Genetic distances for species in the *C. flavescens* complex. COI p-distances in the lower left triangle, and 28S p-distances in upper right. The two samples of *C. flavescens* are from Uganda (U) and Cameroon (C).

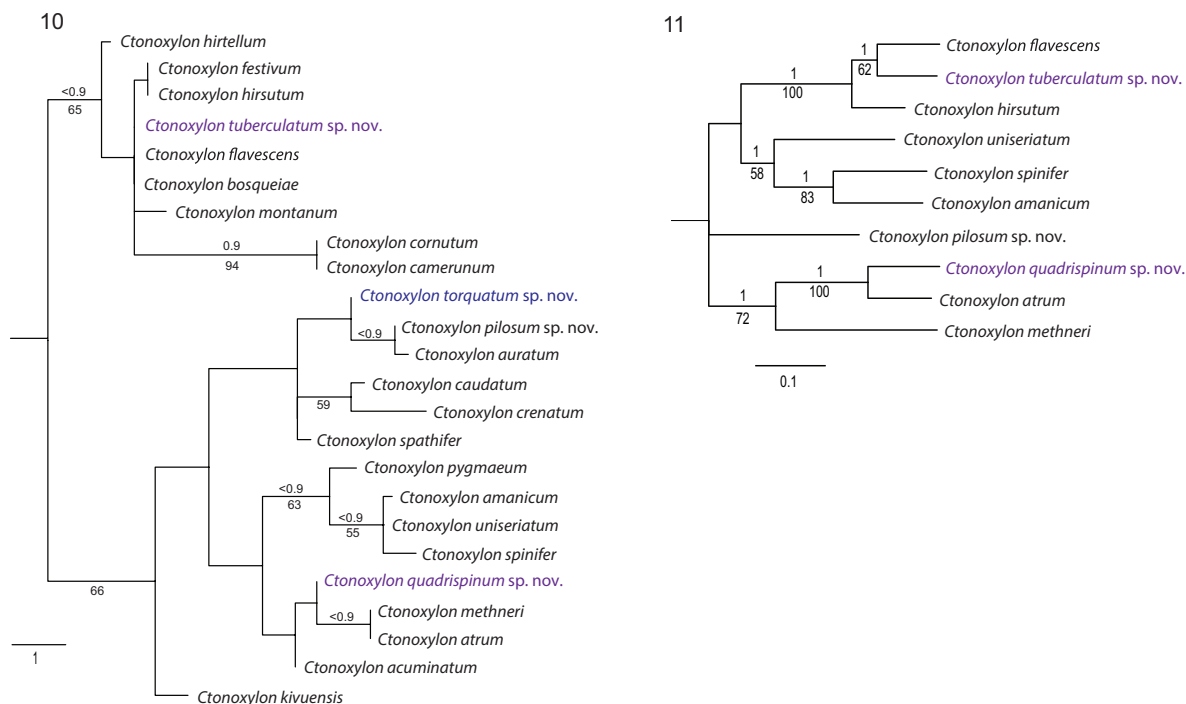
		28S			
		<i>flavescens</i> - U	<i>flavescens</i> - C	<i>hirsutum</i>	<i>tuberculatum</i>
COI	<i>flavescens</i> - U	–	0.0	2.6	1.8
	<i>flavescens</i> - C	10.3	–	2.6	1.8
	<i>hirsutum</i>	16.3	15.4	–	1.0
	<i>tuberculatum</i>	13.2	12.2	14.9	–

Table 5. Reproductive biology observed for *Ctonoxylon* species (*records from Schedl 1961). All observed species form monogynous pairs at the early stage of mating and egg laying. The two last columns indicate the offspring developmental stage where parents have permanently left the nest.

Species	Host family (majority)	Diam (cm)	egg tunnel direction	Brood size	males leave	females leave
<i>Ctonoxylon acuminatum</i> *	Apocynaceae	5	transverse	36		
<i>Ctonoxylon amanicum</i>	(liana)	0.6–2.0	irregular			
<i>Ctonoxylon flavescens</i>	Moraceae	15	longitudinal	19–23	egg	pupa
	Malvaceae	7	longitudinal	20–30	larva	
	Apocynaceae*	2–4	longitudinal	30–45		
<i>Ctonoxylon methneri</i>	Oleaceae	2–60	transverse	8–48	egg	larva
<i>Ctonoxylon quadrispinum</i>	(liana)	4	transverse	50–60		pupa?
<i>Ctonoxylon uniseriatum</i>	(liana)	0.8–3	longitudinal	3–8	egg	larva



Figures 1–9. Novel characters in the identification of *Ctonoxylon* species. Curly brackets illustrate **1** widely separated eye parts and **4** a narrow separation by less than half the size of upper part. Black arrows indicate **1** a sharply pointed eye scraper or **6** a reduced and rounded nodule. White arrows indicate **1–2** the position of a sharp carina running from just above the eye scraper to procoxa, or in that same position **3** an elongated groove, or **4–6** a series of deep pits. Yellow arrows indicate **5–7** the position of a propleural pit. Dark blue arrow **8** points at the swollen mark from the mesotibia's resting position. The pale blue arrow **9** indicates unusually broad and elongated setae on the posterior part of the metaventrite.



Figures 10–11. Phylogeny of *Ctonoxylon*. Node support is given as posterior probabilities above and parsimony bootstrap values below nodes **10** tree topology resulting from the parsimony analysis of 14 morphological characters for all species using implied weighting (Goloboff et al. 2018) **11** partial tree topology redrawn from a previously published Bayesian tree topology based on 1958 nucleotide position from three gene fragments (Jordal 2023). Species found in Madagascar marked in purple.

Taxonomy

Genus *Ctonoxylon* Hagedorn, 1910

Type species. *Ctonoxylon auratum* Hagedorn, 1910: 4, subsequent designation by Hopkins (1914): 119.

Diagnosis. Typical for subtribe Xyloctonina, with stout and rounded body shape, eyes divided, and protibia on its anterior face with a deep groove. Antennal funiculus 7-segmented, club with oblique lateral septum, sutures faint or obscure, asymmetrical; pronotum with pair of teeth in females at the anterior margin, in males just behind anterior margin, teeth occasionally fused, or divided into four parts. Elytral declivity steep, abdominal ventrites flat or gently rising towards elytral apex.

Sexual dimorphism. Dimorphism between males and females has not been clearly formulated in previous work. Nevertheless, the male pronotum has a pair of raised teeth located a little behind the front margin whereas the females have the pair of teeth at the margin and slightly closer to each other. Occasionally the male frons is also slightly modified in some species, either with the central area shinier, or with longer setae, or with patterns of transverse wrinkles. In at least one species (*C. montanum*) the degree of inflation of the elytral apex differs between the sexes (Schedl 1972).

Comments. Recent phylogenetic analyses (Jordal 2023) supported a separate position of *Ctonoxylon* in Xyloctonina as the sister lineage to the three other genera *Scolytomimus*, *Xyloctonus*, and *Cryphalomimus*.

***Ctonoxylon hirtellum* Schedl**

Figs 12, 15, 18

Ctonoxylon hirtellum Schedl, 1971: 9.

Type material. Holotype, male: Congo Belge [Democratic Republic of the Congo], Yangambi, 2.VII.1952, K.E. Schedl leg. [NHMW].

Diagnosis. Length 1.5 mm, 2.1× as long as wide, colour pale brown. Eye parts closely separated (by scapus thickness); pronotal eye scraper weakly developed, faint carina near anterior lateral margin from scraper to coxa, without associated groove or propleural pit; scutellar shield at same level as elytra; elytral striae impressed, punctures slightly elongated, separated by 2–3× their diameter; elytral vestiture consisting of long hairlike setae separated within rows by a little less than their length; elytral apex slightly extended with sharp tubercles along the posterior margin.

Distribution. Democratic Republic of the Congo.

Biology. Nothing known except collected in a tropical lowland rainforest.

***Ctonoxylon festivum* Schedl**

Figs 13, 14, 16, 17, 19, 20

Ctonoxylon festivum Schedl, 1941: 389.

Ctonoxylon dentigerum Schedl, 1941: 388, syn. nov.

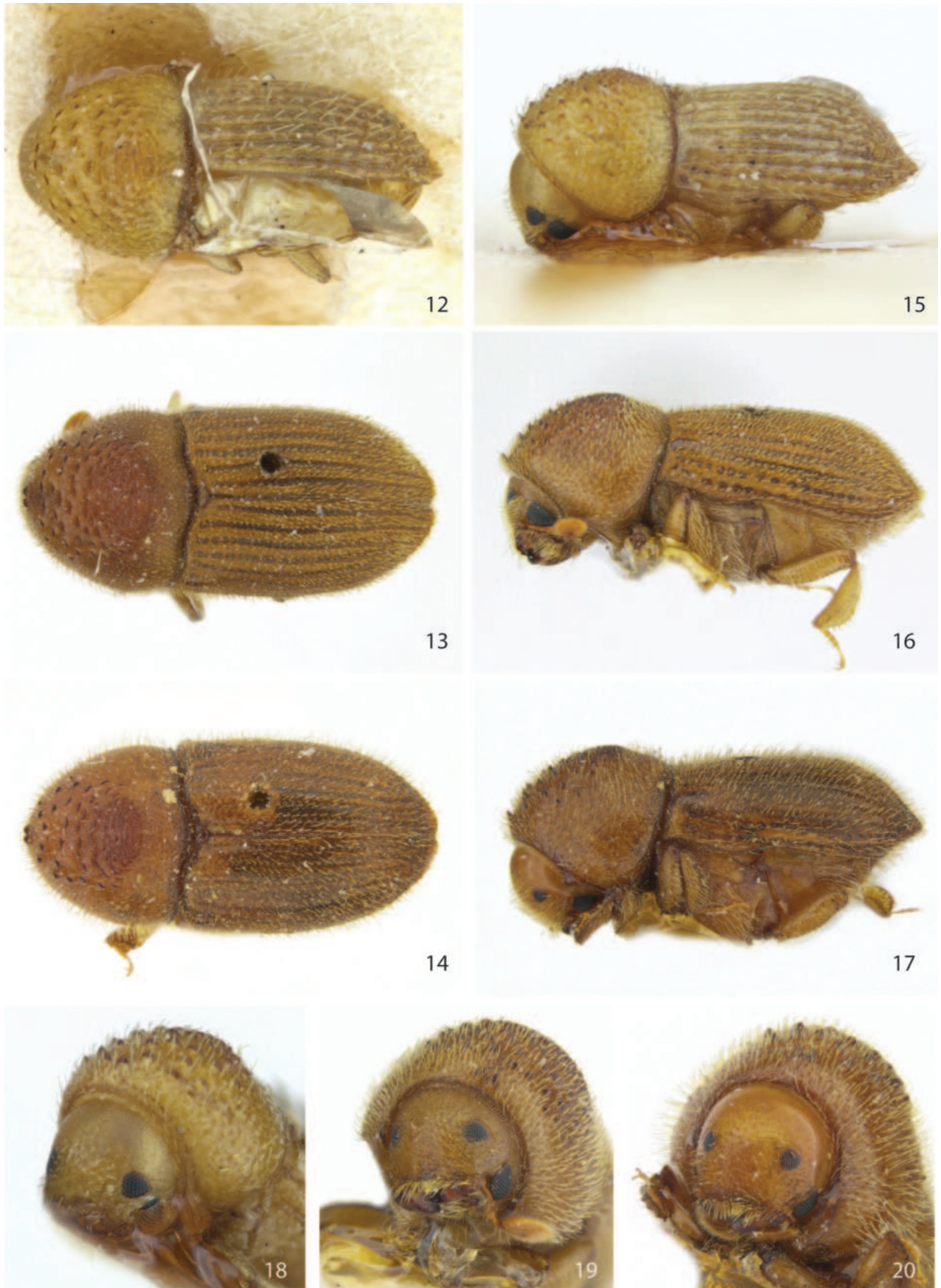
Type material. Holotype, female: Kamerun, Soppo, 800 m, XII 1912, v. Rothkirch S.G. Holotype of *C. dentigerum*, male: Spanish Guinea [Equatorial Guinea]. [both in NHMW].

Diagnosis. Length 3.1–3.2 mm. 2.1–2.2× as long as broad; colour brown. Upper and lower eye parts separated by more than width of upper part; pronotal eye scraper acutely pointed; a sharp carina running from scraper to procoxa, without associated groove or propleural pit; scutellar shield at level with elytra; striae slightly impressed; main interstrial setae and ground vestiture similar and evenly distributed, each seta a little shorter than width of an interstriae; elytral apex slightly emarginated; resting position of mesotibiae marked on metaventrite.

Distribution. Cameroon, Equatorial Guinea, Tanzania (new country record).

New record. Tanzania, Morogoro, Kimboza Forest Reserve [GIS: -7.023, 37.806], S.S. Madoffe, leg. [1, NHMUK].

Comments. Using the principle of first reviser the name *festivum* is given priority as there is nothing particularly dentigerous about this species. Differences noted between the holotypes of *C. dentigerum* and *C. festivum* are likely due to sexual dimorphism, with the male *dentigerum* having the anterior pair of teeth on pronotum a little behind the anterior margin and in *festivum* along the front margin. Minor variation in the length of elytral setae can also be due to dimorphism, or simply due to variation between individuals as often observed in similar species. Biology unknown, except collected in low- to mid-altitude rainforest.



Figures 12–20. Dorsal, lateral, and front views of 12, 15, 18 *Ctonoxylon hirtellum* male holotype 13, 16, 19 *Ctonoxylon festivum* female holotype, and 14, 17, 20 *Ctonoxylon dentigerum* male holotype, syn. nov. (= *Ctonoxylon festivum*).

***Ctonoxylon flavescens* Hagedorn**

Figs 21, 24, 27

Ctonoxylon flavescens Hagedorn, 1910: 4.

Ctonoxylon flavescens usambaricum Eggers, 1920: 38.

Ctonoxylon flavescens opacum Strohmeyer, nom. dub. – not published.

Type material. Holotype: Kamerun [ZMHB]; 'type' of *C. flavescens opacum*: Kamerun [SDEI]. Holotype of *C. flavescens usambaricum*: Mkulumusiberg 1000 m, bei Sigi Ostafrika [NHMW].

Diagnosis. Length 2.2–3.1 mm. 2.1–2.3× as long as broad; colour brown, dull. Upper and lower eye parts separated by more than width of upper part; pronotal eye scraper acutely pointed; a sharp carina running from scraper to procoxa, without associated groove or propleural pit; scutellar shield at level with elytra; striae distinctly impressed; interstrial setae bristle-like, variable in length and placed irregularly in partly confused rows, without ground vestiture; elytral apex slightly emarginated; resting position of mesotibiae marked on metaventrite.

Distribution. Guinea, Ghana, Cameroon, Democratic Republic of the Congo, Gabon, Uganda (new country record), Tanzania.

New records. Uganda, Masindi, Budongo, Nyabyeya [GIS: 1.673, 31.540], 3. July. 1998, ex *Ficus* branch, B. Jordal, leg. [ZMUB]; Budongo, BFP Station, Sonso [1.723, 31.545], 6.10.2004, T. Wagner leg. [1, ZFMK]; Kichwamba [0.71, 30.20], 25.04.1968, P.J. Spangler [1, USNM]; Cameroon, Limbe, Ekande [GIS: 4.081, 9.172], 1000 m. alt., 20. Nov. 2007, ex *Cola acuminata* standing tree, B. Jordal, leg [ZMUB]; [Ghana], 'Gold Coast', Takoradi [4.90, -1.75], 10.12.1946, ex bark of mahogany logs [*Khaya ivorensis*] [4, USNM].

Biology. Very little is known about this species despite frequent collections from many African countries. This study reports *Cola* as a new host plant genus in the same family Malvaceae as for the previously recorded *Triplochiton* (see Schedl 1961). Another new record from *Ficus* is in line with some other collections of closely related species taken from various Moraceae genera (see below). It is also reported here from African mahogany logs (Meliaceae), demonstrating a rather broad assembly of host plants. Records are generally from the bark of larger branches and trunks where the maternal egg tunnel is cut longitudinally. The male may stay at least until eggs are hatched, but not much longer (Table 5). Brood size is moderately large, with 19–45 eggs or larvae.

Comments. This species and the next three are morphologically very similar and can easily be confused. DNA sequence data for COI and 28S from three of the species nevertheless clearly separate them (Table 4, Fig. 11). Eastern and western populations of *C. flavescens* are also deeply, albeit less, diverged in the mitochondrial COI gene, but, more importantly, identical at the nuclear 28S gene. It is advisable to apply DNA sequence data to identify species in this complex group. The record from Madagascar is likely confused with the new species *C. tuberculatum* described in this work.

***Ctonoxylon bosqueiae* Schedl**

Figs 22, 25, 28

Ctonoxylon bosqueiae Schedl, 1962: 66.

Type material. *Holotype* and additional non-types from the type locality of *C. bosqueiae*: Ghana, Bobiri, Kumasi [NHMUK].

Diagnosis. Body length 2.2–2.5 mm, 2.2–2.3× as long as broad; colour dark brown, dull. Upper and lower eye parts separated by more than width of upper part; pronotal eye scraper acutely pointed; a sharp carina running from scraper to procoxa, without associated groove or propleural pit; scutellar shield at level with elytra; striae distinctly impressed; interstrial setae bristle-like, variable in length and placed irregularly in rows, without ground vestiture; elytral apex entire; resting position of mesotibiae marked on metaventrite.

Distribution. Ghana.

Comments. This species is very similar to *C. flavescens* but differs by the nearly closed gap between the apical tip of each elytron. Genetic data are needed to test the validity of this species. It is only known from the type locality in Ghana. Other published records are removed on the suspicion being the similar and commonly occurring *C. flavescens* or *C. hirsutum*. The hostplant *Trilepisium* is in the plant family Moraceae, similar to many other host records for the *flavescens* group.

***Ctonoxylon hirsutum* Hagedorn, stat. rev.**

Figs 23, 26, 29

Ctonoxylon camerunum hirsutum Hagedorn, 1910: 4.

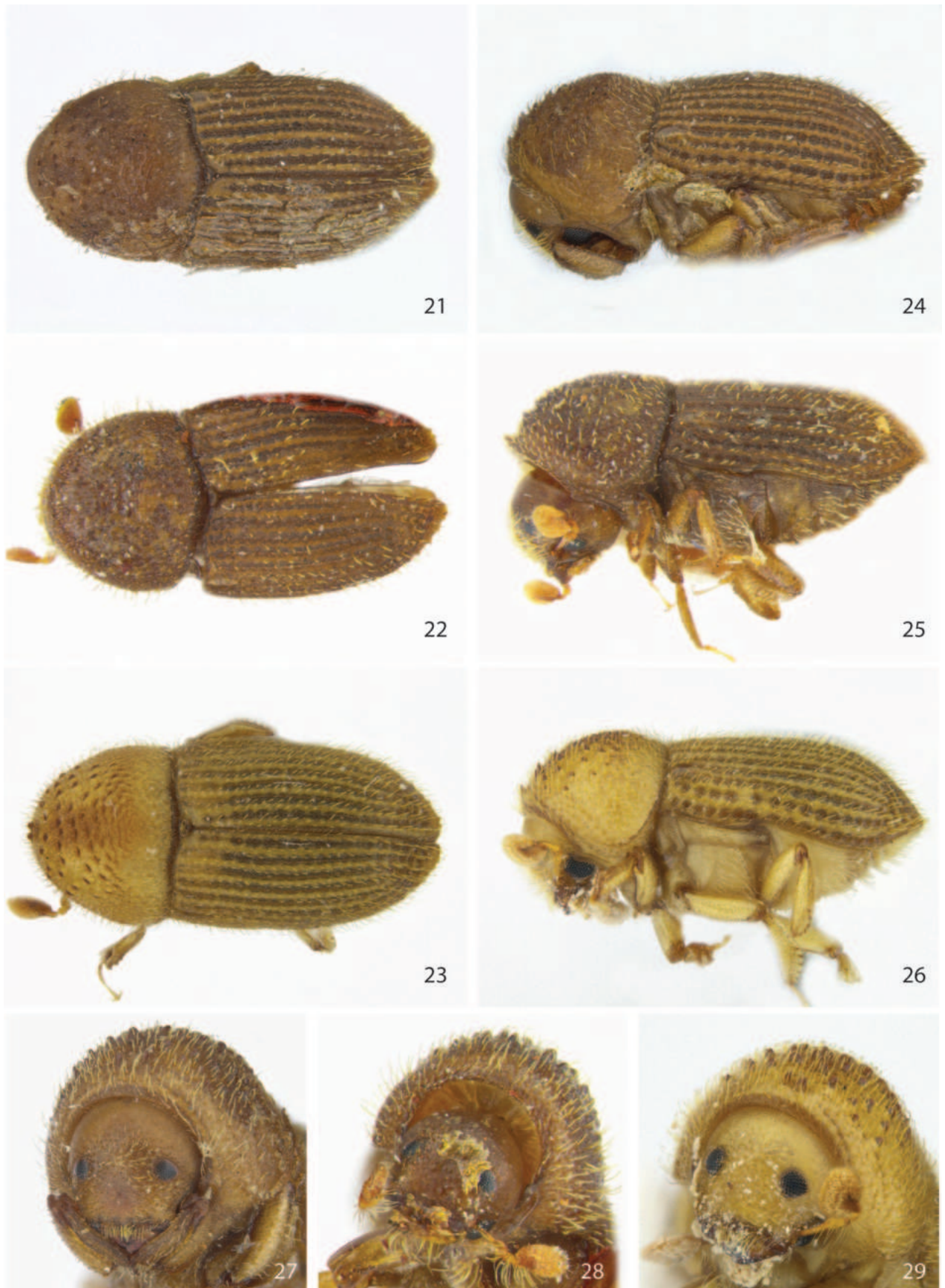
Ctonoxylon flavescens hirsutum Hagedorn, transfer by Eggers 1920 and Schedl 1961.

Type material. *Syntype* (metatype *sensu* Eggers): Kamerun, Conradt leg. [NHMW].

Diagnosis. Body length 2.5–3.0 mm, 2.2–2.3× as long as broad; colour pale brown. Male frons slightly flattened on lower half, very slightly shrivelled, surface finely rugose above, female frons smooth, vestiture in the frons of both sexes consisting of fine setae. Eye parts separated by the size of upper eye; antennal club sutures not clearly marked; anterior lateral margin of prothorax at middle with acute eye scraper; a sharp carina running from eye scraper to near procoxa; propleural pit absent; elytral vestiture on each interstriae consisting of two irregular rows of slightly curved bristle-like setae and scattered very fine hair-like setae; elytral suture straight; elytral apex slightly emarginated, a few small and sharp tubercles along the posterior margin. Metanepisternum with mixed short plumose and hair-like setae; metaventrite with simple hair-like setae; these sclerites on its anterior third glabrous, with a vertically curved swollen trace of mesotibia's resting position.

Distribution. Ghana, Cameroon, Democratic Republic of the Congo, Gabon.

New records. Cameroon, Ekande, 5 km N Limbe [GIS: 4.081, 9.172], 1100 m alt., ex unknown liana, 18.XI.2007, A. Breistøl, leg. [1, ZMUB]; Cameroon, Mbalmayo



Figures 21–29. Dorsal, lateral, and front views of male 21, 24, 27 *Ctonoxylon flavescens* 22, 25, 28 *Ctonoxylon bosqueiae* holotype, and 23, 26, 29 *Ctonoxylon hirsutum* stat. rev.

Forest Reserve, Eboufek [GIS: 3.499, 11.883], 28.07.1993, FIT [1, NHMUK]; Republic of the Congo, 40–60 km ESE of Bomassa [2.04, 16.59], 18.04.1993, D.H. Chadwick leg. [1, USNM].

Biology. All records are from lowland rainforest sites in the western parts of Africa. It was previously collected from latex rich lianas (Schedl 1961). In the current study two further specimens were dissected from a dead liana together with specimens of *C. pilosum* sp. nov. One specimen was also collected in a flight intercept trap [NHMUK].

Comments. Very similar to *C. flavescens*, except the elytral interstriae have fine pubescent ground vestiture and the two teeth near the anterior margin of the pronotum are subcontiguous. Previously designated as a variety of *C. flavescens*, but with a type designated, a subspecies name given and published by Hagedorn (1910). Sufficient diagnostic features as detailed by Eggers (1920), and molecular data demonstrating deep divergence from *C. flavescens* (Table 4), strongly support species status for the name *hirsutum*. Records from Ghana and Gabon (see Schedl 1961) could not be verified but these seem likely given several validated records from nearby countries.

***Ctonoxylon tuberculatum* sp. nov.**

<https://zoobank.org/0921A825-BD54-4309-90AD-2345527F0034>

Figs 30, 33, 36

Type material. *Holotype*, male: Madagascar, Diana prov., Montagne d'Ambre [GIS: -12.54, 49.17], 1000 m alt., ex *Ficus* branch, 03.11.2019, B. Jordal, leg. [ZMUB]. Allotype [ZMUB] and paratype [NHMW]: same data as holotype.

Diagnosis. Two teeth along the anterior margin of pronotum separated by more than width of a tooth; scattered interstitial setae separated within uniseriate rows by more than their length; posterior margin of elytra and declivital interstriae with sharp tubercles, largest tubercles on interstriae 1 and 3.

Description. Male. Body length 3.0–3.1 mm, 2.1–2.2× as long as broad; colour brown. **Frons** flattened from upper level of eyes to epistoma, surface shrivelled; vestiture of fine short setae. Eyes divided, each part separated by a little more than size of upper half. Antennal funiculus 7-segmented; club setose, sutures and septum barely indicated. **Pronotum** coarsely asperate on anterior three quarters, two front teeth separated by little more than width of a tooth, located behind the margin. Anterior lateral margin of prothorax at middle with prominent eye scraper; a sharp carina running from eye scraper to near procoxa; propleural pit absent. **Scutellar shield** wider than long, oval. **Elytral** striae impressed, punctures irregular and small; interstriae rounded, densely micropunctate, vestiture consisting of uniseriate rows of slightly curved bristle-like setae and fine dense ground vestiture along the suture; elytral suture straight; elytral apex slightly emarginated, along the posterior margin and at each declivital interstriae with small sharp tubercles, at interstriae 1 and 3 tubercles 2–3× larger. **Metanepisternum** with mixed short bifid and longer bristle-like setae; metaventrite with simple hair-like setae; these sclerites on its anterior third partly glabrous and with small bifid setae, and with a swollen trace of mesotibia's resting position. **Female** as in male, except anterior pair of teeth more closely placed and located along the anterior margin of the pronotum, and surface of the frons smooth.

Etymology. The Latin adjective *tuberculatus* in its neuter form, reflecting the tubercles on declivital interstriae which are more prominent than in related species.

Distribution and biology. Only known from the holotype locality in Madagascar where it was collected from very thick bark of a fallen *Ficus* branch (Moraceae), 7 cm in diameter. Two pairs were collected at the early stage of tunnel construction, including a mating niche with a short egg tunnel.

Comments. Previous records of *C. flavescens* from Madagascar are most likely *C. tuberculatum* as these two species are very similar. This could also be the case for records of *C. montanum* (recorded as *C. longipilum*), in which the female mainly differs by the more closely set anterior teeth on the pronotum, and the stouter body. These two species are therefore removed from the list of Malagasy species.

***Ctonoxylon montanum* Eggers**

Figs 31, 34, 37 [female]; 32, 35, 38 [male]

Ctonoxylon montanum Eggers, 1922: 170.

Ctonoxylon longipilum Eggers, 1935: 308, syn. nov.

Ctonoxylon nodosum Eggers, 1940: 236, syn. nov.

Links. https://www.barkbeetles.info/photos_target_species.php?lookUp=7979.
https://www.barkbeetles.info/photos_target_species.php?lookUp=2193.

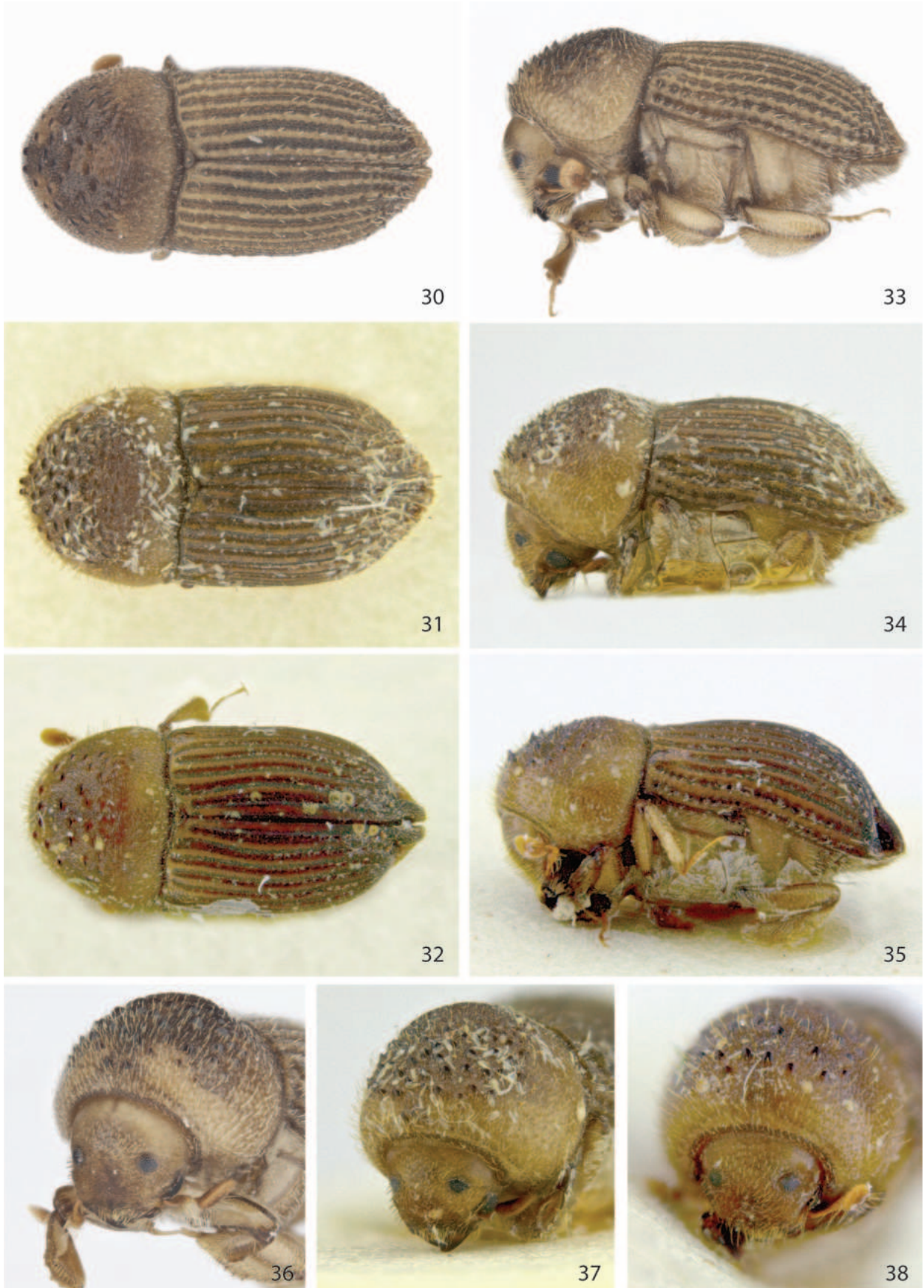
Type material. **Holotype** female: Kamerun, Buea, XII.10, Hintz, leg. Type 60341 [USNM]. **Holotype** of *Ctonoxylon longipilum*, female: [Tanzania] Mulange, Br. O. Afr. Type 60340 [USNM]. **Holotype** of *C. nodosum*, male: [Democratic Republic of the Congo] Congostaat, Mongbwalu [1.93, 30.05], [1200 m alt.] Mm Scholtz [RMCA].

Diagnosis. Length 3.2–3.6 mm. 2.0–2.1× as long as broad; colour brown. Upper and lower eye parts separated by 1.5× the width of upper part; pronotal eye scraper acutely pointed; a sharp carina running from scraper to procoxa, without associated groove or propleural pit; scutellar shield at level with elytra; striae distinctly impressed, interstriae rounded, interstitial setae curved and bristle-like, variable in length and scattered irregularly within rows, denser on declivity, without ground vestiture; elytral apex in females slightly extended, entire, in males apical interstriae 1 and 2 fused and strongly inflated; resting position of mesotibiae marked on metaventricle.

Distribution. Ivory Coast, Ghana, Nigeria, Cameroon, Democratic Republic of the Congo, Uganda, Kenya, Tanzania

New records. Ghana, Ashanti region, Kwadaso, 320 m., N6.42' – W1.39', Dr. S. Endrödy-Younga, mixed light, 25.II.1969 [1, NHMW]; Ghana, Western Region, Ankasa, Nkwanta Camp, 8.6.2005, KB Miller, leg. [1, ZMUB]; Nigeria, Ibadan [7.40, 3.85], 01.11.1964, M.L. Jerath leg. [2, USNM]; Nigeria, Ife, W. State [7.48, 4.48], 01.08.1971, T. Medler [3, USNM]; Cameroon, Libamba, 10 km E of Makak [3.54, 11.09], 11.02.1974, black light, J.A. Gruwell leg. [1, USNM].

Comments. Type specimens of *C. longipilum* and *C. montanum* are near identical and synonymised. The first species has only slightly longer curved elytral setae, but this feature varies between specimens. All specimens of the two nominal taxa are females as characterised by the pair of raised teeth along the anterior



Figures 30–38. Dorsal, lateral, and front views of **30, 33, 36** *Ctonoxylon tuberculatum* sp. nov. male holotype **31, 34, 37** *Ctonoxylon longipilum* female (= *C. montanum*), and **32, 35, 38** *Ctonoxylon nodosum* male holotype (= *C. montanum*).

margin of the pronotum. Previously Schedl (1972) synonymised *C. nodosum* with *C. longipilum* due to the presumed sexual dimorphism expressed in the inflated elytral apex and the lack of raised teeth along the pronotal margin. Schedl's view is supported and the synonym *C. nodosum* is therefore moved to *C. montanum*.

The record from Madagascar as *C. longipilum* (see Schedl 1977) is likely a misidentified female specimen of *C. tuberculatum* sp. nov. and is removed from the distribution list. Basically nothing is known about its biology except coming to light at lower to middle altitudes.

***Ctonoxylon camerunum* Hagedorn**

Figs 39, 42, 45

Ctonoxylon camerunum Hagedorn, 1910: 4.

Ctonoxylon fuscum Hagedorn, 1910: 5. Synonym by Eggers 1920.

Ctonoxylon conradti Schedl, 1939: 171, syn. nov.

Type material. Holotype: Kamerun [ZMHB]. **Holotype** *C. conradti*, female: [Tanzania] Insel Ukerewi [NHMW].

Diagnosis. Length 3.4–3.8 mm. 2.0–2.1× as long as broad; colour brown. Upper and lower eye parts separated by 1.5× the width of upper part; pronotal eye scraper acutely pointed; a sharp carina running from scraper to procoxa, without associated groove or propleural pit; scutellar shield at level with elytra; striae weakly impressed; interstrial setae sort, bristle-like, dense, confused with similar type of ground vestiture; elytral apex slightly emarginated; elytral suture buckled on disk; resting position of mesotibiae marked on metaventricle.

Distribution. Liberia (new country record), Ivory Coast, Nigeria, Cameroon, Equatorial Guinea, Gabon, Democratic Republic of the Congo, Angola, Tanzania.

New records. Liberia, Suakoko [6.98, -9.54], 28.1–5.5.1952, light trap, Blickenstaff leg (47); Cape Mount [6.72, -11.34], 1940, M. Mann (1) [USNM]; Nigeria, Ife, W. State [7.48, 4.48], 25.03.1969, J.T. Medler [1, USNM]; Cameroon, Yangamo, 100 km NE Bertoua [GIS: 5.00, 14.025], 25.03.1984, Kunze & Nagel, leg. [ZFMK]; 10 km S of Tongo [4.91, 10.77], 02.03.1972, black light, J.A. Gruwell [USNM].

Comments. The holotype of *C. conradti* was compared to a specimen of *C. camerunum* determined by Hagedorn in ZMHB, which is possibly the holotype. The type of *C. conradti* has slightly shorter elytral setae and is less shiny than *camerunum*, but this is very likely within species variation.

***Ctonoxylon cornutum* Eggers**

Figs 40, 43, 46

Ctonoxylon cornutum Eggers, 1943: 246.

Type material. Holotype: Kamerun, coll Strohmeyer [SDEI].

Diagnosis. Length 3.8–4.1 mm. 1.9–2.0× as long as broad; colour dark brown. Upper and lower eye parts separated by 1.5× the width of upper part; pronotal eye scraper acutely pointed; a sharp carina running from scraper to procoxa, without associated groove or propleural pit; anterior pair of teeth



Figures 39–47. Dorsal, lateral, and front views of **39, 42, 45** *Ctonoxylon camerunum* female **40, 43, 46** *Ctonoxylon cornutum* female holotype, and **41, 44, 47** *Ctonoxylon torquatium* sp. nov. female holotype.

on pronotum much larger than other asperities; scutellar shield at level with elytra; striae weakly impressed; interstitial setae short and bristle-like, dense, confused with similar type of ground vestiture; elytral apex nearly entire, very slightly emarginated; elytral suture buckled a little behind scutellar shield; resting position of mesotibiae marked on metaventrite.

Distribution. Cameroon.

***Ctonoxylon torquatum* sp. nov.**

<https://zoobank.org/F984EE78-7737-4824-8E00-76B31109A4B1>

Figs 41, 44, 47

Type material. *Holotype*, Madagascar, Toliara, Sept Lacs [GIS: 23.527, 44.155], MGF076, 02.03.2002, B. Fischer, leg. [CAS]. *Paratypes*, same data as holotype [CAS (2), NHMW (2), MSUC (2), ZMUB (2)].

Diagnosis. Protibiae with shallow anterior groove of depth < 1/3 width of the tibia; anterior margin of prothorax from coxa to top with an indented row of deep circular pits; scutellar shield and elytral suture with soft white setae; elytral apex with pair of tubercles.

Description. Body length 1.9–2.5 mm, 2.0–2.1× as long as broad; mature colour dark brown. *Frons* flattened from just below upper level of eyes to epistoma, surface finely punctured and granulated, central third smooth and impunctate; vestiture of fine short setae, nearly glabrous in middle. Eyes divided, each part separated by 2/3 the size of upper half. Antennal funiculus 7-segmented; club with two asymmetrically and strongly procurved sutures, suture one partly grooved, club segments 1 and 2 each with a dark septum clearly indicated. *Pronotum* asperate on central half of anterior three quarters, two front teeth separated by little less than width of a tooth, located at the margin, one additional pair of larger teeth a little behind the front teeth. Lateral anterior margin of prothorax with indented row of deep circular pits running from pronotal teeth to coxa; propleural pit longitudinally elongated, located between coxa and lateral costa on pronotum. *Scutellar shield* slightly detached from elytra, slightly sunken, broader than long, with fine white setae. *Elytral* striae impressed, punctures round or subquadrate, spaced by less than their diameter; interstriae raised, profile rounded, cuticle rough, vestiture consisting of confused, dense, bristle-like setae, with densely placed soft white setae along a straight elytral suture; apex with a pair of small tubercles. *Metanepisternum* with short plumose setae; metaventrite with scattered simple setae. *Protibiae* on anterior face with shallow groove for reception of tarsus, ~ 1/3 as deep as width of tibia.

Etymology. The Latin adjective *torquatus* in its neuter form, meaning adorned with a collar, referring to the row of deep pits along the front margin of the prothorax.

Distribution and biology. Only known from a long series of specimens collected at the type locality in the dry forest of south-western Madagascar.

***Ctonoxylon auratum* Hagedorn**

Figs 48, 51, 54

Ctonoxylon auratum Hagedorn, 1910: 4.

Type material. *Holotype*: Kamerun, Conradt [leg.], coll Kraatz, Hagedorn det. [SDEI].

Diagnosis. Length 2.1–2.2 mm. 2.4–2.5× as long as broad; colour brown. Eyes divided, separated by 2/3 the width of upper part; setae in frons mainly scale-like; anterior margin of pronotum with two teeth fused; anterior margin of prothorax from top to coxa with row of deep circular pits; propleural pit present; elytral vestiture of irregular interstitial rows of scalelike setae mixed with smaller and softer bristle-like setae, appearing somewhat fluffy; elytral apex emarginated; protibiae on anterior face with shallow groove, depth ~ 1/3 of tibia width.



Figures 48–56. Dorsal, lateral, and front views of **48, 51, 54** *Ctonoxylon auratum* female holotype **49, 52, 55** *Ctonoxylon pilosum* sp. nov. female holotype, and **50, 53, 56** *Ctonoxylon pygmaeum* female syntype [ZMHB].

Distribution. Cameroon, Democratic Republic of the Congo.

Remarks. The female holotype of this species is located in Muncheberg [SDEI], not Berlin as stated in Wood and Bright (1992).

***Ctonoxylon pilosum* sp. nov.**

<https://zoobank.org/4F557860-8B61-4BC3-8B06-921E1D3916C8>

Figs 49, 52, 55

Type material. *Holotype*, female: Cameroon, Ekande near Limbe [GIS: 4.081, 9.172], 1100 m alt., 18.11.2007, ex thin liana, A. Breistøl, leg. [ZMUB]. *Allotype* [ZMUB] and one *paratype* [NHMW]: same data as holotype.

Diagnosis. Protibiae with shallow anterior groove of depth $< 1/3$ the width of the tibia; anterior margin of prothorax from coxa to top with indented row of deep circular pits; elytral interstriae with dense, soft, golden ground vestiture in addition to longer, curved, bristle-like main setae.

Description. Body length 1.4–1.8 mm, 2.2–2.4× as long as broad; colour yellowish brown. *Frons* flattened from just below upper level of eyes to epistoma, surface finely punctured below, reticulate above, vestiture consisting of sparse, fine, short setae. Eyes divided, each part separated by $2/3$ the size of upper half. Antennal funiculus 7-segmented; club with two asymmetrically and strongly procurved sutures, suture one partly grooved with a dark partial septum along the front margin of the suture. *Pronotum* coarsely asperate on central two-thirds of anterior two-thirds, two front teeth at margin subcontiguous, not particularly larger than other asperities. Anterior lateral margin of prothorax with indented row of deep circular pits running from the anterior pronotal teeth to coxa; a round propleural pit located between coxa and lateral costa on pronotum. *Scutellar shield* flush with elytra, with fine golden dorsal setae. *Elytral* striae impressed, punctures round, irregularly sized and spaced; interstriae flat to slightly rounded, vestiture consisting of irregular rows of curved bristle-like setae, with ground vestiture consisting of more densely placed, soft, golden, hair-like setae; elytral suture straight, apex weakly emarginated. *Metanepisternum* and upper metaventrite with short plumose setae, simple and longer setae elsewhere. *Protibiae* on anterior face with shallow groove for reception of tarsus, $\sim 1/3$ as deep as width of tibia.

Male nearly identical to female, except frons more distinctly impressed below upper level of eyes, and the anterior pair of pronotal teeth is located just slightly behind the front margin.

Etymology. The Latin adjective *pilosus* in its neuter form, meaning hairy, referring to the dense ground vestiture of fine, short, golden setae.

Distribution and biology. Only known from the type locality in Cameroon where specimens were collected from a climbing plant, ~ 2 cm in diameter.

***Ctonoxylon pygmaeum* Eggers**

Figs 50, 53, 56

Ctonoxylon pygmaeum Eggers, 1920: 39.

Type material. *Syntypes*, females: Kamerun, Soppo, 800 m., XII 1912, v. Rothkirch S.G. [ZMHB, NHMW].

Diagnosis. Length 1.6–1.7 mm. 2.2–2.4× as long as broad; colour dark brown. Eyes divided, separated by half the width of upper part; frons nearly glabrous, reticulate; pronotal asperities broadly distributed on anterior three-quar-

ters; lateral anterior margin of prothorax from top to coxa with row of shallow irregular pits; propleural pit present just above coxa; elytral vestiture of regular interstitial rows of scalelike setae only; elytral apex expanded by pair of elongated prong-like tubercles; protibiae on anterior face with deep groove.

Distribution. Cameroon.

***Ctonoxylon caudatum* Schedl**

Figs 57, 60, 63

Ctonoxylon caudatum Schedl, 1971: 8.

Type material. Holotype, male: [Democratic Republic of the] Congo Belge, Stanleyville [Kisangani], 19.6.1952, K.E. Schedl [NHMW].

Diagnosis. Length 3.5 mm. 2.2× as long as broad; colour dark brown and black. Eyes divided, separated by the size of upper part; head black, frons reticulate, with scattered short setae; pronotal asperities broadly distributed on anterior three-quarters; lateral anterior margin of prothorax from middle part to coxa with shallow irregular groove; propleural pit presumably present; elytral vestiture of multiple confused rows of short interstitial scale-like setae; elytral apex expanded by pair of elongated prong-like tubercles; protibiae on anterior face with shallow groove of depth 1/3 the width of tibia.

Distribution. Democratic Republic of the Congo.

***Ctonoxylon crenatum* Hagedorn**

Figs 58, 61, 64

Ctonoxylon crenatum Hagedorn, 1910: 5.

Type material. Holotype, male: Kamerun, Conradt [leg.], coll Kraatz, Hagedorn det. [SDEI].

Diagnosis. Length 2.4–2.5 mm. 2.1× as long as broad; colour brown. Eyes divided, separated by slightly more than the size of upper part; frons lightly punctured, reticulate, glabrous; pronotum strongly domed, summit near posterior margin; pronotal asperities low, broad, subcontiguous, distributed on anterior three-quarters; lateral anterior margin of prothorax from middle part to coxa with shallow irregular groove; propleural pit presumably present; elytra glabrous, shiny, striae impressed; elytral apex expanded by pair of elongated prong-like tubercles.

Distribution. Cameroon, Republic of the Congo (new country).

New record. Republic of the Congo, Dimonika, Mayumbe [GIS: -4.46, 12.45] [1, NHMW].

***Ctonoxylon kivuensis* Schedl**

Figs 59, 62, 65

Ctonoxylon kivuensis Schedl, 1957: 44.



Figures 57–65. Dorsal, lateral, and front views of **57, 60, 63** *Ctonoxylon caudatum* male holotype **58, 61, 64** *Ctonoxylon crenatum* male holotype, and **59, 62, 65** *Ctonoxylon kivuensis* male holotype.

Type material. Holotype, male: [Democratic Republic of the] Congo Belge, Kivu, Mulungu, 2.VIII.1952, ex *Popowia*, KE Schedl, leg. [RMCA, paratype in NHMW].

Diagnosis (male). Length 1.6 mm. 2.2× as long as broad; colour brown. Eyes divided, separated by slightly more than the size of upper part; antennal club setose, sutures obscure; male frons slightly impressed, smooth and glabrous in centre, with fine soft setae closer to eyes and vertex; pronotum roughly punctured, with sharp asperities on anterior half, anterior pair of teeth small, located behind front margin; lateral anterior margin of prothorax from middle part to coxa with shallow irregular groove; propleural pit round, deep; elytral striae impressed, punctures large, separated by their diameter or less; vestiture consisting of irregular rows of long, soft bristle-like setae; elytral suture slightly buckled at midlength, apex entire.

Distribution. Democratic Republic of the Congo.

Biology. Only known from the medium altitude (732 m) type locality in the Congo basin, breeding in a *Popowia* branch (Annonaceae).

***Ctonoxylon quadrispinum* sp. nov.**

<https://zoobank.org/7345B8EE-8158-414F-860F-3A7F5DE6B9CD>

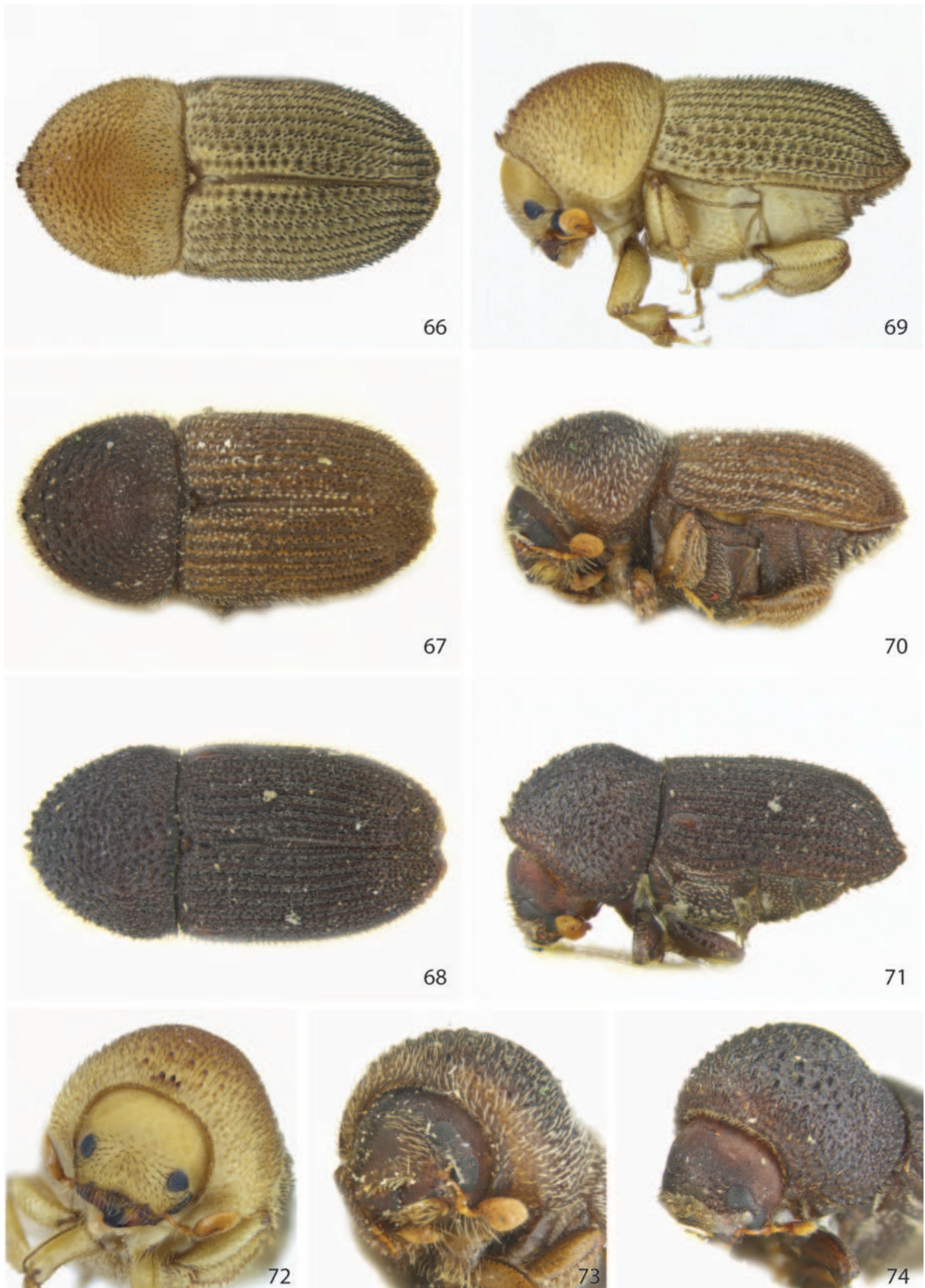
Figs 66, 69, 72

Type material. Holotype, female: Madagascar, Ankarafantsika NP [GIS: -16.264, 46.828], 200 m alt., 8.5.2015, ex liana, B. Jordal, leg. [ZMUB]. **Paratypes**: same data as holotype [NHMW, ZMUB].

Diagnosis. Anterior teeth on the pronotum quadrifid; lateral anterior margin of prothorax with elongated groove; propleural pit present; scutellar shield detached; elytral suture strongly curved just behind scutellar shield, a little buckled further behind.

Description. Female. Body length 2.6–3.0 mm, 2.1× as long as broad; immature colour pale brown. **Frons** convex, surface reticulate, vestiture consisting of sparse, short setae. Eyes divided, each part separated by 2/3 the size of upper half. Antennal funiculus 7-segmented; club with two asymmetrically and strongly procurved sutures, suture one more distinctly marked, with a dark partial septum along its front margin. **Pronotum** broadly asperate on anterior two-thirds, anterior margin with pair of two bifid raised teeth (quadrifid). Anterior lateral margin of prothorax with pointed eye scraper at level of eyes, a deep groove from this point to coxa; a transverse propleural groove located between coxa and lateral costa on pronotum. **Scutellar shield** detached from elytra. **Elytral** suture strongly curved immediately behind scutellar shield and slightly buckled at midlength; striae strongly impressed, punctures round, large and deep, spaced by their diameter or less; interstriae raised, vestiture consisting of irregular and partly confused rows of short scale-like setae, with ground vestiture consisting of shorter setae of the same type and density; apex slightly emarginated. **Metanepisternum** and metaventrite with scant simple setae; last abdominal ventrite with small concavity. **Protibiae** on anterior face with groove for reception of tarsus as deep as width of tibia.

Male nearly identical to female, except frons impunctate and glabrous in a narrow band from epistoma to upper level of eyes, front teeth along the pronotal margin very slightly behind the position in females, and last abdominal ventrite flat.



Figures 66–74. Dorsal, lateral, and front views of **66, 69, 72** *Ctonoxylon quadrispinum* female holotype **67, 70, 73** *Ctonoxylon methneri* male, and **68, 71, 74** *Ctonoxylon atrum* female holotype.

Etymology. Composed by the Latin prefix *quadri-* meaning four, and the Latin adjective *spinum* in its neuter form derived from *spina*, meaning thorn, referring to the four sharp teeth along the front margin of the pronotum.

Distribution and biology. Only known from the type locality in Madagascar where broods containing pupae and teneral, but not parents, were collected from a liana 4 cm in diameter, with thick bark. Egg tunnels were biramous and cut transversely to the grain. Brood sizes ranged from 50–60 ($n = 20$).

***Ctonoxylon methneri* Eggers**

Figs 67,70, 73

Ctonoxylon methneri Eggers, 1922: 170.

Ctonoxylon griseum Schedl, 1941: 389, syn. nov.

Ctonoxylon hamatum Schedl, 1941: 400, syn. nov.

Type material. Holotype ('type'): [Tanzania] Udzungwa-Berge 1300–1600 m., 26.XI.1912, Methner, coll. [ZMHB, not found]. **Holotype** of *C. hamatum* male: [Kenya] Nairobi [NHMW]. **Holotype** of *C. griseum*, female: [Kenya] Brit. O. Africa, Kikuyu [-1.27, 36.68], E. Thomas [NHMW].

Diagnosis. Length 2.3–4.2 mm. 2.1–2.3× as long as broad; colour dark brown, dorsal setae variegated. Male frons flat, smooth, impunctate and glabrous within a triangular pattern of short setae near eyes and epistoma; female frons finely granulated with short setae; eye parts separated by almost the size of upper half; anterior lateral margin of prothorax with elongated groove near front of coxa; propleural pit present just above coxa; scutellar shield detached from elytra; elytral suture slightly buckled at midlength; apex emarginated; interstitial vestiture consisting of confused rows of variegated scale-like setae of similar length and colour as the ground vestiture.

Distribution. Kenya, Tanzania, South Africa.

New records. South Africa, E. Cape Prov., Katberg [GIS: -32.479, 26.673], 01.11.1933, R.E. Turner, leg. [2, NHMUK]; W. Cape province, Knysna, Diepwalle [GIS: -33.957, 23.152], 7.11.2006, ex *Olea capensis* trunk, B. Jordal, leg; same data except Goudveld, Krisjan Se-Nek [GIS: -33.913, 22.948], 5.11.2006; Goudveld, Woodcutters [GIS: -33.927, 22.976], 4.11.2006; Gouna, Grootdrai [GIS: -33.946, 23.054], 6.11.2006; Nature's Valley [GIS: -33.965, 23.562], 8.11.2006; Tsitsikamma, Goesa walk [GIS: -33.983, 23.887], 12.11.2006; Tsitsikamma, Platboos walk [GIS: -33.980, 23.910], 14.11.2006 [all in ZMUB]; Kenya, Ngong Forestry [-1.31, 36.73], 12.01.1968, Malaise trap, Krombein & Spangler leg. [1, USNM].

Biology. This species is exclusively associated with black ironwood, *Olea capensis* (Oleaceae) where it is usually present whenever branches and trees are down. Recent field studies in the Knysna forests in the Cape region indicated no particular preference for breeding material size, ranging from 2-cm thick branches to the largest tree trunks of > 60 cm diameter. It breeds in the same host tree as *Lanurgus jubatus* Jordal, 2021, and *Lanurgus xylographus* Schedl, 1961, but even though it is found in the same forest localities, *C. methneri* only co-occurred with these species in the same tree one out of ten collecting events. Brood size was not smaller in the thinnest branches examined and broods with larvae or older stages ranged from 17–48 (Table 5). Very few

broods with larvae had a male parent present with the female, and then only at very early larval stage. In the large majority of dissected broods, the male left before all eggs were laid or hatched. The female left her offspring before pupal stage. Egg tunnels were always cut transversely to the wood grain and eggs deposited vertically in deep pits packed with frass.

Remarks. Some specimens of *C. methneri* differ from those of *C. hamatum* by having slightly shorter setae on interstriae 1 and 2 but this appears to be intraspecific variation. The differences in frons and pronotum between the types of *C. hamatum* and *C. methneri* on one side, and *C. griseum*, is due to sexual dimorphism otherwise typical for the genus.

***Ctonoxylon atrum* Browne, stat. rev.**

Figs 68, 71, 74

Ctonoxylon atrum Browne, 1965: 190.

Type material. Holotype, male: Nigeria, Idanre [GIS: 7.12, 5.10], 30.9.1964, ex *Canthium* [NHMUK].

Diagnosis. Length 3.4 mm. 2.1–2.2× as long as broad; colour pitch black. Male and female frons slightly impressed and impunctate on lower half, finely granulated above with short scattered setae; eye parts separated by 2/3 the size of upper half; anterior lateral margin of prothorax with elongated groove near procoxa; propleural pit present just above procoxa; pronotum with large and deep irregular punctures; elytral suture buckled at midlength, striae punctures longitudinally elongated, subquadrate; interstriae rough, with irregular punctures and rugosities; elytral apex emarginated; interstitial vestiture of confused rows of short, black, scale-like setae.

Distribution. Ghana, Cameroon (new country).

New record. Cameroon, Limbe, Ekande [GIS: 4.081, 9.172], 19. Nov. 2007, ex water liana, B. Jordal, leg [1, ZMUB].

Remarks. This species is rather similar to *C. methneri* and was synonymised with *C. hamatum* by Schedl (1970). However, *C. atrum* is darker, with shorter elytral setae, the striae punctures are narrowly elongated and more separated, and the pronotal punctures are larger. It is genetically clearly separated from *C. methneri* and instead forms a sister relationship with *C. quadrispinum* sp. nov. (Fig. 11).

***Ctonoxylon acuminatum* Schedl**

Figs 75, 77, 79

Ctonoxylon acuminatum Schedl, 1957: 45.

Type material. Holotype, male: [Democratic Republic of the] Congo Belge, Yangambi, 9.IX.1952, ex *Clitandra staudtii*, KE Schedl, leg. [RMCA, paratype in NHMW].

Diagnosis. Length 2.6 mm. 2.3× as long as broad; colour pale brown. Male frons reticulate with short fine setae; eye parts separated by the size of upper half; anterior lateral margin of prothorax with obtuse eye scraper, from this point to coxa with elongated groove; propleural pit present; elytral suture



Figures 75–80. Dorsal, lateral, and front views of **75, 77, 79** *Ctonoxylon acuminatum* female holotype, and **76, 78, 80** *Ctonoxylon spathifer* male.

slightly buckled at midlength; apex entire, slightly extended and upcurved in lateral view; interstitial vestiture of regular rows of long bristle-like setae.

Biology. One host plant is known, *Orthopichonia visciflua* (K.Schum. ex Hallier f.) Vonk (Apocynaceae), a thin climbing plant (Schedl 1961).

Comments. Superficially similar to *C. kivuensis* but has shorter setae and the elytral apex in lateral view has a slightly curved extension (Fig. 77).

***Ctonoxylon spathifer* Schedl**

Figs 76, 78, 80

Ctonoxylon spathifer Schedl, 1951: 39.

Type material. Syntypes: [Ivory Coast] Cote d'Ivoire, Reserve du Banco [5.39, -4.05] [MNHN, NHMW].

Diagnosis. Length 2.6–3.1 mm. 2.3–2.4× as long as broad; colour reddish brown. Eyes divided, separated by the size of upper part; antennal club setose, sutures obscure; male frons roughly punctured, glabrous in middle, with short coarse setae close to the eyes; pronotum with dense subconfluent asperities on anterior two-thirds, a fused pair of teeth just behind front margin; lateral anterior margin of prothorax from middle part to coxa with shallow irregular groove; propleural pit round, deep; elytral striae impressed, punctures large, deep, narrowly separated; vestiture on interstriae consisting of densely confused, short, scale-like setae; elytral suture straight, apex narrowly rounded, entire.

Distribution. Ivory Coast, Ghana (new country), Tanzania.

New record. Ghana, Samreboi [5.61, -2.55], ex *Trichilia rubescens*, 10.IX.1962, F.G. Browne, leg. [2, NHMUK].

Biology. Known to breed in *Olea welwitschii* (Oleaceae), *Pachylobus deliciosus* (Burseraceae), *Strombosia postulata* (Olacaceae), and *Trichilia rubescens* (Meliaceae), an unusually broad assemblage of host plants for a true bark beetle.

***Ctonoxylon amanicum* Hagedorn**

Figs 81, 84, 87

Ctonoxylon amanicum Hagedorn, 1912: 42.

Ctonoxylon intermedium Schedl, 1971: 10, syn. nov.

Type material. Holotype: [Tanzania] D.O. Afrika, Amani [ZMHB]. **Holotype**, *C. intermedium*: Kamerun, C. Conradt leg. [NHMW].

Diagnosis. Length 1.6–1.9 mm. 2.2–2.4× as long as broad; colour brown. Female frons slightly impressed on central lower half, glabrous and impunctate in middle, with short stiff setae around central area; eye parts narrowly separated by half the size of upper eye part; lateral anterior margin of prothorax with obtuse eye scraper, further below near coxa with short elongated groove; propleural pit present above coxa; elytral suture a little buckled at midlength; apex entire; interstitial vestiture consisting of regular rows of narrowly spatulate setae; posterior part of the metaventricle with unusually long, broad setae.

Distribution. Cameroon, Tanzania.

New record: Tanzania, Morogoro prov. Udzungwa [GIS: -7.85, 36.89], ex liana, 29.6.2010, B. Jordal leg. [ZMUB]. Cameroon, Limbe, Ekande [GIS: 4.081, 9.172], 1100 m alt., ex thin liana, 18.11.2007, A. Breistøl, leg.

Biology. One specimen was collected in each of two localities, in countries with type localities for the two synonymised species *C. amanicum* and *C. intermedium*. Both specimens were tunnelling in thin lianas, one under bark and one in pith of a stem nodule in which only a short irregular tunnel was made.



Figures 81–89. Dorsal, lateral, and front views of **81, 84, 87** *Ctonoxylon amanicum* female **82, 85, 88** *Ctonoxylon uniseriatum* female, and **83, 86, 89** *Ctonoxylon spinifer* female.

Comments. The holotype of *C. amanicum* was supposed to be lost in the museum of Hamburg but was rediscovered in Berlin (ZMHB). The holotype of *C. intermedium* is identical to *C. amanicum* in all important characteristics and therefore synonymised.

***Ctonoxylon uniseriatum* Schedl**

Figs 82, 85, 88

Ctonoxylon uniseriatum Schedl, 1965: 114.

Ctonoxylon capensis Schedl, 1971: 8, synonym by Beaver 2011.

Cryphalostenus erratum Schedl, genus et species nomen nudum.

Type material. Holotype: [Namibia] Deutsch S.W. Afrika [NHMW]. **Holotype** of *C. capensis*: [South Africa] Umgeberge, Cape Town, 1899 [NHMW].

Diagnosis. Length 2.3–2.8 mm. 2.3–2.4× as long as broad; colour dark brown. Male frons slightly inflated, smooth and impunctate with short setae near eyes and epistoma; female frons finely punctured with short erect setae; eye parts separated by the size of upper half; lateral anterior margin of prothorax with short elongated groove near front of procoxa; propleural pit large; scutellar shield detached from elytra; elytral suture a little buckled at mid-length; apex entire; punctures on discal interstriae obscure, interstriae 1–7 with uniseriate, spatulate, curved setae, interstriae 8–10 sometimes with variably confused rows of setae, on declivital interstriae 1 and 2 setae partly confused, directed sideways; posterior metaventrite with unusually broad and long setae.

Distribution. Namibia, South Africa.

New records. South Africa, W. Cape province, 10 km N Hoekwil, Woodville [GIS: -33.933, 22.639], 1.Nov.2006; Knysna, Diepwalle [GIS: -33.957, 23.152], 3.11.2006 and 7.11.2006; Knysna, Goudveld, Krisjan Se-Nek [GIS: -33.913, 22.948], 5.11.2006, all collections ex liana, B. Jordal, leg. [ZMUB].

Biology. A common species found exclusively in thin lianas ~ 1 cm in diameter. Females were excavating longitudinal tunnels in the pith and wood of rather fresh material which still exuded latex. Males had left the female either before egg laying or just after the first eggs were laid. Broods were small, with 3–8 eggs per female (Table 5).

Remarks. A specimen in NHMW marked as the holotype of *Cryphalostenus erratum* det. Schedl is not published. It is clearly the same species as *C. uniseriatum*.

***Ctonoxylon spinifer* Eggers**

Figs 83, 86, 89

Ctonoxylon spinifer Eggers, 1920: 39.

Ctonoxylon setifer Eggers, 1920: 39, syn. nov.

Links. https://www.barkbeetles.info/photos_target_species.php?lookUp=7983.

Type material. Lectotype, male of *C. spinifer*: Kamerun, Soppo, 1912, v. Rothkirch leg. [USNM]; **paratype**, female, same data [NHMW]. **Holotype** *C. setifer*: [Tanzania] Amani [lost]; **paratype** [NHMW].

Diagnosis. Length 2.2–2.8 mm. 2.2–2.3× as long as broad; colour brown. Female frons sparsely punctured, lightly granulated with short erect setae; male frons flat, smooth, impunctate and glabrous on central third, with longer setae near eyes and epistoma; eye parts separated by the size of upper half; anterior lateral margin of prothorax with faint eye scraper, below this point with a short elongated groove near front of procoxa; propleural pit present above coxa; scutellar shield detached from elytra; elytral suture a little buckled at midlength; apex entire; interstitial vestiture of mainly regular rows of bristle-like erect setae, interstitial punctures on both disc and declivity dense, distinct; posterior metaventrite with unusually broad and long setae.

Distribution. Burkino Faso (new country record), Ivory Coast, Cameroon, Democratic Republic of the Congo; Kenya, Tanzania, Madagascar (new country record).

New records. Burkina Faso, Foret de Boulon [10.343, -4.510], 270 m, piege interception (1), piege limeneux (1), 9.7.2006, F. Genier, leg. [CMNC]; Cameroon, Adamoua, 20 km S. Minim [6.49, 12.52], 1200 m alt., 8.3.1982, Flacke & Nagel, leg. [1, ZFMK]; Tanzania, Udzungwa National Park HQ, Mang'ula [GIS: -7.845, 36.880], 200 m alt., ex liana, 9.11.2009 and 29.6.2010, B. Jordal, leg.; Mang'ula [GIS:-7.850, 36.883], ex liana, 14.11.2009, B. Jordal, leg. [ZMUB]; Morogoro, Kimboza Forest Reserve [-7.023, 37.806], S.S. Madoffe, leg. [1, NHMUK]; Madagascar, Reserve speciale de l'Ankarana, 22.9 km SW Anivoran [-12.93, 49.16], B. Fischer, leg. [1, CAS].

Biology. Specimens were dissected from the pith of thin lianas, 0.6–1.0 cm diameter, still exuding latex.

Comments. The co-types (paratypes) of *C. spinifer* are identical to those of *C. setifer*. Because the holotype of *C. setifer* is lost, and using the principle of first reviser, the name *spinifer* is given priority. Eggers' descriptions are very similar and not useful to distinguish specimens. There is some variation within series of various other collections, particularly in the regularity of interstitial rows of setae but this variation follows no predictable pattern. This species is very similar to *C. uniseriatum* but differs by the erect interstitial setae, particularly on the declivity where setae are not directed sideways as in *uniseriatum*, by the densely placed interstitial punctures, and in males also by the less inflated upper central frons. Genetic data supported a sister relationship to *C. amanicum* instead of *C. uniseriatum* (Fig. 11).

A single specimen is recorded from near the north-west coast of Madagascar. This is not too surprising given the broad Afrotropical distribution of this species.

Removed from taxon list

Ctonoxylon alutaceus (Schaufuss, 1897), *nom. dub.*

The type for this taxon is lost from the Hamburg Museum collection. It was examined by Eggers (1922) who stated that the specimen could not be studied due to the partial inclusion in resin. It is therefore not possible to validate species status and is therefore a *nomen dubium*.

Identification key to species

- 1 Near anterior lateral margin of the prothorax with a sharp carina running down to front of procoxa, without pleural pit above the coxa (Fig. 1); anterior part of metaventrite with a flattened field and swollen posterior margin demarcating position of resting mesotibia (Fig. 8); prothoracic eye scraper usually acuminate (Fig. 1) (except for one small species, see next couplet)..... **2**
- Near anterior lateral margin of the prothorax with with a deep elongated groove (Fig. 3) or row of deep circular pits (Fig. 4) running down towards procoxa; a distinct propleural pit or transverse groove present between coxa and pronotum (Fig. 5); metaventrite not modified; prothoracic eye scraper either a round faint nodule or entirely absent **10**
- 2 Elytral interstriae with sparse but very long, curved setae, longer than width of metatibia; upper and lower eye parts separated only by scapus thickness; anterior lateral margin of prothorax without eye scraper; body length 1.5 mm..... ***C. hirtellum***
- Elytral interstriae with various types of vestiture; upper and lower eye parts separated by more than width of upper eye; eye scraper large and triangular; body size much larger, length 2.2–4.2 mm..... **3**
- 3 Elytral apex in dorsal view entire, pointed in both sexes, in males strongly inflated ***C. montanum***
- Elytral apex emarginated **4**
- 4 All elytral vestiture bristle- or scale-like; setae on posterior part of metaventrite narrow scales..... **5**
- Main interstitial setae fine bristles or hair-like; setae on metaventrite hair-like **6**
- 5 Elytral ground vestiture consisting of very short scales; anterior median pair of teeth on pronotum large and strongly raised, each tooth ~ the size of 1/2 an upper eye ***C. cornutum***
- All vestiture longer than width of interstriae; anterior pronotal teeth of normal size..... ***C. camerunum***
- 6 Elytral ground vestiture of the same length and confused with the main row of setae ***C. festivum***
- Main interstitial setae much longer than ground vestiture or ground vestiture absent (*flavescens* group) **7**
- 7 Interstriae 1 and 3 on declivity with sharp tubercles almost as large as one tarsomere; interstriae 2 less raised near apex (Madagascar)..... ***C. tuberculatum* sp. nov.**
- Declivital interstriae with much smaller granules; interstriae 2 and 3 equal (Africa) **8**
- 8 Apical margin of the elytra nearly smooth or with only few fine granules; elytral ground vestiture consisting of fine short hair-like setae ***C. hirsutum***
- Apical margin of the elytra granulated; elytral ground vestiture absent **9**
- 9 Elytral apex almost entire, with very shallow emargination, in lateral view declivity short and straight ***C. bosqueiae***
- Elytral apex deeply emarginated, in lateral view apex slightly extended ***C. flavescens***

- 10 Just behind the anterior lateral margin of prothorax with a row of deep circular pits reaching near front of procoxae **11**
- Just behind the anterior lateral margin of prothorax with an elongated groove (sometimes with many small confluent pits squeezed into a groove)..... **13**
- 11 Pronotum with small asperities, the majority of these are smaller than the width of a funicular segment; elytral apex at suture with two small tubercles; declivital interstriae 1 with dense fine pale-coloured setae.....
..... **C. torquatum sp. nov.**
- Pronotal asperities ~ as broad as the scutellar shield; elytral apex rounded or weakly emarginated; all elytral setae of the same golden colour..... **12**
- 12 Setae in frons and elytral interstriae mainly spatulate; anterior margin of pronotum with a single fused tooth **C. auratum**
- Setae in frons and elytral ground vestiture hair-like, main interstitial setae of curved fine bristles; two teeth at anterior margin of pronotum separated **C. pilosum sp. nov.**
- 13 Elytral apex extended into a pair of short contiguous spines (Figs 50, 57, 58) **14**
- Elytral apex rounded or emarginated **16**
- 14 Elytra mainly glabrous **C. crenatum**
- Elytral interstriae with setae **15**
- 15 Elytral interstriae with multiple confused rows of short setae, each seta shorter than width of interstriae; elytral interstriae ridged **C. caudatum**
- Elytral interstriae with a single row of erect bristles, each longer than width of interstriae; elytral interstriae flat **C. pygmaeum**
- 16 Elytral setae very long and thin..... **C. kivuensis**
- Elytral setae of erect bristles or spatulate setae..... **17**
- 17 Interstitial setae in multiple confused rows **18**
- Interstitial setae mainly in single rows, multiple confused rows may occur on interstriae 8–10..... **21**
- 18 Frons coarsely granulated; a single (fused) pronotal tooth near anterior margin; elytra apex narrowly rounded **C. spathifer**
- Frons almost smooth; two teeth at pronotal margin separated; elytral apex emarginated..... **19**
- 19 Anterior margin of pronotum with pair of bidentate teeth, appearing four-toothed; right elytron just behind scutellar shield with a sharp loop (Madagascar) **C. quadrispinum sp. nov.**
- Anterior margin of pronotum with two uniform teeth; area near scutellar shield only slightly curved..... **20**
- 20 Colour dark brown or black; most elytral setae narrow and bristle-like, shorter than width of an interstria; strial punctures separated by 2–3× their diameter **C. atrum**
- Colour brown to black, setae on elytra variegated, scale-like, longest setae as long or longer than width of an interstriae; strial punctures closely set, separated by less than their diameter..... **C. methneri**
- 21 Setae laterally on the metaventrite hair-like; lower elytral declivity in lateral view curved with apex extended slightly posteriorly..... **C. acuminatum**
- Setae laterally on the metaventrite short and plumose on anterior half, with increasingly long scales posteriorly near margin for reception of metafemur; lower declivity in lateral view more or less straight **22**

- 22 Elytral interstriae with scattered setae placed in single rows, each seta as long or longer than width of one interstriae ***C. amanicum***
- Interstriae 810 often with multiple confused rows of densely placed setae, all interstitial setae shorter than width of an interstria, separated within rows by less than their length..... **23**
- 23 Elytral interstriae with the majority of setae spatulate, curved or semirecumbent, setae on declivital interstriae 1 and 2 obliquely directed sideways; interstitial punctures scattered, shallow (South Africa)..... ***C. uniseriatum***
- All elytral setae bristle-like, erect; interstitial punctures distinct, densely placed (tropical Africa, Madagascar)..... ***C. spinifer***

Acknowledgments

Many thanks to A. Breistøl for assistance in the Cameroon field work and two reviewers for correcting the manuscript.

Additional information

Conflict of interest

The author has declared that no competing interests exist.

Ethical statement

No ethical statement was reported.

Funding

Collecting and export permits for Madagascar were kindly facilitated by MICET and granted by Direction générale de l'environnement et des forêts 2012, 2015 and 2019. Collecting and research permit for Tanzania (COSTECH) was provided by TAWIRI 2009–2010. Permit for collecting and research in the Cape provinces of South Africa 2006 was granted by Cape Nature no. AAA-004-00062-0035. Research in Cameroon 2007 was executed under the broader umbrella project of the Limbe Botanical Garden.

Author contributions

The author solely contributed to this work.

Author ORCIDs

Bjarte H. Jordal  <https://orcid.org/0000-0001-6082-443X>

Data availability

All of the data that support the findings of this study are available in the main text.

References

- Beaver RA (2011) New synonymy and taxonomic changes in bark and ambrosia beetles (Coleoptera: Curculionidae: Scolytinae, Platypodinae). *Koleopterologische Rundschau* 81: 277–289.
- Eggers H (1920) 60 Neue Borkenkäfer (Ipidae) aus Afrika, nebst zehn neuen Gattungen, zwei Abarten. (Fortsetzung). *Entomologische Blätter* 16: 33–45.

- Eggers H (1922) Neue Borkenkäfer (Ipidae) aus Afrika. (Nachtrag I). Entomologische Blätter 18: 163–174.
- Eichhoff WJ (1878) Ratio, descriptio, emendatio eorum Tomycinorum qui sunt in Dr. Me-din. Chapuisii et autoris ipsius collectionibus et quos praeterea recognovit scriptor. Mémoires de la Société Royale des Sciences de Liège 8: 1–581.
- Goloboff PA, Torres A, Arias JS (2018) Weighted parsimony outperforms other meth-ods of phylogenetic inference under models appropriate for morphology. Cladistics 34(4): 407–437. <https://doi.org/10.1111/cla.12205>
- Hagedorn JM (1910) Diagnosen bisher unbeschriebener Borkenkäfer. Deutsche Ento-mologische Zeitschrift 1910(1): 1–13. <https://doi.org/10.1002/mmnd.4801910101>
- Hopkins AD (1914) List of generic names and their type-species in the coleopterous su-perfamily Scolytoidea. Proceedings of the United States National Museum 48(2066): 115–136. <https://doi.org/10.5479/si.00963801.2066.115>
- Hopkins AD (1915) Contributions toward a monograph of the Scolytid beetles. II. Pre-liminary classification of the superfamily Scolytoidea. United States Department of Agriculture, Technical Series 17: 165–232.
- Jordal BH (2023) Glostatina, a new xyloctonine subtribe for *Glostatus* (Coleoptera: Cur-culionidae), based on clear genetic and morphological differences. European Journal of Entomology 120: 199–232. <https://doi.org/10.14411/eje.2023.025>
- Jordal BH (2024) Integrated taxonomy and biogeography of the Afrotropical genus *Xy-loctonus* and other Xyloctonini reveals contrasting colonisation patterns for Mada-gascar. Deutsche Entomologische Zeitschrift 71: 67–84. <https://doi.org/10.3897/dez.71.116185>
- Linder HP, de Klerk HM, Born J, Burgess ND, Fjeldså J, Rahbek C (2012) The partitioning of Africa: Statistically defined biogeographical regions in sub-Saharan Africa. Journal of Biogeography 39(7): 1189–1205. <https://doi.org/10.1111/j.1365-2699.2012.02728.x>
- Morrone JJ, Ebach MC (2022) Toward a terrestrial biogeographical regionalisation of the world: Historical notes, characterisation and area nomenclature. Australian Sys-tematic Botany 35(3): 89–126, 138. <https://doi.org/10.1071/SB22002>
- Schedl KE (1956) Breeding habits of arboricole insects in Central Africa. Proceedings of the Xth International Congress of Entomology, Montreal 1: 183–197.
- Schedl KE (1957) Scolytoidea nouveaux du Congo Belge, II. Mission R. Mayne - K.E. Schedl 1952. Musée Royale du Congo Belge Tervuren, Ser 8. Sciences Zoologiques 56: 1–162.
- Schedl KE (1961) Scolytidae und Platypodidae Afrikas. Band I (part). Familie Scolytidae. Revista de Entomologia de Moçambique 4: 335–742.
- Schedl KE (1970) Zur Synonymie der Borkenkäfer XX 272. Beitrag zur Morphologie und Systematik der Scolytoidea. Annalen des Naturhistorischen Museums in Wien 74: 221–231.
- Schedl KE (1972) Entomological explorations in Ghana by Dr. S. Endrody-Younga, 8. Zur Scolytoidea Fauna von Ghana (Coleoptera). 284 Beitrag. Annales Historico-Naturales Musei Nationalis Hungarici 64: 277–294.
- Schedl KE (1977) Die Scolytidae und Platypodidae Madagaskars und einiger nahelieg-ender Inselgruppen. Mitteilungen der Forstlichen Bundes-Versuchsanstalt Wien 119: 1–326.
- Wood SL, Bright DE (1992) A catalog of Scolytidae and Platypodidae (Coleoptera). Part 2: Taxonomic index. Great Basin Naturalist Memoirs 13: 1–1553.

Fishes (Actinopterygii) of the rapids and associated environments in the lower Vaupés River Basin: an undiscovered Colombian Amazon diversity

Alexander Urbano-Bonilla¹, Jorge E. Garcia-Melo², Mateo Esteban Peña-Bermudez¹, Omar Eduardo Melo-Ortiz¹, Oscar Stiven Ordoñez¹, Sandra Bibiana Correa³, Tiago P. Carvalho¹, Javier A. Maldonado-Ocampo^{1†}

1 Laboratorio de Ictiología, Unidad de Ecología y Sistemática (UNESIS), Departamento de Biología, Facultad de Ciencias, Pontificia Universidad Javeriana, Carrera 7 N° 43-82, Bogotá, 110231, D.C., Colombia

2 Universidad de Ibagué, Facultad de Ciencias Naturales y Matemáticas, Programa de Biología Ambiental, Tolima-Colombia, Ibagué, Colombia

3 Department of Wildlife, Fisheries and Aquaculture, Mississippi State University, Mississippi, USA

Corresponding author: Alexander Urbano-Bonilla (bio.ictiologia@gmail.com), Tiago P. Carvalho (pitiago@javeriana.edu.co)



Academic editor: Felipe Ottoni

Received: 16 January 2023

Accepted: 9 February 2024

Published: 30 May 2024

ZooBank: <https://zoobank.org/314DD623-21AC-4F8D-A10E-9EC83422A617>

Citation: Urbano-Bonilla A, Garcia-Melo JE, Peña-Bermudez ME, Melo-Ortiz OE, Ordoñez OS, Correa SB, Carvalho TP, Maldonado-Ocampo JA (2024) Fishes (Actinopterygii) of the rapids and associated environments in the lower Vaupés River Basin: an undiscovered Colombian Amazon diversity. ZooKeys 1203: 131–158. <https://doi.org/10.3897/zookeys.1203.100642>

Copyright: This is an open access article distributed under the terms of the CC0 Public Domain Dedication.

Abstract

The Vaupés River stands out as one of the few within the Amazon basin due to its numerous rapids. These riverine fast-flowing sections not only provide habitat to highly specialized fishes but also function as natural barriers hindering the movement of fish along its course. During a fish-collecting expedition in the lower Vaupés River basin in Colombia, 95 species were registered belonging to 30 families and seven orders. Despite recent inventories in the region, our comprehensive sampling efforts particularly focused on the rapids and associated rheophilic fauna, allowing us to contribute the first records of four fish species in Colombia (*Myloplus lucienae* Andrade, Ota, Bastos & Jégu, 2016, *Tometes makue* Jégu, Santos & Jégu, 2002, also first record of the genus, *Leptodoras praelongus* (Myers & Weitzman, 1956), and *Eigenmannia matintapereira* Peixoto, Dutra & Wosiacki, 2015) and six presumably undescribed species (i.e., *Jupiaba* sp., *Moenkhausia* sp., *Phenacogaster* sp., *Bunocephalus* sp., *Hemiancistrus* sp., and *Archolaemus* sp.). In this study, a commented list of the ichthyofauna of these environments is presented, as well as a photographic catalog of fish species integrated into the CaVFish Project – Colombia.

Key words: Conservation, freshwater, Neotropical fishes, new records, PhotoFish System, range expansion, taxonomy

Introduction

The Neotropical Region is the biogeographic region with the highest number of freshwater fish species globally, and recent estimates suggest approximately 9,000 species (Reis et al. 2016; Birindelli and Sidlauskas 2018; Dagosta and de Pinna 2019). Some localities in the Amazon River basin often exhibit remarkably high fish species richness that surpasses the hundreds (Albert and Reis 2011). The extraordinary radiation of fishes that occurred in the Neotropical region is often explained as the product of geographic events over extended

† Deceased.

geological periods (Albert and Crampton 2010; Albert and Reis 2011; Albert et al. 2020), but also lineage diversification related to habitat utilization and trophic specialization (Lujan et al. 2012; Lujan and Conway 2015; Arbour and López-Fernández 2016; Roxo et al. 2017; Kolmann et al. 2021). The Vaupés River and its fish have a long history of expeditions that began in the 18th and 19th centuries by early naturalists, such as Alexandre Rodrigues Ferreira, Alexander Von Humboldt, and Alfred Russel Wallace (Lima et al. 2005). Recent analyses of fish biodiversity and hotspots in Amazonia suggested that the Vaupés hydrographic basin in its entirety has high values of species richness and endemism (Jézéquel et al. 2020a), species with high levels of irreplaceability, representativeness, and degree of vulnerability (Jézéquel et al. 2020b). Unlike other tributaries of the Amazon, the numerous rapids of the Vaupés River serve as habitat and provide food (e.g., Podostemaceae aquatic plants) for fish (Lima et al. 2005); in addition, rapids act as natural barriers that affect the dispersal of some fish and harbor rheophilic and endemic fish species (Londoño-Burbano and Urbano-Bonilla 2018; Urbano-Bonilla et al. 2023).

The River Negro Basin, of which Vaupés River is a major tributary, has a rich ichthyofauna, with 1,165 species known to science. A large portion of these species are shared with adjacent basins (i.e., Orinoco), but ~ 15% are endemic (156 species; Beltrão et al. 2019). The western Rio Negro tributaries are known for their distinctive rheophilic fish fauna (Lima et al. 2005). A total of 224 fish species are known to occur in the Vaupés River in Colombia (Bogotá-Gregory et al. 2020, 2022a); some of these species are endemic to this basin, while others are widely distributed in the Amazon basin and adjacent basins such as the Orinoco and those within the Guiana Shield (van der Sleen and Albert 2017; Beltrão et al. 2019; Bogotá-Gregory et al. 2020, 2022a, 2022b; Taphorn et al. 2022).

Despite historic and contemporary sampling efforts, the Vaupés River remains largely under-sampled mainly because of its remote geographical location and numerous rapids, preventing access and navigation. Also, after putting an end to a 60-year conflict between the Colombian state and one of the oldest guerrilla organizations in the world (Fuerzas Armadas Revolucionarias de Colombia-Ejército del Pueblo FARC-EP), biological expeditions were carried out filling an important information gap relative to this previously unreachable area (Botero 2020; Irwin 2023). Recent studies evaluating the sampling efforts to inventory Amazon River basin ichthyofauna reveal that extensive areas in southwestern Colombia remain almost unsampled (Jézéquel et al. 2020a). Recent reviews purported new records for the basin and Colombia suggesting that the biodiversity knowledge of the area is still incipient (Bogotá-Gregory et al. 2020, 2022a).

Here we describe the results of an expedition to the lower Vaupés River basin with the goal of investigating fish species associated with the rapids and surrounding environments in the Vaupés arc (Miocene \approx 10 Mya; see Fig. 1). Tragically during this expedition Colombian, in the Matapí Rapids in the Vaupés River, the boat transporting researchers capsized, and the leader of the expedition, ichthyologist Javier Maldonado-Ocampo passed away (read more in Urbano-Bonilla et al. 2021). This document is a tribute to the effort of Javier, who dedicated his life to the generation and transmission of knowledge aimed at recognizing the diversity of Colombian fishes and rescuing ancestral knowledge.

Materials and methods

Study area and site characterization

This study was carried out in the lower Vaupés River basin in Colombia, more specifically in the Municipality of Mitú, Department of Vaupés. The fish collections were conducted within the indigenous communities of Trubón, Villa Fátima, Nana, Macucú, and Matapí (Fig. 1). We characterized the river channel depth profile from shore to shore. First, we measured the river width with a laser Rangefinder (Nikon Forestry Pro) and divided the river into 5–10 segments. We conducted readings at each location by driving the boat across the river while reading depth on a Hummingbird water depth sonde (model Fishfinder 525) connected to a transducer mounted on an external pole that was carried on the side of the boat. Distance was tracked with a GPS unit (Garmin 76CSx). We measured water transparency with a Secchi disk. Temperature and dissolved oxygen was measured at the water surface (YSI Pro 20).

Sampling methods

We sampled along a stretch of ~ 140 km of the main river course. Fish collection follows animal care guidelines provided by the American Society of Ichthyologists and Herpetologists 2013 (<https://www.asih.org/resources>).

Collections were conducted during the low water period (from February 21 to March 3, 2019), in which we carried standardized sampling with different fishing gear in rapids and surrounding habitats. Four monofilament nylon gillnets: two multi-panel gill nets, 25 m long × 2.5 m depth with five equal length panels of different mesh sizes (2.54, 3.81, 5.08, 6.35, and 7.62 cm stretched mesh size); one 50 m long and one 100 m long, both 14.7 cm stretched mesh size, were deployed at rapids, shallow areas of the main channel, and beaches directly below rapids for 3 hours (morning and night; 6 hrs total per day). Beaches were additionally sampled by five passes with beach seines (3 m long, 2 m high, and 0.5 cm mesh size) and ten cast net throws. Five passes were made with a seine net (3 m long, 2 m high, and 0.5 cm mesh) in streams surrounding the rapids during the day (Fig. 2). This sampling was coupled with 1.5 hours of nocturnal collections with dip nets. Opportunistic sampling was conducted by snorkeling and dip netting in shallow areas.

Photo and CaVFish Project - Colombia database

Each species was photographed alive in the field using the PhotoFish System (García-Melo et al. 2019) in white and black backgrounds. Subsequently, the images were processed assigning the taxonomy established in the laboratory or by direct visual inspection when the voucher was not available. Likewise, tagging and editing were performed using the pipeline developed by the CaVFish Project - Colombia (<https://cavfish.unibague.edu.co/>). A few species not photographed in the field were photographed in the laboratory following similar protocols.

Specimen preservation

The collected specimens were euthanized by overdose with clove oil (*Syzygium aromaticum* (L.) Merr. y Perry, 1939, 0.3 ml/0.25L; Lucena et al. 2013). Fishes were fixed in 10% formaldehyde and later preserved in 70% ethanol for storage. Before formalin fixation in the field, we conducted tissue sampling on euthanized specimens, preserving muscles or fin clips in 2 ml vials containing 96% ethanol. Identification followed taxonomic keys for genus-level assignment (van der Sleen and Albert 2017), specialized literature for species-level identification, and comparison with reference material deposited in the Javeriano Museum of Natural History “Lorenzo Uribe Uribe S.J” (MPUJ) collection. Databases of this study are available at https://ipt.biodiversidad.co/sib/resource?r=peces_del_rio_vaupes. Additionally, photographs of live specimens were sent to taxonomic experts for verification and identification (see acknowledgments section). The classification system follows Fricke et al. (2023) and Dornburg and Near (2021) within which fish orders, families, genera, and species were listed alphabetically.

Unfortunately, a small portion of these fishes were lost during the expedition and therefore were represented only by photographs (or pictures + tissue samples) and are not associated with vouchered specimens.

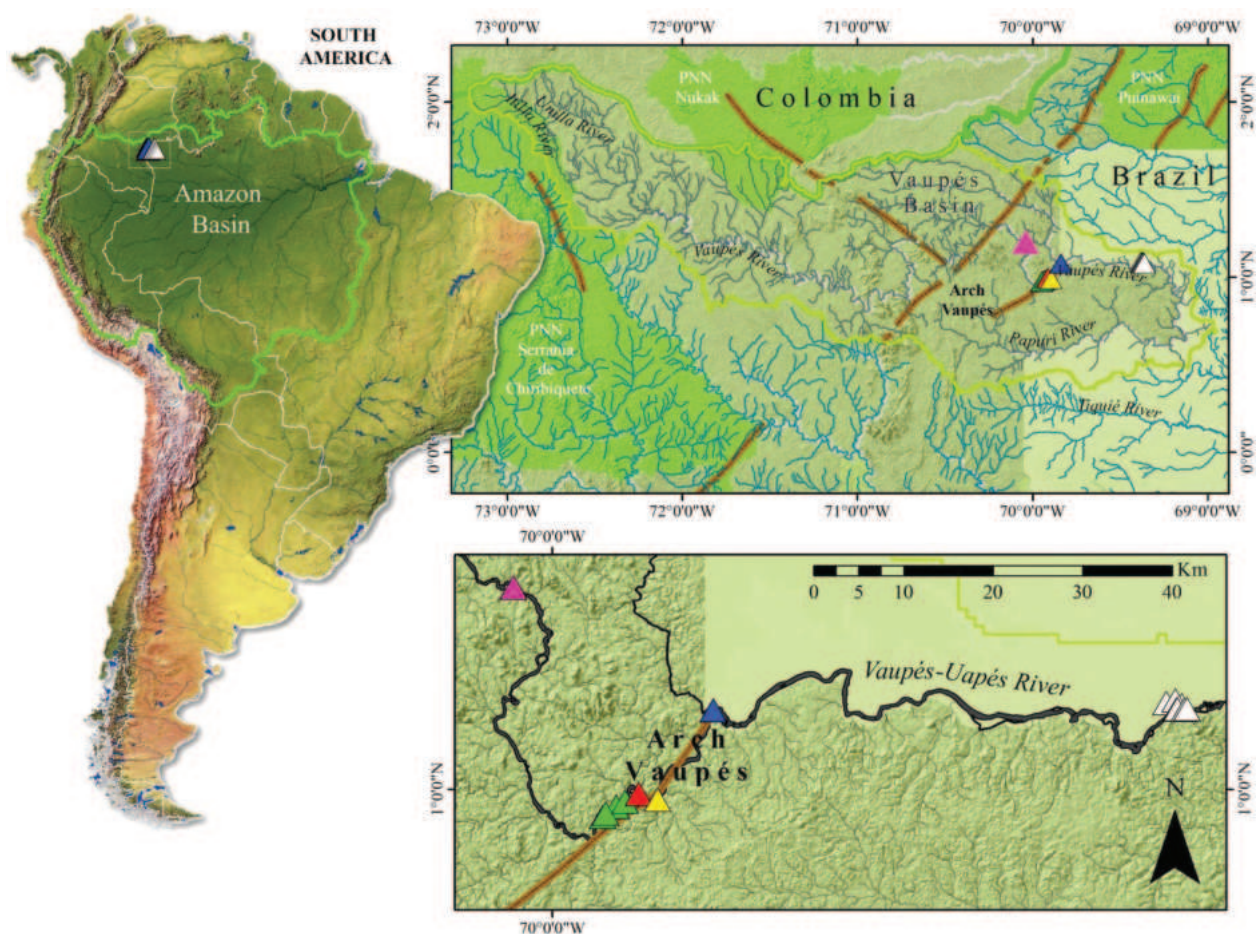


Figure 1. Location of the Vaupés River in Colombia and distribution of sampling sites along the lower Vaupés River. Key: pink triangle – Trubón Community Rapids; green triangle – Villa Fátima Community Rapids; red triangle – Nana Community Rapids; yellow triangle – Macucú Community Rapids; white triangle – Matapí Community Rapids, and blue triangle – military base.

Results

Sampling stations and water physicochemical characteristics

In the lower Vaupes River, in total, we sampled 16 sites (Figs 1, 2, Table 1). The drainage network includes streams, lagoons, river beaches, and river rapids ranging from 2–3 m wide up to 380 m in the main channel. In the latter, the depth varied from a few centimeters at the shore to 18 m. The water is dark in color (brown-black) with relatively high transparency (assessed by Secchi disk, mean and standard deviation ranging between 108 to 122.50 ± 10.61 cm). Temperature ranged between 28.15 ± 0.21 and 29.65 ± 0.21 °C, and surface dissolved oxygen between 6.41 ± 0.01 and 7.63 ± 0.25 mg/L.

Composition

We collected 95 species (Tables 2, 3), 85 of those identified at the species level and ten at the genus level. These species are distributed in 30 families and seven orders. The orders Characiformes (54 spp.) and Siluriformes (21 spp.) represent more than 78% of the total diversity of fish; the remaining orders have between five and nine species (Table 2). In addition, 44 new records are added to the previous list of fishes from the Vaupés River basin of Bogotá-Gregory et al. (2022a).

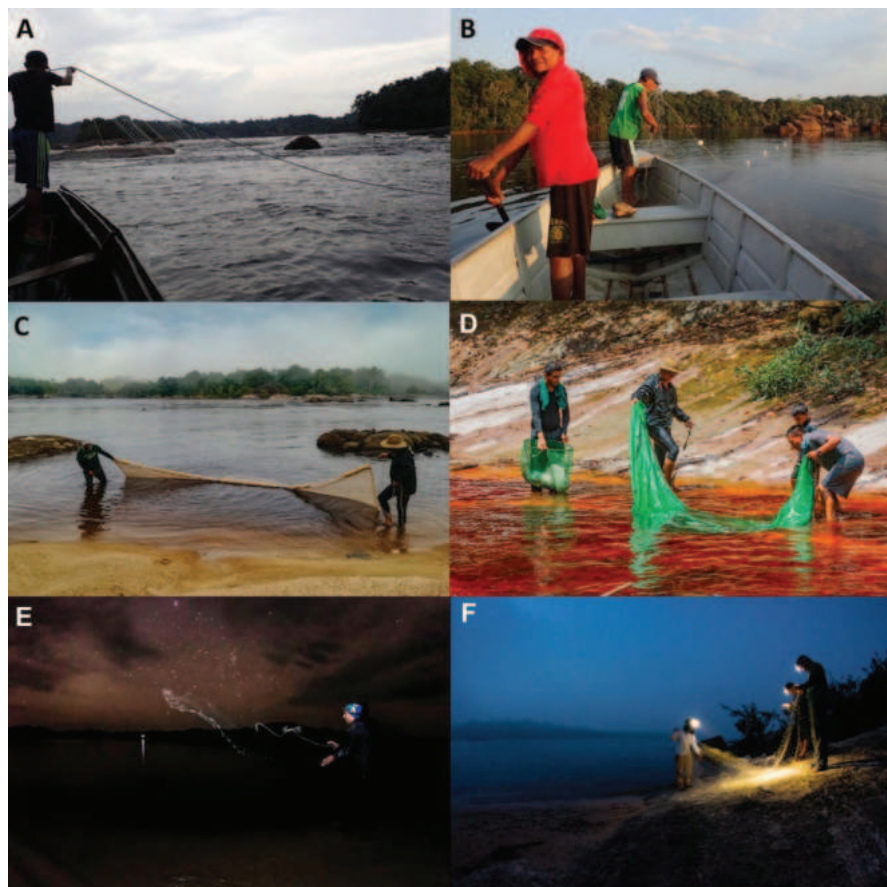


Figure 2. Gear and habitats sampled in the lower Vaupés River, Mitú, Colombia. Gillnets deployed on **A** rapids and **B** beaches below rapids (photographs by SBC). Seine-net used on the beaches of the **C** rapids and **D** associated stream; night fishing with **E** cast net and **F** gillnets (photographs by JEG-M).

Table 1. Description of sampled sites in the lower Vaupés River, Amazon basin, Colombia. Coordinates in degrees, minutes, seconds' format, and altitude in meters above sea level. Localities are ordered by altitude.

Locality description	GPS coordinates	Altitude
Sandy beach on Vaupés River at Resguardo Trubón	1°12'8"N, 70°2'20"W	164
Caño Danta creek tributary to Vaupés River near Villa Fátima	0°58'57"N, 69°56'9"W	168
Vaupés river rapids area, in front of Villa Fátima	0°58'21"N, 69°56'58"W	150
Sandy beach on Vaupés River at Villa Fátima	0°58'33"N, 69°56'47"W	148
Sandy beach and rocky shore on Vaupés River downstream Villa Fátima	0°59'16"N, 69°55'36"W	148
Vaupés River at rapids in front of community of Naná	0°59'44"N, 69°54'48"W	147
Macucú Rapids and sandy beach at community of Macucú	0°59'22"N, 69°53'39"W	144
Vaupés River near Militar Base	1°4'46"N, 69°50'18"W	144
Downstream of the rapids of Caño Almidón, tributary to Vaupés River, upstream of community of Matapí	1°5'11"N, 69°23'1"W	150
Creek tributary to Vaupés River near community of Matapí	1°5'5"N, 69°22'5"W	146
Sandy beach at Vaupés River upstream <i>cachivera</i> Tapira Geral near community of Matapí	1°5'21"N, 69°22'27"W	138
Sandy beach at community of Matapí	1°4'49"N, 69°21'50"W	134
Laguna Arcoiris, small lagoon adjacent to Vaupés River at community of Matapí	1°4'48"N, 69°22'23"W	133
Sandy beach ~ 300 m downstream <i>cachivera</i> Tapira Geral near community of Matapí	1°4'49"N, 69°22'20"W	133
Caño Colibrí, near community of Matapí	1°4'47"N, 69°21'54"W	132
Sandy beach and rocky shore on Vaupés River River at community of Matapí	1°4'49"N, 69°21'45"W	129

Table 2. Number and percentage of families, genera, and species per order.

Order	Family	%	Genus	%	Species	%
Characiformes	15	50	30	46.88	54	56.84
Siluriformes	8	26.67	19	29.69	21	22.11
Bleniiformes	3	10	7	10.94	10	10.53
Gymnotiformes	1	3.33	4	6.25	4	4.21
Acanthuriformes	1	3.33	2	3.13	4	4.21
Gobiiformes	1	3.33	1	1.56	1	1.05
Synbranchiformes	1	3.33	1	1.56	1	1.05
	30	100	64	100	95	100

First records of species photographs in life

This article is one of the first to implement a workflow that associates photographs of live specimens in the field with the meticulous taxonomy carried out in the laboratory and its subsequent upload to the CaVFish Project, Colombia. Many of these species did not have adequate visual records in life, and therefore this study represent a great advance in the knowledge of the ichthyofauna of the Vaupés River, both for specialists and for the broader public. All species photographed can be accessed from the project page using the following URL: <https://cavfish.unibague.edu.co>.

New records for Colombia

This study records for the first time in Colombia the following four species: *Myloplus lucienae* Andrade, Ota, Bastos & Jégu, 2016, *Tometes makue* Jégu, Santos & Jégu, 2002 also a first record of the genus, *Leptodoras praelongus* (Myers & Weitzman, 1956), and *Eigenmannia matintapereira* Peixoto, Dutra & Wosiacki, 2015. These species were absent from recent lists of fish species of Colombia (DoNascimento et al. 2017, 2024; Bogotá Gregory et al. 2020, 2022a) (Fig. 3A–D).

Table 3. List of fish species collected in the lower Vaupés River and their respective voucher numbers at MPUJ, figure numbers, and literature that support taxonomic identification. Species with ¹ represent new records for Colombia; ² represents putative new species; and ³ represents records not included in Bogotá-Gregory et al. (2022a).

ORDER/Family/Species	Voucher	fig.	Literature
CHARACIFORMES			
Acestrorhynchidae			
<i>Acestrorhynchus microlepis</i> (Jardine, 1841)	uncatalogued, photo voucher only	Suppl. material 1: fig. S1	López-Fernández and Winemiller 2003
Anostomidae			
<i>Gnathodolus bidens</i> Myers, 1927	MPUJ 14496	Suppl. material 1: fig. S2	Mendes and Jégu 1987
<i>Leporinus brunneus</i> Myers, 1950	MPUJ 14504, 14507	Suppl. material 1: fig. S3	Chernoff et al. 1991
<i>Leporinus fasciatus</i> (Bloch, 1794)	MPUJ 14369, 14478	Suppl. material 1: fig. S4	Taphorn 2003
<i>Leporinus niceforoi</i> Fowler, 1943 ³	MPUJ 14476, 14539	Suppl. material 1: fig. S5	Sidlauskas et al. 2011
<i>Leporinus yophorus</i> Eigenmann, 1922 ³	MPUJ 14506	Suppl. material 1: fig. S6	Taphorn 2003
Bryconidae			
<i>Brycon pesu</i> Müller & Troschel, 1845	MPUJ 14382, 14389, 14405, 14449, 14472, 14473, 14516, 14517, 14531, 14383	Suppl. material 1: fig. S7	Lima 2017
Characidae			
<i>Bryconamericus orinocoensis</i> Román-Valencia, 2003	MPUJ 14379, 14386, 14423, 14438, 16524	Suppl. material 1: fig. S8	Román-Valencia 2003
<i>Creagrutus maxillaris</i> (Myers, 1927)	MPUJ 14388, 14428, 14429, 14430, 14534	Suppl. material 1: fig. S9	Vari and Harold 2001
<i>Creagrutus vexillapinnus</i> Vari & Harold, 2001 ³	MPUJ 14394, 14413, 14434	Suppl. material 1: fig. S10	Vari and Harold 2001
<i>Hemigrammus analis</i> Durbin, 1909	MPUJ 14480, 14486	Suppl. material 1: fig. S11	Géry 1977
<i>Hemigrammus bellottii</i> (Steindachner, 1882)	MPUJ 14455, 14456, 14484, 14491, 14546	Suppl. material 1: fig. S12	Géry 1977
<i>Hemigrammus geisleri</i> Zarske & Géry, 2007 ³	MPUJ 14421, 14540, 16520	Suppl. material 1: fig. S13	Zarske and Géry 2007
<i>Hemigrammus luelingi</i> Géry, 1964	MPUJ 14545	Suppl. material 1: fig. S14	Géry 1977
<i>Jupiaba anteroides</i> (Géry, 1965)	MPUJ 14487	Suppl. material 1: fig. S15	Zanata 1997; Ferreira et al. 2009
<i>Jupiaba scologaster</i> (Weitzman & Vari, 1986) ³	MPUJ 14436, 16515	Suppl. material 1: fig. S16	Zanata 1997; Ferreira et al. 2009
<i>Jupiaba zonata</i> (Eigenmann, 1908)	MPUJ 14435	Suppl. material 1: fig. S17	Zanata 1997; Ferreira et al. 2009
<i>Jupiaba</i> sp. ²	MPUJ 14385, 14424, 14440, 14446, 14467, 14475, 14488, 14538, 14370	Suppl. material 1: fig. 4A	Zanata 1997; Ferreira et al. 2009
<i>Knodus</i> sp. 1 ³	MPUJ 14447	Suppl. material 1: fig. S19	Van der Sleen et al. 2018
<i>Knodus</i> sp. 2 ³	MPUJ 14536	Suppl. material 1: fig. S20	Van der Sleen et al. 2018
<i>Knodus</i> sp. 3	MPUJ 14452, 14407	Suppl. material 1: fig. S21	Van der Sleen et al. 2018
<i>Microschemobrycon callops</i> Böhlke, 1953	MPUJ 14533	Suppl. material 1: fig. S22	Lima et al. 2013
<i>Microschemobrycon casiquiare</i> Böhlke, 1953	MPUJ 14422, 14448, 16521	Suppl. material 1: fig. S23	Lima et al. 2013
<i>Moenkhausia browni</i> ³ Eigenmann, 1909	MPUJ 14397, 16514, 16517	Suppl. material 1: fig. S24	Géry 1977
<i>Moenkhausia ceros</i> Eigenmann, 1908	MPUJ 14366, 14541	Suppl. material 1: fig. S25	Géry 1977
<i>Moenkhausia collettii</i> (Steindachner, 1882)	MPUJ 14457, 14460, 14492, 14537, 14544	Suppl. material 1: fig. S26	Géry 1977
<i>Moenkhausia cotinho</i> Eigenmann, 1908	MPUJ 14494	Suppl. material 1: fig. S27	Mathubara and Toledo-Piza 2020
<i>Moenkhausia lata</i> Eigenmann, 1908	MPUJ 14432	Suppl. material 1: fig. S29	Marinho and Langeani 2016
<i>Moenkhausia melogramma</i> ³ Eigenmann, 1903	MPUJ 14543, 14367, 14410, 14437	Suppl. material 1: fig. S30	Soares et al. 2020
<i>Moenkhausia mikia</i> Marinho & Langeani, 2010	MPUJ 14371, 14400, 14414, 14419, 14453, 14489, 14439	Suppl. material 1: fig. S31	Marinho and Langeani 2016

ORDER/Family/Species	Voucher	fig.	Literature
<i>Moenkhausia</i> sp. ²	MPUJ 14427, 14542, 14374, 14411, 14443	Suppl. material 1: fig. 4C	Marinho and Langeani 2016
<i>Phenacogaster</i> sp. 1	MPUJ 14373, 14425	Suppl. material 1: fig. S32	Lucena and Malabarba 2010
<i>Phenacogaster</i> sp. 2 ²	MPUJ 14390, 14364	Suppl. material 1: fig. 4B	Lucena and Malabarba 2010
<i>Tetragonopterus chalceus</i> Spix & Agassiz, 1829	MPUJ 14483	Suppl. material 1: fig. S34	Silva et al. 2016
Chilodontidae			
<i>Caenotropus labyrinthicus</i> (Kner, 1858) ³	MPUJ 14409, 14477, 16516	Suppl. material 1: fig. S35	Vari et al. 1995
Crenuchidae			
<i>Characidium declivirostre</i> Steindachner, 1915 ³	MPUJ 14497	Suppl. material 1: fig. S36	Armbruster et al. 2021
<i>Characidium longum</i> Taphorn, Montana & Buckup, 2006	MPUJ 14365	Suppl. material 1: fig. S37	Taphorn et al. 2006
<i>Characidium pteroides</i> Eigenmann, 1909 ³	MPUJ 14384	Suppl. material 1: fig. S38	Taphorn et al. 2006
Ctenolucidae			
<i>Boulengerella maculata</i> (Valenciennes, 1850)	MPUJ 14502	Suppl. material 1: fig. S39	Vari 1995
Curimatidae			
<i>Cyphocharax leucostictus</i> (Eigenmann & Eigenmann, 1889)	MPUJ 14376, 14399, 14418	Suppl. material 1: fig. S40	Vari 1992
<i>Cyphocharax spilurus</i> (Gunther, 1864)	MPUJ 14368, 14391	Suppl. material 1: fig. S41	Vari 1992
Cynodontidae			
<i>Hydrolycus wallacei</i> Toledo-Piza, Menezes & Santos, 1999	MPUJ 14547	Suppl. material 1: fig. S42	Toledo-Piza et al. 1999
Gasteropelecidae			
<i>Carnegiella strigata</i> (Gunther, 1864)	MPUJ 14493	Suppl. material 1: fig. S43	Weitzman 1960
Hemiodontidae			
<i>Argonectes longiceps</i> (Kner, 1858)	MPUJ 14554, 16519	Suppl. material 1: fig. S44	Langeani 2018
<i>Bivibranchia fowleri</i> (Steindachner, 1908)	MPUJ 14403, 14426, 14442, 14535, 14416	Suppl. material 1: fig. S45	Langeani 2018
<i>Hemiodus thayeria</i> Böhlke, 1955	MPUJ 14377, 14444, 14514	Suppl. material 1: fig. S46	Langeani 2018
Iguanodectinae			
<i>Bryconops giacopinii</i> (Fernández-Yépez, 1950)	MPUJ 14462, 14463	Suppl. material 1: fig. S47	Chernoff and Machado-Alisson 2005
<i>Bryconops collettei</i> Chernoff & Machado-Alisson, 2005 ³	MPUJ 14461, 14464, 16523	Suppl. material 1: fig. S48	Chernoff and Machado-Alisson 2005
Lebiasinidae			
<i>Copella nattereri</i> (Steindachner, 1876)	MPUJ 14548	Suppl. material 1: fig. S49	Marinho and Menezes 2017
Serrasalminidae			
<i>Myloplus lucienae</i> Andrade, Ota, Bastos, 2016 ¹	MPUJ 14524, 14525, 14528	Suppl. material 1: fig. 3A	Andrade et al. 2016
<i>Serrasalmus striolatus</i> Steindachner, 1908 ³	Uncatalogued, photo voucher only	Suppl. material 1: fig. S51	Taphorn 2003
<i>Serrasalmus manuei</i> (Fernández-Yépez & Ramírez, 1967)	MPUJ 14417	Suppl. material 1: fig. S52	Taphorn 2003
<i>Tometes makue</i> Jégu, Santos & Jégu, 2002 ¹	MPUJ 14498, 14527, 14529, 14550, 14553	Suppl. material 1: fig. 3B	Jégu et al. 2002
Triporthidae			
<i>Triporthus albus</i> Cope, 1872	MPUJ 16522	Suppl. material 1: fig. S54	Malabarba 2004
SILURIFORMES			
Aspredinidae			
<i>Bunocephalus</i> sp. ²	MPUJ 14433	Suppl. material 1: fig. 4B	Carvalho et al. 2018
Auchenipteridae			
<i>Ageneiosus inermis</i> (Linnaeus, 1766)	MPUJ 14515	Suppl. material 1: fig. S56	Ribeiro et al. 2017
<i>Tatia intermedia</i> (Steindachner, 1877)	Uncatalogued, photo voucher only	Suppl. material 1: fig. S57	Sarmento-Soares and Martins-Pinheiro 2008

ORDER/Family/Species	Voucher	fig.	Literature
Doradidae			
<i>Amblydoras affinis</i> Kner, 1855	MPUJ 14398	Suppl. material 1: fig. S58	Birindelli and de Souza 2018
<i>Centrocoras hasemani</i> (Steindachner, 1915) ³	Uncatalogued, photo voucher only	Suppl. material 1: fig. S59	Birindelli and de Souza 2018
<i>Doras phlyszakion</i> Sabaj Pérez & Birindelli, 2008 ³	MPUJ 14521, 14523	Suppl. material 1: fig. S60	Sabaj Pérez and Birindelli 2008
<i>Leptodoras praelongus</i> (Myers & Weitzman, 1956) ³	MPUJ 16518	Suppl. material 1: fig. S61-3C	Sabaj 2005
<i>Tenellus ternetzi</i> (Eigenmann, 1925) ³	MPUJ 15522	Suppl. material 1: fig. S62	Birindelli and de Souza 2018
Heptapteridae			
<i>Leptorhamdia nocturna</i> (Myers, 1928) ³	Uncatalogued, photo voucher only	Suppl. material 1: fig. S63	Bockmann and Slobodian 2018
<i>Mastiglanis asopos</i> Bockmann, 1994	MPUJ 14392, 14469	Suppl. material 1: fig. S64	Bockmann and Slobodian 2018
<i>Pimelodella</i> sp.	MPUJ 14402	Suppl. material 1: fig. S65	Bockmann and Slobodian 2018
Loricariidae			
<i>Ancistrus patronus</i> de Souza, Taphorn & Armbruster, 2019 ³	MPUJ 14470, 14482	Suppl. material 1: fig. S66	de Souza et al. 2019
<i>Hemiancistrus</i> sp. ²	MPUJ 14509, 14519, 14520	Suppl. material 1: fig. 4F	Werneke et al. 2005
<i>Loricaria cataphracta</i> Linnaeus, 1758	MPUJ 14401	Suppl. material 1: fig. S68	Isbrücker 1981; Londoño-Burbano et al. 2021
<i>Rineloricaria cachivera</i> Urbano-Bonilla, Londoño-Burbano & Carvalho, 2023 ²	MPUJ 14375, 14451, 14481, 14495	Suppl. material 1: fig. S70	Urbano-Bonilla et al. 2023
<i>Rineloricaria</i> sp. 1	MPUJ 14380, 14530	Suppl. material 1: fig. S69	Urbano-Bonilla et al. 2023
Pimelodidae			
<i>Pimelodus albofasciatus</i> Mees, 1974	MPUJ 14479, 14503	Suppl. material 1: fig. S71	Rocha and Zuanon 2013
<i>Pimelodus ornatus</i> Kner, 1858	MPUJ 14518	Suppl. material 1: fig. S72	Rocha and Zuanon 2013
Pseudopimelodidae			
<i>Pseudopimelodus bufonius</i> (Valenciennes, 1840)	Uncatalogued, photo voucher only	Suppl. material 1: fig. S73	Shibatta and van der Sleen 2018
Trichomycteridae			
<i>Haemomaster venezuelae</i> Myers, 1927 ³	MPUJ 14396, 14465	Suppl. material 1: fig. S74	Fernández 2018
<i>Ochmacanthus reinhardtii</i> (Steindachner, 1882)	MPUJ 14387, 14431	Suppl. material 1: fig. S75	Fernández 2018
GYMNOTIFORMES			
Sternopygidae			
<i>Archolaemus</i> sp. ²	Uncatalogued, photo voucher only	Suppl. material 1: fig. 4E	Vari et al. 2012
<i>Eigenmannia matintapereira</i> Peixoto, Dutra & Wosiacki, 2015 ¹	MPUJ 14420, 14501	Suppl. material 1: fig. S77-3D	Peixoto et al. 2015
<i>Eigenmannia</i> sp.	MPUJ 14393	Suppl. material 1: fig. S78	Peixoto et al. 2015
<i>Sternopygus macrurus</i> (Bloch & Schneider, 1801)	Uncatalogued, photo voucher only	Suppl. material 1: fig. S79	Hulen et al. 2005
GOBIIFORMES			
Eleotridae			
<i>Microphilypnus ternetzi</i> Myers, 1927 ²	MPUJ 14466	Suppl. material 1: fig. S80	Caires and Toledo-Piza 2018
BLENIIFORMES			
Belonidae			
<i>Potamorrhaphis guianensis</i> (Jardine, 1843)	MPUJ 14508	Suppl. material 1: fig. S81	Sant'Anna et al. 2012
Cichlidae			
<i>Aequidens diadema</i> (Heckel, 1840) ²	MPUJ 14454, 14458, 14459, 14490, 14552	Suppl. material 1: fig. S82	Kullander and Ferreira 1990; Kullander et al. 2018

ORDER/Family/Species	Voucher	fig.	Literature
<i>Aequidens tetramerus</i> (Heckel, 1840) ²	MPUJ 14459	Suppl. material 1: fig. S83	Kullander and Ferreira 1990; Kullander et al. 2018
<i>Apistogramma</i> sp. 1	MPUJ 14450, 14471, 14549, 14372	Suppl. material 1: fig. S84	Kullander et al. 2018
<i>Apistogramma</i> sp. 2	MPUJ 14378, 14406, 14551, 14445	Suppl. material 1: fig. S85	Kullander et al. 2018
<i>Cichla temensis</i> Humboldt, 1821	MPUJ 14510	Suppl. material 1: fig. S86	Kullander and Ferreira 2006
<i>Saxatilia alta</i> (Eigenmann 1912) ²	MPUJ 14474, 14532	Suppl. material 1: fig. S87	Ploeg, 1991; Varella et al. 2023
<i>Lugubria lenticulata</i> (Heckel 1840)	MPUJ 14505	Suppl. material 1: fig. S88	Ploeg, 1991; Kullander and Varella 2015; Varella et al. 2023
<i>Geophagus abalios</i> López-Fernández & Taphorn, 2004	MPUJ 14381, 14404, 14415, 14468, 14513, 14526	Suppl. material 1: fig. S89	López-Fernández and Taphorn 2004
Rivulidae			
<i>Anablepsoides</i> sp.	MPUJ 14485	Suppl. material 1: fig. S90	Amorim and Bragança 2018
SYNBRANCHIFORMES			
Synbranchidae			
<i>Synbranchus marmoratus</i> Bloch, 1795	MPUJ 14500	Suppl. material 1: fig. S91	Van Der Sleen and Albert 2017
ACANTHURIFORMES			
Sciaenidae			
<i>Pachyurus gabrielensis</i> Casatti, 2001	MPUJ 14412, 14441	Suppl. material 1: fig. S92	Casatti 2001
<i>Pachyurus junki</i> Soares & Casatti, 2000	MPUJ 14511	Suppl. material 1: fig. S93	Casatti 2001
<i>Pachyurus schomburgki</i> Gunther, 1860	MPUJ 14512	Suppl. material 1: fig. S94	Casatti 2001
<i>Plagioscion squamosissimus</i> (Haeckel, 1840)	Uncatalogued, photo voucher only	Suppl. material 1: fig. S95	Casatti 2005

Myloplus lucienae Andrade, Ota, Bastos & Jégu, 2016

Specimens collected in this expedition contributed three lots (MPUJ 14524-3 spec.; 14525-1 spec.; 14528-1 spec.; Fig. 3A; Table 3). This species was recently described, and its known distribution was restricted to the Negro River between Manaus and São Gabriel da Cachoeira in Brazil (Andrade et al. 2016). This species is found in blackwater rivers and typically inhabits rapids. *Myloplus lucienae* can be distinguished from other congeners by the combination of an elongated body, small pre-pelvic spines that reach anteriorly just to the middle of the abdomen, and large scales on flanks resulting in lower scale counts (Andrade et al. 2016).

Tometes makue Jégu, Santos & Jégu, 2002

There are five lots from our expedition (MPUJ 14498-7 spec.; 14527-1 spec.; 14529-1 spec.; 14550-1 spec.; 14553-1 spec.; Fig. 3B; Table 3). This species is known to occur in the Negro and Orinoco River basins. In the Negro River, it was reported in several tributaries, including the Rio Uaupés in Brazil at Cachoeira de Ipanoré (Jégu et al. 2002). These represent the first records upstream of that location within Colombian territory. This species is diagnosed among its congeners by the combination of great number of teeth in the inferior jaw (11 teeth) in specimens greater than 100 mm SL in comparison to congeneric species; fewer pre-pelvic serrae (1–9), total serrae (10–23), and horizontal mouth.

Leptodoras praelongus (Myers & Weitzman, 1956)

There is a single lot from our expedition (MPUJ 16518-2 spec.; Fig. 3C; Table 3). This species is known from blackwater drainages in Brazil and Venezuela, associated with large river cataracts on the upper Orinoco and Negro rivers, and occurs in several localities along the Amazon River (Sabaj 2005). This species is diagnosed based on the combination of the following characters: half of dorsal fin without a black spot or blotch; dorsal spine not extended as a long flexible filament; absence of dark nuchal saddle; and flap-like posterior extensions at corners of lower lip narrow and long, finishing beyond tips of similar extensions at corners of upper lip; sum of midlateral plates usually < 75 (range 70–76) and anterior midlateral plates shallow; height of 2nd midlateral plate less than or equal to vertical diameter of eye; anterior nuchal plate usually narrow, permitting suture between supraoccipital and middle nuchal plate; profile of snout weakly concave (Sabaj 2005).

Eigenmannia matintapereira Peixoto, Dutra & Wosiacki, 2015

There are two lots from our expedition (MPUJ 14420-1 spec.; 14501-4 spec.; Fig. 3D; Table 3). The species was described from the Negro River in Brazil (Peixoto et al. 2015) and previous records were known from the Uneixi and Urubaxi

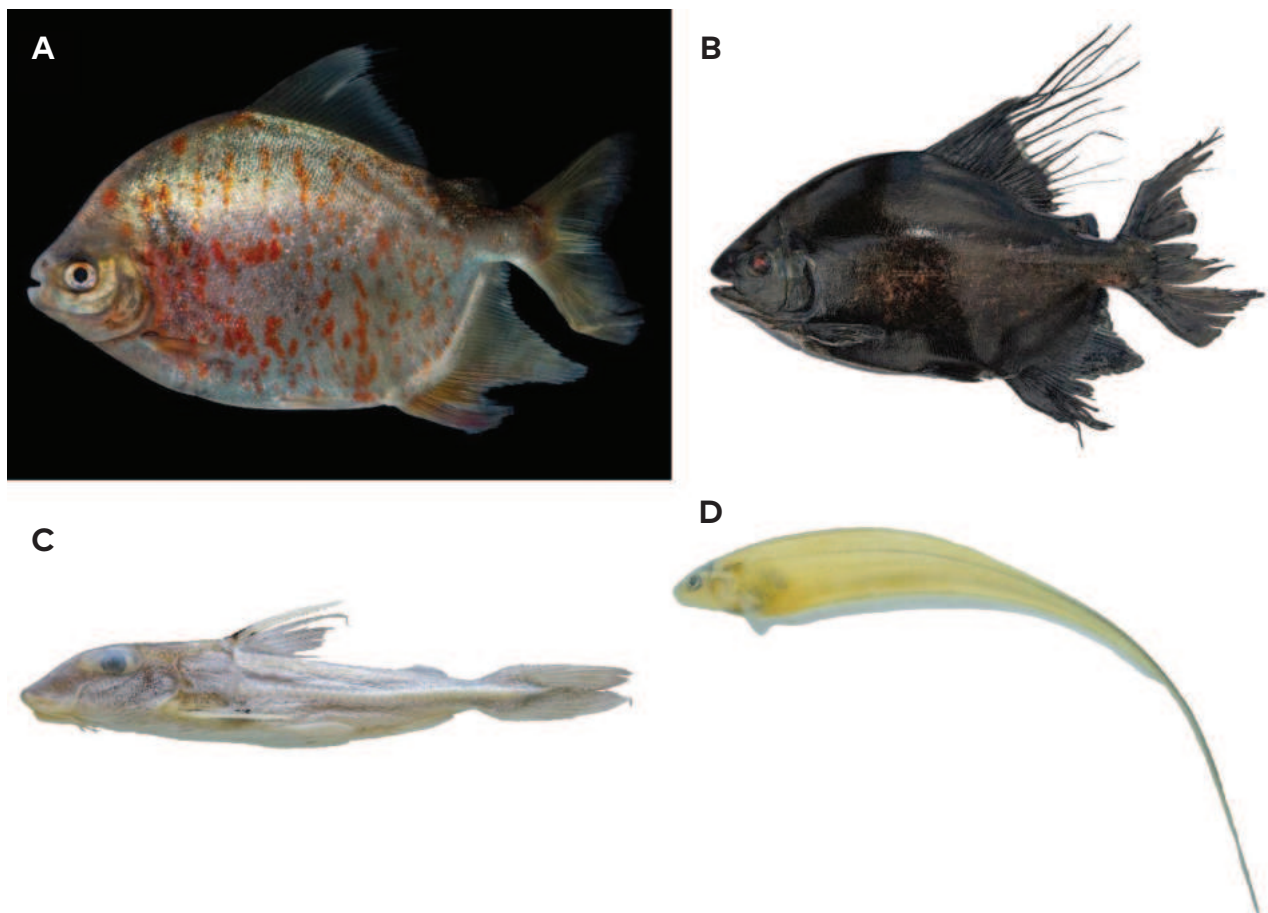


Figure 3. New records for Colombia **A** *Myloplus lucienae* 335.1 mm SL **B** *Tometes makue* 395 mm SL lost and uncatalogued **C** *Leptodoras praelongus* 175.2 mm SL **D** *Eigenmannia matintapereira* 249.1 mm SL.

rivers, tributaries to the Negro River, near Santa Isabel do Rio Negro in Brazil. This species is diagnosed among species of the *Eigenmannia trilineata* group López & Castello, 1966 by having the pectoral fin with a dusky coloration or with a conspicuous dark blotch, and 16-17 branched pectoral-fin rays (Peixoto et al. 2015).

Presumably undescribed species

We found six undescribed species in the lower Vaupés River in Colombia. When verifying their diagnostic characters, they did not coincide with recent taxonomic revisions of each of the genera (Fig. 4A–F). There are genera such as *Eigenmannia* Jordan & Evermann, 1896, *Knodus* Eigenmann, 1911, and *Apistogramma* Regan, 1913 that require taxonomic revisions and under further scrutiny may represent undescribed species.

Jupiaba Zanata, 1997

There are several lots from our expedition of an undescribed species of *Jupiaba* (MPUJ 14385-13 spec.; 14424-3 spec.; 14440-1 spec.; 14446-8 spec.; 14467-5.; 14475-8 spec.; 14488-2 spec.; 14538-1 spec.; 14370; Table 3). This species of *Jupiaba* (Fig. 4A) is most similar to *J. atypindi* Zanata, 1997 and *J. poekotero* Zanata & Lima, 2005 by sharing the combination of premaxillary teeth cusps similar in shape and size; dentary teeth gradually decreasing in size posteriorly; third infraorbital not contacting preopercle ventrally; dark humeral blotch vertically elongated, bordered by clear areas; and teeth of the inner series of premaxilla usually with 7, 9, or 11 cusps (Netto-Ferreira et al. 2009). It differs from *J. atypindi* and *J. poekotero* by its shallower body and distinct coloration pattern on the caudal fin (caudal blotch not reaching ventral and lower margin of caudal peduncle and caudal rays mostly hyaline).

Phenacogaster Eigenmann, 1907

There are two lots from our expedition (MPUJ 14390-5 spec.; MPUJ 14364-1 spec.; Table 3) of an undescribed species of *Phenacogaster* (Fig. 4B). This species has a unique posteriorly displaced humeral spot at a level below dorsal-fin origin that is similar to *P. tegatus* (Eigenmann, 1911), a species distributed in the Paraguay River basin (Lucena and Malabarba 2010). Differing from *P. tegatus*, this species has a complete lateral line (vs an incomplete lateral line).

Moenkhausia Eigenmann 1903

There are seven lots from our expedition (MPUJ 14542-11 spec.; 14543-2 spec.; 14408-13 spec.; 14411-5 spec.; 14427-7 spec.; 14443-7 spec.; 14374-3 spec.; Table 3) of an undescribed species belonging to the *Moenkhausia lepidura* group (Kner, 1858; Fig. 4C). Specimens of this species are similar to *Moenkhausia hasemani* Eigenmann, 1917 also in the *M. lepidura* group by having the combination of predorsal scales arranged in a single median row; it has a humeral spot, conspicuous, which is narrow, vertically elongated, and located on the third to fifth lateral-line scale; five longitudinal scale rows above the lateral line and with 34 or 35 perforated scales on the lateral line; unbranched dorsal-fin rays

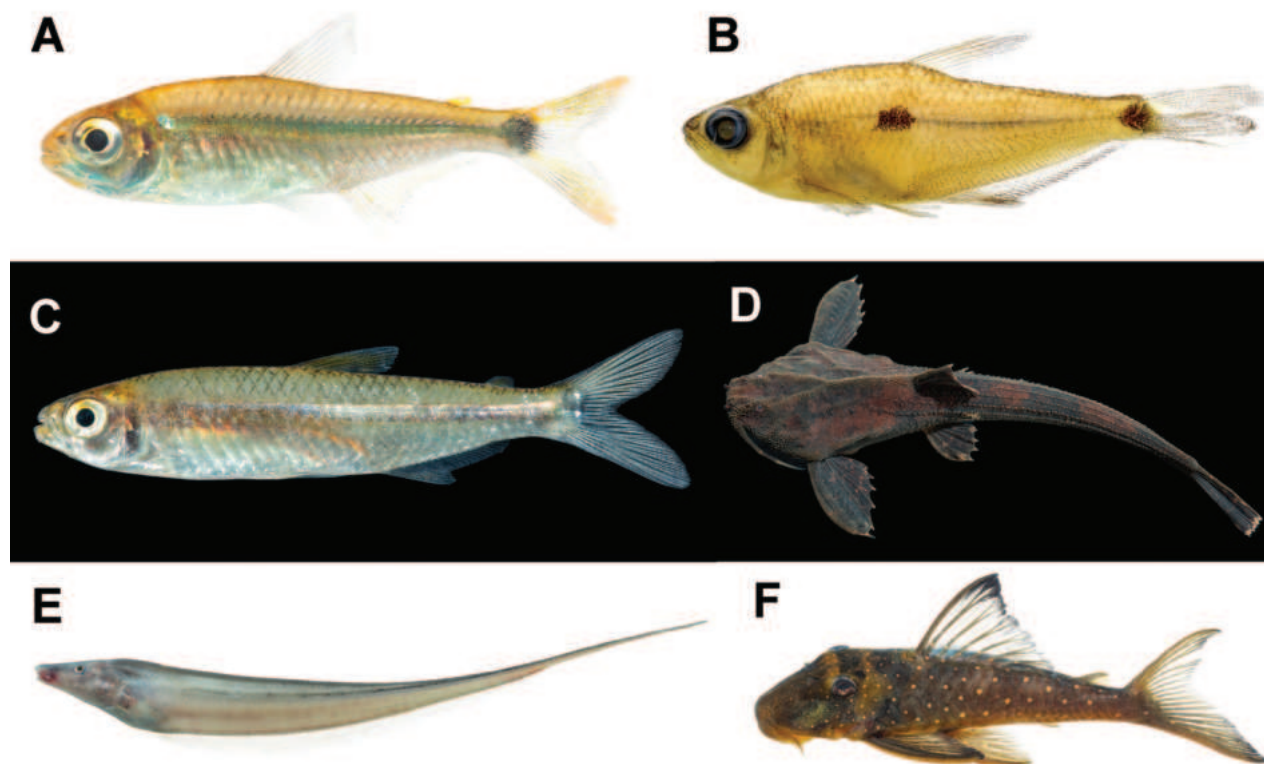


Figure 4. Presumably undescribed species **A** *Jupiaba* sp. 32.6 mm SL **B** *Phenacogaster* sp. 31.3 mm SL **C** *Moenkhausia* sp. 33.1 mm SL **D** *Bunocephalus* sp. 42.5 mm SL **E** *Archolaemus* sp. Lost and uncatalogued copy **F** *Hemiancistrus* sp. 115.3 mm SL.

hyaline, and a longitudinal dark line extending from the humeral spot (or slightly posterior to it), becoming wider at vertical through the posterior third of dorsal fin to the caudal peduncle; caudal-fin lobe mark variable, frequently presenting a semicircular darker spot on its middle portions, and faintly on middle caudal-fin rays (Marinho and Langeani 2016). It differs from *M. hasemani* by having a lower anal-fin ray count with 17–20 branched rays (mode 19) contrasting with 20–23 branched rays in *M. hasemani* (M. Marinho pers. comm. 29 Nov 2021).

Bunocephalus Kner, 1985

There is a single record from our expedition (MPUJ 14433-1 spec; Table 3) of an undescribed species of *Bunocephalus* (Fig. 4D). Species delimitation in *Bunocephalus* is based mainly on morphometric characters and a few meristic features such as fin-ray counts (Mees 1989; Carvalho et al. 2015). The collected species in the Vaupés River represents a species previously identified in a phylogeny whose geographic distribution is the upper Negro and Orinoco river basins (Carvalho et al. 2018); the species could not be identified to species level based on the current literature and likely represents an undescribed species.

Archolaemus Korringa, 1970

The specimen illustrated in Fig. 4E is the first record of the genus *Archolaemus* in Colombia. Unfortunately, it was lost and not catalogued, and there is only a

photographic record and a tissue sample (MPUJ_P_T3796) representing this specimen. The genus *Archolaemus* was reviewed by Vari et al. (2012), and its six known species are distributed in Amazon tributaries draining the Brazilian and the Guiana Shields and in the São Francisco River basin in Brazil. Each species of *Archolaemus* is endemic to a single basin and the geographically closest records of *Archolaemus* to the Vaupés River are of *A. ferrerae* Vari, de Santana & Wosiacki, 2012 in the Uraricoera, a tributary of the Branco River, Negro River basin, Brazil. Based on the photo voucher, the species is most similar to *A. luciae* Vari, de Santana & Wosiacki, 2012 in sharing the combination of traits with a large mouth extending posterior to a vertical through the posterior naris, and a caudal-appendage depth of 3.3–4.8% of the caudal appendage length, which is ~ 4.7% SL. It can be tentatively distinguished from *A. luciae* by having more anal-fin rays (216 vs 192–213; Vari et al. 2012). Given its disjunct geographic distribution from *A. luciae* and other species of the genus, this new record may represent an undescribed species.

Hemiancistrus Bleeker, 1862

There are several records from our expedition (MPUJ 14509-4 spec.; 14519-4 spec.; 14520-1 spec.; Table 3) of an undescribed species of *Hemiancistrus* (Fig. 4F). This species looks like *H. subviridis* Werneke, Sabaj Pérez, Lujan & Armbruster, 2005 by the shared presence of golden yellow spots on the body, but contrasts with *H. subviridis*; however, the species has spots distributed all over the body (vs spots concentrated in the anterior half of the body) and a conspicuous darker posterior margin of the dorsal fin.

Discussion

The Amazon Basin has the greatest freshwater fish biodiversity on the planet (Tisseuil et al. 2013; Dagosta and de Pinna 2019). The Negro River basin and its main drainages have been explored for the last three centuries (Lima et al. 2005). Historical analyses (1821–2019), however, suggest that species richness in the Negro basin is far from being fully known, given that the rate of species descriptions has not stabilized (Beltrão et al. 2019) and there are still areas unexplored scientifically (Jézéquel et al. 2020a). In the Brazilian part of the basin, the uniqueness of the headwater ichthyofaunas are well-documented (Lima et al. 2005), resulting in recent descriptions of more than 30 new species (Beltrão et al. 2019; Bogotá-Gregory et al. 2022a). Recent rigorous work resulted in recording 1,165 fish species associated with different aquatic environments in the basin (Beltrão et al. 2019). Of this compilation, Bogotá-Gregory et al. (2022a) recorded 224 species in the middle Vaupés River basin, of which ten are new records for Colombia and 26 are new records for the Colombian Amazon basin. Our research in the lower Vaupés River basin adds four new records for Colombia and 44 new records (see Table 3) not included in Bogotá-Gregory et al. (2022a), resulting in 268 fish species now known in the middle and lower portions of the Vaupés River basin.

Based on these recent lists of fish species composition (Beltrão et al. 2019; Bogotá-Gregory et al. 2022a) and our results, the entire Negro River basin reaches an approximate richness of 1,210 species. This richness value is still under the predicted estimates that vary between 1,466 and 1,759 species (Beltrão et al. 2019). Despite this, our expedition revealed new records for Colombia, and

undescribed species to science, demonstrating that fish diversity in the region is still far from completely known (Bogotá-Gregory et al. 2020).

Although the Vaupés drainages located to the southwest of our study area have been well sampled (rivers Papuri, Cuduyari Paca, Mituceño, and Tiquié), this study adds new records for the country. Therefore, it is essential to continue monitoring fishes from rheophilic environments and especially those that live in the headwaters of the Vaupés (e.g., Itilla and Unilla rivers; see Fig. 1). This area is recognized for its high degree of species endemism (Hernández-Camacho et al. 1992), the singularity of its fish fauna (Londoño-Burbano and Urbano-Bonilla 2018; Lima et al. 2020), and its connectivity with two protected natural area, the Serranías de la Macarena and Chiribiquete National Parks (Botero and Serrano 2019).

Two new records for Colombia are represented by the serrasalmids *Myloplus lucienae* and *Tometes makue*. From the expeditions of Alfred Russel Wallace (1850–1852) along the Vaupés River, there are illustrations of 43 specimens, representing ~ 40 serrasalmid species (Toledo-Piza 2002). Of these, the fish named “pacu-muritinga” and “pacu-tinga” came to be recognized as *Myloplus lucienae*, a species associated with both rapids and more slowly running waters (Andrade et al. 2016). Therefore, despite the long-known occurrence of this species downstream in the Negro River, this is the first record of this species upstream in the Colombian portion of this basin.

Before the present record of *Myloplus lucienae* in Colombia, the genus was represented by four species in the country, *M. asterias* (Müller & Troschel, 1844), *M. rubripinnis* (Müller & Troschel, 1844), *M. schomburgkii* (Jardine, 1841), and *M. torquatus* (Kner, 1858). The genus *Tometes*, however, was not yet recorded in Colombia (Bogotá-Gregory et al. 2022a; DoNascimento et al. 2024). The populations of *M. lucienae* are distributed in the Negro River basin in Brazil (Andrade et al. 2016) and those of *Tometes makue* in the middle and upper basin of the Negro River in Brazil and the Orinoco River in Venezuela (Jégu et al. 2002); we now document for Colombia the sympatric occurrence of *M. lucienae* (Fig. 3A) and *T. makue* (Fig. 3B). These fishes live in rocky rapids preferably associated with habitats with abundant aquatic vegetation (Podostemaceae). Sympatric fish assemblages form through dispersal and ecological coexistence (Thomaz et al. 2019; Albert et al. 2020).

In *T. makue*, the stomach contents of adult specimens reveal that Podostemaceae plants represent a very important part of the diet of these fishes (Jégu et al. 2002; Lima et al. 2005). On the other hand, *Myloplus* species are generalist herbivorous, with seeds as the main food source, and occasionally feeding on small aquatic animals (van der Sleen and Albert 2017; Correa and Winemiller 2018). In an analysis of the evolution of the diet in the Serrasalminidae family, associated changes in dentition highlight ecomorphological diversity (Kolmann et al. 2021). Podostemaceae makes up most of the diet (based on relative volume) of *Tometes* compared with *Myloplus* (Kolmann et al. 2021), which may explain their sympatric existence.

Between 1923 and 1925 ichthyologist Dr. Carl Ternetz traveled the Amazon from Manaus, up the Negro River and across to the Orinoco River, accruing collections that resulted in descriptions of several new species (Lima et al. 2005). During this expedition, the collected specimens of a fish would be described as *Hassar praelongus* Myers & Weitzman, 1956 (currently *Leptodoras praelongus*) 38 years later, distributed in Brazil and Venezuela (Sabaj 2005; Beltrão et al. 2019). Species of the genus *Leptodoras* are widely distributed in the Amazon, Orinoco

and Essequibo River basins (Sabaj 2005; Birindelli et al. 2008; van der Sleen and Albert 2017; Taphorn et al. 2022). In the Negro River basin (Brazil), seven species [(*Leptodoras acipenserinus* (Günther, 1868), *L. cataniai* Sabaj Pérez, 2005, *L. copei* (Fernández-Yépez, 1968), *L. hasemani* (Steindachner, 1915), *L. juruensis* Boulenger, 1898, *L. linnelli* Eigenmann, 1912, and *L. praelongus* (Myers & Weitzman, 1956)] are known (Beltrão et al. 2019) while for the entire Colombian Amazon five species are known [(*L. acipenserinus*, *L. copei*, *L. juruensis*, *L. linnelli*, and *L. myersi* Böhlke, 1970; Bogotá-Gregory et al. 2022a; DoNascimento et al. 2024)]. Of these, four are shared with drainages of the Colombian Amazon and the Negro River (*L. acipenserinus*, *L. copei*, *L. juruensis*, and *L. linnelli*); two species live in this last river (*L. cataniai* and *L. hasemani*) that are absent in the Colombian Amazon, and that does have records of *L. myersi*, currently absent in the Negro River (Beltrão et al. 2019; DoNascimento et al. 2024). In the rapids of the Macucú community (Mitú), a single specimen of *Leptodoras praelongus* (Fig. 3C) was collected from benthic habitats in deep, fast flowing waters. Some species in the genus (e.g., *L. juruensis* and *L. myersi*) are restricted to deep habitats (50 m; Sabaj 2005). *Leptodoras praelongus* possibly lives in sympatry with *L. copei*, recorded for the middle Vaupés River basin (Bogotá-Gregory et al. 2022a), contrasting with *L. cf. linnelli* that lives downstream in the rapids of Carurú, at the border between Brazil and Colombia (Lima et al. 2005).

Within the electric glassfishes, we recorded new species for Colombia in the genus *Eigenmannia* Jordan & Evermann, 1896. This genus represents the most diverse group in the family Sternopygidae and is distributed throughout Central and South America (Fricke et al. 2023), with its greatest diversity in the Amazon basin (Peixoto and Ohara 2019). It has 24 valid species distributed into two groups; one is called *E. trilineata* group, which includes 22 species (Dutra et al. 2022), with a complex taxonomy, and until recently, *E. virescens* (Valenciennes, 1836) and *E. trilineata* López & Castello, 1966 were erroneously cited as occurring in several Amazon basin drainages. We indicate the presence of two species belonging to the *E. trilineata* group: *E. matintapereira* and an unidentified species. Although there are specimens identified as *Eigenmannia* sp. in other recent inventories in the region (Lima et al. 2005: 256; Bogotá-Gregory et al. 2022a), it is difficult to confirm if these species belong to *E. matintapereira* or even the *E. trilineata* group. Despite that, the present study highlights the sympatry of at least two morphotypes of *Eigenmannia* that occur in the lower basin of the Vaupés River associated with rocky rapids and sandy beaches.

Oberdorff et al. (2019) evaluated 97 Amazon basin drainages and found the size of the habitat, the modern and past climates, and isolation due to natural waterfalls contribute to explain patterns of endemic richness. Naturally, the Vaupés River and the breaks in the relief represented by numerous rapids are common in some of its main drainages. An example of this is the Tiquié River, a tributary of the Vaupés (Fig. 1), which in its route through the different rapids (i.e., Pari-Cachoeira, Pedra Curta, Comprida, and Carurú) shows gradients in fish communities in the downstream-upstream direction; upstream of the Carurú rapids, the absence of some genera (*Phenacogaster* Eigenmann, 1907 and *Serrasalmus* Lacepède, 1803) or species [(*Moenkhausia collettii* (Steindachner, 1882), *Anduzedoras oxyrhynchus* (Valenciennes, 1821), *Pseudoplatystoma tigrinum* (Valenciennes, 1840), *Ageneiosus inermis* (Linnaeus, 1766)] (Lima et al. 2005) is evident. This seems to be consistent with our results, with the exception

of *A. inermis*, which is one of the 92 species of fish identified by the inhabitants of the Tiquié communities in Colombia (Campuzano-Zuluaga 2019).

Contrary to what was observed in the upper part of the Tiquié River, the rapids of the Vaupés River in Colombia (e.g., Fig. 1: rapids upstream between the Colombia-Brazil border to the town of Mitú: Carurú, Matapí, Tapira Geral, La Mojarrá, Macucú, Nana, Villa Fátima rapids) present a different pattern in the occurrence of species since most species listed above are also found in this part of the drainage. In this sense, the rapids at the headwaters of the Vaupes River possibly act as dispersal filters for some species of fishes.

Records are located in the Vaupés Arc, a Miocene origin arch that represents the divide between the Amazon-Orinoco river basins, and represents a semi-permeable barrier for fish dispersal (Winemiler and Willis 2011: table 14.3). Anecdotally, local communities refer to an absence of species upstream of the rapids of Carurú (1°5'8.81"N, 69°19'39"W) that constitutes an important barrier for fish dispersal. An example is the absence of freshwater sting-rays *Potamotrygon* Garman, 1877), the electric eel (*Electrophorus* Gill, 1864), and large migratory catfish (*Brachyplatystoma* Bleeker, 1862) as evidenced in Table 3 and previously published lists of the middle Vaupés River basin in Colombia (Bogotá-Gregory et al. 2022a). In our expedition, we sampled only upstream of this barrier and we did not collect any of these groups.

From another territorial perspective, the historical and traditional knowledge of indigenous communities makes it possible to identify the anthropic displacement of species for subsistence purposes in the Amazon basin (Lima et al. 2005; Camacho-García 2013; Campuzano-Zuluaga 2019). In 1950, in the upper Tiquié River basin, the community transported upstream of the Pedra Curta rapids a fish for consumption, *Satanoperca jurupari* (Heckel, 1840), and it was anticipated that it would colonize the headwaters of the river on the Colombian side (Lima et al. 2005). The coexistence of this species with locally native fish was confirmed 14 years later (Campuzano-Zuluaga, 2019). In addition, it was known that this species was already found naturally in the middle basin of the Vaupés (Bogotá-Gregory et al. 2022a) including its headwaters, i.e., the Unilla and Itilla rivers (Prada-Pedrerós et al. 2018). Likewise, in 1990 another fish used by the communities, *Lugubria johanna* (Heckel, 1840) was transported from the Japurá-Caquetá River basin (in Brazil) to the headwaters of the Tiquié (on the Colombian side) (Lima et al. 2005; Campuzano-Zuluaga 2019) and today inhabits the entire Vaupés River basin, including the main channel, lagoons and main drainages (Beltrão et al. 2019).

Transporting fish species among subbasins of the upper Vaupés River in Colombia threatens both the aquatic biodiversity and the fisheries production of this region. The historical and traditional records reveal the introduction of non-native species, mostly cichlids [(e.g., *Lugubria johanna*, *Heros* sp., *Mesonauta insignis* (Heckel, 1840), *Satanoperca jurupari*)] and an Erythrinidae (*Hoplias lacerdae* Ribeiro, 1908) in the upper Tiquié (Lima et al. 2005; Campuzano-Zuluaga, 2019) that could be related to the decline in the populations of the region's native fish fauna, and threaten the security and food security of the peoples present there (Campuzano-Zuluaga, 2019). Although these species are widely distributed in the Amazon, Orinoco, and Guyanese Shield basins (Beltrão et al. 2019), historical data show translocation of these fish in areas where they did not occur before, and isolated to a certain extent by a series of rapids but living in sympatry with natural populations (Lima et al. 2005).

Regarding cichlids, an example of the extinction of the endemic fauna is known when *Lates niloticus* (Linnaeus, 1758) was introduced to Lake Victoria (Witte et al. 1992). Species checklists and photos document the composition of fish (native and non-native) of the upper Tiquié River, which rises in the southeast of the Colombian territory, in a lagoon system called Ewura (Campuzano-Zuluaga 2019), on its way through Brazilian territory they give way to countless rapids that can act as barriers (Lima et al. 2005). In recent years, endemic (native) fish species have recently been discovered from specific areas of the Tiquié River basin in Brazil [(e.g., *Corydoras desana* Lima & Sazima, 2017; *Hypostomus kopeyaka* and *H. weberi* Carvalho, Lima & Zawadzki, 2010, *Rhinotocinclus yaka* (Lehmann A., Lima & Reis, 2018)] and from the Vaupés River in Colombia (i.e., *Rineloricaria jurupari* Londoño-Burbano & Urbano-Bonilla, 2018, *Hemigrammus xaveriellus* Lima, Urbano-Bonilla, Prada-Pedrerros, 2020 and *Rineloricaria cachivera* Urbano-Bonilla, Londoño-Burbano & Carvalho, 2023). The introduction of non-native fish such as Cichlids generates irreversible effects (displacement, extinction of species, and loss of the gene pool of native species) due to (intra-specific) competition and direct predation (Ogutu-Ohwayo 1993).

In the Amazon Basin, sub-basins with greater accessibility (i.e., shorter travel times from cities or closer to river ports) generally experience greater inventory effort in terms of location density and number of years inventoried, if compared to sites with less accessibility, which is one of the main limitations in fish inventories (Herrera-R et al. 2023). In the study of fish from different geomorphic habitats of the Amazonian lowlands (rivers, alluvial plains, terra firme streams, and shield streams), it is suggested to consider the temporal dynamics of habitat types and variation in hydrological seasonality (Bogotá-Gregory et al. 2023). In this sense, the basin of the Vaupés River in Colombia offers unique and incomparable study opportunities due to its remote and difficult-to-access location, in addition to its geological history, temporal and spatial variability created by rapids, make these results fill gaps of information in areas never before sampled.

The Vaupés River born in the foothills of the eastern Colombian mountain range and flows through outcrops of the Guiana Shield and sandy-soils of the Amazonian lowlands. The water chemistry of this basin is therefore a combination of sediment-rich Andean whitewaters (Unilla river sub-basin; see Fig. 1) and acidic blackwaters that drain sandy lowland rainforest soils (i.e., oxisols) of the peri-Guiana shield region (Itilla River sub-basin; see Fig. 1). The large information gaps in the area (Jézéquel et al. 2020a), the presence of endemic rheophilic species (*Rineloricaria jurupari* Londoño-Burbano & Urbano-Bonilla, 2018, *R. daraha* Rapp Py-Daniel & Fichberg, 2008, *R. cachivera* Urbano-Bonilla Londoño-Burbano & Carvalho, 2023), and various undescribed species (*Odontocharacidium* Buck-up, 1993, *Tetragonopterus* Cuvier, 1816, *Tyttocharax* Fowler, 1913, *Ituglanis* Costa & Bockmann, 1993, *Myoglanis* Eigenmann, 1912, *Nemuroglanis* Eigenmann & Eigenmann, 1889 and *Aequidens* Eigenmann & Bray, 1894; Bogotá-Gregory et al. 2022a) including those in this study (i.e., *Jupiaba* sp., *Moenkhausia* sp., *Phenacogaster* sp., *Bunocephalus* sp., *Hemiancistrus* sp., and *Archolaemus* sp.) support the need to strengthen scientific expeditions and community monitoring of fish. This research should be accomplished in partnership with local indigenous communities or settlers that depend on fish for their subsistence, especially those who live in the rapids of the Vaupés River (i.e., Carurú, Matapí, Tapira Geral, La Mojarra, Macucú, Nana, Villa Fátima, and its headwaters, the Itilla and Unilla).

Conclusions

This study contributes new fish records for the Vaupes Arch region, a biodiverse but poorly explored region of the Colombian Amazon of high geological importance with extensive and well-preserved forested and aquatic habitats. These results increase the documented fish diversity of this region to 95 species, identify several putatively new species to science, and further document geographic and habitat distribution patterns. Continued systematic sampling of this region at larger spatial and temporal scales will advance progress in the knowledge of the species, populations, communities, and their habitats, especially the rapids of the Vaupés River. The taxonomic lists and high-resolution photographs made available from on public consultation platforms (CaVFfish Project - Colombia), represent important resources for monitoring, conservation, and fisheries management of the Vaupés River basin, at local, regional, national and international levels for waters shared among Brazil, Venezuela and Colombia.

Acknowledgments

We want to thank several people in indigenous communities in the region for their support: William González-Torres y Arturo Hernández (Trubón community, Cubeo ethnic group), Emilio Márquez y Anderson Márquez (Villa Fátima community, Guanano ethnic group); Adelmo Santacruz (Nana community, Guanano ethnic group); Jaider Ramírez-Samaniego (Macucú community, Desano ethnic group), Julio V. Vélez y Silvio Vélez (Matapi community, Desano ethnic group). Additionally, we thank the following people for help during the expedition Alejandro Campuzano-Zuluaga (Fundación Conservando); Luis F. Jaramillo-Hurtado (Instituto Amazónico de Investigaciones Científicas SINCHI), and Mariana A. Moscoso (Ictiología y Cultura). Thanks to Alejandro Londoño-Burbano, Angela Zanata; Bárbara Calegari; Cárison Oliveira, Carlos DoNascimento, Dario Faustino-Fuster, Fernando Jerep, Fernando Carvalho, Flávio Lima, Guilherme Dutra, Gustavo Ballen, Henrique Varela, Hernan López Fernandez, Henry Agudelo, José Birindelli, Manoela Marinho, Marcelo Andrade, Matthew Kolmann, Nathan Lujan, Mark Sabaj, and Priscila Madoka Ito, for help with the taxonomic identification of species. We also thank Saul Prada Pedreros for curatorial assistance in the Museo Javeriano de Historia Natural (MPUJ) fish collection, where the fishes are housed.

Additional information

Conflict of interest

The authors have declared that no competing interests exist.

Ethical statement

No ethical statement was reported.

Funding

National Geographic funded the expedition (Grant # 8981-11 to S.B. Correa). The assemblage of this species list received the support from Pontificia Universidad Javeriana with the "Carta Encíclica Laudato Si" grant in the project entitled "Ictiología y

Cultura: Aproximación biológica y cultural a los datos obtenidos en la expedición en las cachiveras del río Vaupés” (#20112). S.B. Correa was supported by the Forest and Wildlife Research Center of Mississippi State University, USA (MISZ-081700).

Author contributions

AU-B: Field data collection and laboratory analysis; study design, data analysis, and manuscript writing. JEG-M: Field data collection, photography (PhotaFish), and data processing and analysis (CaVFish Project). MEP-B: Data collection and laboratory photography. OEM-O: Collection and analysis of laboratory data. OSO: Laboratory data collection and analysis. SBC: Field data collection; analysis of the information and writing of the manuscript. TPC: data analysis, and writing of the manuscript. JMO: Field data collection and project manager.

Author ORCIDs

Alexander Urbano-Bonilla  <https://orcid.org/0000-0002-0190-8913>

Jorge E. Garcia-Melo  <https://orcid.org/0000-0003-2885-5652>

Mateo Esteban Peña-Bermudez  <https://orcid.org/0000-0003-3900-3826>

Sandra Bibiana Correa  <https://orcid.org/0000-0003-4466-6923>

Tiago P. Carvalho  <https://orcid.org/0000-0001-5901-1634>

Data availability

All of the data that support the findings of this study are available in the main text or Supplementary Information.

References

- Albert JS, Crampton WGR (2010) The geography and ecology of diversification in Neotropical freshwaters. *Nature Education Knowledge* 1: 13–19. <https://doi.org/10.1525/california/9780520268685.003.0001>
- Albert JS, Reis RE (2011) Introduction to Neotropical freshwaters. *Historical biogeography of Neotropical freshwater fishes* 1: 3–20. <https://doi.org/10.1525/california/9780520268685.003.0002>
- Albert JS, Tagliacollo VA, Dagosta F (2020) Diversification of Neotropical freshwater fishes. *Annual Review of Ecology, Evolution, and Systematics* 51(1): 27–53. <https://doi.org/10.1146/annurev-ecolsys-011620-031032>
- Amorim P, Bragança PHN (2018) Family Rivulidae—Rivuline Killifishes. In: van der Sleen P, Albert JS (Eds) *Field guide to the fishes of the Amazon, Orinoco, and Guianas*. Field Guides, Vol. 115. Princeton, NJ: Princeton University Press, 350–359.
- Andrade MC, Ota RP, Bastos DA, Jegu M (2016) A new large *Myloplus* Gill 1896 from rio Negro basin, Brazilian Amazon (Characiformes: Serrasalminidae). *Zootaxa* 4205(6): 571–580. <https://doi.org/10.11646/zootaxa.4205.6.5>
- Arbour JH, López-Fernández H (2016) Continental cichlid radiations: functional diversity reveals the role of changing ecological opportunity in the Neotropics. *Proceedings of the Royal Society B: Biological Sciences* 283(1836): 1–9. <https://doi.org/10.1098/rspb.2016.0556>
- Armbruster JW, Lujan NK, Bloom DD (2021) Redescription of the Guiana Shield darter species *Characidium crandellii* and *C. declivirostre* (Crenuchidae) with descriptions of two new species. *Ichthyology & Herpetology* 109(1): 102–122. <https://doi.org/10.1643/i2019299>

- Beltrão H, Zuanon J, Ferreira E (2019) Checklist of the ichthyofauna of the Rio Negro basin in the Brazilian Amazon. *ZooKeys* 881: 53–89. <https://doi.org/10.3897/zookeys.881.32055>
- Birindelli JLO, de Sousa LM (2018) Family Doradidae-Thorny Catfishes. In: In van der Sleen P, Albert JS (Eds) *Field guide to the fishes of the Amazon, Orinoco, and Guianas. Field Guides, Vol. 115.* Princeton, NJ: Princeton University Press, 222–232.
- Birindelli JL, Sidlauskas BL (2018) Preface: How far has Neotropical Ichthyology progressed in twenty years? *Neotropical Ichthyology* 16(3): 1–8. <https://doi.org/10.1590/1982-0224-20180128>
- Birindelli JL, Sousa LM, Pérez MHS (2008) New species of thorny catfish, genus *Leptodoras* Boulenger (Siluriformes: Doradidae), from Tapajós and Xingu basins, Brazil. *Neotropical Ichthyology* 6(3): 465–480. <https://doi.org/10.1590/S1679-62252008000300020>
- Bockmann F, Slobodian V (2018) Family Heptapteridae—Three-Barbeled Catfishes. In: van der Sleen P, Albert JS (Eds) *Field guide to the fishes of the Amazon, Orinoco, and Guianas. Field Guides, Vol. 115.* Princeton, NJ: Princeton University Press, 234–252.
- Bogotá-Gregory JD, Lima FC, DoNascimento C, Acosta-Santos A, Navarro-Villa FA, Córdoba EA (2020) First records of freshwater fish species in Colombia: Extending the distribution of 17 Amazonian and Orinoco fish species. *Check List* 16(5): 1395–1406. <https://doi.org/10.15560/16.5.1395>
- Bogotá-Gregory JD, Lima FC, DoNascimento C, Acosta-Santos A, Villa-Navarro FA, Usma-Oviedo J, Ortega-Lara A, Castro-Pulido W, Córdoba EA (2022a) Fishes of the Mitú Region: middle basin of the río Vaupés, Colombian Amazon. *Biota Neotropical* 22(1): 2–22. <https://doi.org/10.1590/1676-0611-bn-2021-1244>
- Bogotá-Gregory JD, DoNascimento C, Lima FCT, Acosta-Santos A, Villa-Navarro FA, Urbano-Bonilla A, Mojica JI, Córdoba EA (2022b) Peces de la región de la Amazonia Colombiana: Composición de especies de los sistemas fluviales del bioma de selva húmeda. *Biota Neotropica* 22(4): 2–59. <https://doi.org/10.1590/1676-0611-bn-2022-1392>
- Bogotá-Gregory JD, Jenkins DG, Lima FC, Magurran AE, Crampton WG (2023) Geomorphological habitat type drives variation in temporal species turnover but not temporal nestedness in Amazonian fish assemblages. *Oikos* 2023(11): 2–13. <https://doi.org/10.1111/oik.09967>
- Botero CA (2020) La paz produce ciencia. Expediciones biológicas en reemplazo de la guerra. *Biodiversidad En La Práctica* 5(1): 1–14. <http://revistas.humboldt.org.co/index.php/BEP/article/view/758>
- Botero P, Serrano H (2019) Caracterización Biofísica del área de ampliación: geología, geomorfología y suelos. In: Rojas et al., expediciones científicas en las nuevas áreas del PNN Serranía de Chiribiquete. Fundación para la Conservación y el Desarrollo Sostenible-FCDS. Bogotá, D.C., Colombia, 21–30.
- Caires RA, Toledo-Piza M (2018) A New Species of Miniature Fish of the Genus *Microphilypnus* (Gobioidae: Eleotridae) from the Upper Rio Negro Basin, Amazonas, Brazil. *Copeia* 106(1): 49–55. <https://doi.org/10.1643/CI-17-634>
- Camacho García KA (2013) *Tejiendo Sueños, atrapando peces. Hilando historias y conocimientos sobre el medio ambiente de la pesca en áreas de la Cuenca Amazónica.* Bogotá-Colombia, 250 pp.
- Campuzano-Zuluaga A (2019) *Conhecimento tradicional e modo de vida para pensar na gestão comunitária do recurso pesqueiro na zona Aatizot, Alto Tiquié, Alto Rio Negro, Amazônia Colombiana.* Master's Thesis, Instituto Nacional De Pesquisas Da Amazônia - Inpa-Brazil, 221 pp.

- Carvalho TP, Cardoso AR, Friel JP, Reis RE (2015) Two new species of the banjo catfish *Bunocephalus* Kner (Siluriformes: Aspredinidae) from the upper and middle rio São Francisco basins, Brazil. *Neotropical Ichthyology* 13(3): 499–512. <https://doi.org/10.1590/1982-0224-20140152>
- Carvalho TP, Arce M, Reis RE, Sabaj MH (2018) Molecular phylogeny of Banjo catfishes (Ostariophysi: Siluriformes: Aspredinidae): A continental radiation in South American freshwaters. *Molecular Phylogenetics and Evolution* 127: 459–467. <https://doi.org/10.1016/j.ympev.2018.04.039>
- Casatti L (2001) Taxonomia do gênero sul-americano *Pachyurus* Agassiz, 1831 (Teleostei: Perciformes: Sciaenidae) e descrição de duas novas espécies. *Comunicações do Museu de Ciências e Tecnologia da PUCRS. Série Zoologia* 14(2): 133–178.
- Casatti L (2005) Revision of the South American freshwater genus *Plagioscion* (Teleostei, Perciformes, Sciaenidae). *Zootaxa* 1080(1): 39–64. <https://doi.org/10.11646/zootaxa.1080.1.4>
- Chernoff B, Machado-Allison A (2005) *Bryconops magoi* and *Bryconops collettei* (Characiformes: Characidae), two new freshwater fish species from Venezuela, with comments on *B. caudomaculatus* (Günther). *Zootaxa* 1094(1): 1–23. <https://doi.org/10.11646/zootaxa.1094.1.1>
- Chernoff B, Machado-Allison A, Saul WG (1991) Morphology, variation and biogeography of *Leporinus brunneus* (Pisces: Characiformes: Anostomidae). *Ichthyological exploration of freshwaters. Munchen* 1(4): 295–306.
- Correa SB, Winemiller K (2018) Terrestrial–aquatic trophic linkages support fish production in a tropical oligotrophic river. *Oecologia* 186(4): 1069–1078. <https://doi.org/10.1007/s00442-018-4093-7>
- Dagosta FC, de Pinna M (2019) The fishes of the Amazon: Distribution and biogeographical patterns, with a comprehensive list of species. *Bulletin of the American Museum of Natural History* 2019(431): 1–163. <https://doi.org/10.1206/0003-0090.431.1.1>
- De Souza LS, Taphorn DC, Armbruster JW (2019) Review of *Ancistrus* (Siluriformes: Loricariidae) from the northwestern Guiana Shield, Orinoco Andes, and adjacent basins with description of six new species. *Zootaxa* 4552(1): 1–67. <https://doi.org/10.11646/zootaxa.4552.1.1>
- DoNascimento C, Herrera-Collazos EE, Herrera-R GA, Ortega-Lara A, Villa-Navarro FA, Usma Oviedo JS, Maldonado-Ocampo JA (2017) Checklist of the freshwater fishes of Colombia: A Darwin Core alternative to the updating problem. *ZooKeys* 25(708): 25–138. <https://doi.org/10.3897/zookeys.708.13897>
- DoNascimento C, Agudelo-Zamora HD, Bogotá-Gregory JD, Méndez-López A, Ortega-Lara A, Lasso C, Cortés-Hernández MA, Albornoz Garzón JG, Villa-Navarro FA, Netto-Ferreira AL, Lima FTC, Thomaz A, Arce HM (2024) Lista de especies de peces de agua dulce de Colombia / Checklist of the freshwater fishes of Colombia. v2.16. Asociación Colombiana de Ictiólogos. Dataset/Checklist. <https://doi.org/10.15472/numrso>
- Dornburg A, Near TJ (2021) The emerging phylogenetic perspective on the evolution of actinopterygian fishes. *Annual Review of Ecology, Evolution, and Systematics* 52(1): 427–452. <https://doi.org/10.1146/annurev-ecolsys-122120-122554>
- Dutra GM, Ramos TPA, Menezes NA (2022) Description of three new species of *Eigenmannia* (Gymnotiformes: Sternopygidae) from the rio Mearim and rio Parnaíba basins, Northeastern Brazil. *Neotropical Ichthyology* 20(1): 1–23. <https://doi.org/10.1590/1982-0224-2021-0117>
- Fernández L (2018) Family Trichomycteridae—Pencil Catfishes, Torrent Catfishes, and Parasitic Catfishes (Candirús). In: van der Sleen P, Albert JS (Eds) *Field guide to the*

- fishes of the Amazon, Orinoco, and Guianas. Field Guides, Vol. 115. Princeton University Press, Princeton, NJ, 311–322.
- Ferreira AL, Zanata AM, Birindelli JLO, Sousa LM (2009) Two new species of *Jupiaba* (Characiformes: Characidae) from the rio Tapajós and rio Madeira drainages, Brazil. *Zootaxa* 2262(1): 53–68. <https://doi.org/10.11646/zootaxa.2262.1.3>
- Fricke R, Eschmeyer WN, Van der Laan R (2023) Eschmeyer's Catalog of Fishes: Genera, Species, References. [Online] <http://researcharchive.calacademy.org/research/ichthyology/catalog/fishcatmain.asp> [Accessed Jan 8, 2023]
- García-Melo JE, García-Melo LJ, García-Melo JD, Rojas-Briñez DK, Guevara G, Maldonado-Ocampo JA (2019) Photafish system: An affordable device for fish photography in the wild. *Zootaxa* 4554(1): 141–172. <https://doi.org/10.11646/zootaxa.4554.1.4>
- Géry J (1977) Characoids of the world. TFH Pub., Neptune City, New Jersey, 672 pp.
- Hernández-Camacho JI, Hurtado-Guerra A, Ortiz-Quijano R, Walschburger T (1992) Unidades biogeográficas de Colombia. En G. Halffter (Comp.), La diversidad biológica de Iberoamérica. Xalapa: Acta Zoológica Mexicana, 105–151.
- Herrera-R GA, Tedesco PA, DoNascimento C, Jézéquel C, Giam X (2023) Accessibility and appeal jointly bias the inventory of Neotropical freshwater fish fauna. *Biological Conservation* 284: 2–12. <https://doi.org/10.1016/j.biocon.2023.110186>
- Hulen KG, Crampton WG, Albert JS (2005) Phylogenetic systematics and historical biogeography of the Neotropical electric fish *Sternopygus* (Teleostei: Gymnotiformes). *Systematics and Biodiversity* 3(4): 407–432. <https://doi.org/10.1017/S1477200005001726>
- Irwin A (2023) The race to understand Colombia's exceptional biodiversity. *Nature* 619: 450–453. <https://doi.org/10.1038/d41586-023-02300-6>
- Isbrücker I (1981) Revision of *Loricaria* Linnaeus, 1758 (Pisces, Siluriformes, Loricariidae). *Beaufortia* 31(3): 51–96.
- Jégu M, Santos GD, Belmont-Jégu E (2002) *Tometes makue* n. sp. (Characidae: Serrasalminae), une nouvelle espèce du bouclier guyanais décrite des bassins du Rio Negro (Brésil) et de l'Orénoque (Venezuela). *Cybium* 26(4): 253–274.
- Jézéquel C, Tedesco PA, Bigorne R, Maldonado-Ocampo JA, Ortega H, Hidalgo M, Martens K, Torrente-Vilara G, Zuanon J, Acosta A, Agudelo E, Barrera Maure S, Bastos DA, Bogotá Gregory J, Cabeceira FG, Canto ALC, Carvajal-Vallejos FM, Carvalho LN, Cella-Ribeiro A, Covain R, Donascimento C, Dória CRC, Duarte C, Ferreira EJJ, Galuch AV, Giarrizzo T, Leitão RP, Lundberg JG, Maldonado M, Mojica JI, Montag LFA, Ohara WM, Pires THS, Pouilly M, Prada-Pedreras S, de Queiroz LJ, Rapp Py-Daniel L, Ribeiro FRV, Ríos Herrera R, Sarmiento J, Sousa LM, Stegmann LF, Valdiviezo-Rivera J, Villa F, Yunoki T, Oberdorff T (2020a) A database of freshwater fish species of the Amazon Basin. *Scientific Data* 7(1): 1–9. <https://doi.org/10.1038/s41597-020-0436-4>
- Jézéquel C, Tedesco PA, Darwall W, Dias MS, Frederico RG, Hidalgo M, Hugueny B, Maldonado-Ocampo J, Martens K, Ortega H, Torrente-Vilara G, Zuanon J, Oberdorff T (2020b) Freshwater fish diversity hotspots for conservation priorities in the Amazon Basin. *Conservation Biology* 34(4): 956–965. <https://doi.org/10.1111/cobi.13466>
- Kolmann MA, Hughes LC, Hernandez LP, Arcila D, Betancur-R R, Sabaj MH, López-Fernández H, Ortí G (2021) Phylogenomics of piranhas and pacus (Serrasalminidae) uncovers how dietary convergence and parallelism obfuscate traditional morphological taxonomy. *Systematic Biology* 70(3): 576–592. <https://doi.org/10.1093/sysbio/syaa065>
- Kullander SO, Ferreira EJ (1990) A new *Aequidens* species from the río Trombetas, Brasil, and redescription of *Aequidens pallidus* (Teleostei, Cichlidae). *Zoologica Scripta* 19(4): 425–433. <https://doi.org/10.1111/j.1463-6409.1990.tb00269.x>

- Kullander SO, Ferreira EJ (2006) A review of the South American cichlid genus *Cichla*, with descriptions of nine new species (Teleostei: Cichlidae). *Ichthyological Exploration of Freshwaters* 17(4): 289–398.
- Kullander SO, Varella HR (2015) Wallace's pike cichlid gets a name after 160 years: a new species of cichlid fish (Teleostei: Cichlidae) from the upper Rio Negro in Brazil. *Copeia* 103(3): 512–519. <https://doi.org/10.1643/C1-14-169>
- Kullander SO, López-Fernández H, van der Sleen P (2018) Family Cichlidae—Cichlids. In: van der Sleen P, Albert JS (Eds) *Field guide to the fishes of the Amazon, Orinoco, and Guianas. Field Guides, Vol. 115*. Princeton University Press, Princeton, NJ, 359–385.
- Langeani F (2018) Family Hemiodontidae—Halftooths. In: van der Sleen P, Albert JS (Eds) *Field guide to the fishes of the Amazon, Orinoco, and Guianas. Field Guides, Vol. 115*. Princeton University Press, Princeton, NJ, 161–163.
- Lima FCT, Ramos T, Barreto A, Cabalzar G, Tenório A, Barbosa F, Tenório ASR (2005) Peixes do Alto Tiquié - Ictiologia e conhecimentos dos tukuya e tukano. In: Cabalzar A (Org.) *Peixe e Gente no Alto Rio Tiquié*. São Paulo, Instituto Socioambiental, 111–282.
- Lima FCT (2017) A revision of the cis-andean species of the genus *Brycon* Müller & Troschel (Characiformes: Characidae). *Zootaxa* 4222(1): 1–189. <https://doi.org/10.11646/zootaxa.4222.1.1>
- Lima FCT, da Silva Pires TE, Ohara W, Jerep F, Rogério-Carvalho F, Marinho MM, Zuanon J (2013) *Peixes do rio Madeira, Volume 1. Dialeto*, São Paulo, Brazil, 402 pp.
- Lima FCT, Urbano-Bonilla A, Prada-Pedrerros S (2020) A new *Hemigrammus* from the upper Río Vaupés, Colombia (Characiformes: Characidae), with a discussion on the presence of an enlarged urogenital papilla in the family. *Journal of Fish Biology* 96(4): 868–876. <https://doi.org/10.1111/jfb.14267>
- Londoño-Burbano A, Urbano-Bonilla A (2018) A new species of *Rineloricaria* (Teleostei: Loricariidae) from the upper Vaupés River, Amazon River basin, Colombia. *Ichthyological Exploration of Freshwaters* IEF-1071: 1–10. <https://doi.org/10.23788/IEF-1071>
- López-Fernández H, Taphorn DC (2004) *Geophagus abalios*, *G. dicrozoster* and *G. winemilleri* (Perciformes: Cichlidae), three new species from Venezuela. *Zootaxa* 439(1): 1–27. <https://doi.org/10.11646/zootaxa.439.1.1>
- López-Fernández H, Winemiller KO (2003) Morphological variation in *Acestrorhynchus microlepis* and *A. falcatus* (Characiformes: Acestrorhynchidae), reassessment of *A. apurensis* and distribution of *Acestrorhynchus* in Venezuela. *Ichthyological Exploration of Freshwaters* 14(3): 193–208.
- Lucena ZMSD, Malabarba LR (2010) Descrição de nove espécies novas de *Phenacogaster* (Ostariophysi: Characiformes: Characidae) e comentários sobre as demais espécies do gênero. *Zoologia* 27(2): 263–304. <https://doi.org/10.1590/S1984-46702010000200014>
- Lucena CAS, Calegari BB, Pereira EHL, Dallegre E (2013) O uso de óleo de cravo na eutanásia de peixes. *Boletim Sociedade Brasileira de Ictiologia* 105: 20–24.
- Lujan NK, Conway KW (2015) Life in the fast lane: a review of rheophily in freshwater fishes. *Extremophile fishes: Ecology, evolution, and physiology of teleosts in extreme environments*, 107–136. https://doi.org/10.1007/978-3-319-13362-1_6
- Lujan NK, Winemiller KO, Armbruster JW (2012) Trophic diversity in the evolution and community assembly of loricariid catfishes. *BMC Evolutionary Biology* 12(1): 1–13. <https://doi.org/10.1186/1471-2148-12-124>
- Malabarba MCS (2004) Revision of the Neotropical genus *Triportheus* Cope, 1872 (Characiformes: Characidae). *Neotropical Ichthyology* 2(4): 167–204. <https://doi.org/10.1590/S1679-62252004000400001>

- Marinho MM, Langeani F (2016) Reconciling more than 150 years of taxonomic confusion: the true identity of *Moenkhausia lepidura*, with a key to the species of the *M. lepidura* group (Characiformes: Characidae). *Zootaxa* 4107(3): 338–352. <https://doi.org/10.11646/zootaxa.4107.3.3>
- Marinho MM, Menezes NA (2017) Taxonomic review of *Copella* (Characiformes: Lebiasinidae) with an identification key for the species. *PLOS ONE* 12(8): 1–53. <https://doi.org/10.1371/journal.pone.0183069>
- Mathubara K, Toledo-Piza M (2020) Taxonomic study of *Moenkhausia cotinho* Eigenmann, 1908 and *Hemigrammus newboldi* (Fernández-Yépez, 1949) with the description of two new species of *Moenkhausia* (Teleostei: Characiformes: Characidae). *Zootaxa* 4852(1): 1–40. <https://doi.org/10.11646/zootaxa.4852.1.1>
- Mees GF (1989) Notes on the genus *Dysichthys*, subfamily Bunocephalinae, family Aspredinidae (Pisces, Nematognathi). *Proceedings of the Koninklijke Nederlandse Akademie van Wetenschappen. Series C. Biological and Medical Sciences* 92(2): 189–250.
- Santos GM, Jégu M (1987) Novas ocorrências de *Gnathodolus bidens*, *Synaptolaemus cingulatus* e descrição de duas espécies novas de *Sartor* (Characiformes, Anostomidae). *Amazoniana. Limnologia et Oecologia Regionalis Systematis Fluminis Amazonas* 10(2): 181–196.
- Netto-Ferreira AL, Zanata AM, Birindelli JLO, Sousa LM (2009) Two new species of *Jupiaba* (Characiformes: Characidae) from the rio Tapajós and rio Madeira drainages, Brazil. *Zootaxa* 2262(1): 53–68. <https://doi.org/10.11646/zootaxa.2262.1.3>
- Oberdorff T, Dias MS, Jézéquel C, Albert JS, Arantes CC, Bigorne R, Carvajal-Valleros FM, De Wever A, Frederico RG, Hidalgo M, Hugueny B, Leprieur F, Maldonado M, Maldonado-Ocampo J, Martens K, Ortega H, Sarmiento J, Tedesco PA, Torrente-Vilara G, Winemiller KO, Zuanon J (2019) Unexpected fish diversity gradients in the Amazon basin. *Science Advances* 5(9): 1–10. <https://doi.org/10.1126/sciadv.aav8681>
- Ogutu-Ohwayo R (1993) The effects of predation by Nile perch, *Lates niloticus* L., on the fish of Lake Nabugabo, with suggestions for conservation of endangered endemic cichlids. *Conservation Biology* 7(3): 701–711. <https://doi.org/10.1046/j.1523-1739.1993.07030701.x>
- Peixoto LAW, Ohara WM (2019) A new species of *Eigenmannia* Jordan & Evermann (Gymnotiformes: Sternopygidae) from rio Tapajós, Brazil, with discussion on its species group and the myology within Eigenmanniinae. *PLOS ONE* 14(8): 1–30. <https://doi.org/10.1371/journal.pone.0220287>
- Peixoto LA, Dutra GM, Wosiacki WB (2015) The electric glass knifefishes of the *Eigenmannia trilineata* species-group (Gymnotiformes: Sternopygidae): monophyly and description of seven new species. *Zoological Journal of the Linnean Society* 175(2): 384–414. <https://doi.org/10.1111/zoj.12274>
- Ploeg A (1991) Revision of the South American Cichlid Genus *Crenicichla* Heckel, 1840: With Descriptions of Fifteen New Species and Considerations on Species Groups, Phylogeny and Biogeography;(pisces, Perciformes, Cichlidae). Thesis. University Amsterdam, Amsterdam.
- Prada-Pedrerros S, Herrera-Collazos EE, Maldonado-Ocampo JA, Pinto-Carvalho TP (2018) Colección de peces del Museo de Historia Natural de la Pontificia Universidad Javeriana. v4.10. Pontificia Universidad Javeriana. Dataset/Occurrence. <http://doi.org/10.15472/uozvak>
- Py-Daniel LHR, Fichberg I (2008) A new species of *Rineloricaria* (Siluriformes: Loricariidae: Loricariinae) from rio Daraá, rio Negro basin, Amazon, Brazil. *Neotropical Ichthyology* 6(3): 339–346. <https://doi.org/10.1590/S1679-62252008000300007>

- Reis RE, Albert JS, Di Dario F, Mincarone MM, Petry P, Rocha LA (2016) Fish biodiversity and conservation in South America. *Journal of Fish Biology* 89(1): 12–47. <https://doi.org/10.1111/jfb.13016>
- Ribeiro FRV, Rapp Py-Daniel LH, Walsh SJ (2017) Taxonomic revision of the South American catfish genus *Ageneiosus* (Siluriformes: Auchenipteridae) with the description of four new species. *Journal of Fish Biology* 90(4): 1388–1478. <https://doi.org/10.1111/jfb.13246>
- Rocha MS, Zuanon J (2013) Peixes do rio Madeira, Volume III. Diaeto, São Paulo, Brazil.
- Román-Valencia C (2003) Three new species of the genus *Bryconamericus* (Teleostei: Characidae) from Venezuela. *Dahlia* 6: 7–15.
- Roxo FF, Lujan NK, Tagliacollo VA, Waltz BT, Silva GS, Oliveira C, Albert JS (2017) Shift from slow-to fast-water habitats accelerates lineage and phenotype evolution in a clade of Neotropical suckermouth catfishes (Loricariidae: Hypoptopomatinae). *PLOS ONE* 12(6): 1–17. <https://doi.org/10.1371/journal.pone.0178240>
- Sabaj MH (2005) Taxonomic assessment of *Leptodoras* (Siluriformes: Doradidae) with descriptions of three new species. *Neotropical Ichthyology* 3(4): 637–678. <https://doi.org/10.1590/S1679-62252005000400020>
- Sabaj MH, Birindelli JL (2008) Taxonomic revision of extant *Doras* Lacepède, 1803 (Siluriformes: Doradidae) with descriptions of three new species. *Proceedings of the Academy of Natural Sciences of Philadelphia* 157(1): 189–233. [https://doi.org/10.1635/0097-3157\(2008\)157\[189:TROEDL\]2.0.CO;2](https://doi.org/10.1635/0097-3157(2008)157[189:TROEDL]2.0.CO;2)
- Sant’Anna VB, Delapieve MLS, Reis RE (2012) A new species of *Potamorhaphis* (Beloniformes: Belonidae) from the Amazon Basin. *Copeia* 2012(4): 663–669. <https://doi.org/10.1643/CI-12-032>
- Sarmiento-Soares LM, Martins-Pinheiro RF (2008) A systematic revision of *Tatia* (Siluriformes: auchenipteridae: Centromochlinae). *Neotropical Ichthyology* 6(3): 495–542. <https://doi.org/10.1590/S1679-62252008000300022>
- Shibatta OA, van der Sleen P (2018) Family Pseudopimelodidae—Bumblebee Catfishes, Dwarf-Marbled Catfishes. In: van der Sleen P, Albert JS (Eds) *Field guide to the fishes of the Amazon, Orinoco, and Guianas*. Field Guides, Vol. 115. Princeton, NJ: Princeton University Press, 308–310. <https://doi.org/10.1515/9781400888801>
- Sidlauskas BL, Mol JH, Vari RP (2011) Dealing with allometry in linear and geometric morphometrics: a taxonomic case study in the *Leporinus cylindricus* group (Characiformes: Anostomidae) with description of a new species from Suriname. *Zoological Journal of the Linnean Society* 162(1): 103–130. <https://doi.org/10.1111/j.1096-3642.2010.00677.x>
- Silva GS, Melo BF, Oliveira C, Benine RC (2016) Revision of the South American genus *Tetragonopterus* Cuvier, 1816 (Teleostei: Characidae) with description of four new species. *Zootaxa* 4200(1): 1–46. <https://doi.org/10.11646/zootaxa.4200.1.1>
- Soares IM, Ota RP, Lima FC, Benine RC (2020) Redescription of *Moenkhausia melogramma* (Characiformes: Characidae), a poorly known tetra from the western Amazon basin. *Neotropical Ichthyology* 18(3): 1–17. <https://doi.org/10.1590/1982-0224-2020-0025>
- Steindachner F (1915) Beiträge zur Kenntniss der Flussfische Südamerikas. 1–13. In *Komm. bei Alfred Hölder*. v. 93: 1–106.
- Taphorn D (2003) The Characiform fishes of the Apure river drainage, Venezuela. *Biollania*. Edición Especial 4: 1–537.
- Taphorn DCB, Montaña CG, Buckup PA (2006) *Characidium longum* (Characiformes: Crenuchidae), a new fish from Venezuela. *Zootaxa* 1247: 1–12. <https://doi.org/10.11646/zootaxa.1247.1.1>

- Taphorn DC, Liverpool E, Lujan NK, DoNascimento C, Hemraj DD, Crampton WGR, Kolmann MA, Fontenelle JP, de Souza LS, Werneke DC, Ram M, Bloom DD, Sidlauskas BL, Holm E, Lundberg JG, Sabaj MH, Bernard C, Armbruster JW, López-Fernández H (2022) Annotated checklist of the primarily freshwater fishes of Guyana. *Proceedings of the Academy of Natural Sciences of Philadelphia* 168(1): 1–95. <https://doi.org/10.1635/053.168.0101>
- Thomaz AT, Carvalho TP, Malabarba LR, Knowles LL (2019) Geographic distributions, phenotypes, and phylogenetic relationships of *Phalloceros* (Cyprinodontiformes: Poeciliidae): insights about diversification among sympatric species pools. *Molecular Phylogenetics and Evolution* 132: 265–274. <https://doi.org/10.1016/j.ympev.2018.12.008>
- Tisseuil C, Cornu JF, Beauchard O, Brosse S, Darwall W, Holland R, Huguény B, Tedesco PA, Oberdorff T (2013) Global diversity patterns and cross-taxa convergence in freshwater systems. *Journal of Animal Ecology* 82(2): 365–376. <https://doi.org/10.1111/1365-2656.12018>
- Toledo-Piza M (2002). *Fishes of the Rio Negro*. Alfred Russel Wallace. Editora da Universidade de São Paulo, São Paulo, 518 pp.
- Toledo-Piza M, Menezes NAD, Santos GMD (1999) Revision of the neotropical fish genus *Hydrolycus* (Ostariophysi: Cynodontinae) with description of two new species. *Ichthyological Exploration of Freshwaters* 10(3): 255–280.
- Urbano-Bonilla A, Roa-Varon A, Arce HM (2021) Dr. Javier Alejandro Maldonado-Ocampo. *Ichthyology & Herpetology* 109(4): 1073–1074. <https://doi.org/10.1643/t2021115>
- Urbano-Bonilla A, Londoño-Burbano A, Carvalho TP (2023) A new species of rheophilic armored catfish of *Rineloricaria* (Siluriformes: Loricariidae) from the Vaupés River, Amazonas basin, Colombia. *Journal of Fish Biology* 103(5): 1073–1084. <https://doi.org/10.1111/jfb.15500>
- van der Sleen P, Albert JS [Eds] (2017) *Field guide to the fishes of the Amazon, Orinoco, and Guianas*. Field Guides, Vol. 115. Princeton University Press, Princeton, NJ. <https://doi.org/10.2307/j.ctt1qv5r0f>
- Varella HR, Kullander SO, Menezes NA, Oliveira C, López-Fernández H (2023) Revision of the generic classification of pike cichlids using an integrative phylogenetic approach (Cichlidae: tribe Geophagini: subtribe Crenicichlina). *Zoological Journal of the Linnean Society* 198(4): 982–1034. <https://doi.org/10.1093/zoolinnean/zlad021>
- Vari RP (1992) Systematics of the neotropical characiform genus *Cyphocharax* Fowler (Pisces: Ostariophysi). *Smithsonian Contributions to Zoology* 529: 1–1137. <https://doi.org/10.5479/si.00810282.529>
- Vari RP, Harold AS (2001) Phylogenetic study of the Neotropical fish genera *Creagrutus* Günther and *Piabina* Reinhardt (Teleostei: Ostariophysi: Characiformes), with a revision of the cis-Andean species. *Smithsonian Contributions to Zoology* 613(613): 1–239. <https://doi.org/10.5479/si.00810282.613>
- Vari RP, Castro R, Raredon SJ (1995) The Neotropical fish family Chilodontidae (Teleostei: Characiformes): a phylogenetic study and a revision of *Caenotropus* Günther. *Smithsonian Contributions to Zoology* 577(577): 1–32. <https://doi.org/10.5479/si.00810282.577>
- Vari RP, De Santana CD, Wosiacki WB (2012) South American electric knifefishes of the genus *Archolaemus* (Ostariophysi, Gymnotiformes): Undetected diversity in a clade of rheophiles. *Zoological Journal of the Linnean Society* 165(3): 670–699. <https://doi.org/10.1111/j.1096-3642.2012.00827.x>
- Weitzman SH (1960) Further notes on the relationships and classification of the South American characid fishes of the subfamily Gasteropelecinae. *Stanford Ichthyological Bulletin* 7(4): 217–239.

- Werneke DC, Sabaj MH, Lujan NK, Armbruster JW (2005) *Baryancistrus demantoides* and *Hemiancistrus subviridis*, two new uniquely colored species of catfishes from Venezuela (Siluriformes: Loricariidae). *Neotropical Ichthyology* 3(4): 533–542. <https://doi.org/10.1590/S1679-62252005000400011>
- Winemiller KO, Willis SC (2011) The vaupes arch and casiquiare canal. Historical biogeography of neotropical freshwater fishes. University of California Press, Berkeley 225–242. <https://doi.org/10.1525/california/9780520268685.003.0014>
- Witte F, Goldschmidt T, Wanink J, van Oijen M, Goudswaard K, Witte-Maas E, Bouton N (1992) The destruction of an endemic species flock: Quantitative data on the decline of the haplochromine cichlids of Lake Victoria. *Environmental Biology of Fishes* 34(1): 1–28. <https://doi.org/10.1007/BF00004782>
- Zanata AM (1997) *Jupiaba*, um novo gênero de Tetragonopterinae com osso pélvico em forma de espinho (Characidae, Characiformes). *Iheringia, Série Zoologia* 83: 99–136.
- Zarske A, Géry J (2007) *Hemigrammus geisleri* sp. n. a new glass characid fish from the central Amazon basin, with a supplementary description of *Hemigrammus minus* Böhlke, 1955 (Teleostei: Characiformes: Characidae). *Vertebrate Zoology* 57(1): 5–15. <https://doi.org/10.3897/vz.57.e30866>

Supplementary material 1

Photographic atlas of voucher specimens

Authors: Alexander Urbano-Bonilla, Jorge E. Garcia-Melo, Mateo Esteban Peña-Bermudez, Omar Eduardo Melo-Ortiz, Oscar Stiven Ordoñez, Sandra Bibiana Correa, Tiago P. Carvalho, Javier A. Maldonado-Ocampo

Data type: docx

Explanation note: Photographic atlas of voucher specimens collected on the lower Vaupés River, Vaupés, Colombia. Measurements are presented as standard length (SL). All species photographed in life are uploaded to the CaVFish Colombia Project.

Copyright notice: This dataset is made available under the Open Database License (<http://opendatacommons.org/licenses/odbl/1.0/>). The Open Database License (ODbL) is a license agreement intended to allow users to freely share, modify, and use this Dataset while maintaining this same freedom for others, provided that the original source and author(s) are credited.

Link: <https://doi.org/10.3897/zookeys.1203.100642.suppl1>

A remarkable new species of *Paraparatrechina* Donisthorpe (1947) (Hymenoptera, Formicidae, Formicinae) from the Eastern Himalayas, India

Ramakrishnaiah Sahanashree¹, Aswaj Punnath², Dharma Rajan Priyadarsanan¹

¹ Ashoka Trust for Research in Ecology and the Environment, Royal Enclave, Srirampura, Jakkur Post, Bengaluru – 560064, Karnataka, India

² Entomology and Nematology Department, University of Florida, 1881 Natural Area Drive, Gainesville, FL, 32611, USA

Corresponding author: Dharma Rajan Priyadarsanan (priyan@atree.org)

Abstract

A new ant species, *Paraparatrechina neela* **sp. nov.**, with a captivating metallic-blue color is described based on the worker caste from the East Siang district of Arunachal Pradesh, northeastern India. This discovery signifies the first new species of *Paraparatrechina* in 121 years, since the description of the sole previously known species, *P. aseta* (Forel, 1902), in the Indian subcontinent.

Key words: Abor Expedition, Arunachal Pradesh, aspirator, East Siang, taxonomy



Academic editor: Jeffrey Sosa-Calvo
Received: 15 October 2023
Accepted: 16 April 2024
Published: 30 May 2024

ZooBank: <https://zoobank.org/F5F74325-7B54-4728-90A2-441F83F6FABD>

Citation: Sahanashree R, Punnath A, Rajan Priyadarsanan D (2024) A remarkable new species of *Paraparatrechina* Donisthorpe (1947) (Hymenoptera, Formicidae, Formicinae) from the Eastern Himalayas, India. ZooKeys 1203: 159–172. <https://doi.org/10.3897/zookeys.1203.114168>

Copyright: © Ramakrishnaiah Sahanashree et al. This is an open access article distributed under terms of the Creative Commons Attribution License (Attribution 4.0 International – CC BY 4.0).

Introduction

The formicine ant genus *Paraparatrechina* was originally described by Donisthorpe (1947) as a subgenus of *Paratrechina* Motschoulsky, 1863, with *Pa. (Paraparatrechina) pallida* (Donisthorpe, 1947) as type species by monotypy. Later, Brown (1973) treated *Paraparatrechina* as a provisional junior synonym of *Paratrechina*, and Trager (1984) confirmed this synonymy, citing the lack of monophyly of the subgenus based on a morphological assessment. However, LaPolla et al. (2010a) redefined *Paratrechina* as a monotypic genus with *Pa. longicornis* (Latreille, 1802) based on a phylogenetic analysis of the *Prenolepis* genus-group. That study also recovered *Paraparatrechina* as a valid monophyletic genus, distinguishable from its sister taxa by the uniform, erect setal pattern on the mesosoma. Currently, the *Prenolepis* genus-group comprises the genera *Euprenolepis* Emery, 1906, *Nylanderia* Emery, 1906, *Paraparatrechina*, *Paratrechina*, *Prenolepis* Mayr, 1861, and *Pseudolasius* Emery, 1887 (LaPolla et al. 2010a).

Paraparatrechina are generally small ants, measuring 1–2 mm long, and they are typically found in the Afrotropical, Australasian, Indomalayan, Oceanian, and Palearctic biogeographic regions (LaPolla et al. 2010b; AntWeb 2023a). The genus can be easily distinguished from other formicine ant genera by a unique mesosomal setal pattern, which includes two pairs of erect pronotal setae, one pair of mesonotal setae, and one pair of propodeal setae

(LaPolla et al. 2010a). The genus is often confused with *Nylanderia*. However, *Nylanderia* lacks a pair of erect propodeal setae and has six mandibular teeth instead of five (LaPolla et al. 2010b).

Paraparatrechina is present in various tropical environments, ranging from rainforests to forest clearings, and can be found in a wide spectrum of habitats, ranging from leaf litter on the ground to high up in the canopy (LaPolla et al. 2010b). Afrotropical species, for example *P. weissii* (Santschi, 1910) and *P. bufona* (Wheeler, 1922), are the only known polymorphic species of *Paraparatrechina*, displaying several morphological characteristics indicative of a hypogaeic lifestyle (LaPolla et al. 2010a).

Currently, *Paraparatrechina* encompasses 38 valid species and four valid subspecies (Bolton 2023). The Indomalayan biogeographic region has 14 known species, while *P. aseta* (Forel, 1902) is the only known species in the Indian subcontinent until now (Bharti and Wachkoo 2014). This species has been reported in several states of India, including Gujarat, Himachal Pradesh, Jammu and Kashmir, Sikkim, Nagaland, and West Bengal (Bharti et al. 2016; Janicki et al. 2016; Guénard et al. 2017). In this study, we describe and illustrate *P. neela* sp. nov., which was discovered in the foothills of the Eastern Himalayas of India. This find comes 121 years after the discovery of the only previously known Indian species, *P. aseta*.

During the period of colonial rule in India, a scientific expedition to document the natural history and geography of the Siang Valley of the Eastern Himalayas accompanied a punitive military expedition against the indigenous people there in 1911–12 (Army Intelligence Branch 1911). Originally known as the Abor Expedition, the findings of the expedition were published in several volumes from 1912 to 1922 in the *Records of the Indian Museum*. Now, a century later, a team of researchers has been engaged in a series of expeditions under the banner “Siang Expedition”, funded by the National Geographic Society through the wildlife-conservation expedition grant (NGS-71945c-20), to resurvey the biodiversity of the region. In May 2022, among several other ant species from various genera, we collected two worker specimens of *P. neela* sp. nov. from Yingku village, in East Siang District of Arunachal Pradesh, northeastern India. This remarkable new species represents the first documented occurrence of the genus in Arunachal Pradesh and only the second *Paraparatrechina* species known from the Indian subcontinent.

Materials and methods

Two worker specimens belonging to *Paraparatrechina* were collected from a secondary forest at an elevation of 803 m in Yingku village, which is located in East Siang District of Arunachal Pradesh, northeastern India (Fig. 1). East Siang District is encompassed between latitudes 27°43'N to 29°20'N and longitudes 94°42'E to 95°35'E and has an area of 4005 km². It has tropical and humid-subtropical climate, with temperatures of 18–28 °C and an average annual rainfall of 4168 mm (Yumnam et al. 2013; Yogesh Kumar et al. 2022). These specimens were collected from debris in a hole in a tree trunk 3 m above the ground. We used an aspirator to extract the specimens and preserved them in absolute alcohol. The specimens were point mounted and examined under a Zeiss SteREO Discover.V8 microscope.

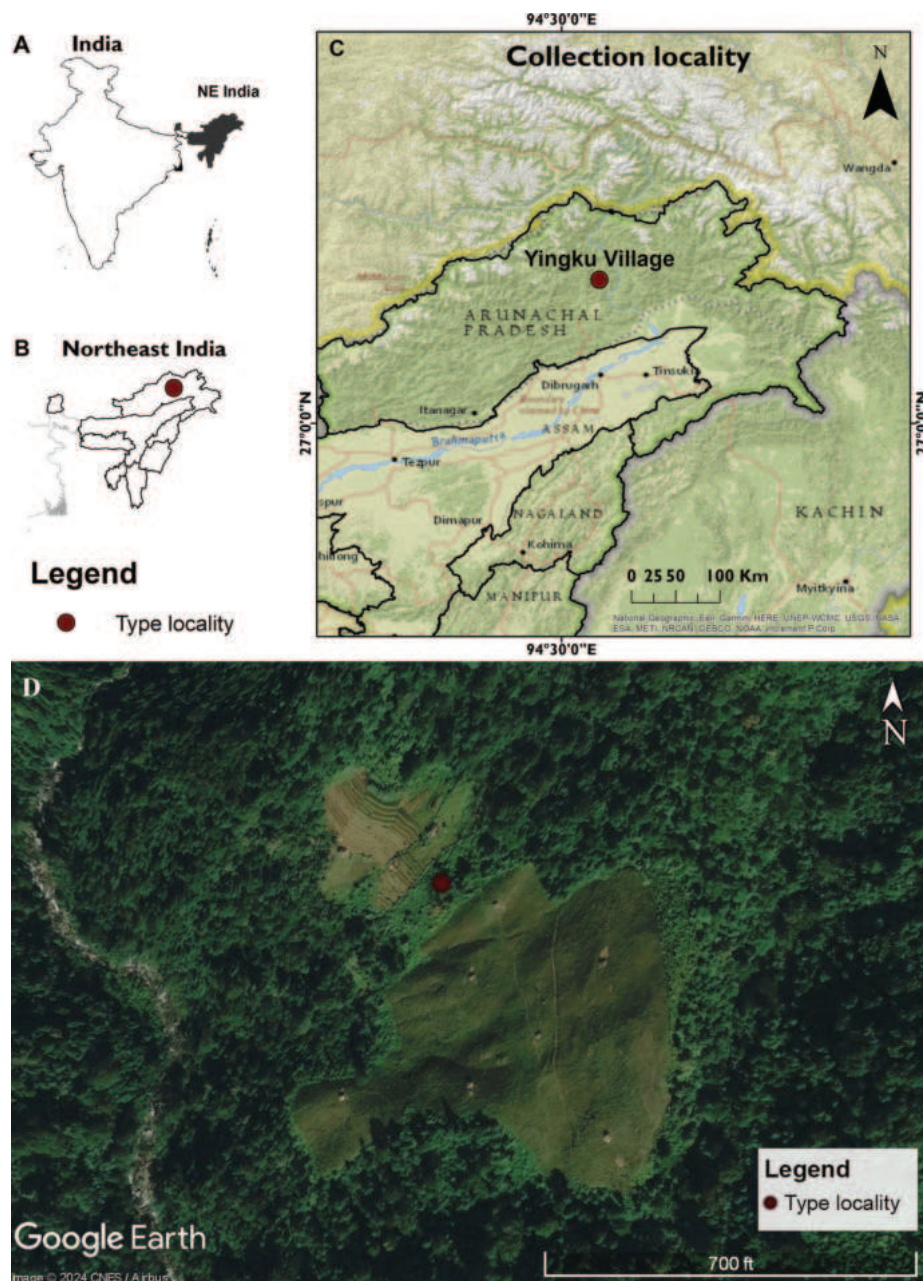


Figure 1. Map showing the type locality of *P. neela* sp. nov. in the Yingku Village, Arunachal Pradesh, northeastern India **A** India, with the North East Region (NER) shown in gray **B** states of the NER with type locality in Arunachal Pradesh **C** Arunachal Pradesh showing the location of the type locality (Yingku village) **D** Google Earth satellite image showing the type locality (Source: Google Earth Pro 2023, accessed on 11 February 2024).

The identifications of the specimens were made by referring to available taxonomic keys by LaPolla et al. (2010a, 2010b) and comparing them with images of the types of all known *Parapatrechina* species, except for *P. bufona*, *P. kongming* (Terayama, 2009), *P. nana* (Santschi, 1928), *P. sakuya* Terayama, 2013, *P. sordida* (Santschi, 1914), and *P. tapinomoides* (Forel, 1905), which are not available on AntWeb (2023a). We checked original descriptions and available illustrations for specimens that did not have type images. The unique metallic-blue coloration of the body, in combination with the head shape, sculpture and

pubescence patterns, helped us to confirm the status of new species. Stacked focus montage images of the new species were captured at 200× magnification using a Keyence VHX 6000 digital microscope. Final figures were prepared using Adobe Photoshop v. 25. The map was prepared using ArcGIS v. 10.4.1 (ArcGIS 2023). The holotype and paratype specimens are deposited in ATREE Insect Museum, Bangalore, India (**AIMB**). Body measurements are in millimeters and were taken with AxioVision v. 4.8 software (Carl Zeiss, Germany) and recorded with two decimal places. Body measurements and indices (Fig. 2) follow LaPolla and Fisher (2014).

Eye length (**EL**): maximum length of compound eye in full-face view.

Head length (**HL**): the length of the head proper, excluding the mandibles; measured in full-face view from the midpoint of the anterior clypeal margin to a line drawn across the posterior margin from its highest points.

Head width (**HW**): the maximum width of the head in full-face view.

Scape length (**SL**): the maximum length of the antennal scape excluding the condylar bulb.

Pronotal width (**PW**): the maximum width of the pronotum in dorsal view.

Weber's length (**WL**): in lateral view, the distance from the posteriormost border of the metapleural lobe to the anteriormost border of the pronotum, excluding the neck.

Gaster length (**GL**): the length of the gaster in lateral view from the anteriormost point of the first gastral segment (third abdominal segment) to the posteriormost point.

Total length (**TL**): $HL + WL + GL$.

Cephalic index (**CI**): $(HW / HL) \times 100$.

Relative eye length index (**REL**): $(EL / HL) \times 100$.

Scape index (**SI**): $(SL / HW) \times 100$.

Results

Parapatrechina Donisthorpe, 1947

Parapatrechina Donisthorpe 1947: 192, as a subgenus of *Paratrechina*. Type species: *Paratrechina pallida*, by monotypy.

Parapatrechina as junior synonym of *Paratrechina*: Brown 1973: 183; Trager 1984: 58.

Status as genus. LaPolla et al. 2010a: 128.

Diagnosis. Worker (adapted from LaPolla et al. 2010a): *Parapatrechina* workers can be identified by the following combination of characters: antenna with 12 segments; mandible with 5 or 6 teeth; maxillary palp and labial palp 6- and 4-segmented, respectively; erect setae on head form a distinct pattern consisting of 4 setae along posterior margin and 6 or 7 rows of paired setae from posterior margin to clypeal margin; erect setae absent on antennal scapes and legs; head excluding clypeal surface and mesonotal dorsum with dense pubescence; eyes typically well developed and positioned laterally towards the midline of head; erect mesosomal setae distinctly paired—2 pairs on pronotum, 1 pair on mesonotum, and 1 pair on propodeum; propodeum dorsal face



Figure 2. *Paraparatrechina umbranatis* LaPolla & Cheng, 2010, showing schematic representation of the body measurements. Abbreviations are defined in materials and methods. Photo credit: April Nobile, www.antweb.org, CASENT0178764 (AntWeb 2024).

typically short compared to its longer posterior face; general overall mesosoma shape compact, although a few species have elongated mesosoma.

Queen (adapted from Cantone 2018): antennae filiform with 12 segments, extending beyond occipital margin; antennal socket located near posterior edge of clypeus; forewings exhibit typology III, formica type, with a closed marginal cell; hindwings display typology II, lacking anal 2 vein;

mandibles triangular and dentate; palp formula 6:4, or in *P. bufona* and *P. weissi*, maxillary palp consists of 5 segments; mesosomal setal pattern same as in workers; metatibiae with a single spur.

Male (adapted from Cantone 2017): antennae with 13 segments, with the scape extending beyond occipital margin; first funicular segment longer and wider than second; forewings exhibit typology III, with a closed marginal cell; hindwings correspond to typology II; mandibles edentate.

Key to *Parapatrechina* species of the Indian subcontinent based on the worker caste

We recognize the uncertainty in the taxonomy of Indomalayan *Parapatrechina*, as some species do not have the typical characteristics of the genus, and for this reason, we have not provided a key to the Indomalayan species. A comprehensive revision is necessary before reliable taxonomic key to the Indomalayan *Parapatrechina* can be made.

The Indian subcontinent has only two species of *Parapatrechina*, *P. aseta* and *P. neela* sp. nov. See the worker description of *P. neela* for a detailed comparison with *P. aseta*.

- 1 Body uniformly light brown; head subrectangular; mandible with 6 teeth in the masticatory margin..... ***P. aseta***
- Body largely metallic blue; head subtriangular; mandible with 5 teeth in the masticatory margin ***P. neela* sp. nov.**

***Parapatrechina neela* sp. nov.**

<https://zoobank.org/E1CB7812-6BF7-4CCC-A319-0D75A493416F>

Figs 3, 4

Material examined. Holotype: worker, point mounted. Original label: "India: Arunachal Pradesh, East Siang District, Yingku Village, 28.4606°N, 94.8841°E, 803 m a.s.l., aspirator, 7 May 2022, Priyadarsanan DR leg."; AIMB/Hy/Fr 25006.

Paratype: 1 worker; same data as holotype; AIMB/Hy/Fr 25007.

Worker description. Measurements (in mm) and indices:

Holotype worker: EL 0.14; HL 0.50; HW 0.42; SL 0.51; PW 0.29; WL 0.53; GL 0.66; TL 1.69; CI 84; REL 28; SI 121.

Paratype worker: EL 0.13; HL 0.59; HW 0.43; SL 0.50; PW 0.28; WL 0.57; GL 0.66; TL 1.76; CI 72; REL 22; SI 116.

Diagnosis. *Parapatrechina neela* sp. nov. has the following unique combination of characters: 1) body opaque and largely metallic blue, except antennae, mandibles, and legs; 2) total length < 2 mm; 3) eyes large relative to head length (REL > 22); 3) scape with appressed pubescence and scape surpasses posterior margin of head by approximately length of first 4 funicular segments; 4) propodeal dorsal face short and angular, with a long declivitous face.

Head. In full-face view (Fig. 3A), subtriangular, 1.2× longer than wide; posterior margin of head convex. Mandible triangular, masticatory margin with 5 teeth (Fig. 4A), 1 long apical tooth followed by acutely triangular tooth, 2 minute denticles and a triangular basal tooth: maxillary palp and labial palp with palp



Figure 3. *Parapatrechina neela* sp. nov., holotype worker AIMB/Hy/Fr 25006 **A** head in full-face view **B** body in dorsal view **C** body in profile view.

formula, PF (6:4). Antennae with 12 segments; scape surpasses posterior margin of head approximately by the length of first 4 funicular segments. In profile view, clypeal disc projects, medially carinate. In full-face view, anterior clypeal margin convex. Eyes large, REL 22–28, oval; ocelli present, only median ocellus visible, other two ocelli relatively concealed, indistinct (Fig. 3A).



Figure 4. *Parapatrechina neela* sp. nov., holotype worker AIMB/Hy/Fr 25006 **A** clypeus and mandibles **B** mesosoma in profile view **C** mesosoma in dorsal view **D** gaster in dorsal view.

Mesosoma. Compact in lateral view, pronotum convex with short dorsal face in lateral view (Figs 3C, 4B). Mesonotum sloping towards metanotum, propleura and mesopleura demarcated by a distinct promesonotal suture; mesopleura and metapleura demarcated by indistinct metanotal groove; propodeum raised, propodeal dorsal face short, angular, with a long declivitous face; propodeal spiracle distinct (Fig. 3C).

Metasoma. Petiole length 0.05 mm, strongly compressed antero-posteriorly. Gaster with 5 tergites, anterior margin concave and forming sharp edges in dorsal view (Figs 3B, 4D). Acidopore distinct apically (Fig. 3C).

Sculpture. Body covered with fine punctures; mandibles with longitudinal striations (Fig. 4A); clypeus, mesopleura, and propodeal declivity smooth and shiny (Fig. 4A–C).

Pilosity. Short, decumbent pubescence covers most of the body. Distinctly paired dark setae present from anterior clypeal margin to propodeum; 8 pairs on head from posterior region to clypeus; 2 pairs on pronotum, 2 pairs on mesonotum, 1 pair on propodeum (Figs 3C, 4B). Setae shorter on head posterior to eyes and gaster and longer on anterior of head and mesosoma.

Color. Body largely iridescent blue, with a purple tinge and white pubescence; legs and antennae brown at base, dark to yellowish brown at middle, white at the tip; mandible yellowish brown. Gaster blue in anterior region, brown towards posterior end.

Etymology. The specific epithet *neela* is a noun in apposition, signifying the color blue in most Indian languages. It is used to describe the unique blue or sapphire color of this species.

Species comparison. *Paraparatrechina neela* sp. nov. is easily distinguishable from all known species of *Paraparatrechina* by its metallic-blue body. It can be separated from *P. aseta*, the only other known species from the Indian subcontinent (Fig. 5A–C) by the following characteristics: 1) body largely metallic blue, except antennae, mandibles, and legs in *P. neela* (body uniformly light brown in *P. aseta*); 2) in full-face view, head subtriangular with strongly convex lateral margin in *P. neela* (head subrectangular with gently convex lateral margin in *P. aseta*); 3) anterior clypeal margin convex in *P. neela* (anterior clypeal margin medially concave in *P. aseta*); 4) mandible with five teeth in the masticatory margin in *P. neela* (mandible with six teeth in *P. aseta*); 5) propodeal dorsal face in lateral view raised in *P. neela* (propodeal dorsal margin flat and continuous with rest of mesosoma in *P. aseta*). *Paraparatrechina neela* is similar to *P. butteli bryanti* (Forel, 1916), another Indomalayan species (Wheeler 1919), in body size, eye length, antennal scape surpassing occipital margin, and a raised propodeal dorsal face with a long declivitous face. However, *P. neela* can be easily separated from *P. butteli bryanti* by the following characteristics: 1) body largely metallic blue in *P. neela* (body castaneous brown; head, thorax, and gaster with metallic reflections in *P. butteli bryanti*); 2) legs with thick appressed pubescence in *P. neela* (legs with sparse pubescence in *P. butteli bryanti*); 3) overall body opaque with fine punctures in *P. neela* (thorax and gaster distinctly shagreened in *P. butteli bryanti*); 4) head subtriangular, longer than wide in *P. neela* (head subrectangular, as long as wide in *P. butteli bryanti*).

Discussion

Paraparatrechina is a relatively underexplored genus but with an expected species diversity much higher than what is currently known (LaPolla et al. 2010b; LaPolla and Fisher 2014). Previous studies indicate that the *Prenolepis* genus-group, which includes *Paraparatrechina*, originated and diversified during the late Paleocene and Eocene, between 45 and 60 mya (Blaimer et al. 2015; Matos-Maraví et al. 2018). Blaimer et al. (2015) estimated ancestral crown age of the genus ranges from 26.8 to 31.4 Ma. Similarly, the estimated crown age of a clade within *Paraparatrechina* is 23.5 Ma (Matos-Maraví et al. 2018). Matos-Maraví et al. (2018) suggested that the *Prenolepis* genus-group most likely originated in continental Southeast Asia. It points to the possibility of dispersal and colonization of this group from Southeast Asia to India. Further explorations are imperative to unravel the influence of the Himalayas and the Western Ghats on this group's evolution and dispersal.

Paraparatrechina species are typically found at elevations below 800 m, although a few inhabit elevations around 1500 m (AntWeb 2023a). However, a few species, such as *P. minutula* (Forel, 1901) and *P. kongming* (Terayama, 2009), are known to occupy higher elevations above 2000 m (2300 m and 2500 m,



Figure 5. *Parapatrechina aseta*, syntype worker **A** head in full-face view **B** body in dorsal view **C** body in profile view. Photo credit: Will Ericson, www.antweb.org, CASENT0910999 (AntWeb 2023b).

respectively). *Parapatrechina neela* sp. nov. was collected from an elevation of 803 m. This species showcases a unique metallic blue coloration not observed in any other species within this genus. However, some *Parapatrechina* species do exhibit color reflections or iridescence, like *P. iridescens* (Donisthorpe, 1942).

Blue coloration in animals, except in marine sponges, is a relatively rare phenomenon. However, there are several blue species of vertebrates, like fish, frogs, and birds, as well as invertebrates, such as spiders (Bagnara et al. 2007; Doucet and Meadows 2009; Umbers 2013; Chomphuphuang et al. 2023).

While blue coloration is common among many insects, particularly in hymenopterans such as Apoidea, Chrysididae and Ichneumonidae, it is very rare in Formicidae. Blue colour in insects is usually produced by the arrangement of biological photonic nanostructures rather than pigments, and it has independently evolved in various groups (Prum 1999; Seago et al. 2009; Hsiung et al. 2015; Chomphu-phuang et al. 2023). This vibrant feature raises intriguing questions. Does it help in communication, camouflage, or other ecological interactions? Delving into the evolution of this conspicuous coloration and its connections to elevation and the biology of *P. neela* presents an exciting avenue for research.

Acknowledgements

We are grateful to Ganesh N Shinde for helping us to prepare the maps. We extend our profound gratitude to Dr Ranjith, A.P., Dr John S. LaPolla, Dr Andrea Lucky, and Dr Jason Williams for their invaluable insights while preparing this manuscript. We express our sincere gratitude to Dr Jeffrey Sosa Calvo, Dr Peter Hawkes, Dr Rodolfo Probst, and an anonymous reviewer for their constructive and insightful comments and suggestions on our manuscript.

Additional information

Conflict of interest

The authors have declared that no competing interests exist.

Ethical statement

No ethical statement was reported.

Funding

We express our gratitude to the Department of Environment and Forest, Government of Arunachal Pradesh for granting research permits, Yingku village head and council for providing accommodation, and logistical support in the field. RS and DRP are thankful to the National Geographic Society (NGS- 71945c-20) for providing financial support in the wildlife-conservation category for the Siang expedition research project “100 years of Solitude? Exploring Changes in Biodiversity of Abor Hills, Eastern Himalayas since the 1911 Expedition” awarded to ATREE and Felis Creations, Bangalore. AP acknowledges the National Science Foundation (NSF), USA, for their financial support (DEB 2026772).

Author contributions

Conceptualization: RS, AP, DDRP. Funding acquisition: DDRP. Methodology: AP, DDRP, RS. Project administration: DDRP. Resources: DDRP. Visualization: RS, AP. Writing - original draft: RS, AP. Writing - review and editing: AP, RS, DDRP.

Author ORCIDs

Ramakrishnaiah Sahanashree  <https://orcid.org/0000-0002-3040-2102>

Aswaj Punnath  <https://orcid.org/0000-0001-8034-6578>

Dharma Rajan Priyadarsanan  <https://orcid.org/0000-0001-8137-3404>

Data availability

All of the data that support the findings of this study are available in the main text.

References

- AntWeb (2023a) AntWeb. Version 8.97. California Academy of Science. Genus: *Paraparatrechina* Donisthorpe, 1947. <https://www.antweb.org/> [Accessed on: 22 September 2023]
- AntWeb (2023b) AntWeb. Version 8.97. California Academy of Science. Specimen: CASENT0910999 *Paraparatrechina aseta*. <https://www.antweb.org/specimen.do?name=casent0910999> [Accessed on: 22 September 2023]
- AntWeb (2024) AntWeb. Version 8.103.2. California Academy of Science. Specimen: CASENT0178764 *Paraparatrechina umbranatis*. <https://www.antweb.org/specimen.do?name=casent0178764> [Accessed on: 12 February 2024]
- ArcGIS (2023) Esri Geographic Information System (version 10.4.1). <http://desktop.arcgis.com> [Accessed on: 18 June 2023]
- Army Intelligence Branch (1911) Frontier and Overseas Expeditions from India: Volume VII Abor Expedition 1911–1912. Mittal Publications, New Delhi. Reprinted 1983.
- Bagnara JT, Fernandez PJ, Fujii R (2007) On the blue coloration of vertebrates. *Pigment Cell Research* 20(1): 14–26. <https://doi.org/10.1111/j.1600-0749.2006.00360.x>
- Bharti H, Wachkoo AA (2014) New combination for a little known Indian ant, *Paraparatrechina aseta* (Forel, 1902) comb. n. (Hymenoptera: Formicidae). *Journal of Entomological Research Society* 16: 95–99.
- Bharti H, Guénard B, Bharti M, Economo EP (2016) An updated checklist of the ants of India with their specific distributions in Indian states (Hymenoptera, Formicidae). *ZooKeys* 551: 1–83. <https://doi.org/10.3897/zookeys.551.6767>
- Blaimer BB, Brady SG, Schultz TR, Lloyd MW, Fisher BL, Ward PS (2015) Phylogenomic methods outperform traditional multi-locus approaches in resolving deep evolutionary history: A case study of formicine ants. *BMC Evolutionary Biology* 15(1): 271. <https://doi.org/10.1186/s12862-015-0552-5>
- Bolton B (2023) An online catalog of the ants of the world. <https://www.antcat.org/catalog/429976> [Accessed on: 18 June 2023]
- Brown Jr WL (1973) A comparison of the Hylean and Congo-West African rain forest ant faunas. In: Meggers BJ, Ayensu ES, Duckworth WD (Eds) *Tropical Forest Ecosystems in Africa and South America: a Comparative Review*. Smithsonian Institution Press, Washington DC, 161–185.
- Cantone S (2017) Winged ants – The male. Dichotomous key to genera of winged male ants in the world. Behavioral ecology of mating flight. Autopubblicato, São Paulo, 318 pp.
- Cantone S (2018) Winged Ants, The Queen. Dichotomous key to genera of winged queen ants in the world. The wings of ants: morphological and systematic relationships. Stefano Cantone, Catania, Italy, 244 pp.
- Chomphuphuang N, Sippawat Z, Sriranan P, Piyatrakulchai P, Songsangchote C (2023) A new electric-blue tarantula species of the genus *Chilobrachys* Karsh, 1892 from Thailand (Araneae, Mygalomorphae, Theraphosidae). *ZooKeys* 1180: 105–128. <https://doi.org/10.3897/zookeys.1180.106278>
- de Motschoulsky V (1863) Essai d'un catalogue des insectes de l'île Ceylan (suite). *Bulletin de la Société Impériale des Naturalistes de Moscou* 36(3): 1–153.
- Donisthorpe H (1942) Descriptions of a few ants from the Philippine Islands, and a male of *Polyrhachis bihamata* Drury from India. *Annals & Magazine of Natural History* 11(49): 64–72. <https://doi.org/10.1080/03745481.1942.9755466>
- Donisthorpe H (1947) Some new ants from New Guinea. *Annals and Magazine of Natural History (Series 11)* 14: 183–197. <https://doi.org/10.1080/00222934708654624>

- Doucet SM, Meadows MG (2009) Iridescence: A functional perspective. *Journal of the Royal Society, Interface* 6(suppl_2): S115–S132. <https://doi.org/10.1098/rsif.2008.0395.focus>
- Emery C (1887) [1886] Catalogo delle formiche esistenti nelle collezioni del Museo Civico di Genova. Parte terza. Formiche della regione Indo-Malese e dell’Australia [part]. *Annali del Museo Civico di Storia Naturale Giacomo Doria (Genova) Serie 2* 4(24): 241–256.
- Emery C (1906) Note sur *Prenolepis vividula* Nyl. et sur la classification des espèces du genre *Prenolepis*. *Annales de la Société Entomologique de Belgique* 50: 130–134. <https://doi.org/10.5962/bhl.part.19942>
- Forel A (1901) Formiciden aus dem Bismarck-Archipel, auf Grundlage des von Prof. Dr. F. Dahl gesammelten Materials. *Mitteilungen aus dem Zoologischen Museum in Berlin* 2: 4–37.
- Forel A (1902) Variétés myrmécologiques. *Annales de la Société Entomologique de Belgique* 46: 284–296.
- Forel A (1905) Ameisen aus Java. Gesammelt von Prof. Karl Kraepelin 1904. *Mitteilungen aus dem Naturhistorischen Museum in Hamburg* 22: 1–26.
- Forel A (1916) Fourmis du Congo et d’autres provenances récoltées par MM. Hermann Kohl, Luja, Mayné, etc. *Revue Suisse de Zoologie* 24: 397–460. <https://doi.org/10.5962/bhl.part.4645>
- Google Earth Pro (2023) Version 7.3.6.9750. <https://www.google.com/earth/about/versions/> [Accessed on: 11 February 2024]
- Guénard B, Weiser MD, Gómez K, Narula N, Economo EP (2017) The Global Ant Biodiversity Informatics (GABI) database: synthesizing data on the geographic distribution of ant species (Hymenoptera: Formicidae). *Myrmecological News* 24: 83–89. https://doi.org/10.25849/myrmecol.news_024:083
- Hsiung BK, Deheyn DD, Shawkey MD, Blackledge TA (2015) Blue reflectance in tarantulas is evolutionarily conserved despite nanostructural diversity. *Science Advances* 1(10): e1500709. <https://doi.org/10.1126/sciadv.1500709>
- Janicki J, Narula N, Ziegler M, Guénard B, Economo EP (2016) Visualizing and interacting with large-volume biodiversity data using client-server web-mapping applications: The design and implementation of antmaps.org. *Ecological Informatics* 32: 185–193. <https://doi.org/10.1016/j.ecoinf.2016.02.006>
- LaPolla J, Fisher B (2014) Two new *Paraparatrechina* (Hymenoptera, Formicidae) species from the Seychelles, with notes on the hypogaecic *weissi* species-group. *ZooKeys* 414: 139–155. <https://doi.org/10.3897/zookeys.414.7542>
- LaPolla JS, Brady SG, Shattuck SO (2010a) Phylogeny and taxonomy of the *Prenolepis* genus-group of ants (Hymenoptera: Formicidae). *Systematic Entomology* 35(1): 118–131. <https://doi.org/10.1111/j.1365-3113.2009.00492.x>
- LaPolla JS, Cheng CH, Fisher BL (2010b) Taxonomic revision of the ant (Hymenoptera: Formicidae) genus *Paraparatrechina* in the Afrotropical and Malagasy Regions. *Zootaxa* 2387(1): 1. <https://doi.org/10.11646/zootaxa.2387.1.1>
- Latreille PA (1802) Histoire naturelle des fourmis, et recueil de mémoires et d’observations sur les abeilles, les araignées, les faucheurs, et autres insectes. Impr. Crapelet (chez T. Barrois), Paris, xvi + 445 pp. <https://doi.org/10.5962/bhl.title.11138>
- Matos-Maraví P, Clouse RM, Sarnat EM, Economo EP, LaPolla JS, Borovanska M, Rabelling C, Czekanski-Moir J, Latumahina F, Wilson EO, Janda M (2018) An ant genus-group (*Prenolepis*) illuminates the biogeography and drivers of insect diversification in the Indo-Pacific. *Molecular Phylogenetics and Evolution* 123: 16–25. <https://doi.org/10.1016/j.ympev.2018.02.007>

- Mayr G (1861) Die europäischen Formiciden. Nach der analytischen Methode bearbeitet. C. Gerolds Sohn, Vienna, 80 pp. <https://doi.org/10.5962/bhl.title.14089>
- Prum RO (1999) The anatomy and physics of avian structural colours. In: Adams NJ, Slotow RH (Eds) Proceedings of the 22nd International Ornithological Congress. Bird Life South Africa, Durban, South Africa.
- Santschi F (1910) Formicides nouveaux ou peu connus du Congo français. Annales de la Société Entomologique de France 78: 349–400.
- Santschi F (1914) Formicides of West and Southern Africa from the trip of Mr. Professor F. Silvestri. Bollettino del Laboratorio di Zoologia Generale e Agraria della Reale Scuola Superiore d'Agricoltura. Portici 8: 309–385.
- Santschi F (1928) New Ants from Australia. Bulletin of the Vaudoise Society of Natural Sciences 56: 465–483.
- Seago AE, Brady P, Vigneron J-P, Schultz TD (2009) Gold bugs and beyond: A review of iridescence and structural colour mechanisms in beetles (Coleoptera). Journal of the Royal Society, Interface 6(suppl_2): S165–S184. <https://doi.org/10.1098/rsif.2008.0354.focus>
- Terayama M (2009) A synopsis of the family Formicidae of Taiwan (Insecta: Hymenoptera). Research Bulletin of Kanto Gakuen University. Liberal Arts 17: 81–266.
- Terayama M (2013) Additions to knowledge of the ant fauna of Japan (Hymenoptera; Formicidae). Memoirs of the Myrmecological Society of Japan 3: 1–24.
- Trager JC (1984) A revision of the genus *Paratrechina* (Hymenoptera: Formicidae) of the continental United States. Sociobiology 9: 49–162.
- Umbers KDL (2013) On the perception, production and function of blue colouration in animals. Journal of Zoology (London, England) 289(4): 229–242. <https://doi.org/10.1111/jzo.12001>
- Wheeler WM (1919) The ants of Borneo. Bulletin of the Museum of Comparative Zoology 63: 43–147.
- Wheeler WM (1922) Ants of the American Museum Congo Expedition. Bulletin of the American Museum of Natural History 45: 1–1139.
- Yogesh Kumar, Haffis Mohammed, Aditya Pratap Singh, Thiyam Jefferson Singh, Tantulung Tatan, Kabir K, Sagar Tasing, Telek Yoka and Hashim Mohammed S (2022) Plant Composition in traditional homegardens of Berung Village, East Siang, Arunachal Pradesh. International Journal of Theoretical & Applied Sciences 14(1): 01–07
- Yumnam J, Tripathi OP, Khan ML (2013) Soil dynamic of agricultural landscape in East Siang District of Arunachal Pradesh, Eastern Himalaya. African Journal of Plant Science 7(1): 43–52. <https://doi.org/10.5897/AJPS12.139>

A new mountain pitviper of the genus *Ovophis* Burger in Hoge & Romano-Hoge, 1981 (Serpentes, Viperidae) from Yunnan, China

Xian-Chun Qiu^{1*}, Jin-Ze Wang^{1*}, Zu-Yao Xia², Zhong-Wen Jiang^{3,4}, Yan Zeng³, Nan Wang⁴, Pi-Peng Li¹, Jing-Song Shi^{3,5}

¹ Institute of Herpetology, Shenyang Normal University, Shenyang, Liaoning 110034, China

² Department of Evolution, Ecology & Biodiversity, University of California, Davis, CA 95616, USA

³ Institute of Zoology, Chinese Academy of Sciences, Beijing 100101, China

⁴ School of Ecology and Nature Conservation, Beijing Forestry University, Beijing 100083, China

⁵ Institute of Vertebrate Paleontology and Paleoanthropology, Chinese Academy of Sciences, Beijing 100044, China

Corresponding authors: Nan Wang (wangnan761227@bjfu.edu.cn); Pi-Peng Li (104466606@qq.com); Jing-Song Shi (shijingsong@ivpp.ac.cn)

Abstract

Based on a molecular phylogenetic analysis and morphological comparison, a new species of mountain pitviper, *Ovophis jenkinsi* **sp. nov.**, is described. The new species was collected in Yingjiang County, Yunnan Province, China. It can be distinguished from congeneric species by the following characters: (1) internasals in contact or separated by one small scale; (2) second supralabial entire and bordering the loreal pit; (3) dorsal scales in 23 (25)–21 (23, 25)–19 (17, 21) rows; (4) 134–142 ventrals; (5) 40–52 pairs of subcaudals; (6) third supralabial larger than fourth in all examined specimens of *Ovophis jenkinsi* **sp. nov.**; (7) deep orange-brown or dark brownish-grey markings on dorsal head surface; (8) background color of dorsal surface deep orange-brown or dark brownish-grey; (9) both sides of dorsum display dark brown trapezoidal patches; (10) scattered small white spots on dorsal surface of tail.

Key words: Morphology, *Ovophis jenkinsi* sp. nov., snake, taxonomy, Yingjiang County



Academic editor: Minh Duc Le

Received: 21 January 2024

Accepted: 1 May 2024

Published: 30 May 2024

ZooBank: <https://zoobank.org/86CD1FAF-8A41-41D2-BF2E-B28EBC805789>

Citation: Qiu X-C, Wang J-Z, Xia Z-Y, Jiang Z-W, Zeng Y, Wang N, Li P-P, Shi J-S (2024) A new mountain pitviper of the genus *Ovophis* Burger in Hoge & Romano-Hoge, 1981 (Serpentes, Viperidae) from Yunnan, China. ZooKeys 1203: 173–187. <https://doi.org/10.3897/zookeys.1203.119218>

Copyright: © Xian-Chun Qiu et al.

This is an open access article distributed under terms of the Creative Commons Attribution License (Attribution 4.0 International – CC BY 4.0).

Introduction

The subfamily Crotalinae (pitvipers) is the largest group of family Viperidae, with 294 species in 23 genera, and widely distributed in Asia and America (Speybroeck et al. 2016; Uetz et al. 2024). The mountain pitviper (*Ovophis*) is a group of medium-sized venomous snakes that are mainly distributed through eastern Asia, the southern Himalayas, and the northern Indochina Peninsula (Che et al. 2020). Within the genus, the distribution of *O. monticola* (Günther, 1864), *O. makazayazaya* (Takahashi, 1922), *O. tonkinensis* (Bourret, 1934), and *O. zayuensis* (Jiang, 1977) in China was supported and defined preliminarily by Malhotra et al. (2011) by molecular phylogenetic analyses (12S, 16S, cytb, and ND4) and comparative morphology. Subsequently, Zeng et al. (2023) revised the molecular phylogeny (cytb, ND4, BACH1, c-mos, NT3, and Rag1) with additional specimens. The result restricted the distribution of *O. monticola* to Zhangmu County (southern Xizang)

* These authors contributed equally to this work.

in China, demarcated the populations that are distributed through Sichuan–Yunnan in the west to Taiwan in the east as *O. makazayazaya*, and introduced *O. malhotrae* Zeng et al., 2023 as a new species representing the southern Yunnan population with its holotype description presented in non-paginated supporting documents. The distribution of *O. malhotrae* is currently recorded only in Jinping and Pingbian, Yunnan and Lao Cai, Vietnam. MtDNA phylogenetic inference of the genus *Ovophis* and partial species of the rest of family Viperidae indicated when "*O.*" *okinavensis* (Boulenger, 1892) is included, genus *Ovophis* is polyphyletic, while "*O.*" *okinavensis* sistering *Trimeresurus gracilis* Oshima, 1920 (Malhotra and Thorpe 2000, 2004; Shi et al. 2021). Although the epithet change of "*O.*" *okinavensis* has not yet been declared, this species is no longer included in genus *Ovophis* in some recent taxonomic studies (Malhotra et al. 2011; Zeng et al. 2023). Currently, therefore, the genus *Ovophis* includes six species: *O. monticola*, *O. convictus* (Stoliczka, 1870), *O. makazayazaya*, *O. tonkinensis*, *O. zayuensis*, and *O. malhotrae* (Malhotra et al. 2011; Zeng et al. 2023; Uetz et al. 2024).

In 2018 and 2023, five specimens of genus *Ovophis* were collected in Yingjiang County, Yunnan. With applied comparative morphology and molecular phylogenetic analysis, these specimens were revealed as distinct from the other *Ovophis* species. Thus, we described here this new population as a new species.

Materials and methods

Sampling

Five specimens (IOZ 002679, IOZ 002680, YJ201801, YJ201802, and YJ201803) were collected by Zhong-Wen Jiang and Xian-Chun Qiu in October 2018 and 2023 from Tongbiguan Township, Yingjiang County, Yunnan Province, China. After euthanasia, liver tissues of specimens IOZ 002679 and IOZ 002680 were extracted and preserved in 95% ethanol for molecular analyses. All specimens were fixed in 10% buffered formalin and then transferred to 75% ethanol for permanent preservation. The specimens IOZ 002679 and IOZ 002680 are deposited in the Institute of Zoology, Chinese Academy of Sciences (IOZ, Beijing, China). The specimens YJ201801, YJ201802, and YJ201803 are deposited in Beijing Forestry University (BFU, Beijing, China).

Morphometrics

Morphological descriptions are accorded to Zhao (2006). Abbreviations are accorded to Darko et al. (2022). A total of 24 morphological characters were examined, including 11 mensural characters and 13 scalation characters. Morphological measurements were taken with digital calipers (Guanglu 111N-101V, accuracy 0.03 mm, Guanglu Digital Instruments, Guilin) to the nearest 0.1 mm. Abbreviations are as follows: **SVL** snout–vent length (distance from tip of snout to posterior margin of cloacal plate); **TAL** tail length (distance from posterior margin of cloacal plate to tip of tail); **TL** total length (distance from tip of snout to tip of tail); **HL** head length (distance from tip of rostral to posterior end of jaw); **HW** head width (maximum width of head); **HH** head height (maximum height between dorsal and ventral surfaces of head); **ED** eye diameter (horizontal eye diameter); **IOD** interorbital distance (distance between the top margin of eyes); **IN** internarial distance (distance

between nostrils); **RH** maximum rostral height; **RW** maximum rostral width; **LOR** loreal; **PRO** preoculars; **PO** postoculars; **SBO** suboculars; **ATEM** anterior temporals; **PTMP** posterior temporals; **SL** supralabials; **IL** infralabials; **CS** chin shields; **DSR** dorsal scale rows (counted at one head length behind head, at midbody, and one head length before vent); **PRV** preventral scales (elongated scales situated beneath the head before the ventrals); **VS** ventral scales (elongated scales situated beneath the body between neck and vent); **SC** subcaudal scales.

Other morphological characters of *Ovophis* species were obtained from Zhao et al. (1998), Li et al. (2010), Neang et al. (2011), Sharma et al. (2013), Che et al. (2020), Guo et al. (2021), Huang (2021), and Zeng et al. (2023).

Phylogenetic analyses

Four mtDNA sequences are specifically amplified in this study: 12S rRNA using primers 12SFPhe and 12SRVal (Knight and Mindell 1993); 16S rRNA using primers 16sFL and 16sRH (Palumbi et al. 1991); cytochrome b (cytb) using primers L14910 and H16064 (Burbrink et al. 2000); and NADH dehydrogenase subunit 4 (ND4) using primers ND4F and LEUR (Arévalo et al. 1994). The standard PCR protocol is performed in 20 µl of reactant with at least 20 ng of template DNA and 10 pmol of primers. The PCR conditions: initial denaturation for 3 min at 94 °C, followed by 35 cycles, denaturation at 94 °C for 30 s, 30 s of annealing at different temperatures (52 °C for 12S, 50 °C for 16S, 56 °C for ND4, and 48 °C for cytb), and then elongation at 72 °C for 60 s, then finalized with elongation step of 10 min at 72 °C. Sequencing was conducted by Beijing Tianyi Huiyuan Bio-tech Co., Ltd. Sequence data were uploaded to GenBank (Table 1).

Table 1. Samples and sequences used for phylogenetic analysis in this study.

Species	Locality	Voucher	GenBank accession number			
			12S	16S	cytb	ND4
<i>Ovophis jenkinsi</i> sp. nov.	Yingjiang, Yunnan, China	IOZ 002679	PP574250	PP574252	PP171456	PP171459
<i>O. jenkinsi</i> sp. nov.	Yingjiang, Yunnan, China	IOZ 002680	PP574249	PP574251	PP171455	PP171458
<i>O. monticola</i>	Gandaki, Nepal	ZMB 70216	HQ325260	HQ325078	HQ325138	HQ325199
<i>O. monticola</i>	Gandaki, Nepal	ZMB 70218	HQ325253	HQ325071	HQ325131	HQ325192
<i>O. convictus</i>	Cameron Highlands, Pahang, Malaysia	AM B628	HQ325264	HQ325082	HQ325141	–
<i>O. convictus</i>	Pulau Langkawi, Malaysia	AM B629	HQ325265	HQ325083	HQ325142	–
<i>O. convictus</i>	Cameron Highlands, Pahang, Malaysia	AM B580	–	–	HQ325129	HQ325190
<i>O. malhotrae</i>	Yunnan, China	GP 2041	–	–	OP441841	OP441784
<i>O. malhotrae</i>	Jinping, Yunnan, China	GP 2053	–	–	OP441842	OP441785
<i>O. malhotrae</i>	Lao Cai, Vietnam	ROM 39381	HQ325283	HQ325102	HQ325160	HQ325218
<i>O. zayuensis</i>	Bomi, Xizang, China	GP 713	–	–	OP441890	OP441833
<i>O. zayuensis</i>	Chayu, Xizang, China	GP 1505	–	–	OP441892	OP441836
<i>O. makazayazaya</i>	Huili, Sichuan, China	GP 21	–	–	OP441856	OP441798
<i>O. makazayazaya</i>	Luquan, Yunnan, China	KIZ 02143	–	–	OP441860	OP441802
<i>O. makazayazaya</i>	Weixi, Yunnan, China	YPX 53011	–	–	OP441861	OP441803
<i>O. tonkinensis</i>	Maoming, Guangdong, China	GP 1665	–	–	OP441876	OP441818
<i>O. tonkinensis</i>	Xuan Son, Phu Tho, Vietnam	KIZ 011602	–	–	OP441880	OP441822
<i>Vipera berus</i>	Jilin, China	–	–	–	MF945570	MF945570

Note: The missing data are marked as “–”.

Corresponding homologous sequences of *Ovophis* species were obtained from GenBank, and the sequences of *Vipera berus* (Linnaeus, 1758) were used as outgroup in the phylogenetic analysis (Zeng et al. 2023). DNA nucleotide sequences were aligned in MEGA 6 (Tamura et al. 2013) with Clustal W algorithm, default parameters (Thompson et al. 1997). PartitionFinder 2.1.1 (Lanfear et al. 2012) was used to test the best partitioning scheme. Pairwise sequence divergence (uncorrected *p*-distances) was calculated using MEGA 6.

Bayesian inference was performed using MrBayes 3.1.2 (Ronquist et al. 2011). All searches consisted of three heated chains and a single cold chain. Three independent iterations each comprising two runs of 100 million generations, sampled every 10,000 generations, and parameter estimates were plotted against generation. The first 25% of the samples were discarded as burn-in, resulting in a potential scale reduction factor (PSRF) of < 0.005. A maximum-likelihood analysis was run with RaxML (Silvestro and Michalak 2012), and a majority rule consensus tree was calculated with 1,000 bootstrap replicates.

Results

Molecular phylogeny

A total of 2,703 aligned base pairs were obtained including 441 bp from 12S, 465 bp from 16S, 1,110 bp from cytb, and 687 bp from ND4. With respect to the different evolutionary characters of each molecular marker, the dataset was split into five partitions by genes and codon positions as recommended by PartitionFinder 2.1.1 (Table 2). The topological structures of the maximum-likelihood (ML) and Bayesian-inference (BI) trees are generally consistent (Fig. 1). All *Ovophis* samples are

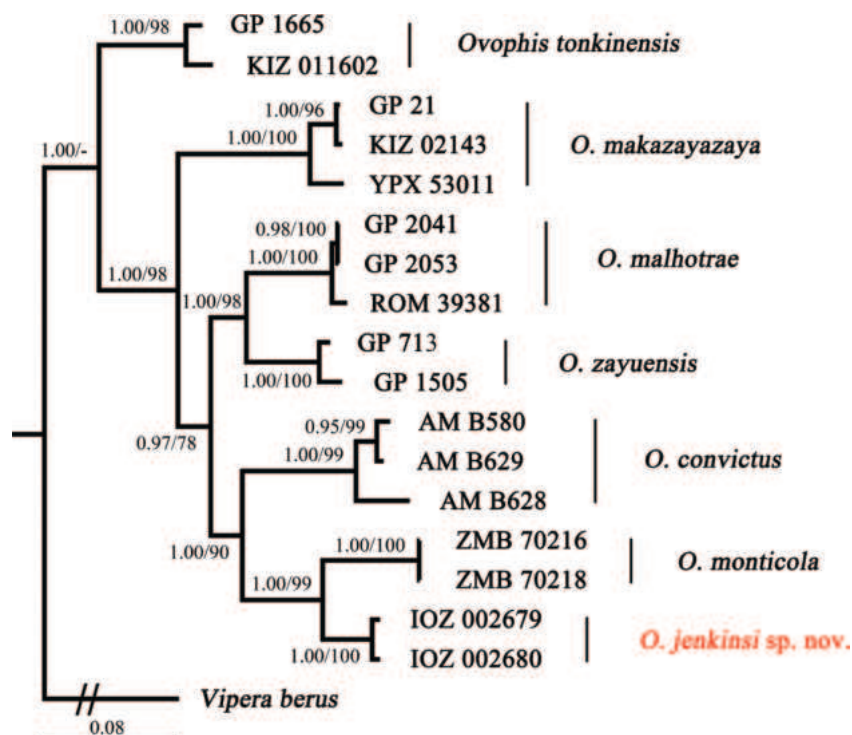


Figure 1. Bayesian-inference tree of *Ovophis* species inferred from the combined fragments of 12S, 16S, cytb, and ND4. Bayesian posterior probabilities/bootstrap support values for the clades are shown adjacent to the node.

divided into seven clades. The cladistic relationship within the group of samples from Yingjiang was resolved with strong support (1.00/100 for BI and ML). The Yingjiang group is sister to the *O. monticola* group with decent support (1.00/99 for BI and ML), and the group of “Yingjiang”+*O. monticola* clustered with *O. convictus*, and formed a larger clade sister to the *O. malhotrae*+*O. zayuensis* lineage.

The uncorrected *p*-distance based on *cytb* gene between the specimens IOZ 002679, IOZ 002680 from Yingjiang, Yunnan and *O. monticola* is 6.2–6.5%, equivalent to those among other recognized species, such as *O. malhotrae* vs. *O. zayuensis* (6.0–6.7%) (Table 3). Thus, the molecular phylogeny supports the validity of *Ovophis jenkinsi* sp. nov.

Table 2. Partitions and their molecular evolution models selected by PartitionFinder 2.1.1.

Partitions	Locus	Length (bp)	Models
Partition 1	12S, <i>cytb</i> pos 1, ND4 pos 3	1,040	TVM+I+G
Partition 2	16S	465	GTR+I
Partition 3	ND4 pos 1, <i>cytb</i> pos 2	599	TRN+I
Partition 4	<i>cytb</i> pos 3	370	TIM+G
Partition 5	ND4 pos 2	229	TIM+G

TVM: transversal substitution model; GTR: General Time-Reversible model; TRN: Tamura-Nei; TIM: transitional substitution model; +I: proportion of invariable sites; +G: rate heterogeneity.

Table 3. Uncorrected *p*-distance among the sequences based on the *cytb* gene fragments of *Ovophis* species in this study.

	1	2	3	4	5	6	7	8	9	10	11	12	13	14	15	16
1 <i>Ovophis jenkinsi</i> sp. nov. IOZ 002679																
2 <i>O. jenkinsi</i> sp. nov. IOZ 002680	0.003															
3 <i>O. monticola</i> ZMB 70216	0.065	0.062														
4 <i>O. monticola</i> ZMB 70218	0.065	0.062	0.000													
5 <i>O. convictus</i> B580	0.097	0.097	0.106	0.106												
6 <i>O. convictus</i> B628	0.118	0.118	0.125	0.125	0.041											
7 <i>O. convictus</i> B629	0.095	0.095	0.101	0.101	0.006	0.038										
8 <i>O. makazayazaya</i> GP21	0.102	0.102	0.111	0.111	0.111	0.110	0.105									
9 <i>O. makazayazaya</i> KIZ02143	0.098	0.098	0.115	0.115	0.117	0.115	0.111	0.007								
10 <i>O. makazayazaya</i> YPX53011	0.100	0.104	0.128	0.128	0.113	0.099	0.107	0.038	0.037							
11 <i>O. malhotrae</i> GP2041	0.102	0.102	0.108	0.108	0.092	0.094	0.086	0.081	0.083	0.084						
12 <i>O. malhotrae</i> GP2053	0.102	0.102	0.108	0.108	0.092	0.094	0.086	0.081	0.083	0.084	0.000					
13 <i>O. malhotrae</i> ROM 39381	0.110	0.110	0.104	0.104	0.095	0.097	0.090	0.079	0.084	0.086	0.007	0.007				
14 <i>O. tonkinensis</i> GP1665	0.105	0.101	0.119	0.119	0.096	0.096	0.094	0.095	0.100	0.109	0.081	0.081	0.083			
15 <i>O. tonkinensis</i> KIZ011602	0.107	0.103	0.120	0.120	0.098	0.102	0.099	0.098	0.103	0.113	0.084	0.084	0.086	0.011		
16 <i>O. zayuensis</i> GP713	0.085	0.085	0.110	0.110	0.090	0.092	0.088	0.085	0.085	0.094	0.060	0.060	0.062	0.089	0.088	
17 <i>O. zayuensis</i> GP1505	0.088	0.088	0.106	0.106	0.092	0.094	0.090	0.087	0.090	0.095	0.065	0.065	0.067	0.094	0.094	0.019

Taxonomic account

Viperidae Oppel, 1811

Ovophis jenkinsi sp. nov.

<https://zoobank.org/45FF4F16-3F01-4ADC-8DA7-24E84E3B810D>

Type material. Holotype. IOZ 002679, an adult male (Figs 2, 3) from Tongbiguan Township, Yingjiang County, Yunnan Province, China (24°36'33"N, 97°39'29"E; 1,343 m a.s.l.) (Fig. 4). It was collected near the road by Zhong-Wen Jiang and Xian-Chun Qiu.



Figure 2. Holotype of *Ovophis jenkinsi* sp. nov. (IOZ 002679) in life.

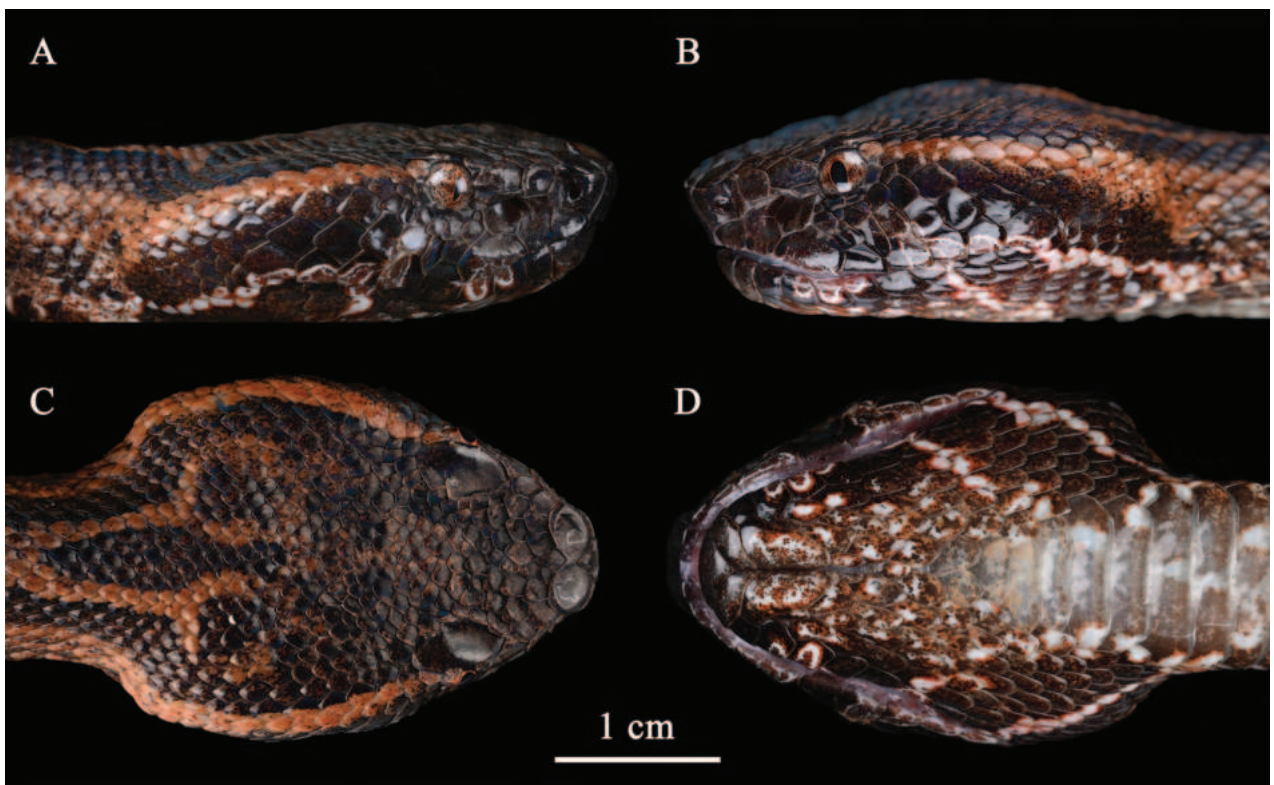


Figure 3. Head of the holotype of *Ovophis jenkinsi* sp. nov. (IOZ 002679) A lateral (right) view B lateral (left) view C dorsal view D ventral view.

Paratype. IOZ 002680 and YJ201801, adult females from Tongbiguan Township, Yingjiang County, Yunnan Province, China (24°35'04"N, 97°41'13"E; 1,321 m a.s.l.) collected by Zhong-Wen Jiang and Xian-Chun Qiu in October



Figure 4. Habitat of *Ovophis jenkinsi* sp. nov. at the type locality in Tongbiguan Township, Yingjiang County, Yunnan Province, China **A** microhabitat, photographed by Sheng-Chao Shi **B** microhabitat, photographed by Guo-Wei Mo **C, D** macrohabitats, photographed by Xiao-Jun Gu.

2023 and 2018; juveniles YJ201802 and YJ201803 from the same locality collected by Zhong-Wen Jiang in October 2018.

Etymology. The specific epithet of the new species is dedicated to Robert “Hank” William Garfield Jenkins AM (August 1947–September 2023), a herpetologist and former chairman of the CITES Animals Committee from Australia, with a passion for snakes, especially pitvipers, and helped China, along with many Asian countries, complete snake census, conservation, and management projects. We suggest the common name “Jenkins’ mountain pitviper” in English and “yíng jiāng lào tiě tóu shé” (盈江烙铁头蛇) in Chinese.

Diagnosis. *Ovophis jenkinsi* sp. nov. can be distinguished by the following combination of morphological characters: (1) internasals in contact or separated by one small scale; (2) second supralabial entire and bordering the loreal pit; (3) dorsal scales in 23 (25)–21 (23, 25)–19 (17, 21) rows; (4) 134–142 ventrals; (5) 40–52 pairs of subcaudals; (6) third supralabial larger than fourth in all examined specimens of *Ovophis jenkinsi* sp. nov.; (7) deep orange-brown or dark brownish-grey markings on dorsal head surface; (8) background color of dorsal surface deep orange-brown or dark brownish-grey; (9) both sides of dorsum display dark brown trapezoidal patches; (10) scattered small white spots on dorsal surface of tail.

Description of holotype. Adult male; body stout and robust, medium-sized, tail slender, TL 515.9 mm (SVL 421.0 mm, TAL 94.9 mm, TAL/TL: 0.23); head triangular in dorsal view, moderately distinct from neck, longer than width,

HL 26.6 mm, HW 18.6 mm (HW/HL: 0.70). Snout blunt and rounded, rostral trapezoidal, broader than high, RW 4.6 mm, RH 3.5 mm (RW/RH: 1.31; RW/HW: 0.25), upper edge visible from dorsum; eye small, ED 2.7 mm (ED/HL 0.10), pupil vertical; nostril subcircular, located in the middle of nasal; nasal divided into two scales by nostril; two internasals, elliptical, separated anteriorly by a small scale and bordered by the upper edge of rostral, connected posteriorly; loreal single; two preoculars, in contact with eye posteriorly; two postoculars, upper one in contact with the lower edge of supraocular; subocular single and elongate, respectively separated by two small scales from the third, fourth and fifth supralabials; supraocular single, the largest scales on the dorsal surface of head, separated by 7–8 scales; supralabials eight, first and second in contact with nasal, second entire and bordering the loreal pit, third larger than fourth; 11 infralabials on left (seventh and eighth infralabials bipartitioned relative to right), 10 infralabials on right, first pair in broad contact with each other, first to third in contact with chin shields; mental triangular; one pair of chin shields, meeting in midline, the right one slightly larger than the left; dorsal scales in 25–21–19 rows, bluntly keeled, except outer row; 134 ventrals, excluding six preventrals; subcaudal scales 49, paired, excluding tail tip; cloacal plate entire.

Coloration in life. Dorsal head surface black, with deep-orange blotches; a deep orange marking resembling an open pair of surgical scissors exists on the front of neck; a deep-orange stripe exists from the upper postocular to the anterior nape, the stripe demarcated from black dorsal head at top, gradually transitioning to black at bottom, approximately one scale row in width behind orbit of eye, after three scales, approximately two scales rows in width, enlarge to 3–4 scales rows in width on the posterior of head. Lateral head surface black, tiny white and vermilion spots exist on the surface of scales near snout; an irregular stripe extends from subocular to the fifth and sixth infralabials, the outermost ring of vermilion, subtle, second ring of white, obvious; the stripe splits in two at fifth and sixth supralabials, one extending backward through seventh, eighth supralabials and the last two infralabials, the other extending downward through seventh and eighth infralabials (left) and seventh infralabial (right), converging at the outer row of dorsal scales; similar markings exist on the third supralabial and third to fifth infralabials. Background color of ventral head surface deep orange, mixed with irregular white blotches with vermilion edges. Pupil black; iris deep orange mixed with white and black.

Background color of dorsal surface deep orange, with 18 connected or disconnected dark brown patches on both sides of body and three similar spots on anterior section of tail visible from dorsum; dorsal blotches predominantly trapezoidal, approximately 2–6 scales in length, and 4–5 scales rows in width, mottled with a few deep orange tiny spots on most dark brown patches; two clusters of lateral dark brown patches exist under each dorsal dark brown patch, each patch covers 2–3 dorsal scales and separated from ventral scales by 2–3 rows of dorsolateral scales. Posterior section of tail pink, 21 tiny spots exist on the dorsal surface, spots white with brown edges, no more than a scale in size. Mixed cream and tan on ventral surface of anterior tail and body, clean pink on posterior section of tail.

Table 4. Scalation data and measurements (in mm) of *Ovophis jenkinsi* sp. nov.

	IOZ 002679 Holotype	IOZ 002680 Paratype	YJ201801 Paratype	YJ201802 Paratype	YJ201803 Paratype
Sex	Male	Female	Female	Juvenile	Juvenile
TL	515.9	402.3	690.0	261.0	279.0
TAL	94.9	66.9	91.1	43.8	45.0
HL	26.6	26.0	38.3	16.2	16.8
HW	18.6	20.6	28.8	11.7	11.2
HW/HL	0.70	0.79	0.75	0.72	0.67
PRO	2	2	2	2	2
SBO	1	3	2	2	2
PO	2	3	2	2	3
SL	8/8	9/9	8/10	8/-	8/8
IL	11/10	12/12	11/11	11/11	11/11
DSR	25–21–19	25–23–19	25–25–21	23–21–19	23–23–17
VS	134	142	138	134	135
SC	49	40	40	50	52

Note: the missing data are marked as “-”.

Table 5. Morphological comparison of *Ovophis* species.

	DSR	VS	SC	Does the 2 nd SL border the loreal pit	3 rd and 4 th SL	Dorsal head surface	Dorsal background color	Dorsal patches	White spots on dorsal surface of tail
<i>Ovophis jenkinsi</i> sp. nov.	23 (25)–21 (23, 25)–19 (17, 21)	134–142	40–52, paired	Yes	3 rd > 4 th	Patterned	Deep orange-brown or dark brownish-grey	Mostly trapezoidal	Scattered
<i>O. monticola</i>	23 (21)–23 (21)–19	141–172	37–58, paired	Yes	3 rd > 4 th	Patterned	Yellowish-brown	Mostly rectangular	Scattered
<i>O. convictus</i>	25–25–18	136	17–31, paired	Yes	3 rd > 4 th	Unpatterned	Yellowish-brown	Mostly rectangular	Scattered
<i>O. makazayazaya</i>	25 (27, 29)–23 (25, 21)–19 (21)	131–159	34–52, paired	Yes or no	3 rd < 4 th	Patterned or unpatterned	Yellowish-brown or dark-grey	Rectangular or irregular patches	Scattered
<i>O. malhotrae</i>	27–23–19	145	47, paired	Yes	3 rd > 4 th	Patterned	Dark-brown	Mostly rectangular	Continuous
<i>O. tonkinensis</i>	25 (27, 29)–23 (21–25)–19 (21)	128–134	39–49, unpaired	Yes or no	3 rd < 4 th	Unpatterned	Yellowish-brown	Rectangular or irregular patches	Continuous
<i>O. zayuensis</i>	25 (27)–23–19 (17)	160–177	43–64, unpaired	Yes or no	3 rd > 4 th	Patterned or unpatterned	Reddish-brown or brown	Mostly trapezoidal and triangular	No visible white spots

Intraspecific variation. Morphometric data are summarized in Table 4. Dorsal head surface of each paratype specimen has different approximately symmetrical markings respectively. Internasals are separated by one scale, and the dorsal background color is dark brownish-grey in paratypes IOZ 002680 and YJ201801. Light greyish-brown on background color of dorsal body in juveniles YJ201802 and YJ201803. Third to tenth subcaudals unpaired in YJ201803. The patches on dorsal body are mostly rectangular in IOZ 002680.

Comparisons. *Ovophis jenkinsi* sp. nov. can be distinct from other congeneric species by the following characters (Table 5): internasals in contact or separated by one small scale (vs internasals separated by two small scales in *O. malhotrae*); second supralabial entire and bordering the loreal pit (vs second supralabial bordering the loreal pit or separated by a loreal in *O. makazayazaya*, *O. tonkinensis*, and *O. zayuensis*); dorsal scales in 23 (25)–21 (23, 25)–19 (17,

21) rows (vs dorsal scales 23 (21)–23 (21)–19 in *O. monticola*, 25 (27, 29)–23 (21–25)–19 (21) in *O. tonkinensis*, 27–23–19 in *O. malhotrae* and 25 (27)–23–19 (17) in *O. zayuensis*); 134–142 ventrals (vs 141–172 ventrals in *O. monticola*, 145 in *O. malhotrae* and 160–177 in *O. zayuensis*); subcaudal scales in pairs (vs unpaired in *O. tonkinensis* and *O. zayuensis*); 40–52 pairs of subcaudals (vs 17–31 pairs in *O. convictus*); the third supralabial being larger than fourth (vs fourth larger than third supralabial in *O. makazayazaya* and *O. tonkinensis*); deep orange-brown or dark brownish-grey markings on dorsal head surface (vs no markings on dorsal head surface in *O. convictus* and *O. tonkinensis*); background color of dorsal surface deep orange-brown or dark brownish-grey (vs yellowish-brown or dark-grey in *O. makazayazaya*, yellowish-brown in *O. monticola* and *O. tonkinensis*, reddish-brown or brown in *O. zayuensis*); both sides of dorsum display dark brown trapezoidal patches (vs mostly rectangular patches in *O. monticola*); adults HW/HL 0.70–0.79 (vs 0.64–0.65 in *O. monticola*); scattered small white spots on dorsal surface of tail (vs continuous small white spots on dorsal surface of tail in *O. tonkinensis* and *O. malhotrae*).

Distribution and ecology. *Ovophis jenkinsi* sp. nov. is currently known only from Yingjiang County, Yunnan Province, China. It was found in the tropical montane rainforest at an altitude of around 1,300 m. Overlapping herpetofauna includes *Lycodon chapaensis* (Angel & Bourret, 1933), *Trimeresurus popeiorum* Smith, 1937, *Pseudocalotes jingpo* Xu et al., 2024, and other species (Xu et al. 2024). The new species reaches activity peak in autumn and is active nocturnally during light rain or high humidity, at temperatures around 15–22 °C (Fig. 5). The type specimens were collected at night in October. When threatened, these snakes inflate their bodies to make themselves appear larger and strike quickly. The specimen IOZ 002680 had released odour from the cloacal scent glands when captured. We are currently unsure of the feeding habit of *O. jenkinsi* sp. nov. in the wild. They fed on juvenile mice (*Mus musculus* Linnaeus, 1758) in our captivity observations. Therefore, we presume the species prey on small mammals in the wild.



Figure 5. *Ovophis jenkinsi* sp. nov. and its microhabitat. Photographed by Zhong-Wen Jiang in Yingjiang, Yunnan.

Discussion

The phylogenetic topology in this study supports Zeng et al. (2023): *Ovophis malhotrae* sistering *O. zayuensis* (Zeng et al. 2023). However, the phylogenetic topology in this study differs from previous publications (Malhotra et al. 2011; Zeng et al. 2023). In this study, *O. tonkinensis* clustered with all other congeners (excluding "*O.*" *okinavensis*), while it clustered with *O. makazayazaya* in Malhotra et al. (2011) and Zeng et al. (2023). Thus, introducing a larger quantity of genetic dataset is suggested when conducting further phylogenetic studies of genus *Ovophis*.

In recent years, new snake species have been discovered constantly near the Yunnan border (Jiang et al. 2020; Chen et al. 2021; Hou et al. 2021; Lee 2021; Liu et al. 2021; Shi et al. 2022; Ma et al. 2023). Zeng et al. (2023) described the new species *O. malhotrae* based on specimens from southern Yunnan, and its molecular systematic position indicated that several populations from Vietnam and Laos may refer to cryptic species of the genus *Ovophis*. Thus, snake diversity in this region may have been underestimated in previous studies.

According to field surveys and recent publications, we identified updated distribution sites of *Ovophis* species in China (Zhang et al. 2011; Che et al. 2020; Zeng et al. 2023; Uetz et al. 2024) (Fig. 6). In Yunnan, *O. makazayazaya* is widely distributed in most parts of the province, *O. zayuensis* in the Gaoligong Mountain region of western Yunnan, and *O. malhotrae* in Jinping and Pingbian in southeastern Yunnan (Wang et al. 2022; Zeng et al. 2023). In some areas, there may be overlapping distributions of *O. makazayazaya* and other congeners. The specimens of "*Trimersurus monticola*" from Hotha, Longchuan County, Yunnan Province, cited by Anderson (1878a), displayed intra-specific polymorphism: the second supralabial completed or divided from the anterior

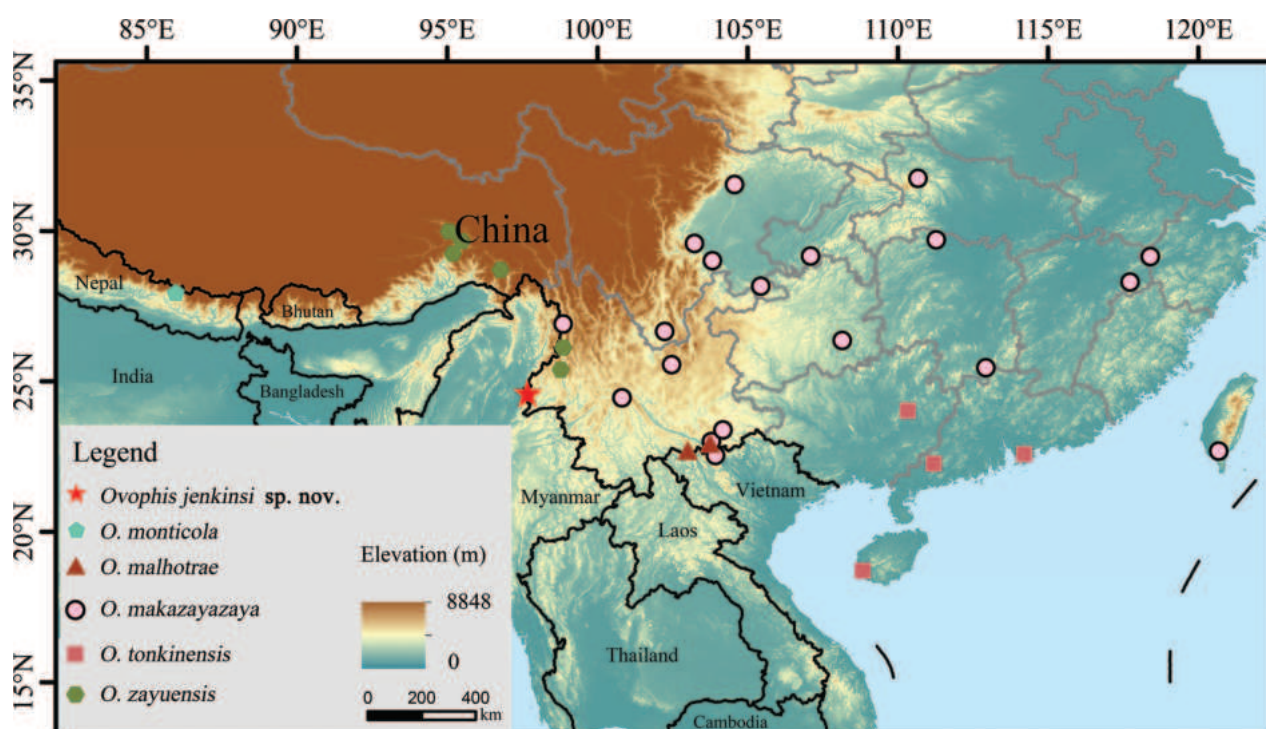


Figure 6. The type locality of *Ovophis jenkinsi* sp. nov. and some distribution sites of *Ovophis* species in China.

of loreal pit, consistent with the character of *O. makazayazaya* (Guo et al. 2021). Further examinations through photos of the specimen that was recorded by Anderson (1878b) were conducted and showed that it displays 10 supralabials, the second divided from the loreal pit and fourth larger than third, suggesting taxonomic placement under *O. makazayazaya*. However, since Longchuan County is adjacent to Yingjiang County, and in specimens from Hotha, Longchuan, the second supralabial also reaches the loreal pit, they should belong to *O. jenkinsi* sp. nov. In addition, Yingjiang County, Yunnan Province is located on the border of China and is adjacent to Myanmar; thus, the new species may also be distributed in Myanmar.

The new species is morphologically most similar to *O. monticola*, but can be distinguished by morphological characters such as wider head, fewer ventrals, trapezoidal patches on dorsal body, and deep orange-brown or dark brownish-grey dorsal surface rather than yellowish brown. In the specimens examined, the new species has a maximum TL of 690 mm (specimen YJ201801), while *O. monticola* appears to be larger, with a maximum TL of 1,300 mm (Sharma et al. 2013). We will collect more specimens of *O. jenkinsi* sp. nov. in the future to supplement the morphological data. Molecular phylogenetic analyses show *O. jenkinsi* sp. nov. is genetically differentiated from *O. malhotrae* (p -distance 10.2–11.0). Currently, only the holotype of *O. malhotrae* is described in supporting documents, the intraspecific variation of this species is unclear. It is, therefore, suggested that additional samples from along the Yunnan border and adjacent areas would enrich the current morphological dataset of *O. jenkinsi* sp. nov., *O. malhotrae*, and other *Ovophis* species and support further biodiversity discoveries.

Acknowledgements

We thank Shuo Qi for helping in the research method. We thank Sheng-Chao Shi, Guo-Wei Mo, and Xiao-Jun Gu for providing habitat photos for this study. We thank Dehong Forestry and Grassland Administration and Tongbiguan Natural Reserve for their support in specimen collection.

Additional information

Conflict of interest

The authors have declared that no competing interests exist.

Ethical statement

No ethical statement was reported.

Funding

This work was supported by National Natural Science Foundation of China (NSFC 42202014, Jingsong Shi); The National Key R&D Program of China (nos. 2022YFC2601200, 2023YFC2604904, Ming Bai); the National Science & Technology Fundamental Resources Investigation Program of China (nos. 2022FY100500, 2023FY100301, Ming Bai); the Second Tibetan Plateau Scientific Expedition and Research Program (2019QZKK0705, Tao Deng and Xi-Jun Ni).

Author contributions

Xian-Chun Qiu: Writing original draft. Jin-Ze Wang: Participating in field surveys; writing original draft. Zu-Yao Xia: Searched for references needed for this thesis; reviewed and revised this thesis. Zhong-Wen Jiang: Participating in the field survey. Yan Zeng: production of distribution maps and the literature search. Nan Wang: Reviewed and revised this thesis. Pi-Peng Li: Supervised the writing of this thesis; reviewed and revised this thesis. Jing-Song Shi: Methodology, funding and review.

Author ORCIDs

Xian-Chun Qiu  <https://orcid.org/0009-0001-5776-711X>

Jing-Song Shi  <https://orcid.org/0000-0001-9168-1734>

Data availability

All of the data that support the findings of this study are available in the main text.

References

- Anderson J (1878a) Anatomical and Zoological Researches: comprising an account of the zoological results of the two expeditions to western Yunnan in 1868 and 1875; and a monograph of the two cetacean genera, *Platanista* and *Orcella*. First Volume—Text. Bernard Quaritch, London, [i–xxv+] 1–985. <https://doi.org/10.5962/bhl.title.55401>
- Anderson J (1878b) Anatomical and Zoological Researches: comprising an account of the zoological results of the two expeditions to western Yunnan in 1868 and 1875; and a monograph of the two cetacean genera, *Platanista* and *Orcella*. Second Volume—Plates. Bernard Quaritch, London. <https://doi.org/10.5962/bhl.title.55401>
- Arévalo E, Davis SK, Sites Jr JW (1994) Mitochondrial DNA sequence divergence and phylogenetic relationships among eight chromosome races of the *Sceloporus grammicus* complex (Phrynosomatidae) in central Mexico. *Systematic Biology* 43(3): 387–418. <https://doi.org/10.1093/sysbio/43.3.387>
- Burbrink FT, Lawson R, Slowinski JB (2000) Mitochondrial DNA phylogeography of the polytypic North American rat snake (*Elaphe obsoleta*): A critique of the subspecies concept. *Evolution; International Journal of Organic Evolution* 54(6): 2107–2118. <https://doi.org/10.1111/j.0014-3820.2000.tb01253.x>
- Che J, Jiang K, Yan F, Zhang YP (2020) Amphibians and Reptiles in Tibet—Diversity and Evolution. Science Press, Beijing, 603 pp. [In Chinese]
- Chen ZN, Shi SC, Gao J, Vogel G, Song ZB, Ding L, Dai R (2021) A new species of *Trimersurus* Lacépède, 1804 (Squamata: Viperidae) from southwestern China, Vietnam, Thailand and Myanmar. *Asian Herpetological Research* 12(2): 167–177. <https://doi.org/10.16373/j.cnki.ahr.200084>
- Darko YA, Voss O, Uetz P (2022) A dictionary of abbreviations used in reptile descriptions. *Zootaxa* 5219(5): 421–432. <https://doi.org/10.11646/zootaxa.5219.5.2>
- Guo P, Liu Q, Wu YY, Zhu F, Zhong GH (2021) Pitvipers of China. Science Press, Beijing, 264 pp. [In Chinese]
- Hou SB, Yuan ZY, Wei PF, Zhao GG, Liu GH, Wu YH, Shen WJ, Chen JM, Guo P, Che J (2021) Molecular phylogeny and morphological comparisons of the genus *Hebius* Thompson, 1913 (Reptilia: Squamata: Colubridae) uncover a new taxon from Yunnan Province, China, and support revalidation of *Hebius septemlineatus* (Schmidt, 1925). *Zoological Research* 42(5): 620–625. <https://doi.org/10.24272/j.issn.2095-8137.2021.093>

- Huang S (2021) Sinoophis. The Straits Publishing and Distributing Group, Fuzhou, 636 pp. [In Chinese]
- Jiang K, Ren JL, Guo JF, Wang Z, Ding L, Li JT (2020) A new species of the genus *Dendrelaphis* (Squamata: Colubridae) from Yunnan Province, China, with discussion of the occurrence of *D. cyanochloris* (Wall, 1921) in China. *Zootaxa* 4743(1): 1–20. <https://doi.org/10.11646/zootaxa.4743.1.1>
- Knight A, Mindell DP (1993) Substitution bias, weighting of DNA sequence evolution, and the phylogenetic position of Fea's viper. *Systematic Biology* 42(1): 18–31. <https://doi.org/10.1093/sysbio/42.1.18>
- Lanfear R, Calcott B, Ho SY, Guindon S (2012) PartitionFinder: Combined selection of partitioning schemes and substitution models for phylogenetic analyses. *Molecular Biology and Evolution* 29(6): 1695–1701. <https://doi.org/10.1093/molbev/mss020>
- Lee JL (2021) Description of a new species of Southeast Asian reed snake from northern Laos (Squamata: Colubridae: Genus *Calamaria* F. Boie, 1827) with a revised diagnosis of *Calamaria yunnanensis* Chernov, 1962. *Journal of Natural History* 55(9–10): 531–560. <https://doi.org/10.1080/00222933.2021.1909165>
- Li PP, Zhao EM, Dong BJ (2010) Amphibians and Reptiles of Tibet. Science Press, Beijing, 226 pp. [In Chinese]
- Liu S, Hou M, Lwin YH, Wang QY, Rao DQ (2021) A new species of *Gonyosoma* Wagler, 1828 (Serpentes, Colubridae), previously confused with *G. prasinum* (Blyth, 1854). *Evolutionary Systematics* 5(1): 129–139. <https://doi.org/10.3897/evolsyst.5.66574>
- Ma S, Shi SC, Aji BD, Jiang JP (2023) A new species of the genus *Hebius* Thompson, 1913 (Serpentes: Natricidae) from Yunnan, China. *Asian Herpetological Research* 14(3): 212–226. <https://doi.org/10.3724/ahr.2095-0357.2023.0008>
- Malhotra A, Thorpe RS (2000) A phylogeny of the *Trimeresurus* group of pit vipers: New evidence from a mitochondrial gene tree. *Molecular Phylogenetics and Evolution* 16(2): 199–211. <https://doi.org/10.1006/mpev.2000.0779>
- Malhotra A, Thorpe RS (2004) A phylogeny of four mitochondrial gene regions suggests a revised taxonomy for Asian pitvipers (*Trimeresurus* and *Ovophis*). *Molecular Phylogenetics and Evolution* 32(1): 83–100. <https://doi.org/10.1016/j.ympev.2004.02.008>
- Malhotra A, Dawson K, Guo P, Thorpe RS (2011) Phylogenetic structure and species boundaries in the mountain pitviper *Ovophis monticola* (Serpentes: Viperidae: Crotalinae) in Asia. *Molecular Phylogenetics and Evolution* 59(2): 444–457. <https://doi.org/10.1016/j.ympev.2011.02.010>
- Neang T, Chhin S, Kris M, Hun S (2011) First records of two reptile species (Gekkonidae: *Hemidactylus garnotii* Dumeril & Bibron, 1836; viperidae: *Ovophis convictus* stoliczka, 1870) from Cambodia. *Cambodian Journal of Natural History* 2: 86–92.
- Palumbi S, Martin A, Romano S (1991) The Simple Fool's Guide to PCR, Version 2.0. University of Hawaii, Honolulu 45: 26–28.
- Ronquist F, Huelsenbeck J, Teslenko M (2011) Draft MrBayes version 3.2 manual: tutorials and model summaries. Distributed with the software from MrBayes. [sourceforge.net/mb3.2_manual.pdf]
- Sharma SK, Pandey DP, Shah KB, Tillack F, Chappuis F, Thapa CL, Kuch U (2013) Venomous Snakes of Nepal. A photographic guide. BP Koirala Institute of Health Sciences, Dharan, 76 pp.
- Shi JS, Liu JC, Giri R, Owens JB, Santra V, Kuttalam S, Selvan M, Guo KJ, Malhotra A (2021) Molecular phylogenetic analysis of the genus *Gloydius* (Squamata, Viperidae, Crotalinae), with descriptions of two new alpine species from Qinghai-Tibet Plateau, China. *ZooKeys* 1061: 87–108. <https://doi.org/10.3897/zookeys.1061.70420>

- Shi SC, Vogel G, Ding L, Rao DQ, Liu S, Zhang L, Wu ZJ, Chen ZN (2022) Description of a new cobra (*Naja Laurenti*, 1768; Squamata, Elapidae) from China with designation of a neotype for *Naja atra*. *Animals (Basel)* 12(24): 3481. <https://doi.org/10.3390/ani12243481>
- Silvestro D, Michalak I (2012) RaxmlGUI: A graphical front-end for RAxML. *Organisms, Diversity & Evolution* 12(4): 335–337. <https://doi.org/10.1007/s13127-011-0056-0>
- Speybroeck J, Beukema W, Bok B, Van Der Voort J (2016) *Field Guide to the Amphibians and Reptiles of Britain and Europe*. Bloomsbury Publishing, London, 430 pp.
- Tamura K, Stecher G, Peterson D, Filipinski A, Kumar S (2013) MEGA6: Molecular Evolutionary Genetics Analysis version 6.0. *Molecular Biology and Evolution* 30(12): 2725–2729. <https://doi.org/10.1093/molbev/mst197>
- Thompson JD, Gibson TJ, Plewniak F, Jeanmougin F, Higgins DG (1997) The CLUSTAL_X windows interface: Flexible strategies for multiple sequence alignment aided by quality analysis tools. *Nucleic Acids Research* 25(24): 4876–4882. <https://doi.org/10.1093/nar/25.24.4876>
- Uetz P, Freed P, Hošek J (2024) The Reptile Database. <http://www.reptile-database.org> [Accessed on 1 Apr. 2024]
- Wang K, Lyu ZT, Wang J, Qi S, Che J (2022) The updated checklist and zoogeographic division of the reptilian fauna of Yunnan Province, China. *Shengwu Duoyangxing* 30(4): 21326. <https://doi.org/10.17520/biods.2021326> [In Chinese]
- Xu YH, Gong YN, Hou M, Weng SY, Liu S, Deng JD, Hu JK, Peng LF (2024) A new species of the genus *Pseudocalotes* (Squamata: Agamidae) from southwest Yunnan, China. *Animals (Basel)* 14(6): 826. <https://doi.org/10.3390/ani14060826>
- Zeng YM, Li K, Liu Q, Wu YY, Hou SB, Zhao GG, Nguyen SN, Guo P, Shi L (2023) New insights into the phylogeny and evolution of Chinese *Ovophis* (Serpentes, Viperidae): Inferred from multilocus data. *Zoologica Scripta* 52(4): 358–369. <https://doi.org/10.1111/zsc.12589>
- Zhang L, Wer QL, Jiang K, Yu BC, Tang XP, Ding XL, Hu HJ (2011) *Ovophis tonkinensis*: A new snake record in Guangdong Province. *Dongwuxue Zazhi* 46(4): 144–146. [In Chinese]
- Zhao EM (2006) *Snakes of China*. Anhui Science and Technology Publishing House, Hefei, 365 pp. [In Chinese]
- Zhao EM, Huang MH, Zong Y (1998) *Fauna Sinica: Reptilia*. Vol. 3. Squamata, Serpentes. Science Press, Beijing, 522 pp. [In Chinese]

First record of the spider family Trechaleidae Simon, 1890 (Araneae) from China

Lu-Yu Wang¹, Yan-Nan Mu², Feng Zhang², Yuri M. Marusik^{3,4,5}, Zhi-Sheng Zhang¹

1 Key Laboratory of Eco-environments in Three Gorges Reservoir Region (Ministry of Education), School of Life Sciences, Southwest University, Chongqing 400715, China

2 The Key Laboratory of Zoological Systematics and Application, Institute of Life Science and Green Development, College of Life Sciences, Hebei University, Baoding, Hebei 071002, China

3 Institute for Biological Problems of the North RAS, Portovaya Str.18, Magadan 685000, Russia

4 Department of Zoology & Entomology, University of the Free State, Bloemfontein 9300, South Africa

5 Altai State University, Lenina Pr., 61, Barnaul, RF-656049, Russia

Corresponding author: Zhi-Sheng Zhang (yurmar@mail.ru, zhangzs327@qq.com)

Abstract

The family Trechaleidae Simon, 1890 is reported for the first time from China, including one new species: *Shinobius cona* **sp. nov.** (♂♀). Morphological descriptions, photos and illustrations of the new species are provided. Taxonomic features of species belonging to the genus are briefly discussed. Photos of the female of *Shinobius orientalis* (Yaginuma, 1967) are also presented to compare it with the new species.

Key words: Description, morphology, new species, taxonomy, Xizang



Academic editor: Alireza Zamani

Received: 5 April 2024

Accepted: 5 May 2024

Published: 30 May 2024

ZooBank: <https://zoobank.org/7BA83309-9861-4A43-A1BD-EB37A6563EF9>

Citation: Wang L-Y, Mu Y-N, Zhang F, Marusik YM, Zhang Z-S (2024) First record of the spider family Trechaleidae Simon, 1890 (Araneae) from China. ZooKeys 1203: 189–195. <https://doi.org/10.3897/zookeys.1203.124808>

Copyright: © Lu-Yu Wang et al.
This is an open access article distributed under terms of the Creative Commons Attribution License (Attribution 4.0 International – CC BY 4.0).

Introduction

The spider family Trechaleidae is relatively small, with 133 named species belonging to 17 genera (WSC 2024). Sixteen genera and 132 species are restricted to the Neotropical Realm, and only one monotypic genus, *Shinobius* Yaginuma, 1991 is known in the Palaearctic Realm (Japan) (WSC 2024).

While studying specimens collected from Xizang, China, we found two specimens of both sexes that are similar to *Shinobius* in somatic morphology and features of the male palp and epigyne. These specimens, observed in the field, construct funnel-shaped webs and carry egg sacs by spinnerets. The goal of this paper is to provide a detailed description of the new species and a brief discussion of the taxonomic position of the genus.

Material and methods

All specimens are preserved in 75% ethanol and were examined, illustrated, photographed, and measured using a Leica M205A stereomicroscope equipped with a drawing tube, a Leica DFC450 camera, and LAS software (v. 4.6). Male palps and epigynes were examined and illustrated after they were dissected.

Epigynes were cleared by immersing them in pancreatin (Álvarez-Padilla and Hormiga 2007). Eye sizes were measured as the maximum diameter. Leg measurements are shown as total length (femur, patella and tibia, metatarsus, tarsus). All measurements are in millimetres. The specimens examined here are deposited in the Collection of Spiders, School of Life Sciences, Southwest University, Chongqing, China (SWUC).

Comparative material: *Shinobius orientalis*: 1♀ Japan, Ibaraki Pref., Saku-ragawa, Hatori, 36°14'10.5"N, 140°05'58.1"E, 23.vi.2018, R. Kuwahara leg.

Abbreviations used in the text: **ALE** – anterior lateral eye; **AME** – anterior median eye; **PLE** – posterior lateral eye; **PME** – posterior median eye.

Taxonomy

Family Trechaleidae Simon, 1890

Genus *Shinobius* Yaginuma, 1991

Type species. *Cispus orientalis* Yaginuma, 1967.

Diagnosis. *Shinobius* is similar to the South American genera *Rhoicinus* Simon, 1898 and *Barrisca* Chamberlin & Ivie, 1936, by the lack of the retrolateral tibial apophysis and having a very large subtegulum composing almost a half of the bulb. However, *Shinobius* can be separated from *Rhoicinus* and *Barrisca* by the cymbial tip shorter than the bulb and a strongly sclerotized posteroretrolateral part of the cymbium (vs. tip of cymbium longer than bulb, basal part of cymbium not modified) and by the presence of a median plate in the epigyne (vs. absent). *Shinobius* differs from other genera considered in the family by the lack of an extending retrolateral tibial apophysis.

Description. Carapace brown. Eight eyes arranged in two rows, posterior row strongly protruding. Fovea longitudinal. Cervical groove indistinct, radial furrows distinct. Chelicerae yellow brown, with three promarginal and three retromarginal teeth. Endites and labium yellow brown, longer than wide. Sternum yellow brown, shield-shaped, with brown setae. Legs yellow brown, with black pigmentation. Leg formula: 4213. Opisthosoma oval. Dorsum yellow brown, with black brown markings. Venter yellowish-brown.

Male palp: tibia without extending retrolateral apophysis (RTA), but with strongly sclerotized kind of hood; cymbium droplet-shaped, with tip shorter than bulb, spines and claws present or absent; posteroretrolateral part strongly sclerotized (Cs, Fig. 3B). Subtegulum large, almost half of bulb, with anterior margin slanting; median apophysis (Ma) short, located on retrolateral half of bulb; conductor finger-shaped, longer than wide; embolus with oval-shaped base, filamentous, round bent at about right angle, tip located close to tip of median apophysis.

Epigyne: epigynal plate slightly wider than long; with a wide septum in type species and round in *S. cona* sp. nov.; fovea divided by septum; septum terminates near epigastral fold.

Composition. *Shinobius cona* sp. nov. and *S. orientalis* (Yaginuma, 1967).

Relationships. *Shinobius* is the only genus of the family found far away from the rest of the genera which are distributed in the Neotropical Realm. *Shinobius*

lacks a developed tibial apophysis (extending in from the tibia) but has instead a kind of hood with a strongly chitinized anterior margin lacking in other members of the family except for *Rhoicinus*. Based on this similarity and the shape of the bulb, Sierwald (1993) considered the two genera in a separate subfamily Rhoicinae Simon, 1898.

Distribution. China (Xizang) and Japan (Fig. 4).

***Shinobius cona* sp. nov.**

<https://zoobank.org/ADFEFF8E-E6C0-4652-AB32-7DB37D101BD8>

Figs 1–3, 5

错那侵蛛

Type material. Holotype ♂ (SWUC-T-TR-01-01): CHINA, Xizang, Cona Co., Mama Township, Lebugou; 27°50'59"N, 91°46'39"E, elev. 2280 m; 4.viii.2020; L.Y. Wang, T. Yuan and Y.M. Hou leg.; **Paratype:** 1♀ (SWUC-T-TR-01-02), same data as holotype.

Etymology. The epithet refers to the type locality.

Diagnosis. The new species is similar to *S. orientalis* (Yaginuma, 1967) (Sierwald 1993: figs 20–22), but differs by having no strong spines on the male palpal tibia and cymbium (vs. present), a median apophysis with one branch (vs. two); a roundly bent and not meandering spermophor (vs. meandering) as well by having the septum of the epigyne wider posteriorly (vs. anteriorly), and slit-like copulatory openings (CO) (vs. round, cf. Fig. 2C and Fig. 4B).

Description. Male holotype (Fig. 1A) total length 5.75. Carapace 2.85 long, 2.37 wide, cephalic part 1.8 times thinner than thoracic; opisthosoma 2.83 long, 2.59 wide. Carapace yellow brown, with distinct pattern: cephalic part behind posterior eye row light brown, anterior part of thoracic part with 2 pairs of light, and submarinal spots, larger anterior and smaller posterior; medially with thin light stripe and 2 thin, and light marginal stripes against coxa III and IV. Cervical groove indistinct, radial furrows distinct. Eye sizes and interdistances: AME 0.12, ALE 0.12, PME 0.18, PLE 0.21; AME–AME 0.13, AME–ALE 0.08, PME–PME 0.14, PME–PLE 0.23, Clypeus height 0.25. Legs yellow brown, with black pigmentation. Tibia I with four pairs of ventral spines; metatarsus I with 3 pairs of ventral spines. Tibia II with 3 pairs of ventral spines; metatarsus II with 3 pairs of ventral spines. Leg measurements: I 10.31 (2.90, 3.52, 2.50, 1.39); II 10.71 (3.03, 3.68, 2.67, 1.33); III 9.14 (2.41, 3.39, 2.21, 1.13); IV 10.84 (2.87, 3.64, 2.93, 1.40). Opisthosoma oval. Dorsum yellow brown, with black brown markings. Venter yellowish-brown.

Palp (Figs 2A, B, 3A–E). Retrolateral tibial edge hood-shaped. Subtegulum large, located on baso-prolateral side of bulb. Tegulum with slanting and meandering thin spermophor. Median apophysis short, medially wide, ventrally with coracoid tip, dorsally with a groove. Conductor digitiform (longer than wide), curving and membranous. Embolus arc-shaped, bent at about right angle, with oval-shaped base (Eb), tip ends in median apophysis groove dorsally.

Female paratype (Fig. 1B–I) total length 5.78. Carapace 2.98 long, 2.55 wide, cephalic part 1.6 times thinner than maximal width of carapace; opisthosoma 3.03 long, 2.41 wide. Eye sizes and interdistances: AME 0.16, ALE 0.15,

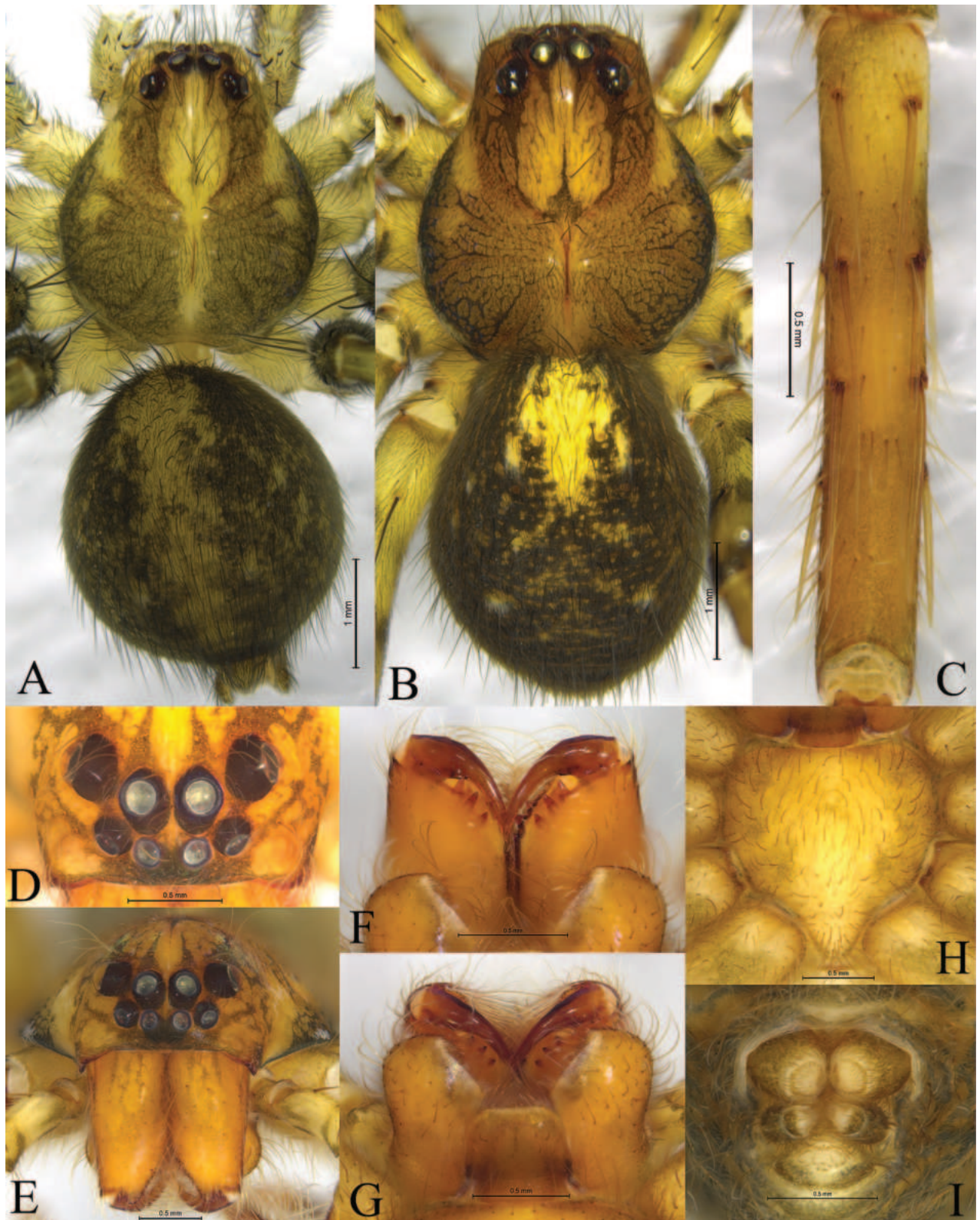


Figure 1. *Shinobius cona* sp. nov. male holotype (A), female paratype (B–I) A male habitus, dorsal view B female habitus, dorsal view C tibia I, ventral view D eyes, dorsal view E eyes and chelicerae, front view F chelicerae, ventral view G chelicerae, endites and labium, ventral view H sternum, ventral view I spinneret, ventral view.

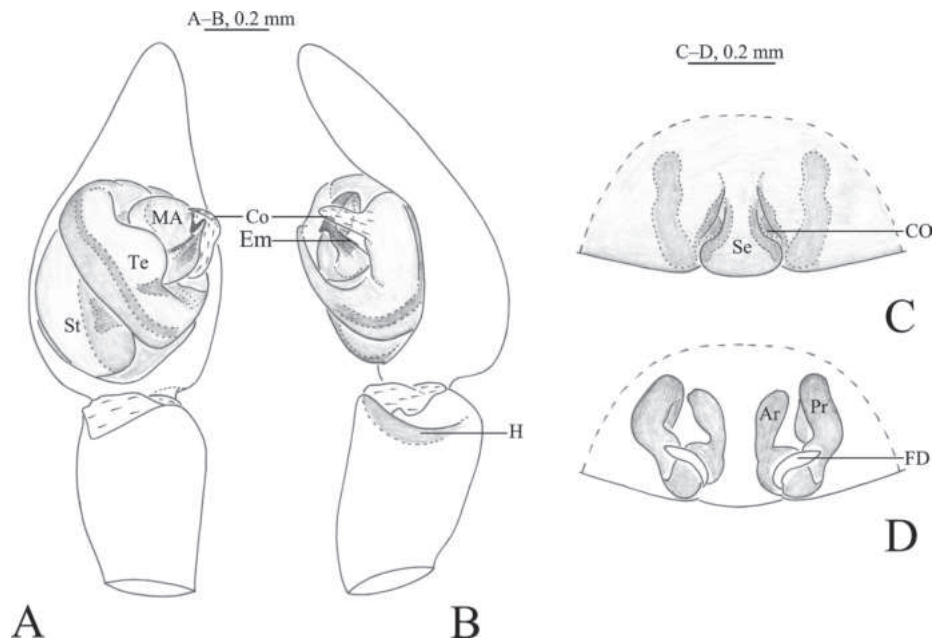


Figure 2. *Shinobius cona* sp. nov. **A, B** holotype male **C, D** paratype female **A** left male palp, ventral view **B** same, retrolateral view **C** epigyne, ventral view **D** vulva, dorsal view. Abbreviations: Ar = anterior receptacle; CO = copulatory opening; Co = conductor; Em = embolus; FD = fertilization duct; MA = median apophysis; Pr = posterior receptacle; H = hood; Se = septum; St = subtegulum; Te = tegulum.

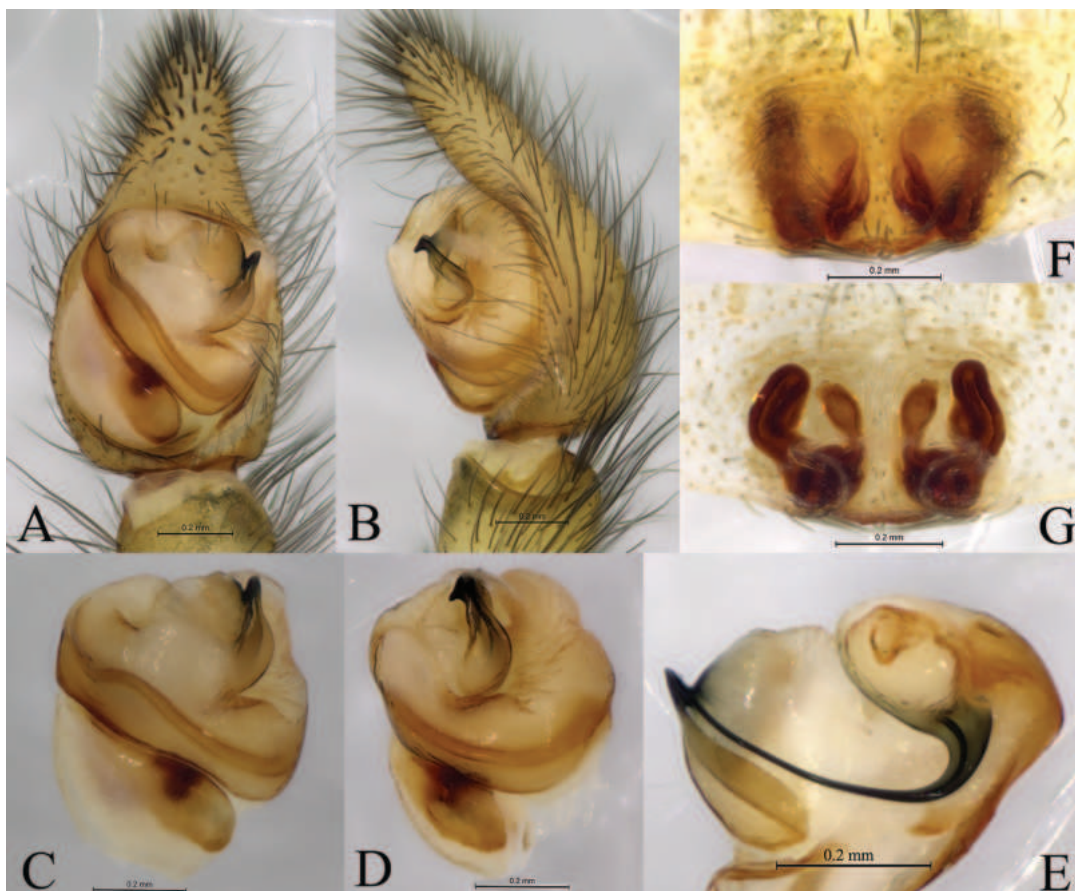


Figure 3. *Shinobius cona* sp. nov. male holotype (**A–E**), female paratype (**F, G**) **A** left male palp, ventral view **B** same, retrolateral view **C** right male palp, bulb, ventral view (overturn) **D** same, retrolateral view (overturn) **E** right male palp, median apophysis and embolus, dorsal view (overturn) **F** epigyne, ventral view **G** vulva, dorsal view.

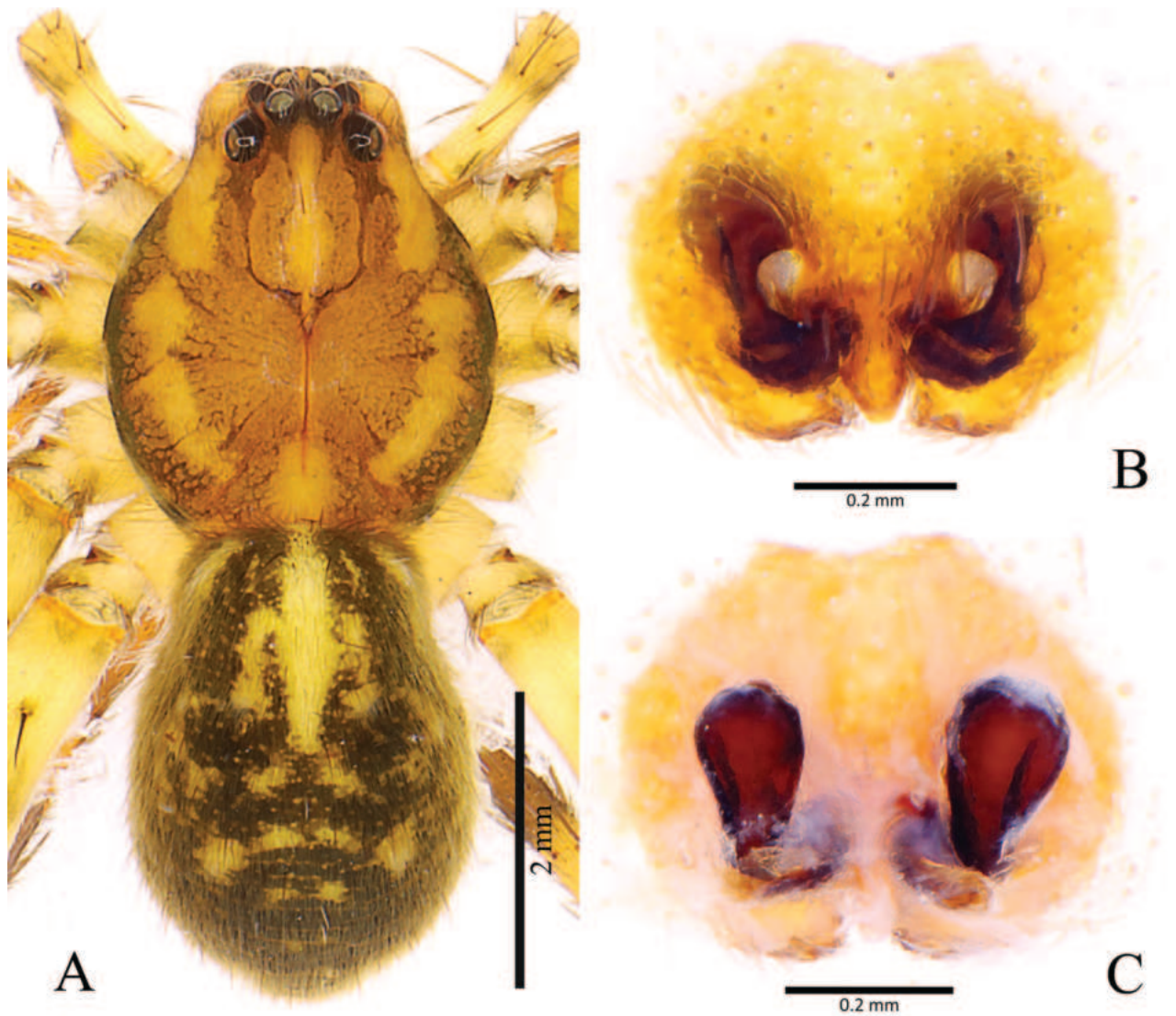


Figure 4. *Shinobius orientalis* (Yaginuma, 1967) **A** female habitus, dorsal view **B** epigyne, ventral view **C** vulva, dorsal view. (courtesy of Francesco Ballarin).

PME 0.24, PLE 0.23; AME–AME 0.12, AME–ALE 0.09, PME–PME 0.14, PME–PLE 0.27. Carapace pattern as in male. Clypeus height 0.15. Leg measurements: I 9.55 (2.71, 3.37, 2.29, 1.18); II 9.70 (2.80, 3.34, 2.39, 1.17); III 8.59 (2.50, 2.88, 2.19, 1.02); IV 10.54 (2.92, 3.48, 2.84, 1.30). Sternum yellowish with 3 pairs of dark round submarginal spots (Fig. 3H)

Epigyne (Figs 2C, D, 3F, G). Epigynal plate 1.2 times wider than long; fovea (atrium) almost totally covered with septum, 1.2 times longer than wide, anterior part of plate 2 times thinner than posterior; copulatory openings (CO) slit-like; Endogyne with 2 pairs of receptacles, posterior receptacles (Pr) crooked; anterior receptacles (Ar) cylindrical, with the oval head covered with sparse glandular pores; Fertilization ducts arc-shaped.

Natural history. Forms a funnel-shaped web on the moss. Female was found with egg-cocoons attached to spinnerets.

Distribution. Known only from the type locality, Xizang, China (Fig. 5).

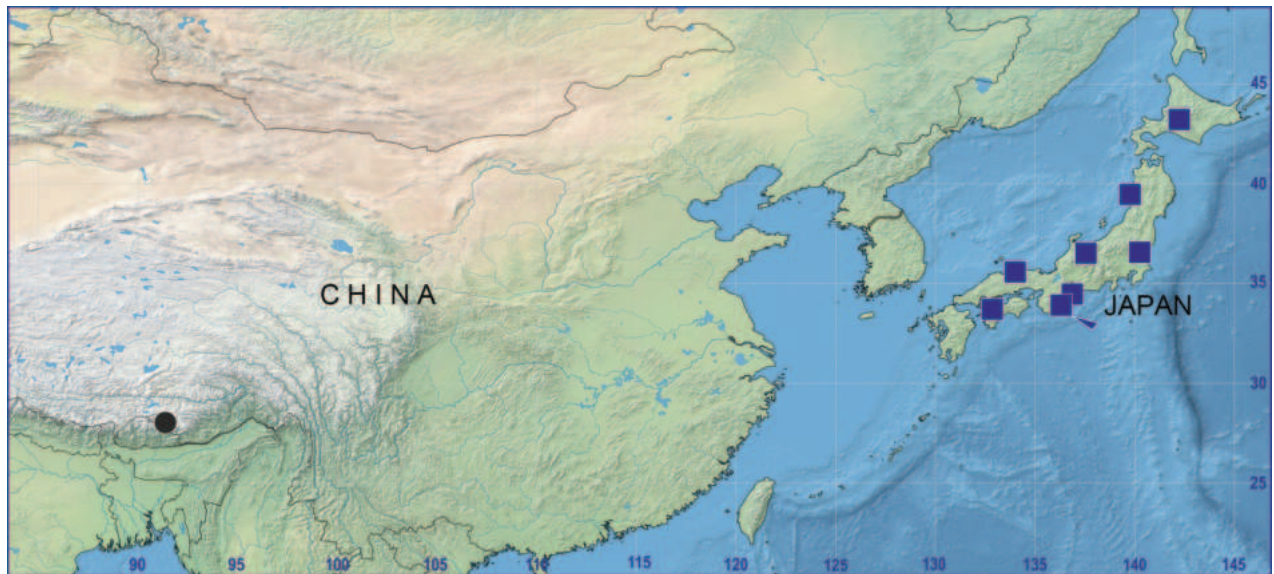


Figure 5. Distribution records of *Shinobius* species: *S. cona* sp. nov. (circle) and *S. orientalis* (square, type locality pointed, only prefecture records are shown).

Acknowledgments

We give great thanks Dr Francesco Ballarin (Tokyo, Japan) for providing the photos. Many thanks are given to Mr Tao Yuan and Yan-Meng Hou (College of Life Sciences, Hebei University, Baoding, China) for their assistance during the fieldwork and collection.

Additional information

Conflict of interest

The authors have declared that no competing interests exist.

Ethical statement

No ethical statement was reported.

Funding

This research was supported by the Science & Technology Fundamental Resources Investigation Program (Grant No. 2022FY202100) and the Survey of Wildlife Resources in Key Areas of Tibet (ZL202203601).

Author contributions

All authors have contributed equally.

Author ORCIDs

Lu-Yu Wang  <https://orcid.org/0000-0002-5250-3473>

Yan-Nan Mu  <https://orcid.org/0000-0002-2504-673X>

Feng Zhang  <https://orcid.org/0000-0002-3347-1031>

Yuri M. Marusik  <https://orcid.org/0000-0002-4499-5148>

Zhi-Sheng Zhang  <https://orcid.org/0000-0002-9304-1789>

Data availability

All of the data that support the findings of this study are available in the main text.

References

- Álvarez-Padilla F, Hormiga G (2007) A protocol for digesting internal soft tissues and mounting spiders for scanning electron microscopy. *The Journal of Arachnology* 35(3): 538–542. <https://doi.org/10.1636/Sh06-55.1>
- Chamberlin RV, Ivie W (1936) New spiders from Mexico and Panama. *Bulletin of the University of Utah* 27(5): 1–103.
- Sierwald P (1993) Revision of the spider genus *Paradossenus*, with notes on the family Trechaleidae and the subfamily Rhoicininae (Araneae, Lycosoidea). *Revue Arachnologique* 10: 53–74.
- Simon E (1898) *Histoire naturelle des araignées*. Deuxième édition, tome second. Roret, Paris, 193–380.
- WSC (2024) World Spider Catalog. Version 25. Natural History Museum Bern, online at <http://wsc.nmbe.ch>. [Accessed 22 January 2024] <https://doi.org/10.24436/2>
- Yaginuma T (1991) A new genus, *Shinobius*, of the Japanese pisaurid spider (Araneae: Pisauridae). *Acta Arachnologica* 40(1): 1–6. <https://doi.org/10.2476/asjaa.40.1>

Current and future potential distribution of two bamboo pests in China: *Anaka burmensis* and *Cicadella viridis* (Hemiptera, Cicadellidae)

Zhengxue Zhao^{1,2,3,4}, Lin Yang^{1,2,3}, Xiangsheng Chen^{1,2,3}

¹ Institute of Entomology, Guizhou University, Guiyang, China

² Provincial Special Key Laboratory for Development and Utilization of Insect Resources of Guizhou, Guizhou University, Guiyang, China

³ Guizhou Key Laboratory for Agricultural Pest Management of Mountainous Region, Guizhou University, Guiyang, China

⁴ College of Agriculture, Anshun University, Anshun, China

Corresponding author: Xiangsheng Chen (chenxs3218@163.com)



Academic editor:

J. Adilson Pinedo-Escatel

Received: 18 January 2024

Accepted: 7 May 2024

Published: 30 May 2024

ZooBank: <https://zoobank.org/094DD97D-26DA-4AD3-BBD5-958331BE2148>

Citation: Zhao Z, Yang L, Chen X (2024) Current and future potential distribution of two bamboo pests in China: *Anaka burmensis* and *Cicadella viridis* (Hemiptera, Cicadellidae). ZooKeys 1203: 197–210. <https://doi.org/10.3897/zookeys.1203.118978>

Copyright: © Zhengxue Zhao et al.
This is an open access article distributed under terms of the Creative Commons Attribution License (Attribution 4.0 International – CC BY 4.0).

Abstract

China's bamboo output is closely associated with its national economy; however, it is currently rapidly declining due to damage from the pests *Anaka burmensis* and *Cicadella viridis*. Identifying regions that are environmentally suitable for these pests is a critical step in their effective control. Therefore, in this study, we used a Maxent model to predict their current and future potential areas of distribution (2021–2040, 2041–2060, and 2061–2080) and explored changes over time using distribution data and related environmental variables. The model results demonstrates that the current potential areas of distribution of *A. burmensis* are predominantly concentrated in several provinces of southern and central China, such as Guizhou, Guangxi, and Hubei, whereas the current potential areas of distribution of *C. viridis* are primarily in many provinces across southern, central, and northeastern China. In the future, the potential distribution of *A. burmensis* will increase and move minimally, whereas the potential distribution of *C. viridis* will decrease and move considerably. The results of the present study provide vital information for predicting the spread and outbreaks of *C. viridis* and *A. burmensis* and provide a reference framework for developing management strategies to control these two pests, thereby minimizing economic loss in the bamboo industry.

Key words: Climate change, distribution areas, Maxent model

Introduction

Bamboo comprises all members of the subfamily Bambusoideae and is the only lineage in the Poaceae family that has adapted and diversified to forest habitats (Judziewicz et al. 1999; Grass Phylogeny Working Group 2001; Bamboo Phylogeny Group 2012). Bamboo plants are mainly distributed in the tropical and subtropical regions of Asia, Africa, and Latin America (Li et al. 2003). The emergence of bamboo has provided several benefits to humans (Sharma et al. 2014). For example, bamboo is a suitable substitute for wood due to its advantages of a short rotation period, strong regeneration ability, good properties for wide use, and excellent performance; these properties are similar to or

even superior to those of wood (Yang et al. 2004). Therefore, a growing number of countries, and especially China, use bamboo as a common building material to save wood (Van der Lugt et al. 2006; Sharma et al. 2014). Bamboo also plays a crucial role in combating degradation of mountain environments, ecosystems, and natural resources (Yang et al. 2004). Furthermore, young, tender bamboo shoots are used as a seasonal vegetable in both rural and urban areas of China (Borah et al. 2008). However, unfortunately, bamboo is vulnerable to damage from herbivorous insect pests throughout its lifetime; thus, pests are the main cause of the massive loss of bamboo in natural and plantation forests (Liese and Köhl 2015).

China has abundant bamboo resources, with 753 species accounting for approximately 50% of the world's bamboo (Shi et al. 2020). Bamboo is widely distributed in China and is found in 27 of the 34 provincial administrative regions (Shu et al. 2015). In China, the output value of bamboo reaches 45 billion yuan per year, which has contributed significantly to China's economic development (Shu et al. 2015). However, in recent years, due to the emergence of numerous bamboo pests, bamboo production has declined sharply (Yang et al. 2011; Shu et al. 2015), causing serious economic losses. Therefore, strengthening the management and control of bamboo pests is conducive to the steady growth of China's economy.

Anaka burmensis Dworakowska, 1993 and *Cicadella viridis* (Linnaeus, 1758) are two important bamboo pests (Xu and Wang 2004; Yang et al. 2007; Dong et al. 2017). Both pests are tiny insects, with body sizes of 3.45–4.05 and 6.2–10.8 mm, respectively (Chen et al. 2012). Owing to this characteristic, they can only be observed when they congregate. Both pests have varying feeding behavior. *Anaka burmensis* feeds on the content of the cells, resulting in the formation of "white spots" or "hopper burn" on the leaf surface. *Cicadella viridis* is a xylem feeder and causes no considerable damage to the leaf surface. They prefer feeding on the stem or larger veins of the plant where they can easily reach the xylem tubes.

Anaka burmensis is distributed across southern China, including Guizhou and Yunnan (Dong et al. 2017), whereas *C. viridis* is more widely distributed in northern China (Liu et al. 2004; Lin et al. 2016; Zhao et al. 2022). Determining the distributional range of a pest is essential for its control; however, the distribution of these two pests has not yet been fully investigated. Traditional manual surveys cannot completely determine the distribution of pests in large geographical areas, such as China, due to limited resources and failure to predict the distributional range of species due to climate change. This frequently results in the use of pest control measures during outbreaks, causing large economic losses. Therefore, preventive methods are urgently required to solve this problem.

Species distribution models use occurrence records and environmental data to produce a model of the species' requirements and a map of its potential distribution (Anderson et al. 2002). Currently, species distribution models have been widely recognized as a useful tool for predicting pest distribution areas (Geng et al. 2011; Kumar et al. 2016; Huang et al. 2019; Xu et al. 2020). Among species distribution models, the Maxent model is the most commonly used, largely because it has significant advantages of requiring only a small sample size and having good performance compared with other models. Phillips et al.

(2006) compared the performance of Maxent and GARP (Genetic Algorithm for Ruleset Prediction) models based on 10 random subsets of the occurrence records for two Neotropical mammal species and found that the Maxent model was almost always higher, suggesting that it better predicted species distribution than the GARP model.

In this study, we used a Maxent model to predict the current and future potential distribution areas of *A. burmensis* and *C. viridis* in China using occurrence records and environmental data. We aim to answer two questions: 1) where are the potential distribution areas, both currently and in the future, and 2) how has the potential distribution area changed over time?

Materials and methods

Occurrence records

We collected the occurrence records of *Anaka burmensis* and *Cicadella viridis* in China from the literature and from the Global Biodiversity Information Facility (GBIF, <https://www.gbif.org/>). Occurrence records that lacked latitude and longitude data were georeferenced using Google Earth. Sampling bias in geographic space frequently arises due to unequal sampling efforts, which can lead to incorrect predictions in species distribution models (Kramer-Schadt et al. 2013; Boria et al. 2014; Fourcade et al. 2014). Therefore, we conducted spatial thinning for the occurrence records with a 10-km distance using the R software package “spThin” to reduce the effect of sampling bias (Aiello-Lammens et al. 2015). After spatial thinning, 18 and 135 occurrence records of *A. burmensis* and *C. viridis* were obtained, respectively (Fig. 1, Suppl. material 1: table S1).

Environmental variables

We used 19 bioclimatic variables (1970–2000) and one elevation datum (altitude) from the current period as the current environment variables. To minimize multicollinearity among environmental variables, we calculated the variance inflation factor for the corresponding environmental variable values of the occurrence records of *A. burmensis* and *C. viridis*. Then, we eliminated the environment variable with the largest variance inflation factor each time until the variance inflation factor values of selected environment variables were less than 5. Finally, four environmental variables were retained for *A. burmensis*: mean diurnal range (bio2), mean temperature of wettest quarter (bio8), precipitation of warmest quarter (bio18), and precipitation of coldest quarter (bio19), whereas five environmental variables were retained for *C. viridis*: isothermality (bio3), mean temperature of wettest quarter (bio8), precipitation of driest month (bio14), precipitation seasonality (bio15), and precipitation of warmest quarter (bio18).

We selected future bioclimatic variables for the periods 2021–2040, 2041–2060, and 2061–2080 from the Coupled Model Intercomparison Project Phase 6 (CMIP 6). Four main emission scenarios driven by different socioeconomic assumptions are provided for CMIP6: SSP126, SSP245, SSP370, and SSP585. However, to avoid extreme simulation, the SSP245 scenario, a moderate emission scenario, was used (Hwang et al. 2022). In addition, due to the uncertainty

The bioclimatic variables and elevation data were obtained from the WorldClim database (<http://www.worldclim.org>), with a 2.5-arc min spatial resolution (~5 km resolution at the equator).

Maxent model

The model was developed in Maxent software v. 3.4.4. Regular multipliers (RM) and feature classes (FC) are closely related to the accuracy of the Maxent model (Phillips and Dudík 2008). Therefore, we used the ENMeval package in R software to choose the best combination of FC and RM values based on the lowest Akaike's Information Corrected Criterion (AICc) score (Muscarella et al. 2014). The RM values ranged from 1 to 4 in increments of 1, while eight FC were used: (i) Linear (L); (ii) Linear and Quadratic (LQ); (iii) Linear, Quadratic, and Hinge (LQH); (iv) Hinge, Product, and Threshold (HPT); (v) Quadratic, Hinge, and Product (QHP); (vi) Linear, Quadratic, Hinge, and Product (LQHP); (vii) Quadratic, Hinge, Product, and Threshold (QHPT); (viii) Linear, Quadratic, Hinge, Product, and Threshold (LQHPT). After the above process, an RM of 3 and the FC LQH were selected for *A. burmensis* and an RM of 1 and the FC LQ were selected for *C. viridis*. In addition, 10,000 background points, five repetitions with cross validation, and logistic output were set to run the model. The performance of the Maxent model was evaluated based on the area under the receiver operating characteristic curve (AUC) and true skill statistic (TSS). The AUC and TSS values greater than 0.75 and 0.6 respectively were considered useful (Elith 2002; Ben Rais Lasram et al. 2010). The importance of environmental variables was measured using the jackknife method. The 10th percentile training presence logistic threshold was used to define the potential distribution areas (Bosso et al. 2016; Fan et al. 2020; Wei et al. 2020; Wei et al. 2021).

Shift in potential distribution areas

To quantify the distributional shifts between the current and future potential distribution areas, centroid analysis was performed using the SDMtoolbox 2.0 tool. This analysis converts the species distribution to a central point (centroid) and creates a vector to describe the direction and magnitude of the change through time (Brown 2014). We obtained the distribution shift by tracking the change of the centroid.

Results

Model validation and important variables

The results showed that the mean test AUC for *Anaka burmensis* and *Cicadella viridis* were 0.887 and 0.869, respectively (Fig. 2). Moreover, mean TSS values for *A. burmensis* and *C. viridis* were 0.691 and 0.614, respectively. The jackknife test revealed that the most important variable that affected the distribution of *A. burmensis* was precipitation in the coldest quarter (bio19), followed by precipitation in the warmest quarter (bio18) (Fig. 3). The mean temperature of the wettest quarter (bio8) was found to be slightly less important than the precipitation in the warmest quarter (bio18). The mean diurnal range (bio2) had

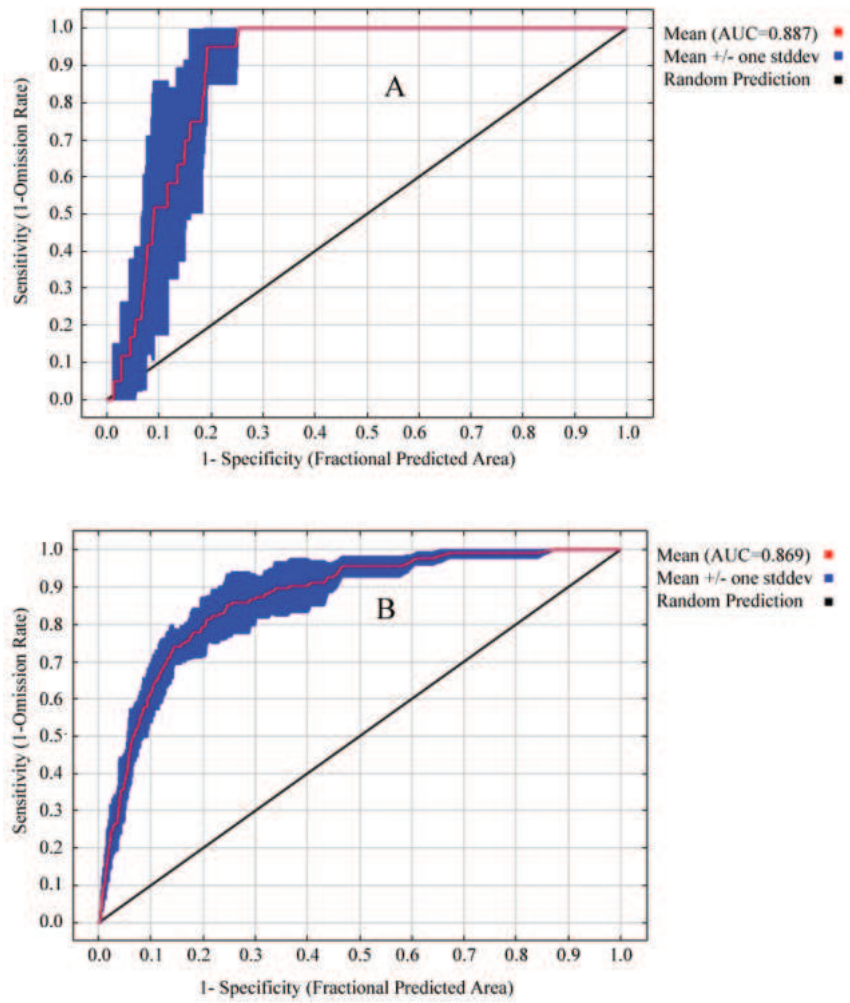


Figure 2. Receiver operating characteristic curve for *Anaka burmensis* (A) and *Cicadella viridis* (B).

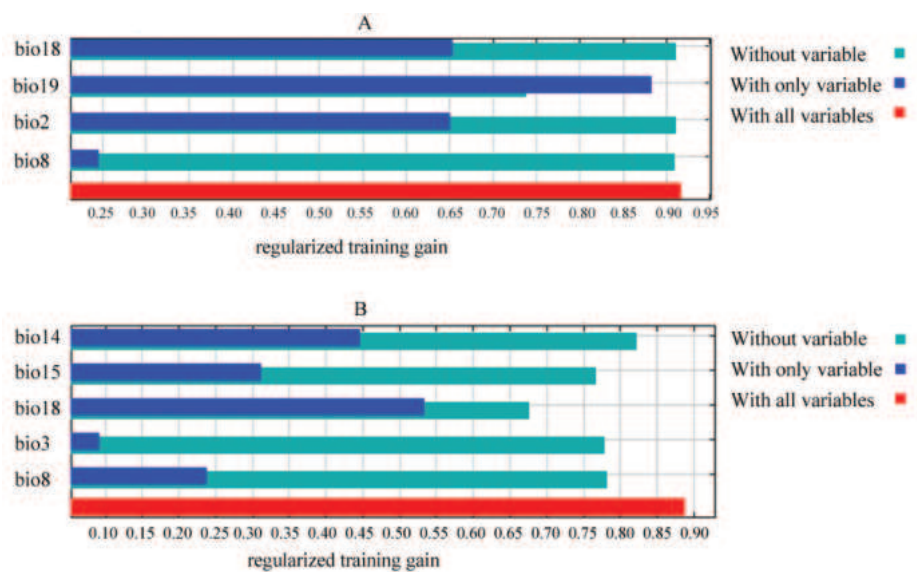


Figure 3. The importance of environmental variables for *Anaka burmensis* (A) and *Cicadella viridis* (B) based on the jackknife test.

the lowest contribution to the distribution of *A. burmensis*. The most important variable that affected the distribution of *C. viridis* was found to be precipitation in the warmest quarter (bio18), followed by precipitation in the driest month (bio14) (Fig. 3). The mean temperature of the wettest quarter (bio8) and precipitation seasonality (bio15) were found to have moderate impacts. The variable with the lowest impact was isothermality (bio3) (Fig. 3).

Potential distribution areas and changes

The current and future potential distribution area for two pests in China was obtained by Maxent model (Figs 4, 5). The current potential distribution area for *A. burmensis* was predicted to be 2.29×10^6 km² (Table 1) and was mainly concentrated in provincial administrative divisions of southern and central China (Fig. 4), including Guizhou, Chongqing, Guangxi, Hunan, Hubei, Guangdong, Jiangxi, Fujian, Anhui, Zhejiang, and Jiangsu. Potential distribution areas have also emerged in Xizang, Sichuan, Yunnan, Hainan, and Taiwan (Fig. 4).

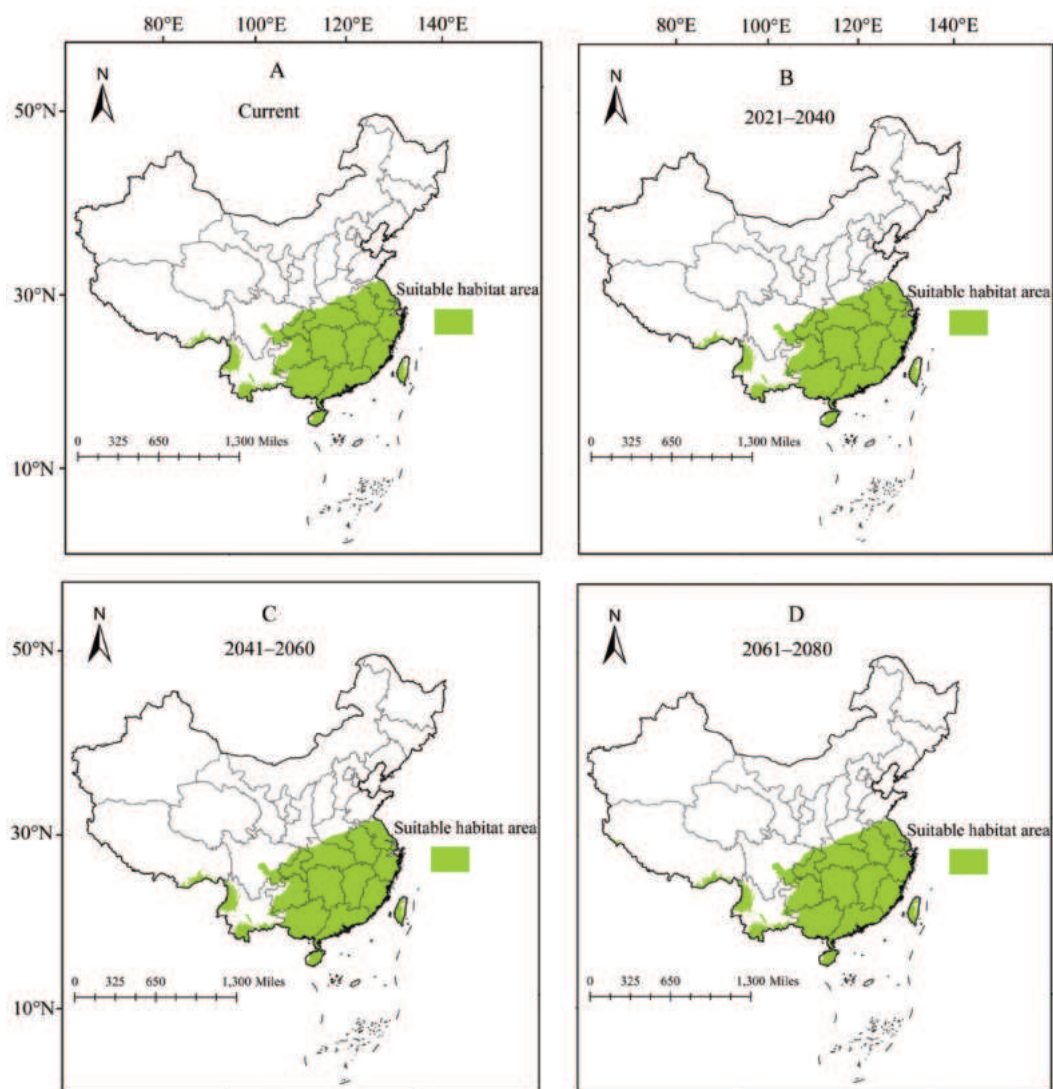


Figure 4. Potential distribution areas of *Anaka burmensis* in China during different periods.

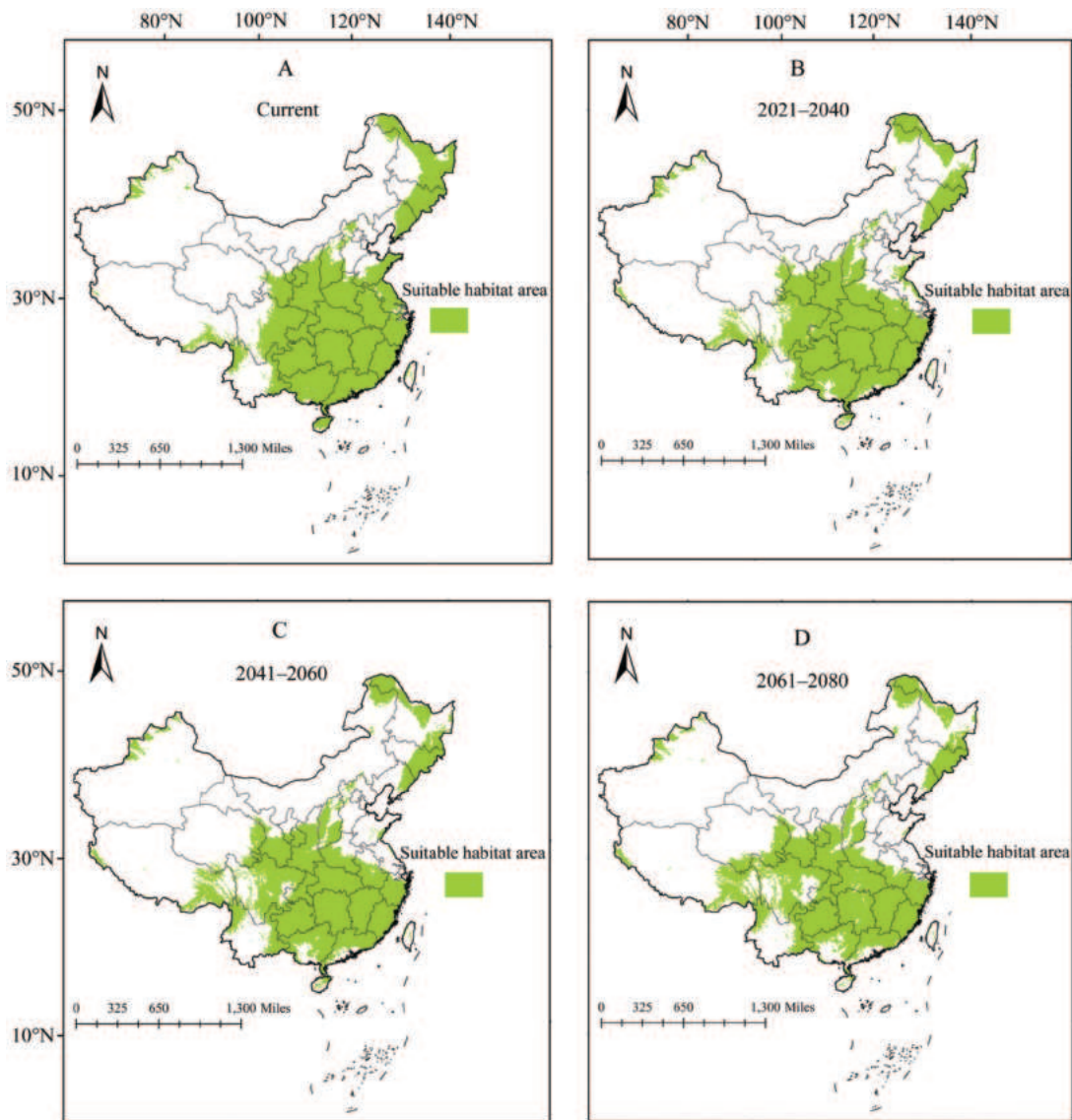


Figure 5. Potential distribution areas of *Cicadella viridis* in China during different periods.

Table 1. Predicted distribution areas (km²) for *Anaka burmensis* and *Cicadella viridis* during different periods in China.

	Current	2021–2040	2041–2060	2061–2080
<i>A. burmensis</i>	2.29×10^6	2.35×10^6 (+2.62%)	2.37×10^6 (+3.49%)	2.42×10^6 (+5.67%)
<i>C. viridis</i>	4.42×10^6	4.16×10^6 (-5.88%)	4.08×10^6 (-7.69%)	4.05×10^6 (-8.37%)

Three future periods showed increases in the size of predicted distribution area for *A. burmensis*, with increases of 2.62%, 3.49%, and 5.67% in 2021–2040, 2041–2060, and 2061–2080, respectively (Table 1). Centroid analysis revealed that centroids representing potential distribution areas moved 7.7 km north in 2021–2040, 8.8 km northwest in 2041–2060, and 17.7 km west in 2061–2080 (Fig. 6). This result revealed a slight shift in potential distribution areas.

The current potential distribution areas for *C. viridis* in China are projected to be 4.42×10^6 km² (Table 1), an area which is larger than that projected for *A. burmensis*. Numerous provincial administrative divisions in central, southern,

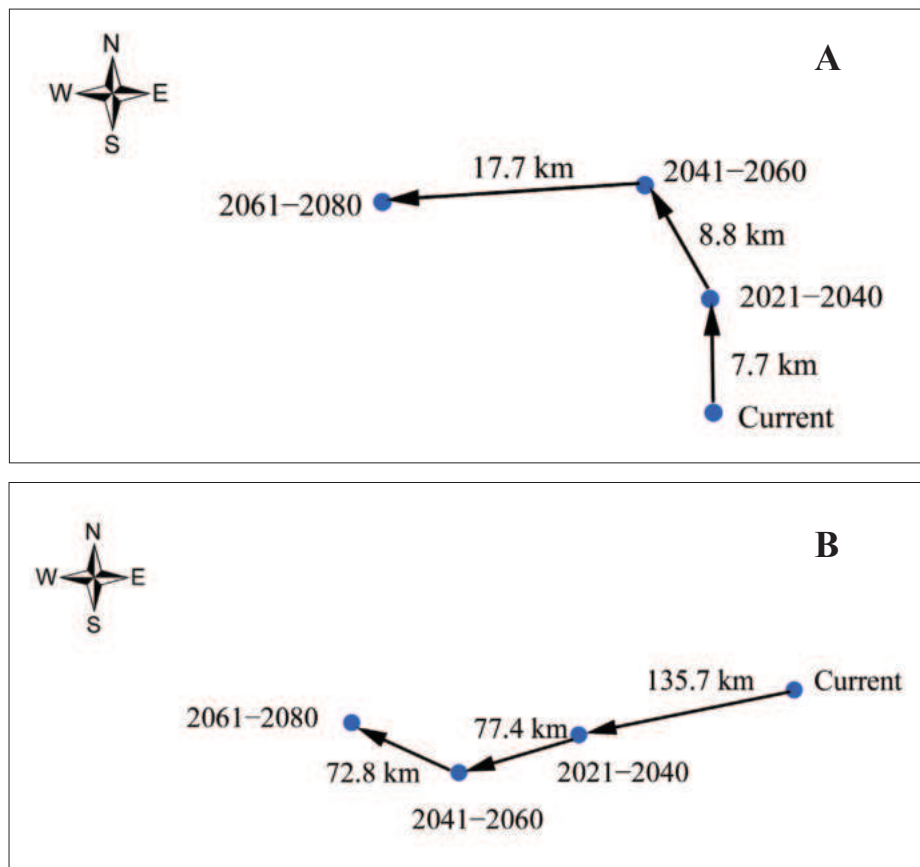


Figure 6. Shift in potential distribution areas of *Anaka burmensis* (A) and *Cicadella viridis* (B) in China.

and northeastern China have become major potential distribution areas for *C. viridis*, such as Guizhou, Hunan, Hubei, and Heilongjiang (Fig. 5). The future potential distribution areas were found to be decreased compared with the current areas by 5.88% in 2021–2040, 7.69% in 2041–2060, and 8.37% in 2061–2080 (Table 1). Overall, potential distribution areas for *C. viridis* are predicted to move toward the southwest in 2021–2040 (135.7 km) and 2041–2060 (77.4 km) and toward the northwest in 2061–2080 (72.8 km) due to climate change (Fig. 6).

Discussion

In the present study, the Maxent model was used to predict the current and future potential distribution areas of two pests that seriously harm bamboo in China. In addition, the spatial variation of potential distribution areas over time was investigated. The mean AUC and TSS value of five runs of the Maxent model for the two pests was high, suggesting that the constructed models have good performance and usefulness.

This study revealed that precipitation is the most important environmental factor driving the distribution of *Anaka burmensis* and *Cicadella viridis*. This is consistent with the findings of previous studies on other pests, such as *Moritzella castaneivora* Miyazaki, 1968 (Wang et al. 2010), *Riptortus pedestris* (Fabricius, 1775) (Zhang et al. 2022), and *Spodoptera frugiperda* (Smith, 1797) (Ramasamy et al. 2022). Therefore, the results of the current and previous studies

suggest that precipitation is a key factor for pest distribution. Furthermore, the current potential distribution areas of *A. burmensis* and *C. viridis*, as predicted by the Maxent model, were not only present in these provinces with occurrence records but also in several other provinces. This result largely reflects serious insufficiency in the current field investigation for the two pests and suggests that the Maxent model can be used as a pest monitoring tool.

The main distribution range of the current and future potential distribution areas of *A. burmensis* and *C. viridis* is the main distribution area of bamboo in China (Xu et al. 2019), which implies that bamboo in China is potentially threatened by these two pests. The potential distribution areas and the spatial change of *A. burmensis* and *C. viridis* identified in this study are extremely important in providing guidance for the management of these pests. For instance, management efforts for *A. burmensis* should continue to be focused on the southern and central China due to insignificant changes in the future. Moreover, the potential distribution areas for *C. viridis* appear to have a slight reduction in the future compared with current, but anticipated expansion of potential distribution areas in Sichuan, Qinhai, and Xizang is predicted; therefore, it is vital to develop effective preemptive strategies (e.g. strict quarantine measures) to prevent the introduction of this pest into these regions.

Zhang et al. (2023) used a Maxent model to predict current and future potential distribution areas of *C. viridis* globally. In their study, many areas in China were found to be environmentally suitable for this pest, but there was a huge difference from our prediction; the distribution of potential distribution areas found in our study revealed a greater range, with northeast Liaoning and northeast Heilongjiang becoming potential distribution. Wei et al. (2023) also obtained potential distribution areas of *C. viridis* in China using the Maxent model and found that most areas have become environmentally suitable. Although the abovementioned two studies have identified potential distribution areas in China, there are common or unique limitations in the modelling process, such as the use of untuned key parameters (i.e., FC and RM) for two studies and outdated future climate data in the study of Wei et al. (2023). Consequently, prediction results of the two studies are highly likely to be biased. Objectively, our results are more accurate due to the use of a more correct modeling process.

Although this study forecasted potential distribution areas for the two pests, the results must be interpreted with caution and some limitations should be acknowledged. All data for the modelling process were derived from GBIF and the literature. It is important to supplement these data with field investigation in future studies and perform the test of prediction. For example, by going to the field where the distribution of the species is predicted, we can confirm that the species is found in the field. Moreover, species distribution is determined by three factors: (1) the capacity to reach a suitable location; (2) the capacity to develop in a certain environmental condition; and (3) the ability to compete with other species occupying the same region (Begon et al. 2005). However, in our study, we only considered the effect of climate on species distribution. Furthermore, the physiological needs of species are plastic and may change over the course of evolution (Thomson et al. 2010), a fact that should be considered in future research.

Conclusions

In summary, the current and future potential distribution areas of *Anaka burmensis* and *Cicadella viridis* in China were obtained using the Maxent model. The results of this study demonstrated that precipitation is the most important environmental factor in shaping the distribution of these two pests. In addition, the findings of this study will assist policymakers and governments in developing appropriate measures for managing and controlling *A. burmensis* and *C. viridis*, thereby decreasing the damage to bamboo and the associated significant economic loss.

Additional information

Conflict of interest

The authors have declared that no competing interests exist.

Ethical statement

No ethical statement was reported.

Funding

This study was supported by the National Natural Science Foundation of China (no. 31860209) and the Science and Technology Support Program of Guizhou Province (no. 20201Y129).

Author contributions

Zhengxue Zhao: distribute data collection, data analysis, and manuscript writing. Lin Yang and Xiangsheng Chen: manuscript revising.

Author ORCIDs

Zhengxue Zhao  <https://orcid.org/0000-0003-1764-8690>

Data availability

All of the data that support the findings of this study are available in the main text or Supplementary Information.

References

- Aiello-Lammens ME, Boria RA, Radosavljevic A, Vilela B, Anderson RB (2015) spThin: An R package for spatial thinning of species occurrence records for use in ecological niche models. *Ecography* 38(5): 541–545. <https://doi.org/10.1111/ecog.01132>
- Anderson RP, Góme-Laverde M, Peterson AT (2002) Geographical distributions of spiny pocket mice in South America: Insights from predictive models. *Global Ecology and Biogeography* 11(2): 131–141. <https://doi.org/10.1046/j.1466-822X.2002.00275.x>
- Bamboo Phylogeny Group (2012) An updated tribal and subtribal classification of the bamboos (Poaceae: Bambusoideae). In: Gielis J, Potters G (Eds) *Proceedings of the 9th World Bamboo Congress, Antwerp, Belgium*.
- Begon M, Townsend CR, Harper JL (2005) *Ecology: from individuals to ecosystems*, 4th edition. Blackwell Publishing, Malden.

- Ben Rais Lasram F, Guilhaumon F, Albouy C, Somot S, Thuiller W, Mouillot D (2010) The Mediterranean Sea as a 'cul-de-sac' for endemic fishes facing climate change. *Global Change Biology* 16(12): 3233–3245. <https://doi.org/10.1111/j.1365-2486.2010.02224.x>
- Borah ED, Pathak KC, Deka B, Neog D, Borah K (2008) Utilization aspects of Bamboo and its market value. *Indian Forester* 134: 423–427.
- Boria RA, Olson LE, Goodman SM, Anderson RP (2014) Spatial filtering to reduce sampling bias can improve the performance of ecological niche models. *Ecological Modelling* 275: 73–77. <https://doi.org/10.1016/j.ecolmodel.2013.12.012>
- Bosso L, Di Febbraro M, Cristinzio G, Zoina A, Russo D (2016) Shedding light on the effects of climate change on the potential distribution of *Xylella fastidiosa* in the Mediterranean basin. *Biological Invasions* 18(6): 1759–1768. <https://doi.org/10.1007/s10530-016-1118-1>
- Brown JL (2014) SDMtoolbox, a python-based GIS toolkit for landscape genetic, biogeographic and species distribution model analyses. *Methods in Ecology and Evolution* 5(7): 694–700. <https://doi.org/10.1111/2041-210X.12200>
- Chen XS, Yang L, Li ZZ (2012) Bamboo-feeding leafhoppers in China. China Forestry Publishing House, Beijing.
- Dong MS, Yang L, Chen XS (2017) Investigation on the distribution and damage of the Bamboo leafhopper pest, *Anaka burmensis* Dworakowska (Hemiptera: Cicadellidae) in China. *Journal of Mountain Agriculture and Biology* 36: 031–034.
- Elith J (2002) Quantitative methods for modeling species habitat: comparative performance and an application to Australian plants. In: Ferson S, Burgman M (Eds) *Quantitative Methods for Conservation Biology*. Springer.
- Fan S, Chen C, Zhao Q, Wei J, Zhang H (2020) Identifying potentially climatic suitability areas for *Arma custos* (Hemiptera: Pentatomidae) in China under climate change. *Insects* 11(10): 674. <https://doi.org/10.3390/insects11100674>
- Fourcade Y, Engler JO, Rodder D, Secondi J (2014) Mapping species distributions with MAXENT using a geographically biased sample of presence data: A performance assessment of methods for correcting sampling bias. *PLoS One* 9(5): e97122. <https://doi.org/10.1371/journal.pone.0097122>
- Geng J, Li ZH, Rajotte EG, Wan FH, Lu XY, Wang ZL (2011) Potential geographical distribution of *Rhagoletis pomonella* (Diptera: Tephritidae) in China. *Insect Science* 18(5): 575–582. <https://doi.org/10.1111/j.1744-7917.2010.01402.x>
- Grass Phylogeny Working Group (2001) Phylogeny and subfamilial classification of the grasses (Poaceae). *Annals of the Missouri Botanical Garden* 88(3): 373–457. <https://doi.org/10.2307/3298585>
- Huang M, Ge X, Shi H, Tong Y, Shi J (2019) Prediction of current and future potential distributions of the Eucalyptus pest *Leptocybe invasa* (Hymenoptera: Eulophidae) in China using the CLIMEX model. *Pest Management Science* 75(11): 2958–2968. <https://doi.org/10.1002/ps.5408>
- Hwang JH, Kim SH, Yoon S, Jung S, Kim DH, Lee WH (2022) Evaluation of spatial distribution of three major *Leptocoris* (Hemiptera: Alydidae) pests using Maxent model. *Insects* 13(8): 750. <https://doi.org/10.3390/insects13080750>
- Judziewicz EJ, Clark LG, London X, Stern MJ (1999) *American Bamboos*. Smithsonian Institution Press, Washington DC.
- Kramer-Schadt S, Niedballa J, Pilgrim JD, Schröder B, Lindenborn J, Reinfelder V, Stillfried M, Heckmann I, Scharf AK, Augeri DM, Cheyne SM, Hearn AJ, Ross J, Macdonald DW, Mathai J, Eaton J, Marshall AJ, Semiadi G, Rustam R, Bernard H, Alfred R, Samejima H, Duckworth JW, Breitenmoser-Wuersten C, Belant JL, Hofer H, Wilting A (2013)

- The importance of correcting for sampling bias in MaxEnt species distribution models. *Diversity & Distributions* 19(11): 1366–1379. <https://doi.org/10.1111/ddi.12096>
- Kumar S, Yee WL, Neven LG (2016) Mapping global potential risk of establishment of *Rhagoletis pomonella* (Diptera: Tephritidae) using Maxent and CLIMEX niche models. *Journal of Economic Entomology* 109(5): 2043–2053. <https://doi.org/10.1093/jee/tow166>
- Li R, Zhang J, Zhang ZE (2003) Values of bamboo biodiversity and its protection in China. *Journal of Bamboo Research* 22: 7–17.
- Liese W, Köhl M (2015) *Bamboo: the Plant and its Uses*. Springer, Berlin. <https://doi.org/10.1007/978-3-319-14133-6>
- Lin SY, Cao WQ, Wang YQ, Hu HY (2016) Primary investigation and study of chalcidoid wasps resources in Xinjiang Manas National Wetland Park where *Cicadella viridis* breaks out. *Xinjiang Nongye Kexue* 53: 1850–1857.
- Liu YJ, Mu YJ, Wang CY (2004) Spatial distribution of mark of ova of *Cicadella viridis* in fruit trees and its application. *Inner Mongolia Forestry Science and Technology* 5: 22–24.
- Muscarella R, Galante PJ, Soley-Guardia M, Boria RA, Kass JM, Uriarte M, Anderson RP, McPherson J (2014) ENMeval: An R package for conducting spatially independent evaluations and estimating optimal model complexity for Maxent ecological niche models. *Methods in Ecology and Evolution* 5(11): 1198–1205. <https://doi.org/10.1111/2041-210X.12261>
- Phillips SJ, Dudík M (2008) Modeling of species distributions with Maxent new extensions. *Ecography* 31(2): 161–175. <https://doi.org/10.1111/j.0906-7590.2008.5203.x>
- Phillips SJ, Anderson RP, Schapire RE (2006) Maximum entropy modeling of species geographic distributions. *Ecological Modelling* 190(3–4): 231–259. <https://doi.org/10.1016/j.ecolmodel.2005.03.026>
- Ramasamy M, Das B, Ramesh R (2022) Predicting climate change impacts on potential worldwide distribution of fall armyworm based on CMIP6 projections. *Journal of Pest Science* 95(2): 841–854. <https://doi.org/10.1007/s10340-021-01411-1>
- Sharma P, Dhanwantri K, Mehta SDKM (2014) Bamboo as a building material. *International Journal of Civil Engineering Research* 5: 249–254.
- Shi JY, Zhou DQ, Ma LS, Yao J, Zhang DM (2020) Diversity and important value of bamboos in China. *World Bamboo Rattan* 18: 55–72.
- Shu JP, Ye BH, Wu X, Zhang Y, Wang H, Xu T (2015) Research advances in bamboo pests and their control measures. *World Forestry Research* 8: 20–57.
- Thomson LJ, Macfadyen S, Hoffmann AA (2010) Predicting the effects of climate change on natural enemies of agricultural pests. *Biological Control* 52(3): 296–306. <https://doi.org/10.1016/j.biocontrol.2009.01.022>
- Van der Lugt P, Van den Dobbelen AAJF, Janssen JJA (2006) An environmental, economic and practical assessment of bamboo as a building material for supporting structures. *Construction & Building Materials* 20(9): 648–656. <https://doi.org/10.1016/j.conbuildmat.2005.02.023>
- Wang XY, Huang XL, Jiang LY, Qiao GX (2010) Predicting potential distribution of chestnut phylloxerid (Hemiptera: Phylloxeridae) based on GARP and Maxent ecological niche models. *Journal of Applied Entomology* 134(1): 45–54. <https://doi.org/10.1111/j.1439-0418.2009.01447.x>
- Wei J, Peng L, He Z, Lu Y, Wang F (2020) Potential distribution of two invasive pineapple pests under climate change. *Pest Management Science* 76(5): 1652–1663. <https://doi.org/10.1002/ps.5684>

- Wei J, Gao G, Wei JF (2021) Potential global distribution of *Daktulosphaira vitifoliae* under climate change based on MaxEnt. *Insects* 12(4): 347. <https://doi.org/10.3390/insects12040347>
- Wei XJ, Xu DP, Zhuo ZH (2023) Predicting the impact of climate change on the geographical distribution of leafhopper, *Cicadella viridis* in China through the MaxEnt model. *Insects* 14(7): 586. <https://doi.org/10.3390/insects14070586>
- Xu TS, Wang HJ (2004) *Main Pests of Bamboo in China*. Chinese Forest Publish House, Beijing.
- Xu Y, Shen ZH, Ying LX, Zang RG, Jiang YX (2019) Effects of current climate, paleo-climate, and habitat heterogeneity in determining biogeographical patterns of evergreen broad-leaved woody plants in China. *Journal of Geographical Sciences* 29(7): 1142–1158. <https://doi.org/10.1007/s11442-019-1650-x>
- Xu D, Li X, Jin Y, Zhuo Z, Yang H, Hu J, Wang RL (2020) Influence of climatic factors on the potential distribution of pest *Heortia vitessoides* Moore in China. *Global Ecology and Conservation* 23: e01107. <https://doi.org/10.1016/j.gecco.2020.e01107>
- Yang YM, Wang KL, Pei SJ, Hao JM (2004) Bamboo diversity and traditional uses in Yunnan, China. *Mountain Research and Development* 24(2): 157–165. [https://doi.org/10.1659/0276-4741\(2004\)024\[0157:BDATUI\]2.0.CO;2](https://doi.org/10.1659/0276-4741(2004)024[0157:BDATUI]2.0.CO;2)
- Yang L, Li ZZ, Jin X (2007) *Anaka burmensis* Dworakowska: a new record leafhopper attacking bamboo (Hemiptera: Cicadellidae: Typhlocybinae) from China. *Journal of Mountain Agriculture and Biology* 26: 444–447.
- Yang L, Li ZZ, Chen XS (2011) Research progress on bamboo-feeding leafhoppers. *Hubei Agricultural Sciences* 50: 2386–2388.
- Zhang HF, Wang Y, Wang ZB, Ding WL, Xu KD, Li LL, Wang YY, Li JB, Yang M, Liu X, Huang X (2022) Modelling the current and future potential distribution of the bean bug *Riptortus pedestris* with increasingly serious damage to soybean. *Pest Management Science* 78(10): 4340–4352. <https://doi.org/10.1002/ps.7053>
- Zhang YB, Zhao ZX, Wang YJ, Liu TL (2023) Suitable habitats for *Cicadella viridis* and *Evacanthus interruptus* (Hemiptera: Cicadellidae) with global climate change. *Journal of Entomological Science* 58(2): 215–229. <https://doi.org/10.18474/JES22-36>
- Zhao Q, Lin SY, Zhulidezi AS, Wen W, Hu HY (2022) Occurrence of *Cicadella viridis* and the biology of its egg parasitoids in Xinjiang. *Zhongguo Shengwu Fangzhi Xuebao* 38: 29–41.
- Zhao ZX, Yang L, Long JK, Chang ZM, Chen XS (2024) Predicting suitable areas for *Metcalfa pruinosa* (Hemiptera: Flatidae) under climate change and implications for management. *Journal of Insect Science* 24(3): ieae053. <https://doi.org/10.1093/jisea/ieae053>

Supplementary material 1

Supplementary data

Authors: Zhengxue Zhao, Lin Yang, Xiangsheng Chen

Data type: xlsx

Copyright notice: This dataset is made available under the Open Database License (<http://opendatacommons.org/licenses/odbl/1.0/>). The Open Database License (ODbL) is a license agreement intended to allow users to freely share, modify, and use this Dataset while maintaining this same freedom for others, provided that the original source and author(s) are credited.

Link: <https://doi.org/10.3897/zookeys.1203.118978.suppl1>

A new species of the *Cyrtodactylus chauquangensis* group (Squamata, Gekkonidae) from the borderlands of extreme northern Thailand

L. Lee Grismer^{1,2,3}, Anchalee Aowphol^{4,5}, Jesse L. Grismer¹, Akrachai Aksornneam^{4,5}, Evan S. H. Quah^{3,6,7}, Matthew L. Murdoch¹, Jeren J. Gregory¹, Eddie Nguyen¹, Amanda Kaatz¹, Henrik Bringsøe⁸, Attapol Rujirawan^{4,5}

1 Herpetology Laboratory, Department of Biology, La Sierra University, 4500 Riverwalk Parkway, Riverside, California 92505, USA

2 Department of Herpetology, San Diego Natural History Museum, PO Box 121390, San Diego, California, 92112, USA

3 Institute for Tropical Biology and Conservation, Universiti Malaysia Sabah, Jalan UMS, 88400, Kota Kinabalu, Malaysia

4 Animal Systematics and Ecology Speciality Research Unit, Department of Zoology, Faculty of Science, Kasetsart University, Bangkok 10900, Thailand

5 Biodiversity Center, Kasetsart University, Bangkok 10900, Thailand

6 Lee Kong Chian Natural History Museum, National University of Singapore, 2 Conservatory Drive, 117377, Singapore

7 School of Biological Sciences, Universiti Sains Malaysia, 11800 Minden, Penang, Malaysia

8 Irisvej 8, DK-4600 Køge, Denmark

Corresponding author: Attapol Rujirawan (fsaciapr@ku.ac.th)



Academic editor: Minh Duc Le

Received: 11 March 2024

Accepted: 3 May 2024

Published: 30 May 2024

ZooBank: <https://zoobank.org/C6B34F96-DFE7-475D-A021-73E0B1D61F3D>

Citation: Grismer LL, Aowphol A, Grismer JL, Aksornneam A, Quah ESH, Murdoch ML, Gregory JJ, Nguyen E, Kaatz A, Bringsøe H, Rujirawan A (2024) A new species of the *Cyrtodactylus chauquangensis* group (Squamata, Gekkonidae) from the borderlands of extreme northern Thailand. ZooKeys 1203: 211–238. <https://doi.org/10.3897/zookeys.1203.122758>

Copyright: © L. Lee Grismer et al.

This is an open access article distributed under terms of the Creative Commons Attribution License (Attribution 4.0 International – CC BY 4.0).

Abstract

Phylogenetic and morphological analyses delimit and diagnose, respectively, a new population of a karst-dwelling *Cyrtodactylus* from extreme northern Thailand. The new species, *Cyrtodactylus phamiensis* **sp. nov.**, of the *chauquangensis* group inhabits karst caves and outcroppings and karst vegetation in the vicinity of Pha Mi Village in Chiang Rai Province, Thailand. Within the *chauquangensis* group, *Cyrtodactylus phamiensis* **sp. nov.** is the earliest diverging species of a strongly supported clade composed of the granite-dwelling *C. doisuthep* and the karst-dwelling sister species *Cyrtodactylus* sp. 6 and *C. erythrosp.* The nearly continuous karstic habitat between the type locality of *Cyrtodactylus phamiensis* **sp. nov.** and its close relatives *Cyrtodactylus* sp. 6 and *C. erythrosp.*, extends for approximately 200 km along the border region of Thailand and the eastern limit of the Shan Plateau of Myanmar. Further exploration of this region, especially the entire eastern ~ 95% of the Shan Plateau, will undoubtedly recover new populations whose species status will need evaluation. As in all other countries of Indochina and northern Sundaland, the continual discovery of new karst-dwelling populations of *Cyrtodactylus* shows no signs of tapering off, even in relatively well-collected areas. This only highlights the conservation priority that these unique karstic landscapes still lack on a large scale across all of Asia.

Key words: Bent-toed gecko, genetics, Indochina, integrative taxonomy, karst, morphology

Introduction

The borderlands of northwestern Thailand, western Laos, and south-central China encompass some of the most complex topography of Indochina. Rugged mountain ranges interleaved by deep gorges; wide, arid basins, and major river drainages, merge imperceptibly with those of the eastern uplands of Myanmar's Shan Plateau. Although many species of *Cyrtodactylus* occupy the karstic borderlands girdling the Shan Plateau, none are yet known to occur within its rugged eastern topography. This collecting artifact is most noticeable in the distribution of the *chauquangensis* group (sec. Grismer et al. 2021) where the eastern border of Myanmar encloses a large unoccupied wedge in the western section of this group's overall range (Fig. 1). The majority of the 28 nominal species of this group inhabit a fairly continuous karstic landscape that stretches from northwestern Thailand and south-central China, eastward through northern Laos to northwestern Vietnam west of the Red River, the exception being *C. gulinqingensis* Liu, Li, Hou, Orlov & Ananjeva, 2021 from Yunnan Province of southern China and *C. luci* Tran, Do, Pham, Phan, Ngo, Le, Ziegler & Nguyen, 2024 from Lao Cai Province in northern Vietnam which lie on the eastern edge of the Red River (Liu et al. 2021, 2023; Tran et al. 2024). Except for *C. taybacensis* Pham, Le, Ngo, Ziegler & Nguyen, 2019 and *C. otai* Nguyen, Le, Pham, Ngo, Hoang, Pham & Ziegler, 2015 of Vietnam (Nguyen et al. 2015a, 2017; Pham et al. 2019), most species in the *chauquangensis* group are known only from their type localities, underscoring the specialized, restrictive life history of karst-dwelling species coupled to the generally fragmented nature of karstic landscapes.

While conducting fieldwork during March of 2023 in the district of Mae Sai along the Thai-Myanmar border in extreme northern Chiang Rai Province, Thailand, we discovered a new population of karst-dwelling *Cyrtodactylus* near Pha Mi Village at the Wat Pa (= temple) Pha Mi as well as from adjacent areas within the same karstic range. Molecular phylogenetic analyses indicated this population was deeply embedded within the *chauquangensis* group and composed the sister species to a lineage containing three other species from northern Thailand. Based on this, and statistically significant diagnostic results from univariate and multivariate analyses, we hypothesize this new population constitutes a new species and as such, describe it below.

Materials and methods

Sampling

The gecko specimens were collected during a field survey at Pha Mi Village, Wiang Phang Kham Subdistrict, Mae Sai District, Chiang Rai Province, Thailand from 25–26 March 2023 (Fig. 1). Geographical coordinates with elevation of each specimen were collected using a Garmin GPSMAP 64st. After collection, the specimens were photographed in life prior to preservation. All specimens were then humanely euthanized using tricaine methanesulfonate (MS-222) solution (Simmons 2015). Liver tissue was immediately dissected from the euthanized specimens, preserved in 95% ethyl alcohol, and stored at -20 °C for genetic analysis. Voucher specimens were then initially fixed in 10% formalin



Figure 1. Distribution of nominal species and unnamed populations of the *Cyrtodactylus chauquangensis* group. The star denotes the type locality of *Cyrtodactylus phamiensis* sp. nov.

and later transferred to 70% ethyl alcohol for long-term storage. The type series and tissue samples were deposited in the herpetological collection of the Zoological Museum, Kasetsart University, Bangkok, Thailand (**ZMKU**).

Molecular data

Genomic DNA was isolated from liver or skeletal muscle samples stored in 95% ethanol using the Qiagen DNeasy™ tissue kit (Valencia, CA, USA). NADH dehydrogenase subunit 2 gene (ND2) and downstream tRNA-Trp, tRNA-Ala, and tRNA-Asn were chosen for phylogenetic analyses with 10 specimens newly sequenced for this work. ND2 was amplified using a double-stranded Polymerase Chain Reaction (PCR) under the following conditions: 2.5 µl genomic DNA (~10–30 ng), 2.5 µl light strand primer (5 µM), 2.5 µl heavy strand primer (5 µM), 1.0 µl dinucleotide pairs (1.0 µM), 2.0 µl 5× buffer (2.0 µM), 1.0 MgCl 10× buffer (1.0 µM), 0.18 µl Taq polymerase (5u/µl), and 9.8s µl ultrapure H₂O at n + 1. PCR reactions were executed on a BIO RAD T-100 Thermal Cycler under the following conditions: initial denaturation at 94 °C for 4 min, followed by a second denaturation at 94 °C for 30 s, annealing at 52 °C for 30 s, followed by a cycle extension at 68 °C for 1:30 min repeated for 35 cycles, followed by a final extension cycle run at 68 °C for 7 min. All PCR products were visualized

on a 1.0% agarose electrophoresis gel. Successful targeted PCR products were outsourced to GENEWIZ® for PCR purification, cycle sequencing, and sequencing. Primers used for amplification and sequencing are presented in Murdoch et al. (2019: table 2). Sequences were analyzed from both the 3' and the 5' ends separately to confirm congruence between the reads. Both the forward and the reverse sequences were uploaded and edited in Geneious™ v. 5.5.6 (Drummond et al. 2011) and were edited therein. The protein-coding region of the ND2 sequence was aligned by eye. Mesquite v. 3.04 (Maddison and Maddison 2015) was used to calculate the correct amino acid reading frame and to confirm the lack of premature stop codons. The GenBank accession numbers for all specimens are in Suppl. material 1.

Phylogenetic analyses

Three different partition schemes, codon, gene, and unpartitioned, were run for three model based phylogenetic analyses – Maximum Likelihood (ML), Bayesian Inference, (BI) and Bayesian Evolutionary Analysis Sampling Trees (BEAST) – in order to search for significant support for the weak nodes in recent analyses (Liu and Rao 2021a, 2021b, 2022; Chomdej et al. 2022) using NADH dehydrogenase subunit 2 (ND2) gene and its flanking tRNAs. *Cyrtodactylus dammathetensis* Grismer, Wood, Thura, Zin, Quah, Murdoch, Grismer, Lin, Kyaw & Lwin, 2017 and *C. sinyineensis* Grismer, Wood, Thura, Zin, Quah, Murdoch, Grismer, Lin, Kyaw & Lwin, 2017 (in Grismer et al. 2018a) were used as outgroups to root the ML and BI trees based on Grismer et al. (2021). Maximum Likelihood (ML) analyses were implemented using the IQ-TREE webserver (Nguyen et al. 2015b; Trifinopoulos et al. 2016). One-thousand bootstrap pseudoreplicates via the ultrafast bootstrap (UFB; Hoang et al. 2018) approximation algorithm were employed, and nodes having UFB values of 95 and above were considered strongly supported (Minh et al. 2013). We considered nodes with values of 90–94 as well-supported. After removing outgroup taxa, uncorrected pairwise sequence divergences were calculated in MEGA 11 (Tamura et al. 2021) using the pairwise deletion option to remove gaps and missing data from the alignment prior to calculation.

Bayesian inference (BI) analyses was implemented in MrBayes 3.2.3 on XSEDE (Ronquist et al. 2012) using CIPRES (Cyberinfrastructure for Phylogenetic Research; Miller et al. 2010). Two simultaneous runs were performed with four chains, three hot and one cold. The simulations ran for 50,000,000 generations, were sampled every 5,000 generations using a Markov Chain Monte Carlo (MCMC), and the first 10% of each run were discarded as burn-in. Stationarity and parameter files from each run were checked in Tracer v. 1.7 (Rambaut et al. 2018) to ensure effective sample sizes (ESS) were above 200 for all parameters. Nodes with Bayesian posterior probabilities (BPP) of 0.95 and above were considered strongly supported (Huelsenbeck et al. 2001; Wilcox et al. 2002). We considered nodes with values of 0.90–0.94 as well-supported.

Input files constructed in BEAUti (Bayesian Evolutionary Analysis Utility) v. 2.4.6 were run in BEAST (Bayesian Evolutionary Analysis Sampling Trees) v. 2.4.6 (Drummond et al. 2012) on CIPRES (Cyberinfrastructure for Phylogenetic Research; Miller et al. 2010) in order to generate BEAST phylogenies. An optimized relaxed clock with unlinked site models and linked tree and clock models

were employed for each run. bModelTest (Bouckaert and Drummond 2017), implemented in BEAST, was used to numerically integrate over the uncertainty of the three input files while simultaneously estimating phylogeny using a Markov Chain Monte Carlo (MCMC). MCMC chains were run using a Yule prior for 50 million generations and logged every 5,000 generations. The BEAST log files were visualized in Tracer v. 1.7 (Rambaut et al. 2018) to ensure effective sample sizes (ESS) were well above 200 for all parameters. Maximum clade credibility trees using mean heights at the nodes were generated using TreeAnnotator v. 1.8.0 (Rambaut and Drummond 2013) with a burn-in of 10%. Nodes with Bayesian posterior probabilities (BPP) of 0.95 and above were considered strongly supported (Huelsenbeck et al. 2001; Wilcox et al. 2002). We considered nodes with values of 0.90–0.94 as well-supported.

Species delimitation

The general lineage concept (GLC: de Queiroz 2007) adopted herein proposes that a species constitutes a population of organisms evolving independently from other such populations owing to a lack of gene flow. By “independently,” it is meant that new mutations arising in one species cannot spread readily into another species (Barraclough et al. 2003; de Queiroz 2007). Under the GLC implemented herein, molecular phylogenies were used to recover monophyletic mitochondrial lineages of individual(s) (i.e., populations) in order to develop initial species-level hypotheses, the grouping stage of Hillis (2019). Discrete color pattern data and morphological data were used to search for unique characters and patterns and compare their consistency with the previous species-level hypotheses designations, the construction of boundaries representing the hypothesis-testing step of Hillis (2019), thus providing lineage diagnoses independent of the molecular analyses. In this way, delimiting (phylogeny) and diagnosing (taxonomy) species are not conflated (Frost and Hillis 1990; Frost and Kluge 1994; Hillis 2019).

Morphological data

Morphological data included morphometric, meristic, and categorical morphological and color pattern characters. Measurements were taken on the left side of the body to the nearest 0.1 mm using Mitutoyo dial calipers under a Nikon SMZ 1500 dissecting microscope and follow Grismer and Grismer (2017) and Grismer et al. (2018a). Measurements taken were: snout-vent length (**SVL**), taken from the tip of the snout to the vent; tail length (**TL**), taken from the vent to the tip of the tail; tail width (**TW**), taken at the base of the tail immediately posterior to the postcloacal swelling; forearm length (**FL**), taken on the ventral surface from the posterior margin of the elbow while flexed 90° to the inflection of the flexed wrist; tibia length (**TBL**), taken on the ventral surface from the posterior surface of the knee while flexed 90° to the base of the heel; axilla to groin length (**AG**), taken from the posterior margin of the forelimb at its insertion point on the body to the anterior margin of the hind limb at its insertion point on the body; head length (**HL**), the distance from the posterior margin of the retroarticular process of the lower jaw to the tip of the snout; head width (**HW**), measured at the angle of the jaws; head depth (**HD**), the maximum height of head measured from the occiput to base of the lower jaw; eye diameter (**ED**),

the greatest horizontal diameter of the eye-ball; eye to ear distance (**EE**), measured from the anterior edge of the ear opening to the posterior edge of the bony orbit; snout length (**ES**), measured from anteriormost margin of the bony orbit to the tip of snout; eye to nostril distance (**EN**), measured from the anterior margin of the bony orbit to the posterior margin of the external naris; interorbital distance (**IO**), measured between the anterior-most edges of the bony orbits; ear length (**EL**), measured as the greatest vertical distance of the ear opening; and internarial distance (**IN**), measured between the nares across the rostrum.

Meristic characters evaluated were the number of supralabial scales (**SL**) counted from the largest scale immediately below the eyeball to the rostral scale; infralabial scales (**IL**) counted from the mental to the termination of enlarged scales just after the upturn of the mouth; the number of paravertebral tubercles (**PVT**) between limb insertions counted in a straight line immediately left or right of the vertebral column; the number of longitudinal rows of body tubercles (**LRT**) counted transversely across the center of the dorsum from one ventrolateral fold to the other; the number of longitudinal rows of ventral scales (**VS**) counted transversely across the center of the abdomen from one ventrolateral fold to the other; the number of expanded subdigital lamellae on the fourth toe (**E4TL**) counted from the base of the first phalanx to the large scale on the digital inflection; the number of unexpanded subdigital lamellae on the fourth toe (**U4TL**) counted from the digital inflection to the end of the digit and including the claw sheath; the total number of expanded subdigital lamellae on the fourth toe (**T4TL** = **E4TL**+**U4TL**) counted from the base of the first phalanx where it contacts the body of the foot to the claw and including the claw sheath (see Murdoch et al. 2019: fig. 2); and the total number of enlarged femoral scales (**FS**) from each thigh combined as a single metric. In some species, only the distalmost FS are greatly enlarged, and the proximal scales are smaller whereas in others, the enlarged scales are continuous with the enlarged precloacal scales. The separation of the two scales rows was determined to be at a point even with the lateral body margin (see Murdoch et al. 2019: fig. 3). The number of enlarged precloacal scales (**PS**); the number of precloacal pores (**PP**) in males; the total number of femoral pores in males (**FP**); the number of rows of enlarged post-precloacal scales (**PPS**) on the midline between the enlarged precloacal scales and the granular scales anterior to the vent; the number of postcloacal tubercles (**PCT**); the number of dark body bands (**BB**) between the nuchal loop (the dark band running from eye to eye across the nape) and the hind limb insertions; and numbers of light-colored (**LCB**) and dark-colored (**DCB**) caudal bands.

Categorical morphological and color pattern characters examined were tubercles extending beyond base of tail or not; femoral pores restricted to distal scales or not; body tubercles low, weakly keeled or raised, moderately to strongly keeled; enlarged femoral and precloacal scales continuous or not; pore-bearing femoral and precloacal scales continuous or not; enlarged proximal femoral scales ~ 1/2 size of distal femorals or not; medial subcaudals two or three times wider than long or not; medial subcaudals extend upward onto lateral surface of tail or not; nuchal loop divided medially or continuous; color of head in hatchlings yellow or not (**HeadCol**); two posterior projections from nuchal loop present or not; nuchal loop with anterior azygous notch or not; triangular marking anterior to nuchal loop; posterior border of nuchal loop projected or

smooth; band on nape present or absent; dorsal banding with paravertebral elements or not; dorsal body bands wider than interspaces or not (**IntSpac**); dorsal body bands with lightened centers or not; dorsal bands edged with white tubercles or not; dorsal tubercles brightly colored or dull (**BodTub**); dorsal bands straight or jagged; dark markings in dorsal interspaces or not; ventrolateral fold whitish or not; top of head diffusely mottled, blotched, or patternless light-colored reticulum on top of head or not (**HeadRetic**); anterodorsal margin of thighs darkly pigmented or not; anterodorsal margin of brachia darkly pigmented or not; white caudal bands with dark markings or not; white caudal bands encircle tail or not; dark caudal bands wider than light caudal bands or not; and mature regenerated tail spotted. HeadCol, IntSpac, BodTub, and HeadRetic were used in the multiple factor analysis (MFA) see below because they could be consistently coded across other taxa.

Statistical analyses

All statistical analyses were conducted using R Core Team (2021). Low sample sizes and incomplete character data throughout species of the *chauquangensis* group, precluded meaningful group-wide univariate analyses. As the next best alternative, we employed a MFA using the R package *FactorMineR* (Husson et al. 2017) and visualized it using the *Factoextra* package (Kassambara and Mundt 2017) for a clade of species from northwestern Thailand to which the Pha Mi population belongs (see below). In so doing, we were able to statistically defend the morphospacial placement of the Pha Mi population as significant (see below). We believe this is superior to the majority of current species diagnoses that provide no statistical analyses and relay only numeric ranges with little to no regard to sample size. The MFA was conducted on a concatenated data set comprised of 12 meristic (SL, IL, PVT, LRT, VS, E4TL, U4TL, T4TL, PS, PPS, FS, and BB), 12 morphometric (SVL, FL, TBL, AG, HL, HW, HD, ED, EE, ES, IO, and IN), and four categorical (HeadCol, IntSpac, BodTub, and HeadRetic) characters. To remove potential effects of allometry in the morphometric characters, size was normalized using the following equation: $X_{adj} = \log(X) - \beta[\log(SVL) - \log(SVL_{mean})]$, where X_{adj} = adjusted value; X = measured value; β = unstandardized regression coefficient for each population; and SVL_{mean} = overall average SVL of all populations (Thorpe 1975, 1983; Turan 1999; Leonart et al. 2000). The morphometrics of each species were normalized separately and then concatenated so as not to conflate intra- with interspecific variation (Reist 1986). All data were scaled to their standard deviation to insure they were analyzed on the basis of correlation and not covariance. MFA is a global, unsupervised, multivariate analysis that incorporates qualitative and quantitative data (Pagès 2015) simultaneously, making it possible to analyze different data types in a nearly total morphological evidence environment. In an MFA, each individual is described by a different set of variables (i.e., characters) which are structured into different data groups in a global data frame, in this case, quantitative data (i.e., meristics and normalized morphometrics) and categorical data (i.e. color pattern characters). In the first phase of the analysis, separate multivariate analyses are carried out for each set of variables: principal component analyses (PCA) for each quantitative data set and a multiple correspondence analysis (MCA) for the categorical data. The data sets are then normalized separately by dividing all their elements by the

square root of their first eigenvalue. For the second phase of the analysis, these normalized data sets are concatenated into a single matrix for a final global PCA of the normalized data. Standardizing the data in this manner prevents one data type from overleveraging another. In other words, the normalization of the data in the first phase prevents data types with the greatest number of characters or the greatest amount of variation from outweighing other data types in the second phase. This way, the contributions of each data type to the overall variation in the data set is scaled to define the morphospacial distance between individuals as well as calculating each data type's contribution to the overall variation in the analysis (Pagès 2015; Kassambara and Mundt 2017).

A non-parametric permutation multivariate analysis of variance (PERMANOVA) from the *vegan* package 2.5–3 in R (Oksanen et al. 2020) was used to determine if the centroid locations and group clusters of each species/population were statistically different from one another (Skalski et al. 2018) based on the MFA load scores of dimensions 1–5. Using loading scores as opposed to raw data, allows for the incorporation of the categorical characters which cannot be run in a PERMANOVA untransformed. The analysis calculates a Euclidean (dis) similarity matrix using 50,000 permutations. A pairwise *post hoc* test calculates the differences between the populations, generating a Bonferroni-adjusted *p* value and a pseudo-*F* ratio (*F* statistic). A $p < 0.05$ is considered significant and larger *F* statistics indicate more pronounced group separation. A rejection of the null hypothesis (i.e., centroid positions and the spread of the data points [i.e., clusters] are no different from random) signifies a statistically significant difference between species/populations.

T-tests were run for each character between the Pha Mi population ($n = 15$) and *Cyrtodactylus doisuthep* Kunya, Panmongkol, Pauwels, Sumontha, Mee-wasana, Bunkhwamdi & Dangsri, 2014 ($n = 3$) to ascertain which means of the numeric characters differed significantly ($p < 0.05$). *F*-tests were run *a priori* to test for homogeneity of variances. If the variances were homogeneous ($p \geq 0.05$), a Student two sample *t*-test was employed. If the variances were not homogeneous ($p < 0.05$), a Welch two sample *t*-test was employed. Both tests employed a Bonferroni correction factor to calculate an adjusted *p*-value. *Cyrtodactylus doisuthep* was chosen for comparison because it was the only species in clade 2 (see below) that had more than two samples. *Cyrtodactylus erythrosp* Bauer, Kunya, Sumontha, Niyomwan, Panitvong, Pauwels, Chanhom & Kunya, 2009 had an $n = 1$ and no data exist for *Cyrtodactylus* sp. 6 (Chomdej et al. 2021). For comparisons with all other species of the *chauquangensis* group, we put together the most complete dataset possible following Pham et al. (2019) and supplemented it with the original descriptions of recently described species (Schneider et al. 2020; Liu and Rao 2021b, 2022; Liu et al. 2021, 2023; Zhang et al. 2021; Chomdej et al. 2022).

Results

No competing topological differences were recovered among nine phylogenies and the codon-partitioned data performed best among the three models (i.e., ML, BI, and BEAST) based on likelihood scores (Table 1). Nodal support among the models differed across the trees and codon-partitioned BI data recovered two polytomies (Fig. 2). Substitution models for the codon-partitioned ML tree

Table 1. Log-likelihood and averaged marginal log-likelihood scores of the nine phylogenetic analyses. Shaded cells denote the likelihood highest scores. Numbers of supported ingroup nodes out of 25 total nodes for the codon-partitioned analyses follow the sequence of strong, moderate, and no support.

	Log-likelihood	Average marginal log-likelihood	Number of supported nodes
Maximum likelihood			
non-partition (1 partition)	-12918.411		
partitioned by gene (2 partitions)	-12869.809		
partitioned by codon & RNA (4 partitions)	-12509.929		15, 6, 5
Bayesian inference			
non-partition (1 partition)		-12941.210	
partitioned by gene (2 partitions)		-12888.095	
partitioned by codon & RNA (4 partitions)		-12524.010	9, 8, 8
BEAST			
non-partition (1 partition)		-12529.162	
partitioned by gene (2 partitions)		-12655.700	
partitioned by codon & RNA (4 partitions)		-12557.950	20, 2, 4

based on the Bayesian Information Criterion (BIC) in ModelFinder (Kalyaanamoorthy et al. 2017) selected HKY+F+I+G4 codon position 1, TPM2+F+G4 for position 2, TPM3+F+G4 for position 3, and TIME+G4 the non-coding RNAs. bModel test was used to co-estimate the site models and the phylogenies simultaneously for the BI and BEAST analyses.

Of the three best performing codon-partitioned phylogenies, the BEAST analysis performed best in that it recovered the greatest number of strongly supported ingroup nodes (20) and the fewest number of moderately and unsupported nodes (Table 1, Fig. 2). Two nodes had no support from any of the nine analyses and one other node was very close to being moderately supported in the ML and BEAST analyses (UFB = 89, BEAST BPP = 0.89). The monophyly of the *chauquangensis* group was strongly supported in all analyses. The ML and BEAST analyses recovered three major clades within the *chauquangensis* group, only one of which (clade 1) was strongly supported in all analyses (100, 1.00, 1.00; ML UFB, BI BPP, and BEAST BPP, respectively and throughout). The earliest diverging clade 1, contains *Cyrtodactylus bichnganae* Ngo & Grismer, 2010 and *C. taybacensis* from the Hoang Lien Son Mountain Range in northwestern Vietnam. Clade 2, strongly supported only in the BEAST analysis (89, 0.60, 0.97), contains *C. doisuthep*, *C. erythrosp*, *Cyrtodactylus* sp. 6, and the Pha Mi population – the latter recovered as the sister taxon to the remaining species. The sister relationship between clades 2 and 3 was strongly supported only in the ML and BEAST analyses (91, 0.70, 0.97). The monophyly of clade 3, variably supported (94, 0.50, 1.00), contains the remaining 21 species that collectively range from the borderlands of western Yunnan, eastward across northern Thailand and Laos and into northwestern Vietnam. Clade 3 is a polytomy in that no analysis offered any support for the basal nodes. Varying support from all three analyses recovered at least four major lineages within clade 3. Although the same equivocation was found in the most recent analyses of this group (Liu and Rao 2021a, 2021b, 2022; Liu et al. 2023; Chomdej et al. 2022; Tran et al. 2024),

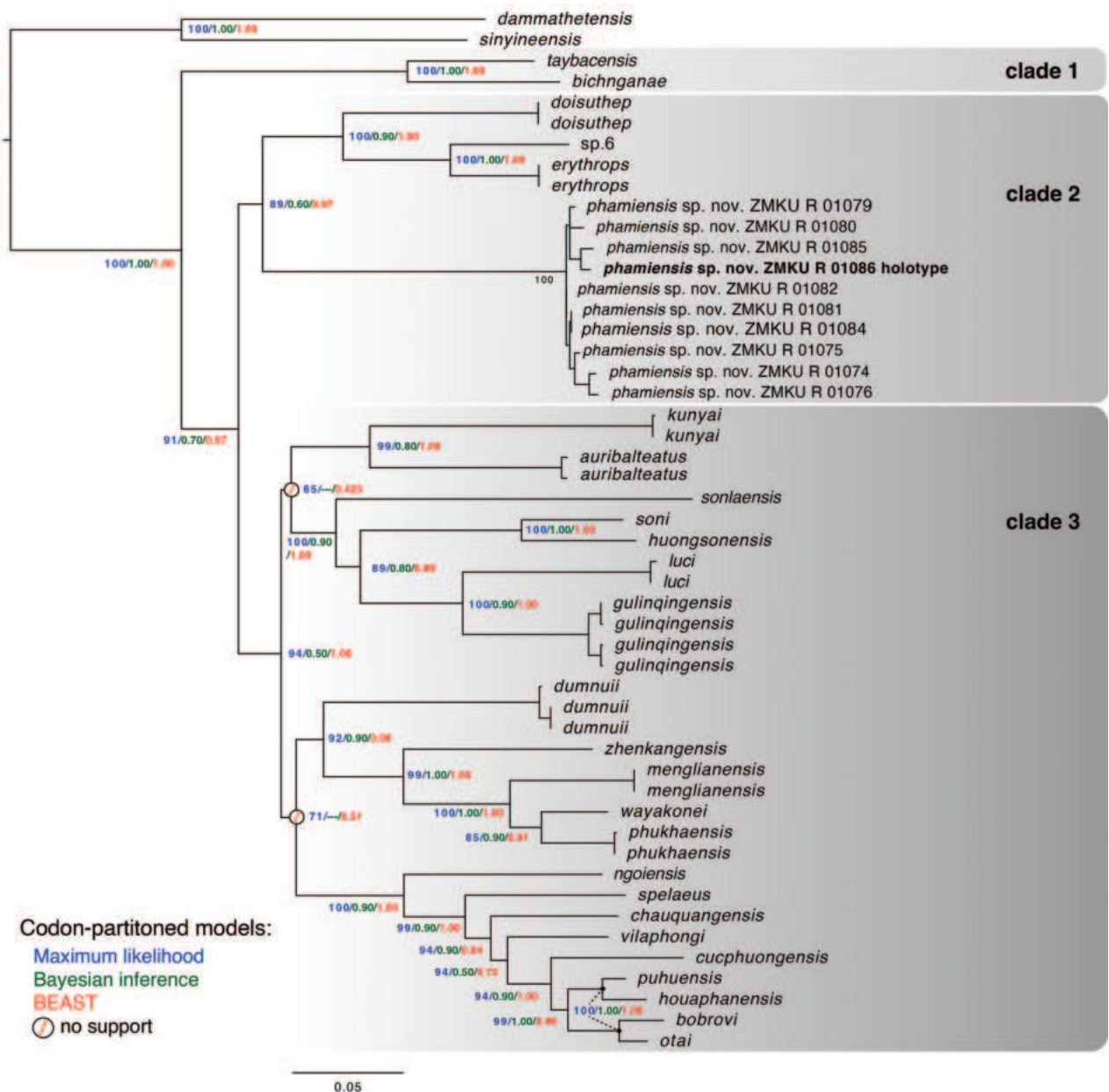


Figure 2. Maximum Likelihood topology of the *Cyrtodactylus chauquangensis* group with nodal support from the three best performing ML, BI, and BEAST analyses.

it went unnoted. The mean uncorrected pairwise sequence divergence between the Pha Mi population and the species of clade 2 ranged from 13.48–14.49%. Genetic distances within the Pha Mi population ranged from 0.00–1.81% and distances between the Pha Mi population and the remaining species of the *chauquangensis* group was 13.72–17.34% (Suppl. material 2).

The MFA analysis recovered all three nominal species of the clade 2 to be widely separated from one another along dimension 1 which accounted for 36.5% of the variation in the data set (Fig. 3A, D). Both *Cyrtodactylus erythropros* and *C. doisuthep* were separated from one another along dimension 2, accounting for an additional 14.2% of the variation, but were not separated from the Pha Mi population (Fig. 3A). Categorical and morphometric characters contributed most of the variation along dimension 1 and meristic data contributed to the

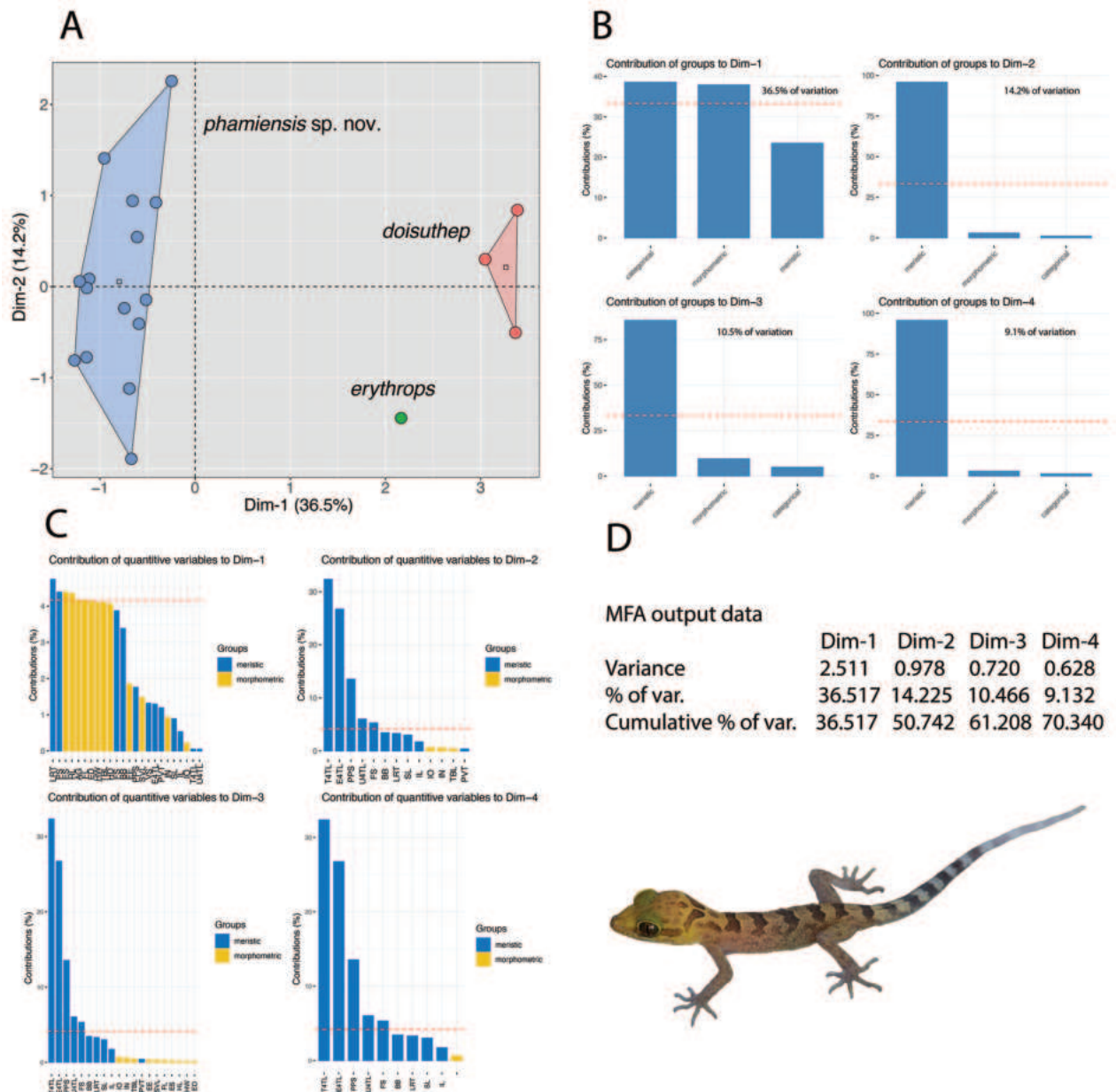


Figure 3. **A** MFA of the species of clade 2 (Fig. 2) **B** Percent contributions of each data type to the inertia of dimensions 1–4 of the MFA. Percentage values on the bar graphs are the amounts of inertia for their respective dimensions **C** Percent contribution of the quantitative variables to the dimensions 1–4 of the MFA. Dotted red line is the mean percentage if all values were equal **D** MFA output data showing the variance, percent variance, and the cumulative percent of 70.3% of the total variance for dimensions 1–4.

majority of the variation along dimension 2 (Fig. 3B). Meristic characters LRT, PS followed by morphometric characters ES, HL, AG, FL, ED, HW, TBL and HD contributed to the majority of the variation along dimension 1 (Fig. 3C). Meristic characters T4TL, and E4TL contributed to the majority of the variation along dimension 2. The PERMANOVA analysis indicated that the Pha Mi population differed significantly in morphospace from *C. doisuthep* but not from *C. erythrosp* (Table 2). The latter case owes to the sample size of *C. erythrosp* ($n = 1$) which precluded its statistically significant differentiation from *C. doisuthep* as well, even though it was widely separated from both species.

Table 2. Summary statistics from the PERMANOVA analysis from the loadings of the MFA comparing *Cyrtodactylus phamiensis* sp. nov. to *C. erythropros* and *C. doisuthep*. Bold fonts denote significant differences.

Species pairs	F.Model	R2	p.value	p.adjusted
<i>C. phamiensis</i> sp. nov. – <i>C. erythropros</i>	1.46607001	0.09479267	0.24835503	0.7450651
<i>C. phamiensis</i> sp. nov.– <i>C. doisuthep</i>	2.97455237	0.15676535	0.01563969	0.04691906
<i>C. erythropros</i> – <i>C. doisuthep</i>	4.56603793	0.69540231	0.25	0.75

Table 3. Means, *t*-, and *p*-values of significantly different meristic and scaled morphometric characters of *Cyrtodactylus doisuthep* and *Cyrtodactylus phamiensis* sp. nov. * = a near significant difference. Character abbreviations are in the Materials and methods.

Character	Mean		t-value	p-value
	<i>C. doisuthep</i> (n = 3)	<i>C. phamiensis</i> sp. nov. (n = 15)		
Student two sample t-test				
SL	11.16667	9.60000	2.2872	0.03614
FS	28.66667	24.20000	3.218	0.005371
SVL*	1.894832	1.703071	2.0945	0.05249
FL	1.102850	0.940363	15.592	4.271e-11
AG	1.534111	1.358982	13.811	2.619e-10
HW	0.1168415	0.1504906	16.842	1.329e-11
ED	0.7892948	0.5728535	15.684	3.906e-11
ES	0.9568607	0.7939798	33.441	3.097e-16
Welch two sample t-test				
PS	6.000000	8.266667	-7.1792	4.715e-06
TBL	1.186221	1.022731	32.605	1.107e-14
HL	1.376238	1.207984	36.999	2.2e-16
HD	0.9829511	0.8017859	22.968	2.179e-13
EE	0.7980227	0.6031066	6.6384	1.06e-05

The results of the *t*-tests (Table 3) mirrored those of the PERMANOVA in that the Pha Mi population differed significantly from *Cyrtodactylus doisuthep* in having fewer supralabials (SL) and enlarged femorals (FS); more preclacals (PS); a shorter axilla-groin length (AG); shorter forelimbs (FL) and tibias (TBL); a shorter, wider, and flatter head (HL, HW, HD, respectively) with a shorter snout (ES) and postorbital region (EE), a smaller eyeball (ED); and a nearly significantly different smaller snout-vent length (SVL). Non-statistical comparisons of a range of other selected characters illustrates how the Pha Mi population may differ from other species in the *chauquangensis* group (Table 4). Raw data would bear these differences out more clearly but were unavailable to us.

Taxonomy

Given that the Pha Mi population is not phylogenetically embedded within any other species of the *chauquangensis* group nor is it sister to any other species (Fig. 2); bears a large, uncorrected pairwise sequence divergence of

Table 4. Comparisons of *Cyrtodactylus phamiensis* sp. nov. to all other species of the *chauquangensis* group except for *Cyrtodactylus* sp. 6. Shaded cells denote potential diagnostic differences. / = data unavailable. Abbreviations are in the Materials and methods.

Species	Max SVL	LRT	VS	FS	FP (in male)	PP (in male)	PS	T4TL	Subcaudals
<i>Cyrtodactylus phamiensis</i> sp. nov.	74.4	19–25	29–37	19–28	9–14	4–6	6–11	19–22	enlarged
<i>C. auribalteatus</i>	98.1	22–24	38–40	10–14	8–10	6	6	18–21	enlarged
<i>C. bichnganae</i>	99.9	16–18	30 or 31	23–26	18	10	/	16–20	enlarged
<i>C. bobrovi</i>	96.4	12–14	40–45	absent	absent	5	5	21 or 22	enlarged
<i>C. chauquangensis</i>	99.3	/	36–38	absent	absent	6	7	19–23	enlarged
<i>C. caixitaoi</i>	89.7	14–15	20–21	22–24	absent	6–8	6–8	22–24	enlarged
<i>C. cucphuongensis</i>	96.0	10	42	28	absent	absent	9	24	enlarged
<i>C. doisuthep</i>	90.5	19 or 20	29–35	28 or 29	absent	6	6	20	enlarged
<i>C. dumnuui</i>	84.2	18–22	40	12 or 13	12–13	5 or 6	7	19	enlarged
<i>C. erythrospis</i>	78.4	18–20	28	28	19	9	9	20	/
<i>C. gulinqingensis</i>	83.9	14–16	28–32	27–29	27–29	7–9	9	19–23	enlarged
<i>C. hekouensis</i>	92.3	10–13	68–72	/	35 or 37 (FP+PP)	/	/	20–23	/
<i>C. houaphanensis</i>	75.8	20	35	absent	absent	6	6	19–23	enlarged
<i>C. huongsonensis</i>	89.8	14–16	41–48	14–18	14–20	6	8	20–23	enlarged
<i>C. kunyai</i>	87.9	19	34	36	11	3	8	21	enlarged
<i>C. luci</i>	89.5	17–19	32–34	25–32	19–24	9–10	9–10	21–23	enlarged
<i>C. martini</i>	96.2	16–19	39–43	30–35	absent	4	/	22–24	not enlarged
<i>C. menglianensis</i>	78.1	18–21	26–29	absent	absent	7	7	21–23	enlarged
<i>C. ngoiensis</i>	95.3	15–21	38–43	14–19	14	7	7	19 or 20	enlarged
<i>C. otai</i>	90.6	11–14	38–43	absent	absent	7 or 8	7 or 8	19–22	not enlarged
<i>C. phukhaensis</i>	82.8	23–28	40–47	absent	absent	7	11	24–28	enlarged
<i>C. puhuensis</i>	79.2	/	36	29	absent	5	8	23	enlarged
<i>C. soni</i>	103.0	10–13	41–45	16–22	12–16	6 or 7	6–8	18–22	enlarged
<i>C. sonlaensis</i>	83.2	13–15	34–42	30–34	29	8	8	18–22	enlarged
<i>C. spelaeus</i>	91.0	10	36–39	/	absent	8 or 9	8 or 9	22–24	enlarged
<i>C. taybacensis</i>	97.5	13–16	30–38	22–26	absent	11–13	11–15	16–20	enlarged
<i>C. vilaphongi</i>	86.1	15 or 16	34–36	absent	/	/	5	18–20	not enlarged
<i>C. wayakonei</i>	86.8	17–19	31–35	absent	absent	6–8	6–8	19–20	enlarged
<i>C. zhenkangensis</i>	87.4	21–24	32–34	25–29	10	8	9	21–23	enlarged

13.5–14.5% from its closest relatives in clade 2, is morphospatially isolated from all other species in clade 2 along the ordination of dimensions 1 and 2 (Fig. 3) and occupies a significantly unique position with respect to *Cyrtodactylus doisuthep* (Table 2); has significantly different mean values from those of *C. doisuthep* in three meristic and 10 adjusted morphometric characters (Table 3); differs from *C. doisuthep* and *C. erythrospis* in lacking a light-colored reticulum on the top of the head; having hatchlings with yellow as opposed to tan colored heads (Fig. 4B); and a range of other potentially different character states from species in clades 1 and 3 (Table 4), we consider the most parsimonious hypothesis based these independent data sets to be that the Pha Mi population is a distinct species.

***Cyrtodactylus phamiensis* sp. nov.**

<https://zoobank.org/DDADBD8A-5234-4183-89A7-C5A3C015456A>

Figs 4–8

Type material. Holotype. Adult male (ZMKU R 01086) collected from Pha Mi Village, Wiang Phang Kham Subdistrict, Mae Sai District, Chiang Rai Province, Thailand (20.40134°N, 99.85369°E; elevation 517 m a.s.l.) on 26 March 2023 by A. Aowphol, A. Rujirawan, A. Aksornneam, L.L. Grismer, J.L. Grismer, E.S.H. Quah, and M.L. Murdoch.

Paratypes. Two adult males (ZMKU R 01085, ZMKU R 01087) and one adult female (ZMKU R 01084) bear the same collection data as the holotype. Four adult females (ZMKU R 01073–01075, ZMKU R 01078) and one adult male (ZMKU R 01081) bear the same collection data as the holotype except collected on 25 March 2023.

Referred specimens. Six hatchlings. ZMKU R 01076–01077, ZMKU R 01079–01080 bear the same collection data as the holotype except were collected on 25 March 2023. ZMKU R 01082–01083 bear the same collection data as the holotype except collected from 20.39800°N, 99.85466°E; elevation 505 m a.s.l., on 25 March 2023.

Diagnosis. *Cyrtodactylus phamiensis* sp. nov. can be separated from all other species of the *chauquangensis* group by the combination of having a maximum SVL = 74.4 mm (female); 8–12 supralabials; 9–11 infralabials; 30–43 paravertebral tubercles; 19–25 rows of longitudinally arranged tubercles; 29–37 longitudinal rows of ventrals; 6–9 expanded subdigital lamellae on the fourth toe; 12–14 unmodified subdigital lamellae on the fourth toe; 19–22 total subdigital lamellae on the fourth toe; 19–28 total number of enlarged femoral scales; 9–14 total number of femoral pores in males ($n = 4$); 6–11 enlarged precloacals; 4–6 precloacal pores in males ($n = 4$); two or three rows of large post-precloacal scales; enlarged femorals and enlarged precloacals continuous; proximal femorals usually smaller than distal femorals; femoral pores restricted to distal scales; body tubercles weakly keeled; small tubercles on forelimbs; tubercles extend beyond base of tail; medial subcaudals 2–3 times wider than long but not extending onto lateral surface of tail; nuchal loop often divided medially, bearing two posteriorly directed projections, no anterior azygous notch, projecting posterior margin; usually no triangular marking anterior to nuchal loop; dark-colored band on nape variably present; dark-colored dorsal bands lack paravertebral elements, have variably lightened centers, are edged with white tubercles, usually jagged in shape, and the same width or wider than interspaces; dark-colored markings in dorsal interspaces; no whitish ventrolateral fold; top of head in adults diffusely mottled, blotched; no light-colored reticulum on top of head; 4–6 dark-colored transverse body bands; 10–13 light-colored caudal bands on an original tail bearing dark-colored markings and not encircling tail ($n = 7$); 9–12 dark-colored caudal bands on an original tail and wider than light-colored caudal bands ($n = 7$); and mature regenerated tail mottled ($n = 3$) (Table 4).

Description of holotype. (Figs 4A, 5, Suppl. material 3) Adult male SVL 68.5 mm; head moderate in length (HL/SVL 0.28), width (HW/HL 0.72), flattened (HD/HL 0.40), distinct from neck, triangular in dorsal profile; lores weakly concave anteriorly, weakly inflated posteriorly; prefrontal region concave; canthus rostralis rounded; snout elongate (ES/HL 0.40), flat, rounded in dorsal profile; eye large

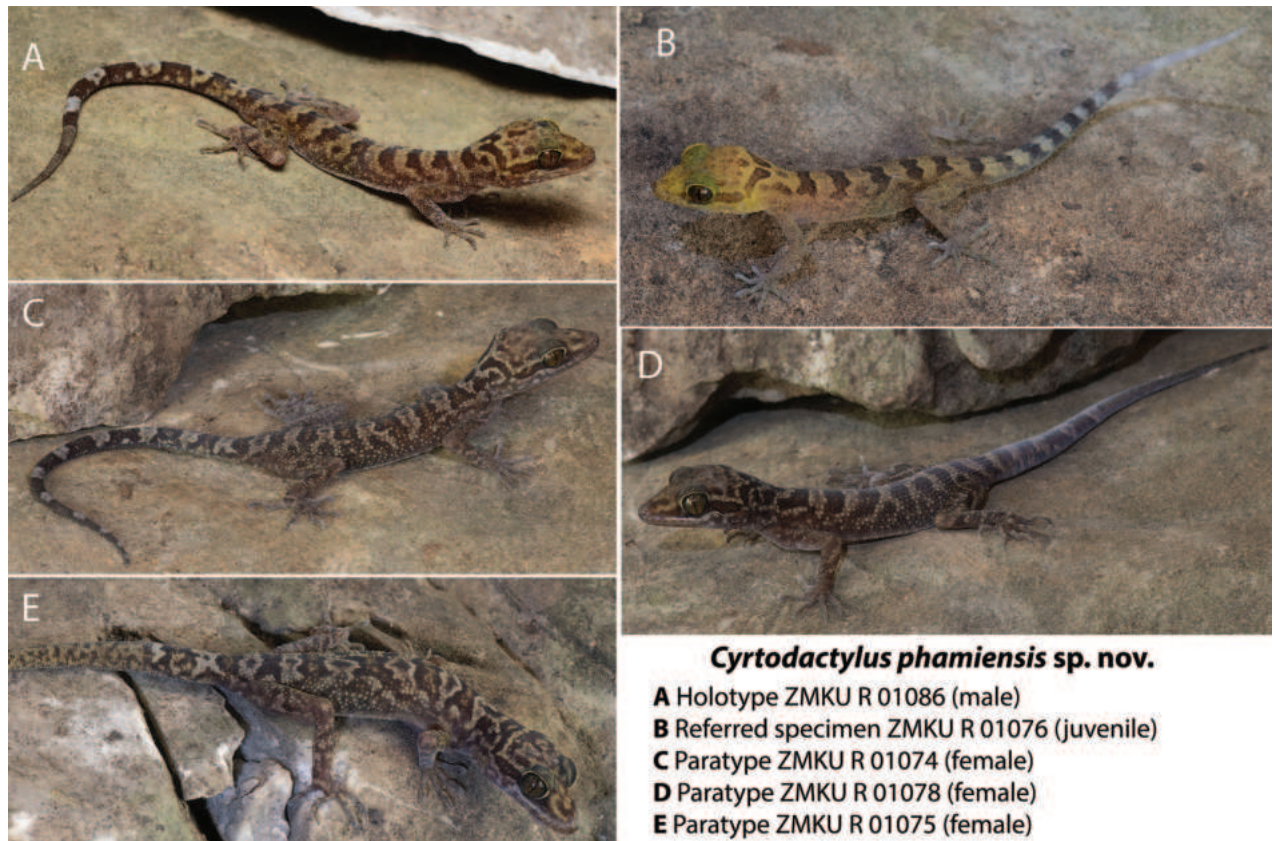


Figure 4. Selected individuals of the type series and referred specimen of *Cyrtodactylus phamiensis* sp. nov. from Pha Mi Village, Wiang Phang Kham Subdistrict, Mae Sai District, Chiang Rai Province, Thailand.

(ED/HL 0.31); ear opening elliptical, obliquely oriented, moderate in size; eye to ear distance slightly greater than diameter of eye; rostral rectangular, partially divided dorsally by inverted Y-shaped furrow, bordered posteriorly by large left and right supranasals, bordered laterally by first supralabials; external nares bordered anteriorly by rostral, dorsally by large supranasal, posteriorly by two moderately sized postnasals, bordered ventrally by first supralabial; nine (R, L) rectangular supralabials tapering abruptly to below midpoint of eye, first–fifth supralabials largest; 11 (R, L) infralabials tapering smoothly to slightly past the termination of enlarged supralabials to corner of mouth; scales of rostrum and lores flat, larger than granular scales on top of head and occiput; scales of occiput intermixed with small, rounded, tubercles; superciliaries elongate, largest dorsally; mental triangular, bordered laterally by first infralabials and posteriorly by large left and right trapezoidal postmentals contacting medially for ~ 65% of their length posterior to mental; one row of enlarged, sublabials extending posteriorly to fifth infralabials (R, L); gular and throat scales small, granular, grading posteriorly into slightly larger, flatter, smooth, imbricate, pectoral and ventral scales.

Body relatively long (AG/SVL 0.46) with well-defined ventrolateral folds; dorsal scales small, granular, interspersed with moderately sized, smooth, rounded, semi-regularly arranged tubercles extending from occiput to slightly beyond base of tail; ~ 25 longitudinal rows of tubercles at midbody; ~ 33 paravertebral tubercles; 33 flat, imbricate, ventral scales much larger than dorsal scales; eight enlarged precloacal scales, six bearing pores; no deep precloacal groove or depression; and two rows of large post-precloacal scales on midline.

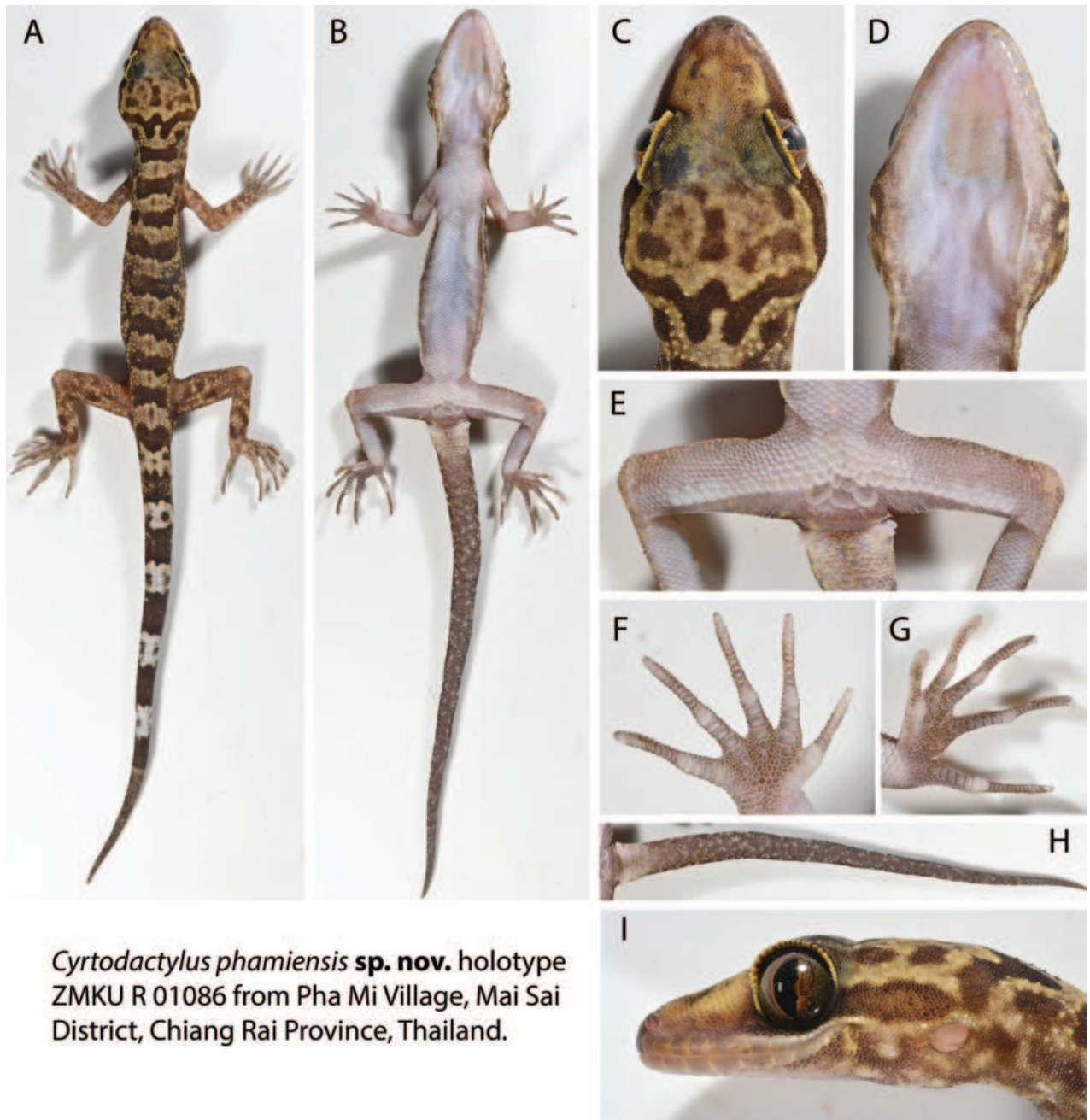


Figure 5. Adult male holotype of *Cyrtodactylus phamiensis* sp. nov. **A** dorsal view **B** ventral view **C** dorsal view of head **D** gular region **E** thighs and precloacal region **F** ventral view of right manus **G** ventral view of left pes **H** subcaudal region **I** lateral view of left side of head. Photographs by Attapol Rujirawan.

Forelimbs moderate in length and stature (FL/SVL 0.16); granular scales of forelimbs slightly larger than those on body, small rounded tubercles on dorsal surface of forearms; palmar scales flat, juxtaposed; digits well-developed, inflected at basal interphalangeal joints, slightly narrower distal to inflections; subdigital lamellae transversely expanded, those proximal to joint inflections much wider than nearly unmodified lamellae distal to inflections; claws well-developed, sheathed by a dorsal and ventral scale; hind limbs robust, wider and longer than forelimbs (TBL/SVL 0.20), covered dorsally by granular scales interspersed with moderately sized tubercles, larger and flat scales anteriorly; ventral scales of thighs flat, imbricate, slightly larger than dorsals; subtibial

scales small, flat, imbricate; one row of 10(R)11(L) enlarged femoral scales terminating distally before knee, continuous with enlarged precloacal scales; proximal femorals nearly same size as distal femorals, all femorals forming an abrupt union with smaller, granular, ventral scales of posteroventral scales of thigh; femoral pores 4(R) 5(L) restricted to distalmost femorals; plantar scales flat, juxtaposed; digits well-developed, inflected at basal interphalangeal joints; claws well-developed, sheathed by a dorsal and ventral scale at base; seven (R, L) wide subdigital lamellae on fourth toe proximal to joint inflection, 12 (R, L) narrower lamellae distal to joint inflection, 19 total subdigital lamellae.

Tail regenerated, long (TL/SVL 1.14), thin, 78.1 mm in length, 6.9 mm wide at base, tapering to a point; dorsal caudal scales small, generally square, juxtaposed; median row of subcaudals significantly larger than dorsal caudals, transversely expanded, not extending dorsally onto lateral side of tail; body tubercles extending slightly beyond base of tail; faint hemipenial swellings at base of tail, two large postcloacal tubercles on both sides; and postcloacal scales flat, imbricate.

Coloration prior to preservation. (Figs 4, 5) Ground color of top of head, limbs, and dorsum straw to pale brown; top of head bearing poorly defined, irregularly shaped, dark brown markings; dark brown, nuchal loop bearing two posterior projections extend between postorbital regions; well-defined, rectangular dark brown band on nape; six dark brown, immaculate, weakly jagged, dorsal body bands terminating above the ventrolateral folds extending from shoulders to groin, same width as straw-colored interspaces, not edged with white or bright-colored tubercles; one darkly colored sacral band; dorsal interspaces faintly mottled, each bearing a brown “fuzzy-edged” longitudinal vertebral marking; forelimbs faintly mottled; hind limbs more darkly mottled, accentuating light-colored tubercles; one post-sacral and five wide, dark brown caudal bands slightly wider whitish caudal bands markings; whitish caudal bands do not encircle tail, bear subcircular dark brown markings; iris reddish gold with thin black reticulations; venter beige with faint, dark shadowing on lateral edges of belly and limbs; and subcaudal region dark-brown, weakly mottled with pale-colored markings.

Etymology. The species name *phamiensis* is in reference to the type locality at Pha Mi Village, Wiang Phang Kham Subdistrict, Mae Sai District, Chiang Rai Province, Thailand (Fig. 1).

Distribution. The type series of *Cyrtodactylus phamiensis* sp. nov. is known only from the type locality at Pha Mi Village, Wiang Phang Kham Subdistrict, Mae Sai District, Chiang Rai Province, Thailand (Fig. 1). On 30 March 2023, a bat researcher from the University of Hong Kong, Ada Chornelia, informed us of this species’ potential presence in a two adjacent karst caves at monastery 5 km north of the type locality in Tham Pha Chom along the same line of large karst formations. Examination of a photograph (Fig. 6) from this locality, tentatively confirms this observation. Furthermore, on 17 December 2022 three *Cyrtodactylus phamiensis* sp. nov. were observed, one of which was photographed, only 50 meters west-southwest of the type locality immediately east of Pha Mi Village by H. Bringsøe (Fig. 7) from the same karstic formations. It is likely that *Cyrtodactylus phamiensis* sp. nov. ranges throughout the karstic landscapes of this region.

Variation. (Table 4) The paratypes closely approach the holotype in general coloration and pattern (Fig. 8). The most notable variation pertains to the shape of the nuchal loop, nape band, the caudal pattern and morphology. In ZMKU R 01073–74, ZMKU R 01081, ZMKU R 01083–84 and ZMKU R 01087, the nuchal



Figure 6. *Cyrtodactylus cf. phamiensis* sp. nov. from 5 km north of the type locality in Tham Pha Chom. Photograph by Ada Chornelia.

loop is medially bifurcated. That of ZMKU R 01075 is irregular and ill-defined. The holotype, ZMKU R 01086, is the only specimen with a complete rectangular nape band. Nape bands of the paratypes are either tripartite or nearly so. ZMKU R 01074, ZMKU R 01084 and ZMKU R 01087 have complete tails. Tails of ZMKU R 01075 and ZMKU R 01078 are three-quarters to one-half regenerated, respectively. ZMKU R 01081 and ZMKU R 01085 lack the majority of their tails. The body bands of ZMKU R 01074–75, ZMKU R 01085 and ZMKU R 01087 have lightened centers. Morphometric, meristic, and categorical data of the type series and referred specimens are listed in Suppl. material 3.

Comparisons. *Cyrtodactylus phamiensis* sp. nov. is embedded in clade 2 and is the sister species to a clade composed of three lineages, *C. doisuthep*, *C. erythrops* and *C. sp. 6*. *Cyrtodactylus phamiensis* sp. nov. differs from those three lineages by mean uncorrected pairwise sequence divergence of 13.5–14.5% and the remaining species in the *chauquangensis* group by 13.7–17.3% (Suppl. material 2). It differs from *C. doisuthep* by having maximum SVL 74.4 mm (vs 90.5 mm); 9–14 total number of femoral pores in males (vs absent); and lack-



Figure 7. *Cyrtodactylus phamiensis* sp. nov. from 50 meters west-southwest of the type locality, immediately east of Pha Mi Village. 17 December 2022. Photograph by Henrik Bringsøe.

ing light-colored reticulum on the top of the head (vs present; Kunya et al. 2014: fig. 1). *Cyrtodactylus phamiensis* sp. nov. differs from *C. erythropterus* by having 29–37 longitudinal rows of ventrals (vs 28 rows); 9–14 total number of femoral pores in males (vs 19 pores); 4–6 precloacal pores in males (vs 9 pores); and hatchlings with yellow-colored heads (vs tan colored; Bauer et al. 2009: fig. 5). Additional comparisons (meristics, morphometrics, and subcaudal scale morphology) between *Cyrtodactylus phamiensis* sp. nov. and the remaining species in the *chauquangensis* group are presented in Table 4.

Natural history. (Fig. 9) All specimens were collected during the evening between 19:30 and 20:50 hours on karst formations, at the entrance of a karst cave, within the cave, or on karst vegetation outside the cave at varying distances from the cave entrance. One specimen was observed during the day in a crack ~ 5 m above the cave floor ~ 20 m in from the entrance. Juveniles



Figure 8. Paratypes of *Cyrtodactylus phamiensis* sp. nov. from Pha Mi Village, Wiang Phang Kham Subdistrict, Mae Sai District, Chiang Rai Province, Thailand. Photographs by Attapol Rujirawan.

(SVL < 40 mm) were found outside the cave less than 1 m above ground level on karst boulders or on the base of small trees. Most were found farther away (~ 20–40 m) from the cave entrance than adults. On 26 March, four or five juveniles (not collected) were also observed far from the cave entrance on karst boulders and on the base of trees. That same night, other juveniles were observed near ground level on small karst outcroppings along a shallow ravine ~ 0.3 m southeast of the type locality. We have noted similar behavior in juveniles of *Cyrtodactylus aunghini* Grismer, Wood, Thura, Win, Grismer, Trueblood & Quah, 2018, *C. bayinnyiensis* Grismer, Wood, Thura, Quah, Murdoch, Grismer, Herr, Lin & Kyaw, 2018, *C. chrysopylos* Bauer, 2003, and *C. shwetaungorum* Grismer, Wood, Thura, Zin, Quah, Murdoch, Grismer, Lin, Kyaw & Lwin, 2017, of unrelated species groups in Myanmar (Grismer et al. 2018a, 2018b, 2018c). All hatchlings of these were found on the ground far from the adults on karst formations. We suspect this may be a way to avoid predation by adults as well as a means to disperse to other karst habitats. The fact that several juveniles of *Cyrtodactylus phamiensis* sp. nov. and no gravid females were observed indicates the reproductive season must have terminated prior to March. The three individuals of *Cyrtodactylus phamiensis* sp. nov. which were found 50 meters from the type locality on 17 December 2022 were adults and were observed on the karst walls outside caves at night between 21:30 and 22:30 hours (Fig. 7).

Other species of herpetofauna observed in the vicinity during this period were two species of frogs, *Sylvirana nigrovittata* (Blyth, 1856) and *Polypedates megacephalus* Hallowell, 1861; four other gecko species, *Gehyra mutilata* (Wiegmann, 1834), *Gekko gekko* (Linnaeus, 1758), *Hemidactylus garnotii* Duméril & Bibron, 1836, and *Hemidactylus platyurus* (Schneider, 1797); and a pitviper *Trimeresurus macrops* Kramer, 1977. We postulate that the high number of adult *Cyrtodactylus phamiensis* sp. nov. that had missing or regenerated tails as well as their skittish nature and that they did not stray far from their shelters could have been due to predation pressures from the large *G. gekko* that were also found on the karst walls and the pitvipers that were observed coiled in ambush position on vegetation beside the karst.



Figure 9. Karst habitat of the type locality from Pha Mi Village, Wiang Phang Kham Sub-district, Mae Sai District, Chiang Rai Province, Thailand. Photograph by Evan S.H. Quah.

Discussion

The computation of nine phylogenies from three model-based analyses using three different partition schemes did not resolve all of the unequivocal nodes variably present in the most recent analyses (Liu and Rao 2021a, 2021b, 2022; Liu et al. 2021; Chomdej et al. 2022; Tran et al. 2024). Direct comparison to the previously published trees is difficult because one used CO1 instead of ND2 (Liu and Rao 2021b) and the others had incomplete species coverage of the group. Our analysis also lacked *Cyrtodactylus caixitaoi* Liu, Rao, Hou, Wang & Ananjeva, 2023, *C. hekouensis* Zhang, Liu, Bernstein, Wang & Yuan, 2021, and *C. martini* Ngo, 2011 (Ngo 2011; Zhang et al. 2021; Liu et al. 2023). Nonetheless, running multiple analyses underscores the necessity to evaluate the performance of more than just one or two models employing a single partition scheme. Had we only run codon-partitioned ML and BI analyses – which is generally standard for most integrative taxonomic studies in herpetology although many drop the BI analysis – we would not have recovered the best resolved tree. Had we not employed the BEAST analysis, the ML analysis would have generated the best phylogeny but with five fewer strongly supported nodes. However, BEAST analyses can inflate nodal support values. With *a priori* knowledge that many of the internal nodes of the clade being tested are not well-supported, running varying partition schemes across different models offers the best chance of recovering the best tree possible given the data. Additionally, it should be noted that if the marker used is highly informative, then all phylogenetic iterations should recover the same well supported phylogeny.

The topology of the tree generated herein is similar to that of Liu and Rao (2022) based on their codon partitioned ML and BI although they recovered five deep nodes with no support as opposed three unsupported nodes herein. The topologies of these trees were inconsistent with that of Chomdej et al. (2022) which used one substitution model for both genes (ND2 and tRNA) in their ML and BI analyses and did not recover the *chauquangensis* group as monophyletic. The differences in the latter case may be due to the choice of outgroups used to root the trees. For the most part, the unresolved nodes in all the trees occur at the ends of deep short internodes, indicating speciation in this part of the trees was rapid as opposed to other parts (Fig. 2). Until other markers are used to resolve these equivocal nodes, the current phylogeny here falls outside the legitimate purview of any comparative phylogenetic methods for character evolution, biogeography, evolution of habitat preference, etc., – all of which could potentially affect plans for conservation management.

The discovery of new species of *Cyrtodactylus* in karstic caves, towers, cones, or hills in Southeast Asia and Indochina has become more of an expectation than a surprise and vast areas of karstic landscapes across these regions remain unexplored. These landscapes are proving to have a far greater number of species across the taxonomic board than previously expected. This is especially true for *Cyrtodactylus* where karst landscapes have been shown to be foci of speciation (Grismer et al. 2021) as opposed to only being refugial “arks”. The growing research in karstic landscapes will continue to underscore their unrealized biodiversity, further emphasizing the need for their conservation, something they woefully lack across all of Asia.

Acknowledgements

We would like to thank Shuo Liu and Cuong Pham for their comments improved the manuscript. We are thankful to Ada Chornelia for sharing information and providing a photograph of *Cyrtodactylus cf. phamiensis*.

Additional information

Conflict of interest

The authors have declared that no competing interests exist.

Ethical statement

The research protocol was approved by Institutional Animal Care and Use Committee, Kasetsart University (ACKU66-SCI-019).

Funding

This research and innovation activity is funded by National Research Council of Thailand (NRCT) (N35E660138), and Centre of Excellence on Biodiversity (MHESI) (BDC-PG1-166008).

Author contributions

Conceptualization: L.L. Grismer, A. Rujirawan. Formal analysis: L.L. Grismer, A. Rujirawan. Investigation: L.L. Grismer, A. Aowphol, J.L. Grismer, A. Aksornneam, E.S.H. Quah, M.L. Murdoch, J.J. Gregory, E. Nguyen, A. Kaatz, H. Bringsøe, A. Rujirawan. Writing – Original draft: L.L. Grismer, A. Rujirawan. Writing – Review and Editing: L.L. Grismer, A. Aowphol, J.L. Grismer, A. Aksornneam, E.S.H. Quah, M.L. Murdoch, H. Bringsøe, A. Rujirawan. Visualization: L.L. Grismer, E.S.H. Quah, H. Bringsøe, A. Rujirawan. Supervision: A. Aowphol, A. Rujirawan. Project administration: A. Aowphol, A. Rujirawan.

Author ORCIDs

L. Lee Grismer  <https://orcid.org/0000-0001-8422-3698>

Anchalee Aowphol  <https://orcid.org/0000-0001-9504-4601>

Jesse L. Grismer  <https://orcid.org/0000-0002-2542-5430>

Akrachai Aksornneam  <https://orcid.org/0000-0003-4780-376X>

Evan S. H. Quah  <https://orcid.org/0000-0002-5357-1953>

Matthew L. Murdoch  <https://orcid.org/0000-0001-5914-6408>

Attapol Rujirawan  <https://orcid.org/0000-0001-9179-6910>

Data availability

All of the data that support the findings of this study are available in the main text or Supplementary Information.

References

- Barraclough TG, Birky Jr CW, Burt A (2003) Diversification in sexual and asexual organisms. *Evolution; International Journal of Organic Evolution* 57(9): 2166–2172. <https://doi.org/10.1111/j.0014-3820.2003.tb00394.x>
- Bauer AM, Kunya K, Sumontha M, Niyomwan P, Panitvong N, Pauwels OSG, Chanhom L, Kunya T (2009) *Cyrtodactylus erythrops* (Squamata: Gekkonidae), a new cave-dwell-

- ing gecko from Mae Hong Son Province, Thailand. *Zootaxa* 2124(1): 51–62. <https://doi.org/10.11646/zootaxa.2124.1.4>
- Bouckaert RR, Drummond AJ (2017) bModelTest: Bayesian phylogenetic site model averaging and model comparison. *BMC Evolutionary Biology* 17(1): 42. <https://doi.org/10.1186/s12862-017-0890-6>
- Chomdej S, Pradit W, Suwannapoom C, Pawangkhanant P, Nganvongpanit K, Poyarkov NA, Che J, Gao YC, Gong SP (2021) Phylogenetic analyses of distantly related clades of bent-toed geckos (genus *Cyrtodactylus*) reveal an unprecedented amount of cryptic diversity in northern and western Thailand. *Scientific Reports* 11(1): e2328. <https://doi.org/10.1038/s41598-020-70640-8>
- Chomdej S, Pradit W, Pawangkhanant P, Kuensaen C, Phupanbai A, Naiduangchan M, Piboon P, Nganvongpanit K, Yuan Z, Zhang Y, Che J, Cucharitakul P, Suwannapoom C (2022) A New *Cyrtodactylus* species (Reptilia: Gekkonidae) from Nan Province, Northern Thailand. *Asian Herpetological Research* 13: 96–108. <https://doi.org/10.16373/j.cnki.ahr.210055>
- de Queiroz K (2007) Species concepts and species delimitation. *Systematic Biology* 56(6): 879–886. <https://doi.org/10.1080/10635150701701083>
- Drummond AJ, Ashton B, Buxton S, Cheung M, Cooper A, Duran C, Field M, Heled J, Kearse M, Markowitz S, Moir R, Stones-Havas S, Sturrock S, Thierer T, Wilson A (2011) Geneious. Version 5.6. <http://www.geneious.com/> [accessed 9 January 2018]
- Drummond AJ, Suchard MA, Xie D, Rambaut A (2012) Bayesian phylogenetics with BEAUti and the BEAST 1.7. *Molecular Biology and Evolution* 29(8): 1969–1973. <https://doi.org/10.1093/molbev/mss075>
- Frost DR, Hillis DM (1990) Species in concept and practice: Herpetological application. *Herpetologica* 46: 87–104.
- Frost DR, Kluge AG (1994) A consideration of the epistemology in systematic biology, with special reference to species. *Cladistics* 10(3): 259–294. <https://doi.org/10.1111/j.1096-0031.1994.tb00178.x>
- Grismer LL, Grismer JL (2017) A re-evaluation of the phylogenetic relationships of the *Cyrtodactylus condorensis* group (Squamata; Gekkonidae) and a suggested protocol for the characterization of rock-dwelling ecomorphology in *Cyrtodactylus*. *Zootaxa* 4300(4): 486–504. <https://doi.org/10.11646/zootaxa.4300.4.2>
- Grismer LL, Wood Jr PL, Thura MK, Zin T, Quah ESH, Murdoch ML, Grismer MS, Lin A, Kyaw H, Lwin N (2018a) Twelve new species of *Cyrtodactylus* Gray (Squamata: Gekkonidae) from isolated limestone habitats in east-central and southern Myanmar demonstrate high localized diversity and unprecedented microendemism. *Zoological Journal of the Linnean Society* 182(4): 862–959. <https://doi.org/10.1093/zoolinnean/zlx057>
- Grismer LL, Wood Jr PL, Thura MK, Quah ESH, Murdoch ML, Grismer MS, Herr MW, Lin A, Kyaw H (2018b) Three more new species of *Cyrtodactylus* (Squamata: Gekkonidae) from the Salween Basin of eastern Myanmar underscore the urgent need for the conservation of karst habitats. *Journal of Natural History* 52(19–20): 19–20, 1243–1294. <https://doi.org/10.1080/00222933.2018.1449911>
- Grismer LL, Wood Jr PL, Thura MK, Win NM, Grismer MS, Trueblood LA, Quah ESH (2018c) A re-description of *Cyrtodactylus chrysopylos* Bauer (Squamata: Gekkonidae) with comments on the adaptive significance of orange coloration in hatchlings and descriptions of two new species from eastern Myanmar (Burma). *Zootaxa* 4527(2): 151–185. <https://doi.org/10.11646/zootaxa.4527.2.1>

- Grismer LL, Wood Jr PL, Poyarkov NA, Le MD, Karunarathna S, Chomdej S, Suwannapoom C, Qi S, Liu S, Che J, Quah ESH, Kraus F, Oliver PM, Riyanto A, Pauwels OSG, Grismer JL (2021) Karstic landscapes are foci of species diversity in the World's Third-Largest Vertebrate genus *Cyrtodactylus* Gray, 1827 (Reptilia: Squamata; Gekkonidae). *Diversity* 13(5): 183. <https://doi.org/10.3390/d13050183>
- Hillis DM (2019) Species delimitation in herpetology. *Journal of Herpetology* 53(1): 3–12. <https://doi.org/10.1670/18-123>
- Hoang DT, Chernomor O, von Haeseler A, Minh BQ, Vinh LS (2018) UFBoot2: Improving the ultrafast bootstrap approximation. *Molecular Biology and Evolution* 35(2): 518–522. <https://doi.org/10.1093/molbev/msx281>
- Huelsenbeck JP, Ronquist F, Nielsen R, Bollback JP (2001) Bayesian inference of phylogeny and its impact on evolutionary biology. *Science* 294(5550): 2310–2314. <https://doi.org/10.1126/science.1065889>
- Husson F, Josse J, Le S, Mazet J (2017) FactoMine R: exploratory data analysis and data mining. R package, version 1.36.
- Kalyanamoothy S, Minh BQ, Wong TK, von Haeseler A, Jermiin LS (2017) ModelFinder: Fast model selection for accurate phylogenetic estimates. *Nature Methods* 14(6): 587–589. <https://doi.org/10.1038/nmeth.4285>
- Kassambara A, Mundt F (2017) Factoextra: extract and visualize the result of multivariate data analyses. R package, version 1.0.5.999.
- Kunya K, Panmongkol A, Pauwels OSG, Sumontha M, Meewasana J, Bunkhwamdi W, Dangsri S (2014) A new forest-dwelling Bent-toed Gecko (Squamata: Gekkonidae: *Cyrtodactylus*) from Doi Suthep, Chiang Mai Province, northern Thailand. *Zootaxa* 3811(2): 251–261. <https://doi.org/10.11646/zootaxa.3811.2.6>
- Liu S, Rao D (2021a) A new species of *Cyrtodactylus* Gray, 1827 (Squamata: Gekkonidae) from Western Yunnan, China. *Journal of Natural History* 55(11–12): 713–731. <https://doi.org/10.1080/00222933.2021.1921871>
- Liu S, Rao D (2021b) A new species of *Cyrtodactylus* Gray, 1827 (Squamata, Gekkonidae) from Yunnan, China. *ZooKeys* 1021: 109–126. <https://doi.org/10.3897/zookeys.1021.60402>
- Liu S, Rao D (2022) A new species of *Cyrtodactylus* Gray, 1827 (Squamata, Gekkonidae) from southwestern Yunnan, China. *ZooKeys* 1084: 83–100. <https://doi.org/10.3897/zookeys.1084.72868>
- Liu S, Li QS, Hou M, Orlov NL, Ananjeva NB (2021) A New Species of *Cyrtodactylus* Gray, 1827 (Squamata, Gekkonidae) from Southern Yunnan, China. *Russian Journal of Herpetology* 28(4): 185–196. <https://doi.org/10.30906/1026-2296-2021-28-4-185-196>
- Liu S, Rao D, Hou M, Wang Q, Ananjeva NB (2023) A new species of *Cyrtodactylus* Gray, 1827 (Squamata, Gekkonidae), previously confused with *C. wayakonei* Nguyen, Kingsada, Rösler, Auer et Ziegler, 2010. *Russian Journal of Herpetology* 30(6): 529–538. <https://doi.org/10.30906/1026-2296-2023-30-6-529-538>
- Lleonart J, Salat J, Torres GJ (2000) Removing allometric effects of body size in morphological analysis. *Journal of Theoretical Biology* 205(1): 85–93. <https://doi.org/10.1006/jtbi.2000.2043>
- Maddison WP, Maddison DR (2015) Mesquite: a modular system for evolutionary analysis. Version 3.04. <https://doi.org/10.1093/sysbio/42.2.218> [accessed 25 August 2020]
- Miller MA, Pfeiffer W, Schwartz T (2010) Creating the CIPRES Science Gateway for inference of large phylogenetic trees. In: Gateway Computing Environments Workshop (GCE), New Orleans (USA), November 2010, IEEE, 1–8. <https://doi.org/10.1109/GCE.2010.5676129>

- Minh Q, Nguyen MAT, von Haeseler A (2013) Ultrafast approximation for phylogenetic bootstrap. *Molecular Biology and Evolution* 30(5): 1188–1195. <https://doi.org/10.1093/molbev/mst024>
- Murdoch ML, Grismer LL, Wood Jr PL, Neang T, Poyarkov NA, Ngo VT, Nazarov RA, Aowphol A, Pauwels OSG, Nguyen HN, Grismer JL (2019) Six new species of the *Cyrtodactylus intermedius* complex (Squamata: Gekkonidae) from the Cardamom Mountains and associated highlands of Southeast Asia. *Zootaxa* 4554(1): 1–62. <https://doi.org/10.11646/zootaxa.4554.1.1>
- Ngo VT (2011) *Cyrtodactylus martini*, another new karst-dwelling *Cyrtodactylus* Gray, 1827 (Squamata: Gekkonidae) from Northwestern Vietnam. *Zootaxa* 2834(1): 33–46. <https://doi.org/10.11646/zootaxa.2834.1.3>
- Nguyen TQ, Le MD, Pham AV, Ngo HN, Hoang VH, Pham CT, Ziegler T (2015a) Two new species of *Cyrtodactylus* (Squamata: Gekkonidae) from the karst forest of Hoa Binh Province, Vietnam. *Zootaxa* 3985(3): 375–390. <https://doi.org/10.11646/zootaxa.3985.3.3>
- Nguyen LT, Schmidt HA, von Haeseler A, Minh BQ (2015b) IQ-TREE: A fast and effective stochastic algorithm for estimating maximum likelihood phylogenies. *Molecular Biology and Evolution* 32(1): 268–274. <https://doi.org/10.1093/molbev/msu300>
- Nguyen TQ, Pham AV, Ziegler T, Ngo HT, Le MD (2017) A new species of *Cyrtodactylus* (Squamata: Gekkonidae) and the first record of *C. otai* from Son La Province, Vietnam. *Zootaxa* 4341(1): 25–40. <https://doi.org/10.11646/zootaxa.4341.1.2>
- Oksanen J, Blanchet FG, Friendly M, Kindt R, Legendre P, McGlinn D, Minchin PR, O'Hara RB, Simpson GL, Solymos P, Stevens MHH, Szoecs E, Wagner H (2020) Package 'vegan'. Version 2.5–7. <https://cran.r-project.org/web/packages/vegan/>
- Pagès J (2015) Multiple Factor Analysis by Example Using R. CRC Press, New York, 272 pp. <https://doi.org/10.1201/b17700-10>
- Pham AV, Le MD, Ziegler T, Nguyen TQ (2019) A new species of *Cyrtodactylus* (Squamata: Gekkonidae) from northwestern Vietnam. *Zootaxa* 4544(3): 360–380. <https://doi.org/10.11646/zootaxa.4544.3.3>
- R Core Team (2021) R: A language and environment for statistical computing. R foundation for statistical computing, Vienna, Austria. <https://www.R-project.org>
- Rambaut A, Drummond AJ (2013) TreeAnnotator version 1.8.0 MCMC Output Analysis. <https://doi.org/10.1017/CBO9780511819049.020>
- Rambaut A, Drummond AJ, Xie D, Baele G, Suchard MA (2018) Posterior summarization in Bayesian phylogenetics using Tracer 1.7. *Systematic Biology* 67(5): 901–904. <https://doi.org/10.1093/sysbio/syy032>
- Reist JD (1986) An empirical evaluation of coefficients used in residual and allometric adjustment of size covariation. *Canadian Journal of Zoology* 64(6): 1363–1368. <https://doi.org/10.1139/z86-203>
- Ronquist F, Teslenko M, van Der Mark P, Ayres DL, Darling A, Höhna S, Larget B, Liu L, Suchard MA, Huelsenbeck JP (2012) MrBayes 3.2: Efficient Bayesian phylogenetic inference and model choice across a large model space. *Systematic Biology* 61(3): 539–542. <https://doi.org/10.1093/sysbio/sys029>
- Schneider N, Luu VQ, Sitthivong S, Teynié A, Le MD, Nguyen TQ, Ziegler T (2020) Two new species of *Cyrtodactylus* (Squamata: Gekkonidae) from northern Laos, including new finding and expanded diagnosis of *C. bansocensis*. *Zootaxa* 4822(4): 503–530. <https://doi.org/10.11646/zootaxa.4822.4.3>
- Simmons JE (2015) Herpetological collecting and collections management, 3rd ed. Society for the Study of Amphibians and Reptiles Herpetological Circular No. 42. Salt Lake City, UT, 191 pp.

- Skalski JR, Richins SM, Townsend RL (2018) A statistical test and sample size recommendations for comparing community composition following PCA. *PLoS One* 13(10): e0206033. <https://doi.org/10.1371/journal.pone.0206033>
- Tamura K, Stecher G, Kumar S (2021) MEGA11: Molecular evolutionary genetics analysis version 11. *Molecular Biology and Evolution* 38(7): 3022–3027. <https://doi.org/10.1093/molbev/msab120>
- Thorpe RS (1975) Quantitative handling of characters useful in snake systematics with particular reference to intraspecific variation in the Ringed Snake *Natrix natrix* (L.). *Biological Journal of the Linnean Society* 7(1): 27–43. <https://doi.org/10.1111/j.1095-8312.1975.tb00732.x>
- Thorpe RS (1983) A review of the numerical methods for recognising and analysing racial differentiation. In: Felsenstein J (Ed.) *Numerical Taxonomy*. NATO ASI Series, Volume 1. Springer, Berlin, Heidelberg, 404–423. https://doi.org/10.1007/978-3-642-69024-2_43
- Tran TT, Do QH, Pham CT, Phan TQ, Ngo HT, Le MD, Ziegler T, Nguyen TQ (2024) A new species of the *Cyrtodactylus chauquangensis* species group (Squamata, Gekkonidae) from Lao Cai Province, Vietnam. *ZooKeys* 1192: 83–102. <https://doi.org/10.3897/zookeys.1192.117135>
- Trifinopoulos J, Nguyen LT, von Haeseler A, Minh BQ (2016) W-IQ-TREE: A fast online phylogenetic tool for maximum likelihood analysis. *Nucleic Acids Research* 44(W1): 232–235. <https://doi.org/10.1093/nar/gkw256>
- Turan C (1999) A note on the examination of morphometric differentiation among fish populations: The Truss System. *Turkish Journal of Zoology* 23: 259–263.
- Wilcox TP, Zwickl DJ, Heath TA, Hillis DM (2002) Phylogenetic relationships of the dwarf boas and a comparison of Bayesian and bootstrap measures of phylogenetic support. *Molecular Phylogenetics and Evolution* 25(2): 361–371. [https://doi.org/10.1016/S1055-7903\(02\)00244-0](https://doi.org/10.1016/S1055-7903(02)00244-0)
- Zhang Y, Liu X, Bernstein J, Wang J, Yuan Z (2021) A new species of *Cyrtodactylus* (Squamata: Gekkonidae) from the karst forests of Daweishan National Nature Reserve, Yunnan, China. *Asian Herpetological Research* 12(3): 261–270. <https://doi.org/10.16373/j.cnki.ahr.200090>

Supplementary material 1

GenBank accession numbers for the mitochondrial NADH dehydrogenase subunit 2 (ND2) gene and catalog number of voucher specimens used in this analysis

Authors: L. Lee Grismer, Anchalee Aowphol, Jesse L. Grismer, Akrachai Aksornneam, Evan S. H. Quah, Mathew L. Murdoch, Jeren J. Gregory, Eddie Nguyen, Amanda Kaatz, Henrik Bringsøe, Attapol Rujirawan

Data type: pdf

Copyright notice: This dataset is made available under the Open Database License (<http://opendatacommons.org/licenses/odbl/1.0/>). The Open Database License (ODbL) is a license agreement intended to allow users to freely share, modify, and use this Dataset while maintaining this same freedom for others, provided that the original source and author(s) are credited.

Link: <https://doi.org/10.3897/zookeys.1203.122758.suppl1>

Supplementary material 2

Mean uncorrected pairwise genetic distance (%) between species of the *Cyrtodactylus chauquangensis* group based on the mitochondrial NADH dehydrogenase subunit 2 (ND2) gene

Authors: L. Lee Grismer, Anchalee Aowphol, Jesse L. Grismer, Akrachai Aksornneam, Evan S. H. Quah, Mathew L. Murdoch, Jeren J. Gregory, Eddie Nguyen, Amanda Kaatz, Henrik Bringsøe, Attapol Rujirawan

Data type: pdf

Copyright notice: This dataset is made available under the Open Database License (<http://opendatacommons.org/licenses/odbl/1.0/>). The Open Database License (ODbL) is a license agreement intended to allow users to freely share, modify, and use this Dataset while maintaining this same freedom for others, provided that the original source and author(s) are credited.

Link: <https://doi.org/10.3897/zookeys.1203.122758.suppl2>

Supplementary material 3

Morphological and color pattern data for the type series and hatchlings of *Cyrtodactylus phamiensis* sp. nov.

Authors: L. Lee Grismer, Anchalee Aowphol, Jesse L. Grismer, Akrachai Aksornneam, Evan S. H. Quah, Mathew L. Murdoch, Jeren J. Gregory, Eddie Nguyen, Amanda Kaatz, Henrik Bringsøe, Attapol Rujirawan

Data type: pdf

Explanation note: Key: / = data unavailable or inapplicable; m = male; f = female; r = re-generated; b = broken; y = yes; n = no.

Copyright notice: This dataset is made available under the Open Database License (<http://opendatacommons.org/licenses/odbl/1.0/>). The Open Database License (ODbL) is a license agreement intended to allow users to freely share, modify, and use this Dataset while maintaining this same freedom for others, provided that the original source and author(s) are credited.

Link: <https://doi.org/10.3897/zookeys.1203.122758.suppl3>

Population structure of *Taenioides* sp. (Gobiiformes, Gobiidae) reveals their invasion history to inland waters of China based on mitochondrial DNA control region

Chenlian Sun¹, Zhenming Lü¹, Jiaqi Fang¹, Chenhao Yao¹, Shijie Zhao², Yantao Liu¹, Li Gong¹, Bingjian Liu¹, Liqin Liu¹, Jing Liu¹

¹ National Engineering Laboratory of Marine Germplasm Resources Exploration and Utilization, College of Marine Sciences and Technology, Zhejiang Ocean University, Zhoushan 316000, China

² National Engineering Research Center for Facilitated Marine Aquaculture, Zhejiang Ocean University, Zhoushan 316000, China

Corresponding author: Jing Liu (liujing218@foxmail.com)

Abstract

Taenioides sp. is a small temperate fish originally known to inhabit muddy bottoms of brackish waters in coastal areas of China. However, it began to invade multiple inland freshwaters and caused severe damage to Chinese aquatic ecosystems in recent years. To investigate the sources and invasive history of this species, we examined the population structure of 141 individuals collected from seven locations based on partial mitochondrial D-loop regions. The results revealed that the genetic diversity gradually decreased from south to north, with the Yangtze River Estuary and Taihu Lake populations possessing the highest haplotype diversity (Hd), average number of differences (k), and nucleotide diversity (π) values, suggesting that they may be the sources of *Taenioides* sp. invasions. Isolation-by-distance analysis revealed a non-significant correlation ($p = 0.166$) between genetic and geographic distances among seven populations, indicating that dispersal mediated through the regional hydraulic projects may have played an essential role in *Taenioides* sp. invasions. The population genetic structure analysis revealed two diverged clades among seven populations, with clade 2 only detected in source populations, suggesting a possible difference in the invasion ability of the two clades. Our results provide insights into how native estuary fish become invasive through hydraulic projects and may provide critical information for the future control of this invasive species.

Key words: D-loop, eel goby, hydraulic engineering, population differentiation

Introduction

Biological invasion is considered one of the leading causes of global biodiversity loss. The successful reproduction and spread of alien species pose a severe threat and lasting impact on the balance of native ecosystems (Roy et al. 2014). Identifying the sources of alien species might help to establish efficient management to prevent invasion (Daane et al. 2018), and determining the invasion routes can improve understanding of potential invasion risks (Corin et al.



Academic editor:

Maria Elina Bichuette

Received: 21 January 2024

Accepted: 5 April 2024

Published: 30 May 2024

ZooBank: <https://zoobank.org/55ED6ECD-DECD-4A05-B548-8A15D31C6A4A>

Citation: Sun C, Lü Z, Fang J, Yao C, Zhao S, Liu Y, Gong L, Liu B, Liu L, Liu J (2024) Population structure of *Taenioides* sp. (Gobiiformes, Gobiidae) reveals their invasion history to inland waters of China based on mitochondrial DNA control region. ZooKeys 1203: 239–251. <https://doi.org/10.3897/zookeys.1203.119133>

Copyright: © Chenlian Sun et al.
This is an open access article distributed under terms of the Creative Commons Attribution License (Attribution 4.0 International – CC BY 4.0).

2008). Both are vital factors for controlling and managing the spread of invasive species (Hulme 2009; Yue et al. 2021).

The eel goby, *Taenioides* sp., is a newly confirmed candidate species of the genus *Taenioides* (Gobiidae, Amblyopinae) which is frequently mistaken as a form of *Taenioides cirratus* (Yao et al. 2022). It is a small temperate fish initially known to be widely distributed in Chinese coastal waters from the Yangtze River to the Nandu River. It inhabits muddy bottoms in brackish waters areas, such as estuaries, mangrove swamps, and inner bays (Murphy and Randall 2002; Yao et al. 2022). However, massive propagates of *Taenioides* sp. entered major inland freshwaters of China, including rivers, lakes, and reservoirs, making it a common invasive species in recent years. The most affected areas are Taihu, Gaoyou, Luoma, and Nansi lakes and their nearby regions in China (Ni and Wu 2006; Qin et al. 2019). The boom of *Taenioides* sp. is considered a severe threat to local benthic organisms, and it may cause damage to the ecological environment (Liang et al. 2020). Although substantial work on this invasive species' morphological, behavioral, and physiological characteristics has been described and recorded (Liang et al. 2020; Yao et al. 2022), the sources and mechanisms of the *Taenioides* sp. invasions have never been studied.

The rapid development of molecular biology, coupled with a decreased cost of classical methodologies such as microsatellite, mitochondrial and nuclear DNA sequencing (Darling and Blum 2007; Okada et al. 2007; Chen et al. 2017) has primarily contributed to the extensive use of molecular tools in population genetic structuring analysis. Mitochondrial DNA is applied to be an efficient genetic marker to determine the genetic variation and population structure in native habitats and invasion areas because of their high mutation rate and maternal inheritance (Cameron et al. 2008), which can be further used to infer the source populations (Freshwater et al. 2009; Diaz et al. 2015) and invasion mechanisms of introduced species (Cheng et al. 2008; Betancur-R et al. 2011). The D-loop-containing region is considered the most variable region of mtDNA because of no coding pressure and is widely used to analyze the genetic variation of fish populations (Saeidi et al. 2014; Parmaksiz 2018; Fang et al. 2022). *Taenioides* sp. is an invasive species with short invasion history and presumed tiny genetic difference, of which the D-loop-containing region is sensitive for genetic variation detection.

Here, we assessed the genetic diversity and population structure of *Taenioides* sp. populations collected from the Yangtze River Estuary (YE), to which they are native, and six inland lakes of introduced habitats with mitochondrial D-loop-containing regions. The phylogeographic analysis revealed invasion sources and forces of the *Taenioides* sp. populations in inland freshwaters of China. The results would provide important information for the future control of this invasive species.

Materials and methods

Sample collection and DNA extraction

A total of 141 *Taenioides* sp. samples were collected from seven localities, including Yangtze River Estuary, Taihu Lake (TH), Gaoyou Lake (GY), Hongze Lake (HZ), Luoma Lake (LM), Weishan Lake (WS) and Chaohu lake (CH) during

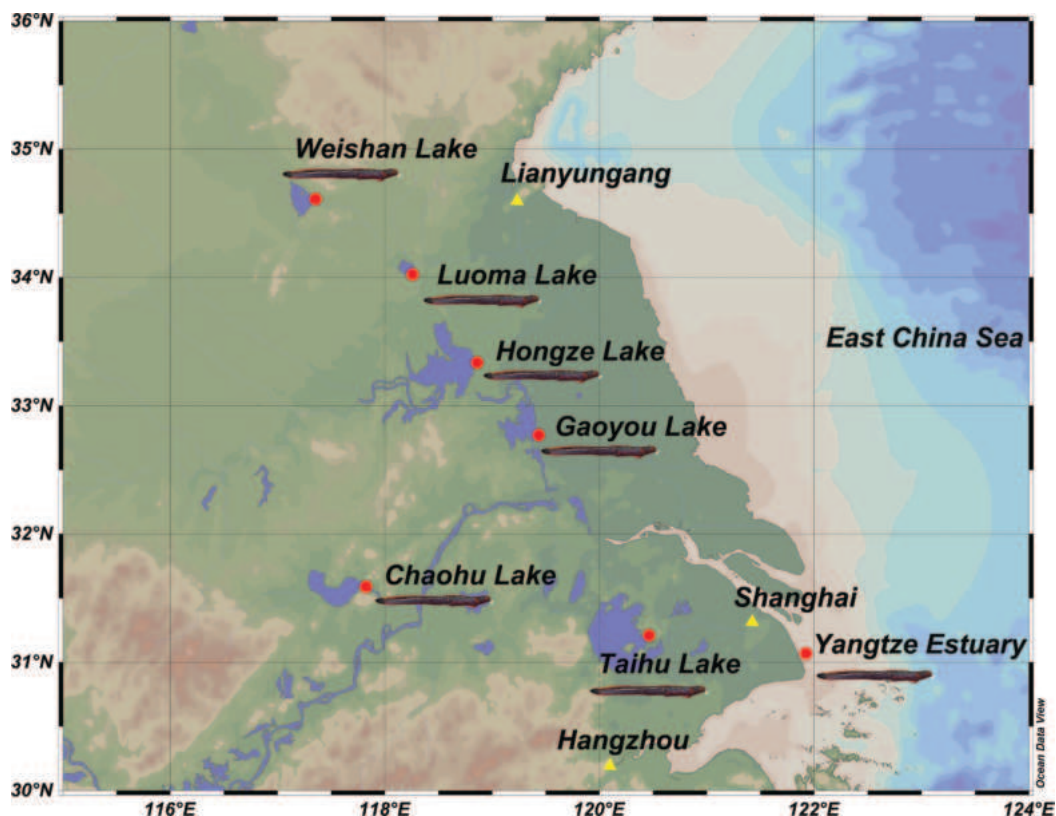


Figure 1. The distribution of sampling locations of *Taenioides* sp.

Table 1. Genetic diversity and neutral test of *Taenioides* sp. populations based on D-loop-containing regions.

Locations	Number of individuals	Code	Number of haplotypes	Haplotype diversity (Hd)	Average number of differences (<i>k</i>)	Nucleotide diversity (π)	Tajima's <i>D</i>	Fu's <i>F_s</i>
Yangtze River Estuary	29	YE	7	0.7710	5.3000	0.0074	0.5425	3.1047
Taihu Lake	24	TH	6	0.8080	8.7570	0.0122	2.3158	6.5903
Gaoyou Lake	14	GY	4	0.6590	1.0440	0.0015	-0.5601	-0.3268
Hongze Lake	21	HZ	4	0.5330	1.9240	0.0027	-0.0364	1.7497
Luoma Lake	20	LM	6	0.6840	1.8320	0.0025	0.2645	-0.5145
Weishan Lake	20	WS	4	0.4320	1.3680	0.0019	-0.6083	0.7452
Chaohu lake	13	CH	2	0.1540	0.1540	0.0002	-1.1492	-0.5371

2021 and 2022, using ground cages (Fig. 1, Table 1). According to our previous study (Yao et al. 2022), all individuals were identified based on morphological and molecular characteristics. Briefly, the total number of vertebrae, dorsal-fin elements, and barbels on the ventral surface of head were counted in morphological observation. Partial fragments of the *COI* gene were amplified and sequenced. Muscle tissues were preserved in 95% ethanol after dissection and transported to the laboratory. The total genomic DNA was isolated following the salt-extraction method (Aljanabi and Martinez 1997). Agarose gel electrophoresis (1.5%) was used to examine the integrity and purity of the extracted DNA. The electrophoresis was performed using 12 μ L final volume containing 3 μ L extracted DNA, 2 μ L 6 \times loading buffer, and 7 μ L double-distilled H₂O.

Mitochondrial DNA amplification and sequencing

Primers (D-loop-F: TTGCCTATGCCATCCTTC; D-loop-R: ATTTGGGCACTTGTT) were designed using the complete mitochondrial genome sequences of *Taenioides* sp. available from the NCBI (accession number: OL625024) to amplify the target mitochondrial D-loop fragment with Primer Premier (version 6.0) (Premier Biosoft, Palo Alto, CA, USA). The PCR assay was performed in a total volume of 25 μ L, which contained 1.25 U Taq DNA polymerase (Promega, USA), 50 ng template DNA, 200 μ M forward and reverse primers, 200 μ M of each dNTP, 1 \times reaction buffer and 1.5 mM MgCl₂. PCR amplifications were performed in a Bio-Rad C1000 Touch Thermal Cycler with the following PCR programs: initial denaturation at 94 °C for 3 min, 34 cycles at 94 °C for 45 s, annealing at 55 °C for 45 s, extending at 72 °C for 90 s and a final extension at 72 °C for 10 min. PCR products were examined by electrophoresis on 1.5% agarose gel and sent to Sangon Biotech (Shanghai) Co., Ltd for sequencing.

Data analysis

The obtained nucleotide sequences were aligned using Clustal X (version 1.83) (Thompson et al. 1997) with manual correction. DNA Sequence Polymorphism (DnaSP, version 5.0) (Librado and Rozas 2009) was used to calculate the number of haplotypes (n), haplotype diversity (Hd), the average number of pairwise differences (k), and nucleotide diversity (π) of each population. Phylogenetic analysis was carried out using the maximum-likelihood (ML) method based on the Hasegawa-Kishino-Yano (HKY) model (Hasegawa et al. 1985) with 1,000 bootstrap replicates in MEGA X (Kumar et al. 2018) to determine the genetic relationships of the populations. The Hasegawa-Kishino-Yano model was selected as the best-fit substitution model based on BIC scores among 24 models in MEGA X (Paria et al. 2021). The D-loop control region from *Odontamblyopus rubicundus* and *Amblyotrypauchen arctcephalus*, two species of the same subfamily Amblyopinae, were used as outgroups. The median-joining network of haplotypes was constructed by POPART (version 1.7) (Leigh and Bryant 2015) to estimate the genealogical relationships in *Taenioides* sp. Analysis of molecular variance (AMOVA) was performed using Arlequin (version 3.11) software (Excoffier et al. 2007) to analyze the degree of genetic variability between and within populations. The pairwise genetic differentiation coefficient (F_{st}) values were obtained based on the compute pairwise distances model (Nei and Li 1979) with 10,000 permutations using Arlequin to estimate the genetic differentiation among populations. Pairwise genetic distances between populations were calculated based on the Tamura 3-parameter modeled by using a discrete Gamma distribution (T92+G) (the best-fit substitution model) in MEGA X. IBD (version 1.5.3) (Bohonak 2002) was used for isolation-by-distance (IBD) analysis to evaluate the relationship between geographic and pairwise genetic distances among population pairs. The pairwise geographic distances between each pair of populations were calculated using an online tool (<https://www.liddgo.net/convert/distance>) based on their latitudes and longitudes. Default parameters were used in Arlequin to investigate Tajima's D test and Fu's F_s test to examine historical population dynamics.

Results

Population genetic diversity

A D-loop fragment of 722 bp was obtained and analyzed based on 141 sequences from seven populations. Gene sequence analyses revealed that there were 15 haplotypes in the D-loop fragments of the mtDNA (Table 1). A total of 26 polymorphic sites were identified, of which 23 were parsimony-informative sites and three were singleton variable sites. A total of five indel sites were identified. The genetic diversity of seven *Taenioides* sp. populations was analyzed (Table 1). The indices of haplotype diversity (H_d), the average difference (k), and nucleotide diversity (π) in different populations ranged from 0.1540 to 0.8080, 0.1540 to 8.7570 and 0.0002 to 0.0122, respectively. Among them, the YE and TH populations, two southernmost populations in this study, harbored the highest genetic diversity with the highest H_d , k , and π values among all locations (0.8080, 8.7570, and 0.0122), and the WS and CH populations harbored the lowest. The genetic diversity of these populations, except for the CH population, showed a decreasing trend from the southernmost population (YE and TH) to the northernmost (WS) from a geographic point of view.

Phylogeny and genetic structure

According to the sequenced fragments, we built the maximum-likelihood phylogenetic tree with 15 haplotypes in seven populations (Fig. 2). The tree exhibited two main lineages: clade 1 consisted of individuals mainly from the YE, TH, GY, HZ, LM, WS, and CH populations, and clade 2 consisted of individuals only from the YE and TH populations. Hap_5, Hap_8, Hap_13, and Hap_14 formed a subclade in clade 1, consisting of individuals from the YE, TH, HZ, LM, and WS populations. The phylogenetic tree did not separate seven populations.

The haplotype network could also be divided into two branches (Fig. 3), which showed a consistent topology with two clades of the ML phylogenetic tree. The network showed that the common haplotypes in clade 1 and clade 2 were Hap_7 and Hap_9, respectively. Hap_7 was shared in seven populations in clade 1 and occupied a central position, indicating that it might be the original haplotype. Hap_9 was in only one population (TH) in clade 2. Hap_5 and Hap_2 were also shared by most populations.

The pairwise F_{st} analysis performed on seven *Taenioides* sp. populations showed that F_{st} values ranged from -0.0353 to 0.6670 , and the majority of the populations were significantly differentiated ($p \leq 0.05$) (Table 2). AMOVA analysis based on populations showed significant genetic differentiation ($F_{st} = 0.2666$, $p \leq 0.05$) among seven sample locations. The results revealed that 73.34% of the variation occurred within populations, while 26.66% of the variation occurred among populations, suggesting that the genetic variation within the populations was the primary source of total variation (Table 3).

The sequence analysis results based on the D-loop regions showed that the genetic distances between different *Taenioides* sp. populations ranged from 0.0010 to 0.0120. The IBD results showed moderate ($r = 0.341$) and non-significant evidence ($p = 0.166$) of a positive relationship between genetic and geographic distances among populations of *Taenioides* sp. obtained from different locations (Fig. 4), revealing that the invasion of *Taenioides* sp. was not driven by active dispersal.

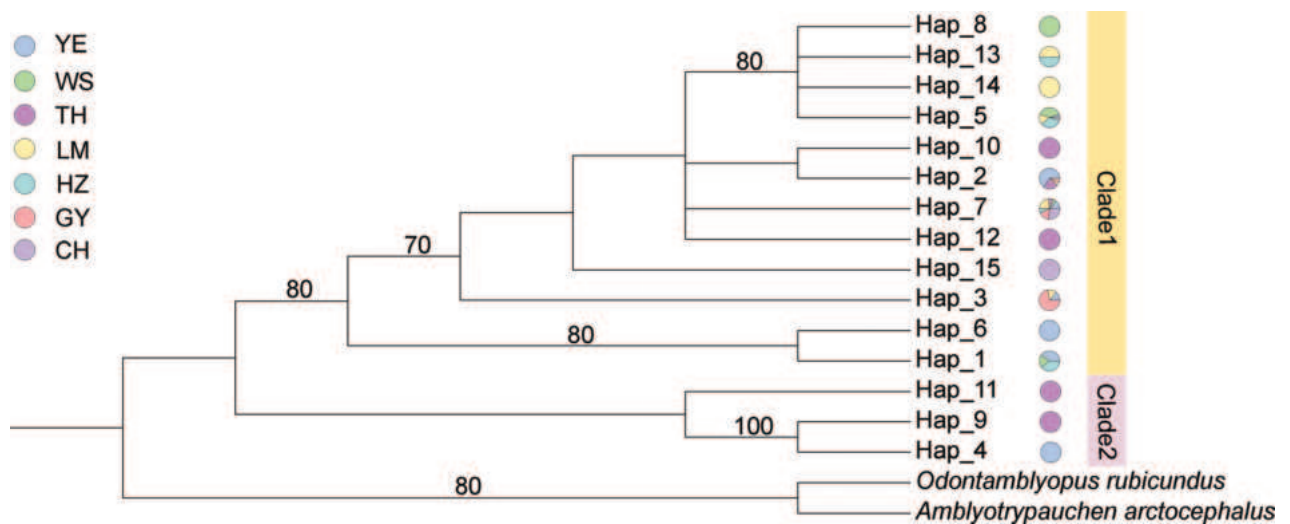


Figure 2. Maximum-likelihood phylogenetic tree constructed from mitochondrial D-loop regions of seven *Taenioides* sp. populations using 15 haplotypes. The number of nodes represents bootstrap values (%) for ML analysis.

Table 2. Pairwise *Fst* (below the diagonal) and genetic distances (above the diagonal) among seven populations of *Taenioides* sp. based on mtDNA D-loop regions.

Populations	YE	TH	GY	HZ	LM	WS	CH
YE		0.0110	0.0053	0.0067	0.0060	0.0068	0.0051
TH	0.0861		0.0105	0.0120	0.0112	0.0120	0.0104
GY	0.1130*	0.2767*		0.0037	0.0025	0.0037	0.0010
HZ	0.2204*	0.3477*	0.4213*		0.0029	0.0022	0.0036
LM	0.1326*	0.3039*	0.1737*	0.0955		0.0027	0.0021
WS	0.2715*	0.3767*	0.5405*	-0.0353	0.1753*		0.0036
CH	0.1674*	0.3085*	0.1610*	0.5414*	0.2805*	0.6670*	

*Statistically significant values ($p \leq 0.05$).

Table 3. AMOVA results among seven *Taenioides* sp. populations using D-loop regions.

Source of variation	df	Sum of squares	Variance components	Percentage of variation (%)	<i>Fst</i>
Among populations	6	85.7240	0.6300 Va	26.66	0.2666*
Within populations	134	232.2620	1.7333 Vb	73.34	
Total	140	317.9860	2.3633		

*Statistically significant values ($p \leq 0.05$).

Population demographic history

Tajima’s *D* and Fu’s *Fs* neutral tests were used to predict the demographic history of *Taenioides* sp. The results of neutral tests showed that the Tajima’s *D* or Fu’s *Fs* values of the GY, HZ, LM, WS, and CH populations were negative (Table 1), revealing that these populations probably experienced population expansion.

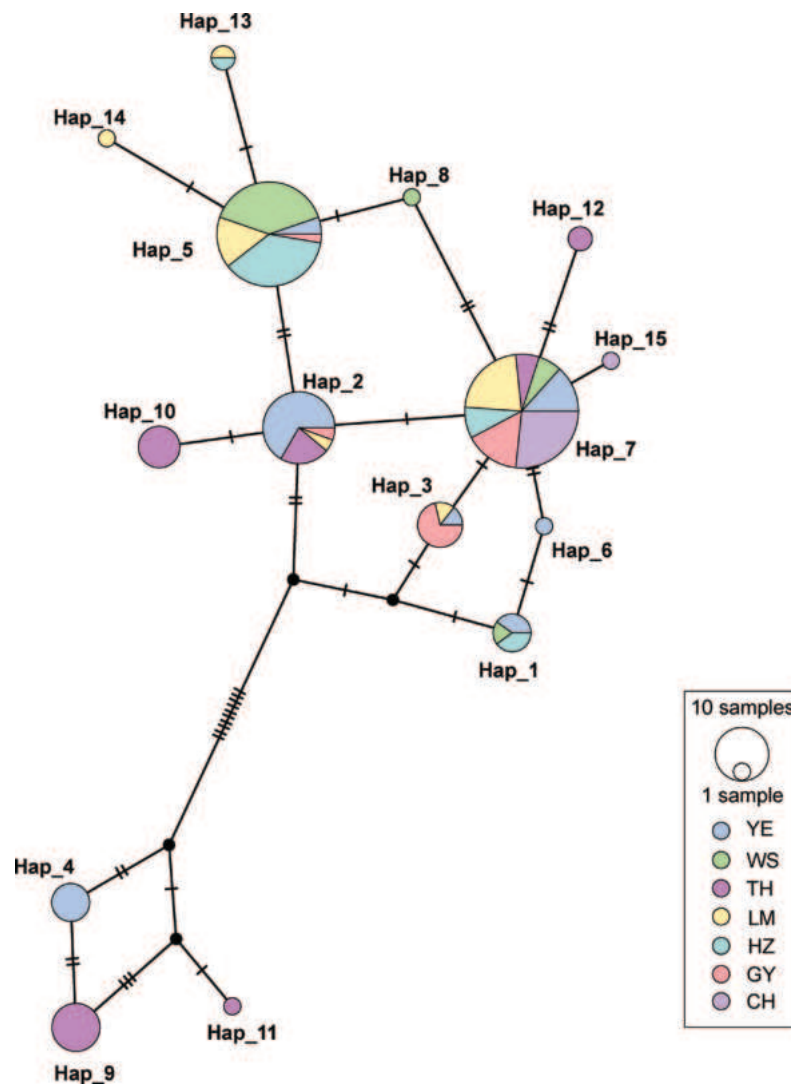


Figure 3. Haplotype network of seven *Taenioides* sp. populations developed with D-loop data. Each circle represents an observed haplotype; the colors reflect the sampling location, the unlabeled small black dots represent missing haplotypes, the small black lines represent the number of mutation steps, and the circle sizes are proportional to the number of samples per haplotype.

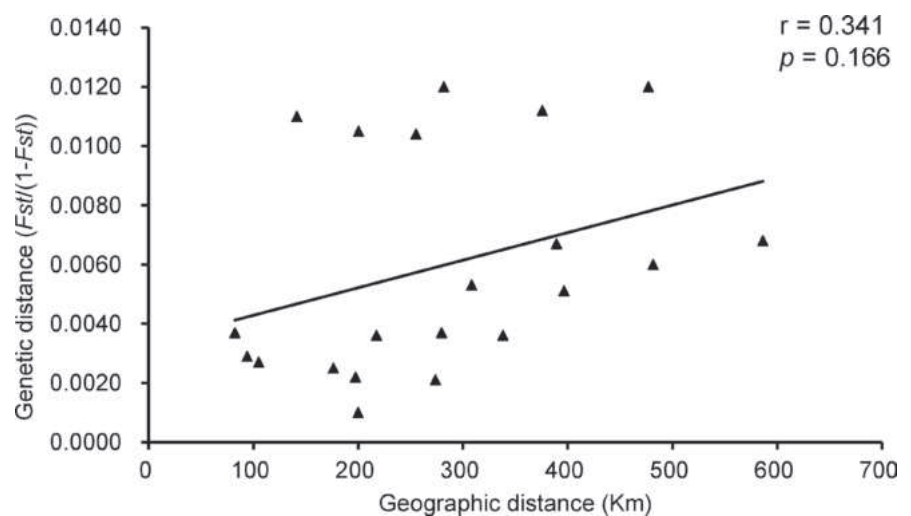


Figure 4. Scatter plots of genetic and geographic distances of *Taenioides* sp. populations.

Discussion

Genetic diversity generally refers to the sum of the genetic variation of individuals within a species or a population (Wu et al. 2020), which is critical for evolution to adapt to the changing environment. It is traditionally believed that high genetic diversity will help invasive species better adapt to new habitats, making it easier to colonize successfully (Crawford and Whitney 2010). However, during invasions, the genetic diversity of alien species tends to suffer many deprivations, mainly attributed to the founder effects, genetic bottlenecks, or gene drift (Shi et al. 2010). The highest genetic diversity of seven *Taenioides* sp. populations was found in two southernmost sample locations, the Yangtze River Estuary and Taihu Lake. The H_d , k , and π values of the YE, TH, GY, HZ, LM, and WS *Taenioides* sp. populations showed a descending trend, revealing that the genetic diversity decreased from south to north. This trend is consistent with the regular pattern that the population's genetic diversity would gradually reduce during the invasion. Combined that the Yangtze River Estuary is one of the conventional habitats of *Taenioides* sp. in China (Wu and Zhong 2008), we speculate that *Taenioides* sp. from the YE and TH populations are the original individuals that invaded the inland waters of China. According to the records, Taihu Lake was first invaded by *Taenioides* sp. in 1960 (Ni and Wu 2006), making it the first inland freshwater lake to be invaded. *Taenioides* sp., which has resided in Taihu Lake for a long period, may have established a relatively stable population capable of maintaining high genetic diversity. *T. cirratus*, one of the representative invasive species of the genus *Taenioides*, has invaded Gaoyou Lake, Luoma Lake, Weishan Lake, and Chaohu Lake (Wang et al. 2017; Qin et al. 2019; Liang et al. 2020), also originating from the Yangtze Estuary and Taihu Lake (Qin et al. 2022). Similar cases have already been described in several invasive species, such as the Europe-introduced red swamp crayfish *Procambarus clarkii* (Barbaresi et al. 2007) and the Japan-introduced bluegill *Lepomis macrochirus* (Yonekura et al. 2007). The CH population, which has the shortest invasion history, may suffer from the most severe founder effect, resulting in the lowest genetic diversity. Considering that the Yangtze River and Taihu Lake are connected by rivers such as the Wangyu River, *Taenioides* sp. in Taihu Lake may come from the Yangtze River Estuary (Dai et al. 2018).

IBD is a common spatial pattern in invasive species (Johansson et al. 2018; Qin et al. 2022). However, IBD analysis for seven *Taenioides* sp. populations detected no significant association ($p = 0.166$) between genetic and geographic distances, revealing that the invasion of *Taenioides* sp. did not follow the active dispersal strategy. IBD is affected mainly by landscape connectivity and invasive species dispersal ability (Sherpa and Després 2021). Combined with that *Taenioides* sp. is a weakly swimming benthic fish (Wu and Zhong 2008), we inferred that active dispersal may not be the only way of invasion. The dam construction of a series of water conservancy projects since the 1960s, such as the water diversion to the northern plains of Jiangsu province, the South-to-North Water Diversion Project, and the water diversion to Chaohu Lake, reconstructed river connectivity and supplied a way for long-distance dispersal of *Taenioides* sp., resulted in a large number of *Taenioides* sp. introductions from the Yangtze River Estuary. Considering that the invasion time of *Taenioides* sp. at each site of the South-to-North Water Diversion Project roughly coincides with the construction time of the project, and the most severely invaded area is also an important node of the project, we infer

that human-mediated dispersal likely played an essential role in the invasion of *Taenioides* sp. A similar situation was described in the quagga mussel, a recent invader of the Thames River in Great Britain (Gallardo and Aldridge 2018). There was a severe risk of the mussel further spread through extensive water abstraction of the Thames Valley, which provided a direct link of isolated water basins. Water transfer projects are becoming one of the main approaches to freshwater invasions (Jażdżewski 1980; Leuven et al. 2009; Zhan et al. 2015; Zhao et al. 2019). Therefore, the potential risk of aquatic species invasion should be taken into consideration when constructing water transfer projects.

Interestingly, the *Taenioides* sp. individuals from the source populations (YE and TH) were found to diverge into two branches. One was clade 2, consisting of individuals that did not invade inland waters, and the other was clade 1, consisting of individuals which clustered with those from inland waters, from GY, HZ, LM, WS, and CH populations. Similar situations are common in invasive species, such as *Eurytemora affinis* (Winkler et al. 2008). *Eurytemora affinis*, a freshwater invasive copepod in the St. Lawrence River drainage basin, exhibited two clades of individuals inhabiting saline-alkali waters in its phylogenetic tree. One of the clades invaded freshwaters with the opening of the waterway, while the other was still limited to its original habitats. The results of physiological studies under a food-insufficient situation showed that some of the individuals from the saline-alkali environment can tolerate fresh water, while others cannot. Hence, we speculated that the reason *Taenioides* sp. from clade 2 failed to invade inland waters is attributed to the enormous differences in salinity between the sea and fresh waters. They failed to adapt to the freshwater environment. More studies are needed to explore the mechanism behind the difference in the invasion ability of the two clades. Individuals from YE, TH, HZ, LM, and WS populations were divided into two branches in clade 1 of the phylogenetic tree (Fig. 2), which suggested a graded invasion of *Taenioides* sp. in inland waters of China. The new subclade consisting of Hap_5, Hap_8, Hap_13, and Hap_14, with a higher degree of invasion, has already formed. To protect the local species diversity, stronger measures should be implemented to prevent the further spread of *Taenioides* sp. in the freshwaters of China.

Conclusions

Our study analyzed the genetic diversity and population structure of seven *Taenioides* sp. populations based on mitochondrial D-loop regions. The YE and TH populations held the highest genetic diversity and might be the source of other populations that invaded inland freshwater lakes. Combined with IBD analysis and the history of water conservancy projects, we hypothesized that water diversion may have contributed to the invasion of *Taenioides* sp. in inland lakes. We investigated how water conservancy projects transform an indigenous species into an invasive one and provided insights into assessing the potential impact of water conservancy projects on the natural ecosystem.

Acknowledgements

We are grateful to all members of the National Engineering Research Center for Marine Germplasm Resources Exploration and Utilization of the College of

Marine Sciences and Technology of Zhejiang Ocean University who contributed in any way to the success of this research.

Additional information

Conflict of interest

The authors have declared that no competing interests exist.

Ethical statement

The study was approved by the Animal Ethics Committee of Zhejiang Ocean University (ZOUMGREU-2023-000401).

Funding

This research was funded by the National Natural Science Foundation of China (NSFC), grant numbers 42171069.

Author contributions

Conceptualization, Zhenming Lü and Jing Liu; Data curation, Liqin Liu; Formal analysis, Chenhao Yao and Yantao Liu; Funding acquisition, Zhenming Lü; Investigation, Li Gong; Methodology, Jiaqi Fang; Project administration, Jing Liu; Resources, Zhenming Lü and Shijie Zhao; Software, Chenlian Sun; Supervision, Li Gong, Bingjian Liu and Liqin Liu; Validation, Chenlian Sun, Zhenming Lü and Jing Liu; Visualization, Bingjian Liu; Writing – original draft, Chenlian Sun; Writing – review & editing, Zhenming Lü and Jing Liu. All authors have read and agreed to the published version of the manuscript.

Author ORCIDs

Chenhao Yao  <https://orcid.org/0000-0002-1743-2155>

Data availability

Data available in a publicly accessible repository. The data presented in this study are openly available in NCBI at accession numbers PP001065–PP001079.

References

- Aljanabi SM, Martinez I (1997) Universal and rapid salt-extraction of high quality genomic DNA for PCR-based techniques. *Nucleic Acids Research* 25(22): 4692–4693. <https://doi.org/10.1093/nar/25.22.4692>
- Barbaresi S, Gherardi F, Mengoni A, Souty-Grosset C (2007) Genetics and invasion biology in fresh waters: a pilot study of *Procambarus clarkii* in Europe. In: Gherardi F (Eds) *Biological Invaders in Inland Waters: Profiles, Distribution, and Threats*. Springer, Dordrecht, 381–400. https://doi.org/10.1007/978-1-4020-6029-8_20
- Betancur-R R, Hines A, Acero PA, Ortí G, Wilbur AE, Freshwater DW (2011) Reconstructing the lionfish invasion: Insights into Greater Caribbean biogeography. *Journal of Biogeography* 38(7): 1281–1293. <https://doi.org/10.1111/j.1365-2699.2011.02496.x>
- Bohonak AJ (2002) IBD (isolation by distance): A program for analyses of isolation by distance. *The Journal of Heredity* 93(2): 153–154. <https://doi.org/10.1093/jhered/93.2.153>
- Cameron EK, Bayne EM, Coltman DW (2008) Genetic structure of invasive earthworms *Dendrobaena octaedra* in the boreal forest of Alberta: Insights into introduction

- mechanisms. *Molecular Ecology* 17(5): 1189–1197. <https://doi.org/10.1111/j.1365-294X.2007.03603.x>
- Chen X, Wang J, Huang L, Yue W, Zou J, Yuan C, Lu G, Wang C (2017) Evolutionary relationship of three mitten crabs (*Eriocheir* sp) revealed by mitogenome and 5S ribosomal DNA analysis. *Aquaculture and Fisheries* 2(6): 256–261. <https://doi.org/10.1016/j.aaf.2017.10.004>
- Cheng XY, Cheng FX, Xu RM, Xie BY (2008) Genetic variation in the invasive process of *Bursaphelenchus xylophilus* (Aphelenchida: Aphelenchoididae) and its possible spread routes in China. *Heredity* 100(4): 356–365. <https://doi.org/10.1038/sj.hdy.6801082>
- Corin SE, Ritchie PA, Lester PJ (2008) Introduction pathway analysis into New Zealand highlights a source population 'hotspot' in the native range of the red imported fire ant (*Solenopsis invicta*). *Sociobiology* 52(1): 129–143.
- Crawford KM, Whitney KD (2010) Population genetic diversity influences colonization success. *Molecular Ecology* 19(6): 1253–1263. <https://doi.org/10.1111/j.1365-294X.2010.04550.x>
- Daane KM, Middleton MC, Sforza RFH, Kamps-Hughes N, Watson GW, Almeida RPP, Correa MCG, Downie DA, Walton VM (2018) Determining the geographic origin of invasive populations of the mealybug *Planococcus ficus* based on molecular genetic analysis. *PLoS ONE* 13(3): e0193852. <https://doi.org/10.1371/journal.pone.0193852>
- Dai J, Wu S, Wu X, Xue W, Yang Q, Zhu S, Wang F, Chen D (2018) Effects of water diversion from Yangtze River to Lake Taihu on the phytoplankton habitat of the Wangyu River channel. *Water (Basel)* 10(6): 759. <https://doi.org/10.3390/w10060759>
- Darling JA, Blum MJ (2007) DNA-based methods for monitoring invasive species: A review and prospectus. *Biological Invasions* 9(7): 751–765. <https://doi.org/10.1007/s10530-006-9079-4>
- Diaz F, Endersby NM, Hoffmann AA (2015) Genetic structure of the whitefly *Bemisia tabaci* populations in Colombia following a recent invasion. *Insect Science* 22(4): 483–494. <https://doi.org/10.1111/1744-7917.12129>
- Excoffier L, Laval G, Schneider S (2007) Arlequin (version 3.0): An integrated software package for population genetics data analysis. *Evolutionary Bioinformatics Online* 1: 47–50. <https://doi.org/10.1177/117693430500100003>
- Fang D, Luo H, He M, Mao C, Kuang Z, Qi H, Xu D, Tan L, Li Y (2022) Genetic diversity and population differentiation of naked carp (*Gymnocypris przewalskii*) revealed by cytochrome oxidase subunit I and D-loop. *Frontiers in Ecology and Evolution* 10: 827654. <https://doi.org/10.3389/fevo.2022.827654>
- Freshwater DW, Hines A, Parham S, Wilbur A, Sabaoun M, Woodhead J, Akins L, Purdy B, Whitfield PE, Paris CB (2009) Mitochondrial control region sequence analyses indicate dispersal from the US East Coast as the source of the invasive Indo-Pacific lionfish *Pterois volitans* in the Bahamas. *Marine Biology* 156(6): 1213–1221. <https://doi.org/10.1007/s00227-009-1163-8>
- Gallardo B, Aldridge DC (2018) Inter-basin water transfers and the expansion of aquatic invasive species. *Water Research* 143: 282–291. <https://doi.org/10.1016/j.watres.2018.06.056>
- Hasegawa M, Kishino H, Yano T (1985) Dating of the human-ape splitting by a molecular clock of mitochondrial DNA. *Journal of Molecular Evolution* 22(2): 160–174. <https://doi.org/10.1007/BF02101694>
- Hulme P (2009) Trade, transport and trouble: Managing invasive species pathways in an era of globalization. *Journal of Applied Ecology* 46(1): 10–18. <https://doi.org/10.1111/j.1365-2664.2008.01600.x>

- Jażdżewski K (1980) Range extensions of some gammaridean species in European inland waters caused by human activity. *Crustaceana* (Supplement 6): 84–107.
- Johansson ML, Dufour BA, Wellband KW, Corkum LD, MacIsaac HJ, Heath DD (2018) Human-mediated and natural dispersal of an invasive fish in the eastern Great Lakes. *Heredity* 120(6): 533–546. <https://doi.org/10.1038/s41437-017-0038-x>
- Kumar S, Stecher G, Li M, Knyaz C, Tamura K (2018) MEGA X: Molecular evolutionary genetics analysis across computing platforms. *Molecular Biology and Evolution* 35(6): 1547–1549. <https://doi.org/10.1093/molbev/msy096>
- Leigh JW, Bryant D (2015) POPART: Full-feature software for haplotype network construction. *Methods in Ecology and Evolution* 6(9): 1110–1116. <https://doi.org/10.1111/2041-210X.12410>
- Leuven RSEW, van der Velde G, Bajens I, Snijders J, van der Zwart C, Lenders HJR, bij de Vaate A (2009) The river Rhine: A global highway for dispersal of aquatic invasive species. *Biological Invasions* 11(9): 1989–2008. <https://doi.org/10.1007/s10530-009-9491-7>
- Liang Y, Fang T, Li J, Yang K, Zhao X, Cui K, Lu W (2020) Age, growth and reproductive traits of invasive goby *Taenioides cirratus* in the Chaohu Lake, China. *Journal of Applied Ichthyology* 36(2): 219–226. <https://doi.org/10.1111/jai.14024>
- Librado P, Rozas J (2009) DnaSP v5: A software for comprehensive analysis of DNA polymorphism data. *Bioinformatics* (Oxford, England) 25(11): 1451–1452. <https://doi.org/10.1093/bioinformatics/btp187>
- Murdy EO, Randall JE (2002) *Taenioides kentalleni*, a new species of eel goby from Saudi Arabia (Gobiidae: Amblyopinae). *Zootaxa* 93(1): 1–6. <https://doi.org/10.11646/zootaxa.93.1.1>
- Nei M, Li WH (1979) Mathematical model for studying genetic variation in terms of restriction endonucleases. *Proceedings of the National Academy of Sciences of the United States of America* 76(10): 5269–5273. <https://doi.org/10.1073/pnas.76.10.5269>
- Ni Y, Wu H (2006) *Fishes of Jiangsu province*. China Agriculture Press, Beijing, 34 pp.
- Okada M, Ahmad R, Jasieniuk M (2007) Microsatellite variation points to local landscape plantings as sources of invasive pampas grass (*Cortaderia selloana*) in California. *Molecular Ecology* 16(23): 4956–4971. <https://doi.org/10.1111/j.1365-294X.2007.03568.x>
- Paria P, Behera BK, Mohapatra PKD, Parida PK (2021) Virulence factor genes and comparative pathogenicity study of *tdh*, *trh* and *tli* positive *Vibrio* parahaemolyticus strains isolated from Whiteleg shrimp, *Litopenaeus vannamei* (Boone, 1931) in India. *Infection, Genetics and Evolution* 95: 105083. <https://doi.org/10.1016/j.meegid.2021.105083>
- Parmaksiz A (2018) Population genetic diversity of Yellow Barbell (*Carasobarbus luteus*) from Kueik, Euphrates and Tigris rivers based on mitochondrial DNA D-loop sequences. *Turkish Journal of Fisheries and Aquatic Sciences* 20(1): 79–86. https://doi.org/10.4194/1303-2712-v20_1_08
- Qin J, Cheng F, Zhang L, Schmidt BV, Liu J, Xie SG (2019) Invasions of two estuarine gobiid species interactively induced from water diversion and saltwater intrusion. *Management of Biological Invasions : International Journal of Applied Research on Biological Invasions* 10(1): 139–150. <https://doi.org/10.3391/mbi.2019.10.1.09>
- Qin J, Victor SB, Zhang L, Cheng F, Xie SG (2022) Patterns of genetic diversity: Stepping-stone dispersal of an invasive fish introduced by an inter-basin water transfer project. *Freshwater Biology* 67(12): 2078–2088. <https://doi.org/10.1111/fwb.13997>

- Roy HE, Peyton J, Aldridge DC, Bantock T, Blackburn TM, Britton R, Clark P, Cook E, Dehnen-Schmutz K, Dines T, Dobson M, Edwards F, Harrower C, Harvey MC, Minchin D, Noble DG, Parrott D, Pocock MJ, Preston CD, Roy S, Salisbury A, Schonrogge K, Sewell J, Shaw RH, Stebbing P, Stewart AJ, Walker KJ (2014) Horizon scanning for invasive alien species with the potential to threaten biodiversity in Great Britain. *Global Change Biology* 20(12): 3859–3871. <https://doi.org/10.1111/gcb.12603>
- Saeidi Z, Gilkolaei SR, Soltani M, Laloei F (2014) Population genetic studies of *Liza aurata* using D-Loop sequencing in the southeast and southwest coasts of the Caspian Sea. *Iranian Journal of Fisheries Science* 13(1): 216–227.
- Sherpa S, Després L (2021) The evolutionary dynamics of biological invasions: A multi-approach perspective. *Evolutionary Applications* 14(6): 1463–1484. <https://doi.org/10.1111/eva.13215>
- Shi W, Geng Y, Ou X (2010) Genetic diversity and invasion success of alien species: Where are we and where should we go? *Shengwu Duoyangxing* 18(6): 590. <https://doi.org/10.3724/SP.J.1003.2010.590>
- Thompson JD, Gibson TJ, Plewniak F, Jeanmougin F, Higgins DG (1997) The CLUSTAL_X windows interface: Flexible strategies for multiple sequence alignment aided by quality analysis tools. *Nucleic Acids Research* 25(24): 4876–4882. <https://doi.org/10.1093/nar/25.24.4876>
- Wang Y, Li X, Ke H, Cong X, Shi J (2017) Application of DNA barcoding gene *COI* for identifying *Taenioides cirratus* in Nansi Lake. *Shuichanxue Zazhi* 30(6): 12–18.
- Winkler G, Dodson JJ, Lee CE (2008) Heterogeneity within the native range: Population genetic analyses of sympatric invasive and noninvasive clades of the freshwater invading copepod *Eurytemora affinis*. *Molecular Ecology* 17(1): 415–430. <https://doi.org/10.1111/j.1365-294X.2007.03480.x>
- Wu H, Zhong J (2008) *Fauna Sinica: Ostichthyes Perciformes (V) Gobioidae*. Science Press, Beijing, 922 pp.
- Wu X, Duan L, Chen Q, Zhang D (2020) Genetic diversity, population structure, and evolutionary relationships within a taxonomically complex group revealed by AFLP markers: A case study on *Fritillaria cirrhosa* D. Don and closely related species. *Global Ecology and Conservation* 24(2): e01323. <https://doi.org/10.1016/j.gecco.2020.e01323>
- Yao C, Zhao S, Chen J, Zhu K, Fang J, Liu L, Lü Z (2022) Molecular and morphological analyses suggest cryptic diversity of eel gobies, genus *Taenioides* (Gobiidae), in coastal waters of China. *Journal of Ichthyology* 62(6): 1025–1033. <https://doi.org/10.1134/S0032945222060315>
- Yonekura R, Kawamura K, Uchii K (2007) A peculiar relationship between genetic diversity and adaptability in invasive exotic species: Bluegill sunfish as a model species. *Ecological Research* 22(6): 911–919. <https://doi.org/10.1007/s11284-007-0357-0>
- Yue GH, Feng JB, Xia JH, Cao SY, Wang CM (2021) Inferring the invasion mechanisms of the red swamp crayfish in China using mitochondrial DNA sequences. *Aquaculture and Fisheries* 6(1): 35–41. <https://doi.org/10.1016/j.aaf.2020.04.003>
- Zhan A, Zhang L, Xia Z, Ni P, Xiong W, Chen Y, Douglas Haffner G, MacIsaac HJ (2015) Water diversions facilitate spread of non-native species. *Biological Invasions* 17(11): 3073–3080. <https://doi.org/10.1007/s10530-015-0940-1>
- Zhao N, Xu M, Blanckaert K, Qiao C, Zhou H, Niu X (2019) Study of factors influencing the invasion of golden mussels (*Limnoperna fortunei*) in water transfer projects. *Aquatic Ecosystem Health & Management* 22(4): 385–395. <https://doi.org/10.1080/14634988.2019.1698860>

An annotated catalogue of selected historical type specimens, including genetic data, housed in the Natural History Museum Vienna

Anja Palandačić^{1,2}, Min J. Chai¹, Gennadiy A. Shandikov¹, Nesrine Akkari³, Pedro R. Frade⁴, Susanne Randolph⁵, Hans-Martin Berg⁶, Ernst Mikschi¹, Nina G. Bogutskaya^{1,7}

1 Fish collection, First Zoological Department, Natural History Museum Vienna, Burgring 7, 1010 Vienna, Austria

2 Department of Biology, Biotechnical Faculty, University of Ljubljana, Jamnikarjeva 101, SI-1000 Ljubljana, Slovenia

3 Myriapoda collection, Third Zoological Department, Natural History Museum Vienna, Burgring 7, 1010 Vienna, Austria

4 Evertebrata Varia collection, Third Zoological Department, Natural History Museum Vienna, Burgring 7, 1010 Vienna, Austria

5 Neuropterida-Orthopteroidea-Insecta Varia collection, Second Zoological Department, Natural History Museum Vienna, Burgring 7, 1010 Vienna, Austria

6 Bird collection, First Zoological Department, Natural History Museum Vienna, Burgring 7, 1010 Vienna, Austria

7 BIOTA j.d.o.o., Dolga Gora 2, 3232 Ponikva, Slovenia

Corresponding author: Anja Palandačić (anja.palandacic@nhm-wien.ac.at)



Academic editor: Fedor Konstantinov

Received: 21 December 2023

Accepted: 8 April 2024

Published: 30 May 2024

ZooBank: <https://zoobank.org/74DDEA6C-E7BA-4731-99E9-092F8BC32EAB>

Citation: Palandačić A, Chai MJ, Shandikov GA, Akkari N, Frade PR, Randolph S, Berg H-M, Mikschi E, Bogutskaya NG (2024) An annotated catalogue of selected historical type specimens, including genetic data, housed in the Natural History Museum Vienna. ZooKeys 1203: 253–323. <https://doi.org/10.3897/zookeys.1203.117699>

Copyright: © Anja Palandačić et al.

This is an open access article distributed under terms of the Creative Commons Attribution License (Attribution 4.0 International – CC BY 4.0).

Abstract

Museum collections are an important source for resolving taxonomic issues and species delimitation. Type specimens as name-bearing specimens, traditionally used in morphology-based taxonomy, are, due to the progress in historical DNA methodology, increasingly used in molecular taxonomic studies. Museum collections are subject to constant deterioration and major disasters. The digitisation of collections offers a partial solution to these problems and makes museum collections more accessible to the wider scientific community. The Extended Specimen Approach (ESA) is a method of digitisation that goes beyond the physical specimen to include the historical information stored in the collection. The collections of the Natural History Museum Vienna represent one of the largest non-university research centres in Europe and, due to their size and numerous type specimens, are frequently used for taxonomic studies by visiting and resident scientists. Recently, a version of ESA was presented in the common catalogue of the Fish and Evertebrata Varia collections and extended to include genetic information on type specimens in a case study of a torpedo ray. Here the case study was extended to a heterogeneous selection of historical type series from different collections with the type locality of Vienna. The goal was to apply the ESA, including genetic data on a selected set of type material: three parasitic worms, three myriapods, two insects, twelve fishes, and one bird species. Five hundred digital items (photographs, X-rays, scans) were produced, and genetic analysis was successful in eleven of the 21 type series. In one case a complete mitochondrial genome was assembled, and in another case ten short fragments (100–230 bp) of the cytochrome oxidase I gene were amplified and sequenced. For five type series, genetic analysis confirmed their taxonomic status as previously recognised synonyms, and for one the analysis supported its status as a distinct species. For two species, genetic information was provided for the first time. This catalogue thus demonstrates the usefulness of ESA in providing digitised data of types that can be easily made available to scientists worldwide for further study.

Key words: Biodiversity, digitisation, historical DNA, type locality Vienna, zoological collections

Introduction

Museum collections are the largest archives of biodiversity, encompassing taxonomic, spatial, and temporal variation (Webster 2017). As such, they are an important source for studying demographic (Hoeksema and Koh 2009; van der Meij et al. 2009; Hoeksema et al. 2011; Meineke et al. 2018) and climatic changes (van der Meij et al. 2010; Robbirt et al. 2014), as well as for resolving taxonomic questions (Stoev et al. 2013; Silva et al. 2017, 2019; Antić and Akkari 2020; Kehlmaier et al. 2020; Straube et al. 2021) and the species delimitation (Agne et al. 2022a, 2022b) of (sometimes) extinct species (Feigin et al. 2017; Palandačić et al. 2023). Type specimens as name-bearing specimens, traditionally used in morphology-based taxonomy (Maxted 1992; Winston 1999), are, due to the progress in historical DNA (as defined in Raxworthy and Smith 2021) methodology, increasingly used in molecular taxonomy studies (e.g., Federhen 2014; Li et al. 2015; Straube et al. 2021; Agne et al. 2022a; Sullivan et al. 2022). While barcoding projects have provided a method for rapid species identification (Goldstein and DeSalle 2011; Kress and Erickson 2012), only genotyping of the type specimen(s) provides an explicit link between a genetic lineage (or in some cases a specific sequence) and the species name (Prosser et al. 2016; Castañeda-Rico et al. 2022). Nevertheless, there is often a (taxonomic) ambiguity associated with the type series and the specimens it contains (e.g., van Steenberge et al. 2016; Agatha et al. 2021), and therefore a careful examination of the associated historical information should be carried out in order to contextualise the acquired genetic data appropriately (Durette-Desset and Digiani 2010; Renner 2016; Kehlmaier et al. 2020).

Museum collections are subject to gradual but constant deterioration, as well as catastrophes of major proportions (recently reviewed in Tyler et al. (2023)). The digitisation of collections offers a partial solution to these problems and, although digital data can never replace the physical specimen, it can be seen as an insurance policy. At the same time, through online databases or other shared resources (Lendemmer et al. 2020; Monfils et al. 2022; Hardisty et al. 2023), digitisation makes museum collections more accessible to the wider scientific community and to researchers from disadvantaged or distant countries who may not have the opportunity to see the specimen in person (open science concept). The Extended Specimen Approach (ESA; Webster 2017; Lendemmer et al. 2020) is a method of digitisation that goes beyond the physical specimen, e.g., photographs, X-rays, CT scans (Stoev et al. 2013; Akkari et al. 2015, 2018), but also includes all its attributes, such as historical information stored in the collection in the form of acquisition and inventory books, inventory cards and labels (Haston et al. 2012; Albano et al. 2018; Price et al. 2018; Zahiri et al. 2021; Bogutskaya et al. 2022; Takano et al. 2024).

Founded more than 270 years ago, the collections of the Natural History Museum Vienna (NHMW) represent one of the largest non-university research centres in Europe, with both historic and recent specimens of most animal groups. The collections date back to the United Imperial Royal Natural History Cabinet of the early 18th century and are the result of many expeditions and material collected by naval personnel on special missions, as well as many specimens donated, purchased, or exchanged (Kähsbauer 1959; Fischer et al. 1976; Hamann 1976; Schefbeck 1996; Herzig-Straschil 1997). Due to their size and extensive representation of type specimens, the collections are repeatedly used in taxonomic studies by

visiting and resident scientists. Currently, the collections are in various stages of digitisation (e.g., Fig. 1) and a museum-wide database covering all NHMW collections is being developed, but none of the collections are yet available online. Thus, the holdings of the museum have been reviewed in a series of 20 volumes of Catalogues of the scientific collections of the Natural History Museum Vienna (Kataloge der wissenschaftlichen Sammlungen des Naturhistorischen Museums in Wien) published 1978–2007, and are regularly presented in illustrated and annotated catalogues of different taxonomic groups (e.g., Wirkner et al. 2002; Schileyko and Stagl 2004; Stagl and Stoev 2005; Stagl and Zapparoli 2006; Schifter et al. 2007; Ilie et al. 2009; Zettel et al. 2022, 2023; van den Elzen et al. 2023), by collectors or authors (e.g., Albano et al. 2018), or only type specimens by taxa or/and authors (e.g., Saint Quentin 1970; Schifter 1991; Gemel et al. 2019).

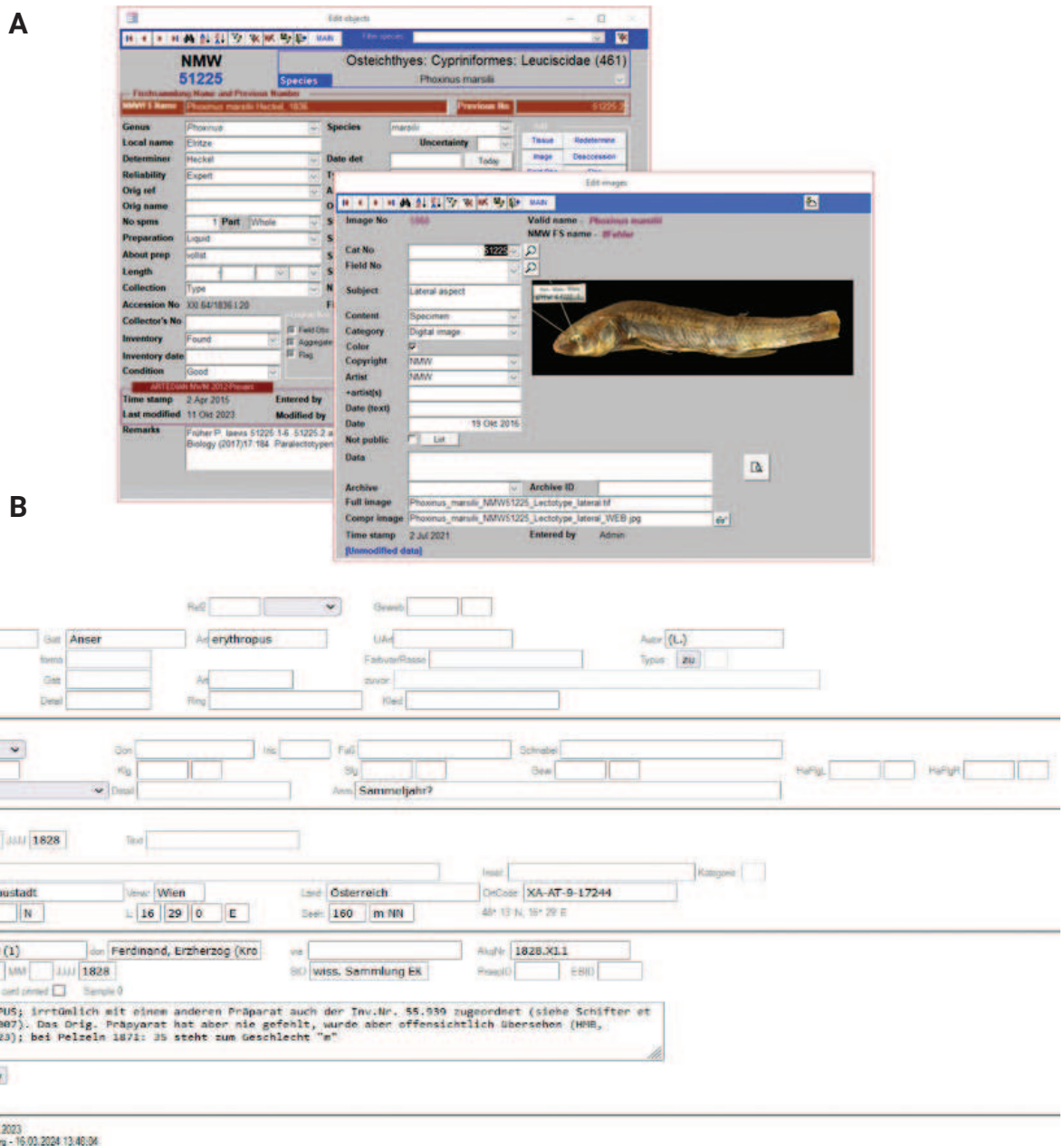


Figure 1. **A** an example of the Fish collection and **B** bird collection databases presenting lectotype of *Phoxinus marsilii* Heckel, 1836 and *Anser brevirostris* Brehm, 1831.

Similarly, a version of this approach was presented in the common catalogue of the NHMW Fish and Evertebrata Varia collections published recently (Bogutskaya et al. 2022), and extended to include genetic information on type specimens in a case study of a torpedo ray (Palandačić et al. 2023). Here, this case study has been extended to heterogeneous selection of historical type series from different collections, with the common denominator of the type locality Vienna. Thus, the goal of this catalogue is to apply the ESA as presented earlier (digitisation of physical specimens, associated historical information; Bogutskaya et al. (2022)) and including genetic data (where possible; see Palandačić et al. (2023: fig. 1)), on a wide variety of type material: three parasitic-worm, three myriapod, two insect, twelve fish, and one bird species. The catalogue includes historical information and literature in which they were mentioned, as well as genetic data where the analysis was successful.

Background on the authors of the species names

Chromadorea and Trematoda type series

The Chromadorea and Trematoda type series represented in this catalogue are a part of the Parasitic-worms collection (for further reading see Sattmann et al. (2000, 2001), Sattmann (2002), Stagl and Sattmann (2013)), which is a part of the larger Evertebrata Varia (EV) collection, and were described by Maximilian Braun, Leopold Karl Böhm, and Rudolf Supperer.

Maximilian Braun (1850–1930) was an ornithologist, zoologist, and physician whose main focus was on the trematode parasites of birds. As an anatomist, Braun contributed greatly to the medical field of parasitology. Born in Myslowitz in 1850, Braun studied medicine and natural sciences before obtaining his doctorate in 1877. Braun was a full Professor of zoology and comparative anatomy at the University of Rostock and later in Königsberg (now Kaliningrad), where he was director of the Zoological Museum and where he would die in 1930. In 1916–1917 he was president of the German Zoological Society. During his career, Maximilian Braun published several zoological books, such as *Developmental history of the Tapeworm (Entwicklungsgeschichte des Bandwurms)* (Braun 1883), and also on parasitology, such as *A handbook of Practical Parasitology (Ein Handbuch der praktischen Parasitologie)* (Braun and Lühe 1910).

Leopold Karl Böhm (1886–1958) was a veterinarian, zoologist, and parasitologist. Born in Vienna in 1886, Böhm received his doctorate in 1910 and his veterinary degree in 1916, becoming an associate Professor in 1924 and a Professor in 1937. Böhm went on to head the Institute of General Zoology and Parasitology at the University of Veterinary Medicine in Vienna, and later serving as its rector (1948–1950) and vice-rector (1950–1952). In 1941, Böhm became a full member of the Austrian Academy of Sciences and died in Vienna in 1958. Böhm published numerous scientific papers in zoological and veterinary journals and was co-editor of several journals (e.g., the *Vienna Veterinary Monthly (Wiener Tierärztliche Monatsschrift)*, the *Journal of Scientific Biology (Zeitschrift für wissenschaftliche Biologie)*, the *Journal of Parasitology (Zeitschrift für Parasitenkunde)*, and the *Austrian Zoological Journal (Österreichische Zoologische Zeitschrift)*).

Rudolf Supperer (1918–2006) was a veterinary surgeon and student of Leopold Karl Böhm, who later became Professor of Parasitology and General Zoology at the University of Veterinary Medicine in Vienna. Born in Kirchstetten in 1918, Supperer was also rector of the University of Veterinary Medicine from 1967 to 1969. Together with Böhm, Supperer established the genus name *Wehrdikmansia*, in honour of the work of Wehr and Dikmans, who described numerous filarioid nematodes (family Filariidae; Wehr and Dikmans (1935)) associated with various diseases of North American mammals such as sheep, deer, or elk.

Diplopoda type series

The Diplopoda type series represented in this catalogue are a part of Myriapoda collection (MY; for further reading see Stagl 2006) and were described by Robert Latzel and Carl Attems.

Robert Latzel (1845–1919), a pioneer in myriapodology, was born in Silesia (today's Czech Republic). Although his main profession at that time was a teacher of natural history at high schools and later a principal of the main grammar school in Klagenfurt, Carinthia, since 1875, he studied myriapods. His major work (Latzel 1884) was considered a turning point in millipede systematics, as he was the first to emphasize on the importance of the gonopods (modified legs used for copulation in millipedes) for the taxonomy of the group. Latzel sold large collections to the NHMW in 1884 and in 1919, the year of his death. The collection contained ca 545 species and 8098 specimens. The main issue with these samples is that Latzel did not give precise information on the localities of the species, neither in the original description of new species and variations, nor on the labels in the jars of his collection. This information could however be retrieved only from the book of acquisitions for 1884, written in red ink by Latzel himself (Stagl 2006).

The collection owes its value also to the imminent Austrian myriapodologist Carl Attems (1894–1952), examined material from nearly all parts of the world, described ca 1700 species and published 138 papers, monographs, and textbooks.

Insecta type series

The Insecta type series represented in this catalogue are a part of the Neuropterida-Orthopteroidea-Insecta Varia collection (ORTH; for further reading see Kaltenbach 2001) and were described by Vinzenz Kollar and Hermann Krauss.

Detailed biographical data on Vinzenz Kollar (1797–1860) can be found in von Wurzbach (1864) and in two obituaries by Schiner (1860) and Schrötter (1861). The latter includes a bibliography and dates of birth and death that differ from other sources. Recent publications deal with different aspects of this versatile researcher (Thaler and Gruber 2003; Rabitsch 2006; Christian 2008; Zuna-Kratky 2017). The following is a brief summary of Kollar's life and work in relation to the insect collection.

Vinzenz Kollar was born in Kranowitz (then Prussian Silesia, now Poland) on 15 January 1797. After completing his education, he moved to Vienna in 1815 to study medicine. His growing interest in entomology led him to the Natural History Cabinet in 1817, where he met the curator of the insect collection, Franz

Anton Ziegler (1760–1842). Under his guidance, Kollar began to examine the existing collections and put them into a systematic order. Initially an unpaid volunteer, he was eventually given a permanent position and finally became the director of the Imperial Court Zoological Cabinet in 1851.

His first publication was a systematic work on a genus of beetles, inspired by the many collections made by explorers in Brazil (Kollar 1824). But far more than the diversity of forms, he seems to have been fascinated by the distribution, life-style, and development of insects. Over the years, in addition to faunistic works (e.g., Kollar 1831a, 1831b, 1833a, 1850), he published mainly on insects that were directly harmful to humans or indirectly harmful as pests in agriculture and forestry (e.g., Pohl and Kollar 1832; Kollar 1833b, 1837, 1842, 1850, 1855). Kollar's extensive collecting activities greatly increased the number of known locust species in Upper and Lower Austria. He listed 51 species and described four species new to science (Kollar 1833a). One of them still bears his name in its German common name: Kollars Höhlenschrecke, *Troglophilus cavicola* (Kollar, 1833).

Vinzenz Kollar was a member of the Austrian Academy of Sciences, awarded the Ritterkreuz of the Franz-Joseph Order and appointed a Geheimer Regierungsrat. After his death on 30 May 1860, he was buried in an honorary grave in the Vienna Central Cemetery.

The largest and most valuable addition to the Orthoptera collection was the Brunner von Wattenwyl collection, acquired by the Museum in 1901. At that time, it was one of the most important Orthoptera collections in the world, with some 79,500 specimens of 10,600 species. Carl Brunner von Wattenwyl (1823–1914) was a Swiss geologist who established telegraphy in Switzerland in 1851 and became director of the Austrian Post and Telegraph Administration in 1857 (Brunner 1914). His great passion for Orthoptera led him to start his own collection. As director of telegraphy he was also responsible for the expansion of the telegraph network in south-eastern Europe and Turkey. The collection also includes Orthoptera collected during his business trips to these areas (Directories I–VI of Brunner von Wattenwyl/2nd Zoological Department).

Not only did he collect himself, but he also actively traded and added to his collection through purchases. In 1859 he received from Rudolf Türk some alpine groundhoppers collected on the banks of the Danube. Not much is known about Rudolf Türk. His date of birth is given as “around 1820” (Zuna-Kratky et al. 2009) and his main occupation was probably imperial court secretary (Krauss 1876). In his publications he abbreviated his first name to “Rud.”. Türk summarised the results of his intensive collecting activities in Lower Austria in a detailed fauna listing 78 different species (Türk 1858, 1860, 1862).

The physician and entomologist Hermann Krauss (1848–1939) was in active correspondence with Brunner von Wattenwyl for several decades (Entomological letter collection Brunner von Wattenwyl (Entomologische Briefsammlung Brunner von Wattenwyl)/Second Zoological Department/NHMW) and worked as an assistant at the Natural History Court Museum (k. k. Naturhistorisches Hofmuseum) from 1876 to 1880. Later he returned to Tübingen and opened a medical practice (Kaltenbach 2001). The first description of a new species dates from his time in Vienna, which he named *Tetrix tuerki* in honour of Türk as a collector and for his faunistic works (Krauss 1876). In the description he noted that the species was only found in a few localities at the time and attributed this to the “reorganisation of the whole terrain”. The reorganisation refers to the

regulation of the Danube, which began in 1870 and led to the rapid and complete disappearance of the sandy, gravelly, sparsely vegetated alluvial soils so important for this species (Zuna-Kratky et al. 2009).

Actinopteri type series

The Actinopteri type series represented in this catalogue are a part of the Fish collection (FS from *Fischsammlung* in German; for further reading see Herzig-Straschil 1997; Mikschi 2009) and were described by Johann Jakob Heckel.

A detailed description of the life and scientific career of Johann Jakob Heckel (1790–1857) can be found in historical (Anonymous 1857a; von Wurzbach 1862; Carus 1880) and recent (Herzig-Straschil 1997; Svojtka et al. 2009, 2012) publications. In the following, we present a brief summary of Heckel's life and activities relevant to the subject of this study.

Johann Jakob Heckel, born on 23 January 1790 in Churpfalz (now Mannheim), began his career in 1818 as a volunteer taxidermist in the United Imperial Royal Natural History Cabinet in Vienna. In 1819–1820, Heckel travelled through Germany, Switzerland, and Italy, and in August 1820 he was officially employed as a taxidermist in the vertebrate department of the Natural History Cabinet in Vienna under the curator Joseph Natterer Jr. He began scientific studies of terrestrial and freshwater molluscs, birds, and fishes, paying particular attention to the Fish collection, which at that time consisted of only ca 700 specimens.

Under the guidance of the curator Leopold Joseph Fitzinger (1802–1884), Heckel participated in the preparation of a detailed inventory of Austrian fish fauna, first of the Danube, then of Lake Neusiedl, Lake Balaton, and the Upper Austrian lakes. In 1824 he travelled to Upper Austria and Salzburg for several months and made some useful acquaintances, including the well-known Swiss ichthyologist Louis J. R. Agassiz (1807–1873), who then spent a long period in Vienna in 1830. A number of fish specimens collected during these trips are still extant in the NHMW Fish collection (e.g., acquisitions 1824.II; Fig. 2).

On 26 February 1832, Heckel was appointed curator of the Fish collection of the Natural History Cabinet. A number of stuffed fishes collected by him were given to the Vienna University Museum (Fitzinger 1856), the so-called Old Collection



Figure 2. Directory I of the Brunner von Wattenwyl collection.

(Alte Sammlung); some collections were later returned to the NHMW. In 1835 Heckel was appointed second curator and soon after, in 1836, first curator, responsible for overseeing the incorporation of the collections from the disbanded “Brazilian Museum” and the subsequent rearrangement of the collections in the Natural History Cabinet. In the following years, Heckel also undertook expeditions to southern Hungary and Croatia (in 1839), Dalmatia and western Herzegovina (in August–September 1840, together with Rudolf Kner), and to the Tisza region, which enriched his knowledge, especially of the cyprinoids. These expeditions were extremely productive and a large number of new species were described.

Heckel was a skilled artist; his original drawings of scales, bones, teeth, and whole fishes were used as illustrations in his publications (e.g., Heckel 1843; Heckel and Kner 1857). Over 100 drafts of illustrations, still deposited in the NHMW Archive (in a sketchbook of Heckel, who used an instrument he developed to draw precise outlines), were made by Heckel “with mathematical accuracy using his ichthyometer” (Heckel 1852a: 109: “Sämmtliche Tafeln sind mittelst meines Ichthyometers mit mathematischer Genauigkeit angefertigt worden”). Heckel was particularly interested in some osteological features of the fishes he studied, such as the scale structure and the pharyngeal bones and teeth of cypriniforms. Many of his new species (including those discussed in this catalogue) were described on the basis of the shape and structure of the pharyngeal teeth. Heckel’s collection of cypriniform pharyngeal bones is still deposited in the NHMW Fish collection and comprises 184 catalogue numbers. Heckel also established a classification of cypriniform fishes based on the structure of the pharyngeal bones and teeth (“Dispositio systematica familiae Cyprinorum”, Heckel 1843: 1013–1043).

During the 1840s and 1850s, Heckel authored or contributed to more than 30 publications on recent fishes (e.g., Heckel 1850, 1851a, 1851c, 1851d, 1852a, 1852b), including the new species descriptions discussed in this catalogue (for a full bibliographic list, see Svojtka et al. (2012)). By this time, his reputation and expertise had brought him into close contact with the most eminent ichthyologists in Europe: Prince Charles Bonaparte, Johannes Müller, Louis Agassiz, and Achille Valenciennes.

In 1851, Emperor Franz Joseph ordered the reorganisation of the United Imperial Royal Natural History Cabinet into three administratively separate cabinets, and Heckel was appointed deputy curator of the Fish collection of the Court Zoological Cabinet. Johann Jakob Heckel died of ‘wasting’ (a long-term infection or tuberculosis) on 1. March 1857. He did not live to see the publication of the summary results on the fishes of Austria (Heckel and Kner 1857).

Aves type series

The two Aves types represented in this catalogue are a part of the Bird collection (VS from Vogelsammlung in German; for further reading see Bauernfeind 2003; Schifter 2010; Berg 2016) and were described by Christian Ludwig Brehm.

Christian Ludwig Brehm (1787–1864) was born on 24 January 1787 in Schönau vor dem Walde near Gotha, Thuringia, the son of a pastor. He studied theology at Jena and began a career as a tutor in 1810. In 1812 he became a pastor in Drackendorf, near Jena, and from 1813 until his death on 23 June 1864 he was the parish priest in Renthendorf, near Neustadt, Thuringia (Hildebrandt 1929; Kleinschmidt 1955; Gebhardt 1964).

Throughout his life, Brehm's deep interest in the world of birds coexisted with his pastoral duties, earning him an honoured position in German ornithology. His early fascination with birds, coupled with his expertise in taxidermy and bird collecting, culminated in a collection of at least 9000 bird specimens. This collection laid the foundation for his research into the differentiation of bird species. Initiated by Pastor Otto Kleinschmidt and Ernst Hartert, a significant part of Brehm's collection found its way to the Rothschild Museum in Tring, UK, and then to New York. Some parts of the collection eventually returned to the Alexander Koenig Museum in Bonn. Brehm's attention to minute morphological distinctions led to several species and subspecies descriptions, most notably in his comprehensive work *Handbook of the natural history of all birds in Germany (Handbuch der Naturgeschichte aller Vögel Deutschlands)* (Brehm 1831). Despite criticism of his typological taxonomic views, his descriptions of some 60 bird taxa remain valid to day (Hildebrandt 1929; Kleinschmidt 1955; Gebhardt 1964).

Brehm's other notable works include *Contributions to Ornithology (Beiträge zur Ornithologie, 3 volumes, 1820–1822)*, the world's first ornithological journal, *Ornis or the newest and most important of ornithology (Ornis oder das neueste und wichtigste der Vögelkunde; 3 issues, 1824–1827)* and *The entire bird catch (Der gesamte Vogelfang)* (Brehm 1855).

It is evident that Brehm was in contact with Johann Jakob Heckel, as a note at *Anser brevirostris* "Heckel" in the copy of *Handbook of the natural history of all birds in Germany* (Brehm 1831: 844–845), which is still kept in the department, indicates. Furthermore, an entry in the acquisition list of the NHMW's Bird collection for the year 1828 (1828.X.1–20) records the acquisition of 22 bird skins through an exchange with C.L. Brehm. In return, Brehm received an 'old *Crocodylus niloticus*' and a 'skin of *Equus zebra*', both of which were given to Heckel. This entry also shows the scientific exchange between Brehm and Heckel (Hildebrandt 1929; Kleinschmidt 1955; Gebhardt 1964).

Materials and methods

Extended Specimen Approach (ESA) as applied to the NHMW collections in this catalogue

The ESA, as previously applied to the NHMW collections (Bogutskaya et al. 2022; Palandačić et al. 2023) and adopted in this catalogue, includes the following information: (i) external morphological image files per specimen, including individual body parts and structures (structures of particular taxonomic importance in the groups concerned (e.g., the mouth to show the shape of the lips, the disc, the serration of the fin rays, the barbels in fish; or cuticular structures in insects); (ii) radiographs where appropriate; (iii) georeferencing of geographic localities (where possible), country, and comments clarifying the locality; (v) scanned or photographed copies of labels, acquisition and/or inventory records, original description; and (vi) comments on the nomenclatural status of the type specimen(s).

It is impossible to publish all the imagery and other prepared files, so these data have been linked to the associated physical voucher specimens via a database (Fig. 1) and/or are available from the authors on request.

Dates in the species accounts are given as they appear on the labels, catalogue cards, acquisition book and main inventory book. In some cases, it is not possible to distinguish between the date of collection, acquisition, and inventory (registration) based on existing written collection information sources. However, special searches were made for historical data on the routes and times of the collection trips under consideration, and the dates of collection and geographical location of type localities were clarified.

Recent preservation condition of type specimens was evaluated by a six-point grade: very poor – poor – bad – average – good – very good. The descriptions of the conditions are based on the definitions given in the Fish collection data base and are summarised in Table 1.

Table 1. The descriptions used for describing the preservation condition of specimens are based on the descriptions given in the Fish collection data base and are summarised here.

Condition	Description
Very poor	Fallen apart, completely destroyed; worse than dissected, maybe should be discarded.
Poor	Specimen not good for some systematic work, e.g., scale counts, colour or shape analysis.
Bad	Specimen not good but still suitable for some systematic work, e.g., shape analysis or radiography.
Average	Suitable for systematic work like some measurements and counts.
Good	Specimen well suitable for morphological analysis and photography or demonstration, but some damage to, e.g., fins.
Very good	Nice specimen suitable for photography or demonstration characters but not completely excellent.
Excellent	100% intact specimen; should be treated with great care.

Abbreviations

BL, body length; **ESA**, Extended Specimen Approach; **NHMW**, Natural History Museum of Vienna (Naturhistorisches Museum Wien); **NMW**, a traditional abbreviation used here for the Fish collection of NHMW catalogue numbers; **TL**, total length, **SL**, standard length. Abbreviations for conservation status of species follow those used in the IUCN Red List of Categories and Criteria (IUCN 2012).

Acquisition information

The set of Acquisition Sheets is a reliable source of original primary information that accompanied the specimens at the time of their accession to the collection. However, the earliest Acquisition Sheets (1806 to 1850s) do not constitute a true register analogous to a collection catalogue (they do not contain catalogue numbers), but rather a register to identify the materials in terms of from whom they were received: purchased (with the money paid indicated), donated, or exchanged. Identifications follow a sender or a person who filled in the acquisition list, and were sometimes later corrected or some information added. Localities are not always given, have been added later, or are not accurate, as the information would have been given on labels accompanying the specimens. However, these have often faded, been damaged or lost over time. As a result, the date of collection has often been lost or omitted, and only the date of acquisition is known. See also the Remarks section in the catalogue list.

A comment on the acquisition information in the Orthoptera collection relevant to this catalogue

There are no acquisition lists for the Orthoptera collection, apart from the directories (Figs 2, 3) kept by Brunner von Wattenwyl, in which he listed the acquisitions. He assigned over 26,500 numbers, with each number representing an average of 3 specimens.

A comment on the acquisition information in the Fish collection relevant to this catalogue

After the acquisition of the material, the identifications follow either a sender or a person who filled in the acquisition list (Josef Natterer, Fitzinger or Heckel), with later corrections and additions by Heckel (who was the only one to study the collection taxonomically at the time). Localities were sometimes added later by Heckel (an example is shown in Fig. 4). Information was sometimes later revised by Victor Pietschmann and later curators Paul Kähsbauer, Rainer Hacker, Barbara Herzig, and Ernst Mikschi.

The source of a large number of fish specimens received (purchased) by the Fish collection in the 1825–1840s, named ‘Laboratorio’ or ‘Laboratorium’, is not entirely clear. Judging by the context, it could have been a laboratory of the Natural History Cabinet itself, which was organisationally not part of the collections and was managed separately (M. Svojtka, pers. comm.); at least this “laboratory” was involved in some kind of aquatic studies or fisheries control. It is important to note that although no localities were given in the acquisition sheets (only “purchased from Laboratory”), many (but not all) labels on (in) jars and recorded in the inventory book contain localities (mostly Vienna (“Wien”)), but also Lake Neusiedl (“Neusidlersee”) and some others; all reasonably close to Vienna. This obviously means that at least when Victor Pietschmann (curator of the Fish collection 1919–1946) started the Inventory Book (presumably, late 1940s), the old (now lost) labels existed.

Samples

The sample set contains type series of 21 nominal species: three of parasitic worms, three of myriapods, two of insects, twelve of fishes, and one bird. Vernacular names are used here and throughout the text where generalisation is necessary, and original names when Latin names are given, for detailed classification see Table 2. They were collected within the present-day borders of the state of Vienna. However, as the type series also include specimens collected

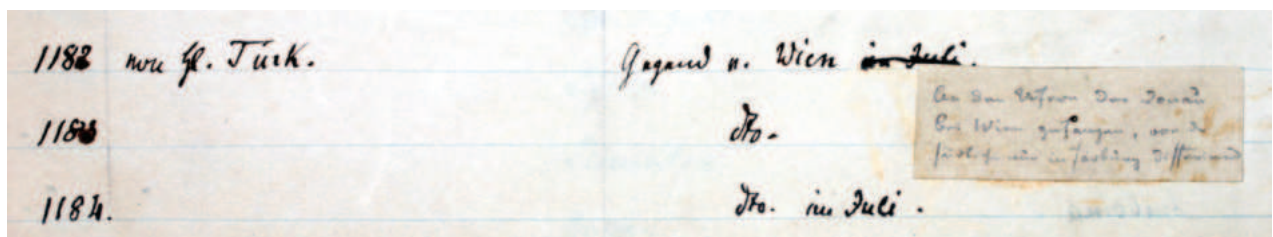


Figure 3. Handwritten entry 1859 of Brunner von Wattenwyl in his directory I with glued-in note.

1824
Sept. Von G. Heckel's Reise nach Oberösterreich II
3^{te} Kauf 2^{ter} Hof, C.M.G.

	Stück	Wegh.
1. <i>Salmo labellinus</i> -----	4.	Alb. - C. Sp. - Paris
2. <i>alpinus</i> -----	5.	Langhoff - Wien - 2 ^{te} Paris
3. <i>speciosa</i> var! -----	3.	Wien - Wien - 1 ^{te} Paris
4. <i>Tritta</i> -----	1.	Wien - Wien
5. <i>Fario</i> -----	3.	Wien
6. <i>Thymallus</i> -----	4.	Wien - Wien - 1 ^{te} Paris
7. <i>Maxana</i> -----	4.	Wien - Wien - 1 ^{te} Paris
8. <i>Cyprinus Wimba</i> -----	1.	Wien
9. <i>erythrophthalmus</i> -----	2.	Wien - Wien
10. <i>rutilus</i> -----	1.	Wien - Wien
11. <i>Alburnus Heckelii</i> -----	3.	Wien - Wien - 1 ^{te} Paris
	21	Stück Wien 7. Paris

7 Doublett
24
31.

Figure 4. Acquisition Sheet "1824.II" for samples purchased from Heckel, collected during his trip to Upper Austria; 1824.II.10 record is for [*Cyprinus*] *mento* (here as *heckelii*; see the account on *Aspius mento* for history of this species name).

elsewhere (e.g., Lower Austria), these have also been included in the catalogue and genetic analysis. The specimens were collected between the years 1824 and 1935 and are held in the NHMW collections, preserved in alcohol or dry mounted. Details are given in Table 3.

Genetic analysis

Different tissue types were sampled depending on the animal group. For myriapods and parasitic worms, a damaged (incomplete) syntype was selected and digested for DNA extraction. For insects, a leg was carefully removed from

Table 2. Classification of type series presented in this catalogue. The classification of fishes follows Van der Laan et al. (2023).

Coll.	Phylum	Subphylum	Class	Order	Family	Original name	Name
EV	Platyhelminthes		Trematoda	Plagiorchiida	Dicrocoeliidae	<i>Lyperosomum corrigia</i> Braun, 1901	parasitic worm
EV	Platyhelminthes		Trematoda	Plagiorchiida	Orchepedidae	<i>Orchepedum tracheicola</i> Braun, 1901	parasitic worm
EV	Nematoda		Chromadorea	Rhabditida	Onchocercidae	<i>Wehrdikmansia rugosicauda</i> Böhm & Supperer, 1935	parasitic worm
MY	Arthropoda	Myriapoda	Diplopoda	Polydesmida	Polydesmidae	<i>Brachydesmus superus</i> Latzel, 1884	myriapod
MY	Arthropoda	Myriapoda	Diplopoda	Julida	Julidae	<i>Cylindroiulus ignoratus</i> Attems, 1927; <i>Iulus scandinavicus</i> Latzel, 1884	myriapod
ORTH	Arthropoda		Insecta	Orthoptera	Rhaphidophoridae	<i>Locusta cavicola</i> Kollar, 1833	insect
ORTH	Arthropoda		Insecta	Orthoptera	Tetrigidae	<i>Tetrix tuerki</i> Krauss, 1876	insect
FS	Chordata		Actinopteri	Cypriniformes	Leuciscidae	<i>Abramis leuckartii</i> Heckel, 1836; <i>Abramis schreibersii</i> Heckel, 1836; <i>Alburnus breviceps</i> Heckel & Kner, 1858; <i>Aspius mento</i> Heckel, 1837; <i>Blicca argyroleuca</i> Heckel, 1843; <i>Cyprinus acuminatus</i> Heckel & Kner, 1858; <i>Idus melanotus</i> Heckel & Kner, 1858; <i>Idus miniatus</i> Heckel & Kner, 1858; <i>Leuciscus virgo</i> Heckel, 1852; <i>Phoxinus marsilii</i> Heckel, 1836; <i>Squalius delineatus</i> Heckel, 1843; <i>Squalius lepusculus</i> Heckel, 1852	fish
VS	Chordata		Aves	Anseriformes	Anatidae	<i>Anser brevirostris</i> Brehm, 1831	goose

Coll. – collection; EV – Evertebrata Varia; MY - Myriapoda collection; ORTH – Orthoptera collection; FS – Fish collection (from Fische Sammlung in German); VS – Bird collection (from Vogel Sammlung in German); Name – vernacular name used throughout the text when generalisation is necessary.

a topotype (collected with the holotype) and digested for DNA extraction. For fish, gill rakes were taken from the right side of the body, while for dry specimens, small pieces of tissue were cut from the (historical) incision used to stuff the fish. For bird species, small pieces of toe pads were used. The insect species *L. cavicola* is represented by only one poorly preserved syntype, which is already missing a leg and was therefore considered too valuable to be further damaged for genetic analysis. See Table 3 for more information.

Laboratory procedures were carried out in accordance with all requirements for working with museum material, including the use of UV-irradiated equipment, a clean room and negative extraction controls. For alcohol preserved samples, DNA was extracted from air-dried tissue using the QIAamp® DNA Blood and Tissue Micro Kit (Qiagen) following the manufacturer's protocol, but with the addition of 40 µl of 100 mM dithiothreitol to the lysis buffer (to enhance lysis, following Hawkins et al. 2022). For dry samples, tissue (toe pads, leg) was first pre-washed with water to remove dust and potential contaminants and then the same extraction protocol was followed. For lysis, samples were incubated overnight, but the time was extended if necessary until the tissue was completely dissolved.

After DNA extraction, the amount of double-stranded DNA was assessed by fluorometry (Qubit; ThermoFisher Scientific) using the Double-stranded DNA

Table 3. Type series described in this catalogue.

Collection	Original name	Valid name	Inventory number	Type status	Year	Preservation
EV	<i>Lyperosomum corrigia</i> Braun, 1901	<i>Lyperosomum corrigia</i>	4429	SYN	1858	Ethanol
EV	<i>Orchipedum tracheicola</i> Braun, 1901	<i>Orchipedum tracheicola</i>	4472	SYN	1857	Ethanol
EV	<i>Wehrdikmansia rugosicauda</i> Böhm & Supperer, 1935	<i>Cercopithifilaria rugosicauda</i>	6352	SYN	1952	Ethanol
MY	<i>Brachydesmus superus</i> Latzel, 1884	<i>Brachydesmus superus</i>	3661	SYN	1884	Ethanol
MY	<i>Cylindroiulus ignoratus</i> Attems, 1927	<i>Cylindroiulus parisiorum</i>	8170	SYN	1884	Ethanol
MY	<i>Iulus scandinavicus</i> Latzel, 1884	<i>Julus scandinavicus</i>	2749	SYN	1884	Ethanol
ORTH	<i>Locusta cavicola</i> Kollar, 1833	<i>Troglophilus cavicola</i>	-	SYN	1831	Dry Mounted
ORTH	<i>Tetrix tuerki</i> Krauss, 1876	<i>Tetrix tuerki</i>	-	HOLO, PARA	1859	Dry Mounted
FS	<i>Abramis leuckartii</i> Heckel, 1836	hybrid	55331, 94754	SYN	1836	Ethanol
FS	<i>Abramis schreibersii</i> Heckel, 1836	<i>Ballerus sapa</i>	16584, 79462–63 74963	SYN	1825	Dry Mounted
FS	<i>Alburnus breviceps</i> Heckel & Kner, 1858	<i>Alburnus alburnus</i>	55539	HOLO	1856	Ethanol
FS	<i>Aspius mento</i> Heckel, 1837	<i>Alburnus mento</i>	16261, 16441, 50440, 55630, 55650, 55652, 94795	SYN	1824, 1836	Ethanol, Dry Mounted
FS	<i>Blicca argyroleuca</i> Heckel, 1843	<i>Blicca bjoerkna</i>	16901, 54918–20, 94767	SYN	1836	Ethanol
FS	<i>Cyprinus acuminatus</i> Heckel & Kner, 1858	<i>Cyprinus carpio</i>	52846, 52854–55, 52927–29, 52950, 53403, 94708	SYN	1836, 1840	Ethanol
FS	<i>Idus melanotus</i> Heckel & Kner, 1858	<i>Leuciscus idus</i>	53434, 53436, 53438–39, 53455, 53467, 58775, 94805	SYN	1825, 1840	Ethanol, pharyngeal teeth
FS	<i>Idus miniatus</i> Heckel & Kner, 1858	<i>Leuciscus idus</i>	53432, 94807	SYN	1852	Ethanol, pharyngeal teeth
FS	<i>Leuciscus virgo</i> Heckel, 1852	<i>Rutilus virgo</i>	22373, 50626, 94733	SYN	1825, 1836	Ethanol
FS	<i>Phoxinus marsilii</i> Heckel, 1836	<i>Phoxinus marsilii</i>	51225, 98672	LECTO, paralecto	1825 or 1836	Ethanol
FS	<i>Squalius delineatus</i> Heckel, 1843	<i>Leucaspius delineatus</i>	49783, 50794, 94777	SYN	1840	Ethanol, pharyngeal teeth
FS	<i>Squalius lepusculus</i> Heckel, 1852	<i>Leuciscus leuciscus</i>	49345, 49347–48, 49359, 49393	SYN	1825, 1840	Ethanol
VS	<i>Anser brevirostris</i> Brehm, 1831	<i>Anser erythropus</i>	55170, 20928	SYN	1824, 1828	Dry Mounted

The abbreviations are official abbreviation used in the collections and also a part of the inventory numbers (e.g., NHMW-ZOO (for zoological collections)-EV4429; EV – Evertebrata Varia; MY - Myriapoda collection; ORTH – Orthoptera collection; FS- Fish collection (from Fische Sammlung in German); VS – Bird collection (from Vogelsammlung in German); Year – year of collection is given, but sometimes it cannot be distinguished from the year of acquisition.

High Sensitivity Assay Kit. The average DNA fragment length was measured on the TapeStation system (Agilent) using High Sensitivity DNA Screen Tape. Depending on the results of these two measurements, the DNA was either sent for shotgun sequencing (IGA Technology Services, Udine, Italy). The raw sequences were then trimmed and complete mitochondrial genomes were assembled

from a subset of 15 million pair-end reads using Geneious v 10.2.6 (<http://www.geneious.com>; for details see Palandačić et al. (2023)). Alternatively, two overlapping fragments of the cytochrome oxidase I (COI) barcode region were amplified by polymerase chain reaction (PCR) using specific primers designed in this study (see Table 4). For two parasitic worm species no COI sequences were available in GenBank to use as a basis for primer design, so 18S and 28S sequences were used instead. The proportions and conditions of the PCR reactions followed the protocol described in Antognazza et al. (2023), with an annealing temperature of 54 °C. The PCR products were then purified using the PCR Purification Kit (Qiagen) and sent to Mycosynth (Balgach, Switzerland) for bidirectional sequencing using PCR primers.

Table 4. Primers used for polymerase chain reaction and sequencing.

Collection - Original name - Valid name - Gene	Primer Name	Sequence (5'-3' direction)
EV - <i>Lyperosomum corrigia</i> - <i>Corrigia corrigia</i> - 28S	LcorriF1	TTCATCGAGCTTCCTTGCCA
	LcorriR1	GCTAACGAGCTACCTGCCAT
	LcorriF2	GTAAACCGGCCTTGCGATG
	LcorriR2	ACAGAACCATCACGGTCAGC
EV - <i>Orchipedum tracheicola</i> - <i>Orchipedum tracheicola</i> - 18S	OtracheiiF1	CGCTGCTCGTATTCTGGTCC
	OtracheiiR1	AACCGCAAGTGGAACTCAC
	OtracheiiF2	GTGAGTCGGTGTCTGGTT
	OtracheiiR2	GAAGCATGCCAACCAACCG
EV - <i>Wehrdikmansia rugosicauda</i> - <i>Cercopithifilaria rugosicauda</i> - COI	WrugoF1	GACCAGGAAGTAGTTGAA
	WrugoR1	CAGCCTCACTAATAATACCA
MY - <i>Brachydesmus superus</i> - <i>Brachydesmus superus</i> - COI	BrachySuperF1	GCACCCGATATGGCTTTTCC
	BrachySuperR1	AGACCACTAGCCAAAGGAGGA
	BrachySuperF2	GGAAATTGGGGTTGGTACTGGA
	BrachySuperR2	AGAAGAAGCCCCAGCTAAGT
MY - <i>Cylindroiulus ignoratus</i> - <i>Cylindroiulus parisiorum</i> - COI	CylinIgnoF1	TCCGCTGTTGAAAAAGGTGC
	CylinIgnoR1	ATGAAGCACCCGCTAAGTGT
	CylinIgnoF2	GATATGGCCTTCCCCGTTT
	CylinIgnoR2	ACAGAAGGACCTGAGTGTGA
MY - <i>Iulus scandinavicus</i> - <i>Iulus scandinavicus</i> - COI	JulScandiF1	ACCCTGGGAGTTTAATTGGAGA
	JulScandiR1	AATCGAGGGAAAGCTATGTC
	JulScandiF2	AATTGATTAGTACCTTTAAT
	JulScandiR2	AGGGCCAGAGTGAGAAATGT
ORTH - <i>Tetrix tuerki</i> - <i>Tetrix tuerki</i> - COI	Ttuerki_F1	TTCATCTTCGGGCATGAGC
	Ttuerki_R1	AATCGGAGGGTTTGGTAATTGA
	Ttuerki_F2	TAGTAGTAACAGCTCACGCATTTAT
	Ttuerki_R2	AGATATGGCATTCCCGCAATA
FS - <i>Abramis leuckartii</i> – hybrid - COI	FishF1	TCAACCAACCACAAAGACATTGGCAC
	AleuckR1	TATTACGAAGGCGTGGGCAGT
	AleuckF2	AACGTCATCGTTACTGCCCA
	AleuckR2	ACGATGGGGGTAGAAGTCAGA
FS - <i>Abramis schreibersii</i> - <i>Ballerus sapa</i> - COI	FishF1	TCAACCAACCACAAAGACATTGGCAC
	BsapaR1	AGAAAATTATTACGAAGGCGTGGG
	BsapaF2	GTCACCTTTTAGGCGATGACCAAT
	BsapaR2	TCGTGGGAATGCTATATCAGGT

Collection - Original name - Valid name - Gene	Primer Name	Sequence (5'-3' direction)
FS - <i>Alburnus breviceps</i> - <i>Alburnus alburnus</i> - COI FS - <i>Aspius mento</i> - <i>Alburnus mento</i> - COI FS - <i>Blicca argyroleuca</i> - <i>Blicca bjoerkna</i> - COI FS - <i>Leuciscus virgo</i> - <i>Rutilus virgo</i> - COI	FishF1	TCAACCAACCACAAAGACATTGGCAC
	BlicR1	CGTGGGCGGTAACGATGACA
	BlicF2	CTAAGCCAACCCGGGTCAC
	BlicR2	TCAGGCGCACCGATTATTAGT
FS - <i>Idus melanotus</i> - <i>Leuciscus idus</i> - COI FS - <i>Idus miniatus</i> - <i>Leuciscus idus</i> - COI	FishF1	TCAACCAACCACAAAGACATTGGCAC
	LeuiduR1	TGGTCATCGCCTAAAAGTGACCC
	LeuiduF2	CCCTAAGCCTCCTTATTTCGGG
	LeuiduR2	AGTCAATTTCCGAACCCGCC
FS - <i>Squalius delineatus</i> - <i>Leucaspius delineatus</i> - COI	FishF1	TCAACCAACCACAAAGACATTGGCAC
	SdeliR1	TCATCGCCTAAAAGTGACCCAGG
	SdeliF2	GGAATAGTGGGGACTGCCTT
	SdeliR2	ATCGGGCGCACCAATCATT
FS - <i>Squalius lepusculus</i> - <i>Leuciscus leuciscus</i> - COI	FishF1	TCAACCAACCACAAAGACATTGGCAC
	Leuleu_R1	CGTGGGCGGTAACGATAACATTG
	Leuleu_F2	GCCGAACCTAAGCCAACCCG
	Leuleu_R2	GCCAATCATTAGTGGGACGAG
VS - <i>Anser brevirostris</i> - <i>Anser erythropus</i>	Aerythro F1	GCACCGCACTCAGCCTATTA
	Aerythro R1	CAGTTGCCGAATCCTCCGAT
	Aerythro F2	ACCGCTCACGCCCTTTGTAATA
	Aerythro R2	TGGATGAGGCTAGTAGGAGGAG

FishF1 (Ward et al. 2005) is a general barcoding primer used for fishes.

After sequencing, smaller sequence fragments were visually inspected, aligned using MEGA 6.0 (Tamura et al. 2013) and, if multiple fragments were successfully amplified and sequenced, combined into single sequences. During this process, overlapping fragments were checked for congruence. Sequences of the same taxa and, where available, of geographical proximity, were then downloaded from GenBank. The programme MEGA 6.0 (Tamura et al. 2013) was used to construct simple neighbour-joining trees to compare the genetic information of the species with the sequences from GenBank.

Results

Extended specimen approach and samples

A total of 16 original descriptions, 17 drawings and illustrations, 64 acquisitions, registries, and labels, 48 catalogue cards, 91 radiographs, 239 image files (photographs and scans) were produced (Table 5).

Genetic analysis

The results of the DNA extraction are shown in Table 6. The highest DNA concentration was measured in the goose sample (30.4 ng/μl), whereas all parasitic-worm samples seem to be devoid of DNA, or at least the DNA is below the detection limit. Based on DNA concentration and fragmentation, two fish samples were sent for shotgun sequencing: Cacu1 (NMW (FS) 52846, *Cyprinus acuminatus*) and Imini1 (NMW (FS) 53432, *Idus miniatus*). For

Table 5. Digital items (image files, pdfs) prepared in the course of the project.

Category of digital item	Content	Collection					Total
		EV	MY	ORTH	FS	VS	
Original descriptions	Printed text	2	3	2	14	1	22
Drawings, illustrations	Graphic				17		17
Acquisition books, registries, labels	Handwritten text	9	5	3	38	9	64
Catalogue cards	Text		3		48	1	52
Radiographs	Digitised x-ray films				89	2	91
Image files (photos and scans)	Specimens (different aspects), specimen parts	18	25	18	174	6	241
Genetic information	Deposited at GenBank		1	1	10	1	13
TOTAL		29	37	24	390	20	= 500

Table 6. DNA concentration.

Collection	Original name	Valid name	Inv. No.	Lab ID	DNA concentration (ng/μl)	Result
EV	<i>Lyperosomum corrigia</i>	<i>L. corrigia</i>	4429	Lcorr	too low	PCR not successful
EV	<i>Orchipedum tracheicola</i>	<i>Orchipedum tracheicola</i>	4472	Otrache	too low	PCR not successful
EV	<i>Wehrdikmansia rugosicauda</i>	<i>Cercopithifilaria rugosicauda</i>	6352	Wrugo	too low	PCR not successful
MY	<i>Brachydesmus superus</i>	<i>Brachydesmus superus</i>	3661	Bsuper1	0,184	C1+C2 COI fragments 214 bp long with primers 167 bp long without primers GB No. PP576055
MY	<i>Cylindroiulus ignoratus</i>	<i>Cylindroiulus parisiorum</i>	8170	Cigno	0,144	PCR not successful
MY	<i>Iulus scandinavicus</i>	<i>Iulus scandinavicus</i>	2749	Jscandi	7,96	PCR not successful
ORTH	<i>Troglophilus cavicola</i>	<i>Troglophilus cavicola</i>	/	/		Only one damaged syntype, not sampled
ORTH	<i>Tetrix tuerki</i>	<i>Tetrix tuerki</i>	/	Ttuerki	0,404	C2 COI fragment 147 bp long with primers 101 bp long without primers GB No. PP579753
FS	<i>Abramis leuckartii</i>	hybrid	55331	Aleu1	0,6	PCR not successful
FS	<i>Abramis schreibersii</i>	<i>Ballerus sapa</i>	79462	Abram2	0,568	C1+C2 COI fragments 266 bp long with primers 217 bp long without primers GB No. PP576053
FS	<i>Abramis schreibersii</i>	<i>Ballerus sapa</i>	16584	Abram1	0,302	PCR not successful
FS	<i>Alburnus breviceps</i>	<i>Alburnus alburnus</i>	55539	Abrevi1	0,188	C2 reverse sequence turns out to be a contamination
FS	<i>Aspius mento</i>	<i>Alburnus mento</i>	55630	Amento1	3,34	C1 COI fragment 162 bp long with primers 114 bp long without primers GB No. PP579756
FS	<i>Aspius mento</i>	<i>Alburnus mento</i>	55629	Amento2	3,84	PCR not successful
FS	<i>Aspius mento</i>	<i>Alburnus mento</i>	50440	Amento3	1,68	C1 COI fragment 162 bp long with primers 114 bp long without primers GB No. PP579755
FS	<i>Aspius mento</i>	<i>Alburnus mento</i>	55650	Amento4	1,67	PCR not successful
FS	<i>Aspius mento</i>	<i>Alburnus mento</i>	55652	Amento5	2,56	C1 COI fragment 162 bp long with primers 114 bp long without primers GB No. PP579754
FS	<i>Aspius mento</i>	<i>Alburnus mento</i>	16441	Amento6	2,1	PCR not successful

Collection	Original name	Valid name	Inv. No.	Lab ID	DNA concentration (ng/μl)	Result
FS	<i>Aspius mento</i>	<i>Alburnus mento</i>	16261	Amento7	0,134	PCR not successful
FS	<i>B. argyroleuca</i>	<i>B. bjoerkna</i>	54918	Bargy4	1,33	C2 COI fragment 152 bp long with primers 112 bp long without primers GB No. PP579757
FS	<i>Cyprinus acuminatus</i>	<i>Cyprinus carpio</i>	52846	Cacu1	16,2	Shot-gun Reads after trimming 68 895 309 Complete mitochondrial genome Possibility of a draft genome assembly. GB No. (COI) PP576059 GB No. (complete mt) PP621518
FS	<i>Idus melanotus</i>	<i>Leuciscus idus</i>	53434	Imel1	2,4	C1+C2 COI fragments 243 bp long with primers 193 bp long without primers GB No. PP576058
FS	<i>Idus melanotus</i>	<i>Leuciscus idus</i>	58775	Imel2	0,26	PCR not successful
FS	<i>Idus melanotus</i>	<i>Leuciscus idus</i>	53432	Imini1	6,69	Shot-gun: only contaminates C2 COI fragment 170 bp long with primers 149 bp long without primers GB No. PP579758
FS	<i>Leuciscus virgo</i>	<i>Rutilus virgo</i>	50626	Lvir1	0,9	C1+C2 COI fragments 250 bp long with primers 218 bp long without primers GB No. PP576056
FS	<i>Phoxinus marsilii</i>	<i>Phoxinus marsilii</i>	51225	/	/	Three previously published partial sequences of the genes: MF408203 (partial cytb) MF407956 (partial COI) MN818242 (partial ITS1)
FS	<i>Squalius delineatus</i>	<i>Leucaspius delineatus</i>	50794	Sdeli1	0,929	PCR not successful
FS	<i>Squalius lepusculus</i>	<i>Leuciscus leuciscus</i>	49345_1	Sleb1	1,1	C1+C2 COI fragments 242 bp long with primers 192 bp long without primers GB No. PP576057
VS	<i>Anser brevirostris</i>	<i>Anser erythropus</i>	55170	Aerythro	30,4	C1+C2 COI fragments 262 bp long with primers 220 bp long without primers GB No. PP576054

PCR – polymerase chain reaction, COI – cytochrome oxidase I, cytb – cytochrome b, ITS1 – internal transcribed spacer 1; GB No. - GenBank Accession Number; mt - mitochondrion.

Cacu1, the sequences obtained allowed the assembly of a complete mitochondrial genome (coverage >35) and can possibly be used for the assembly of the draft genome, whereas for Imini1 most of the sequences turned out to be contaminations.

Two overlapping fragments of COI (designated C1 and C2) were successfully amplified and sequenced in the myriapod Bsuper1 (NMW (MY) 3661, *Brachydesmus superus*), fish samples Abram2 (NMW (FS) 16584, *Abramis schreibersii*), Imel1 (NMW (FS) 53434, *Idus melanotus*), Lvir1 (NMW (FS) 50626, *Leuciscus virgo*), Sleb1 (NMW (FS) 49345, *Squalius lepusculus*), and the bird species Aerythro1 (NMW (VS) 55170 *Anser brevirostris*). While in the insect sample Ttuerki (no inv. number given; *Tetrix tuerki*) and the fish samples Abrevi1 (NMW (FS) 55539, *Alburnus breviceps*), Amento1 (NMW (FS) 55630, *Aspius mento*), Bargy4 (NMW (FS) 54918, *Blicca argyroleuca*) and Imini1 (NMW (FS) 53432, *Idus miniatus*) either C1 or C2 was successfully amplified and sequenced. In the remaining samples, DNA extraction, amplification, and/or sequencing were not successful.

Catalogue of nomenclatural types of taxa described based on specimens from the state of Vienna

Chromadorea and Trematoda type series

Trematoda: Plagiorchiida: Dicrocoeliidae

1. *Lyperosomum corrigia* Braun, 1901

Original publication of the name. Braun (1901: 946).

Syntypes. NHMW EV4429 (old inventory number 5678, 15 specimens in alcohol) (Fig. 5a, b); all 15 are currently found, of which one whole animal was used for DNA extraction. Preservation condition: average (Fig. 6).

Remarks. The year 1858 given in the Inventory Book (Fig. 5) is the date of acquisition rather than collecting; the host specimen was registered in the old collection (Wiener Sammlung) under the number 376 (Braun 1901: 946).

Type locality. Vienna; from the intestine of *Tetrao tetrix* (Linnaeus, 1758) (= *Lyrurus tetrix*, the black grouse).

Distribution. Gastrointestinal parasite of Galliformes in the Alpine area (Italy, France, Austria) (Tizzani et al. 2021).

Etymology. The species name is a Latin noun meaning shoelace or tie, from *corrigō* (smooth out, make straight).

Taxonomic status. Valid as *Corrigia corrigia* (Braun, 1901).

Conservation status. Not assessed for the IUCN Red List.

Genetic information. Genetic analysis was not successful.

Trematoma: Plagiorchiida: Orchipediidae

2. *Orchipedum tracheicola* Braun, 1901

Original publication of the name. Braun (1901: 943).

Syntypes. NHMW EV4472 (old inventory number 5677, 8 specimens) (Fig. 5a, c); seven (in alcohol) are currently found, of which one whole animal used for DNA extraction. Preservation condition: good (Fig. 7).

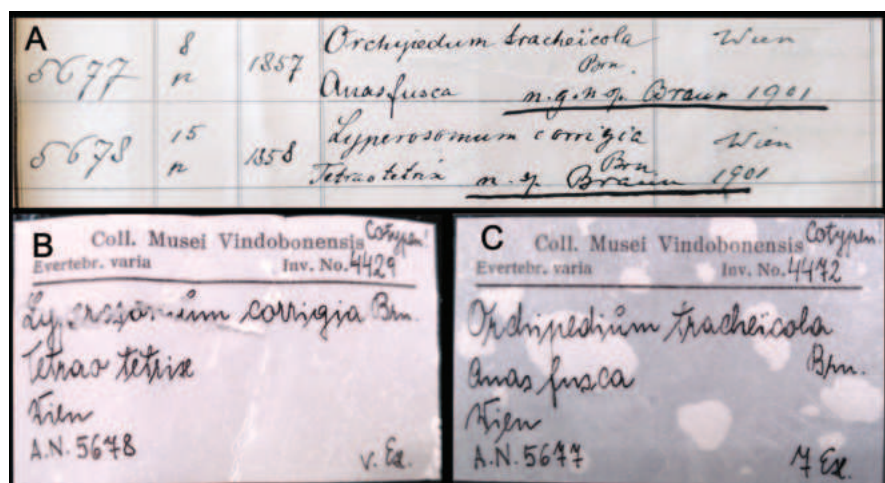


Figure 5. A old inventory records for syntypes of *Lyperosomum corrigia* (No. 5678) and B, C *Orchipedum tracheicola* (No. 5677), present-day labels.

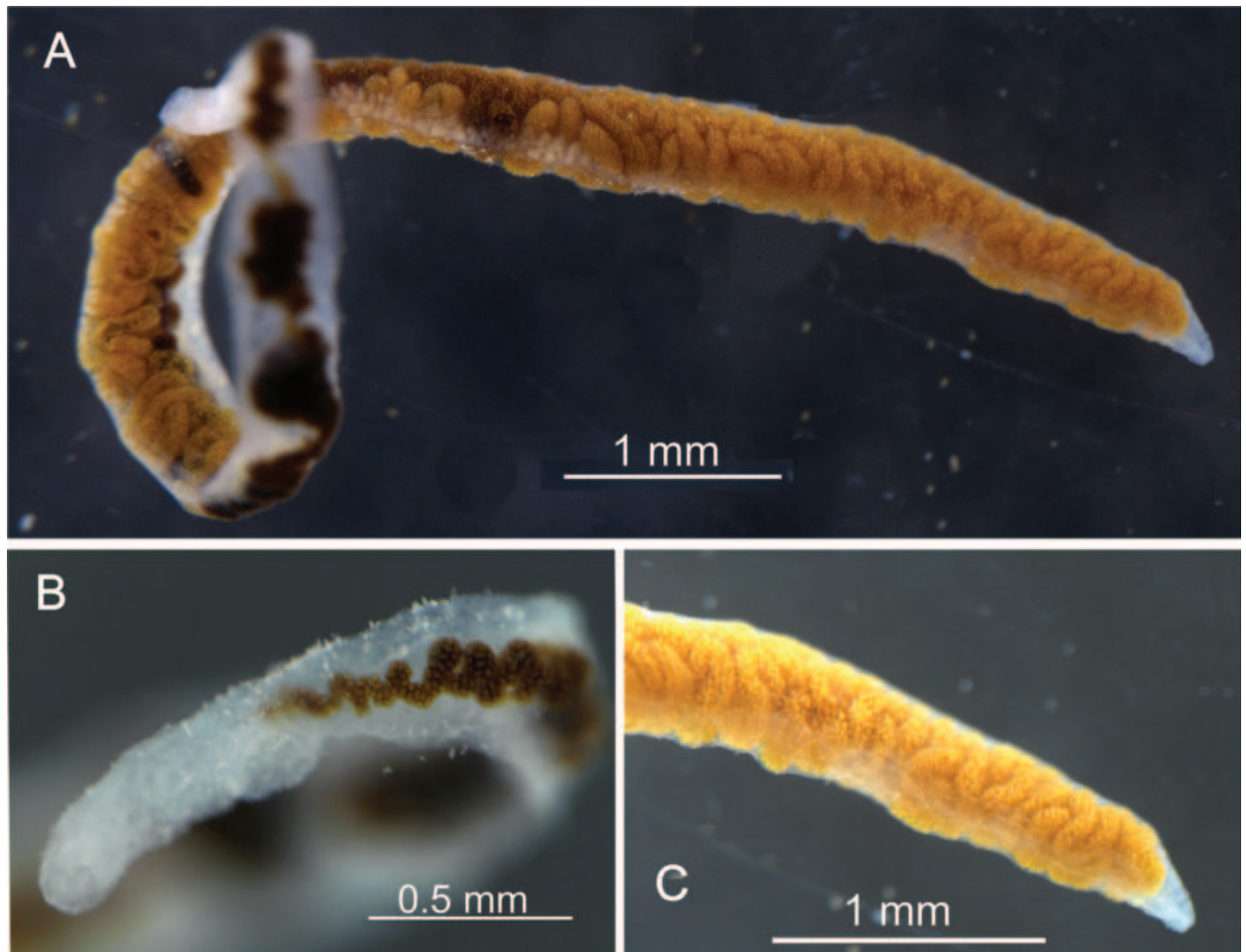


Figure 6. A syntype of *Lyperosomum corrigia* (EV4429) **A** total view **B** anterior **C** posterior end of the body.

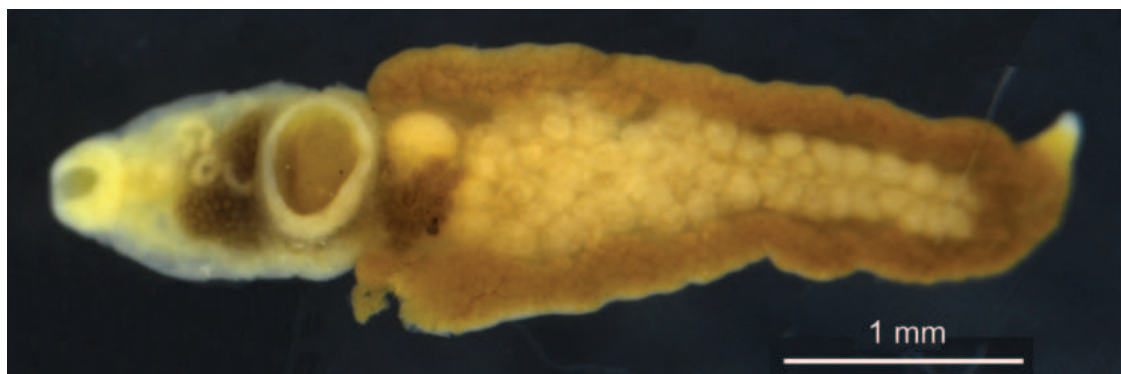


Figure 7. A syntype of *Orchipedum tracheicola* Braun, 1901 (EV4472).

Type locality. Vienna; in the trachea of *Anas fusca* Linnaeus, 1758 (the velvet scoter), collected in October 1857 (Braun 1901: 943).

Remarks. The host specimen was registered in the old collection (Wiener Sammlung) in 1857 under the number 377.

Distribution. *Orchipedum tracheicola* is reported from trachea of water birds in North America and Europe (Webster 1959).

Etymology. The name *tracheicola* is a Latin compound noun, from *trachea* (windpipe) and *cola* (inhabitor, one who inhabits), referring to the finding of the syntypes in trachea of an avian host.

Taxonomic status. Valid as *Orchipedum tracheicola* Braun, 1901.

Conservation status. Not assessed by the IUCN.

Genetic information. Genetic analysis was not successful.

Chromadorea: Rhabditida: Onchocercidae

3. *Wehrdikmansia rugosicauda* Böhm & Supperer, 1953

Original publication of the name. Böhm and Supperer (1953: 96).

Syntypes. NHMW EV6352 (old inventory number 18019, three specimens, donated by Böhm and Supperer in 1955; Fig. 8a, b); three (in alcohol) are currently found, of which one half was used for DNA extraction. Preservation condition: good (Fig. 8c).

Remarks. The species was described based on four syntypes in total: three female and one male (Böhm and Supperer 1953: 95).

Type locality. Vienna; from the subcutaneous connective tissue of the back in the lumbar region of *Capreolus capreolus* (Linnaeus, 1758) (roe deer, collected in March 1952 (Böhm and Supperer 1953: 96).

Distribution. The species is a subcutaneous filarial nematode of roe deer *Capreolus capreolus* (Linnaeus, 1758) in Europe (Lefoulon et al. 2014), mainly in Central Europe, Britain, Ireland, and southern Scandinavia. Also introduced into New Zealand and North America.

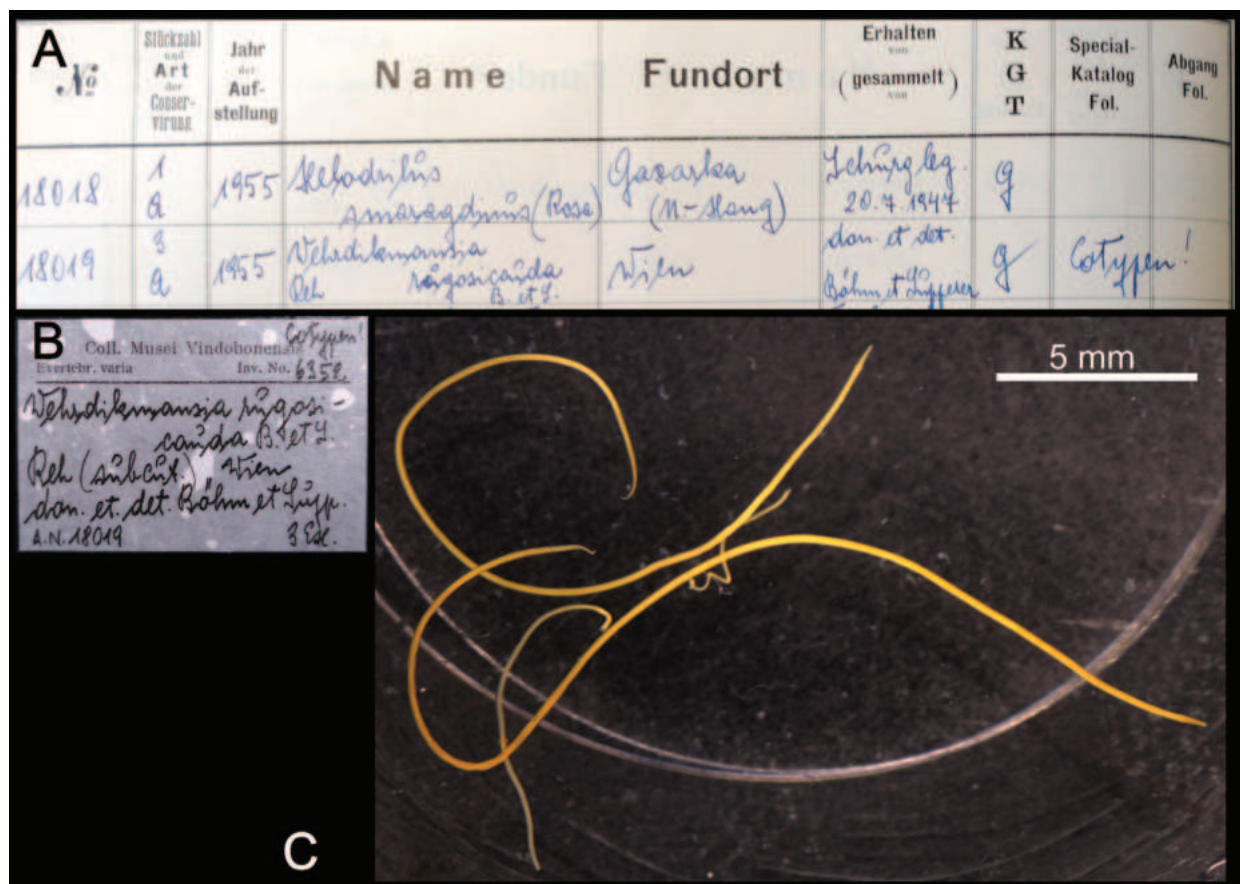


Figure 8. A old inventory record for syntypes of *Wehrdikmansia rugosicauda* (No. 18019) B present-day label (Nr. 6352) B, C total view of three extant syntypes.

Etymology. The species name is a feminine Latin adjective, from *rugosa* (with wrinkles, folds, or creases) and *cauda* (tail), referring to the area *rugosa*, a peculiar feature in males.

Taxonomic status. Valid as *Cercopithifilaria rugosicauda* (Böhm & Supperer, 1953).

Conservation status. Not assessed by the IUCN.

Genetic information. Genetic analysis was not successful.

Diplopoda type series

Diplopoda: Polydesmida: Polydesmidae

1. *Brachydesmus superus* Latzel, 1884

Original publication of the name. Latzel (1884: 130).

Syntypes. NHMW MY3661; two males, two females, one juvenile, three fragments (in alcohol), one micro-preparation with gonopods, “Nr 67.”, Latzel leg. (Fig. 9). Preservation condition: good.

Remarks. Latzel (1884) mentioned he had studied more than 60 specimens, most of which are from the Prater in Vienna. Other type localities mentioned in Latzel (1884: 132) are “Mähren, Ober und Westungarn”, corresponding today to Czech Republic, Slovakia, and west Hungary. All the syntypes in NHMW are from Prater.

Type locality. Vienna, Prater.

Etymology. Not mentioned in the original description. However, the prefix *super* (above/upper) might indicate the fact that the species lives in the upper soil layers, but this remains a tentative explanation.

Distribution. Nearly Pan-European species. Anthropochorous and has spread beyond its natural range.

Taxonomic status. Valid. To date, around 21 subspecies of *Brachydesmus superus* have been described, mostly by Verhoeff (1891, 1895, 1907, 1928, 1930a, 1930b, 1932, 1941, 1942, 1951, 1952) and Attems (1908, 1927).

Conservation status. Not assessed by the IUCN.

Genetic information. Two overlapping fragments of the mitochondrial COI region (LabID Bsuper1; 167 bp in total, GenBank Accession No. PP576055) were successfully amplified. Nucleotide blast search with a subsequent alignment of the sequences and simple neighbour-joining tree analysis showed the closest relative to be *B. superus*, GenBank Accession No. HQ966183, from Lombardy, Italy. In this case, sequencing of the type has irreversibly connected this COI fragment with the species name *B. superus*, which will be helpful in the subsequent taxonomic and barcoding projects.

Diplopoda: Julida: Julidae

2. *Cylindroiulus ignoratus* Attems, 1927

Original publication of the name. Attems (1927: 199).

Syntypes. NHMW MY8170; three males, three females, three subadults (in alcohol), “Nr 103 *Julus luscus* Meinert”, Niederösterreich, Prater bei Wien, Latzel



Figure 9. *Brachydesmus superus* Latzel, 1884, male syntype (MY3661) **A** habitus, dorsolateral view **B** head and anterior-most bodyrings **C, D** labels.

don. leg. (Fig. 10). NHMW MY 8171; several specimens Styria, Graz, Leechwald, Rhabarberbeet, Attems leg. NHMW MY 8172; 15 specimens, one micro-preparation, Lower Austria, Laxenburg. Preservation condition: good.

Type locality. Vienna, Lower Austria, Styria.

Distribution. Mainly Central Europe, Britain, Ireland, and southern Scandinavia. Also introduced into New Zealand and North America.



Figure 10. *Cylindroiulus ignoratus* Attems, 1927, male syntype (MY8170) **A** habitus lateral view **B** head and anteriormost body rings, lateral view **C**, **D** labels.

Taxonomic status. Not valid. A junior subjective synonym of *Cylindroiulus parisorum* (Brölemann & Verhoeff, in Brölemann 1896).

Conservation status. Not assessed by the IUCN.

Genetic information. Genetic analysis was not successful.

3. *Iulus scandinavicus* Latzel, 1884

Original publication of the name. Latzel (1884: 322).

Syntypes. NHMW MY2749; two males, one female (in alcohol) (Fig. 11). Preservation condition: good.

Remarks. As many of the types of Robert Latzel, the original type locality of this species was not provided with precision and mentioned by Latzel (1884) as the Austro-Hungarian Empire, the crown lands of Lower Austria, Upper Austria, Bohemia, Moravia and Western Hungary. Five specimens are listed in the the acquisition book in 1884.I.117, whereas only three exist in the collection. The whereabouts of the remaining syntypes is unknown. An additional label "*Julus ligulifer*" is also contained in the jar. This label must have been added subsequently as *Julus ligulifer* Latzel, in Verhoeff, 1891 is a junior subjective synonym of *Julus scandinavicus*.

Type locality. Lower Austria; Vienna, Prater, Upper Austria, Kirchdorf.

Etymology. Not mentioned in the original description but the name refers to the fact the author believed the species is rare in Central Europe and should most probably come from Scandinavia and Denmark (Latzel 1884: 324). The name is used as an adjective.

Distribution. A very common species in Central Europe with a wide distribution range. Mostly encountered in woodlands although also recorded on heaths, wetlands, humid open grassland, and sand dunes (Kime and Enghoff 2017).

Taxonomic status. Valid.

Conservation status. Not assessed by the IUCN.

Genetic information. Genetic analysis was not successful.

Insecta type series

Insecta: Orthoptera: Rhabdophoridae

1. *Locusta cavicola* Kollar, 1833

Original publication of the name. Kollar (1833a: 80).

Syntype. One male (dry mounted; Fig. 12). Preservation condition: poor.

Remarks. The original description is based on several male individuals, found by Carl von Schreibers (1775–1852), director of the United Natural History Cabinet, in the cave "Schelmenloch" south of Vienna around 1831 (Kollar 1833a; Christian 2008). Handwritten labels write Kollar det. A. Corey, 2003.

Type locality. Schelmenloch (cave), Baden, south of Vienna, Lower Austria.

Etymology. the species name is a noun, coming from the Latin word *cavum*, meaning cave dweller. The current combination *Trogophilus cavicola* by Krauss

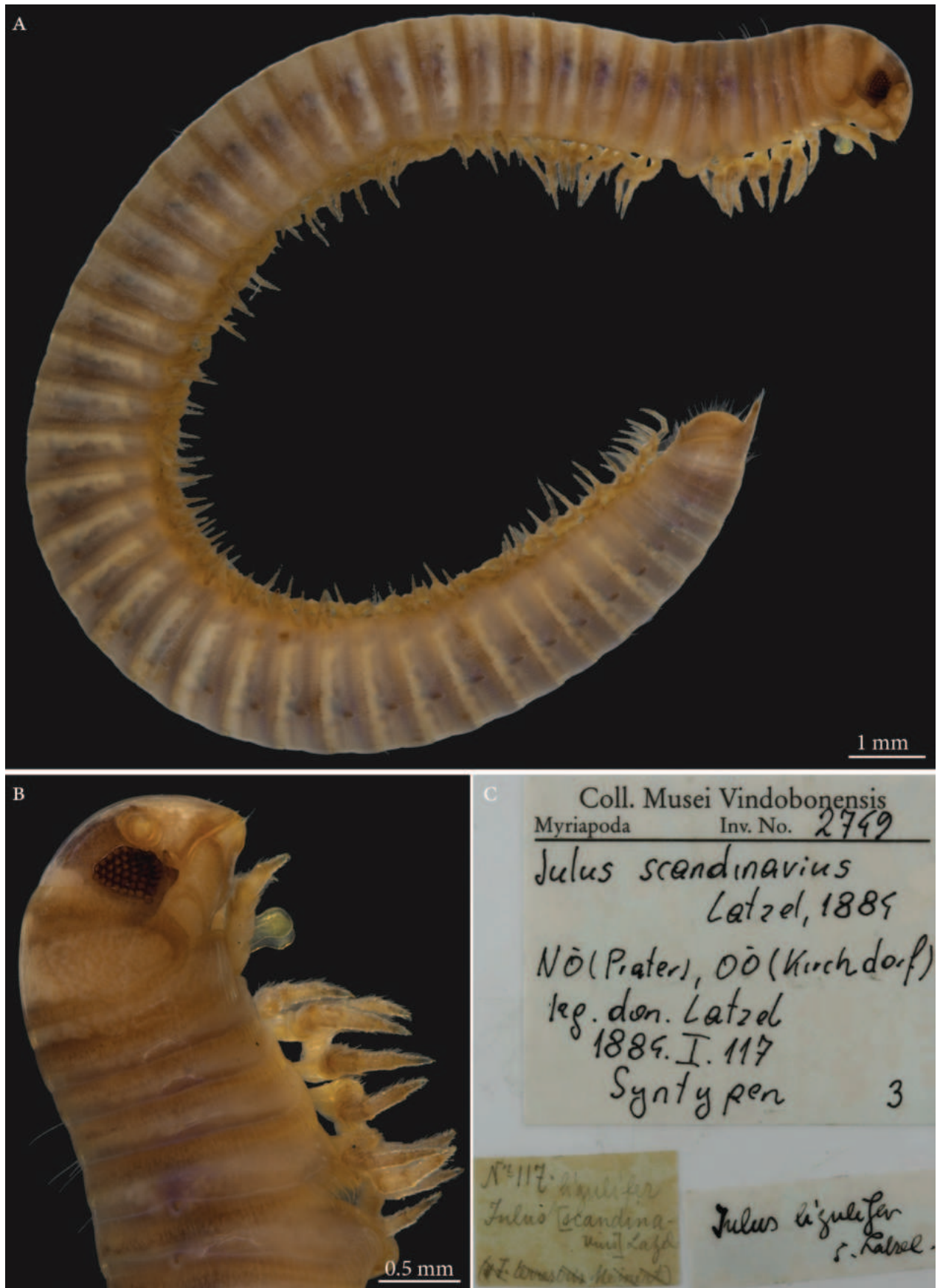


Figure 11. *Iulus scandinavicus* Latzel, 1884, male syntype (MY2749) **A** habitus, lateral view **B** head and anteriormost body rings, lateral view **C** labels.



Figure 12. *Troglophilus cavicola*, Syntype, male, lateral view and labels.

(1878) [1879] is a tautological combination of the Greek word *troglophil*, meaning cave-loving, therefore “the cave-loving cave dweller” (Christian 2008).

Taxonomic status. Valid as *Troglophilus cavicola* (Kollar, 1833).

Distribution. The main distribution area of *Troglophilus cavicola* is in south-eastern Europe. From central Greece, the range extends across the Balkan Peninsula to the Bergamo Alps, the south of Graubünden to Austria. The northern limit of distribution is south of Vienna (Moog 1982; Christian 2008).

Conservation. *Troglophilus cavicola* is in the LC category (Europe and Austria) (Hochkirch et al. 2016; Zuna-Kratky et al. 2017).

Genetic information. As there is only one, already damaged, syntype left, no genetic analysis was performed.

Insecta: Orthoptera: Tetrigidae

2. *Tetrix tuerki* Krauss, 1876

Original publication of the name. Krauss (1876: 103)

Holotype. One male (dry mounted; Fig. 13). Preservation condition: good.

Remarks. In Brunner von Wattenwyl’s directory I (Fig. 2), the specimens in question are listed with the number 1183 from the year 1859. On a glued-in note next to it is written in handwriting: “An den Ufern der Donau bei Wien gefangen, von d. südlichen nur in Färbung differierend” (“Caught on the banks of the Danube near Vienna, differing from the southern one(s) only in coloration”) (Fig. 3). This note was presumably written by Türk and handed over to Brunner von Wattenwyl together with the specimens. As southern species he probably means *T. depressa* and *T. meridionalis*, which were available to him as comparative material from the Mediterranean region. As Krauss (1876) notes, Türk described *T. tuerki* (Krauss 1876) as *T. depressa* Brisout de Barneville, 1848 (Türk 1860) and *Paratettix meridionalis* (Rambur, 1838) as *T. meridionalis* (Türk 1862).

Type locality. Vienna, on flat, sandy banks of the Danube, washed by water, sparsely vegetated, in the Prater, Brigittenau, near Klosterneuburg and in several other places (Krauss 1876: 104).



Figure 13. *Tetrix tuerki*, Holotype, male, lateral view and labels.

Etymology. The species name is a patronym, a noun in the genitive, named after Rudolf Türk.

Taxonomic status. Valid.

Distribution. *Tetrix tuerki* is a Pontomediterranean faunal element that is native to the Alps and mountain ranges of eastern and southern Europe, but also occurs east of the Black Sea region (Zuna-Kratky et al. 2017).

Conservation. *Tetrix tuerki* is in the VU category for Europe (Hochkirch et al. 2016) and in the EN category for Austria (Zuna-Kratky et al. 2017).

Genetic information. To refrain from damaging the types, a topotype specimen (Fig. 14, female) collected together with the holotype was used for genetic analysis. Genetic analysis was successful for one fragment of the COI region (LabID Ttuerki; 101 bp in total, GenBank Accession No. PP579753). This short sequence is identical to the unpublished COI sequences from the GenBank (GU706152–GU706154) collected at the Austrian-Germany border (47.50 N; 11.50 E).



Figure 14. *Tetrix tuerki*, Topotype, female, lateral view and labels.

Actinopteri type series

Actinopteri: Cypriniformes: Leuciscidae*

classification according to van der Laan et al. (2023).

1. *Abramis leuckartii* Heckel, 1836

Original publication of the name. Heckel (1836: 229, pl. XX, fig. 5).

Remarks. This paper (Heckel 1836) was published in the Annals of the Vienna Museum of Natural History (Annalen des Wiener Museums der Naturgeschichte), which was a short living journal; only two volumes have been published, the first one, as commonly cited, in 1836 (for 1835) and the second one, in parts, in 1837–1840 (Ahnelt and Mikschi 2008). However, the volume (or some part of it) was possibly published in 1835; there is also a separate dated 1835.

Syntypes. NMW 55331 (a specimen in alcohol), 94754 (a pair of pharyngeal bones with teeth). Recent measurements: TL ca 130 mm (the caudal fin damaged), SL 105 mm (Fig. 15). Preservation condition: good.

Remarks. The original description is based on more than one individual (the numbers of countable feature are given as ranges, e.g., the number of branched anal-fin rays is 15–17). The extant syntype (NMW 55331) has 15 (if two last rays are counted as one, as it was accepted at the time), similar to a syntype in the original drawing (Fig. 16). Acquisition record 1836.I.10 indicates three specimens.

Type locality. “Schnellfliessenden Stellen der Donau bei Fischment unter Wien” (“Fast-flowing parts of the Danube near Fischment downstream of Vienna”) in the original description (Heckel 1836: 230); acquisition 1836.I.10 reads only “Danube”.



Figure 15. *Abramis leuckartii* syntype, NMW 55331, SL 105 mm **A** left lateral view **B** radiograph.

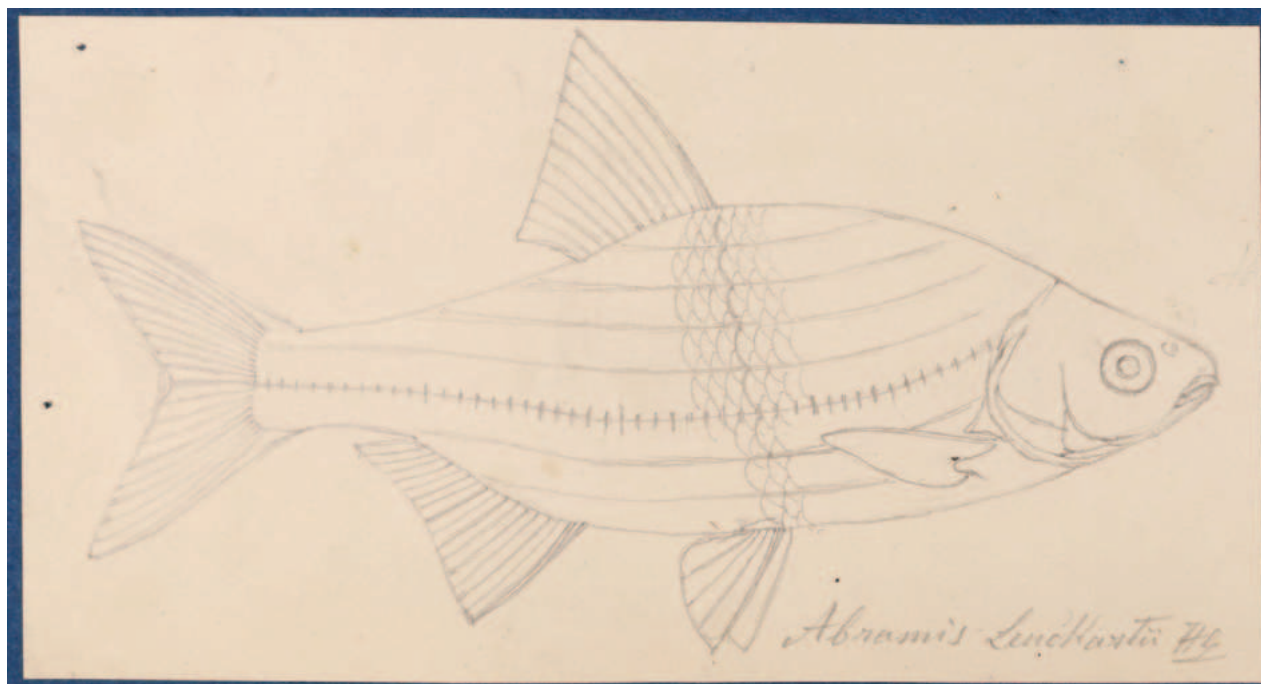


Figure 16. A draft by Heckel of *Abramis leuckartii* for Heckel (1836: pl. XX, fig. 5) (NHMW Archive).

Etymology. The species name is a patronym, a noun in the genitive; named for Friedrich Sigismund Leuckart, a German naturalist (1794–1843).

Taxonomic status. Hybrid between *Rutilus rutilus* (Linnaeus, 1758) × *Abramis brama* (Linnaeus, 1758) (Günther 1868: 214). This opinion is correct as the specimen has character states intermediate between *Rutilus* and *Abramis* (especially, the shape of the posterior process of the basioccipital and the number of branched anal-fin rays). The availability of the name is not affected if it is applied to a taxon later found to be of hybrid origin, Art. 17 of the Code (International Commission on Zoological Nomenclature 1999).

Distribution. Only known by the syntypes.

Conservation status. None (a hybrid).

Genetic information. Genetic analysis was not successful.

2. *Abramis schreibersii* Heckel, 1836

Original publication of the name. Heckel (1836: 227, pl. XX, fig. 4)

Syntypes. NMW 16584 (1), 79462–63 (1, 1); all are stuffed individuals. Recent measurements (TL, SL): NMW 16584 ca 255 mm, ca 215 mm (Fig. 17); 79462 ca 223 mm, ca 185 mm; 79463 ca 230 mm, ca 195 mm. Preservation condition: average.

Remarks. The original description is based on more than one individual (the numbers of countable feature are given as ranges, e.g., the number of branched anal-fin rays is 39–43); 38 branched anal-fin rays in the illustrated individual. The extant syntypes are all with Acquisition Number 1825.V.32 which indicates three specimens.

Type locality. "Schnellfließenden Stellen der Donau unter Wien, auch in der March kommt er vor" ("Fast-flowing parts of the Danube below Vienna, also in



Figure 17. *Abramis schreibersii* syntype, NMW 16584, SL ca 215 mm, left lateral view.

the March") (Heckel, 1836: 228). Acquisition 1825.V.32 (as *Balerus* (sic) *neu* species): "II. Semester 1825, vom Laboratorio zukaufft".

Etymology. The species name is a patronym, a noun in the genitive; named for Carl Franz Anton Ritter von Schreibers (1775–1852), an Austrian naturalist and botanist, the director of the Natural History Cabinet since 1806.

Taxonomic status. Treated as a synonym of *Abramis sapa* (Pallas, 1814) since as early as Heckel and Kner (1857: 115), now in the genus *Ballerus*.

Distribution. *Ballerus sapa* is native in large rivers draining to Black, Azov, Caspian, and Aral seas. Introduced elsewhere (Northern Dvina, Volkhov, Rhine, Vistula) (Freyhof and Kottelat 2008a).

Conservation. IUCN: *Ballerus sapa* is in the LC category (Freyhof and Kottelat 2008a). In the Red Data List of Lower Austria (Wolfram and Mikschi 2007: 110) as Not Endangered ("nicht gefährdet").

Genetic information. DNA extraction was performed on scales from two stuffed specimens, NMW 16584 and 79462, but genetic analysis was successful only on the latter. Two overlapping fragments of the mitochondrial COI regions (LabID Abram2; 217 bp in total, GenBank Accession No. PP576053) were successfully amplified in the specimen NMW 79462. The sequence was identical to the *Ballerus sapa* sequences from Austria (Zangl et al. 2022).

3. *Alburnus breviceps* Heckel & Kner, 1857

Original publication of the name. Heckel and Kner (1857: 134, fig. 69).

Although dated 1858, the book (Heckel and Kner 1857) was already printed in December 1857 as shown by Svojtka et al. (2012: 60). Rudolf Kner donated it to the library of the Zoological-Botanical Society at the meeting on 2 December 1857 (Anonymous 1857b: 158).

Holotype. NMW 55539 (in alcohol). Recent measurements: TL 152 mm, SL 124 mm. Preservation condition: average.

Remarks. The original description is based on one individual of 5 Zoll (Viennese inches) of total length (= 131.7 mm) (Fig. 18a). Recent measurements (TL, SL): 132 mm, 114 mm. The length, number of branched anal-fin rays (19) and the lateral-line scales (50) suit to those in the 55539 specimen (Fig. 18b, c). Acquisition number, 1856.VII.63, indicates one specimen (as "*Alburnus breviceps* Heckel").

Type locality. Not provided in the original description (Heckel and Kner 1857: 134–135). Acquisition entry 1856.VII.63: Danube, Vienna. Acquisition 1856.VII contains a remark that it had been earlier recorded as 1856.I. (this number is still indicated in respective labels and cards).

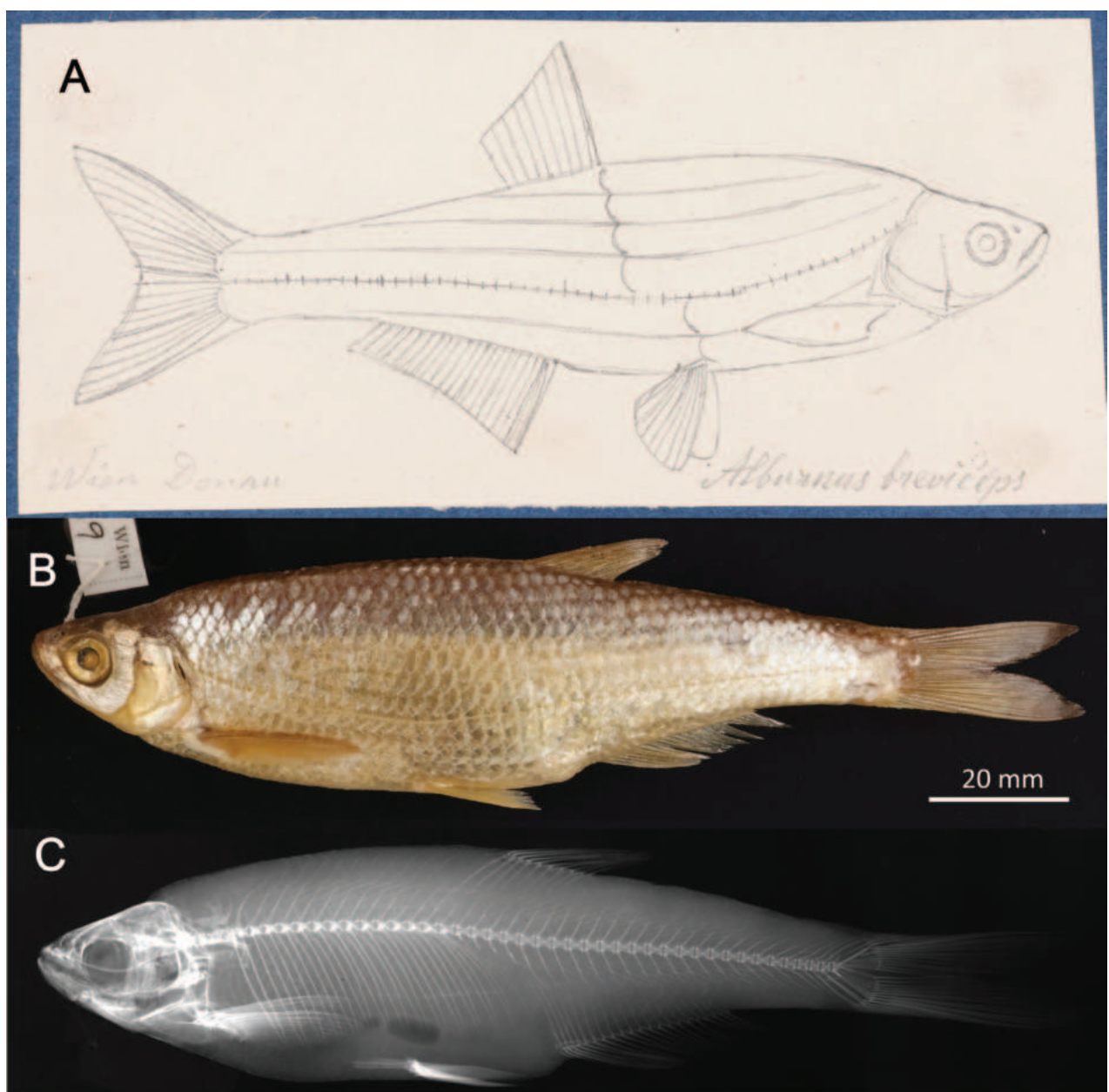


Figure 18. *Alburnus breviceps* holotype, NMW 55539, SL 124 mm **A** a draft drawing by Heckel of the described specimen from the Danube at Vienna, for Heckel and Kner (1857: fig. 69) (NHMW Archive) **B** left lateral view **C** radiograph.

Etymology. The species name is an adjective, short-headed, comes from the Latin word *brevis*, meaning short, and *ceps*, head.

Taxonomic status. Synonymised with *Alburnus alburnus* (Linnaeus, 1758) soon after the description (e.g., Günther 1868: 313).

Distribution. *Alburnus alburnus* is native in most of Europe north of Caucasus, Pyrénées, and Alps, eastward to Ural and Emba. Locally introduced elsewhere (Spain, Italy, the Rtysh River) (Freyhof and Kottelat 2008b).

Conservation. IUCN: *Alburnus alburnus* is in the LC category (Freyhof and Kottelat 2008b). In the Red Data List of Lower Austria (Wolfram and Mikschi 2007: 111) as Not Endangered (“nicht gefährdet”).

Genetic information. Genetic analysis was not successful.

4. *Aspius mento* Heckel, 1836

Original publication of the name. Heckel (1836: 225, pl. XIX, fig. 3).

Remarks. The name of the species in the acquisition records (listed below) (e.g., Fig. 4) are given as *heckelii* because Fitzinger (1832: 335) had already published this name (unavailable as neither indication (reference) nor description were provided) as “*Aspius Heckelii*. Mihi. Im Gebirge; in Flüssen. Bisher nur in Ober-Oesterreich gefunden; in der Traun. Sehr selten” (In the mountains; in rivers. So far only found in Upper Austria; in Traun. Very rare).

On the other hand, Heckel knew that Agassiz was going to describe the species as the two ichthyologists were well acquainted. At the time Agassiz stayed in Vienna in 1830, he was preparing a multi-volume monography titled ‘*Histoire naturelle des poissons d’eau douce de l’Europe centrale, ou description anatomique et historique des poissons qui habitent les lacs et les fleuves de la chaîne des Alpes et les rivières qu’ils reçoivent dans leur cours*’ (‘Natural history of the freshwater fishes of Central Europe, or anatomical and historical description of the fishes which inhabit the lakes and rivers of the Alps and the rivers which they receive in their course’). This work, which remained unfinished, has a curious history. Agassiz undertook it in 1828, in Munich, having the plates of his future work drawn by Joseph Dinkel. On August 30, 1830, Agassiz published a prospectus in German and French announcing the book: “In the arrangement of the materials I followed the procedure that I am going to indicate: everything is arranged by natural families, each of which is the subject of a particular monograph. General considerations on the class of fishes should first serve as an introduction to my work, but what I have to say cannot be appreciated until after the publication of all the particular facts, I have had to return these generalities at the end of the work. Each monograph therefore begins with the indication of the general external characteristics, and the main organizational features of a detailed exposition of the characters of each genus, I have given the anatomy as complete and as concise as possible of the species...” (Surdez 1973: 69–70). However, only three volumes, on Salmonidae, were published while the volumes on cyprinids have never appeared. It can be assumed that Heckel decided to publish the new species by himself but with attribution to Agassiz, as *Aspius mento* Ag. (Heckel 1836: 226): “Später erhielt das hiesige Museum durch die Güte des Herrn Professor Agassiz sehr schöne Exemplare seines *Aspius Mento* aus München; ich habe nun diese Exemplare auf das

sorgfältigste mit jenen aus der Traun verglichen, ..." ("Later, the local museum received by the generosity of Professor Agassiz very beautiful specimens of his *Aspius Mento* from Munich; I have now most carefully compared these specimens with those from the Traun...").

Syntypes. NMW 16261 (1) and 16441 (1), both stuffed; 50440 (1), 55630 (1), 55650 (2) and 55652 (1), in alcohol; NMW 94795 (a pair of pharyngeal bones).

Recent measurements (SL): NMW 16261, 140 mm; NMW 16441, 134 mm, NMW 50440, 221 mm; NMW 55630, 190 mm; NMW 55650, 157 and 137.5 mm, NMW 55652, 219 mm. Preservation condition: poor to good.

Remarks. The original description (Heckel 1836: 225–226) clearly indicates the three samples of specimens on which it was based. All three samples are still present among specimens labelled as syntypes.

1. NMW 16261 and 16441: specimens collected by Heckel during his travel to Upper Austria in September 1824 in Lake Traun at Gmunden (the acquisition number 1824.II.10); two specimens are still in NMW (16261 and 16441) (Fig. 19), and one was sent to Muséum national d'Histoire naturelle in Paris (MNHN-IC-0000-3894). NMW 94795, a pair of pharyngeal bones (locality: Gmunden; labelled (handwritten by Heckel) as *Aspius Heckelii*) apparently belongs to one of the two stuffed specimens. The two NMW specimens have a standard length (139.8 mm and 134 mm, respectively) which corresponds to total length equalling "Spanne" [Handspanne] (the distance between the end of the little finger and the end of the thumb that is ca 18–22 cm), mentioned in the original description.
2. NMW 50440, 55650 and 55652: specimens received later [than 1824] from Agassiz. These specimens are most probably those registered under the acquisition number 1830.II.3. The acquisition 1830.II contains seven entries in total (e.g., 1830.II.1 is for *Gobio uranoscopus*) and reads "Bavaria. November 1829. Von Herrn Leopold Fitzinger durch Kauf". This acquisition is made by Jos. Natterer and 1830.II.3 refers to later by Heckel, 6 individuals (4 were sent to Lüttich (Liege) on exchange). The labels for NMW 50440, 55650, and 55652 (with the acquisition number 1830.II.3) reading "Durch Agassiz aus München" (by Agassiz from Munich) appeared later, at Steindachner's time, and are most probably based on information from the Heckel's description of *Aspius mento* Agassiz as a synonym of *Aspius heckelii* Fitzinger (Heckel 1836: 225).
3. NMW 55630: one specimen, 9 Zoll (Viennese inches) long (total length; 237 mm) from the Danube near Vienna. This specimen (Fig. 20) was registered under the acquisition number 1836.I.19: Danube at Vienna. November 1835.

Type locality. The original description reads (Heckel 1836: 225–226): 1. "... bei Gmunden in Ober-Oesterreich in September 1824, und zwar ziemlich häufig unter der über die Traun führenden Brücke" (near Gmunden in Upper Austria in September 1824, quite often under the bridge over the Traun) (the acquisition number 1824.II.10: Traun, ... Heckels Reise durch Oberösterreich... Nr. 80); 2. Bavaria. November 1829 (acquisition number 1830.II.3, purchased from Leopold Fitzinger; 3. Danube at Vienna. November 1835 (acquisition number 1836.I.19).



Figure 19. *Aspius mento* A a draft drawing by Heckel of a syntype from Gmunden, for Heckel (1836: pl. XIX, fig. 3) (NHMW Archive) B syntype NMW 16441, SL 140 mm, right lateral view.



Figure 20. *Aspius mento*, syntype, NMW 55630, SL 188 mm, Danube, Vienna A left lateral view B radiograph.

Etymology. The species name is a noun in apposition; an Italian *mento* for chin, mentum, reflecting a peculiar feature of the fish, its protruding chin.

Taxonomic status. After recent revisions of the genus *Alburnus*, it is commonly considered that *Alburnus mento* is a valid species (e.g., Bogutskaya and Naseka 2004: 79; Freyhof and Kottelat 2007: 214, 217; Kottelat and Freyhof 2007: 171; Bogutskaya et al. 2017: 106; Freyhof et al. 2018: 130). Lectotypification may be required as the syntypes include both the lacustrine form, the “true *Alburnus mento*” in its modern concept (the syntypes from Traunsee, Austria, and from Bavaria), and a riverine fish (NMW 55630, from Vienna) that belongs to a recently described species, *Alburnus sava* Bogutskaya, Zupančič, Jelić, Diripasko & Naseka, 2017 (Bogutskaya et al. 2017).

Distribution. *Alburnus mento* is a lacustrine species in most subalpine lakes in Germany and Austria.

Conservation. IUCN: *Alburnus mento* is in the LC category (Freyhof and Kottelat 2008c). In the Red Data List of Lower Austria (Wolfram and Mikschi 2007: 21, as *Chalcalburnus chalcoides mento*) not referred to any of threatened categories.

Genetic information. Amplification and sequencing of only the first of the two overlapping fragments of the mitochondrial COI region (LabIDs Amento1, Amento3, Amento5; 114 bp in total, GenBank Accession Nos. PP579754–PP579756) was successful in two lacustrine (NMW 50440 and 55652) and one riverine specimen (NMW 55630). In this short fragment, all three sequences of all three specimens differ in one nucleotide base. Nucleotide blast search puts them in the same group as *A. mento* and other “shemayas” from Turkey (e.g., GenBank Accession Nos. MT407383, NC019574, MG182572, MT407410, MW649504). In the publication reporting on Austrian DNA barcode inventory of fish species (Zangl et al. 2022), *A. mento* was not mentioned. Thus, further research is needed to resolve the taxonomic status of this group and of the type specimens.

5. *Blicca argyroleuca* Heckel, 1843

Original publication of the name. Heckel (1843: 1007, pl. 1).

Remarks. Heckel (1843) is a part of the Vol. 1, Part 2, of Russeger's *Reisen in Europa, Asien und Afrika mit besonderer Rücksicht auf die naturwissenschaftlichen Verhältnisse der betreffenden Länder, unternommen in den Jahren 1835 bis 1841*. Also published as a special print under the title *Abbildungen und Beschreibungen der Fische Syriens nebst einer neuen Classification und Charakteristik sämtlicher Gattungen der Cyprinen* (Illustrations and descriptions of the fish of Syria along with a new classification and characteristics of all genera of cyprinids). It contains pp. 1001–1012 Zahn-System der Cyprinen (Tooth system of the cyprinids), pp. 1013–1043 Dispositio systematica familiae Cyprinorum (Systematic arrangement of the family Cyprinidae), and pp. 1044–1099 Süßwasser-Fische Syriens (Freshwater fishes of Syria). A volume of figures for this publication was published later, presumably in 1843–1838, in Stuttgart.

In the original publication, Heckel only refers to the structure of the pharyngeal teeth of a single specimen (Heckel 1843: pl. 1), and the description is unambiguously available as providing a clear diagnosis referring to a single species name. Though, in later times, the date and authorship of the species name

was often thought to be Heckel and Kner (1857: 120), presumably following Günther (1868: 306) and Berg (1916: 305).

It is not quite clear why Heckel did not refer in his publications to the Linnaeus' (1758) name of the species, *Cyprinus bjoerkna*, and is always only citing the species name as *blicca*, e.g., *Cyprinus blicca* of Bloch (1782) and Fries and Eckstrom (Fries et al. 1837: tab.12) (Heckel 1843: 1032; Heckel and Kner 1857: 120). As Heckel (1843: 1032) established a new genus, *Blicca*, with pharyngeal teeth 2.5–5.2 (in contrast to 3.5–5.3 in *Abramis*), it seems quite probable that the new name *argyroleuca* was given just to avoid Strikland's tautonymy (to avoid the *Blicca blicca* combination) as it was a common practice at the time (also, see *Idus melanotus* below).

Holotype or a syntype. NMW 94767, left pharyngeal bone (uppermost tooth in the longer row broken) (Fig. 21).

Remarks. A single (left) pharyngeal bone is now kept in the collection. As mentioned in Introduction, in many cases, individuals from which the pharyngeal bones were taken for a special study, are still kept in NHMW. We failed to find any individual lacking pharyngeal bones that could be a source of the original description. Although it is worth mentioning, that Heckel had apparently examined more than one whole individual identified by him as *Blicca argyroleuca* before he published the description as his original drawing represents the fish collected in the Danube in July 1841 (Fig. 22) with counts given as ranges, e.g., 19–21 anal-fin branched rays. At present, there are no specimens of *Blicca* in the Fish collection that could be confirmed as collected in July 1841 from the Danube. However, we cannot exclude that pharyngeal teeth morphology was studied in more than one specimen.

Apparently due to the misinterpretation of the date and authorship, all specimens in NMW lots, historically (since Heckel's time) labelled as *Blicca argyroleuca*, became considered as syntypes of the species: NMW 16901 (2; 1840, Fish market in Berlin), 54918 (6; 1836, Vienna), 54919 (4; 1836, Neusiedlersee), 54920 (1; 1842, Pommern). All 13 of them have the pharyngeal bones intact.

Among the mentioned above possible syntypes, NMW 54918 (6 specimens, SL 111–222 mm) (Fig. 23) is the only lot with individuals collected in the Danube at Vienna (acquisition 1836.I.9).



Figure 21. Possible holotype (or a syntype) of *Blicca argyroleuca*, NMW 94767, left pharyngeal bone.

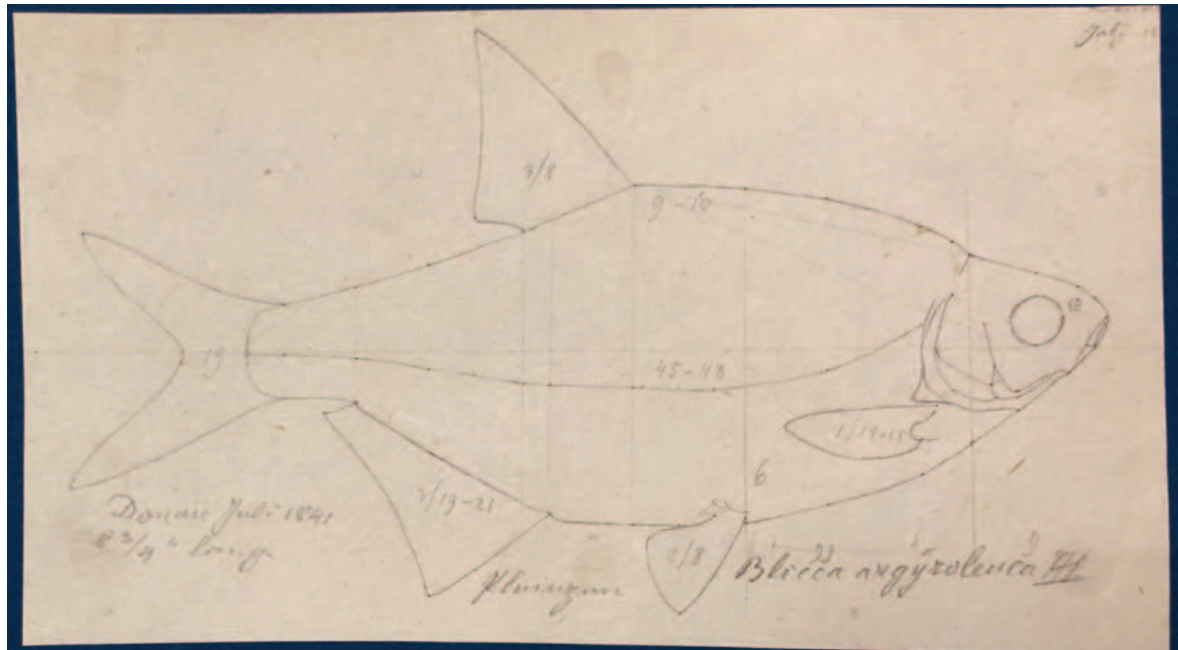


Figure 22. A draft by Heckel of the drawing of a specimen (or a possible syntype) of *Blicca argyroleuca*, representing a fish collected in the Danube in July 1841; this may be a composite (note ranges of counts) (NMH Archive).



Figure 23. *Blicca argyroleuca* NMW 54918:2, SL 156 mm, Danube at Vienna **A** left lateral view **B** radiograph, with intact pharyngeal bones.

Type locality. Not provided in the original description (Heckel 1843: 1007). The label of the possible holotype NMW 94767 reads Oder that is later included in the range of the species by Heckel and Kner (1857: 122).

Etymology. The species name is a patronym, a noun in the genitive; named for Friedrich Sigismund Leuckart, a German naturalist (1794–1843).

Taxonomic status. Synonym of *Blicca bjoerkna* (Linnaeus, 1758).

Distribution. *Blicca bjoerkna* is native to North, Baltic, White, Black (south to Rioni drainage) and Caspian Sea basins, Atlantic basin southward to Adour drainage and Mediterranean basin in France (Hérault and Rhône drainages), in Aral, Marmara and Anatolian Black Sea basins west of Ankara. Locally introduced elsewhere (Spain, northeastern Italy, France) (Freyhof and Kottelat 2008d).

Conservation status. IUCN: *Blicca bjoerkna* is in the LC category (Freyhof and Kottelat 2008d). In the Red Data List of Lower Austria (Wolfram and Miksch 2007: 113) as Not Endangered (“nicht gefährdet”).

Genetic information. Amplification and sequencing of only the second of the two overlapping fragments of the mitochondrial COI region (LabID Bargy4; 112 bp in total, GenBank Accession No. PP579757) was successful in the specimen NMW 54918. This short fragment is identical to sequences of *Blicca bjoerkna* collected in Austria (Zangl et al. 2022).

6. *Cyprinus acuminatus* Heckel & Kner, 1857

Original publication of the name. Heckel and Kner (1857: 57, fig. 22).

Remarks. The name is objectively invalid being a junior homonym of *Cyprinus acuminatus* Richardson, 1846.

The original description is based on more than one individual (the numbers of countable feature are given as ranges, e.g., the number of branched dorsal-fin rays is 18–20). Besides, Heckel refers to two of his earlier species (unavailable, nomina nuda): *Cyprinus angulatus* and *Cyprinus thermalis* “Heck. nov. spec. (Hungaria)” (Heckel 1843: 1013). Fig. 24 represents a draft (made by Heckel) of the original drawing used in the original publication (Heckel and Kner 1857: fig. 22) of an individual from the Danube at Vienna.

Syntypes. NMW 52846 (2), acquisition 1836.I.2, Vienna; 52854 (1) and 52855 (1), acquisition 1836.I.22, Neusiedlersee, coll. Lestrin; 52927 (1), 52928 (1), 52929 (1), 53403 (2), acquisition 1840.III.3, Plattensee (Balaton), received from “Laboratorium”; 52950 (9), acquisition 1840.III.4, Kesythely (Keszthely, Balaton), received from “Laboratorium”; 94708 (a pair of pharyngeal bones; before 1857, Heckel).

Recent measurements of the Viennese syntypes, NMW 52846 (TL, SL): 230 mm, 182.5 mm (Fig. 25) and 123.5 mm, 97 mm. Preservation condition good.

Type locality. Danube, Neusiedler Lake and Plattensee (Balaton Lake) in the original description (Heckel and Kner 1857: 60); these localities refer to the localities of the syntypes.

Etymology. The species name is a Latin adjective, past participle of *acuminare* “to sharpen”, from *acumen* “a point”, and refers to the shape of the snout.

Taxonomic status. The name has been considered a synonym of *Cyprinus carpio* Linnaeus, 1758, or its variety, from as early as at least Günther (1868: 26).

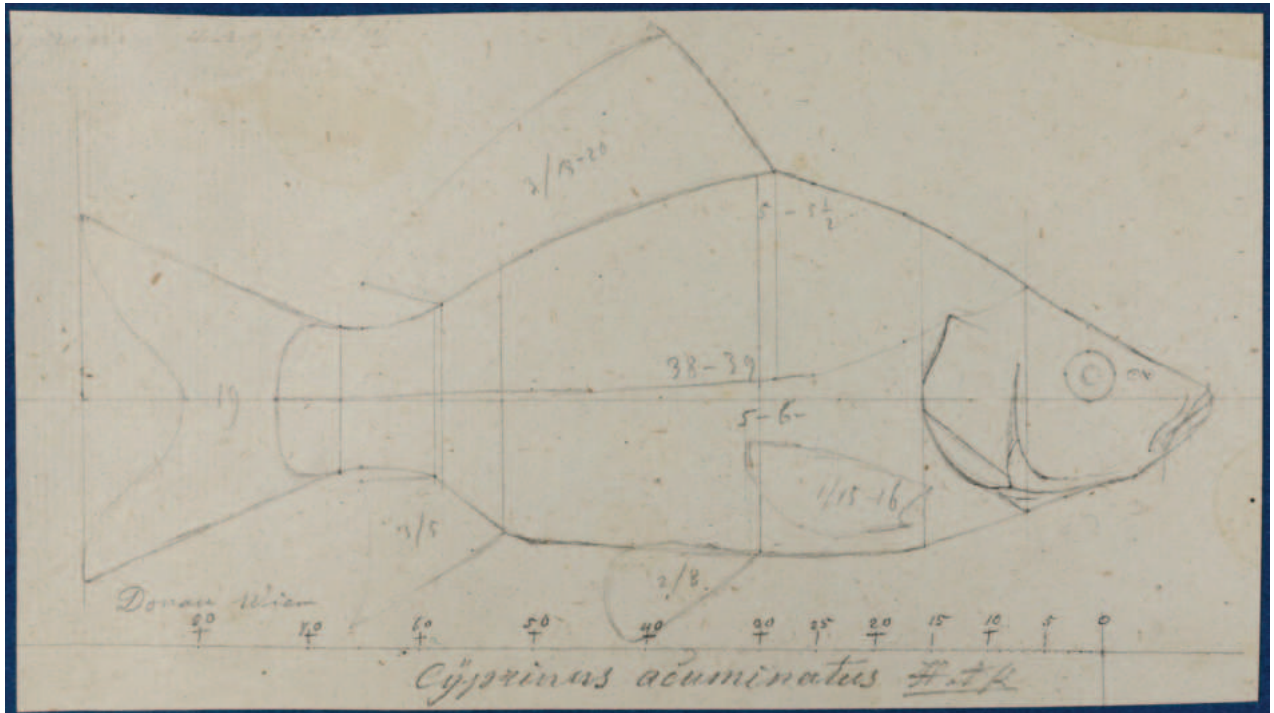


Figure 24. A draft by Heckel of his drawing of *Cyprinus acuminatus* for Heckel and Kner (1857: fig. 22), Danube, Vienna (NHMW Archive).

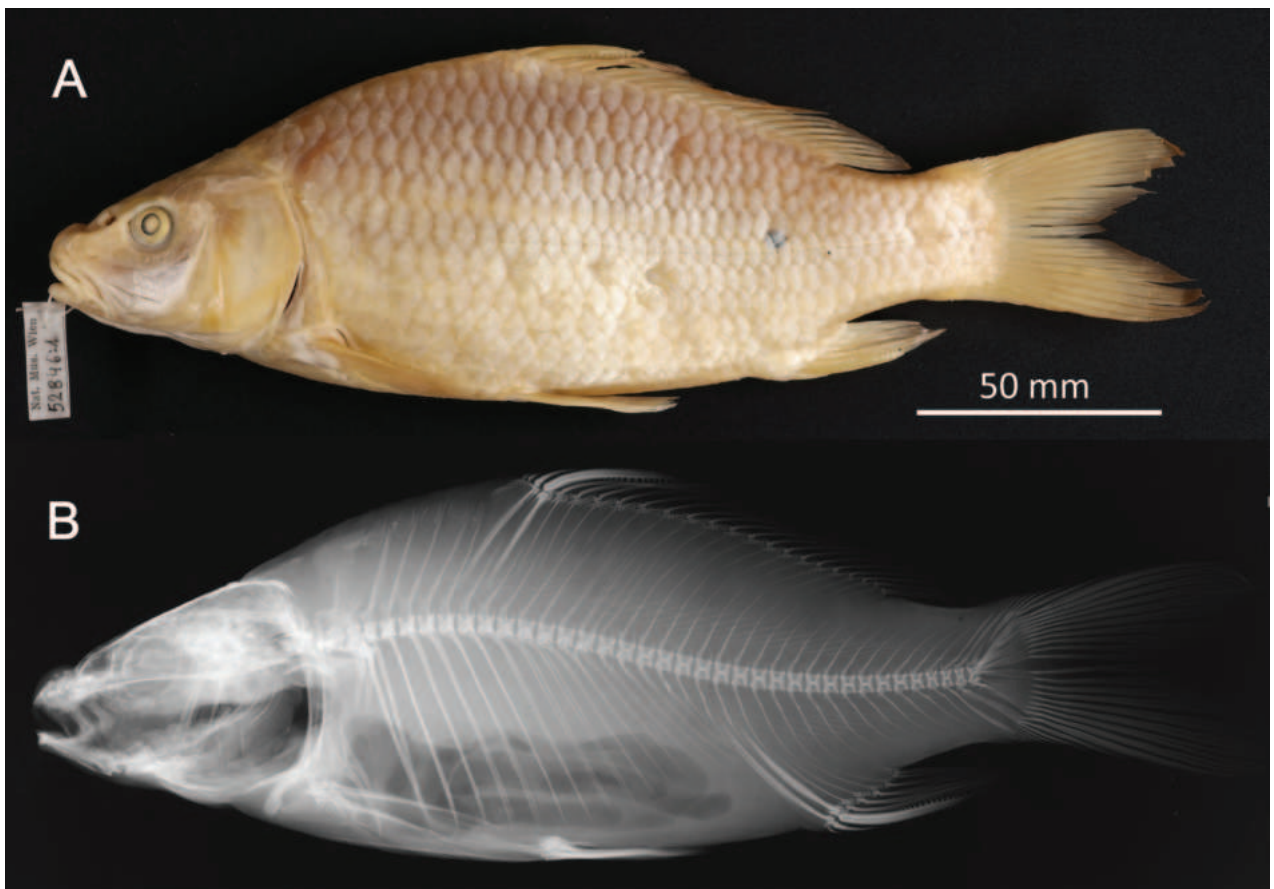


Figure 25. A syntype of *Cyprinus acuminatus*, NMW 52846:1, SL 182.5 mm, Danube, Vienna A left lateral view B radiograph.

Distribution. Wild European *Cyprinus carpio* is native to Black, Caspian and Aral Sea basins. Introduced throughout the world. Cultivated in large quantities for human food and stocked for sport fishing (Balon 1995).

Conservation status. IUCN: wild native European *Cyprinus carpio* is in the category VU (under criteria A2ce) (Freyhof and Kottelat 2008e). Important to emphasize, that common carp (*Cyprinus carpio*) is the world's oldest domesticated and the most important aquaculture species, but the native populations are slowly but continuously declining due to diverse reasons, first of all, competition with domesticated introduced common carp. In Western Europe, there is even a debate if native common carp still exist. Also, hybridisation with domesticated introduced stocks, East Asian congeners, and their hybrids, is a serious long-term threat for the species. However, superficially pure carp (currently, it is impossible to identify pure carp by genetic analysis) are still abundant in the lower parts of rivers within its native range. Most likely, only very few stocks remain "genetically unpolluted" as a result of this long-lasting process. The average age of the spawners is estimated to be between 20–25 years, as they are a long-lived species (up to 50 years). Although no population data exists, it is suspected that in the past 60 to 75 years within the species native range, river regulation (due to channelization and dams), which impacts the species as they need flooded areas at very specific times to successfully spawn, and hybridisation with introduced stock, has caused a population decline of over 30% (Freyhof and Kottelat 2008e).

In the Red Data List of Lower Austria (Wolfram and Mikschi 2007: 38) the wild native carp is in the category 2, Critically Endangered ("stark gefährdet").

Genetic information. Shot-gun sequencing resulted in over 68 million pair-end reads. Based on a subset of 15 million reads, a complete mitochondrial genome was assembled (LabID Cacu1; GenBank Accession No. for COI PP576059; for complete mitochondrial genome PP621518). According to a nucleotide blast search, the sequence with the highest identity score is OL693871, *C. carpio* from Eugene, Portland, USA. Further analysis is beyond the scope of this paper, and will be presented elsewhere.

7. *Idus melanotus* Heckel, 1843

Original publication of the name. Heckel (1843: 1008, pl. I).

Remarks. In the original publication, Heckel only refers to the structure of the pharyngeal teeth, and the description is unambiguously available as providing a clear diagnosis referring to a single species name. Though, in later times, the date and authorship of the species name was often thought to be Heckel (1852a: 56, 66) (Günther 1868: 230) or Heckel and Kner (1857: 147, figs 77, 78), apparently following, e.g., Berg (1912: 163).

As Heckel (1843: 1037) established a new genus *Idus* in the same publication, it seems quite probable that the new name *melanotus* was given to just avoid Strickland's tautonymy (to avoid the *Idus idus* combination) as it was a common practice at the time (similar to *Blicca argyroleuca* above).

Syntypes. 1. NMW 94805, a pair of pharyngeal bones (Fig. 26) labelled *Idus melanotus* Heckel, that may belong to NMW 58775:1 (Fig. 27). 2. Specimens



Figure 26. Syntype of *Idus melanotus*, NMW 94805, a pair of pharyngeal bones, which apparently belongs to NMW 58775:1 (Fig. 27 below, see the text for explanation).



Figure 27. Syntype of *Idus melanotus* NMW 58775:1 (with its pharyngeal bones separated as NMW 94805, Fig. 22) **A** left lateral view **B** radiograph; arrow indicates the lack of the pharyngeal bones.

collected or received in the Fish collection before 1843 and lacking pharyngeal bones that may indicate that Heckel examined the teeth and used these data in the original description, as follows: "Alte Sammlung" (Vienna): 53434 (1); Acquisition 1840.VII.10–11 (Berlin, leg. Rammelsberg): 53436 (1), 53438 (1), 53467 (1); Acquisition 1825.V.35a (Bayern, leg. Langthaler): 53439 (1); Acquisition 1842.I.13 (Pommern, coll. Hornschuh): 53455 (1); Acquisition 1825.V.34 (Vienna): 58775:1. 3. The specimen in a draft of the drawing, collected in the Danube in May 1841, 1 ¼ inches long (296 mm) (Fig. 28) (absent at present from the collection).

Recent measurements of NMW 58775:1 (TL, SL): 380 mm, 291 mm. Preservation condition: good.

Remarks. As explained in Introduction, in many cases, cypriniform specimens from which the pharyngeal bones were taken for a special study by Heckel, were still kept in the collection. We assumed that the pharyngeal bones NMW 94805 belong to the individual under the number NMW 58775 as they suit each other by size, and NMW 58775:1 is the only one extant individual collected at Vienna before 1843, which lacks pharyngeal bones, among the whole set of extant Heckel's *I. melanotus* specimens.

Type locality. Not provided in the original description (Heckel 1843: 1008). The NMW 94805 and 58775 (possibly representing one and the same individual) are from Vienna. The Danube by Vienna is also included in the range of distribution of the species by Heckel and Kner (1857: 148).

Etymology. The species name is a Latinized Greek adjective, *melano*, meaning black and *melanotus*, meaning the black-coloured one, alluding to the predominantly black dorsal colouration of the fish.

Taxonomic status. Synonym of *Leuciscus idus* (Linnaeus, 1758) since soon after the description (e.g., Günther 1868: 230).

Distribution. *Leuciscus idus* is native to Baltic, Black, northern Caspian and North Sea basins, Atlantic basin southward to Seine and lower Loire drainages (France). Introduced to Great Britain and northern Italy (Freyhof and Kottelat 2008f).

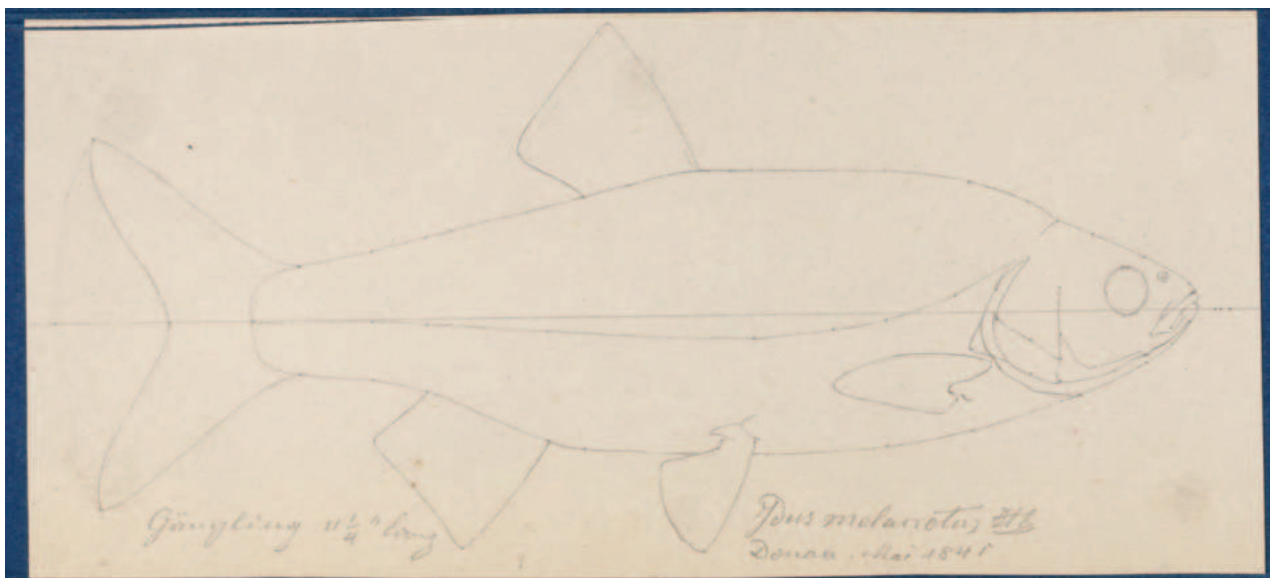


Figure 28. A draft by Heckel of the drawing of a specimen (a possible syntype) *Idus melanotus*, representing a fish collected in the Danube in May 1841 (NHMW Archive).

Conservation status. IUCN: *Leuciscus idus* is in the LC category (Freyhof and Kottelat 2008f). In the Red Data List of Lower Austria (Wolfram and Mikschi 2007: 113) in the category 3, Endangered (“gefährdet”).

Genetic information. DNA extraction was performed on two specimens, NMW 53434 and 58775, but genetic analysis was successful only on the first. Two overlapping fragments of the mitochondrial COI region (LabID Imel1; 217 bp in total, GenBank Accession No. PP576058) were successfully amplified. The sequence is identical to the *L. leuciscus* or *L. idus* (which, based on COI sequences, exhibit no differences) sequences from Austria (Zangl et al. 2022).

8. *Idus miniatus* Heckel & Kner, 1857

Original publication of the name. Heckel and Kner (1857: 151, no figure).

Remarks. In an earlier publication, Heckel (1843: 1038) introduced the name *Idus miniatus* but did not provide any reference, figure or description leaving the name nomen nudum. Similar to the case of *Idus melanotus*, described above, a pair of pharyngeal bones is kept labelled as “*Idus miniatus* Heckel. Hofgarten” among the Heckel’s collection of cyprinid pharyngeal bones, NMW 94807. The name became available in Heckel and Kner (1857) as above, and, as an exception, no figure of the fish is provided.

Holotype. NMW 53432 and a pair of pharyngeal bones, NMW 94807 (Fig. 29), that apparently belongs to this individual. Preservation condition: very poor (decomposed).

Remarks. The original description per se is based on a single specimen; and only one specimen was registered as *Idus miniatus* Heckel from “Hofgarten” – acquisition entry 1852.XV.1, Royal Gardens of Burg (k.k. Hofgarten), received from Court gardener (Hofgärtner) Antoine, is handwritten by Heckel. However, the text in Heckel and Kner (1857: 151–152) mentions observations on size of the species: “Reaching the size and weight of the Orfe, our longest specimens do not measure a full foot”.

Type locality. The species name is applied to captive fish; they had been kept in the pond of the Imperial court garden of the castle in Vienna but originated from Tyrol (Heckel and Kner 1857: 151): “For many years, numerous specimens of a fish very close to the orfe have lived in the pond of the imperial court garden of the castle in Vienna, which was supposedly first brought here from Tyrol, but which maintains and reproduces constantly in its own characteristics. Although it is therefore only a cultured fish and is limited to a single locality, we believe that we should not ignore it and distinguish it as *Idus miniatus*, a new species”. So, according to Art. 76.1.1 of the Code (International Commission on Zoological Nomenclature 1999), the type locality is Tyrol.

Etymology. The species name is a Latin first/second-declension adjective meaning scarlet, cinnabar-red in reference to the reddish (“blasser rot”) colouration of the back of the fish.

Taxonomic status. Synonym of *Leuciscus idus* (Linnaeus, 1758).

Distribution. As *Leuciscus idus* (above).

Conservation status. As *Leuciscus idus* (above).

Genetic information. Amplification and sequencing of only the second of the two overlapping fragments of the mitochondrial COI region (LabID Imini1; 149 bp



Figure 29. *Idus miniatus* syntype, NMW 94807, a pair of pharyngeal bones, apparently dissected out of NMW 53432 (now decomposed).

in total, GenBank Accession No. PP579758) was successful in the specimen NMW 53432. The sequence is identical to the *L. leuciscus* or *L. idus* (which based on COI sequences exhibit no differences) sequences from Austria (Zangl et al. 2022).

9. *Leuciscus virgo* Heckel, 1852

Original publication of the name. Heckel (1852a: 69, pl. VI, figs 1–8, mature male with breeding tuberculation, and pl. VII, figs 1–5).

Remarks. This paper is published in the Proceedings of the Academy of Sciences in Vienna, Mathematics and Natural Sciences class (Sitzungsberichte der Akademie der Wissenschaften in Wien, Mathematisch-Naturwissenschaftliche Klasse), Vol. 9 (1) with pagination 49–123, and numbers of plates of figures VI–XIII, and, also, as a separate with different pagination, 127–201, and numbers of plates of figures, XI–XVIII. It is one of six papers by Heckel (1850, 1851a, 1851b, 1851c, 1852a, 1852b) in Sitzungsberichte as a series of reports on his travel to the Alps area.

The original description is based on a number of individuals, the length of the described specimens is 6–15 Zoll (Viennese inches) (= 158–395 mm) (Heckel 1852a: 76); one of them was apparently dissected as the numbers of vertebrae is given, and at least four specimens are presented by the pharyngeal bones.

Syntypes. NMW 22373 (1) and NMW 50626 (1), whole individuals in alcohol, pharyngeal bones intact; NMW 94733 (4 pairs of pharyngeal bones from fish of a variety of size). It is not clear to which acquisition numbers these individuals

refer to; there are at least three acquisition entries referring to this species: 1. 1825.IV.4 (one specimen), 2. 1825.IV.4 (one specimen), both purchased in the first semester of 1825 from “Laboratorium” (supposedly, Danube at Vienna); 3. 1836.I.12 (two specimens), Danube, no other data; all three acquisition records were made by Heckel, first as *Leuciscus Jeses* but then the species name corrected (in pencil) to *virgo*. In 1825.IV.4 entry, there is a later note by Heckel in pencil “[sent] to Munich”. One more syntype, apparently not preserved as a whole fish or lost, is the one in the figures (Heckel 1852a: pl. VI–VII), collected in the Danube in June 1841, 14 $\frac{3}{4}$ Zoll (Viennese inches) long (389 mm) (Fig. 30).

Recent measurements of the extant syntypes collected at Vienna (TL, SL): NMW 22373 (Fig. 31), 225 mm, 180 mm; 50626, 210 mm, 152 mm. Also, NMW 94733, a pair of pharyngeal bones. Preservation condition: good.

Type locality. Not clearly provided in the original description but apparently the Danube. The syntypes are from Vienna and from the Danube without specification.

Etymology. The species name is a Latin word for virgin or maiden, which serves both as adjective and substantive.

Taxonomic status. Commonly treated as a synonym of *Rutilus pigus* (Lacepède, 1803) in earlier literature (e.g., Berg 1912: 79; Kottelat 1997: 79); a valid species, *Rutilus virgo* (Heckel, 1852), in most recent publications (Bogutskaya and Iliadou 2006: 294, Kottelat and Freyhof 2007: 247; many others).

Distribution. Danube drainage upriver of Iron Gate; most abundant in Save drainage (Freyhof and Kottelat 2008g).

Conservation status. IUCN: *Rutilus virgo* is in the LC category (Freyhof and Kottelat 2008g). In the Red Data List of Austria (Wolfram and Mikschi 2007: 47) (as *R. pigus virgo*) in the category 2, Critically Endangered (“stark gefährdet”).

Genetic information. Two overlapping fragments of the mitochondrial COI region (LabID Lvir1; 217 bp in total, GenBank Accession No. PP576056) were successfully amplified in the specimen NMW 50626. The sequence is identical to the Austrian *R. virgo* sequences (Zangl et al. 2022) and clearly distant from both *Rutilus rutilus* (Linnaeus, 1758) and *R. pigus* (Fig. 32).

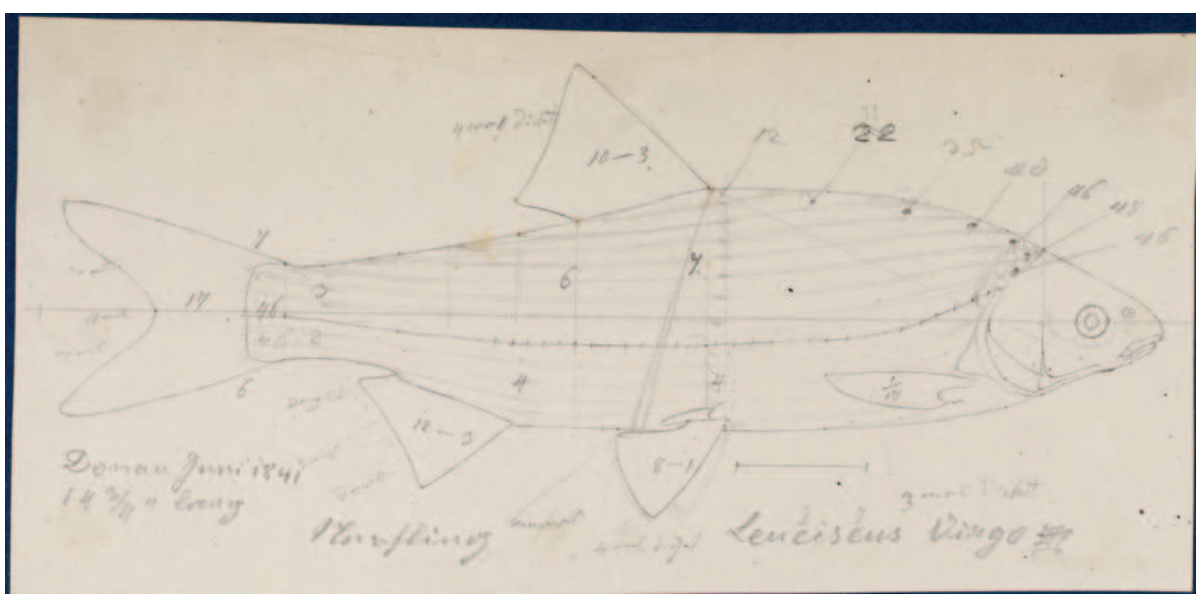


Figure 30. A draft by Heckel of the drawing of *Leuciscus virgo* published in Heckel (1852a: pl. VI and VII), Danube, June 1841 (NHMW Archive).



Figure 31. A syntype of *Leuciscus virgo*, NMW 22373, SL 180 mm, possibly Vienna **A** left lateral view **B** radiograph.

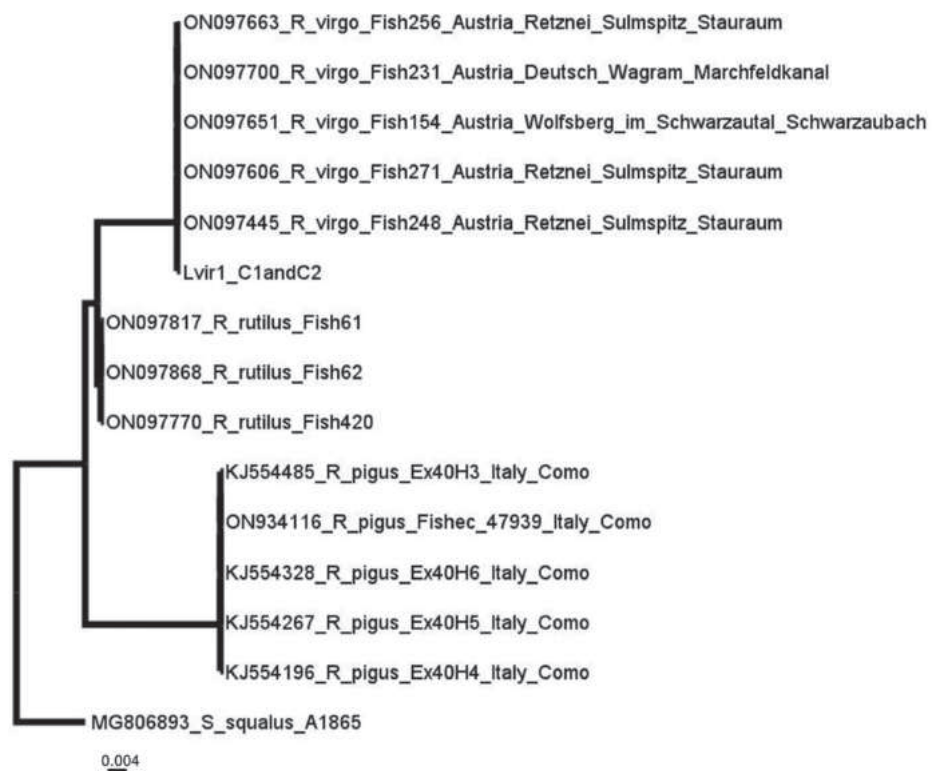


Figure 32. A simple neighbour-joining tree (MEGA 6.0; Tamura et al. (2013)) calculated based on a 218-bp long cytochrome oxidase I fragment and sequences downloaded from GenBank. Species names, localities, and accession numbers are given.

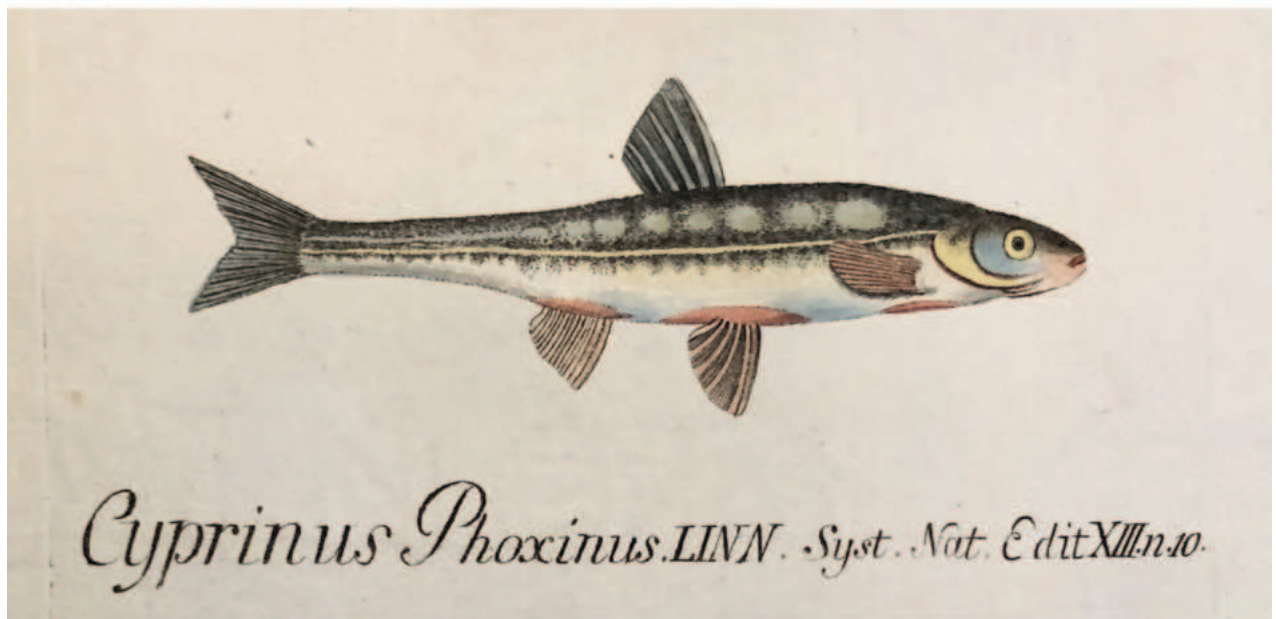
10. *Phoxinus marsilii* Heckel, 1836

Original publication of the name. Heckel (1836: 232).

Remarks. The original description does not contain any specification of the examined specimens but makes clear that Heckel had examined (or observed) many. Heckel also refers to *Cyprinus aphy* of von Meidinger (1786: pl. XV) (Fig. 33a), *Cyprinus phoxinus* of von Meidinger (1790: pl. XXXIX) (Fig. 33b) and *Phoxinus laevis* of Fitzinger (1832: 337).



A



B

Figure 33. A *Cyprinus aphy* from von Meidinger (1786: pl. XV); note the handwritten identification made by Heckel **B** *Cyprinus phoxinus* from von Meidinger (1790: pl. XXXIX).

He also provides a comparison of *Phoxinus* from the upper Danube in Germany (that could represent *P. csikii* in present understanding) and the new species: “Our museum owes many specimens of this species to the kindness of Professor Agassiz, who found them in Bavaria, and sent to the Cabinet Collection under the name *Phoxinus laevis*. How closely this species approaches our local *Phoxinus Marsilii* in colour, from which it differs slightly by its larger scales and the lateral line that disappears in front of the tail, I do not dare to determine from specimens in alcohol; meanwhile, the black spot on the caudal fin is clearly visible, the back appears light brown with darker spots, the sides are mottled black along its length and the belly is silver; in terms of size they are at least 1/3 larger than the following [*P. marsilii*]”.

Lectotype. NMW 51225, male (Fig. 34) (former 51225:2). Lectotype designated by Palandačić et al. (2017b: 2). Recent measurement of the lectotype: SL 65.5 mm. Preservation condition: bad (desiccated). Former syntypes (51225:1 and 51225:3–6), now paralectotypes, are NMW 98672.

The sample NMW 51225 was apparently registered (included into the inventory book) in Pietschmann’s time (judging from the number of the record and the handwriting) as belonging to the acquisition record 1836.I.20 for “*Phoxinus marsilii* Donau”, but the locality was given as Vienna, possi-



Figure 34. Lectotype of *Phoxinus marsilii*, NMW 51225, lectotype, SL 65.5 mm, male, possibly, at Vienna **A** lateral view, **B** ventral view of head and breast to show a distinguishing feature of the species, continuous patches of breast scales (type 6 as defined in Bogutskaya et al. 2019: table 2) **C** radiograph.

bly based on some information (e.g., labels that have been lost). However, there were only two (not six) individuals in the acquisition entry 1836.I.20 and the species name was given as already existing (known) that may indicate that the sample had been collected (received) after the species description. The six specimens which were considered syntypes, NMW 51225:1–6 (now 51225 and 98672) are in a very similar preservation condition (dried apparently long ago), so, all six specimens may belong to one and the same sample. We would assume that Heckel had seen all museum samples that were present in the collection before he described the species in 1836. These could be as follows.

1. 1825.IV.16 (eight specimens, bought from Laboratorium; possibly, Danube at Vienna or nearby).
2. 1826.VI.10 (two specimens, Moosbrunn in the south of Vienna);
3. 1830.II.5 for *Leuciscus Aphyia*, 11 specimens (three from them were sent to Lüttich (Liege) on exchange) and 1830.II.6 for *Leuciscus Phoxinus*, ten specimens; in total, these acquisitions include seven samples (records) received from Leopold Fitzinger (see also the account on *Aspius mento* above) and, apparently, the identifications were made by him; localities not specified but apparently the Danube.

Type locality. The original description does not specify neither examined individuals nor localities. However, it is clear from the context (Heckel 1836: 232–233) that the name is assigned to a *Phoxinus* from the Austrian part of the Danube: “Man findet unser Fischchen sehr häufig und in grossen Gesellschaften in allen klaren Bächen der Wiener-Gegend und weiter” (“Our little fish can be found very often and in large groups in all clear streams in the Vienna area and beyond”), which is compared with the Bavarian *P. laevis* (Heckel 1836: 232). As Heckel also refers to *Cyprinus aphyia* and *Cyprinus phoxinus* of von Meidinger (1786: tab. XV and 1890: XXXIX, respectively) and *Phoxinus laevis* of Fitzinger (1832: 337), he apparently defines the range of the species as, at least, Danube within the [former] Austrian Empire.

As shown above, the exact locality of the lectotype is not quite clear; it is still probable that it belongs to the acquisition 1836.I.20 and the locality is Vienna. Genetic analysis presented in Palanadačić et al. (2017a, 2020) shows that the same mitochondrial genetic lineage (lineage 9) has been distributed in Vienna in the last 200 years.

Etymology. The species name is a patronym, a noun in the genitive; named after Count Luigi Ferdinando Marsili (or Marsigli, Latin Marsilius; 1658–1730), an Italian scholar and natural scientist, an author of “Danubius Pannonico-Mysicus”, richly illustrated work in six volumes containing much valuable historic and scientific information on the river Danube (published in 1726).

Taxonomic status. Recently re-established as a valid species (Palanadačić et al. 2017a); earlier, it was commonly treated as a synonym of *Phoxinus phoxinus* (Linnaeus, 1758).

Distribution. Danube drainage in Austria and Germany; also, Odra drainage in Germany (J. Freyhof, personal communication).

Conservation status. Not evaluated by IUCN. In the Red Data List of Lower Austria (Wolfram and Mikschi 2007: 91) (as *P. phoxinus*) in the category 4,

Potentially Endangered (“potentiell gefährdet”); evaluation of the conservation status of all three *Phoxinus* species distributed in Austria according to most recent revisions (Palandačić et al. 2017a, 2020) is strongly required.

Genetic information. Three previously published partial sequences of the genes cytochrome b (cytb, MF408203), COI (MF407956) and internal transcribed spacer 1 (ITS1, MN818242).

11. *Squalius delineatus* Heckel, 1843

Original publication of the name. Heckel (1843: 1041).

Remarks. The original description is based on more than one individual (the number of lateral-line scales is given as a range, and two localities are mentioned).

Syntypes. NMW 49783 (7) and 50794 (6) (Fig. 35), in alcohol, both from the acquisition record (made by Heckel) 1840.IX.4 (15 specimens, purchased from “Laboratorio”; Aderklaa); NMW 50796, in alcohol, acquisition record 1842.IV.33 (ten specimens (11 in the jar), Datschitz, Mähren [Dačice, Moravia]; NMW 94777 (a pair of pharyngeal bones, Vienna). Recent measurement of the syntypes (SL): NMW 49783: 57–59 mm; NMW 50794: 56.5–65 mm; NMW 50796: 39.5–67 mm. Preservation condition: average.

Type locality. In the original description as “in der Ebene des Marchfelds bei Wien, so wie auch in Mahren die einzelnen Feldlachen hautig bewohnt” (“in the plain of the Marchfeld near Vienna, as well as in Moravia”) (Heckel 1843: 1041). The Marchfeld is an area right in the north-east of Vienna on the left bank of the Danube; the locality Aderklaa belongs to this region (and is currently within the administrative boundaries of the city of Vienna).

Etymology. The species name is an adjective from Latin *delineatus*, past participle of *delineare* (to sketch out, from *de-* completely) + *lineare* (draw lines, from *linea* line), that refers to a peculiar feature of the species, a very shortened (reduced) lateral line.

Taxonomic status. A valid species since it was described, in a genus of its own, *Leucaspius* Heckel & Kner (1857: 145).

Distribution. *Leucaspius delineatus* is native to Europe from lower Rhine and northern Germany eastward to southern Baltic basin, Black Sea basin south to Rioni drainage, Aegean Sea basin (from Maritsa to Nestos), and in northern Caspian basin; in Asia, native to western Caspian basin (south to Kura drainage). Introduced elsewhere (France, Great Britain, Switzerland, western Siberia in the Ob drainage in Russia and Kazakhstan) (Freyhof and Kottelat 2008h).

Conservation status. IUCN: *Leucaspius delineatus* is in the LC category (Freyhof and Kottelat 2008h). In the Red Data List of Lower Austria (Wolfram and Mikschi 2007: 70) in the category 3, Endangered (“gefährdet”).

Genetic information. Genetic analysis was not successful.

12. *Squalius lepusculus* Heckel, 1852

Original publication of the name. Heckel (1852a: 109, pl. XII, figs 1–8).

Syntypes. The original description is mostly based on a single individual eight Viennese inches (= 158 mm) long (Heckel 1852a: 110, pl. XI, figs 1–4).



Figure 35. Syntypes of *Squalius delineatus*, NMW 50794:1, 3, Aderklaa **A** left lateral view **B** radiograph.

However, there are clear indications that Heckel used more than one specimen for the description. First, two drafts by Heckel represent different fishes: one (Fig. 36a) is apparently taken from a real fish collected in the Danube in January 1841, and the other one (Fig. 36b) may be a composite as it contains the number of lateral-line scales as a range (49–50) and a note, added apparently later (in ink) “vertebrae 21 abdominal and 19 caudal”. Second, as the number of vertebrae is given, then, apparently, a specimen (or specimens) was/were dissected; indeed, there are two entirely laterally dissected specimens among the specimens considered syntypes of the species, NMW 49347:1 (Fig. 37) and 49359:2. Third, individuals NMW 49354:1, 59348, and 49359:1 lack the pharyngeal bones that may indicate that one of these specimens were used

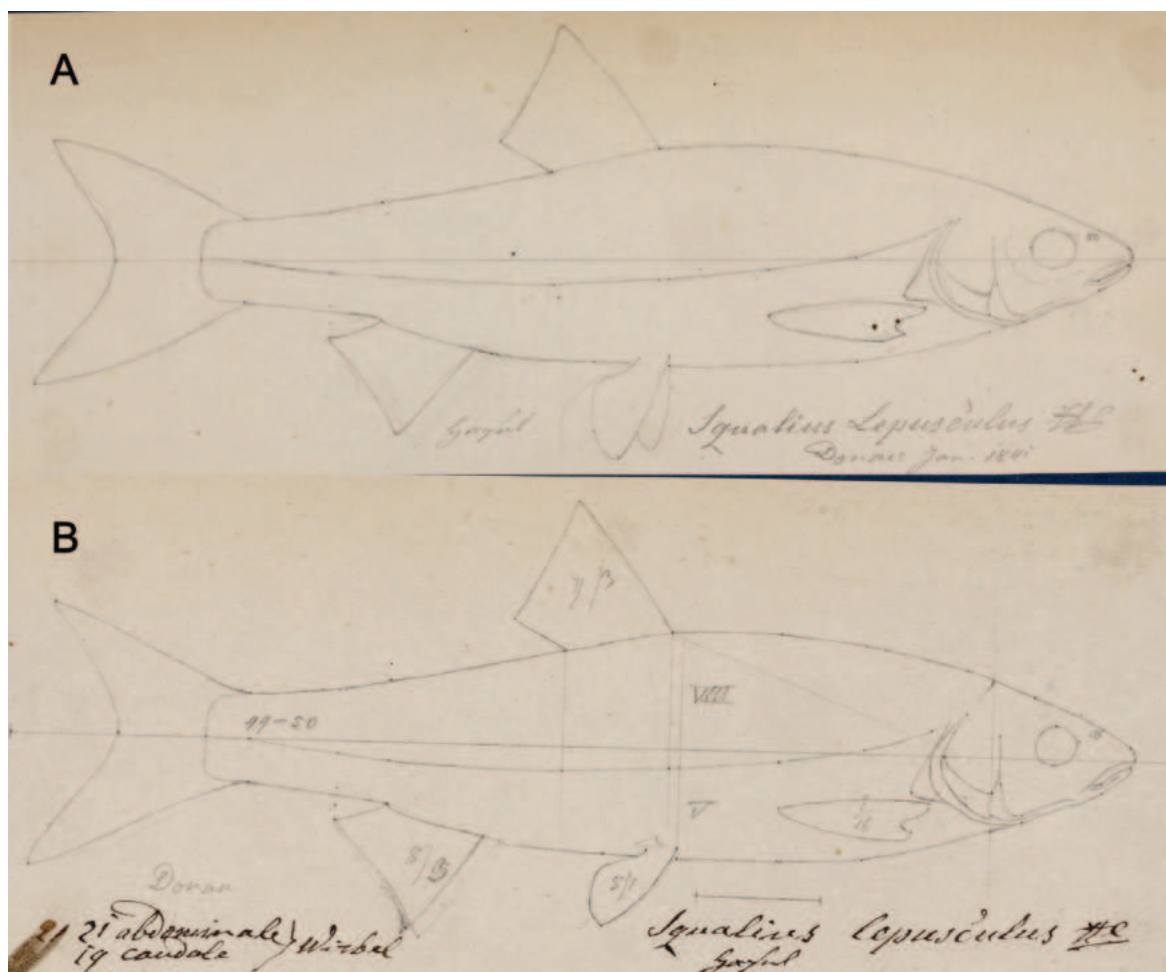


Figure 36. **A** *Squalius lepusculus*, original drafts by Heckel for the lithograph of the species presented in the original description (Heckel, 1852a: 109, pl. XII) and, later, in Heckel and Kner (1857: fig. 104) **B** a specimen collected in the Danube in January 1841 (NHMW Archive).

for the drawing of the pharyngeal bones (Heckel 1852a: pl. XI, fig. 3). NMW specimens historically labelled as syntypes of the species (all collected before 1852) are as follows: NMW 49345 (2), 49347 (2), 49348 (1), all three samples belong to the Acquisition 1825.IV.12–13, purchased from Laboratorio, Vienna; 49359 (2) and 49393 (2), both from the acquisition 1840.IX.8, purchased from Laboratorio, Moosbrunn (in the south of Vienna). Recent measurements (SL): NMW 49345 (2): 129 mm, 94 mm; 49347: 128.5 mm, 109 mm, 49348 (1): 146 mm; 49359 (2): 143 mm, 118.5 mm; and 49393 (2): 127 mm, 119 mm.

Type locality. Danube near Vienna and Moosbrunn (defined by the possible syntypes as above). In the original description, the type locality is not specified per se; specimens seen by Heckel (including those deposited in the collection at the time) are from Upper Danube, Vienna, Vltava near České Budějovice, Olsa at Teschen (Cieszyn), upper reaches of the Elbe, and the Oder.

Etymology. The species name is a Latin masculine noun, diminutive of *lepus* + *-culus*, meaning a young hare, or leveret.

Taxonomic status. Synonymised with *Leuciscus leuciscus* (Linnaeus, 1758) (= *Leuciscus vulgaris* auct.) soon after the description (Günther 1868: 226).

Distribution. *Leuciscus leuciscus* is native to North, Baltic, White, Barents, Caspian (Volga and Ural), Black Sea (Danube to Dnieper) basins (Freyhof 2011).



Figure 37. Possible syntype of *Squalius lepusculus*, NMW 49347:1, SL 128.5 mm, Vienna **A** left and **B** right lateral views **C** radiograph.

Conservation status. IUCN: *Leuciscus leuciscus* is in the LC category (Freyhof 2011). In the Red Data List of Lower Austria (Wolfram and Mikschi 2007: 118) as Not Endangered (“nicht gefährdet”)

Genetic information. Two overlapping fragments of the mitochondrial COI region (LabID Sleb1; 192 bp in total, GenBank Accession No. PP576057) were successfully amplified in the specimen NMW 49345:1. The sequence is identical to the *L. leuciscus* or *L. idus* (which based on COI sequences exhibit no differences) sequences from Austria (Zangl et al. 2022).

Aves type series

Aves: Anseriformes: Anatidae

1. *Anser brevirostris* Brehm, 1831

Original publication of the name. Brehm (1831: 844).

Syntypes. 1. AMNH 730708, 2. RMNH 87330, 3. NHMW 55.170 additional 4. NHMW 20.928.

Syntypes in the bird collection Natural History Museum Vienna:

NHMW 55.170 dry mounted (Fig. 38a); Acqu. No. 1824.VIII.19, female, adult; Seefeld; leg. et don. Graf Hardegg [Johann Dominik von Hardegg] (Fig. 38b); date of collecting is not given, presumably 1824. Preservation condition: good.

NHMW 20.928 dry mounted; Acqu. No. 1828.XI.1 (Fig. 39), female; Aspern; leg.: shot by H. [Herrn] Herzog; don. Erzherzog Kronprinz [Ferdinand]; date of collecting is not given, presumably 1828; though Marschall and Pelzeln (1882) states 27.11.[1828]. Preservation condition: good.

Remarks. Syntype status of AMNH 730708, RMNH 87330, 3. NHMW 55.170 was confirmed by Mlikovsky (2023), syntype status of NHMW 20.928 confirmed by Schifter et al. (2007).

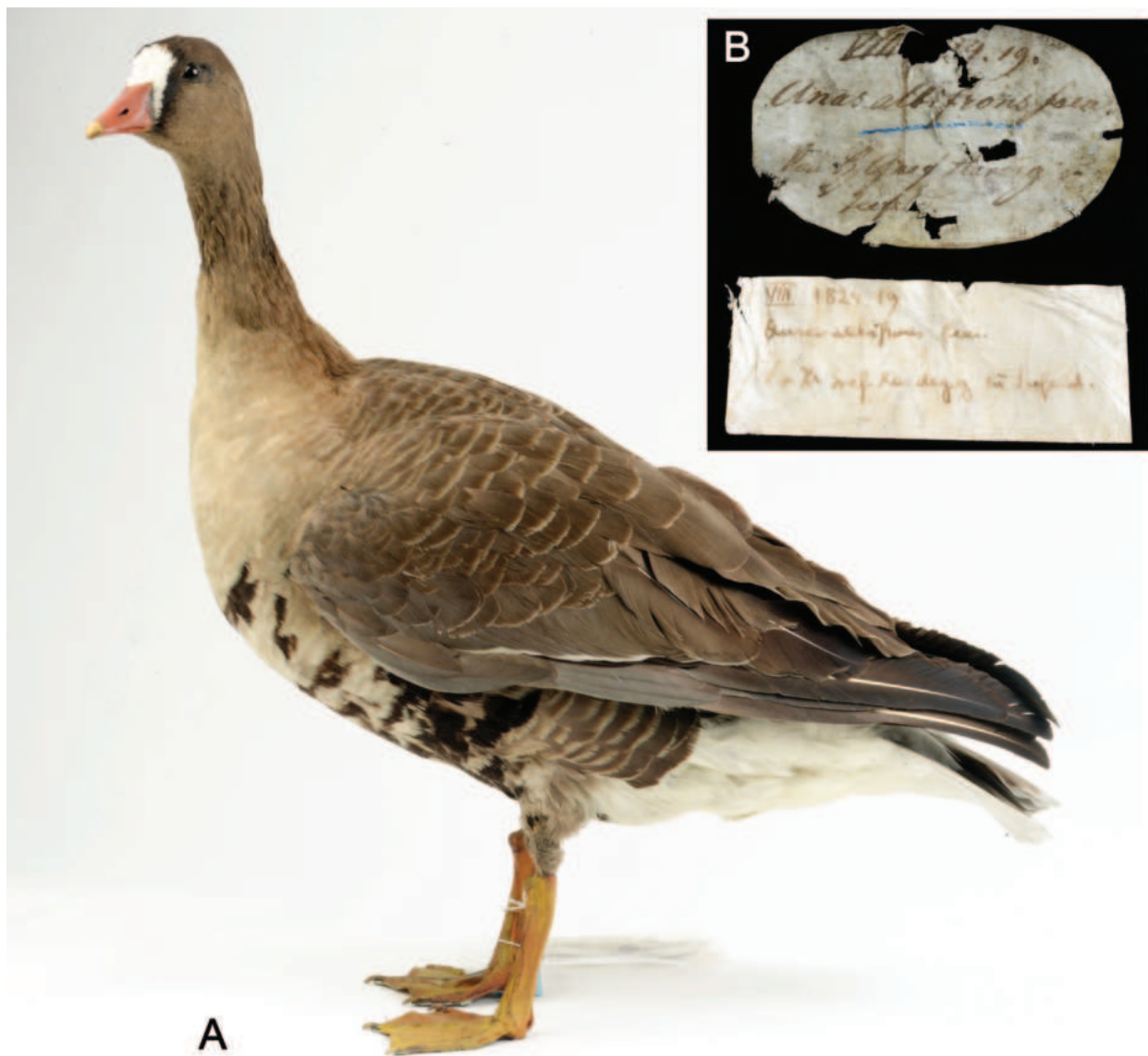


Figure 38. Syntype of *Anser brevirostris* **A** syntype of *Anser brevirostris* "Heckel" C.L. Brehm, 1831, NMW 55.170 **B** corresponding original labels, removed from pedestal.

Vogel-Sammlung. XI

1828
Oktober. *Königl. Acquisitionsprotokoll, welches eingetut in
Laufe des Jahres eines k. k. Hofrathes
verordnet*

Species	Individua
1. <i>Anas albifrons</i> f. in Aspern <u>von H. Schmidt (Hr. Jäger) in Mitterteufen.</u>	1
2. <i>Falco columbarius</i> m. <u>von H. Schmidt (Hr. Jäger) in Mitterteufen.</u>	1 Dobl.
3. <i>Falco cristatus</i> mas. <u>von H. Schmidt (Hr. Jäger) in Mitterteufen.</u>	1
4. <i>Falco Bonelli</i> adult. <u>von H. Schmidt (Hr. Jäger) in Mitterteufen.</u>	1
5. <i>Falco Bonelli</i> juv. <u>von H. Schmidt (Hr. Jäger) in Mitterteufen.</u>	1
6. <i>Anas modiolata</i> pull. m. <u>von H. Schmidt (Hr. Jäger) in Mitterteufen.</u>	1
7. <i>Columba domestica</i> ^{fabiana} <u>von H. Schmidt (Hr. Jäger) in Mitterteufen.</u>	1
8. <i>Falco gallus</i> <u>von H. Schmidt (Hr. Jäger) in Mitterteufen.</u>	1
9. <i>Trochilus giganteus</i> <u>von H. Schmidt (Hr. Jäger) in Mitterteufen.</u>	1
<i>J. P. Schaller</i> Cust.	
7 für die Sammlung 2 — Dobl. <hr/> 9	

Figure 39. Acquisition Sheet “1828.XI”, record 1828.XI.1. Entry for year 1828 in the acquisition book of the bird collection/NHM Vienna for the specimen of *Anser erythropus* (here sub *Anas albifrons*), NMW 20.928 (= syntype of *Anser brevisrostris* “Heckel” C.L. Brehm, 1831).

Type locality. 1. presumably Austria (from Vienna Market), 2. “Europe”, 3. Seefeld [Seefeld-Kadolz, Lower Austria; 48°43'N, 16°10'E]; 4. Aspern [48°13'N, 16°29'E Lower Austria; today 22nd district of Vienna].

Etymology. The species name *brevirostris* is from Latin *brevis* (short), *rostrum* (beak).

Taxonomic status. Synonym of *Anser erythropus* (Linnaeus, 1758).

Distribution. Breeds in discontinuous narrow band across Arctic Eurasia from Norway to E Siberia. Winters from C and SE Europe east to Iran and in some regions of E Asia (Carboneras and Kirwan 2020).

Conservation status. In the IUCN category VU (BirdLife International 2018).

Genetic information. Two overlapping fragments of the mitochondrial COI region (LabID Aerythro; 220 bp in total, GenBank Accession No. PP576054) were successfully amplified in the specimen NHMW 55.170. Unfortunately, the sequence was not long enough to unambiguously connect the type specimen with a certain mitochondrial genetic lineage. Thus, further molecular analysis of the type(s) is needed.

Conclusions

This catalogue presents and annotates historical type series of three parasitic worms, three myriapods, two insects, twelve fish, and one bird species with type locality in the state of Vienna. The catalogue includes historical information and the references to the literature in which they are mentioned, as well as photographs of specimens and their labels, scans of acquisition records, and radiographs where available. A total of 500 digital items have been produced, including the digitisation of 22 original descriptions, 17 drawings and illustrations, 64 acquisition books, registers, and labels, 52 catalogue cards, 91 radiographs, 241 image files, 12 short COI sequences, and one complete mitochondrial genome.

Genetic analysis was at least partially successful in 11 of the 21 type series, but only one extraction produced DNA of a quality that allowed shotgun sequencing, whereas in ten type series short fragments (100–230 bp) of COI were amplified and sequenced. The only existing *L. cavicola* syntype is already damaged and missing a leg, so genetic analysis was not attempted. Of the 27 specimens used for DNA extraction, genetic analysis provided at least some results in 13 specimens (48%), which is higher than previously reported for the NHMW Fish collection (Palandačić et al. 2020).

For the myriapod *Brachydesmus superus*, the genetic analysis provided the first genetic information of this species in Austria and a genetic reference for the species name to be used in further (barcoding) projects. For the insect *Tetrix tuerki*, the COI fragment obtained was identical to the COIs originating from specimens collected from the Austrian-German border. For the fish species *Abramis schreibseri*, *Blicca argyroleuca*, *Cyprinus acuminatus*, *Idus melanotus*, and *Idus miniatus*, the genetic analysis confirmed their taxonomic status as synonyms of *Ballerus sapa*, *Blicca bjoerkna*, *Cyprinus carpio*, *Leuciscus idus*, and *L. idus*, respectively. For *Rutilus virgo*, the genetic analysis confirmed the difference from *R. pigus* and the genetic identity with *R. virgo* recently collected in Austria (Zangl et al. 2022). For *Aspius mento*, the DNA fragment obtained did not contain sufficient genetic information to resolve the taxonomic ambiguity associated with the lacustrine and riverine forms (for details see Results), of which the type series probably consists, and further research is therefore required. However, this study provides the first genetic record of *A. mento* in Austria, as this species was not included in the Austrian Barcode of Life project (Zangl et al. 2022). Similar to *A. mento*, the DNA fragment obtained from the bird species *Anser brevirostris* did not contain sufficient genetic information to assign the type specimen to any of the currently valid *Anser* species.

Despite the partial success of the genetic analyses, this catalogue demonstrates the usefulness of ESA with the addition of genetic data. The catalogue contains digitised data from 21 type series, making them available to scientists around the world for further study.

Acknowledgements

We would like to thank Matthias Svojtka for discussing some of the historical aspects of this catalogue. NA is grateful to Oliver Macek and Nathalie Fial (NHMW) for their help in photographing the types and assembling the figure plates. We would like to thank the editor, Dr Fedor Konstantinov, and the reviewer, Dr Bert W. Hoeksema, as well as two other anonymous reviewers, for a detailed review which helped us to improve the manuscript.

Additional information

Conflict of interest

The authors have declared that no competing interests exist.

Ethical statement

No ethical statement was reported.

Funding

This study was partially funded by grant H-868630/2022 awarded by Hochschuljubiläumsstiftung der Stadt Wien, Vienna, Austria.

Author contributions

AP – conceptualization, general methodology, genetic analysis, original draft, reviewing and editing, supervision, project administration, funding acquisition; MC – laboratory work and genetic analysis; GS – photographing, x-rays, pre- and post- production, methodology; PF – Parasitic worms, reviewing and editing; NA – Myriapods, reviewing and editing; SR - Orthoptera, reviewing and editing; EM - Fishes, reviewing and editing; HMB - Birds, reviewing and editing; NB – Fishes, conceptualization, methodology, original draft, reviewing and editing, supervision.

Author ORCIDs

Anja Palandačić  <https://orcid.org/0000-0002-4555-5240>

Min J. Chai  <https://orcid.org/0009-0003-6213-2973>

Nesrine Akkari  <https://orcid.org/0000-0001-5019-4833>

Pedro R. Frade  <https://orcid.org/0000-0002-4010-255X>

Susanne Randolph  <https://orcid.org/0000-0002-2402-3077>

Nina G. Bogutskaya  <https://orcid.org/0000-0002-9153-0095>

Data availability

All of the data that support the findings of this study are available in the main text.

References

- Agatha S, Ganser MH, Santoferrara LF (2021) The importance of type species and their correct identification: A key example from tintinnid ciliates (Alveolata, Ciliophora, Spirotricha). *The Journal of Eukaryotic Microbiology* 68(6): e12865. <https://doi.org/10.1111/jeu.12865>
- Agne S, Naylor GJP, Preick M, Yang L, Thiel R, Weigmann S, Paijmans JLA, Barlow A, Hofreiter M, Straube N (2022a) Taxonomic identification of two poorly known lantern

- shark species based on mitochondrial DNA from wet-collection paratypes. *Frontiers in Ecology and Evolution* 10: 910009. <https://doi.org/10.3389/fevo.2022.910009>
- Agne S, Preick M, Straube N, Hofreiter M (2022b) Simultaneous barcode sequencing of diverse museum collection specimens using a mixed RNA bait set. *Frontiers in Ecology and Evolution* 10: 909846. <https://doi.org/10.3389/fevo.2022.909846>
- Ahnelt H, Mikschi E (2008) The type of *Gobius semilunaris* Heckel, 1837 (Teleostei: Gobiidae). *Annalen des Naturhistorischen Museums in Wien* 109B: 67–72. https://www.zobodat.at/pdf/ANNA_109B_0067-0072.pdf
- Akkari N, Enghoff H, Metscher BD (2015) A new dimension in documenting new species: High-detail imaging for myriapod taxonomy and first 3D cybertype of a new millipede species (Diplopoda, Julida, Julidae). *PLOS ONE* 10(8): e0135243. <https://doi.org/10.1371/journal.pone.0135243>
- Akkari N, Ganske A-S, Komerički A, Metscher B (2018) New avatars for Myriapods: Complete 3D morphology of type specimens transcends conventional species description (Myriapoda, Chilopoda). *PLOS ONE* 13(7): e0200158. <https://doi.org/10.1371/journal.pone.0200158>
- Albano PG, Schnedl S-M, Eschner A (2018) An illustrated catalogue of Rudolf Sturany's type specimens in the Naturhistorisches Museum Wien, Austria (NHMW): Deep-sea Eastern Mediterranean molluscs. *Zoosystematics and Evolution* 94(1): 29–56. <https://doi.org/10.3897/zse.94.20116>
- Anonymous (1857a) Nekrolog. Johan Jacob Heckel. *Verhandlungen und Mitteilungen des Siebenbürgischen Vereins für Naturwissenschaften zu Hermannstadt* 8: 119–124. https://www.zobodat.at/pdf/VerhMittNaturwissHermannstadt_8_0119-0124.pdf
- Anonymous (1857b) [Herr Prof. Dr. R. Kner übergab ein Exemplar des von ihm in Verbindung mit dem verewigten Custos J. Heckel herausgegebenen Werkes]. *Sitzungsberichte – Verhandlungen der Zoologisch-Botanischen Gesellschaft in Wien* 7: 3–163. https://www.zobodat.at/pdf/VZBG_7_0003-0163.pdf
- Antić D, Akkari N (2020) *Haasea* Verhoeff, 1895—a genus of tumultuous history and chaotic records—redefinition, revision of taxonomy and geographic distributions, with descriptions of two new species from Austria and Serbia (Diplopoda, Chordeumatida, Haaseidae). *Zootaxa* 4798 (1): 001–077. <https://doi.org/10.11646/zootaxa.4798.1.1>
- Antognazza CM, Palandačić A, Delmastro GB, Crosa G, Zaccara S (2023) Current and historical genetic variability of native brown trout populations in a southern Alpine ecosystem: Implications for future management. *Fishes* 8(8): 411. <https://doi.org/10.3390/fishes8080411>
- Attems CMT Graf von (1908) Myriopoden von Elba. *Zoologische Jahrbücher, Abteilung für Systematik, Ökologie und Geographie der Tiere* 26(2): 181–195. <https://www.biodiversitylibrary.org/partpdf/75062>
- Attems CMT Graf von (1927) Über palaearktische Diplopoden. *Archiv für Naturgeschichte* 92(1–2): 1–256. https://www.zobodat.at/pdf/Archiv-Naturgeschichte_92A_1_0001-0144.pdf
- Balon EK (1995) Origin and domestication of the wild carp, *Cyprinus carpio*: From Roman gourmets to the swimming flowers. *Aquaculture (Amsterdam, Netherlands)* 129(1–4): 3–48. [https://doi.org/10.1016/0044-8486\(94\)00227-F](https://doi.org/10.1016/0044-8486(94)00227-F)
- Bauernfeind E (2003) The Vienna Bird Collection: History and Main Research Focus. *Bonn Zoological Bulletin* 51: 147–149. https://www.zobodat.at/pdf/Bonner-Zoologische-Beitraege_51_0147-0149.pdf
- Berg LS (1912) Faune de la Russie et des pays limitrophes fondés principalement sur les collections du Musée Zoologique de l'Académie Impériale des Sciences de

- St.-Pétersbourg. Poissons (Marsipobranchii et Pisces). Vol. III. Ostariophysi. Part 1. Izdanije Imperatorskoj Akademii Nauk, St. Petersburg, 336 pp. <https://archive.org/details/faunedelarussiee1191berg> [In Russian]
- Berg LS (1916) Les Poissons des eaux douces de la Russie. Ryabushinskiy, Moscow, 563 pp. [In Russian]
- Berg H-M (2016) Die Vogelsammlung im Naturhistorischen Museum Wien. Vogelschutz in Österreich. Mitteilungen von BirdLife Österreich 40: 20–21.
- BirdLife International (2018) *Anser erythropus*. The IUCN Red List of Threatened Species 2018: e.T22679886A132300164. <https://doi.org/10.2305/IUCN.UK.2018-2.RLTS.T22679886A132300164.en> [Accessed on 19 December 2023]
- Bloch ME (1782) D. Marcus Elieser Bloch's, ausübenden Arztes zu Berlin;..., Oeconomische Naturgeschichte der Fische Deutschlands. Mit Sieben und Dreissig Kupfer tafeln nach Originalen. Theil 1. Auf Kosten des Verfassers und in Commission bei dem Buchhändler Hr. Hesse, Berlin, 128 pp. <https://archive.org/details/DMarcusElieserB00BlocC/page/n5/mode/2up>
- Bogutskaya NG, Iliadou K (2006) *Rutilus panosi*, a new roach from western Greece (Teleostei: Cyprinidae). Zoosystematica Rossica 14(2): 293–298. <https://doi.org/10.31610/zsr/2005.14.2.293>
- Bogutskaya NG, Naseka AM (2004) Catalogue of agnathans and fishes of fresh and brackish waters of Russia with comments on nomenclature and taxonomy. KMK Scientific Press, Moscow, 389 pp. [In Russian]
- Bogutskaya NG, Zupančič P, Jelić D, Diripasko OA, Naseka AM (2017) Description of a new species of *Alburnus* Rafinesque, 1820 (Actinopterygii, Cyprinidae, Leuciscinae) from the Kolpa River in the Sava River system (upper Danube drainage), with remarks on the geographical distribution of shemayas in the Danube. ZooKeys 688: 81–110. <https://doi.org/10.3897/zookeys.688.11261>
- Bogutskaya NG, Jelić D, Vucić M, Jelić M, Diripasko OA, Stefanov T, Klobučar G (2019) Description of a new species of *Phoxinus* from the upper Krka River (Adriatic Basin) in Croatia (Actinopterygii: Leuciscidae), first discovered as a molecular clade. Journal of Fish Biology 96(2): 378–393. <https://doi.org/10.1111/jfb.14210>
- Bogutskaya NG, Mikschi E, Riedl M, Szeiler S, Frade P, Palandačić A (2022) An annotated catalogue of the type specimens described by Maximilian Holly housed in the Natural History Museum of Vienna. Part. 1. Chordata. Annalen des Naturhistorischen Museums in Wien 124B: 19–92. https://www.zobodat.at/pdf/ANNA_124B_0019-0092.pdf
- Böhm LK, Supperer R (1953) Beobachtungen über eine neue Filarie (Nematoda), *Wehrdikmansia rugosicauda* Böhm and Supperer, 1953, aus dem subkutanen Bindegewebe des Rehes. Sitzungsberichte der Akademie der Wissenschaften Mathematisch-Naturwissenschaftliche Klasse 162: 95–104. https://www.zobodat.at/pdf/SBAWW_162_0095-0104.pdf
- Braun M (1883) Zur Entwicklungsgeschichte des breiten Bandwurms (*Bothriocephalus latus* Brehms). A. Stuber, Würzburg, 72 pp. <https://babel.hathitrust.org/cgi/pt?id=uc1.b3371776&seq=3>
- Braun M (1901) Zur Revision der Trematoden der Vögel. II. Centralblatt für Bakteriologie. Parasitenkunde und Infektionskrankheiten 29(23): 941–948.
- Braun M, Lühe M (1910) A handbook of practical parasitology. Translated by L. Forter. John Bale, Sons & Danielson, London, 208 pp. <https://doi.org/10.5962/bhl.title.27217>
- Brehm CL (1831) Handbuch der Naturgeschichte aller Vögel Deutschlands. Bernhard Friedrich Voigt, Ilmenau, 844 pp. <https://doi.org/10.5962/bhl.title.169254>

- Brehm CL (1855) Der vollständige Vögelsang: Eine gründliche Anleitung alle europäischen Vögel. B. Voigt, Weimar, 416 pp. <https://doi.org/10.5962/bhl.title.15791>
- Brisout de Barneville L (1848) Catalogue des Acrididés qui se trouvent aux environs de Paris. Annales de la Société Entomologique de France 6: 411–445. <https://www.biodiversitylibrary.org/page/9485831#page/417/mode/1up>
- Brölemann HW (1896) Matériaux pour servir a une faune des myriapodes de France. Feuille des jeunes naturalistes 26(311): 214–218.
- Brunner B (1914) Zur Erinnerung an Carl Brunner von Wattenwyl (1823–1914). <https://hls-dhs-dss.ch/de/articles/028793/2003-01-30/>
- Carboneras C, Kirwan GM (2020) Lesser White-fronted Goose (*Anser erythropus*), version 1.0. In: del Hoyo J, Elliott A, Sargatal J, Christie DA, de Juana E (Eds) Birds of the World. Cornell Lab of Ornithology, Ithaca, NY, USA. <https://doi.org/10.2173/bow.lwfgoo.01> [Accessed on 19 December 2023]
- Carus JV (1880) Heckel, Johann Jakob. In: Allgemeine Deutsche Biographie (ADB). Band 11, Duncker und Humblot, Leipzig, 205. https://de.wikisource.org/wiki/ADB:Heckel,_Johann_Jakob
- Castañeda-Rico S, Edwards CW, Hawkins MTR, Maldonado JE (2022) Museomics and the holotype of a critically endangered cricetid rodent provide key evidence of an undescribed genus. *Frontiers in Ecology and Evolution* 10: 930356. <https://doi.org/10.3389/fevo.2022.930356>
- Christian E (2008) Höhlenheuschrecken - Zum Jubiläum einer Wortschöpfung. *Die Höhle* 59(1–4): 48–58. https://www.zobodat.at/pdf/Hoehle_059_0048-0058.pdf
- Durette-Desset M-C, Digiani MC (2010) Taxonomic revision of the type specimens of Ethiopian Nippostrongylineae (Nematoda) deposited at the Natural History Museum of London. *Zootaxa* 2494(1): 1–28. <https://doi.org/10.11646/zootaxa.2494.1.1>
- Federhen S (2014) Type material in the NCBI Taxonomy Database. *Nucleic Acids Research* 43(D1): D1086–D1098. <https://doi.org/10.1093/nar/gku1127>
- Feigin CY, Newton AH, Doronina L, Schmitz J, Hipsley CA, Mitchell KJ, Gower G, Llamas B, Soubrier J, Heider TN, Menzies BR, Cooper A, O'Neill RJ, Pask AJ (2017) Genome of the Tasmanian tiger provides insights into the evolution and demography of an extinct marsupial carnivore. *Nature Ecology & Evolution* 2(1): 182–192. <https://doi.org/10.1038/s41559-017-0417-y>
- Fischer M, Schönmann R, Moschner I (1976) Das Naturhistorisches Museum in Wien und seine Geschichte. *Annalen des Naturhistorischen Museums in Wien* 80: 1–24. https://www.zobodat.at/pdf/ANNA_80_0001-0024.pdf
- Fitzinger LJFJ (1832) Ueber die Ausarbeitung einer Fauna des Erzherzogthumes Oesterreich, nebst einer systematischen Aufzählung der in diesem Lande vorkommenden Säugethiere, Reptilien und Fische, als Prodrum einer Fauna derfelben. *Beiträge zur Landeskunde Österreichs unter der Enns*, Vienna 1: 280–340.
- Fitzinger LJFJ (1856) Geschichte des kön. Hof-Naturalien-Cabinetes zu Wien. 1. Abtheilung. Älteste Periode bis zum Tode Kaiser Leopold II, 1792. *Sitzungsberichte der Akademie der Wissenschaften mathematisch-naturwissenschaftliche Klasse* 21: 433–479. https://www.zobodat.at/pdf/SBAWW_21_0433-0479.pdf
- Freyhof J (2011) *Leuciscus leuciscus* (errata version published in 2016). The IUCN Red List of Threatened Species 2011: e.T11887A97808936. <https://doi.org/10.2305/IUCN.UK.2008.RLTS.T11887A3312583.en> [Accessed on 11 October 2023]
- Freyhof J, Kottelat M (2007) Review of the *Alburnus mento* species group with description of two new species (Teleostei: Cyprinidae). *Ichthyological Exploration of Freshwaters* 18(3): 213–225.

- Freyhof J, Kottelat M (2008a) *Ballerus sapa*. The IUCN Red List of Threatened Species 2008: e.T135639A4168069. <https://doi.org/10.2305/IUCN.UK.2008.RLTS.T135639A4168069.en> [Accessed on 11 October 2023]
- Freyhof J, Kottelat M (2008b) *Alburnus alburnus* (errata version published in 2020). The IUCN Red List of Threatened Species 2008: e.T789A174775859. <https://doi.org/10.2305/IUCN.UK.2008.RLTS.T789A174775859.en> [Accessed on 11 October 2023]
- Freyhof J, Kottelat M (2008c) *Alburnus mento*. The IUCN Red List of Threatened Species 2008: e.T135634A4167016. <https://doi.org/10.2305/IUCN.UK.2008.RLTS.T135634A4167016.en> [Accessed on 11 October 2023]
- Freyhof J, Kottelat M (2008d) *Blicca bjoerkna* (errata version published in 2020). The IUCN Red List of Threatened Species 2008: e.T39270A174781952. <https://doi.org/10.2305/IUCN.UK.2008.RLTS.T39270A174781952.en> [Accessed on 11 October 2023]
- Freyhof J, Kottelat M (2008e) *Cyprinus carpio*. The IUCN Red List of Threatened Species 2008: e.T6181A12559362. <https://doi.org/10.2305/IUCN.UK.2008.RLTS.T6181A12559362.en> [Accessed on 09 October 2023]
- Freyhof J, Kottelat M (2008f) *Leuciscus idus*. The IUCN Red List of Threatened Species 2008: e.T11884A3312021. <https://doi.org/10.2305/IUCN.UK.2008.RLTS.T11884A3312021.en> [Accessed on 06 November 2023]
- Freyhof J, Kottelat M (2008g) *Rutilus virgo*. The IUCN Red List of Threatened Species 2008: e.T135722A4193052. <https://doi.org/10.2305/IUCN.UK.2008.RLTS.T135722A4193052.en> [Accessed on 09 October 2023]
- Freyhof J, Kottelat M (2008h) *Leucaspis delineatus*. The IUCN Red List of Threatened Species 2008: e.T11873A3311162. <https://doi.org/10.2305/IUCN.UK.2008.RLTS.T11873A3311162.en> [Accessed on 09 October 2023]
- Freyhof J, Kaya C, Bayçelebi E, Geiger MF, Turan D (2018) Generic assignment of *Leuciscus kurui* Bogutskaya from the upper Tigris drainage, and a replacement name for *Alburnus kurui* Mangit and Yerli (Teleostei: Leuciscidae). *Zootaxa* 4410(1): 113–135. <https://doi.org/10.11646/zootaxa.4410.1.6>
- Fries BF, Ekström CU, Sundevall CJ (1837) Skandiniens fiskar, målade efter lefvande exemplar och ritade på sten af Wilh. von Wright, med text af B. Fr. Fries, och C. U. Ekström. (Pisces Scandinavie.... Versio Latina...), 3. Stockholm, 222 pp. <http://hdl.handle.net/2077/29271>
- Gebhardt L (1964) Brehm, Christian Ludwig. In: Gebhardt L Die Ornithologen Mitteleuropas. 1747 bemerkenswerte Biographien vom Mittelalter bis zum Ende des 20. Jahrhunderts. Brühl, Giessen, 51–52.
- Gemel R, Gassner G, Schweiger S (2019) Katalog der Typen der Herpetologischen Sammlung des Naturhistorischen Museums Wien. *Annalen des Naturhistorischen Museums in Wien* 121B(2018): 33–248. http://verlag.nhm-wien.ac.at/pdfs/121B_033248_Gemel.pdf
- Goldstein PZ, DeSalle R (2011) Integrating DNA barcode data and taxonomic practice: Determination, discovery, and description. *BioEssays* 33(2): 135–147. <https://doi.org/10.1002/bies.201000036>
- Günther A (1868) Catalogue of the fishes in the British Museum. Catalogue of the Physostomi, containing the families Heteropygii, Cyprinidae, Gonorhynchidae, Hyodontidae, Osteoglossidae, Clupeidae, Chirocentridae, Alepocephalidae, Notopteridae, Halosauridae, in the collection of the British Museum, 7. Order of the Trustees, London, 512 pp. <https://www.biodiversitylibrary.org/item/34522#page/11/mode/1up>
- Hamann G [Ed.] (1976) Die Geschichte der Wiener naturhistorischen Sammlungen bis zum Ende der Monarchie. Mit einem Kapitel über die Zeit nach 1919 von M. Fischer, I.

- Moschner u. R. Schönmann. Veröffentlichungen aus dem Naturhistorischen Museum in Wien, Neue Folge 13: 1–98. https://www.zobodat.at/publikation_volumes.php?id=33611
- Hardisty AR, Ellwood ER, Nelson G, Zimkus B, Buschbom J, Addink W, Rabeler RK, Bates J, Bentley A, Fortes JAB, Hansen S, Macklin JA, Mast AR, Miller JT, Monfils AK, Paul DL, Wallis E, Webster M (2023) Digital Extended Specimens: Enabling an Extensible Network of Biodiversity Data Records as Integrated Digital Objects on the Internet. *Bioscience* 72(10): 978–987. <https://doi.org/10.1093/biosci/biac060>
- Haston E, Cubey R, Harris D (2012) Data concepts and their relevance for data capture in large scale digitisation of biological collections. *International Journal of Humanities and Arts Computing* 6(1–2): 111–119. <https://doi.org/10.3366/ijhac.2012.0042>
- Hawkins MTR, Flores MFC, McGowen M, Hinckley A (2022) A comparative analysis of extraction protocol performance on degraded mammalian museum specimens. *Frontiers in Ecology and Evolution* 10: 984056. <https://doi.org/10.3389/fevo.2022.984056>
- Heckel JJ (1836) Über einige neue, oder nicht gehörig unterschiedene Cyprinen, nebst einer systematischen Darstellung der europäischen Gattungen dieser Gruppe. *Annalen des Wiener Museums der Naturgeschichte* 1: 219–234, Taf. 19–21. https://www.zobodat.at/pdf/AWMN_1_0219-0234.pdf
- Heckel JJ (1843) Ichthyologie. In: Russegger J, Reisen in Europa, Asien und Afrika mit besonderer Rücksicht auf die naturwissenschaftlichen Verhältnisse der betreffenden Länder, unternommen in den Jahren 1835 bis 1841. 1. Band, 2. Teil. E. Schweizerbart, Stuttgart, 991–1099. <https://www.biodiversitylibrary.org/item/80448#page/529/mode/1up>
- Heckel JJ (1850) Bericht über das Vorkommen fossiler Fische zu Seefeld in Tirol und Monte Bolca im Venetianischen. *Jahrbuch der k.k. geologischen Reichsanstalt* 1(4): 696–701. https://www.zobodat.at/pdf/JbGeolReichsanst_001_0696-0701.pdf
- Heckel JJ (1851a) Ueber die in den Seen Oberösterreichs vorkommenden Fische. *Sitzungsberichte der kaiserlichen Akademie der Wissenschaften, mathematisch-naturwissenschaftliche Classe* 6(2): 145–149. https://www.zobodat.at/pdf/SBAWW_06_0145-0248.pdf
- Heckel JJ (1851b) Ueber die Ordnung der Chondrostei und die Gattungen *Amia*, *Cyclurus*, *Notaeus*. *Sitzungsberichte der kaiserlichen Akademie der Wissenschaften, mathematisch-naturwissenschaftliche Classe* 6(2): 219–224. https://www.zobodat.at/pdf/SBAWW_06_0145-0248.pdf
- Heckel JJ (1851c) Bericht einer auf Kosten der kais. Akademie der Wissenschaften durch Oberösterreich nach Salzburg, München, Innsbruck, Botzen, Verona, Padua, Venedig und Triest unternommenen Reise. *Sitzungsberichte der kaiserlichen Akademie der Wissenschaften, mathematisch-naturwissenschaftliche Classe* 7(2): 281–333. https://www.zobodat.at/pdf/SBAWW_07_0281-0333.pdf
- Heckel JJ (1851d) Stör-Arten der Lagunen bei Venedig. [Weitere Fortsetzung des Reiseberichtes]. *Sitzungsberichte der kaiserlichen Akademie der Wissenschaften, mathematisch-naturwissenschaftliche Classe* 7(4): 547–563. https://www.zobodat.at/pdf/SBAWW_07_0547-0563.pdf
- Heckel JJ (1852a) Fortsetzung des im Julihefte 1851 enthaltenen Berichtes über eine, auf Kosten der kais. Akademie der Wissenschaften unternommene, ichthyologische Reise. Anhang III. Über die zu den Gattungen *Idus*, *Leuciscus* und *Squalius* gehörigen Cyprinen. *Sitzungsberichte der kaiserlichen Akademie der Wissenschaften, mathematisch-naturwissenschaftliche Classe* 9(1): 49–123. https://www.zobodat.at/pdf/SBAWW_9_0049-0123.pdf

- Heckel JJ (1852b) Verzeichniss der Fische des Donaugebietes in der ganzen Ausdehnung des österreichischen Kaiserstaates. Verhandlungen der Zoologisch-Botanischen Vereins in Wien 2: 28–33. https://www.zobodat.at/pdf/VZBG_2_0001-0120.pdf
- Heckel JJ, Kner R (1857) Die Süßwasserfische der Österreichischen Monarchie, mit Rücksicht auf die angrenzenden Länder. W. Engelmann, Leipzig, 388 pp. https://www.zobodat.at/pdf/MON-V-FISCH_0001_0001-0388.pdf
- Herzig-Straschil B (1997) Franz Steindachner (1834–1919) and other prime contributors to the Ichthyological Collection of the Naturhistorisches Museum Wien. In: Pietsch TW, Anderson Jr WD (Eds) Collection Building in Ichthyology and Herpetology. The American Society of Ichthyologists and Herpetologists, Special Publication 3(1): 101–108.
- Hildebrandt HCM (1929) Christian Ludwig Brehm als Ornithologe. Mitteilungen aus dem Osterlande 20: 23–54.
- Hochkirch A, Nieto A, García Criado M, Cáliz M, Braud Y, Buzzetti FM, Chobanov D, Odé B, Presa Asensio JJ, Willemse L, Zuna-Kratky T, Barranco Vega P, Bushell M, Clemente ME, Correas JR, Dusoulier F, Ferreira S, Fontana P, García MD, Heller K-G, Iorgu IŞ, Ivković S, Kati V, Kleukers R, Krištín A, Lemonnier-Darcemont M, Lemos P, Massa B, Monnerat C, Papapavlou KP, Prunier F, Pushkar T, Roesti C, Rutschmann F, Şirin D, Skejjo J, Szövényi G, Tzirkalli E, Vedenina V, Barat Domenech J, Barros F, Cordero Tapi PJ, Defaut B, Fartmann T, Gomboc S, Gutiérrez-Rodríguez J, Holuša J, Illich I, Karjalainen S, Kočárek P, Korsunovskaya O, Liana A, López H, Morin D, Olmo-Vidal JM, Puskás G, Savitsky V, Stalling T, Tumbrinck J (2016) European Red List of Grasshoppers, Crickets and Bush-crickets. Publications Office of the European Union, Luxembourg, 88 pp. <https://op.europa.eu/en/publication-detail/-/publication/e2d74198-523d-11e7-a5ca-01aa75ed71a1/language-en>
- Hoeksema BW, Koh EGL (2009) Depauperation of the mushroom coral fauna (Fungiidae) of Singapore (1860s–2006) in changing reef conditions. The Raffles Bulletin of Zoology 22(Supplement): 91–101.
- Hoeksema BW, van der Land J, van der Meij SET, van Ofwegen LP, Reijnen BT, van Soest RWM, de Voogd NJ (2011) Unforeseen importance of historical collections as baselines to determine biotic change of coral reefs: The Saba Bank case. Marine Ecology (Berlin) 32(2): 135–141. <https://doi.org/10.1111/j.1439-0485.2011.00434.x>
- Ilie V, Schiller E, Stagl V (2009) Type specimens of the Geophilomorpha (Chilopoda) in the Natural History Museum in Vienna. Kataloge der wissenschaftlichen Sammlungen des Naturhistorischen Museums in Wien. Band 22, Myriapoda Heft 4. Verlag des Naturhistorischen Museums Wien, Vienna, 75 pp.
- International Commission on Zoological Nomenclature (1999) International Code of Zoological Nomenclature, Fourth Edition: adopted by the International Union of Biological Sciences. The International Trust for Zoological Nomenclature, London, 306 pp. <https://code.iczn.org/?frame=1>
- International Union for Conservation of Nature (2012) IUCN Red List Categories and Criteria: Version 3.1. Second edition. IUCN, Gland, Switzerland and Cambridge, UK, 32 pp. <https://portals.iucn.org/library/node/10315>
- Kähsbauer P (1959) Intendant Dr. Franz Steindachner, sein Leben und Werk. Annalen des Naturhistorischen Museums in Wien 63: 1–30. https://www.zobodat.at/pdf/ANNA_63_0001-0030.pdf
- Kaltenbach AP (2001) Die Orthopterensammlung des Naturhistorischen Museums in Wien und ihre Geschichte. Entomologica Austriaca: Zeitschrift der Österreichischen Entomologischen Gesellschaft 4: 21–23. https://www.zobodat.at/pdf/EN-TAU_0004_0021-0023.pdf

- Kehlmaier C, Zinenko O, Fritz U (2020) The enigmatic Crimean green lizard (*Lacerta viridis magnifica*) is extinct but not valid: Mitogenomics of a 120-year-old museum specimen reveals historical introduction. *Journal of Zoological Systematics and Evolutionary Research* 58(1): 303–307. <https://doi.org/10.1111/jzs.12345>
- Kime RD, Enghoff H (2017) Atlas of European millipedes 2: Order Julida (Class Diplopoda). *European Journal of Taxonomy* 346(346): 1–299. <https://doi.org/10.5852/ejt.2017.346>
- Kleinschmidt A (1955) Brehm, Christian Ludwig. *Neue Deutsche Biographie* 2: 570. <https://www.deutsche-biographie.de/pnd116469838.html#ndbcontent>
- Kollar V (1824) *Monographia Chlamydom. Cum tabulis aeneis duabus coloratus*. JG Heubner, Vienna, 49 pp. <https://doi.org/10.5962/bhl.title.52095>
- Kollar V (1831a) *Insekten des Schneebergs*. In: Schmidl A. *Der Schneeberg in Unterösterreich*. Vienna, 36–41.
- Kollar V (1831b) *Über Insecten, als Ursache verschiedener Krankheiten bey Menschen und Thieren*. *Wiener Zeitschrift für Kunst, Literatur, Theater und Mode*: 781–786, 792–795, 799–801.
- Kollar V (1833a) *Systematisches Verzeichnis der im Erzherzogthume Oesterreich vorkommenden geradflügeligen Insecten*. *Beiträge zur Landeskunde Oesterreichs unter der Enns*, Vienna 3: 67–87.
- Kollar V (1833b) *Die Kornschabe, Tinea granella* Lin. *Verhandlungen der K.K. Landwirtschafts-Gesellschaft in Wien, und Aufsätze vermischten ökonomischen Inhaltes*. *Neue Folge* 1(2): 52–59.
- Kollar V (1837) *Naturgeschichte der schädlichen Insecten in Beziehung auf Landwirtschaft und Forstcultur*. *Monografien Entomologie Gemischt* 5: 1–421. https://www.zobodat.at/pdf/MON-E-DIV_0005_0001-0421.pdf
- Kollar V (1842) *Über einige dem Feld- und Gartenbau verderbliche Insecten*. *Verhandlungen der K.K. Landwirtschafts-Gesellschaft in Wien, und Aufsätze vermischten ökonomischen Inhaltes*. *Neue Folge* 11(2): 125–148.
- Kollar V (1850) *Ueber Weinbeschädigung durch einen kleinen Nachtfalter, Tortrix Roserana Fröhl., in den Weingärten von Brunn nächst Mödling*. *Sitzungsberichte der kaiserlichen Akademie der Wissenschaften, mathematisch-naturwissenschaftliche Classe* 5: 89–91. https://www.zobodat.at/pdf/SBAWW_05_0001-0093.pdf
- Kollar V (1855) *Ueber Beschädigung des Roggens durch Apamea basilinea* W.V. (mit Abbild.). *Verhandlungen des Zoologisch-Botanischen Vereins in Wien* 5: 697–700. https://www.zobodat.at/pdf/VZBG_5_0697-0700.pdf
- Kottelat M (1997) *European freshwater fishes*. *Biologia* 52(suppl. 5): 1–271.
- Kottelat M, Freyhof J (2007) *Handbook of European freshwater fishes*. Publications Kottelat, Cornol, Switzerland, 646 pp.
- Krauss HA (1876) *Tettix Türki* nov. spec. (Orthopt.). *Entomologische Monatsblätter*: 103–104.
- Krauss HA (1878) [1879] *Die Orthopteren-Fauna Istriens*. *Sitzungsberichte der kaiserlichen Akademie der Wissenschaften, mathematisch-naturwissenschaftliche Classe* 78(1): 451–544. https://www.zobodat.at/pdf/SBAWW_78_0451-0544.pdf
- Kress JW, Erickson DL (2012) DNA barcodes: methods and protocols. In: Kress JW, Erickson DL (Eds) *Methods in Molecular Biology*, vol. 858. Springer Science+Business Media, 4–8. https://doi.org/10.1007/978-1-61779-591-6_3
- Lacépède BGE (1803) *Histoire naturelle des poissons*. Vol. 5. F. Dufart, Paris, 1–803. <https://archive.org/details/histoinaturel1lacea>
- Latzel R (1884) *Die Myriopoden der Österreichisch-ungarischen Monarchie*. Zweite Hälfte. *Die Symphylen, Pauropoden und Diplopoden*. A. Hölder, Vienna, 414 pp.

- Lefoulon E, Kuzmin Y, Plantard O, Mutafchiev Y, Otranto D, Martin C, Bain O (2014) Re-description of *Cercopithifilaria rugosicauda* (Böhm and Supperer, 1953) (Spirurida: Onchocercidae) of roe deer, with an emended diagnosis of the genus *Cercopithifilaria* and a genetic characterisation. *Parasitology International* 63(6): 808–816. <https://doi.org/10.1016/j.parint.2014.07.011>
- Lendemmer J, Thiers B, Monfils AK, Zaspel J, Ellwood ER, Bentley A, LeVan K, Bates J, Jennings D, Contreras D, Lagomarsino L, Mabee P, Ford LS, Guralnick R, Gropp RE, Revels M, Cobb N, Seltmann K, Aime MC (2020) The extended specimen network: A strategy to enhance US biodiversity collections, promote research and education. *Bioscience* 70(1): 23–30. <https://doi.org/10.1093/biosci/biz140>
- Li C, Corrigan S, Yang L, Straube N, Harris M, Hofreiter M, White WT, Naylor GJP (2015) DNA capture reveals transoceanic gene flow in endangered river sharks. *Proceedings of the National Academy of Sciences of the United States of America* 112(43): 13302–13307. <https://doi.org/10.1073/pnas.1508735112>
- Linnaeus C (1758) *Systema Naturae*, Ed. X. (*Systema naturae per regna tria naturae, secundum classes, ordines, genera, species, cum characteribus, differentiis, synonymis, locis. Tomus I. Editio decima, reformata.*), 1. Laurentii Salvii, Holmiae, 824 pp. <https://doi.org/10.5962/bhl.title.542>
- Marschall AF Graf, Pelzeln A von (1882) *Ornis Vindobonensis. Die Vogelwelt Wiens und seiner Umgebung*. Georg Paul Faesy, Vienna, 192 pp.
- Maxted N (1992) Towards defining a taxonomic revision methodology. *Taxon* 41(4): 653–660. <https://doi.org/10.2307/1222391>
- Meineke EK, Davies TJ, Daru BH, Davis CC (2018) Biological collections for understanding biodiversity in the Anthropocene. *Philosophical Transactions of the Royal Society B: Biological Sciences* 374(1763): 20170386. <https://doi.org/10.1098/rstb.2017.0386>
- Mikschi E (2009) *Geschichte der Fischforschung am Naturhistorischen Museum. Österreichs Fischerei* 62: 292–296.
- Mlikovsky J (2023) *Systematic Catalogue of the Birds of Siberia. Historical Ornithology*, vol. 1. Center for Historical Ornithology, Praha, 3167 pp.
- Monfils AK, Krimmel ER, Linton DL, Marsico TD, Morris AB, Ruhfel BR (2022) Collections education: The extended specimen and data acumen. *Bioscience* 72(2): 177–188. <https://doi.org/10.1093/biosci/biab109>
- Moog O (1982) Die Verbreitung der Höhlenheuschrecken *Troglophilus cavicola* Kollar und *T. neglectus* Krauss in Österreich (Orthoptera, Rhabdiphoridae). *Sitzungsberichte der Akademie der Wissenschaften, mathematisch-naturwissenschaftliche Klasse* 191: 185–207. https://www.zobodat.at/pdf/SBAWW_191_0185-0207.pdf
- Palandačić A, Naseka AM, Ramler D, Ahnelt H (2017a) Contrasting morphology with molecular data: An approach to revision of species complexes based on the example of European *Phoxinus* (Cyprinidae). *BMC Evolutionary Biology* 17(184): 1–17. <https://doi.org/10.1186/s12862-017-1032-x>
- Palandačić A, Naseka AM, Ramler D, Ahnelt H (2017b) Corrigendum to «Contrasting morphology with molecular data: an approach to revision of species complexes based on the example of European (Cyprinidae)» by Palandačić et al. 2017. *Biodiversity Data Journal* 5: e21772[1–5]. <https://doi.org/10.3897/BDJ.5.e21772>
- Palandačić A, Kruckenhauser L, Ahnelt H, Mikschi E (2020) European minnows through time: museum collections aid genetic assessment of species introductions in freshwater fishes (Cyprinidae: *Phoxinus* species complex). *Heredity* 124(3): 410–422. <https://doi.org/10.1038/s41437-019-0292-1>

- Palandačić A, Kapun M, Greve C, Schell T, Kirchner S, Kruckenhauser L, Szucsich N, Bogutskaya NG (2023) From historical expedition diaries to whole genome sequencing: A case study of the likely extinct Red Sea torpedo ray. *Zoologica Scripta* 00: 1–20. <https://doi.org/10.1111/zsc.12632>
- Pallas PS (1814) *Zoographia Rosso-Asiatica, sistens omnium animalium in extenso Imperio Rossico et adjacentibus maribus observatorum recensionem, domicilia, mores et descriptiones anatomem atque icones plurimorum*. Vol. 3. Academia Scientiarum, Petropolis (Sankt Petersburg), 428 pp. <https://archive.org/details/zoographiarossoa22pall>
- Pohl JE, Kollar V (1832) Brasiliens vorzüglich lästige Insecten. In: *Reise im Inneren von Brasilien. Auf allerhöchsten Befehl Seiner Majestät des Kaisers von Österreich Franz des Ersten in den Jahren 1817–1821*: 1–20.
- Price B, Dupont S, Allan E, Blagoderov V, Butcher A, Durrant J, Holtzhausen P, Kokkini P, Livermore L, Hardy H, Smith V (2018). ALICE: Angled Label Image Capture and Extraction for high throughput insect specimen digitisation. <https://doi.org/10.31219/osf.io/s2p73>
- Prosser SWJ, deWaard JR, Miller SE, Hebert PDN (2016) DNA barcodes from century-old type specimens using next-generation sequencing. *Molecular Ecology Resources* 16(2): 487–497. <https://doi.org/10.1111/1755-0998.12474>
- Rabitsch W (2006) Geschichte und Bibliographie der Wanzenkunde in Österreich *Denisia* 19: 41–94. https://www.zobodat.at/pdf/DENISIA_0019_0041-0094.pdf
- Rambur P (1838) Orthoptères. In: Rambur P *Faune entomologique de l'Andalousie: Deux forts volumes in octavo accompagnés de 50 planches*. Vol. 2. A. Bartrand, 12–94.
- Raxworthy CJ, Smith BT (2021) Mining museums for historical DNA: Advances and challenges in museomics. *Trends in Ecology & Evolution* 36(11): 1049–1060. <https://doi.org/10.1016/j.tree.2021.07.009>
- Renner SS (2016) A return to Linnaeus's focus on diagnosis, not description: The use of DNA characters in the formal naming of species. *Systematic Biology* 65(6): 1085–1095. <https://doi.org/10.1093/sysbio/syw032>
- Richardson J (1846) Report on the ichthyology of the seas of China and Japan. Report of the British Association for the Advancement of Science 15th meeting [1845]: 187–320. <https://archive.org/details/reportonichthyol00rich>
- Robbirt KM, Roberts DL, Hutchings MJ, Davy AJ (2014) Potential disruption of pollination in a sexually deceptive orchid by climatic change. *Current Biology* 24(23): 2845–2849. <https://doi.org/10.1016/j.cub.2014.10.033>
- Saint Quentin D (1970) Katalog der Odonaten-Typen im Naturhistorischen Museum Wien. *Annalen des Naturhistorischen Museums in Wien* 74: 253–279. https://www.zobodat.at/pdf/ANNA_74_0253-0279.pdf
- Sattmann H (2002) Anfänge der systematischen Helminthologie in Österreich. *Denisia* 6: 271–290. https://www.zobodat.at/pdf/DENISIA_0006_0271-0290.pdf
- Sattmann H, Konecny R, Stagl V (2000) Die Geschichte der Helminthensammlung am Naturhistorischen Museum in Wien, Teil 1 (1797–1897). *Mitteilungen der Österreichischen Gesellschaft für Tropenmedizin und Parasitologie* 21(1999): 83–92. https://www.zobodat.at/pdf/MOGTP_21_0083-0092.pdf
- Sattmann H, Stagl V, Esberger R, Konecny R (2001) Die Geschichte der Helminthensammlung am Naturhistorischen Museum in Wien, Teil 2 (1898–1998). *Mitteilungen der Österreichischen Gesellschaft für Tropenmedizin und Parasitologie* 22(2000): 25–32. https://www.zobodat.at/pdf/MOGTP_22_0025-0032.pdf
- Schefbeck G (1996) The Austro-Hungarian Deep-sea Expeditions. In: Uiblein F, Ott J, Stachowitsch M (Eds) *Deep-sea and extreme shallow-water habitats: affinities and*

- adaptations. *Österreichische Akademie der Wissenschaften, Biosystematics and Ecology Series* 11: 1–27.
- Schifter H (1991) Typen von Theodor von Heuglin beschriebener Vögel in der Vogelsammlung des Naturhistorischen Museums Wien. *Annalen des Naturhistorischen Museums in Wien* 92B: 59–76. https://www.zobodat.at/pdf/ANNA_92B_0059-0076.pdf
- Schifter H (2010) Specimens in the public galleries reflecting the history of the Bird Collection at the Museum of Natural History in Vienna. In: Bauernfeind E, Gamauf A, Berg H-M, Muraoka Y (Eds) *Proceedings of the 5th International Meeting of European Bird Curators, Nat. Hist. Mus. Vienna, Aug. 29th–31st, 2007*. Publishing House of the Natural History Museum Vienna, Vienna, 237–255.
- Schifter H, Bauernfeind E, Schifter T (2007): *Die Typen der Vogelsammlung des Naturhistorischen Museums Wien. Teil I. Nonpasseres. Katalog der wissenschaftlichen Sammlungen des Naturhistorischen Museums in Wien, Band 20. Aves Heft I. Naturhistorischen Museums, Vienna, 376 pp.* https://www.zobodat.at/pdf/kat-nhmw_20_0003-0376.pdf
- Schileyko A, Stagl V (2004) The collection of Scolopendromorph Centipedes (Chilopoda) in the Natural History Museum in Vienna: A critical re-evaluation of former taxonomic identifications. *Annalen des Naturhistorischen Museums in Wien* 105B: 67–137. https://www.zobodat.at/pdf/ANNA_105B_0067-0137.pdf
- Schiner IJR (1860) Vincenz Kollar. *Wiener Entomologische Monatschrift* 4: 222–224.
- Schrötter A (1861) Vincenz Kollar. *Almanach der kaiserlichen Akademie der Wissenschaften* 11: 154–169.
- Silva PC, Malabarba MC, Malabarba LR (2017) Using ancient DNA to unravel taxonomic puzzles: the identity of *Deuterodon pedri* (Ostariophysi: Characidae). *Neotropical Ichthyology* 15(1): 1–12. <https://doi.org/10.1590/1982-0224-20160141>
- Silva PC, Malabarba MC, Malabarba LR (2019) Integrative taxonomy: Morphology and ancient DNA barcoding reveals the true identity of *Astyanax taeniatus*, a tetra collected by Charles Darwin during the Beagle's Voyage. *Zoologischer Anzeiger* 278: 110–120. <https://doi.org/10.1016/j.jcz.2018.12.007>
- Stagl V (2006) Robert Latzel - his life-work and importance for Myriapodology. *Norwegian Journal of Entomology* 53: 223–236.
- Stagl V, Sattmann H (2013) *Der Herr der Würmer: Leben und Werk des Wiener Arztes und Parasitologen Johann Gottfried Bremser (1767–1827)*. Böhlau, Vienna, 240 pp. <https://doi.org/10.7767/boehlau.9783205789857>
- Stagl V, Stoev P (2005) Type specimens of the order Callipodida (Diplopoda) in the Natural History Museum in Vienna. *Kataloge der wissenschaftlichen Sammlungen des NHMW. Myriapoda, Heft 2. Natural History Museum, Vienna, 26 pp.*
- Stagl V, Zapparoli M (2006) Type specimens of the Lithobiomorpha (Chilopoda) in the Natural History Museum in Vienna. *Kataloge der wissenschaftlichen Sammlungen des NHMW. Myriapoda, Heft 3. Natural History Museum, Vienna, 49 pp.*
- Stoev P, Komerički A, Akkari N, Liu S, Zhou X, Weigand A, Hostens J, Hunter C, Edmunds S, Porco D, Zapparoli M, Georgiev T, Mietchen D, Roberts D, Faulwetter S, Smith V, Penev L (2013) *Eupolybothrus cavernicolus* Komerički and Stoev sp. n. (Chilopoda: Lithobiomorpha: Lithobiidae): the first eukaryotic species description combining transcriptomic, DNA barcoding and micro-CT imaging data. *Biodiversity Data Journal* 1: e1013. <https://doi.org/10.3897/BDJ.1.e1013>
- Straube N, Lyra ML, Paijmans JLA, Preick M, Basler N, Penner J, Rödel M-O, Westbury MV, Haddad CFB, Barlow A, Hofreiter M (2021) Successful application of ancient DNA extraction and library construction protocols to museum wet collection specimens. *Molecular Ecology Resources* 21(7): 2299–2315. <https://doi.org/10.1111/1755-0998.13433>

- Sullivan JP, Hopkins CD, Pirro S, Peterson R, Chakona A, Mutizwa TI, Mukweze Mulelenu C, Alqahtani FH, Vreven E, Dillman CB (2022) Mitogenome recovered from a 19th century holotype by shotgun sequencing supplies a generic name for an orphaned clade of African weakly electric fishes (Osteoglossomorpha, Mormyridae). *ZooKeys* 1129: 163–196. <https://doi.org/10.3897/zookeys.1129.90287>
- Surdez M (1973) *Catalogue des Archives de Louis Agassiz (1807–1873)*. Université de Neuchâtel, Institut de Géologie et Séminaire d'Histoire, 196 pp. [Version informatisée mai 2009 par MDS, Archives de l'Etat de Neuchâtel] https://doc.rero.ch/record/32397/files/PAL_E3549.pdf
- Svojtka M, Salvini-Plawen L, Mikschi E (2009) Biographischer Abriss zu Johann Jakob Heckel (1790–1857). *Österreichs Fischerei* 62(11/12): 285–288.
- Svojtka M, Salvini-Plawen L, Mikschi E (2012) Johann Jakob Heckel (1790–1857), der Begründer der systematischen Ichthyologie in Österreich: Ein biographischer Überblick. *Schriften des Vereins zur Verbreitung Naturwissenschaftlicher Kenntnisse* 148/150: 43–74.
- Takano A, Cole TCH, Konagai H (2024) A novel automated label data extraction and data base generation system from herbarium specimen images using OCR and NER. *Scientific Reports* 14(1): 112. <https://doi.org/10.1038/s41598-023-50179-0>
- Tamura K, Stecher G, Peterson D, Filipski A, Kumar S (2013) MEGA6: Molecular evolutionary genetics analysis version 6.0. *Molecular Biology and Evolution* 30(12): 2725–2729. <https://doi.org/10.1093/molbev/mst197>
- Thaler K, Gruber J (2003) Zur Geschichte der Arachnologie in Österreich 1758–1955. *Denisia* 8: 139–163. https://www.zobodat.at/pdf/DENISIA_0008_0139-0163.pdf
- Tizzani P, Fanelli A, Belleau E (2021) Gastrointestinal parasites of black grouse *Lyrurus tetrix*: A long-term study (1986–2019) in the French Alps. *Research in Veterinary Science* 137: 163–169. <https://doi.org/10.1016/j.rvsc.2021.05.005>
- Türk R (1858) Ueber die in Oesterreich unter der Enns bis jetzt aufgefundenen Orthopteren. *Wiener Entomologische Monatschrift* 2(12): 361–381. https://www.zobodat.at/pdf/WEMS_2_0361-0381.pdf
- Türk R (1860) Mehrere für Niederösterreichs Fauna neue Orthopteren. *Wiener Entomologische Monatschrift* 4: 84–88. https://www.zobodat.at/pdf/WEMS_4_0084-0088.pdf
- Türk R (1862) Für Niederösterreichs Fauna neue Orthopteren. *Wiener Entomologische Monatschrift* 6: 81–82. https://www.zobodat.at/pdf/WEMS_6_0081-0082.pdf
- Tyler MJ, Fucsko L, Roberts D (2023) Calamities causing loss of museum collections: A historical and global perspective on museum disasters. *Zootaxa* 5230(2): 153–178. <https://doi.org/10.11646/zootaxa.5230.2.2>
- van den Elzen R, Berg H-M, Pilat M, Renner SC (2023) Type specimens of Thamnophilidae Swainson, 1824 (Chordata, Animalia) in the Bird Collection of the Natural History Museum Vienna. *Annalen des Naturhistorischen Museums in Wien* 125B: 45–81. https://www.zobodat.at/pdf/ANNA_125B_0045-0081.pdf
- van der Laan R, Fricke R, Eschmeyer WN [Eds] (2023) *Eschmeyer's Catalog of Fishes: classification*. <http://www.calacademy.org/scientists/catalog-of-fishes-classification/> [Electronic version accessed 7 October 2023]
- van der Meij SET, Moolenbeek RG, Hoeksema BW (2009) Decline of the Jakarta Bay molluscan fauna linked to human impact. *Marine Pollution Bulletin* 59(4–7): 101–107. <https://doi.org/10.1016/j.marpolbul.2009.02.021>
- van der Meij SET, Suharsono, Hoeksema BW (2010) Long-term changes in coral assemblages under natural and anthropogenic stress in Jakarta Bay (1920–2005). *Marine Pollution Bulletin* 60(9): 1442–1454. <https://doi.org/10.1016/j.marpolbul.2010.05.011>

- van Steenberge M, Snoeks J, Vreven E (2016) Lingering taxonomic confusion in *Labeo* (Actinopterygii: Cypriniformes: Cyprinidae): correcting the records and basis of type designations for seven Congolese species. *Acta Ichthyologica et Piscatoria* 46(1): 1–8. <https://doi.org/10.3750/AIP2016.46.1.01>
- Verhoeff KW (1891) Ein Beitrag zur mitteleuropäischen Diplopodenfauna. *Berliner Entomologische Zeitschrift* 36(1): 115–166. <https://doi.org/10.1002/mmnd.18910360114>
- Verhoeff KW (1895) Beiträge zur Kenntnis paläarktischer Myriopoden. I. Aufsatz: Über einige neue Myriopoden der österreichisch-ungarischen Monarchie. *Verhandlungen der Zoologisch-botanischen Gesellschaft in Wien* 45: 284–298. https://www.zobodat.at/pdf/VZBG_45_0284-0298.pdf
- Verhoeff KW (1907) Über Diplopoden. 7. (27.) Aufsatz: Europäische Polydesmiden. *Zoologischer Anzeiger* 32(12–13): 337–354.
- Verhoeff KW (1928) Ueber Diplopoden aus Bulgarien gesammelt von Dr. I. Buresch. 3 Aufsatz in Dr. Karl W. Verhoeff in Pasing bei München. Band 1, 28–44.
- Verhoeff KW (1930a) Über Diplopoden aus Italien, namentlich Piemont. 114. Diplopoden-Aufsatz. *Zoologische Jahrbucher. Abteilung für Systematik, Ökologie und Geographie der Tiere* 59: 387–446.
- Verhoeff KW (1930b) Zur Kenntnis italienischer Diplopoden. 119. Diplopoden-Aufsatz. *Zoologische Jahrbucher. Abteilung für Systematik, Ökologie und Geographie der Tiere* 60: 281–326.
- Verhoeff KW (1932) Zur Geographie, Ökologie und Systematik der Diplopoden Nordwestitaliens. *Archiv für Naturgeschichte* 1: 517–645.
- Verhoeff KW (1941) Diplopoden der Insel Ischia, systematisch, morphologisch, phänologisch, ökologisch, geographisch. *Zoomorphology* 38(1): 147–196. <https://doi.org/10.1007/BF02176181>
- Verhoeff KW (1942) Diplopoden der Insel Kapri. *Zoologischer Anzeiger* 139: 213–233.
- Verhoeff KW (1951) Diplopoda, Chilopoda und Isopoda terrestria vom Mt. Soratte in Latium. *Zoologische Jahrbucher. Abteilung für Systematik, Ökologie und Geographie der Tiere* 80: 205–255.
- Verhoeff KW (1952) Weitere Beiträge zur Kenntnis der Isopoden- und Diplopodenfauna von Ischia und Capri. *Bonner Zoologische Beiträge* 3(1–2): 125–150.
- von Meidinger C (1786) *Icones piscium Austriae indigenorum, quos collegit vivisque coloribus expressos edidit C. Baron de Meidinger. Tafeln von J. Lachenbauer und M. Sedlmayer. Vol. 2: Plates X–XX.* Baumeister Press, Vienna.
- von Meidinger C (1790) *Icones piscium Austriae indigenorum, quos collegit vivisque coloribus expressos edidit C. Baron de Meidinger. Tafeln von J. Lachenbauer und M. Sedlmayer. Vol. 4: Plates XXXI–XL.* Baumeister Press, Vienna.
- von Wurzbach C (1862) Heckel, Johann Jacob. In: *Biographisches Lexikon des Kaiserthums Oesterreich*. 8. Theil. Kaiserlich-königliche Hof- und Staatsdruckerei, Vienna, 184–189.
- von Wurzbach C (1864) Kollar, Vincenz. In: *Biographisches Lexikon des Kaiserthums Oesterreich*. 12. Theil. Kaiserlich-königliche Hof- und Staatsdruckerei, Vienna, 333–338.
- Webster GA (1959) *Orchipeum tracheicola* reported from a whistling swan, *Cygnus columbianus*. *Canadian Journal of Zoology* 37(2): 213–213. <https://doi.org/10.1139/z59-023>
- Webster MS [Ed.] (2017) *The Extended Specimen: Emerging Frontiers in Collections-Based Ornithological Research*. Studies in Avian Biology Series, No. 50. CRC Press, Taylor and Francis Group, Boca Raton, FL, USA, 240 pp. <https://doi.org/10.1201/9781315120454>

- Wehr EE, Dikmans G (1935) New nematodes (Filariidae) from North American Ruminants. *Zoologischer Anzeiger* 110: 202–208.
- Winston JE (1999) Describing species: Practical taxonomic procedure for biologists. Columbia University Press, 512 pp. <https://www.jstor.org/stable/10.7312/wins06824>
- Wirkner C, Stagl V, Turk N (2002) Type specimens of the Chordeumatida in the Natural History Museum (Diplopoda). *Kataloge der wissenschaftlichen Sammlungen des Naturhistorischen Museums in Wien, Band 16 Myriapoda, Heft 1*.
- Wolfram G, Mikschi E (2007) Rote Liste der Fische (Pisces) Österreichs. Rote Listen gefährdeter Tiere Österreichs, Teil 2: Kriechtiere, Lurche, Fische, Nachtfalter, Weichtiere. Böhlau Verlag, Wien-Köln-Weimar, 515 pp.
- Zahiri R, Tarmann G, Efetov KA, Rajaei H, Fatahi M, Seidel M, Jaenicke B, Dalsgaard T, Sikora M, Husemann M (2021) An illustrated catalogue of the type specimens of Lepidoptera (Insecta) housed in the Zoological Museum Hamburg (ZMH): Part I. superfamilies Hepialoidea, Cossioidea, and Zygaenoidea. *Evolutionary Systematics* 5(1): 39–70. <https://doi.org/10.3897/evolsyst.5.62003>
- Zangl L, Schäffer S, Daill D, Friedrich T, Gessl W, Mladinić M, Sturmhuber C, Wanzenböck J, Weiss SJ, Koblmüller S (2022) A comprehensive DNA barcode inventory of Austria's fish species. *PLOS ONE* 17(6): e0268694. <https://doi.org/10.1371/journal.pone.0268694>
- Zettel H, Laciny A, Bruckner H (2022) Catalogue of the type specimens of the family Gerridae (Insecta: Hemiptera: Heteroptera) in the Natural History Museum Vienna. *Annalen des Naturhistorischen Museums in Wien* 124B: 193–247. https://www.zobodat.at/pdf/ANNA_124B_0193-0247.pdf
- Zettel H, Bruckner H, Laciny A, Zenz K (2023) Catalogue of the type specimens of the family Hebridae (Insecta: Hemiptera: Heteroptera) in the Natural History Museum Vienna. *Annalen des Naturhistorischen Museums in Wien* 125B: 13–36. https://www.zobodat.at/pdf/ANNA_125B_0013-0036.pdf
- Zuna-Kratky T (2017) Zur Geschichte der Heuschreckenforschung in Österreich. *Denisia* 39: 35–54. https://www.zobodat.at/pdf/DENISIA_0039_0035-0054.pdf
- Zuna-Kratky T, Karner-Ranner E, Lederer E, Braun B, Berg H-M, Denner M, Bieringer G, Ranner A, Zechner L (2009) Verbreitungsatlas der Heuschrecken und Fangschrecken Ostösterreichs. *Naturhistorisches Museum Wien, Vienna*, 303 pp.
- Zuna-Kratky T, Landmann A, Illich I, Zechner L, Essl F, Lechner K, Ortner A, Weißmair W, Wöss G (2017) Die Heuschrecken Österreichs. *Denisia* 39: 1–880.

Taxonomic review of the genus *Ponyalis* Fairmaire, 1899 (Coleoptera, Lycidae), with descriptions of six new species from China

Chen Fang¹, Yuxia Yang^{1,2}, Xingke Yang³, Haoyu Liu¹

1 Key Laboratory of Zoological Systematics and Application, School of Life Sciences, Hebei University, Baoding 071002, China

2 Hebei Basic Science Center for Biotic Interaction, Hebei University, Baoding 071002, China

3 Key Laboratory of Zoological Systematics and Evolution, Institute of Zoology, Chinese Academy of Sciences, Beijing 100101, China

Corresponding authors: Yuxia Yang (yxyang@hbu.edu.cn); Haoyu Liu (liuhy@hbu.edu.cn)

Abstract

The lycid genus *Ponyalis* Fairmaire, 1899 is reviewed. Six new species are described from China, including *P. longicornis* sp. nov., *P. truncata* sp. nov., *P. dabiesshanensis* sp. nov., *P. hainanensis* sp. nov., *P. quadricollimima* sp. nov., and *P. zhejiangensis* sp. nov. Nine previously known species, including *P. alternata* (Pic, 1927), *P. fukiensis* (Bocak, 1999), *P. gracilis* (Bocak, 1999), *P. himalejica* (Bourgeois, 1885), *P. klapperichi* (Bocak, 1999), *P. laticornis* Fairmaire, 1899, *P. nigrohumeralis* (Pic, 1939), *P. quadricollis* (Kiesenwetter, 1874), and *P. variabilis* Li, Bocak & Pang, 2015 are illustrated with images of the habitus and aedeagi to make the comparisons with the new species. In addition, a distribution map and an identification key to all 24 species of *Ponyalis* are provided.

Key words: Aedeagus, alpha taxonomy, antennae, differential diagnosis, distribution, identification key, Net-winged beetles, Oriental Region



Academic editor: Vinicius S. Ferreira

Received: 3 February 2024

Accepted: 26 April 2024

Published: 31 May 2024

ZooBank: <https://zoobank.org/8B648676-1798-4BE3-8AFE-E5B09D7C2FB7>

Citation: Fang C, Yang Y, Yang X, Liu H (2024) Taxonomic review of the genus *Ponyalis* Fairmaire, 1899 (Coleoptera, Lycidae), with descriptions of six new species from China. ZooKeys 1203: 325–354. <https://doi.org/10.3897/zookeys.1203.120166>

Copyright: © Chen Fang et al.
This is an open access article distributed under terms of the Creative Commons Attribution License (Attribution 4.0 International – CC BY 4.0).

Introduction

The genus *Ponyalis* Fairmaire, 1899 is currently classified in the lycid tribe Lyponiini (Bocak and Bocakova 1990, 2008; Kazantsev 2002, 2005; Kusy et al. 2019), which includes one other genus, *Lyponia* Waterhouse, 1878. These two genera have been confused for a long time due to their morphological similarities (e. g., Gorham 1883; Kleine 1924; Pic 1926; Nakane 1961, 1969). It was not until Bocak (1999) conducted a cladistics analysis based on morphological data, where he identified *Ponyalis* as a subgenus of *Lyponia*. Later, Kazantsev (2002) reinstated *Ponyalis* as a separate genus because of its morphological differences from *Lyponia*, which are as follows: basal part of the coxite free, while basally fused in *Lyponia*; antennomere I abruptly widened near base in both sexes, while progressively widened towards apex in *Lyponia*; elytral primary costa III almost reaching apex, while not extending beyond apical fifth in *Lyponia*; aedeagus present with a pair of lateral thorns in the preapical portion of the median lobe, while absent in *Lyponia* (Kazantsev 2002). Kazantsev's (2002) classification system was adopted by Li et al. (2015a) and supported by their molecular phylogenetic results of Lyponiini (Li et al. 2015b).

Prior to this study, a total of 18 *Ponyalis* species are described, which are widely distributed in the eastern Palaearctic and Oriental regions (Bocak 1999; Bocakova and Bocak 2007; Li et al. 2015a). During our study, we assembled a large series of *Ponyalis* material, which made it possible for us to review this genus. After examination and identification, we discovered six new species from China, which are reported in the present study. Meanwhile, some of the previously known species are illustrated in more detail to make them better known, and enable comparison with the new species, allowing a better understanding of the species diversity of the Chinese *Ponyalis* fauna.

Materials and methods

The studied specimens are deposited in the Institute of Zoology, Chinese Academy of Sciences, Beijing, China (**IZAS**), Entomological Museum of China Agricultural University, Beijing, China (**CAU**) and Museum of Hebei University, Baoding, China (**MHBU**).

Studied specimens were first softened in water, and then the genitalia of both sexes were dissected. After dissection, the male genitalia was cleared in a 10% NaOH solution, examined and photographed in glycerol, and finally glued on a paper card for permanent preservation. Images of the adults were taken with a Canon EOS 80D digital camera, and those of the genitalia by a Leica M205A stereomicroscope, which were stacked in Helicon Focus 7. The final plates were edited in Adobe Photoshop CS3.10.0.1.

The measurements were taken with Image J 1.50i (NIH, Bethesda, MD, USA). Body length was measured from the anterior margin of the head to the elytral apex, and the width across the elytral humeri. Pronotal length was measured from the middle of the anterior margin to the middle of posterior margin of the pronotum and the width across its widest part. Eye diameter was measured at the maximal width and the interocular distance at the minimal point. The shapes of male antennomeres were assessed based on the ratio of the apical process to corresponding stem of the antennomere in length. We considered the antennomere as triangular if the ratio was at most 1.0, otherwise as lamellate if a higher value.

The distribution information was collected from the original publications (Bocak 1999; Kazantsev 2002; Li et al. 2015a) and the newly collected material. The distribution map was prepared by the ArcMap 10.8 and edited in Adobe Photoshop CS3.10.0.1.

Taxonomy

Genus *Ponyalis* Fairmaire, 1899

Diagnosis. Body length 9.5–15.0 mm, brown to black, pronotum red or black, elytra uniformly red but sometimes black at margins. Head small, hemispherical eyes prominent. Antennae flabellate in males, while serrate in females; antennomere I abruptly widened near base and nearly globular or flattened dorsally, II very short, III nearly triangular, IV–X triangular to lamellate, IX slender. Pronotum subquadrate, with all margins almost straight. Elytra flat to weakly convex, subparallel-sided, usually wider in female than male; each elytron with four primary and five secondary longitudinal and many transverse costae, elytral cells mostly squared, sometimes strongly transverse. Male genitalia robust,

phallus long and present with a pair of lateral thorns apically, more or less projected distad at apical margin, internal sac usually invaginated, with only apex exposed, which is a slender or thorn-shaped tube, sometimes hardly visible.

Included species. *P. alternata* (Pic, 1927), *P. cincinnatus* Kazantsev, 2002, *P. chifengleei* Kazantsev, 2002, *P. daucus* Kazantsev, 2002, *P. dolosa* (Kleine, 1924), *P. fukiensis* (Bocak, 1999), *P. gestroi* Pic, 1912, *P. gracilis* (Bocak, 1999), *P. himalejica* (Bourgeois, 1885), *P. ishigakiana* (Nakane, 1961), *P. klapperichi* (Bocak, 1999), *P. laticornis* Fairmaire, 1899, *P. nigrohumeralis* (Pic, 1938), *P. oshimana* (Nakane, 1961), *P. quadricollis* (Kiesenwetter, 1874), *P. sichuanensis* (Bocak, 1999), *P. tryznai* (Bocak, 1999), *P. variabilis* Li, Pang & Bocak, 2015., *P. longicornis* sp. nov., *P. truncata* sp. nov., *P. dabiesshanensis* sp. nov., *P. hainanensis* sp. nov., *P. quadricollimima* sp. nov., *P. zhejiangensis* sp. nov.

Distribution (Fig. 1). China (Henan, Shaanxi, Gansu, Anhui, Zhejiang, Hunan, Jiangxi, Hubei, Fujian, Guangdong, Hainan, Guangxi, Chongqing, Sichuan, Guizhou, Yunnan, Xizang), Korea, Japan, Vietnam, Myanmar, Laos, Thailand, India.

Key to the males of *Ponyalis*

- 1 Male antennomere IV present with a long lamella, which is $\geq 2.0\times$ longer than joint itself and extending from middle of the joint (e.g., Figs 2C, 8A, C) **2**
- Male antennomere IV triangular, or present with a short lamella, which is no longer than joint itself and extending from apex of the joint (e.g., Figs 2A, 4A)..... **6**
- 2 Elytra orange **3**
- Elytra red (e.g., Fig. 2C) **4**
- 3 Pronotum bicolored, with a pale brown patch in center of disc; antennal tubercles pale brown; China (Taiwan) (Fig. 1) ***P. dolosa* (Kleine, 1924)**
- Pronotum uniformly orange; antennal tubercles red; China (Taiwan) (Fig. 1) ***P. daucus* Kazantsev, 2002**
- 4 Phallus strongly projected distad at apical margin (e.g., Figs 3D, E, 9A, B) **5**
- Phallus nearly straight at apical margin (Fig. 9D, E); China (Anhui) (Fig. 1) ***P. truncata* sp. nov.**
- 5 Male antennomere III with outer apical angle barely protruding laterally (Fig. 8A); phallus arched at apex in dorsal and ventral views (Fig. 9A, B); China (Anhui) (Fig. 1) ***P. dabiesshanensis* sp. nov.**
- Male antennomere III with outer apical angle strongly protruding laterally (Fig. 2C); phallus narrowly rounded at apex in dorsal and ventral views (Fig. 3D, E); China (Zhejiang, Jiangxi, Fujian, Guangdong) (Fig. 1) ***P. fukiensis* (Bocak, 1999)**
- 6 Male antennomere I nearly globular, elytral cells mostly squared (e.g., Fig. 10A, B)..... **7**
- Male antennomere I flattened dorsally, elytral cells transverse (e.g., Figs 6A, 7A)..... **9**
- 7 Pronotum uniformly black; phallus strongly projected distad at apical margin and narrowly triangular at apex in ventral view (Bocak 1999: fig. 76); China (Sichuan) (Fig. 1) ***P. tryznai* (Bocak, 1999)**
- Pronotum bicolored, black with bright red margins; phallus barely projected distad at apical margin and widely triangular at apex in ventral view (e.g., Fig. 11B)..... **8**

8	Lamella of male antennomere IX 2.5× as long as joint itself (Fig. 10C); China (Sichuan) (Fig. 1)	<i>P. longicornis</i> sp. nov.	
–	Lamella of male antennomere IX 1.5× as long as joint itself; China (Sichuan) (Fig. 1).....	<i>P. sichuanensis</i> (Bocak, 1999)	
9	Pronotum uniformly red or bicolored and at least bright red at margins (e.g., Fig. 7C, D).....		19
–	Pronotum uniformly black (e.g., Figs 2A, B, 7A, B).....		10
10	Elytra bicolored, at least black at humeri (e.g., Fig. 7A, B).....		11
–	Elytra uniformly orange red or brownish red (e.g., Fig. 2A, B)		12
11	Phallus moderately widened at middle part in ventral view (Fig. 5G), weakly bent dorsally in lateral view (Fig. 5I); China (Henan, Shaanxi, Gansu, Hunan, Hubei, Sichuan) (Fig. 1).....	<i>P. nigrohumeralis</i> (Pic, 1938)	
–	Phallus strongly widened at middle part in ventral view (Kazantsev, 2002: fig. 19), obviously bent dorsally in lateral view (Kazantsev, 2002: fig. 20); China (Taiwan) (Fig. 1).....	<i>P. chifengleei</i> Kazantsev, 2002	
12	Lamella of male antennomere VI longer, ≥ 1.8× longer than joint itself (e.g., Fig. 6A).....		13
–	Lamella of male antennomere VI shorter, ≤ 1.3× longer than joint itself (e.g., Fig. 2A).....		18
13	Elytra orange-red, primary costae as strong as secondary ones		14
–	Elytra red to brownish red, primary costae much stouter than secondary ones (e.g., Fig. 6A, B).....		15
14	Antennal tubercles with reddish spots posteriorly; phallus strongly widened at basal part and acute at apex (Kazantsev 2002: figs 25, 27); China (Taiwan) (Fig. 1)	<i>P. cincinnatus</i> Kazantsev, 2002	
–	Antennal tubercles uniformly black; phallus barely widened at basal part and arched at apex (Bocak 1999: fig. 75); China (Taiwan) (Fig. 1)	<i>P. gestroi</i> Pic, 1912	
15	Phallus projected distad at apical margin (e.g., Figs 9G, H, J, K, 11G, H).		16
–	Phallus nearly straight at apical margin (Fig. 5A, B); China (Zhejiang, Jiangxi, Fujian), Korea (Fig. 1)	<i>P. klapperichi</i> Bocak, 1999	
16	Phallus narrowly rounded at apex (Fig. 11G, H); China (Hainan) (Fig. 1)	<i>P. hainanensis</i> sp. nov.	
–	Phallus arched at apex (e.g., Fig. 9G, H)		17
17	Phallus hardly widened at basal part in dorsal and ventral views (Fig. 9J, K); China (Chongqing) (Fig. 1)	<i>P. quadricollimima</i> sp. nov.	
–	Phallus moderately widened at middle part in dorsal and ventral views (Fig. 9G, H); Japan (Fig. 1)	<i>P. quadricollis</i> (Kiesenwetter, 1874)	
18	Lamella of male antennomere X slender and even in width, trunk of VIII 2.8× longer than width in the middle; Japan (Fig. 1).....	<i>P. oshimana</i> (Nakane, 1961)	
–	Lamella of male antennomere X broader and tapering distad, trunk of VIII 1.9× longer than width in the middle (Fig. 2A); China (Guangxi), Vietnam (Fig. 1)	<i>P. alternata</i> (Pic, 1927)	
19	Elytra ≥ 5.5× longer than pronotum (e.g., Figs 4D, 12A).....		20
–	Elytra ≤ 5.0× longer than pronotum (e.g., Fig. 4A–C)		21

- 20 Anterior margin of pronotum straight (Fig. 4D); phallus bisinuate at lateral margins in dorsal and ventral views (Fig. 3J, K); China (Hunan, Fujian) (Fig. 1) ***P. gracilis* (Bocak, 1999)**
- Anterior margin of pronotum arched (Fig. 12A); phallus arcuate at lateral margins in dorsal and ventral views (Fig. 11D, E); China (Zhejiang) (Fig. 1) ***P. zhejiangensis* sp. nov.**
- 21 Elytral primary costae much stouter than secondary ones in whole length (e.g., Fig. 7C, D)..... **22**
- Elytral primary costae nearly as strong as secondary ones (e.g., Figs 4A–C, 6C, D)..... **23**
- 22 Phallus with > 45° angle at apex (Bocak 1999: fig. 74); Japan (Fig. 1)..... ***P. ishigakiana* (Nakane, 1961)**
- Phallus with < 30° angle at apex (Fig. 5J, K); China (Hunan, Hubei, Guizhou) (Fig. 1) ***P. variabilis* Li, Bocak & Pang, 2015**
- 23 Pronotum present with a large black patch, extending to anterior and posterior margins; elytral width at humeri 1.5× wider than posterior margin of pronotum (Fig. 6C, D); China (Yunnan), Vietnam, Myanmar (Fig. 1) ***P. laticornis* Fairmaire, 1899**
- Pronotum unicolored, or present with a dark brown to black patch in center of disc, but never extending to anterior or posterior margin; elytral width at humeri 1.2–1.3× wider than posterior margin of pronotum (Fig. 4A–C); China (Yunnan), Vietnam, Myanmar, Laos, Thailand, India (Fig. 1) ***P. himalejica* (Bourgeois, 1885)**

***Ponyalis alternata* (Pic, 1927)**

Figs 1, 2A, B, 3A–C

Lyponia alternata Pic, 1927: 5; Bocak 1999: 96, figs 41, 78.

Ponyalis alternata: Kazantsev 2002: 205; Li et al. 2015a: 16.

Material examined. CHINA: 2♂1♀ (MHBU), Guangxi, Wuming, Damingshan, 20.V.2011, 1100 m, leg. H. Y. Liu.

Differential diagnosis. This species can be readily identified from all other *Ponyalis* by the combination of the following characters: pronotum uniformly black and elytra red (Fig. 2A, B); male antennomere I flattened dorsally, III long-triangular, IV wide-triangular, lamellae of V–X extended along whole length of corresponding stem and tapered laterally, lamella of VI short and 1.3× longer than joint itself (Fig. 2A); elytral primary costae much stouter than the secondary ones in whole length, cells transverse (Fig. 2A, B); phallus widened at middle part, projected distad at apical margin and narrowly rounded at apex in ventral and dorsal views (Fig. 3A, B).

Descriptive notes. Male (Fig. 2A). Antennae reaching elytral mid-length when inclined, antennomere I flattened dorsally, III long-triangular, 1.3× as long as wide, IV wide-triangular, approximately as long as wide, lamellae of V–X extended along whole length of corresponding stem and tapered laterally, 1.1–2.9× longer than the corresponding antennomere itself, XI fusiform and 4.2× as long as wide.

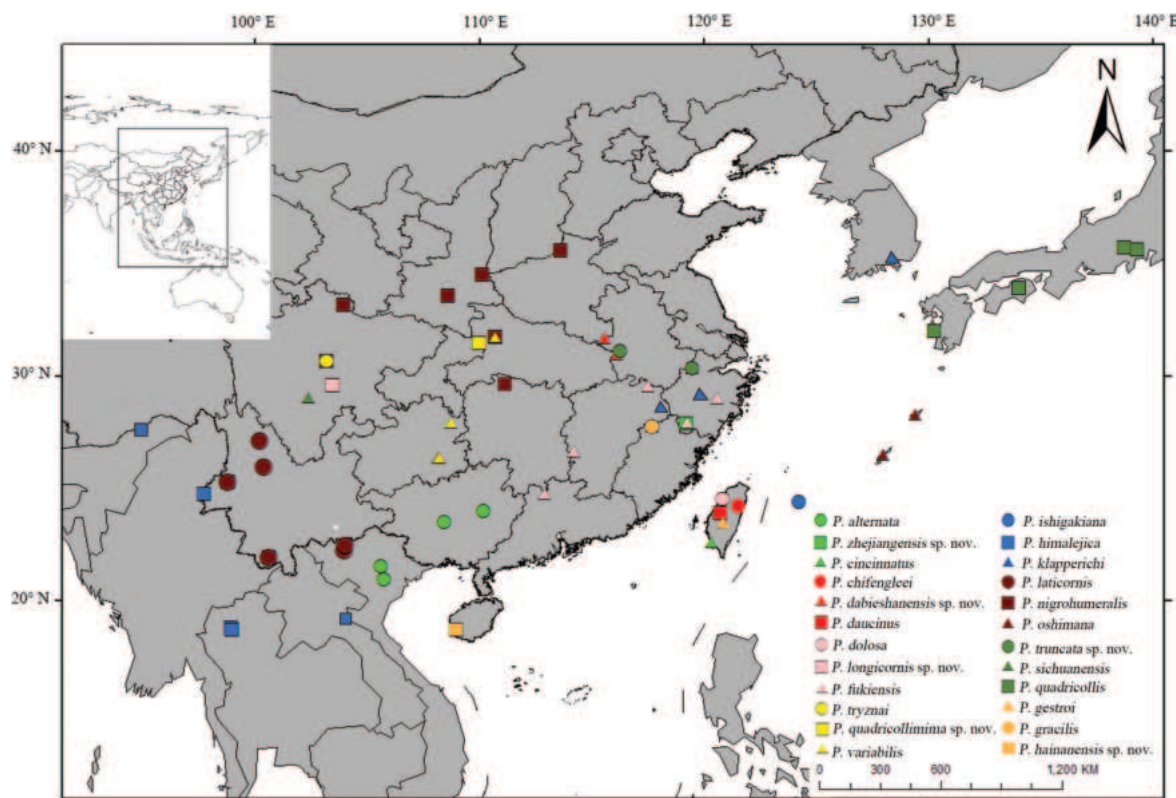


Figure 1. Distribution map of *Ponyalis* in the world.

Aedeagus: phallus stout, 2.4× as long as wide, moderately widened at middle part and arcuate at lateral margins, moderately projected distad at apical margin and narrowly rounded at apex in dorsal and ventral views, with acute latero-apical angles, between which the distance much smaller than maximal width of trunk (Fig. 3A, B); almost even in width and weakly bent dorsally, truncate at ventro-apical 1/4 in lateral view (Fig. 3C).

Female (Fig. 2B). Similar to male, but body stouter, antennomeres III–V all nearly triangular, lamellae of VI–X 1.1–1.8× as long as its corresponding antennomere itself, XI fusiform and 3.0× as long as wide.

Distribution (Fig. 1). China (Guangxi), Vietnam.

Remarks. Bocak (1999) provided illustrations of basal antennomeres of male antenna and ventral view of aedeagus for this species. Here we present the images of habitus of both sexes and aedeagus in ventral, dorsal and lateral views to make its morphology better known.

Ponyalis fukiensis (Bocak, 1999)

Figs 1, 2C, D, 3D–F

Lyponia fukiensis Bocak, 1999: 92, figs 26, 51.

Ponyalis fukiensis: Kazantsev 2002: 206; Li et al. 2015a: 17.

Material examined. CHINA: 1♂ (MHBV), Zhejiang, Longquan, Fengyangshan, 1250 m, 31.III.2007, leg. J. Cao; 1♀ (MHBV), same locality as the preceding, 18.V.2007, leg. D. D. Hu & J. F. Gao; 1♀ (MHBV), same locality as the preceding,

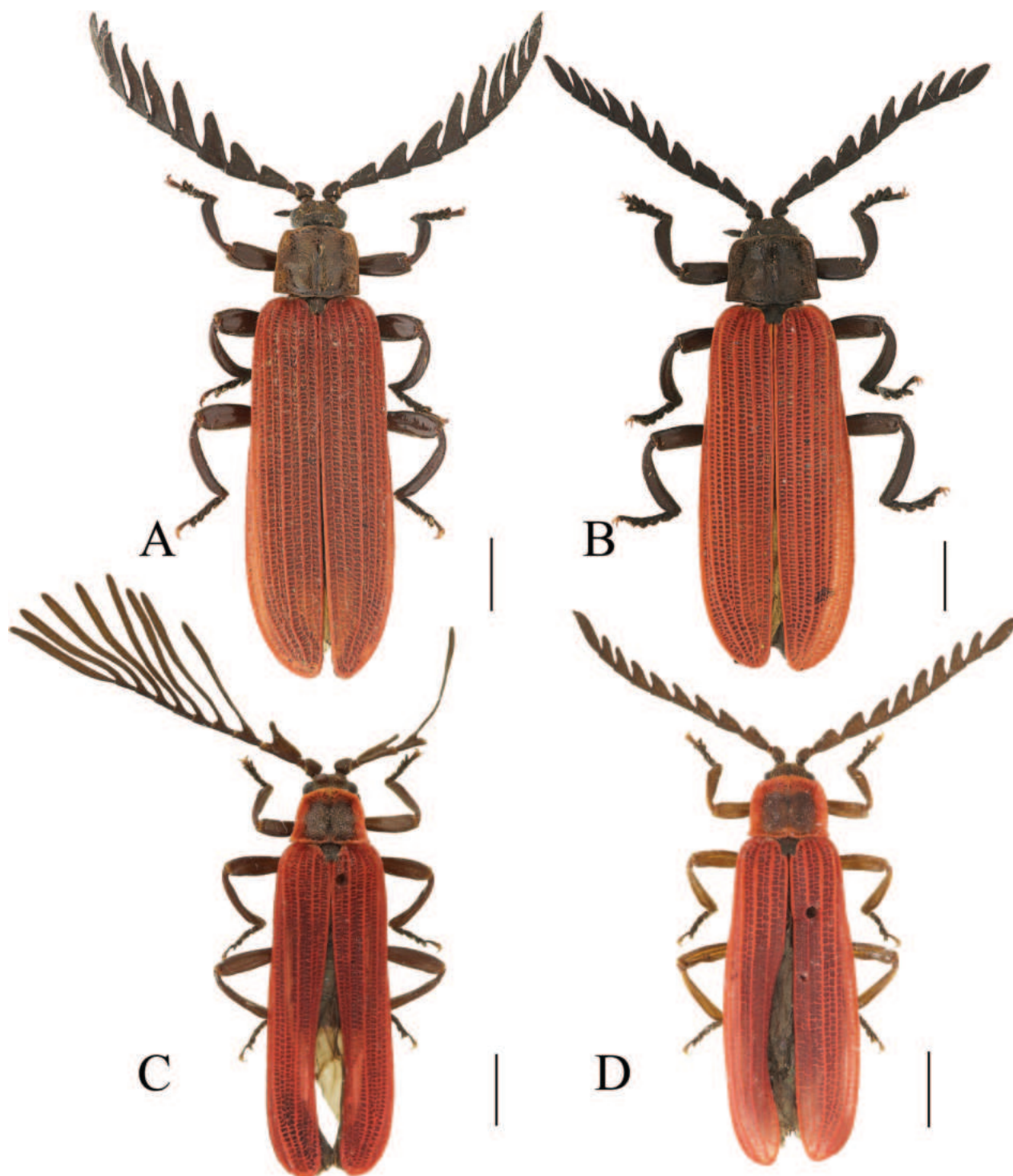


Figure 2. Habitus, dorsal view: *Ponyalis alternata* (Pic, 1927) (A, B); *P. fukiensis* (Bocak, 1999) (C, D). A, C males B, D females. Scale bars: 2.0 mm.

17.V.2007, leg. B. F. Zhou & L. Wang; 1♀ (IZAS), Fujian, Jianyang, Huangkeng, Aotou, 26.V.1973, leg. P. Y. Yu; 1♀ (IZAS), same locality as the preceding, 800–950 m, 5.V.1960, leg. F. J. Pu.

Differential diagnosis. This species can be differentiated from all others of *Ponyalis* by the combination of the following characters: pronotum black, with red margins, elytra red (Fig. 2C, D); male antennomere I nearly globular, III with outer

apical angle strongly protruding laterally, lamellae of IV–X nearly parallel-sided along the whole length, lamella of IV long and 2.0× longer than joint itself, (Fig. 2C); elytral primary costae much stouter than the secondary ones in whole length, cells transverse to squared (Fig. 2C, D); phallus moderately projected distad at apical margin, narrowly rounded at apex in dorsal and ventral views (Fig. 3D, E).

Descriptive notes. Male (Fig. 2C). Antennae reaching apical 1/4 length of elytra when inclined, antennomere I nearly globular, III long-triangular, 1.4× as long as wide, with outer apical angle strongly protruding laterally, lamellae of IV–X abruptly extended laterally and nearly parallel-sided along the whole length, 5.5–7.0× longer than the corresponding antennomere itself, XI parallel-sided and 13.0× as long as wide.

Aedeagus: phallus slender and 3.7× as long as wide, barely widened at basal part and arcuate at lateral margins, moderately projected distad at apical margin and narrowly rounded at apex in dorsal and ventral views, with sharp latero-apical angles, between which the distance barely greater than maximal width of trunk (Fig. 3D, E), almost even in width and nearly straight, truncate at ventro-apical 1/5 in lateral view (Fig. 3F).

Female (Fig. 2D). Similar to male, but body stouter, antennae shorter and reaching elytral apical 1/3 length when inclined, antennomeres III–V all nearly triangular, lamellae of VI–X 1.1–1.5× as long as its corresponding antennomere itself, XI fusiform and 4.0× as long as wide.

Distribution (Fig. 1). China (Zhejiang, Jiangxi, Fujian, Guangdong).

***Ponyalis himalejica* (Bourgeois, 1885)**

Figs 1, 3G–I, 4A–C

Lyponia himalejica Bourgeois, 1885: 79; Bocak 1999: 94, figs 52, 53.

Lyponia waterhousei Gorham, 1890: 543. Synonymized by Bocak 1999: 94.

Lyponia ochraceicollis Pic, 1923: 9. Synonymized by Bocak 1999: 94.

Lyponia aurantiaca Pic, 1927: 5. Synonymized by Bocak 1999: 94.

Lyponia robusticollis Pic, 1939: 165. Synonymized by Bocak 1999: 94.

Ponyalis himalejica: Kazantsev 2002: 205, fig. 30; Li et al. 2015a: 17.

Material examined. CHINA: 1♂1♀ (IZAS), Yunnan, Menghai, Nannuoshan, 1100–1200 m, 28.IV.1957, leg. G. J. Hong; 2♂ (IZAS), same locality as the preceding, 1600 m, 25.IV.1958, leg. G. J. Hong; 1♀ (IZAS), same locality as the preceding, 1100–1500 m, 27.IV.1957, leg. F. J. Pu; 1♀ (IZAS), Yunnan, Menghai, Chachan, 1200–1450 m, 24.IV.1957, leg. S. Y. Wang; 1♂1♀ (IZAS), Yunnan, Xishuangbanna, Mengsong, 1600 m, 26.IV.1958, leg. Y. R. Zhang; 2♂2♀ (MHBU), Yunnan, Yingjiang, Xima, 20.VII.2019, leg. P. Wang.

Differential diagnosis. This species differs from all others of *Ponyalis* by the combination of the following characters: pronotum uniformly red, or present with a dark brown to black patch in center of disc, but never extending to anterior or posterior margin, elytra red (Fig. 4A–C); male antennomere I flattened dorsally, III and IV long-triangular, lamellae of V–X extended along whole length of corresponding stem and tapered laterally (Fig. 4A); elytra 5.0× longer than pronotum, primary costae nearly as strong as secondary ones, cells transverse (Fig. 4A–C); phallus strongly widened at middle part and arcuate at lateral



Figure 3. Aedeagi of *Ponyalis alternata* (Pic, 1927) (A–C); *P. fukiensis* (Bocak, 1999) (D–F); *P. himalejica* (Bourgeois, 1885) (G–I); *P. gracilis* (Bocak, 1999) (J–L). A, D, G, J ventral views B, E, H, K dorsal views C, F, I, L lateral views. Scale bars: 0.5 mm.

margins, moderately projected distad at apical margin and narrowly rounded at apex in dorsal and ventral views (Fig. 3G, H).

Descriptive notes. Male (Fig. 4A). Antennae reaching basal 3/5 length of elytra when inclined, antennomere I flattened dorsally, III and IV long-triangular, 1.3–1.5× as long as wide, with outer apical angles strongly protruding laterally, lamellae of V–X extended along whole length of corresponding stem and tapered laterally, 1.8–3.8× longer than the corresponding antennomere itself, XI fusiform and 5.3× as long as wide.

Aedeagus: phallus stout, 2.0× as long as wide, strongly widened at middle part and arcuate at lateral margins, moderately projected distad at apical margin and narrowly rounded at apex in dorsal and ventral views, with acute latero-apical

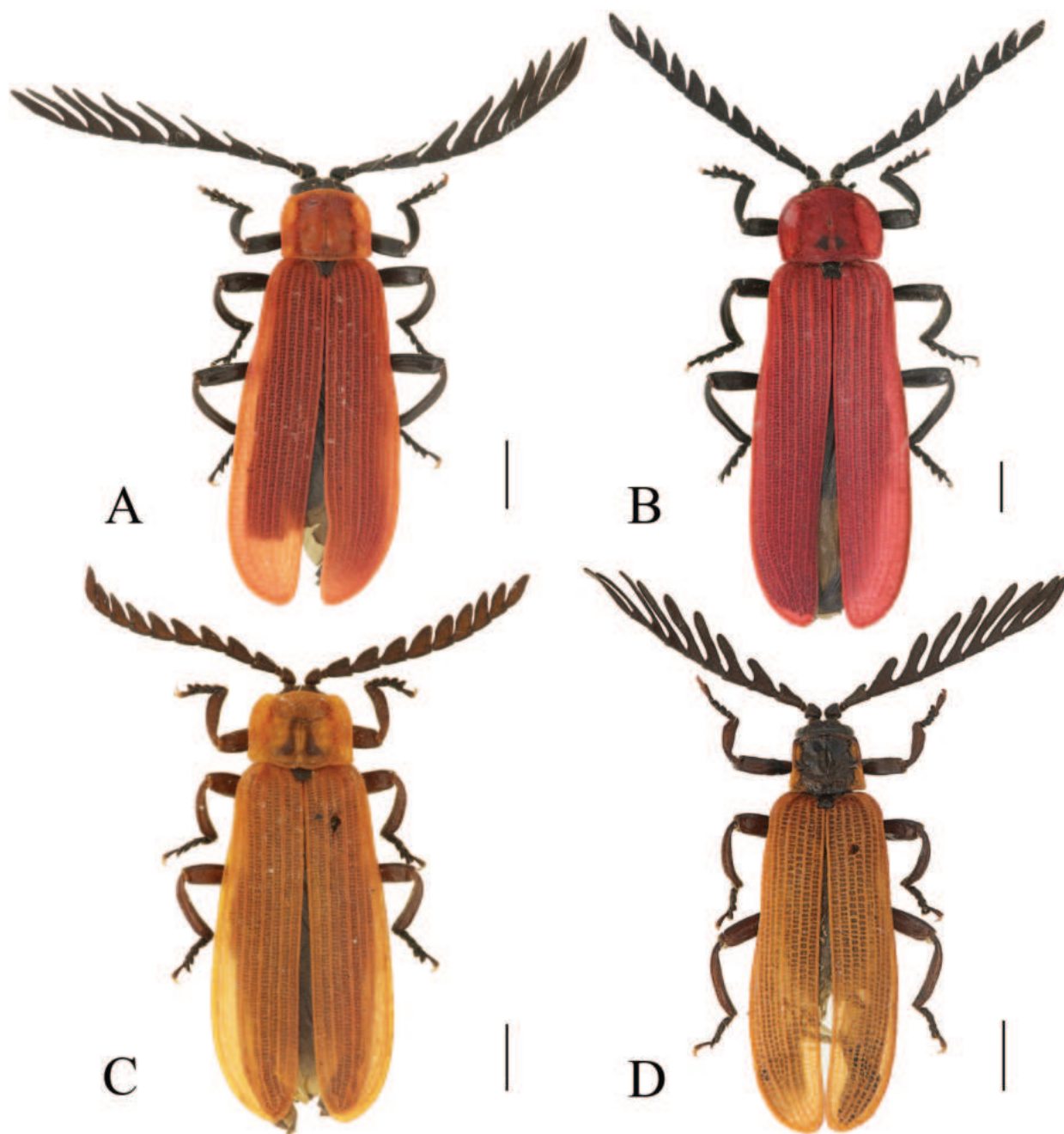


Figure 4. Habitus, dorsal view: *Ponyalis himalejica* (Bourgeois, 1885) (A–C); *P. gracilis* (Bocak, 1999) (D). A, D males B, C females. Scale bars: 2.0 mm.

angels, between which the distance much smaller than maximal width of trunk (Fig. 3G, H), weakly bent dorsally and tapered distad in lateral view (Fig. 3I).

Female (Fig. 4B, C). Similar to male, but body stouter, antennae shorter and reaching elytral mid-length when inclined, antennomeres III–V triangular, lamellae of VI–X 1.1–1.5× as long as its corresponding antennomere itself, XI fusiform and 3.0× as long as wide.

Distribution (Fig. 1). China (Yunnan), Vietnam, Myanmar, Laos, Thailand, India.

Remarks. We provide different habitus macrophotographs (Fig. 4B, C) for this species to show its variability of appearance, probably due to its wide distribution (Bocak 1999).

***Ponyalis gracilis* (Bocak, 1999)**

Figs 1, 3J–L, 4D

Lyponia gracilis Bocak, 1999: 89, fig. 71.

Ponyalis gracilis: Kazantsev 2002: 205; Li et al. 2015a: 17.

Material examined. CHINA: 1♂ (MHBU), Fujian, Wuyishan, Guadun, 29.IV.2004, leg. D. K. Zhou.

Differential diagnosis. This species can be separated from all other *Ponyalis* by the combination of the following characters: pronotum black, with red margins, elytra red (Fig. 4D); antennomere I flattened dorsally, III long-triangular, lamellae of IV–X nearly parallel-sided (Fig. 4D); elytra 5.5× longer than pronotum, primary costae as strong as the secondary ones, cells transverse (Fig. 4D); phallus bisinuate at lateral margins and narrowly rounded at apex in dorsal and ventral views (Fig. 3J, K).

Descriptive notes. Male (Fig. 4D). Antennae reaching elytral mid-length when inclined, antennomere I flattened dorsally, III long-triangular, 1.5× as long as wide, lamellae of IV–X nearly parallel-sided, 1.5–3.6× longer than corresponding antennomere itself, XI parallel-sided and 8.0× as long as wide.

Aedeagus: phallus slender and 3.3× as long as wide, barely widened at basal part and bisinuate at lateral margins, moderately projected distad at apical margin and narrowly rounded at apex in dorsal and ventral views, with acute latero-apical angles, between which the distance barely smaller than maximal width of trunk (Fig. 3J, K), moderately bent dorsally and tapered distad in lateral view (Fig. 3L).

Distribution (Fig. 1). China (Hunan, Fujian).

***Ponyalis klapperichi* (Bocak, 1999)**

Figs 1, 5A–C, 6A, B

Lyponia klapperichi Bocak, 1999: 100, fig. 77.

Ponyalis klapperichi: Kazantsev 2002: 205; Li et al. 2015a: 17.

Material examined. CHINA: 1♂ (IZAS), Fujian, Jianyang, Huangkeng, Aotou, 850–950 m, 29.IV.1960, leg. F. J. Pu; 1♀ (IZAS), Fujian, Chongan, Xingcun, Sangang, 720 m, 16.V.1960, leg. F. J. Pu.

Differential diagnosis. This species can be easily identified from the rest of the *Ponyalis* species by the combination of the following characters: pronotum uniformly black and elytra red (Fig. 6A, B); male antennomere I flattened dorsally, III long-triangular, IV wide-triangular, lamellae of VI–X nearly parallel-sided along the whole length, lamella of VI 2× longer than joint itself (Fig. 6A); elytral primary costae as strong as the secondary ones, cells transverse (Fig. 6A, B); phallus moderately widened at middle part and nearly straight at apical margin in dorsal and ventral views (Fig. 5A, B).

Descriptive notes. Male (Fig. 6A). Antennae reaching apical 1/4 length of elytra when inclined, antennomere I nearly globular, III long-triangular, 1.4× as long as wide, IV wide-triangular and nearly as long as wide, lamella of V extended along whole length of stem and tapered laterally, lamellae of VI–X nearly



Figure 5. Aedeagi of *Ponyalis klapperichi* (Bocak, 1999) (A–C); *P. laticornis* Fairmaire, 1899 (D–F); *P. nigrohumeralis* (Pic, 1939) (G–I); *P. variabilis* Li, Bocak & Pang, 2015 (J–L). A, D, G, J ventral views B, E, H, K dorsal views C, F, I, L lateral views. Scale bars: 0.5 mm.

parallel-sided along the whole length, 2.1–4.1× longer than the corresponding antennomere itself, XI nearly parallel-sided and 6.7× as long as wide.

Aedeagus: phallus slender and 3.7× as long as wide, moderately widened at middle part and arcuate at lateral margins, nearly straight at apical margin in dorsal and ventral views, with sharp latero-apical angles, between which the distance barely smaller than maximal width of trunk (Fig. 5A, B), almost even in width and weakly bent dorsally, truncate at ventro-apical 1/4 in lateral view (Fig. 5C).

Female (Fig. 6B). Similar to male, but body stouter, antennae shorter and reaching elytral mid-length when inclined, antennomeres III–V all nearly triangular, lamellae of VI–X 1.1–1.5× longer than the corresponding antennomere itself, XI fusiform and 3.2× as long as wide.

Distribution (Fig. 1). China (Zhejiang, Jiangxi, Fujian), Korea.

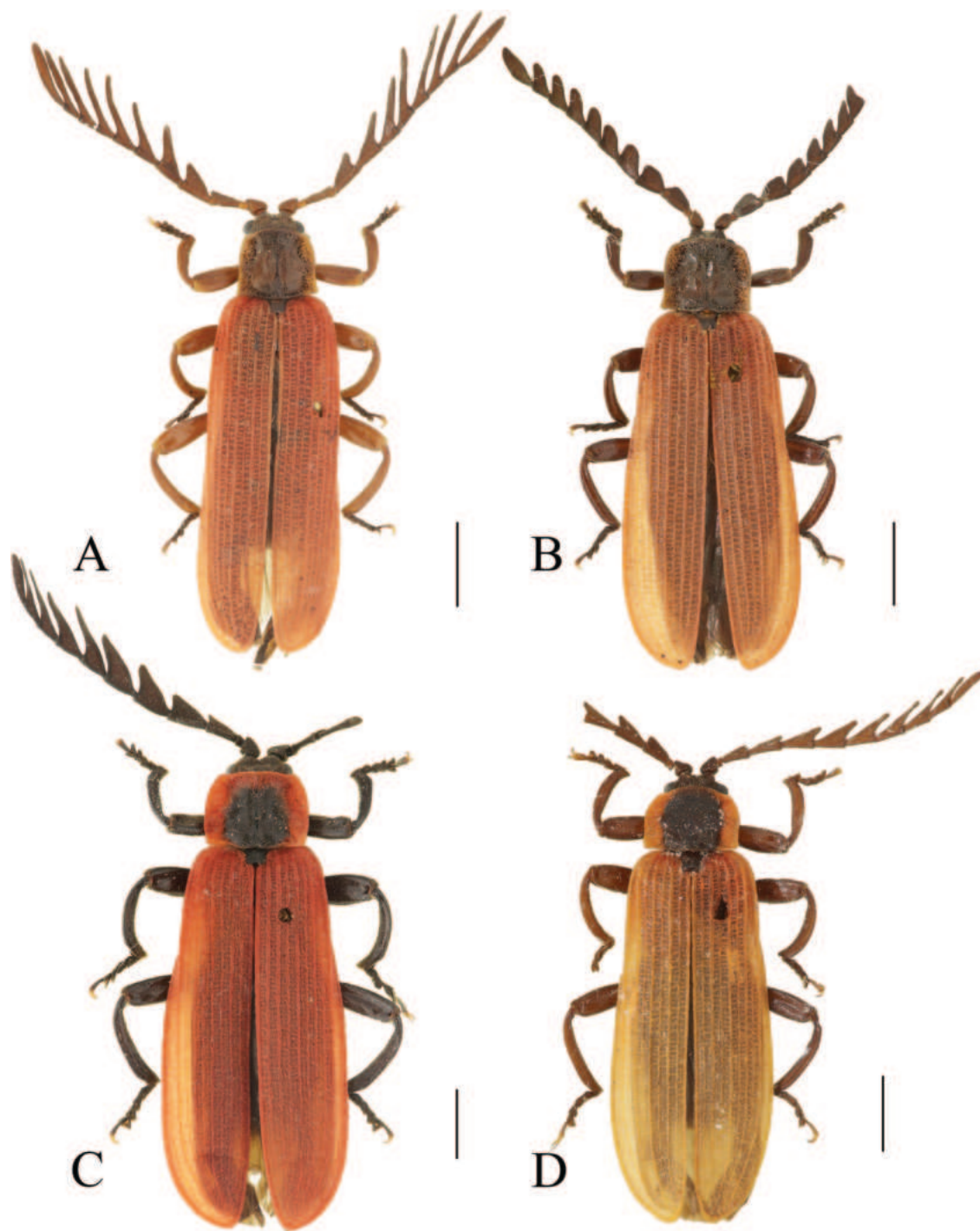


Figure 6. Habitus, dorsal view: *Ponyalis klapperichi* (Bocak, 1999) (A, B); *P. laticornis* Fairmaire, 1899 (C, D). A, C, D males B female. Scale bars: 2.0 mm.

***Ponyalis laticornis* Fairmaire, 1899**

Figs 1, 5D–F, 6C, D

Ponyalis laticornis Fairmaire, 1899: 623; Kazantsev 2002: 205; Li et al. 2015a: 17.

Lyponia robusta Pic, 1922: 13. Synonymized by Bocak and Bocakova 2000: 42.

Lyponia laticornis: Pic, 1926: 69; Bocak 1999: 93, fig. 55.

Lyponia diversicornis Pic, 1926: 70. Synonymized by Bocak and Bocakova 2000: 42.

Lyponia limbaticollis Pic, 1926: 70. Synonymized by Bocak 1999: 93.

Lyponia guerryi Pic, 1939: 165. Synonymized by Bocak and Bocakova 2000: 42.
Lyponia patruelis Kleine, 1939: 17. Synonymized by Bocak 1999: 93.

Material examined. CHINA: 1♂ (IZAS), Yunnan, Lijiang, 3100 m, 27.V.1980, leg. L. Y. Wang; 1♂ (IZAS), Yunnan, Mancheng, 1700 m, 16.IV.1980, leg. P. Gao.

Differential diagnosis. This species can be differentiated from all other *Ponyalis* by the combination of the following characters: pronotum red, present with a large black patch, extending to anterior and posterior margins, elytra red (Fig. 6C, D); male antennomere I flattened dorsally, III–IV long-triangular, lamellae of V–X extended along whole length of corresponding stem and tapered laterally (Fig. 6C); elytra 5.5× longer than pronotum and 1.2–1.3× wider than posterior margin of pronotum, primary costae nearly as strong as the secondary ones, cells transverse (Fig. 6C, D); phallus abruptly widened near middle part, moderately projected distad at apical margin and narrowly rounded at apex in dorsal and ventral views (Fig. 5D, E).

Descriptive notes. Male (Fig. 6C, D). Antennae reaching apical 1/4 length of elytra when inclined, antennomere I flattened dorsally, III and IV long-triangular, 1.3–1.4× as long as wide, lamellae of V–X extended along whole length of corresponding stem and tapered laterally, 1.2–2.2× longer than the corresponding antennomere itself, XI fusiform and 5.0× as long as wide.

Aedeagus: phallus stout, 2.3× as long as wide, abruptly widened near middle part and obtusely angled at lateral margins, moderately projected distad at apical margin and narrowly rounded at apex in dorsal and ventral views, with acute latero-apical angles, between which the distance much smaller than maximal width of trunk (Fig. 5D, E), almost even in width and weakly bent dorsally, truncate at ventro-apical 1/4 in lateral view (Fig. 5F).

Distribution (Fig. 1). China (Yunnan), Vietnam, Myanmar.

Remarks. As noted by others (e.g., Bocak 1999), this species shows some variations in the coloration of pronotum, of which the black patch could be extending to anterior margin (Fig. 6D) or not (Fig. 6C).

***Ponyalis nigrohumeralis* (Pic, 1939)**

Figs 1, 5G–I, 7A, B

Lyponia nigrohumeralis Pic, 1939: 220; Bocak 1999: 100, fig. 79.

Ponyalis nigrohumeralis: Kazantsev 2002: 199, figs 31, 32; Li et al. 2015a: 17.

Material examined. CHINA: 1♂1♀ (MHBU), Shaanxi, Liuba, Miaotaizi, 10–15.VI.2005, leg. Y. B. Ba; 1♀ (MHBU), Shaanxi, Liuba, 10–12.VI.2005, Y. B. Ba leg., 1♂ (IZAS), Shaanxi, Ningshan, Pingheliang, 2106–2448 m, 1.V.2007, leg. M. Y. Lin; 1♂ (IZAS), same locality as the preceding, 1.V.2007, leg. J. Z. Cui; 2♂ (IZAS), Shaanxi, Zhouzhi, Houzhenzi, 1745–2021 m, 26.V.2007, leg. J. Z. Cui; 1♀ (IZAS), same locality as the preceding, 26.V.2007, leg. H. L. Shi; 1♂ (IZAS), Henan, Huixian, Baligou, 9–12.V.2002, leg. Y. F. Hao; 1♂ (MHBU), Gansu, Qin Zhou, Niangniangba, 30.V.2021, leg. R. Liu; 1♂ (MHBU), Gansu, Wenxian, Huangtuling, 2250 m, 9.VII.2003, leg. Y. B. Ba & Y. P. Niu; 1♂ (MHBU), Sichuan, Jiuzhaigou, Wujiao, 15.VII.2009, leg. Z. H. Gao & Y. P. Niu.

Differential diagnosis. This species can be easily separated from all other *Ponyalis* by the combination of the following characters: pronotum uniformly

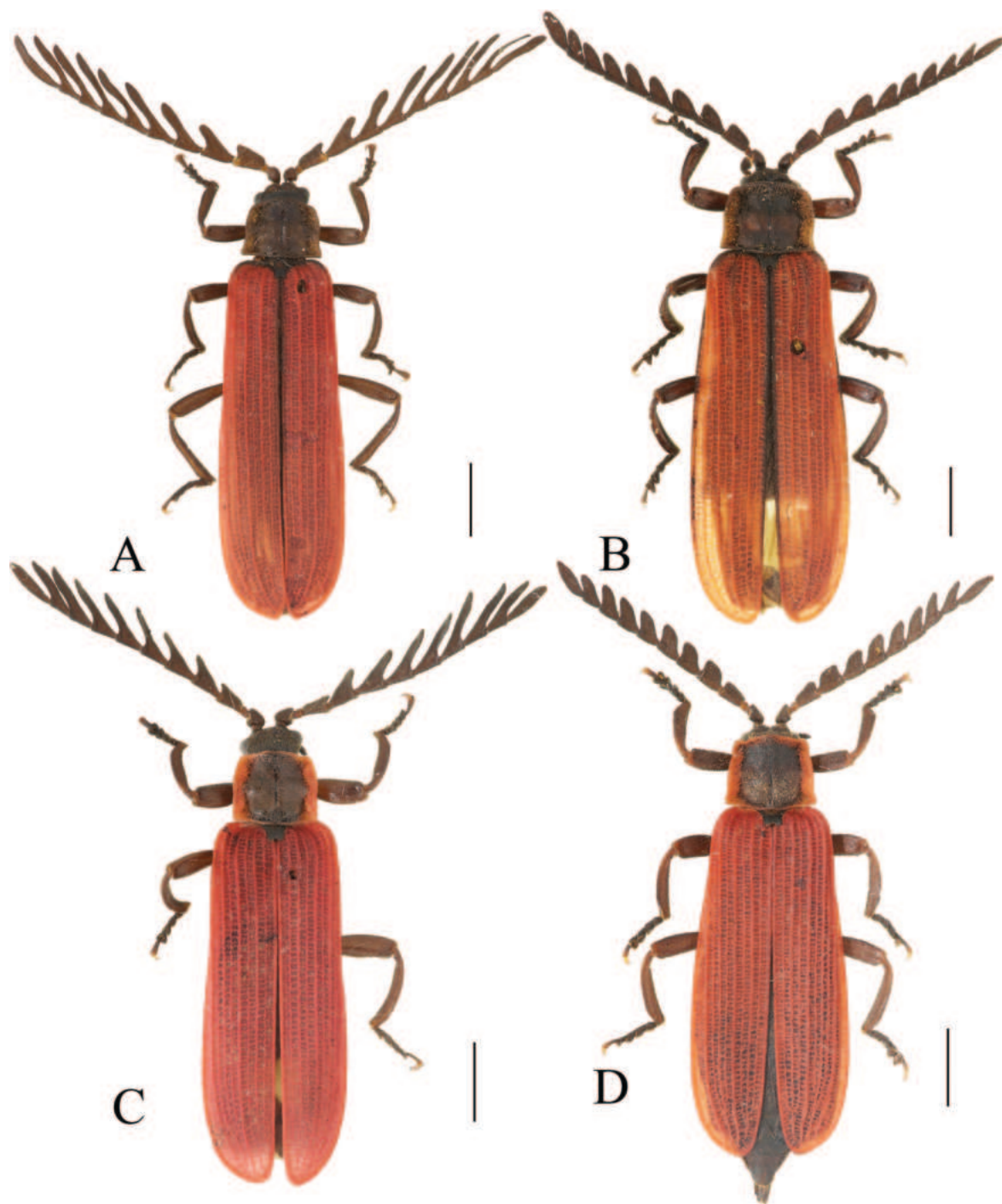


Figure 7. Habitus, dorsal view: *Ponyalis nigrohumeralis* (Pic, 1939) (A, B); *P. variabilis* Li, Bocak & Pang, 2015 (C, D). A, C males; B, D females. Scale bars: 2.0 mm.

black, elytra bicolored, at least black at humeri (Fig. 7A, B); male antennomere I flattened dorsally, III long-triangular, lamellae of IV–X nearly parallel-sided along the whole length (Fig. 7A); elytral primary costae much stouter than the secondary ones in whole length, cells transverse (Fig. 7A, B); phallus moderately widened at middle part and arched at apex in dorsal and ventral views (Fig. 5G, H), weakly bent dorsally in lateral view (Fig. 5I).

Descriptive notes. Male (Fig. 7A). Antennae reaching basal 3/5 length of elytra when inclined, antennomere I flattened dorsally, III long-triangular, 1.4×

as long as wide, lamellae of IV–X nearly parallel-sided along the whole length, 1.5–3.9× longer than the corresponding antennomere itself, XI parallel-sided and 4.2× as long as wide.

Aedeagus: phallus slender and 3.3× as long as wide, moderately widened at middle part and arcuate at lateral margins, strongly projected distad at apical margin and arched at apex in dorsal and ventral views, with rectangular latero-apical angles, between which the distance barely smaller than maximal width of trunk (Fig. 5G, H), weakly bent dorsally and tapered distad in lateral view (Fig. 5I).

Female (Fig. 7B). Similar to male, but body stouter, antennae shorter and reaching elytral mid-length when inclined, antennomeres III–V all nearly triangular, lamellae of VI–X 1.1–1.5× as long as its corresponding antennomere itself, XI fusiform and 2.6× as long as wide.

Distribution (Fig. 1). China (Henan, Shaanxi, Gansu, Hunan, Hubei, Sichuan).

Remarks. Bocak (1999) and Kazantsev (2002) provided the illustration of the aedeagus for this species, and here we present the habitus of male and female for the first time.

***Ponyalis variabilis* Li, Bocak & Pang, 2015**

Figs 1, 5J–L, 7C, D

Ponyalis variabilis Li, Bocak & Pang, 2015: 14, figs 8, 15, 16.

Material examined. CHINA: 1♂ (MHB), Hubei, Qingtianpao, 22.V.2019, leg. P. Wang; 1♀ (MHB), same locality as the preceding, 11.VI.2018, leg. P. Wang.

Differential diagnosis. This species can be readily identified from all other *Ponyalis* by the combination of the following characters: pronotum black, red margins, elytra red (Fig. 7C, D); male antennomere I flattened dorsally, III long-triangular, lamellae of IV–X extended along whole length of corresponding stem and tapered laterally (Fig. 7C); elytra 5.0× longer than pronotum, primary costae much stouter than the secondary ones in whole length, cells transverse (Fig. 7C, D); phallus widened at middle part and moderately projected distad at apical margin and < 30° angle at apex in ventral and dorsal views (Fig. 5J, K).

Descriptive notes. Male (Fig. 7C). Antennae reaching basal 3/5 length of elytra when inclined, antennomere I flattened dorsally, III long-triangular, 1.3× as long as wide, with outer apical angle barely protruding laterally, lamellae of IV–X extended along whole length of corresponding stem and tapered laterally, 2.0–3.2× longer than the corresponding antennomere itself, XI fusiform and 5.0× as long as wide.

Aedeagus: phallus slender and 3.7× as long as wide, strongly widened at middle part and arcuate at lateral margins, moderately projected distad at apical margin and narrowly narrowed at apex, with acute latero-apical angles, between which the distance much smaller than maximal width of trunk (Fig. 5J, K), almost even in width and weakly bent dorsally, truncate at ventro-apical 1/4 in lateral view (Fig. 5L).

Female (Fig. 7D). Similar to male, but body stouter, antennae shorter and reaching elytral mid-length when inclined, antennomeres III–V all nearly triangular, lamellae of VI–IX 1.1–1.7× as long as its corresponding antennomere itself, XI fusiform and 3.0× as long as wide.

Distribution (Fig. 1). China (Hunan, Hubei, Guizhou).

***Ponyalis dabieshanensis* Y. Yang, Fang & Liu, sp. nov.**

<https://zoobank.org/35305630-EE04-48A4-9E34-7CAC75ABB912>

Figs 1, 8A, B, 9A–C

Type material. *Holotype*: ♂ (MHBU), CHINA, Anhui, Yaoluoping Natural Reserve, VII. 2015, leg. J. Fang. *Paratype*: CHINA: 1 ♀ (IZAS), Anhui, Jinzhai, Baojia, Jingangtai, 5.V.2021, leg. K. D. Zhao & X. C. Zhu.

Differential diagnosis. This species differs from all others of *Ponyalis* by the combination of the following characters: pronotum black, with red margins, elytra red (Fig. 8A, B); male antennomere I nearly globular, III with outer apical angle strongly protruding laterally, lamella of IV extending from middle of the joint, extremely long and 2.0× longer than joint itself (Fig. 8); elytral primary costae much stouter than the secondary ones in whole length, cells mostly squared (Fig. 8A, B); phallus moderately projected distad at apical margin and arched at apex in dorsal and ventral views (Fig. 9A, B).

The new species looks like *P. fukiensis* in the body coloration, but differs from it in the following characters: male antennomere III with outer apical angle barely protruding laterally (Fig. 8A), while strongly protruding laterally in *P. fukiensis* (Fig. 2C); phallus arched at apex in dorsal and ventral views (Fig. 9A, B), while narrowly rounded at apex in *P. fukiensis* (Fig. 3D, E); phallus with distance between the latero-apical thorns barely smaller than maximal width of trunk (Fig. 9A, B), while greater in *P. fukiensis* (Fig. 3D, E).

Description. Male (Fig. 8A). Body stout, black to dark brown, pronotum red, with a large black patch in center of disc, elytra red.

Head dorsally flat, antennomere I nearly globular, III long-triangular, 1.4× as long as wide, with outer apical angle barely protruding laterally, lamellae of IV–VII abruptly extended laterally and nearly parallel-sided along the whole length, 4.2–7.2× longer than the corresponding antennomere itself.

Pronotum nearly trapezoidal, flat, and barely wider than long, with rounded anterior angles and acute posterior angles, anterior margin arched, lateral margins weakly sinuate and posterior margin bisinuate. Scutellum barely narrowed posteriorly and obviously emarginate at apex.

Elytra parallel-sided, all primary costae stouter than secondary ones, and primary costae II and IV stouter than other costae in whole length of elytra, most cells rectangular.

Aedeagus: phallus slender and 3.2× as long as wide, barely widened at basal part and arcuate at lateral margins, moderately projected distad at apical margin and arched at apex in dorsal and ventral views, with sharp latero-apical angles, between which the distance barely smaller than maximal width of trunk (Fig. 9A, B), almost even in width and weakly bent dorsally, truncate at ventro-apical 1/5 in lateral view (Fig. 9C).

Female (Fig. 8B). Similar to male, but body stouter, antennae reaching apical 1/3 length of elytra when inclined, antennomeres III–VII triangular, 1.0–1.3× as long as wide, lamellae of VIII–X 1.1–1.3× as long as its corresponding antennomere itself, XI fusiform and 3.0× as long as wide.

Distribution (Fig. 1). China (Anhui).

Etymology. The specific name is derived from the type locality of this new species, Dabieshan, Anhui Province, China.

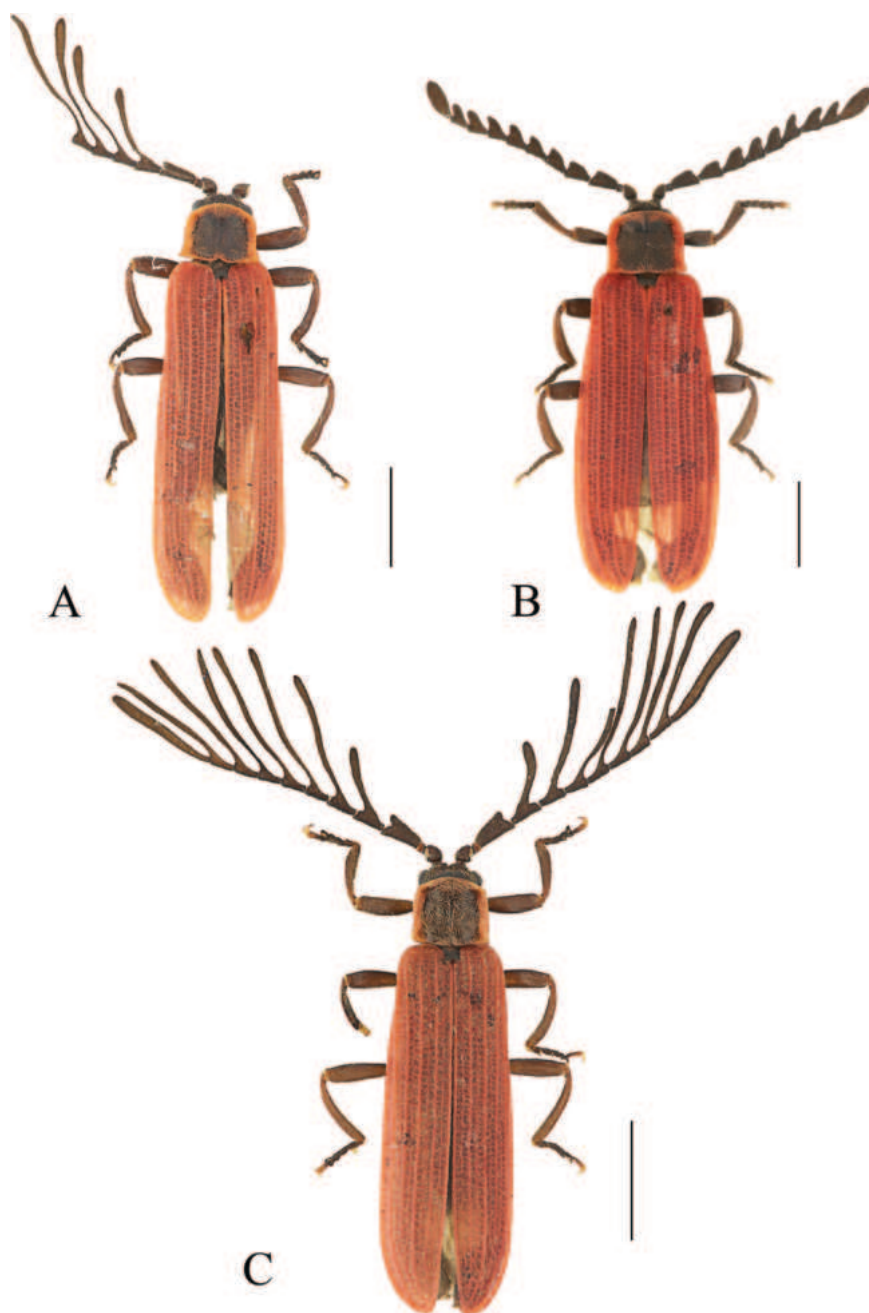


Figure 8. Habitus, dorsal view: *Ponyalis dabieshanensis* sp. nov. (A, B); *P. truncata* sp. nov. (C). A, C males B female. Scale bars: 2.0 mm.

Remarks. The left proleg, left VIII–XI and right III–XI antennomeres of the holotype are missing.

***Ponyalis truncata* Y. Yang, Liu & X. Yang, sp. nov.**

<https://zoobank.org/2CBD74FF-EA53-478D-8D81-56A0D8B1BEA4>

Figs 1, 8C, 9D–F

Type material. *Holotype*: ♂ (IZAS), CHINA, Anhui, Huoshan, Mozitang, Huangni-bao, 902 m, 14.V.2021, leg. K. D. Zhao & X. C. Zhu. *Paratype*: CHINA: 1♂ (CAU), Zhejiang, Xitianmushan, V.1960, leg. J. K. Yang.

Differential diagnosis. This species can be separated from all other *Ponyalis* by the combination of the following characters: pronotum black, with red margins, elytra red (Fig. 8C); male antennomere I nearly globular, III long-triangular, lamellae of IV–X abruptly extended laterally and nearly parallel-sided along the whole length, lamella of IV long and 2× longer than joint itself (Fig. 8C); elytral primary costae much stouter than the secondary ones in whole length, cells most squared (Fig. 8C); phallus widened at apical part and arcuate at lateral margins, nearly straight at apical margin in dorsal and ventral views (Fig. 9D, E).

The new species is similar to *P. fukiensis* in the body coloration and extremely long lamellae of antennomeres IV–X, but can be distinguished from the latter by the following characters: male antennomere III with outer apical angle barely protruding laterally (Fig. 8C), while strongly protruding laterally in *P. fukiensis* (Fig. 2C); phallus nearly straight at apical margin (Fig. 9D, E), while moderately projected distad in *P. fukiensis* (Fig. 3D, E); phallus with distance between the latero-apical thorns barely greater than maximal width of trunk (Fig. 9D, E), while barely smaller in *P. fukiensis* (Fig. 3D, E).

Description. Male (Fig. 8C). Body slender, black to dark brown, pronotum red, with a black patch in the middle of disc, elytra red.

Head dorsally flat, antennae reaching apical 1/5 length of elytra when inclined, antennomere I nearly globular, III long-triangular, 1.6× as long as wide, with outer apical angle barely protruding laterally, lamellae of IV–X abruptly extended laterally and nearly parallel-sided along the whole length, 2.9–7.0× longer than the corresponding antennomere itself, XI nearly parallel-sided and 11.0× as long as wide.

Pronotum nearly trapezoidal, flat, and barely wider than long, with rounded anterior angles and acute posterior angles, anterior margin arched, lateral margins nearly straight and posterior margin bisinuate. Scutellum barely narrowed posteriorly and obviously emarginate at apex.

Elytra barely widened posteriorly, primary costae stouter than secondary ones, and primary costae II and III stouter than others in whole length of elytra, most cells squared to rectangular.

Aedeagus: phallus stout, 2.8× as long as wide, moderately widened at apical part and arcuate at lateral margins, nearly straight at apical margin in dorsal and ventral views, with sharp latero-apical thorns, between which the distance barely smaller than maximal width of trunk (Fig. 9D, E), almost even in width and weakly bent dorsally, truncate at ventro-apical 1/5 in lateral view (Fig. 9F).

Female. Unknown.

Distribution (Fig. 1). China (Anhui, Zhejiang).

Etymology. The specific name is derived from the Latin *truncatus* (cut off), referring to its phallus nearly straight at apical margin.

***Ponyalis quadricollis* (Kiesenwetter, 1874)**

Figs 1, 9G–I, 10A

Celetes quadricollis Kiesenwetter, 1874: 252.

Eros militans Kiesenwetter, 1874: 253. Synonymized by Lewis 1879: 16.

Lyponia quadricollis: Gorham 1883: 404; Bocak 1999: 99: figs 46, 91, 92.

Ponyalis quadricollis: Kazantsev 2002: 199; Li et al. 2015a: 17.

Material examined. JAPAN: 1♂ (IZAS), Japan, Kyoto, 30.V.1932, leg. S. Yie.

Differential diagnosis. This species can be differentiated from all other *Ponyalis* by the combination of the following characters: pronotum uniformly black, elytra red (Fig. 10A); male antennomere I flattened dorsally, III long-triangular, IV and V wide-triangular, lamellae of VI–X nearly parallel-sided along the whole length, lamella of VI longer, 1.8× longer than joint itself (Fig. 10A); elytral primary costae barely stouter than the secondary ones, cells transverse (Fig. 10A); phallus widened at middle part, moderately projected distad at apical margin and arched at apex in dorsal and ventral views (Fig. 9G, H).

Descriptive notes. Male (Fig. 10A). Antennae reaching apical 1/5 length of elytra when inclined, antennomere I flattened dorsally, III long-triangular, 1.2× as long as wide, IV and V widely triangular, approximately as long as wide, with outer apical angles strongly protruding laterally, lamellae of VI–X nearly paral-



Figure 9. Aedeagi of *Ponyalis dabiieshanensis* sp. nov. (A–C); *P. truncata* sp. nov. (D–F); *P. quadricollis* (Kiesenwetter, 1874) (G–I); *P. quadricollimima* sp. nov. (J–L). A, D, G, J ventral views B, E, H, K dorsal views C, F, I, L lateral views. Scale bars: 0.5 mm.

lel-sided along the whole length, 2.0–3.4× longer than the corresponding antennomere itself, XI nearly parallel-sided and 5.1× as long as wide.

Aedeagus: phallus slender and 2.5× as long as wide, moderately widened at middle part and arcuate at lateral margins, moderately projected distad at apical margin and arched at apex, with acute latero-apical angles, between which the distance barely smaller than maximal width of trunk (Fig. 9G, H), weakly bent dorsally and tapered distad in lateral view (Fig. 9I).

Distribution (Fig. 1). Japan.

Remarks. Bocak (1999) provided male antennae and aedeagus illustrations for this species, and we present the male habitus for the first time.

***Ponyalis quadricollimima* Y. Yang, Fang & Liu, sp. nov.**

<https://zoobank.org/C0794C56-8095-487F-8C66-B52C7C97CD40>

Figs 1, 9J–L, 10B

Type material. Holotype: ♂ (MHBU), CHINA, Chongqing, Wuxi, Shuangyang, Yingtiaoling Natural Reserve, Linkouzi, 1224 m, 22.VI.2022, leg. L. Y. Wang.

Differential diagnosis. The new species can be separated from all other *Ponyalis* by the combination of the following characters: pronotum uniformly black, elytral red (Fig. 10B); male antennomere I flattened dorsally, III and IV long-triangular, lamellae of V–X nearly parallel-sided along the whole length, lamella of VI longer, 1.8× longer than joint itself (Fig. 10B); primary costae much stouter than the secondary ones, cells most squared (Fig. 10B); phallus projected distad at apical margin and arched at apex in dorsal and ventral views (Fig. 9J, K).

It is most close to *P. quadricollis* in general appearance, but can be distinguished from the latter by the following characters: primary costae strongly stouter than secondary ones (Fig. 10B), while barely stouter in *P. quadricollis* (Fig. 10A); phallus barely widened at basal part in dorsal and ventral views (Fig. 9J, K), while moderately widened at middle part in *P. quadricollis* (Fig. 9G, H); phallus with distance between the latero-apical thorns barely greater than maximal width of trunk (Fig. 9J, K), while barely smaller in *P. quadricollis* (Fig. 9G, H).

Description. Male (Fig. 10B). Body slender, black to dark brown, pronotum dark-brown, elytra red.

Head dorsally flat, antennae reaching apical 1/5 length of elytra when inclined, antennomere I flattened dorsally, III and IV long-triangular, 1.4–1.5× as long as wide, lamellae of V–X nearly parallel-sided along the whole length, 1.5–2.8× longer than the corresponding antennomere itself, XI fusiform and 5.5× as long as wide.

Pronotum trapezoidal, with rounded anterior angles and rectangular posterior angles, anterior margin arched, lateral margins sinuate and posterior margin nearly straight. Scutellum barely narrowed posteriorly and obviously emarginate at apex.

Elytra parallel-sided, all primary costae stouter than secondary ones, and primary costae I and IV stouter than others in whole length of elytra, most cells rectangular.

Aedeagus: phallus stout, 3.0× as long as wide, hardly widened at basal part, moderately projected distad at apical margin and arched at apex in dorsal and ventral views, with acute latero-apical angles, between which the distance barely greater than maximal width of trunk (Fig. 9J, K), almost even in width and nearly straight, truncate at ventro-apical 1/4 in lateral view (Fig. 9L).

Female. Unknown.

Distribution (Fig. 1). China (Chongqing).

Etymology. The name of the species is derived from the Latin *minus* (imitator), referring to its similarity to *P. quadricollis*.

***Ponyalis longicornis* Y. Yang, Liu & X. Yang, sp. nov.**

<https://zoobank.org/C4B5D587-A4DD-48FB-9CC5-14650BCFB7B9>

Figs 1, 10C, 11A–C

Type material. Holotype: ♂ (MHBU), CHINA, Sichuan, Emeishan, Baoguoshi, 902 m, 29. V. 2010, leg. Q. Yuan & S. Xian.

Differential diagnosis. The new species can be differentiated from the remaining *Ponyalis* species by the combination of the following characters: pronotum black, with red margins, elytra red (Fig. 10C); male antennomere I nearly globular, III long-triangular, lamellae of IV–X nearly parallel-sided along the whole length, lamella of IX 2.5× as long as joint itself (Fig. 10C); elytral primary costae much stouter than the secondary ones, cells most squared (Fig. 10C); phallus widened at middle part, moderately projected distad at apical margin and narrowly rounded at apex in dorsal and ventral views (Fig. 11A, B).

It seems similar to *P. sichuanensis* (Bocak, 1999) on basis of the general appearance, but can be easily distinguished from the latter by the following characters: lamellae of male antennomere IX 2.0× as long as joint itself (Fig. 10C), while 1.5× in *P. sichuanensis*; pronotum with a black patch extending to posterior margin (Fig. 10C), while never reaching in *P. sichuanensis*; phallus arched at apical margin (Fig. 11A, B), while nearly straight in *P. sichuanensis* (Bocak 1999: fig. 73).

Description. Male (Fig. 10C). Body slender, black to dark brown, pronotum pale brown, with a black patch in middle of disc, which extending to posterior margin, elytra red, tibiae paler at bases.

Head dorsally flat, antennae reaching apical 1/5 length of elytra when inclined, antennomere I nearly globular, III long-triangular, 1.3× as long as wide, lamellae of IV–X nearly parallel-sided along the whole length, 2.0–3.6× longer than the corresponding antennomere itself, XI parallel-sided and 6.5× as long as wide.

Pronotum nearly trapezoidal, flat, and barely wider than long, with rounded anterior angles and rectangular posterior angles, anterior margin barely arched, lateral margins nearly straight and posterior margin nearly straight. Scutellum barely narrowed posteriorly and obviously emarginate at apex.

Elytra parallel-sided, primary costae stouter than secondary ones, and primary costae II and IV stouter than others in whole length of elytra, most cells irregular.

Aedeagus: phallus stout, 3.1× as long as wide, moderately widened at middle part and arcuate at lateral margins, moderately projected distad at apical margin and narrowly rounded at apex in dorsal and ventral views, with acute latero-apical angles, between which the distance barely smaller than maximal width of trunk (Fig. 11A, B), almost even in width and weakly bent dorsally, truncate at ventro-apical 1/5 in lateral view (Fig. 11C).

Female. Unknown.

Distribution (Fig. 1). China (Sichuan).

Etymology. The specific name is derived from the Latin *longus* (long) and *cornus* (horn), referring to its long antennae.

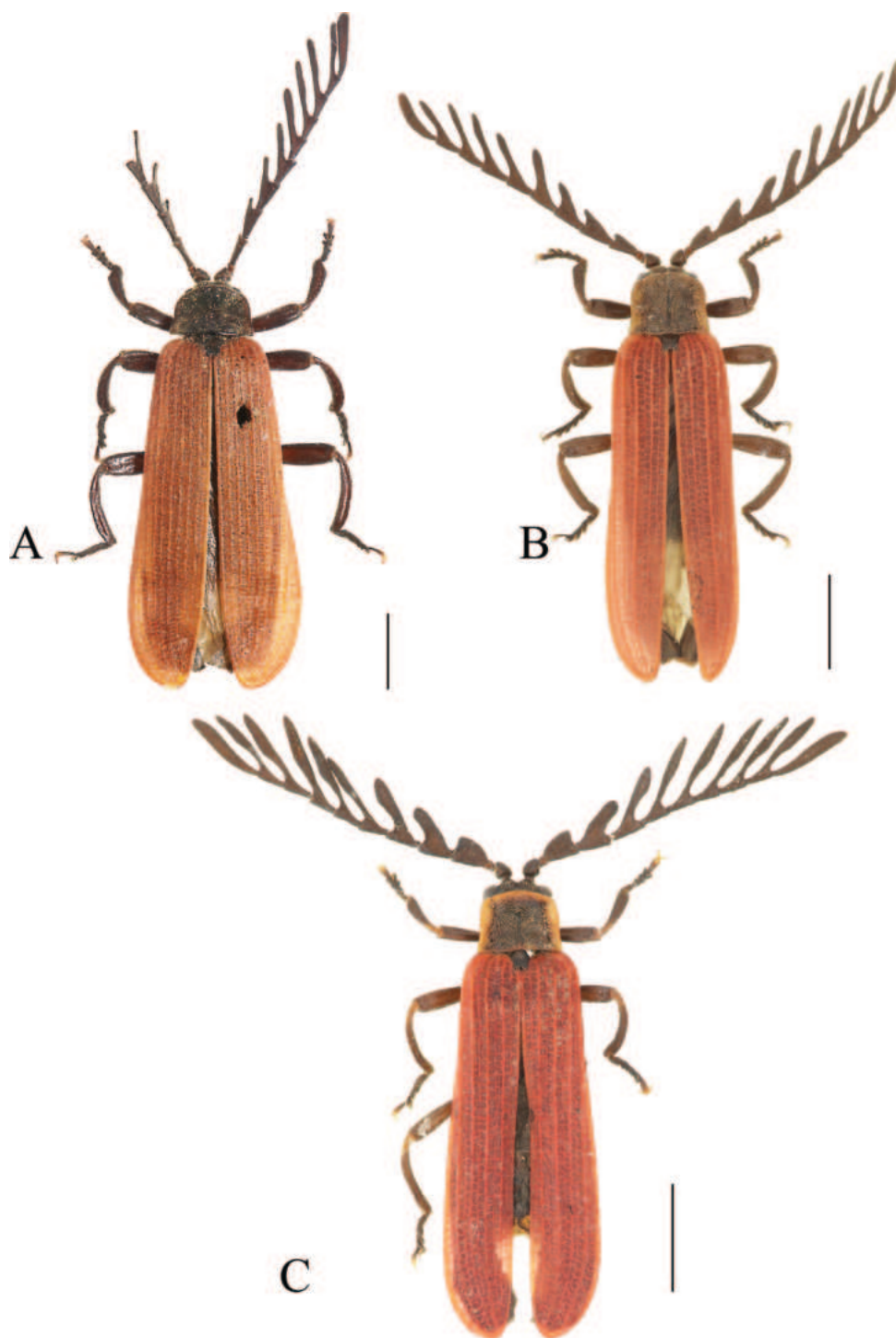


Figure 10. Habitus, dorsal view: *Ponyalis quadricollis* (Kiesenwetter, 1874) (A); *P. quadricollimima* sp. nov. (B); *P. longicornis* sp. nov. (C). A–C males. Scale bars: 2.0 mm.

***Ponyalis zhejiangensis* Y. Yang, Fang & Liu, sp. nov.**

<https://zoobank.org/5A418042-9D95-4DFB-8C75-F552AD1A03F1>

Figs 1, 11D–F, 12A, B

Type material. *Holotype*: ♂ (MHBU), CHINA, Zhejiang, Longquan, Fenyangshan, 1250 m, 17.V.2007, leg. B. F. Zhou & L. Wang. *Paratype*: 1 ♀ (MHBU), same locality as holotype, 1500 m, 15.V.2007, leg. J. H. Xu & L. Q. Liu.

Differential diagnosis. This new species can be separated from all other *Ponyalis* by the combination of the following characters: pronotum black, with red margins, elytra red (Fig. 12A, B); male antennomere I nearly globular, III long-triangular, lamellae of IV–X nearly parallel-sided along the whole length (Fig. 12A); elytra 5.5× longer than pronotum, primary costae barely stouter than the secondary ones only basally, cells transverse (Fig. 12A, B); phallus widened at basal part and narrowly rounded at apex in dorsal and ventral views (Fig. 11D, E).

It looks similar to *P. gracilis* in the coloration, but differs in the following characters: anterior margin of pronotum arched (Fig. 12A), while nearly straight in *P. gracilis* (Fig. 4D); phallus arcuate at lateral margins in dorsal and ventral views (Fig. 11D, E), while bisinuate in *P. gracilis* (Fig. 3J, K); phallus with distance between the latero-apical thorns much smaller than maximal width of trunk (Fig. 11D, E), while barely smaller in *P. gracilis* (Fig. 3J, K).

Description. Male (Fig. 12A). Body stout, black, pronotum cinnabar red, with a black patch in middle of disc, which extending to both anterior and posterior margins, elytra red.

Head dorsally flat, antennae reaching elytral mid-length when inclined, antennomere I flattened dorsally, III long-triangular, 1.3× as long as wide, lamellae of IV–X nearly parallel-sided along the whole length, 1.7–4.7× longer than the corresponding antennomere itself, XI parallel-sided and 6.7× as long as wide.

Pronotum trapezoidal, flat, and wider than long, with rounded anterior angles and acute posterior angles, anterior margin arched, lateral margins nearly straight and posterior margin weakly bisinuate. Scutellum narrowed posteriorly and obviously emarginate at apex.

Elytra barely widened posteriorly, primary costae barely stouter than secondary ones only at the humeral part, cells squared to transverse.

Aedeagus: phallus stout, 3.3× as long as wide, moderately widened at basal part and arcuate at lateral margins, moderately projected distad at apical margin and narrowly rounded at apex in dorsal and ventral views, with acute latero-apical angles, between which the distance much smaller than maximal width of trunk (Fig. 11D, E), weakly bent dorsally and tapered distad in lateral view (Fig. 11F).

Female (Fig. 12B). Similar to male, but body stouter, antennae reaching basal 1/3 length of elytra when inclined, antennomeres III–V all nearly triangular, lamellae of VI–X 1.1–1.5× longer than the corresponding antennomere itself, pronotum with black patch never extending to anterior or posterior margin.

Distribution (Fig. 1). China (Zhejiang).

Etymology. The name of the species is derived from the name of the type locality, Zhejiang Province, China.

***Ponyalis hainanensis* Y. Yang, Liu & X. Yang, sp. nov.**

<https://zoobank.org/55E7F4A5-01DE-4E0E-8758-5931A0EDB583>

Figs 1, 11G–I, 12C, D

Type material. Holotype: ♂ (IZAS), CHINA, Hainan, Jianfeng, 21.V.1980, leg. F. J. Pu. **Paratype:** 1 ♀ (IZAS), same data as the holotype.

Differential diagnosis. This new species can be readily identified from all other *Ponyalis* by the combination of the following characters: pronotum uniformly black, elytra red (Fig. 12C, D); male antennomere I flattened dorsally, III and IV



Figure 11. Aedeagi of *Ponyalis longicornis* sp. nov. (A–C); *P. zhejiangensis* sp. nov. (D–F); *hainanensis* sp. nov. (G–I). A, D, G ventral views B, E, H dorsal views C, F, I lateral views. Scale bars: 0.5 mm.

long-triangular, lamella of VI longer, 1.8× longer than joint itself (Fig. 12C); elytral primary costae much stouter than the secondary ones, cells transverse (Fig. 12C, D); phallus widened near middle and sinuate at lateral margins, projected distad and narrowly rounded at apical margin in dorsal and ventral views (Fig. 11G, H).

It looks like *P. klapperichi* in the general appearance, but can be distinguished from the latter by the following characters: male pronotum broad (0.7× longer than wider) (Fig. 12C), while slender in *P. klapperichi* (0.9–1.0× longer than wider) (Fig. 6A); lamella of antennomere VII 2.3× longer than joint itself (Fig. 12C),

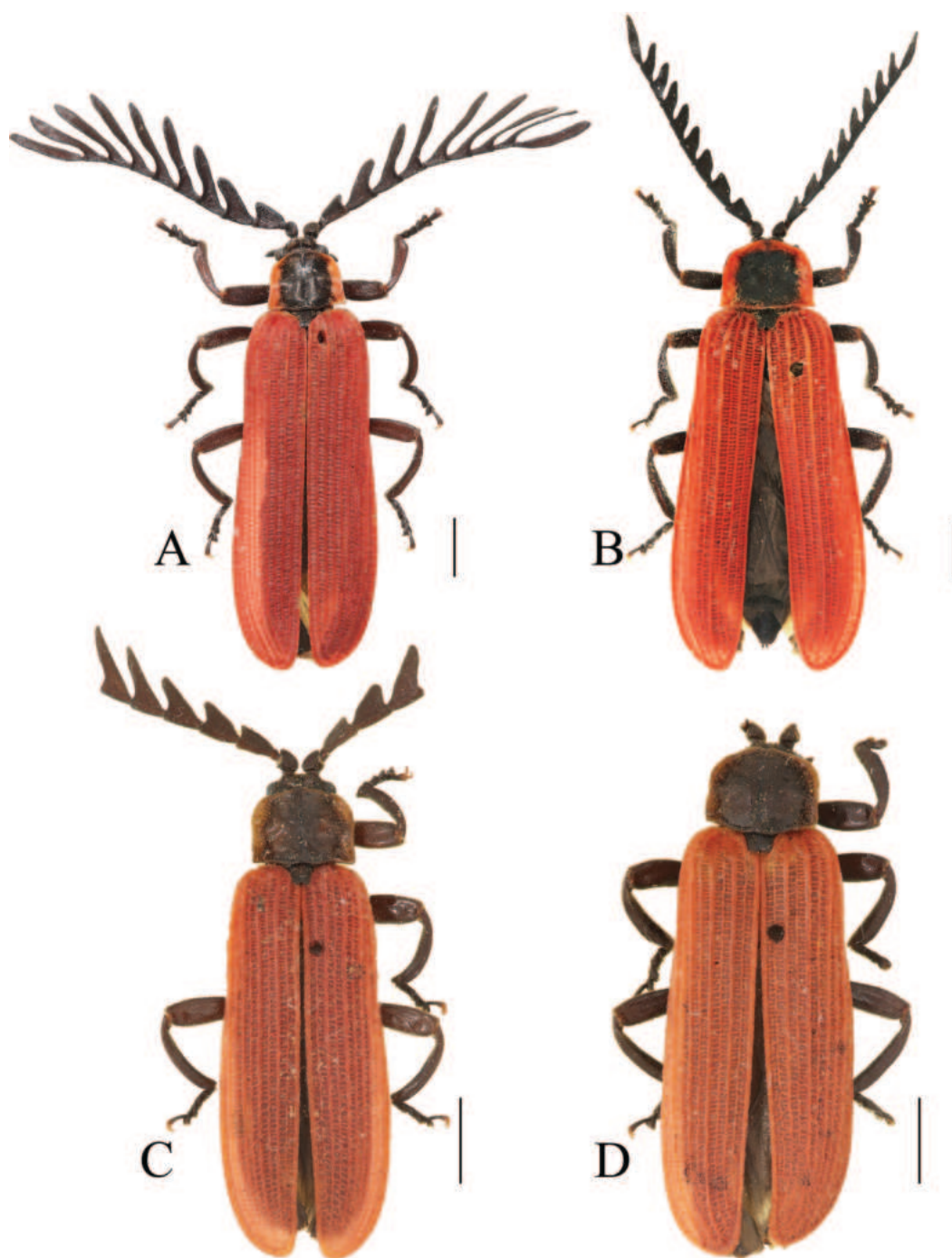


Figure 12. Habitus, dorsal view: *Ponyalis zhejiangensis* sp. nov. (A, B); *P. hainanensis* sp. nov. (C, D). A, C males B, D females. Scale bars: 2.0 mm.

while 3.0× in *P. klapperichi* (Fig. 6A); phallus moderately projected distad at apical margin (Fig. 11G, H), while nearly straight in *P. klapperichi* (Fig. 5A, B).

Description. Male (Fig. 12C). Body stout, black, pronotum dark-brown, elytra cinnabar red.

Head dorsally flat, antennae reaching elytral mid-length when inclined, antennomere I barely flattened dorsally, III–IV long-triangular, 1.3–1.5× as long as wide, lamellae of V–VII extended along whole length of corresponding stem and tapered laterally, 1.5–2.3× longer than the corresponding antennomere itself.

Pronotum trapezoidal, flat, and barely wider than long, with rounded anterior angles and rectangular posterior angles, anterior margin arched, lateral margins weakly sinuate and posterior margin bisinuate. Scutellum barely narrowed posteriorly and obviously emarginate at apex.

Elytra barely widened posteriorly, primary costae stouter than secondary ones, primary costae II, III and IV stouter than others in whole length of elytra, most cells rectangular.

Aedeagus: phallus stout, 2.1× as long as wide, abruptly widened at middle and sinuate at lateral margins, moderately projected distad at apical margin and narrowly rounded at apex in dorsal and ventral views, with acute latero-apical angles, between which the distance much smaller than maximal width of trunk (Fig. 11G, H), almost even in width and weakly bent dorsally, truncate at ventro-apical 1/4 in lateral view (Fig. 11I); internal sac membranous and expanded, densely covered with minute tubercles and short bristles on surface, abruptly thinned into a thorn-like apex (Fig. 11 G–I).

Female (Fig. 12D). Similar to male, but body stouter.

Distribution (Fig. 1). China (Hainan).

Etymology. The name of the species is derived from the name of the type locality, Hainan Island, China.

Remarks. The left pro- and meso-legs, left VIII–XI and right VI–XI antennomeres of the holotype, and both antennomeres II–XI, left proleg, and the right pro- and mesotarsomeres III–V of the paratype are missing.

Discussion

As the number of species descriptions increases, we have a better understanding of the diversity of *Ponyalis*. With six species newly described, we raised the number of known species to 24. In general (Fig. 1), *Ponyalis* are mainly distributed in China (21 species, accounting for 87.5% of species diversity), and most of them are endemic, except for a few that are distributed to adjacent countries, including Vietnam, Myanmar, Laos, Thailand, and India (3 species, 12.5%), and Korea (1 species, 4.1%), respectively. The remaining three species (12.5%) are restricted to Japan. This distribution pattern is similar to that of *Lyponia* (Fang et al. 2024). As noted by others (Nakane 1969; Bocak 1999), there is a high turnover of Lyponiini in species composition amongst mountain ranges in China and between continental Asia and adjacent islands (including Taiwan and Japan). The tribe was inferred to have originated from continental Asia, and the species in adjacent islands were established separately by multiple vicariance or short distance dispersal events (Li et al. 2015b; Masek et al. 2018). Meanwhile, most of the *Ponyalis* species are narrowly distributed (Fig. 1), and limited ranges also have often been documented in other net-winged beetles, which have been ascribed to their low dispersal propensity (e.g., Bocak and Yagi 2010; Malohlava and Bocak 2010; Sklenarova et al. 2013). The present result is congruent with the opinion of Li et al. (2015b) that allopatric speciation is proposed as the predominant mechanism of speciation of *Ponyalis*.

Furthermore, based on the examination and comparison results of more material, we have a better understanding of the morphology of *Ponyalis*. The internal sac of male genitalia is usually invaginated in the phallus and exposed only

apically, making it difficult to be well prepared and retracted for examination. Luckily, we have almost seen the overall structure of internal sac of *P. hainanensis* sp. nov. Our examination shows that the internal sac (Fig. 11G–I) is membranous and densely covered with minute tubercles and short bristles on surface, and it is overall expanded, but abruptly thinned at apex. The apex is a slender or thorn-shaped tube, and either long and evidently exposed (e.g., Figs 3D–F, J–L, 5A–C, G–L) or short even hardly visible (e.g., Figs 3A–C, G–I, 5D–F, 9, 11). However, this is inconsistent with the opinion of Li et al. (2015a), who argued that the apical length of internal sac is a differential diagnosis between *Ponyalis* and *Lyponia* (*Poniella*) Kazantsev, 2002. These have nearly identical shapes of the aedeagus (Li et al. 2015a), but their separation was well supported by the molecular phylogenetic analysis (Li et al. 2015b), also by some morphological differences found in the antennae, elytral costae, and coxite (Kazantsev 2002). This suggests that we should consider and integrate the characters comprehensively, and not base taxonomic decisions on a single character.

Moreover, Li et al. (2015b) noted that the females do not have any diagnostic characters of either the genitalia or antennae, but we found that they are indeed present with some differences in the details of their antennal shapes (e.g., Figs 2B, D, 4B, C, 6B, 7B, D, 8B, 12B). Of course, this requires the material of both sexes available for us to recognize the species comprehensively. Within *Ponyalis*, although the appearance is sometimes variable, such as *P. himalejica* and *P. laticornis*, its antennal shape and aedeagus are relatively conserved and dependable, which are mainly applied in the following identification key to the species.

Acknowledgments

We are grateful to Prof. Xingyue Liu (CAU), Prof. Zhisheng Zhang (Southwest China University, Chongqing, China) and Dr Jie Fang (Anhui University, Hefei, China) for providing some material to us. Thanks are also given to the editor Dr Vinicius S. Ferreira, Dr. Sergey V. Kazantsev (Moscow, Russia), and another anonymous reviewer for their comments which improved the original manuscript, and to Dr Christopher Glasby for his help in polishing our language.

Additional information

Conflict of interest

The authors have declared that no competing interests exist.

Ethical statement

No ethical statement was reported.

Funding

This study is financially supported by the National Natural Science Foundation of China (Nos 32270491, 31772507), the Natural Science Foundation of Hebei Province (No. C2022201005) and the Interdisciplinary Research Program of Natural Science of Hebei University (No. DXK202103), as well as the Fund on survey of spiders and insects from Yintiaoling Nature Reserve.

Author contributions

Conceptualization, CF, YXY, XKY, HYL. Data curation: CF, YXY. Formal analysis: CF, YXY. Methodology: CF, YXY. Investigation: CF, YXY, HYL. Visualization: CF. Supervision: YXY, XKY, HYL. Writing—original draft preparation: CF, YXY. Writing—review and editing: CF, YXY, XKY, HYL. All authors have read and agreed to the published version of the manuscript.

Author ORCIDs

Chen Fang  <https://orcid.org/0009-0005-0483-8446>

Yuxia Yang  <https://orcid.org/0000-0002-3118-6659>

Xingke Yang  <https://orcid.org/0000-0003-3676-6828>

Haoyu Liu  <https://orcid.org/0000-0003-1383-5560>

Data availability

All of the data that support the findings of this study are available in the main text.

References

- Bocak L (1999) A revision and phylogenetic analysis of the genus *Lyponia* C. O. Waterhouse, 1878 (Coleoptera, Lycidae). *Entomologica Basiliensia* 21: 59–103.
- Bocak L, Bocakova M (1990) Revision of the supergeneric classification of the family Lycidae (Coleoptera). *Polskie Pismo Entomologiczne* 59: 623–676.
- Bocak L, Bocakova M (2008) Phylogeny and classification of the family Lycidae (Insecta: Coleoptera). *Annales Zoologici* 58(4): 695–720. <https://doi.org/10.3161/000345408X396639>
- Bocak L, Yagi T (2010) Evolution of mimicry patterns in *Metriorrhynchus* (Coleoptera: Lycidae): the history of dispersal and speciation in South East Asia. *Evolution; International Journal of Organic Evolution* 64(1): 39–52. <https://doi.org/10.1111/j.1558-5646.2009.00812.x>
- Bocakova M, Bocak L (2007) Lycidae. In: Löbl I, Smetana A (Eds) *Catalogue of Palaearctic Coleoptera*, Vol. 4. Apollo Books, Stenstrup, 211–224.
- Bourgeois J (1885) Diagnoses de Lycides nouveaux ou peu connus. 5e partie. *Annales de la Societe Entomologique de France* 5: 71–84.
- Fang C, Yang Y, Yang X, Liu H (2024) A phylogenetic morphometric investigation of interspecific relationships of *Lyponia* s. str. (Coleoptera, Lycidae) based on male genitalia shapes. *Insects* 15(1): 11. <https://doi.org/10.3390/insects15010011>
- Gorham HS (1883) Revision of the genera and species of Malacoderm Coleoptera of the Japanese fauna. Part I. - Lycidae, Lampyridae. *Transactions of the Royal Entomological Society of London* 31: 393–411. <https://doi.org/10.1111/j.1365-2311.1883.tb02955.x>
- Gorham HS (1890) Notes on the species of the families Lycidae and Lampyridae, contained in the Imperial Museum of Calcutta, with descriptions of new species, and a list of the species at present described from India. *Transactions of the Royal Entomological Society of London* 38: 543. <https://doi.org/10.1111/j.1365-2311.1890.tb02707.x>
- Kazantsev SV (2002) Supplementary notes to the revision of the genus *Lyponia* Waterhouse, 1878 (Coleoptera, Lycidae) with description of new taxa. *Russian Entomological Journal* 11(2): 197–206.
- Kazantsev SV (2005) Morphology of Lycidae with some considerations on evolution of the Coleoptera. *Elytron* 2005(17): 49–226.

- Kiesenwetter EA (1874) Die Malacodermes Japans nach dem Ergebnisse der Sammlungen des Herrn G. Lewis während der Jahre 1869–1871. Berliner Entomologische Zeitschrift 18: 241–288. <https://doi.org/10.1002/mmnd.18740180302>
- Kleine R (1924) Die Gattung *Lyponia* Waterhouse. Entomologische Blaetter 20: 170–175.
- Kleine R (1939) Entomological results from the Swedish expedition 1934 to Burma and British India. Coleoptera: Brenthidae und Lycidae, gesammelt von Herrn Rene Malaise. Arkiv för Zoologi 31: 1–23.
- Kusy D, Motyka M, Bocak M, Masek M, Bocak L (2019) Phylogenomic analysis resolves the relationships among net-winged beetles (Coleoptera: Lycidae) and reveals the parallel evolution of morphological traits. Systematic Entomology 44(4): 911–925. <https://doi.org/10.1111/syen.12363>
- Lewis G (1879) A catalogue of Coleoptera from the Japanese archipelago. Taylor and Francis, London, 31 pp.
- Li Y, Pang H, Bocak L (2015a) Description of New Species of Lyponiini from China (Coleoptera: Lycidae). Annales Zoologici 65(1): 9–19. <https://doi.org/10.3161/00034541ANZ2015.65.1.002>
- Li Y, Gunter N, Pang H, Bocak L (2015b) DNA-based species delimitation separates highly divergent populations within morphologically coherent clades of poorly dispersing beetles: Species delimitation in Chinese Lycidae. Zoological Journal of the Linnean Society 175(1): 59–72. <https://doi.org/10.1111/zoj.12262>
- Malohlava V, Bocak L (2010) Evidence of extreme habitat stability in a Southeast Asian biodiversity hotspot based on the evolutionary analysis of neotenic net-winged beetles. Molecular Ecology 19(21): 4800–4811. <https://doi.org/10.1111/j.1365-294X.2010.04850.x>
- Masek M, Motyka M, Kusy D, Bocek M, Li Y, Bocak L (2018) Molecular phylogeny, diversity and zoogeography of net-winged beetles. Insects 9(4): 154. <https://doi.org/10.3390/insects9040154>
- Nakane T (1961) The lycid beetles from the Loochoo islands, with descriptions of a few new forms (Coleoptera). Entomological Review of Japan 13: 11–15.
- Nakane T (1969) Lycidae (Insecta: Coleoptera). Fauna Japonica. Tokyo: Academic Press of Japan, 224 pp.
- Pic M (1912) Notes sur certains genres litigieux ou peu connus. Mélanges exotico-entomologique 3: 1–3. <https://doi.org/10.5962/bhl.title.52304>
- Pic M (1922) Contribution à l'étude des Lycides. L'Échange. Revue Linnéenne 38: 13–28.
- Pic M (1923) Etude des Malacodermes de l'Indochine recueillis par M. R. Vitalis de Salvaza. Faune Entomologique de l'Indochine Française 1: 7–24.
- Pic M (1926) Sur le genre *Lyponia* Wat. (Col. Lycidae). Bulletin Mensuel de la Société Linnéenne de Lyon 5: 70.
- Pic M (1927) Coléoptères de Indochine. Mélanges exotico-entomologique 49: 1–36.
- Pic M (1938) Nouveaux Coléoptères du Siam. Bulletin de la Société Zoologique de France 20: 352–356.
- Pic M (1939) Malacodermes exotiques. L'Échange. Revue Linnéenne 55: 165–172.
- Sklenarova K, Chesters D, Bocak L (2013) Phylogeography of poorly dispersing net-winged beetles: A role of drifting India in the origin of Afrotropical and Oriental fauna. PLoS ONE 8(6): e67957. <https://doi.org/10.1371/journal.pone.0067957>
- Waterhouse CO (1878) On the different forms occurring in the Coleopterous family Lycidae, with descriptions of new genera and species. Transactions of the Royal Entomological Society of London 26(1): 95–118. <https://doi.org/10.1111/j.1365-2311.1878.tb01944.x>

Ameripathidae, a new family of antipatharian corals (Cnidaria, Anthozoa, Hexacorallia, Antipatharia)

Jeremy Horowitz¹, Dennis M. Opresko¹, Santiago Herrera^{1,2}, Colleen M. Hansel³,
Andrea M. Quattrini¹

¹ Department of Invertebrate Zoology, National Museum of Natural History, Smithsonian Institution, Washington, DC, USA

² Department of Biological Sciences, Lehigh University, Lehigh, PA, USA

³ Department of Marine Chemistry and Geochemistry, Woods Hole Oceanographic Institution, Woods Hole, MA, USA

Corresponding author: Jeremy Horowitz (Jerhorowitz@gmail.com)

Abstract

A new family of antipatharian corals, Ameripathidae (Cnidaria: Anthozoa: Antipatharia), is established for *Ameripathes pseudomyriophylla* Opresko & Horowitz, **gen. et sp. nov.** The new family resembles Myriopathidae and Stylopathidae in terms of the morphology of the polyps and tentacles and the pinnulate branching of the corallum. Phylogenetic analysis using a genomic data set of 741 conserved element loci indicates that the new family is sister to a clade containing the Myriopathidae, Stylopathidae, Antipathidae, and Aphanipathidae.

Key words: Deep sea, fauna of Puerto Rico, genome skimming, mesophotic, molecular phylogenetics, new genus, new species, taxonomy, ultraconserved elements



Academic editor: Bert W. Hoeksema

Received: 21 February 2024

Accepted: 16 April 2024

Published: 31 May 2024

ZooBank: <https://zoobank.org/2DF99255-9469-4D5B-B67F-C64ED9F5419C>

Citation: Horowitz J, Opresko DM, Herrera S, Hansel CM, Quattrini AM (2024) Ameripathidae, a new family of antipatharian corals (Cnidaria, Anthozoa, Hexacorallia, Antipatharia). ZooKeys 1203: 355–375. <https://doi.org/10.3897/zookeys.1203.121411>

Copyright: This is an open access article distributed under the terms of the CC0 Public Domain Dedication.

Introduction

Opresko (1972) re-examined Caribbean antipatharian corals originally described by L.F. de Pourtalès (1880). Among syntypes of *Antipathes picea* Pourtalès, 1880, Opresko found one specimen inconsistent with the species description, having only two rows of primary pinnules instead of four. Opresko provisionally identified this and two additional specimens from the Gulf of Mexico and Lesser Antilles as *Antipathes americana* Duchassaing & Michelotti, 1860 (see Opresko 1972: 975–977); however, the type specimen of *A. americana* was not available for examination at that time. Later, a specimen labeled as a syntype of *A. americana* was discovered in the collections of the Regional Museum of Natural Sciences, Turin, Italy (Registration Number 78). This type specimen was considered to represent a valid species in the genus *Stylopathes* Opresko, 2006, in the family Stylopathidae Opresko, 2006 with a pinnulation pattern very different from the syntype of *A. picea* and the other two specimens provisionally assigned to *A. americana* by Opresko (1972). For example, they were unbranched but distinctly pinnulate with three orders of pinnules, with the primary pinnules in three to four rows along the length of the stem, and with secondary and tertiary pinnules in whorls with \leq four members (see Opresko 2006: fig. 4a). It was concluded that the specimens originally referred to *A. americana* by Opresko (1972) represented

a distinct and undescribed species; however, they could not be assigned to any nominal species known at the time. Although the pinnulation pattern of the species resembled that of species of the genus *Myriopathes* Opresko, 2001, the skeletal spines more closely resembled those of species of the family Stylopathidae.

Recently two samples were collected during an exploratory research cruise to the waters surrounding Puerto Rico conducted onboard the R/V Falkor (too) of the Schmidt Ocean Institute. These specimens matched the morphological characters of the specimens examined by Opresko (1972). We used an integrative approach, combining morphological and genomic data, to recognize these corals as representative of a new species, new genus, and new family.

Materials and methods

Specimen collection and deposition

The specimen was collected 7 km east of Desecheo Island, Puerto Rico, in the Mona Passage, which connects the Atlantic Ocean to the Caribbean Sea, at a depth of 165 m during the Schmidt Ocean Institute expedition FKt230417 entitled: 'Health diagnostics of deep-sea coral' (Fig. 1) onboard the R/V Falkor (too). The colony was imaged with high-resolution video and sampled by cutting a 19 cm section of a branch using a manipulator arm of the ROV SuBastian. The holotype is this subsampled portion of the whole colony. One paratype was collected in the same way 6 km east of Desecheo Island. Both specimens are deposited in the collections of the National Museum of Natural History (NMNH), Smithsonian Institution, Washington DC.

The syntype of *Antipathes picea* was collected by the U.S. Coast Survey Steamer Blake in 1879 and is deposited in the collections of the Museum of Comparative Zoology at Harvard University (specimen registration prefix "MCZ:IZ:"). One of the remaining two paratypes was collected by the U.S. Bureau of Commercial Fisheries R/V Silver Bay in 1957 and the other by the R/V Pillsbury of the University of Miami in 1969, and both are deposited in the collections of the Rosenstiel School of Marine, Atmospheric and Earth Science at the University of Miami (specimen registration prefix "UMML"). The locations where the specimens were collected are indicated in Fig. 1.

Morphological analyses

The skeletal elements of the specimens "new to science" were examined using a Zeiss EVO MA 15 scanning electron microscope (SEM). Before scanning, the specimens were coated with a 30–40 nm thick layer of 60% gold: 40% palladium. SEM stubs are deposited at the NMNH. SEM stub numbers are from a series established by the authors at the NMNH. The microscopic skeletal features were measured directly using a Meiji Techno RZ stereo microscope equipped with an ocular micrometer or from the photographs taken with the SEM. Spine height was measured as the distance from the spine tip to the middle of the base of the spine. Polyp and branch characteristics were measured with a dissecting microscope and terminal branch diameter was measured near the base of the branch. The morphological characters of the specimens were compared with all nominal and currently accepted families.

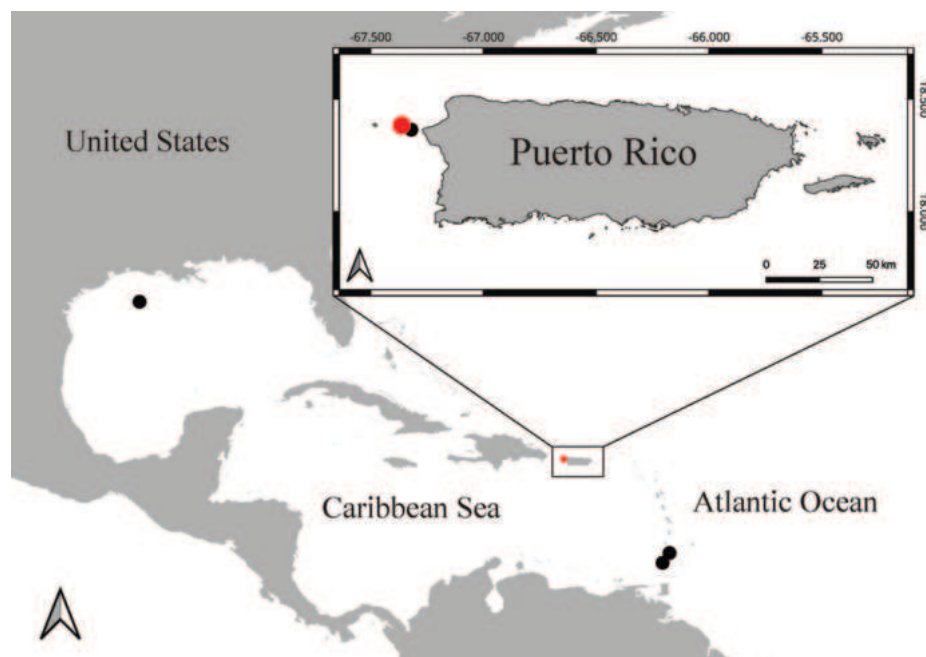


Figure 1. Locations where specimens of *Ameripathes pseudomyriophylla* gen. nov., sp. nov. were collected (red dots indicate the type locality; black dots represent additional sample localities).

Molecular analyses

DNA extractions of the holotype and one paratype were performed using the DNeasy Blood and Tissue Kit (Qiagen, Germany) following the manufacturer's protocol. The DNA was cleaned with a Qiagen Power Clean Pro kit, and concentrations were estimated using a High Sensitivity Qubit 4 Fluorometer (Invitrogen, US). For the new species, DNA was sheared using a QSonica Inc Sonicator Q800R to a target size range of 400–800 bp and then checked via gel electrophoresis on a 1.5% agarose gel. Following shearing, DNA libraries were prepared with the Kappa Hyper Prep protocol using a $\frac{1}{2}$ reaction with iTruSeq adapters and dual indexes following Quattrini et al. (2018). DNA extraction and library preparation were conducted in the Laboratories of Analytical Biology at the NMNH. Paired-end sequencing (150 bp) was performed on an Illumina - NovaSeq X Plus at the Oklahoma Medical Research Foundation Genomics Facility with other samples to obtain 10M paired-end (PE) reads (150 bp) per sample. Raw reads are deposited in the short read archive (SRA) of the National Center for Biotechnology Information (<https://www.ncbi.nlm.nih.gov/>).

Phylogenetic analyses

The conserved loci were bioinformatically obtained from the high-throughput sequencing data. First, raw reads were trimmed using Trimmomatic v. 0.35 (Bolger et al. 2014) and then assembled using Spades v. 3.15 (Prjibelski et al. 2020). Then, UCE and exon loci were extracted using the hexacoral-v2-baitset (Cowman et al. 2020), following the Phyluce pipeline (<https://phyluce.readthedocs.io/en/latest/tutorials/tutorial-1.html>) (Faircloth 2016) with some modifications such as minimum-identity and minimum-coverage thresholds set to 70%. These data were then combined with existing conserved loci extracted from

previous studies. All loci were edge-trimmed and aligned with MAFFT v. 7.130 (Kato and Standley 2013). Then, `phyluce_align_get_only_loci_with_min_taxa` was used to obtain all loci with 50% taxon-occupancy, which were then concatenated using `phyluce_align_concatenate_alignments`. The phylogenomic inference was conducted on the concatenated dataset using maximum likelihood analysis in IQTree v. 2.1 (Minh et al. 2020). A partitioned analysis (Chernomor et al. 2016) was conducted on the dataset using the best model for each locus [-m TESTMERGE (Kalyaanamoorthy et al. 2017)]. Ultrafast bootstrapping [-bb 1000 (Hoang et al. 2018)] and the Sh-like approximate likelihood ratio test [-alrt 1000 (Anisimova et al. 2011)] were also selected. All analyses were run on the Smithsonian's High-Performance Computing Cluster (doi.org/10.25572/SH-PC), except for the phylogeny, which was plotted in FigTree v. 1.4.4.

Taxonomic results

Family Ameripathidae Opresko & Horowitz, fam. nov.

<https://zoobank.org/D9089DA2-C41B-414C-A224-D4DA55B133C7>

Diagnosis. Corallum branched and pinnulate; flabellate. Primary pinnules arranged bilaterally and alternately, secondary pinnules arranged uniseriately. Spines up to 0.06 mm tall, conical, slightly compressed laterally with rounded apex, smooth or with knob-like protuberances. Polyps slightly transversely elongate up to 1.2 mm in transverse diameter, subequal tentacles, sagittals positioned lower than laterals, and a raised oral cone.

Remarks. Examination of SEM images of the spines of the new family revealed that most spines are triangular and smooth with un-ornamented surfaces with a small number of polypar spines possessing a few small, rounded, low-relief, knob-like protuberances (Fig. 2A). Also, the rows become much less regular; however, the number of rows per view, and the density of spines in each row do not differ substantially from that on the pinnules (Fig. 6D–G). These spine characteristics differ from other families, for example: Antipathidae Ehrenberg, 1834 has spines that are either perfectly smooth (Fig. 2B) or are papillose with or without apical bifurcations or multiple knobs (Fig. 2C). Aphanipathidae Opresko, 2004 typically has spines with distinct tubercles (Fig. 2D). Stylopathidae Opresko, 2006 has spines that are small, conical, smooth-surfaced, and distally directed (Fig. 2E). Myriopathidae Opresko, 2001 has blade-like spines, often with very small, elongated papillae or fine striations (Fig. 2F), and in which the spines increased in density on the larger branches and stem. Cladopathidae Kinoshita, 1910 has spines that are smooth, triangular, or conical, and often distally directed (Fig. 2G). Schizopathidae Brook, 1889 has spines that are simple or multi-lobed, smooth, and conical or triangular (Fig. 2H). Leiopathidae Haime, 1849 has small spines that are simple or multi-lobed, smooth and are triangular, conical, or blister-shaped (Fig. 2I); often poorly developed or absent on older parts of the corallum (Molodtsova 2011).

Examination of in situ images of the polyps of the new family revealed a slightly transversely elongated external morphology (Fig. 3A). The tentacles are subequal in length, cylindrical with rounded tips and are relatively short, being no more than 1.5× the transverse diameter of the polyp. The number of mesenteries in the polyps of the Ameripathidae has not yet been determined.

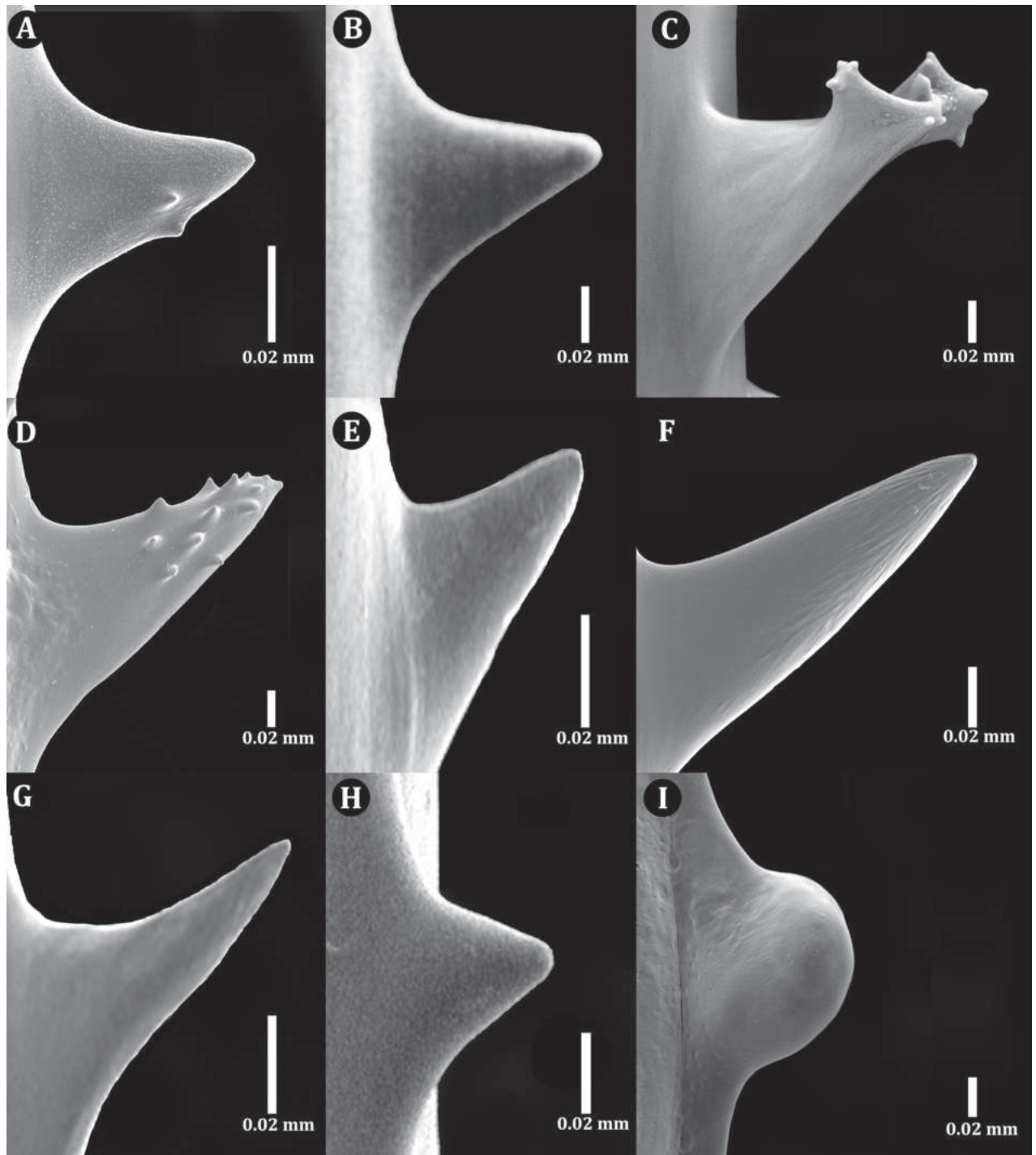


Figure 2. Skeletal spines of antipatharian families **A** Ameripathidae (*Ameripathes pseudomyriophylla* gen. et sp. nov.) **B** Antipathidae (*Antipathes furcata* Gray, 1857) **C** Antipathidae (*Antipathes falkorae* Horowitz, 2022) **D** Aphanipathidae (*Aphanipathes sarothamnoides* Brook, 1889) **E** Stylopathidae (*Stylopathes litocrada* Opresko, 2006) **F** Myriopathidae (*Myriopathes* cf. *japonica* (Brook, 1889)) **G** Cladopathidae (*Cladopathes plumosa* Brook, 1889) **H** Schizopathidae (*Schizopathes affinis* Brook, 1889) **I** Leiopathidae (*Leiopathes* sp. of Hamie 1849).

The new family has polyps like Myriopathidae (Fig. 3B); except in Myriopathidae, polyps are more circular in shape with tentacles equally distributed and positioned around the polyp mouth. The new family also has polyps like Stylopathidae (Fig. 3C, D); except polyps are not as transversely elongated as the new family. The remaining families have different polyp characteristics:



Figure 3. Polyps of live corals representing different antipatharian families **A** Ameripathidae (*Ameripathes pseudo-myriophylla* gen. et sp. nov.) **B** Myriopathidae (*Myriopathes* sp.) **C** Stylopathidae (*Stylopathes* sp.) **D** Stylopathidae (*Stylopathes* sp.) **E** Antipathidae (*Antipathes atlantica* Gray, 1857) **F** Aphanipathidae (*Anozopathes* sp. Opresko & Bo, 2021) **G** Schizopathidae (*Bathypathes* sp.) **H** Cladopathidae (*Heteropathes* sp.) **I** Leiopathidae (*Leiopathes* sp.). Photo credits: **A, C, D** (Schmidt Ocean Institute); **B** (M. Bo); **E** (S. Weinberg); **F, G, H** (NOAA/OER; **I** (P. Etnoyer).

The polyps of the Antipathidae (Fig. 3E) and Aphanipathidae (Fig. 3F) tend to be as long as wide (sometimes transversely compressed), and with expanded tentacles $\leq 3\times$ the transverse diameter of the polyps and tentacles are not subequal in length. The polyps of Schizopathidae (Fig. 3G) and Cladopathidae (Fig. 3H) are more transversely elongated than the new family. Leiopathidae polyps are transversely compressed (Fig. 3I).

Comparative diagnosis Antipathidae differs in corallum pattern with an unpinnulated corallum compared to the pinnulated corallum in the new family. Cladopathidae differs in polyp size and spine ornamentation, with polyps measuring at least 1.8–2.0 mm compared to up to 1.2 mm in transverse diameter in the new family and possessing smooth spines rather than ones with knob-like protuberances. Leiopathidae differs in corallum pattern, possessing an unpinnulated corallum compared to a pinnulated corallum in the new family. Aphanipathidae differs in spine height, spine ornamentation type, and polyp characteristics, possessing spines up to 0.5 mm tall, distinct tubercles on the surfaces of skeletal spines, and polyps that are as long as they are wide or can be transversely compressed, respectively, compared to spine heights 0.06 mm tall, low-relief, knob-like protuberances on the surfaces of skeletal spines, and slightly transversely elongate polyps with short, subequal tentacles with blunt, rounded tips in the new family. Myriopathidae differs in spine ornamentation type with striations on the surfaces of skeletal spines compared to the spines with a few small, rounded, low-relief, knob-like protuberances in the new family. Stylopathidae differs in subpinnule arrangement and spine surface ornamentation, presenting verticils or irregularly bilateral and smooth spines, respectively, compared to uniserially arranged subpinnules and spines with low-relief, knob-like protuberances spines in the new family. Schizopathidae differs in polyp size and spine ornamentation, having larger polyps (2–12 mm in transverse diameter) and smooth spines, respectively, compared to smaller polyps (up to 1.2 mm in transverse diameter) and spines with knob-like protuberances in the new family.

The recognition of the new family is further supported by the phylogenetic analysis (see further below) conducted on the holotype and one paratype showing that Ameripathidae is a distinct lineage sister to the Antipathidae + Aphanipathidae + Myriopathidae + Stylopathidae, representing a novel deep divergence in the order Antipatharia (Fig. 4).

Genus *Ameripathes* Opresko & Horowitz, gen. nov.

<https://zoobank.org/18F1C58B-E0CE-462A-A160-4497CCC150BF>

Type species. *Ameripathes pseudomyriophylla* sp. nov. (see below).

Diagnosis. Corallum sparsely branched, generally in one plane to the seventh order or more. Stem and branches consistently pinnulated to the second order and very rarely to the third order on older sections of the corallum, in some specimens. Primary pinnules 1–2 cm in length, thin; < 0.1 mm in diameter at their midsection. Primary pinnules arranged bilaterally and alternating in two rows. Secondary pinnules 0.5–2 cm in length; arranged uniserially at intervals starting near the base of primary pinnules, projecting anteriorly. Rarely, one or two tertiary pinnules occurring on a very small number of secondary pinnules and usually on the most basal secondary pinnules on the older portions of the corallum. Spines conical, slightly compressed laterally; ≤ 0.06 mm tall on the pinnules; mostly smooth, but some polypar spines possessing small, rounded, low-relief, knob-like protuberances. Spines taller, ≥ 0.14 mm, and needle-like on the thicker branches and stem. Number of spine rows per view and the density of spines in each row do not differ substantially from that on the pinnules.

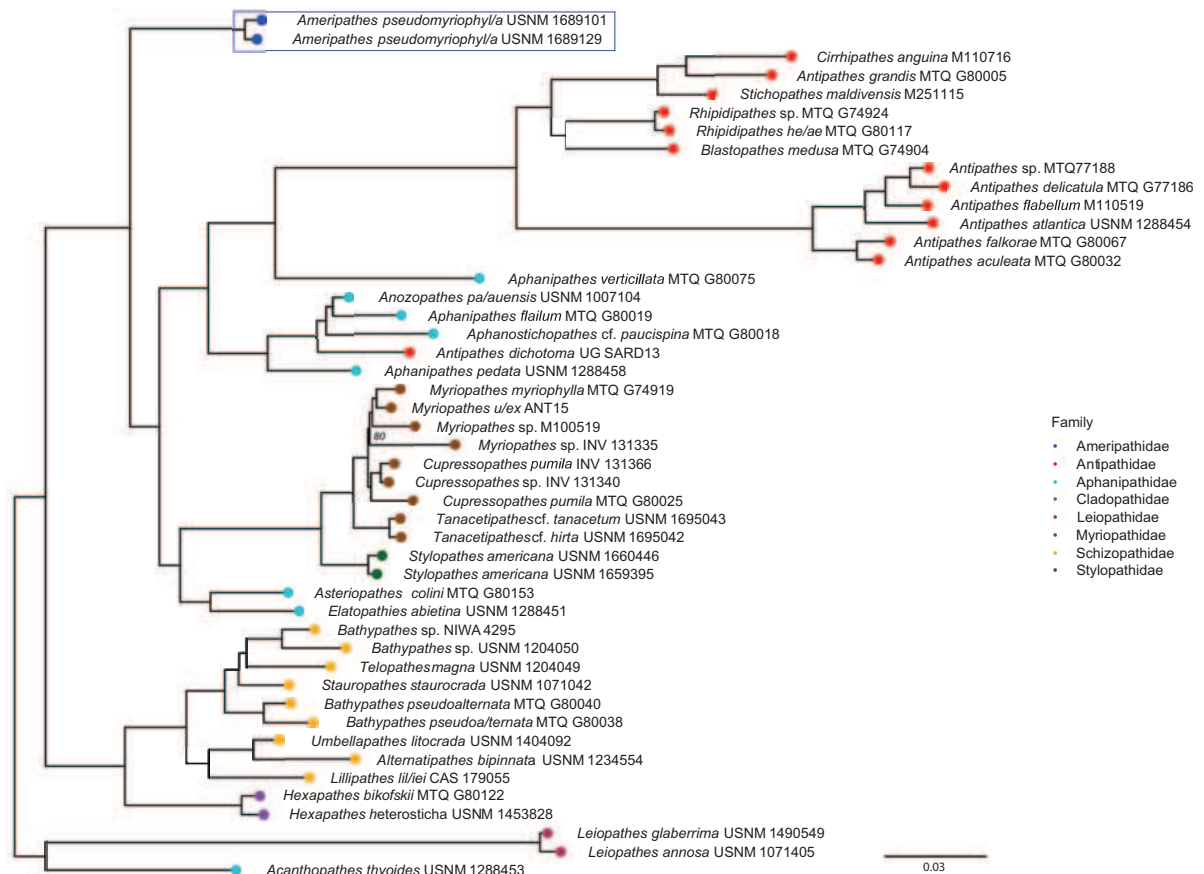


Figure 4. Maximum likelihood phylogeny of all black coral families and the new family based on a 50% complete matrix containing 741 loci. Boxed taxa (blue outline) represent the new species. Ultrafast bootstrap support is 100% at all nodes except for two nodes, which are noted in the phylogeny. The phylogeny was rooted to the Leioopathidae clade based on results from Horowitz et al. (2023b).

Polyps up to 1.25 mm in transverse diameter, appearing elongated transversely, arranged in a single row, with mostly seven or eight polyps per centimeter. Tentacles cylindrical, subequal in size; and when fully extended not much longer than the transverse diameter of the polyps. Tip of expanded tentacles rounded. Oral cone raised.

Remarks. Although the family at present contains only a single genus, a comparison with genera of other families suggests that the major generic morphological feature of *Ameripathes* is the pinnulate nature of the corallum, with two bilateral rows of primary pinnules and one to two orders of subpinnules. This same pinnulation pattern occurs in the genus *Myriopathes* in the family Myriopathidae and in the deep-sea genus *Dendrobathypathes* Opresko, 2002 in the family Schizopathidae. The occurrence of similar branching or pinnulation patterns across families is common among antipatharians.

Another feature that occurs in both *Ameripathes* and *Myriopathes* is an increase in the size of the spines on the branches and stem where they are more cylindrical and needle-like. However, in *Ameripathes* the spines on the stem do not increase in density (number of rows and number per row) and do not become forked or antler-shaped, which is often the case in the *Myriopathes*.

Species assigned to *Ameripathes*. *Ameripathes pseudomyriophylla* sp. nov. is the only species assigned to the newly described genus.

Etymology. In accordance with Article 11.3 of the International Code for Zoological Nomenclature the name of the genus *Ameripathes* can be considered an arbitrary combination of letters; however, it is loosely derived from “americana” in reference to the early association of this taxon with *Antipathes americana* Duchassaing and Michellotti, and the commonly used suffix *-pathes*.

Distribution. The single species assigned to this genus is known only from the Western Central Atlantic, in the Caribbean Sea and the Gulf of Mexico (Fig. 1).

***Ameripathes pseudomyriophylla* Opresko & Horowitz, sp. nov.**

<https://zoobank.org/9D4AFE4A-C83F-49A7-81BE-8E45999B0B56>

Figs 2A, 3A, 5–9, Suppl. material 1, <https://tinyurl.com/SupplMat2>

Antipathes americana Opresko, 1972: 975–979.

Antipathes picea Pourtalès, 1880: 115 (in part).

not *Antipathes americana* Duchassaing & Michelotti, 1860: 56.

Material examined. Holotype: USNM 1689129, 7 km east of Desecheo Island, Puerto Rico, 18.387°N, 67.408°W, 165 m depth, seawater temperature 22 °C. Schmidt Ocean Institute R/V Falkor (too), FKt230417, *Health diagnostic of deep-sea coral*, ROV SuBastian dive 506, April 19, 2023 (SEM stub No. 586–590).

Paratypes: USNM 1689101, 6 km east of Desecheo Island, Puerto Rico, 18.389°N, 67.417°W, 183 m depth, seawater temperature 21 °C. Schmidt Ocean Institute R/V Falkor (too), FKt230417, *Health diagnostic of deep-sea coral*, ROV SuBastian dive 504 April 18, 2023 (SEM stub No. 581–585); UMML 7.669 (schizoparatype USNM 1705331), Lesser Antilles, off Carriacou, 12.3917°N, 61.3600°W, 37–251 m depth. R/V Pillsbury sta. 857, July 3, 1969 (SEM stub No. 223); UMML 7.668 (schizoparatype USNM 1705332), Gulf of Mexico, 28.1167°N, 95.05°W, 55 m depth, R/V Silver Bay sta 190, Sept. 27, 1957; MCZ:IZ:57354, Lesser Antilles, off Grenada, 12.0583°N, 61.7861°W, 532 m depth, USCSS Blake sta. 260, Feb. 28, 1879 (SEM stub No. 207) (syntype of *Antipathes picea* Pourtalès).

Type locality. 7 km east of Desecheo Island, Mona Passage, Puerto Rico, 165 m depth

Diagnosis. As for the genus.

Description of the holotype. The holotype (USNM 1689129) is a 19-cm section of branch (Fig. 5A) from a colony estimated to be ~ 0.75 m tall based on in situ imagery (Fig. 5B). The polyps are white in color, both in situ and in the preserved state. The collected sample is sparsely branched to the second order, and pinnulate to the second order. Pinnulate branches are 4–6 cm in length and occur irregularly, but bilaterally. The primary pinnules, arranged bilaterally and alternately along the branches (Fig. 5C), measure 1–2 cm in length with basal diameters ≤ 0.2 mm, tapering to ~ 0.05 mm midsection and 0.02 mm near the distal end, are spaced 2.0–2.5 mm apart in each row (8 or 9 per centimeter, total for both rows), and incline distally at ~ 75°. The interior angle between the two rows of primaries is ~ 150°. The pinnules also tend to curve posteriorly, towards the abpolypar side of the corallum. The secondary pinnules are arranged uniseriably on the polypar side of the primary pinnules; the most proximal secondary is placed ~ 2 mm from the base of the primary pinnule, and secondary pinnules are spaced between 2–5 mm apart in a row with a maximum of three

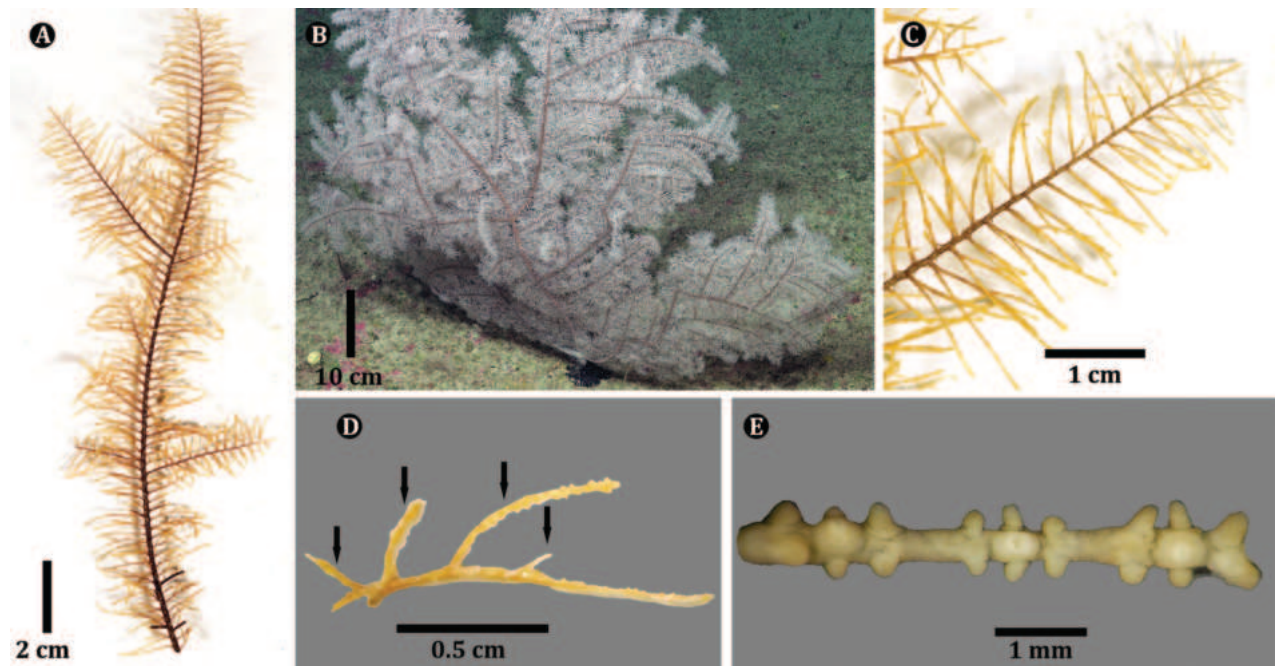


Figure 5. *Ameripathes pseudomyriophylla*, holotype (USNM 1689129) **A** section of the collected specimen **B** colony from which the holotype specimen was collected **C** section of pinnulated branch showing two rows of alternating primary pinnules and uniserial secondary pinnules **D** dorsal view of pinnulation pattern (second-order uniserial pinnules indicated by the arrows) **E** section of pinnule showing preserved polyps with contracted tentacles.

secondary pinnules occurring on one primary pinnule (Fig. 5D). The secondary pinnules are mostly 0.5–2.0 cm long and extending out from the polypar side of the corallum and form 60° distal angles. The longest secondaries can be longer than the primary pinnule from which they arise.

Spines (Fig. 6) on the pinnules are conical, slightly compressed laterally (especially those nearer the tips of the pinnules), with a rounded apex, and smooth or with one to three small, rounded, low-relief, knob-like protuberances 0.003–0.006 mm tall on polypar spines visible in lateral view (Fig. 6A, B). On pinnules ranging between 0.03 and 0.1 mm in diameter, polypar spines are 0.05 to 0.06 mm in height (Fig. 6B), and abpolypar spines range from 0.04 to 0.05 mm (Fig. 6C). The abpolypar spines are more distally directed than polypar spines. The developing spines nearer to the tip of the pinnules, where the axial diameter is 0.02–0.04 mm, have a very elongated and sloping proximal edge, ≤ 0.1 mm long, and a very short distal edge of ~ 0.03 mm or less, which extends out at near right angles to the surface of the pinnule (Fig. 6D). The distance from the tip of the spines to the middle of the base; however, is 0.05–0.06 mm. Three to four rows of spines can be counted in one view. The spines in each row are offset such that they also appear to follow a spiral pattern around the axis (with one spine from each row). Spaces between spines in a row range from 0.18 mm (abpolypar spines) to 0.22 mm (polypar spines), and 6 spines can be counted in 1 mm in each row. Spines on branches become taller and more cylindrical and needle-like; on a branch 1.3 mm in diameter, they are ≤ 0.12 mm tall. The rows become much less regular; however, the number of rows per view, and the density of spines in each row do not differ substantially from that on the pinnules.

Polyps occur in a single row. On the primary pinnules they are confined on or near the side on which the subpinnules occur. The polyps are 1.0–1.25 mm

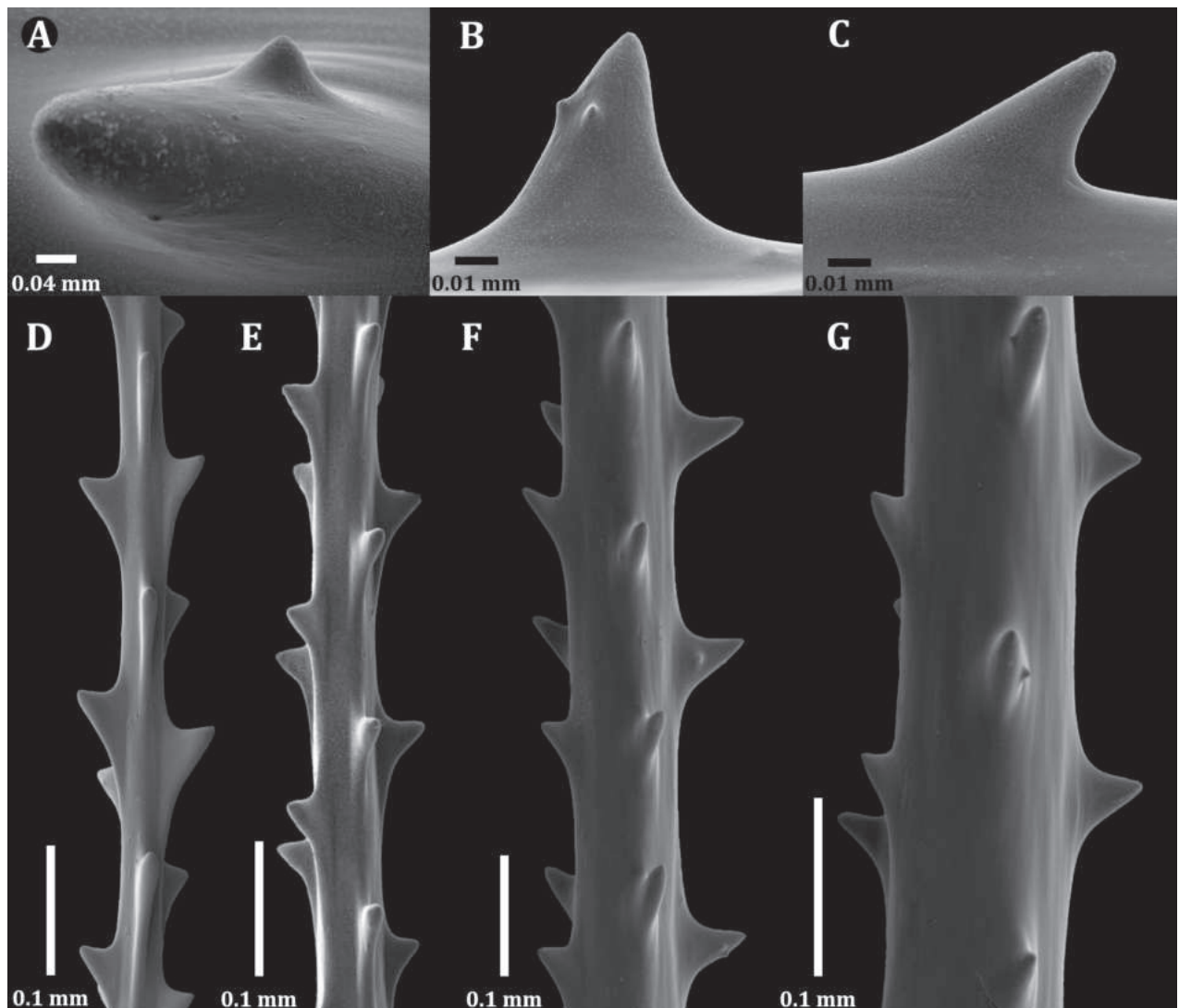


Figure 6. *Ameripathes pseudomyriophylla*, holotype (USNM 1689129) **A** dorsal view of single spine showing a single knob **B** lateral view of a polypar spine showing two knobs **C** lateral view of an abpolypar spine **D–G** sections of pinnules of increasing thickness.

in the transverse diameter (Fig. 5E). They appear elongated due to the small axial diameter of the pinnules. The interpolypar distance (between lateral tentacles of adjacent polyps) is 0.4–0.6 mm, and there are usually seven or eight polyps per centimeter. The tentacles (in preserved state) are subequal in size, 0.4–0.5 mm long, with the sagittals placed lower than the laterals. The oral cone is raised ~ 0.25 mm (Fig. 5E).

Description of colony from which holotype was collected. The colony from which the holotype was collected was imaged in situ (Fig. 5B) and based on a 4K video (<https://tinyurl.com/SupplMat2>), the complete colony was estimated to be approximately 1 m tall and 0.75 m wide. The main stem is ~ 1 m tall and the colony is branched to the seventh order or more and forms a distinct fan shape. Branches are ≥ 20 cm in length, have 75–90° distal angles, and are straight or curved distally near the base of the lower order branch from which they arise, and are slightly curved proximally towards the tip. Branches occur on both sides of lower-order branches.

Description of paratypes. Specimen USNM 11689101 is a 12-cm section of branch from a colony estimated to be ~ 0.3 m tall based on in situ imagery (Fig. 7A). The polyps are white in color in situ and in the preserved state. The collected sample has two orders of branches and pinnulate to the second order. The primary pinnules, arranged bilaterally and alternately along the stem and branches (Fig. 7B), measure 1.0–1.5 cm in length with basal diameters \leq 0.1 mm, tapering to ~ 0.05 mm midsection and 0.03 mm near the distal end, are spaced 2.0 mm apart in each row (9 or 10 per centimeter, total for both rows), and incline distally at ~ 65°. The interior angle between the two rows of primaries is ~ 130°. The pinnules also tend to curve posteriorly, towards the abpolypar side of the corallum. The secondary pinnules are arranged uniseriably on the polypar side of the primary pinnules; the most proximal secondary is placed ~ 2 mm from the base of the primary pinnule and rarely < 1 mm from the base of the primary pinnule. Secondary pinnules are spaced between 2–5 mm apart in a row with a maximum of two secondary pinnules occurring on one primary pinnule (Fig. 7B). The secondary pinnules are mostly 0.5–1.5 cm long and extending out from the polypar side of the corallum and form 60° distal angles. The longest secondaries can be longer than the primary pinnule from which they arise.

Spines on the pinnules are conical, slightly compressed laterally (especially those nearer the tips of the pinnules), with a rounded apex, and smooth or with one to two small, rounded, low-relief, knob-like protuberances 0.003–0.006 mm tall on polypar spines visible in lateral view (Fig. 7C). On pinnules ranging between 0.03 and 0.08 mm in diameter, polypar spines are 0.04–0.07 mm in height, and abpolypar spines range from 0.04 to 0.05 mm. The abpolypar spines are more distally directed than polypar spines. Three rows of spines can be counted in one view. The spines in each row are offset such that they also appear to follow a spiral pattern around the axis (with one spine from each row). Spaces between spines in a row range from 0.2 to 0.23 mm among abpolypar spines and to 0.25–0.3 among polypar spines, and five or six spines can be counted in 1 mm in each row. Spines on branches become taller and more cylindrical and needle-like and less regularly arranged, and sometimes absent on large areas of the axial surface (Fig. 7D). On a branch 0.8 mm in diameter, the spines are \leq 0.13 mm tall, in four irregular rows and with mostly five or six spines per millimeter in each row (Fig. 7D).

Polyps occur in a single row. On the primary pinnules they are confined on or near the side on which the subpinnules occur. The polyps are 1.0–1.25 mm in the transverse diameter (Fig. 7D). They appear elongated due to the small axial diameter of the pinnules. The interpolypar distance (between lateral tentacles of adjacent polyps) is 0.1–0.2 mm and there are usually eight or nine polyps per centimeter. The tentacles (in preserved state) are subequal in size with the sagittals placed lower than the laterals. The oral cone is raised ~ 0.25 mm.

The specimen from R/V Pillsbury sta. 857 (UMML 7.669, Fig. 8A) is mostly flattened in one plane, but with some overlapping branches. It has a height of 28 cm, a width of 22 cm, and a basal stem diameter of ~ 2 mm. It is sparsely branched to the third order, and pinnulate to the second and occasionally third order. The major branches are 5–10 cm in length and spaced 2.5–3 cm apart, and extend out laterally to vertically. As in the holotype, the primary pinnules are arranged bilaterally and alternately along the stem and branches (Fig. 8B,

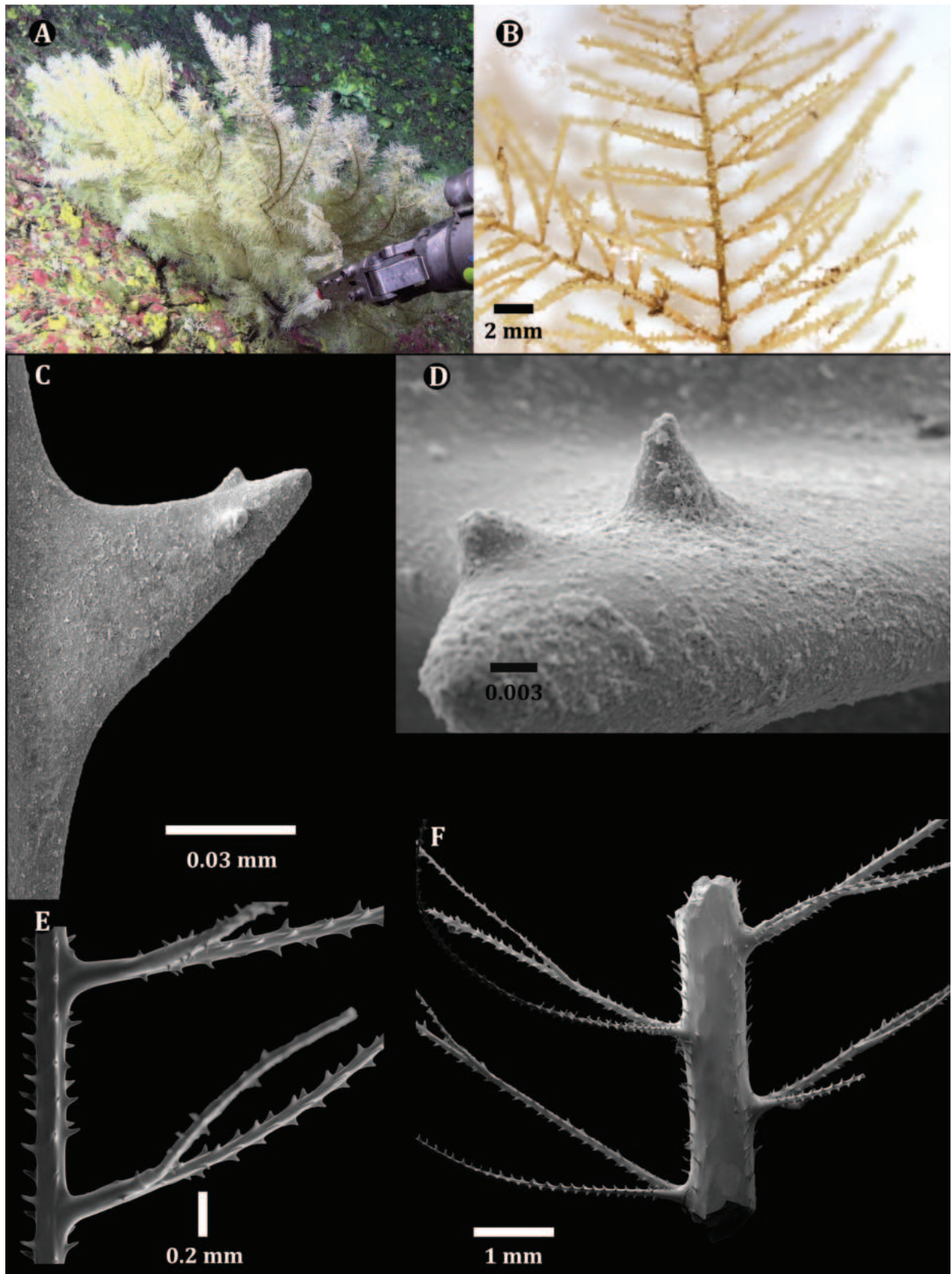


Figure 7. *Ameripathes pseudomyriophylla*, paratype (USNM 1689101) **A** colony from which the paratype was collected **B** section of the collected specimen **C** lateral view of a polypar spine showing two knobs **D** dorsal view of single spine showing two knobs **E** lateral view of a pinnulated branch showing the arrangement of the pinnules and subpinnules **F** lateral view of a branch showing the arrangement of the pinnules and subpinnules.

C). They are 1.5–2.0 cm long, mostly around 0.06 mm thick (up to 0.1 mm near the base), 2.5–3.0 mm apart (eight or nine per centimeter, total for both rows), and most are inclined distally, usually forming an angle of $\sim 60^\circ$ with the branch from which they arise. The interior angle between the two rows of primaries is close to 180° . The pinnules also tend to curve posteriorly, towards the abpolypar side of the corallum. The secondary pinnules are arranged uniseriably on the polypar side of the primary pinnules (Fig. 8C); the lowermost secondary is placed ~ 0.5 mm from the base of the primary, the second is 1.2–2.6 mm from the lowermost one, and the third secondary is 1.7–2.8 mm from the second. There can be as many as four secondary pinnules on the longest primaries. The secondary pinnules are 0.5–2.0 cm long and are inclined distally such that they form a distal angle of $\sim 60^\circ$ with the primary pinnule. The longest secondaries are usually those nearest the base of the primary, and they are sometimes as long, or longer than the primary pinnule from which they arise. One or two tertiary pinnules are rarely present on the polypar side of the lowermost secondary pinnules and sometimes on one of the more distal secondaries (Fig. 8D).

Spines (Fig. 9) on the pinnules are conical, slightly compressed laterally (especially those nearer the tips of the pinnules), with a rounded apex, and smooth or with a few small, rounded, low-relief, knob-like protuberances. The spines on one side are more distally directed than those on the opposite side. On the distal portion of a pinnule, where the axial diameter ranges from ~ 0.03 to 0.06 mm, the polypar spines are mostly 0.05–0.06 mm tall, and the abpolypar spines ~ 0.04 mm (Fig. 9A, B). On a pinnule with an axial diameter of 0.08–0.1 mm, the spines are ~ 0.06 mm (Fig. 9C–F). Spines on branches and stem become taller and more cylindrical and needle-like; on a branch 0.3 mm in diameter, they are ≤ 0.11 mm tall, spaced 0.2–0.3 mm apart (~ 5 per millimeter) and arranged in five rows as seen from one aspect (Fig. 9E).

Polyps occur in a single row. On the primary pinnules they are confined on or near the side on which the subpinnules occur. The polyps are 0.6 mm in transverse diameter near the tips of the pinnules, increasing to ~ 1.1 mm near the base. They appear elongated due to the small axial diameter of the pinnules. The interpolypar distance (between lateral tentacles of adjacent polyps) is 0.1–0.2 mm, and there are usually eight or nine polyps per centimeter, rarely as many as ten per centimeter. The tentacles (in preserved state) are subequal in size, ~ 0.4 mm long, with the sagittals placed lower than the laterals. The oral cone is ~ 0.25 mm high.

The MCZ specimen from *Blake* Sta. 260 is a 6.5-cm long branch or the stem of a small colony (with the basal plate missing). The primary pinnules are 1–2 cm long, ~ 0.17 mm in diameter at their base, and spaced ~ 3.0 mm apart in each row. Primary pinnules longer than ~ 2 cm develop into pinnulated branches with the primary pinnules 3 mm apart in each lateral row. The interior angle formed by the two rows of primary pinnules is 160 – 175° , but the pinnules are curved backwards so that they appear in the plane of the stem/branch. The distal angle of the pinnules is $\sim 75^\circ$. There are ≤ 4 secondary pinnules on each primary; the first is 0.05 mm from the base of the primary, the second 1.5–1.8 mm from the first, the third 2.0–2.5 mm from the second; and the fourth 3 mm from the third. The secondary pinnules are 0.2–0.7 cm long. They extend outward on the convex side of the primaries and are also angled distally $\sim 60^\circ$ to the primary.

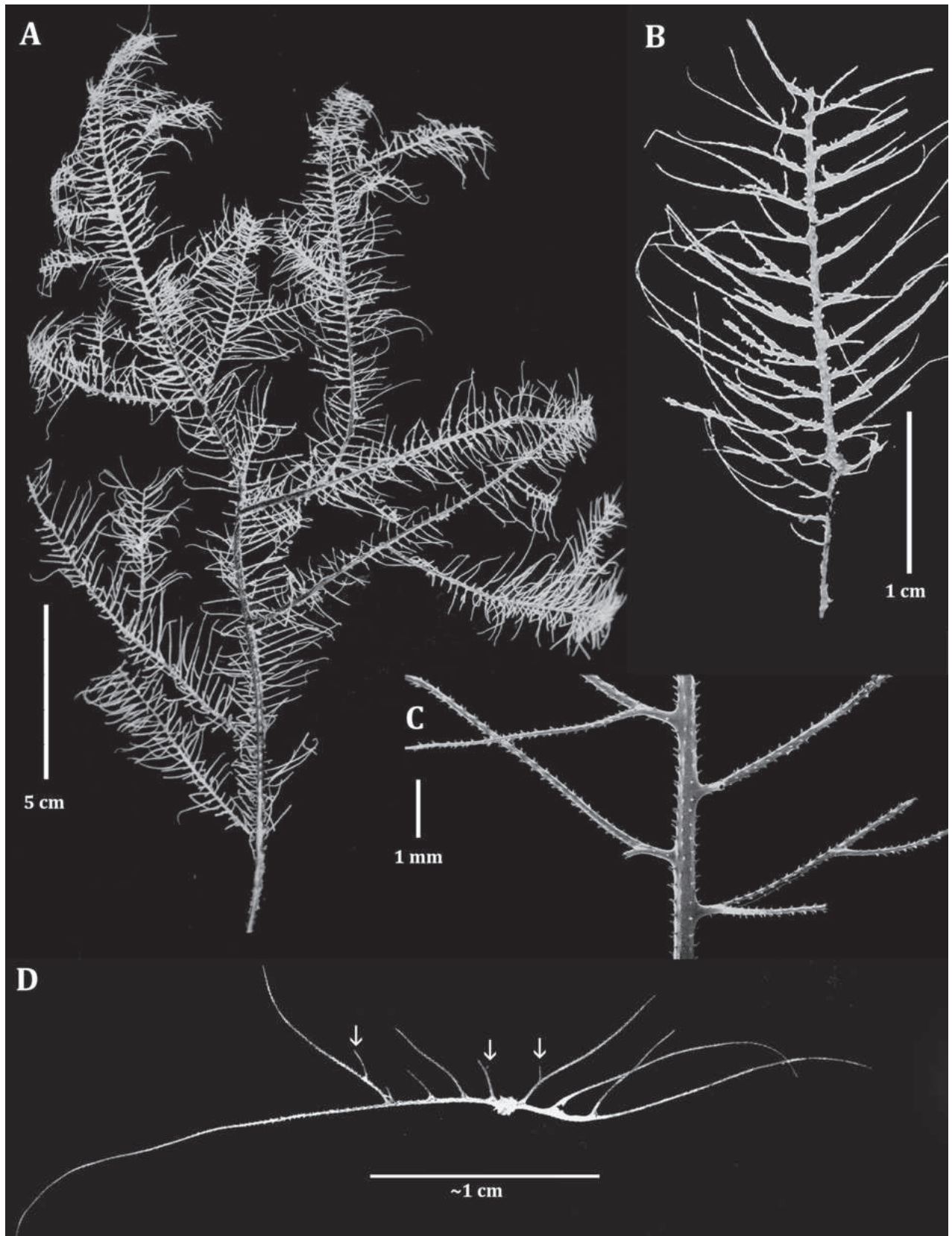


Figure 8. *Ameripathes pseudomyriophylla*, paratype (UMML 7.669) **A** entire corallum **B** section of a branch **C** closeup view showing the arrangement of the pinnules and subpinnules **D** dorsal view of pinnulation pattern (third order pinnules indicated by the arrows).

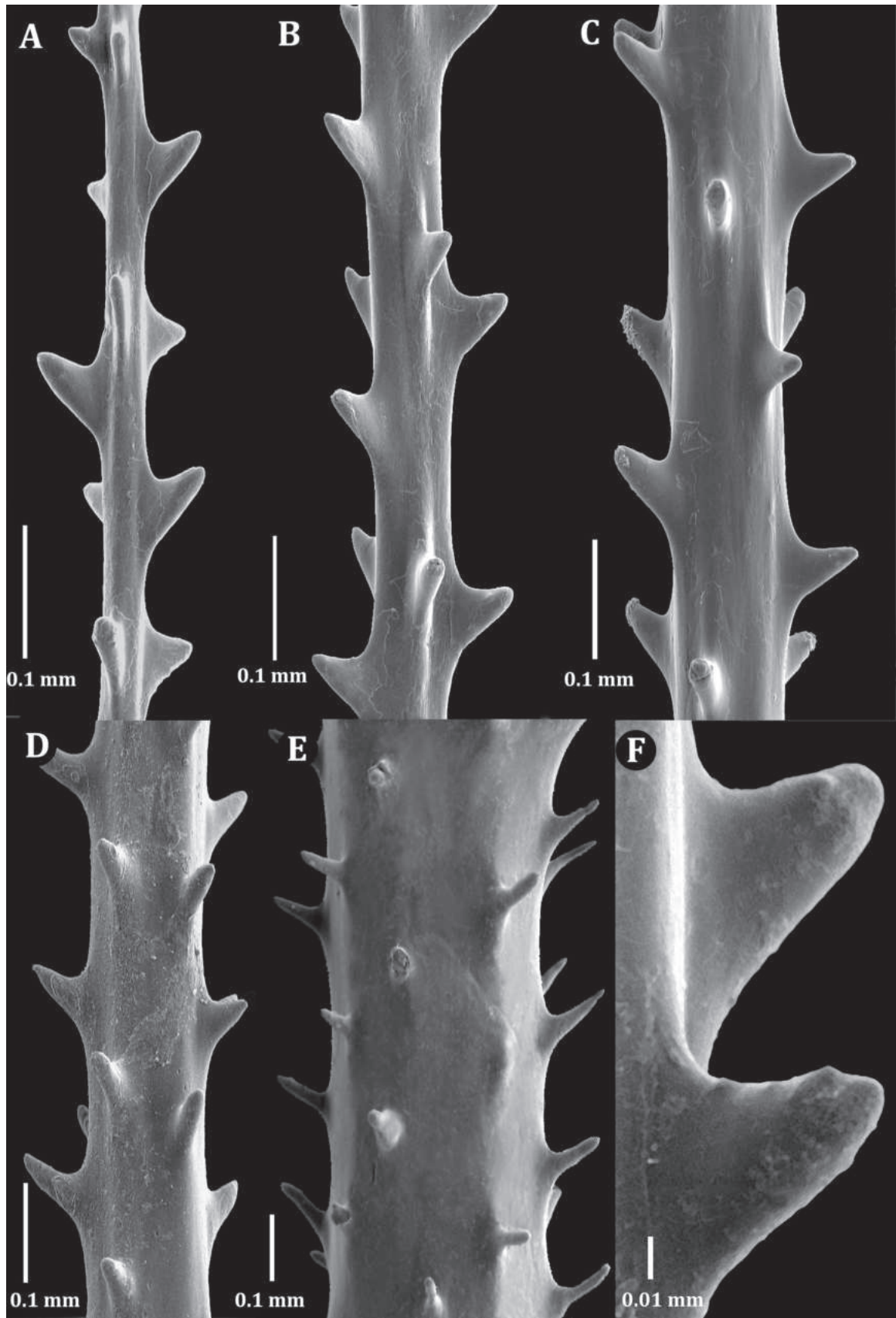


Figure 9. *Ameripathes pseudomyriophylla*, paratype (USNM 1705331, subsample of UMML 7.669) **A–C** sections of pinules **D** branchlet **E** section of thick branch **F** close-up view of two spines showing knob-like protuberances.

Tertiary pinnules are present on a few of the basal-most secondaries and are in the same plane as the secondary or extend upward to be parallel to the branch. The spines are 0.06 mm tall on the pinnules and 2–3× taller on the lower part of the stem/branch (≤ 0.17 mm). They are less regularly arranged near the base of the stem and extend out in various directions. In places, they are completely absent. Polyps are not present.

The specimen from Silver Bay sta. 190 (UMML 7.668) is 15 cm high and 8 cm wide, with a stem ~ 2.5 mm in diameter near its basal end. In this colony, the secondary pinnules are 0.5–1.5 cm long, and tertiary pinnules occur on not only the most basal secondary pinnule but also on the more distal ones. The tertiary pinnules also tend to project upward, parallel to the branch. On the lower part of the stem, the skeletal material of the axis has overgrown the basal portion of the lowermost secondary pinnules. Consequently, the stem appears to have four rows of primary pinnules. This appearance is enhanced by the fact that the secondary pinnules can be longer than the primary pinnules.

Intraspecies variation. The five specimens in the type series are fairly consistent in morphological features. They all form a branched pinnulate corallum with at least two orders of pinnules. The colonies tend to be planar. The occurrence and number of secondary and tertiary pinnules is, however, variable, both within a colony and between colonies, explainable perhaps by the size and age of the colony or the section of the colony sampled. The primary pinnules are always arranged bilaterally and alternately in two rows. The distance between primary pinnules in each row ranges from 2 to 3 mm; the total density for both rows is fairly consistent at eight or nine per centimeter. On the largest specimens, the maximum length of the primary pinnules is 2 cm or slightly longer. Pinnules longer than 2 cm usually develop into pinnulated branches. The pinnules are always very thin, the axial diameter is usually < 0.2 mm near their insertion on a branch and only 0.05–0.06 mm at their midpoint. The number of secondary pinnules per primary pinnule is usually one or two; however, rarely, there are as many as four per primary. Secondary pinnules are variable in length within and between colonies and can be as long as the primary pinnules. Tertiary pinnules are very rare and appear to occur mainly on older sections of the corallum. The fact that tertiary pinnules could not be found on the holotype is most likely due to its being a section taken from the upper, younger part of the colony. When present, tertiary pinnules are very short and are mostly confined to the lowermost secondary pinnules; however, they occasionally can also be found on a more distal secondary pinnule. There are usually only one, and rarely two tertiary pinnules on a secondary. On the pinnules, the maximum size of the polyp spines is consistently 0.06 mm from colony to colony. The spines always increase in size and become more cylindrical and needle-like on the larger branches, and depending on the axial diameter, can be as tall as 0.17 mm. The number of rows of spines varies slightly from colony to colony ranging between three or four to four or five visible in one aspect.

The number of rows, however, does not increase on the larger branches, and the density of the spines is mostly five or six per mm, even on the thickest branches. The maximum size of the polyps varies only slightly between colonies in that the transverse diameter ranges from ~ 1 –1.25 mm, and the density is typically 7–9 per cm. The interpolyp distance ranges from 0.1 to 0.6 mm.

Phylogenetic results. A total of 60–986 conserved element loci were obtained per specimen. Total number of contigs ranged from 16,819 to 1,444,028 base pairs (bp) (average lengths (bp) ranged from 280 to 1,695). The 50% taxon occupancy matrix included 741 loci that were concatenated into an alignment with a total length of 391,648 bp. Read and locus summary statistics are detailed in Suppl. material 1. The maximum likelihood phylogeny includes all eight black coral families with the new family representing a distinct lineage sister to the Antipathidae + Aphanipathidae + Myriopathidae + Stylopathidae (Fig. 4).

Etymology. The species name is derived from *pseudo* (false) and *myriophylla*, in reference to the very similar appearance to species in the genus *Myriopathes* with *M. myriophylla* being the type species of the genus.

Distribution. The species is only known only from the Caribbean and the Gulf of Mexico between 54 and 532 m depth.

Discussion and conclusions

This study describes the first new black coral family discovered in 18 years, underscoring the untapped potential for groundbreaking discoveries even in seemingly well-surveyed areas, such as the Gulf of Mexico. Furthermore, the identification of this new species, alongside another recent species described from the Caribbean Sea off Puerto Rico (Horowitz et al. 2023a), further demonstrates the need to increase exploration efforts of mesophotic and deep coral habitats, particularly in understudied regions. Discoveries such as this are now more feasible than ever, thanks to sophisticated remotely operated vehicles (ROVs) that can collect coral species with precision and provide invaluable in situ data, including imagery that reveals information such as colony color, habitat, and associated invertebrates. Furthermore, the advent of cutting-edge genetic methodologies for black corals—specifically, genome skimming and target enrichment of conserved elements (see Quattrini et al. 2018, 2024)—has revolutionized our ability to place these specimens within a phylogenetic framework with unparalleled accuracy and resolution, thereby bolstering the foundation for erecting new taxa.

Traditionally, the taxonomic classification of black corals has relied heavily on morphological characters, which can be prone to issues of convergence and homoplasy (Horowitz et al. 2023a). This study, however, leverages robust molecular data to navigate the complexities of classification, especially when the new species shares branching, spine, and polyp characteristics with the families Myriopathidae and Stylopathidae. By integrating detailed morphological examinations with advanced molecular analyses, this research confidently positions the new species within a novel genus and family and reinforces the importance of an integrated taxonomic framework. Such research not only contributes to the scientific endeavor of cataloging earth's biodiversity but also has profound implications for conservation strategies, offering insights that are vital for the preservation of vulnerable and often endangered ecosystems.

Acknowledgements

The authors wish to thank W. Keel, W. Moser, and K. Reed for their assistance during visits to the Museum Support Center at the NMNH. The photomicrographs were prepared in the NMNH SEM Laboratory (S. D. Whittaker,

director). Portions of the laboratory and/or computer work were conducted in and with the support of the L.A.B. facilities of the National Museum of Natural History. We also thank the Schmidt Ocean Institute R/V Falkor (too) crew and personnel for their assistance, support, and most importantly their passion for ocean research and exploration. We acknowledge the following museums and universities that made their material available for study: Rosenstiel School of Marine, Atmospheric, and Earth Science (University of Miami); Museum of Comparative Zoology (Harvard University); The Royal Belgian Institute of Natural Sciences; California Academy of Sciences; National Institute of Water and Atmospheric Research (New Zealand); National Museum of Natural History; and the University of Geneva. Research activities in Puerto Rico waters were coordinated with the Departamento de Recursos Naturales y Ambientales under permit # 2023-IC-019 (O-VS-PVSIS-SJ-01354-01022023).

Additional information

Conflict of interest

The authors have declared that no competing interests exist.

Ethical statement

No ethical statement was reported.

Funding

Funding for this project was provided by the Smithsonian Peter Buck Fellowship, Smithsonian Institution Barcode Network Award, and by a grant from the Department of Justice to the Smithsonian Institution. SH was supported by NOAA award NA18OAR0110289 and the National Academies of Sciences, Engineering, and Medicine Gulf Research Program Early-Career Fellowship under award 2000013668.

Author contributions

J.H. and D.M.O conceived the original idea and designed the study. J.H., D.M.O., S.H., C.M.H., and A.M.Q contributed to the overall research direction and planning. C.M.H. conducted the specimen collection. J.H., A.M.Q, and D.M.O developed the methodology and experimental protocols. J.H., D.M.O., S.H., C.M.H., and A.M.Q performed the data analysis and interpretation. J.H. and D.M.O wrote the first draft of the manuscript. J.H., D.M.O., S.H., C.M.H., and A.M.Q provided feedback and suggestions on the draft and edited the manuscript multiple times.

Author ORCIDs

Jeremy Horowitz  <https://orcid.org/0000-0002-2643-5200>

Dennis M. Opresko  <https://orcid.org/0000-0001-9946-1533>

Santiago Herrera  <https://orcid.org/0000-0001-7204-9434>

Colleen M. Hansel  <https://orcid.org/0000-0002-3506-7710>

Andrea M. Quattrini  <https://orcid.org/0000-0002-4247-3055>

Data availability

Raw sequence reads were submitted to GenBank under BioProject # PRJNA1078781. 4K video can be found on <https://tinyurl.com/SupplMat2>.

References

- Anisimova M, Gil M, Dufayard J-F, Dessimoz C, Gascuel O (2011) Survey of Branch Support Methods Demonstrates Accuracy, Power, and Robustness of Fast Likelihood-based Approximation Schemes. *Systematic Biology* 60(5): 685–699. <https://doi.org/10.1093/sysbio/syr041>
- Bolger AM, Lohse M, Usadel B (2014) Trimmomatic: A flexible trimmer for Illumina sequence data. *Bioinformatics (Oxford, England)* 30(15): 2114–2120. <https://doi.org/10.1093/bioinformatics/btu170>
- Chernomor O, von Haeseler A, Minh BQ (2016) Terrace aware data structure for phylogenomic inference from supermatrices. *Systematic Biology* 65(6): 997–1008. <https://doi.org/10.1093/sysbio/syw037>
- Cowman PF, Quattrini AM, Bridge TCL, Watkins-Colwell GJ, Fadli N, Grinblat M, Roberts TE, McFadden CS, Miller DJ, Baird AH (2020) An enhanced target-enrichment bait set for Hexacorallia provides phylogenomic resolution of the staghorn corals (Acroporidae) and close relatives. *Molecular Phylogenetics and Evolution* 153: 106944. <https://doi.org/10.1016/j.ympev.2020.106944>
- de Pourtalès L (1880) Zoological results of the Blake expedition to the Caribbean Sea. *Bulletin of the Museum of Comparative Zoology* 6: 113–118.
- Duchassaing P, Michelotti J (1860) Mémoire sur les coralliaires des Antilles. *Memorie della Reale Accademia delle Scienze di Torino* 2: 279–365. <https://doi.org/10.5962/bhl.title.11388>
- Faircloth BC (2016) PHYLUCE is a software package for the analysis of conserved genomic loci. *Bioinformatics (Oxford, England)* 32(5): 786–788. <https://doi.org/10.1093/bioinformatics/btv646>
- Hoang DT, Chernomor O, von Haeseler A, Minh BQ, Vinh LS (2018) UFBoot2: Improving the Ultrafast Bootstrap Approximation. *Molecular Biology and Evolution* 35(2): 518–522. <https://doi.org/10.1093/molbev/msx281>
- Horowitz J, Opresko DM, González-García MDP, Quattrini AM (2023a) Description of a new species of black coral in the family Aphanipathidae (Anthozoa, Antipatharia) from Puerto Rico. *ZooKeys* 1173: 97–110. <https://doi.org/10.3897/zookeys.1173.104141>
- Horowitz J, Quattrini AM, Brugler MR, Miller DJ, Pahang K, Bridge TCL, Cowman PF (2023b) Bathymetric evolution of black corals through deep time. *Proceedings. Biological Sciences* 290(2008): 20231107. <https://doi.org/10.1098/rspb.2023.1107>
- Kalyaanamoorthy S, Minh BQ, Wong TKF, von Haeseler A, Jermini LS (2017) ModelFinder: Fast model selection for accurate phylogenetic estimates. *Nature Methods* 14(6): 587–589. <https://doi.org/10.1038/nmeth.4285>
- Katoh K, Standley DM (2013) MAFFT Multiple Sequence Alignment Software Version 7: Improvements in Performance and Usability. *Molecular Biology and Evolution* 30(4): 772–780. <https://doi.org/10.1093/molbev/mst010>
- Minh BQ, Schmidt HA, Chernomor O, Schrempf D, Woodhams MD, von Haeseler A, Lanfear R (2020) IQ-TREE 2: New models and efficient methods for phylogenetic inference in the genomic era. Teeling E (Ed.). *Molecular Biology and Evolution* 37: 1530–1534. <https://doi.org/10.1093/molbev/msaa015>
- Molodtsova TN (2011) A new species of *Leiopathes* (Anthozoa: Antipatharia) from the Great Meteor seamount (North Atlantic). *Zootaxa* 3138(1): 52–64. <https://doi.org/10.11646/zootaxa.3138.1.3>
- Opresko DM (1972) Redescriptions and reevaluations of the antipatharians described by L. F. de Pourtalès. *Bulletin of Marine Science* 22: 950–1017.

- Opresko DM (2001) Revision of the Antipatharia (Cnidaria: Anthozoa). Part I. Establishment of a new family, Myriopathidae. *Zoologische Mededelingen, Leiden* 75: 343–370.
- Opresko DM (2004) Revision of the Antipatharia (Cnidaria: Anthozoa). Part IV. Establishment of a new family, Aphanipathidae. *Zoologische Mededelingen, Leiden* 78: 1–15.
- Opresko DM (2006) Revision of the Antipatharia (Cnidaria: Anthozoa). Part V. Establishment of a new family. Stylopathidae *Zoologische Mededelingen, Leiden* 80(4): 109–138.
- Prjibelski A, Antipov D, Meleshko D, Lapidus A, Korobeynikov A (2020) Using SPAdes De Novo Assembler. *Current Protocols in Bioinformatics* 70(1): e102. <https://doi.org/10.1002/cpbi.102>
- Quattrini AM, Faircloth BC, Dueñas LF, Bridge TCL, Brugler MR, Calixto-Botía IF, DeLeo DM, Forêt S, Herrera S, Lee SMY, Miller DJ, Prada C, Rádis-Baptista G, Ramírez-Portilla C, Sánchez JA, Rodríguez E, McFadden CS (2018) Universal target-enrichment baits for anthozoan (Cnidaria) phylogenomics: New approaches to long-standing problems. *Molecular Ecology Resources* 18(2): 281–295. <https://doi.org/10.1111/1755-0998.12736>
- Quattrini AM, McCartin LJ, Easton EE, Horowitz J, Wirshing HH, Bowers H, Mitchell K, Sei M, McFadden CS, Herrera S (2024) Skimming genomes for systematics and DNA barcodes of corals. *Ecology and Evolution* 14(5): e11254. <https://doi.org/10.1002/ece3.11254>

Supplementary material 1

Table of read and locus summary statistics for specimens

Authors: Jeremy Horowitz, Dennis M. Opresko, Santiago Herrera, Colleen M. Hansel, Andrea M. Quattrini

Data type: xlsx

Explanation note: Metadata for molecular data including the number of raw reads, assembly statistics, and NCBI details.

Copyright notice: This dataset is made available under the Open Database License (<http://opendatacommons.org/licenses/odbl/1.0/>). The Open Database License (ODbL) is a license agreement intended to allow users to freely share, modify, and use this Dataset while maintaining this same freedom for others, provided that the original source and author(s) are credited.

Link: <https://doi.org/10.3897/zookeys.1203.121411.suppl1>

